REPORT TITLE PAGE

Estimation and Comparison of Methane, Nitrous Oxide, and Trace Volatile Organic Compound Emissions and Gas Collection System Efficiencies in California Landfills

March 25, 2020

Produced Under Contract By: California Polytechnic State University

Estimation and Comparison of Methane, Nitrous Oxide, and Trace Volatile Organic Compound Emissions and Gas Collection System Efficiencies in California Landfills

Final Report

CalRecycle Contract: DRR16109 and CARB Contract: 16ISD006

Principal Investigators:
James L. Hanson
Nazli Yesiller

Prepared for:
The California Air Resources Board and The California Department of Resources Recycling and Recovery

Prepared by:
James L. Hanson
Nazli Yesiller
Derek C. Manheim
Department of Civil and Environmental Engineering
California Polytechnic State University
One Grand Avenue
San Luis Obispo, CA 93407
(805) 756-6227

March 25, 2020

Prepared as part of contract numbers DRR16109 and *16ISD006, in the total amount of $1,100,000.*

TABLE OF CONTENTS

LIST OF FIGURES

LIST OF TABLES

ACKNOWLEDGMENTS

The research team included Dr. Jean E. Bogner of University of Illinois – Chicago and Dr. Donald R. Blake of University of California-Irvine. Staff of the Rowland-Blake Laboratory at UC-Irvine assisted with analytical testing. Dr. Amro El Badawy and Mr. Nephi Derbidge from California Polytechnic State University assisted with the field test program and the laboratory testing program. Ms. Alexandra D. Limpert assisted with the field testing program and the laboratory testing program. Numerous graduate and undergraduate students from California Polytechnic State University assisted with the field and laboratory tests. Waste Connections Inc., Waste Management Company, City of Santa Maria, and County Tulare – Solid Waste Department coordinated access to the landfill field sites. Staff at the five landfill sites cooperated with the research team and provided support during all phases of the field analysis. CARB and CalRecycle staff provided constructive feedback in finalizing the report.

This Report is submitted in fulfillment of CalRecycle Contract Number: DRR16109 and CARB Contract Number: 16ISD006, total contract amount $1,100,000, pursuant to Government Code Section 7550, provided for the Project entitled “Estimation and Comparison of Methane and Nitrous Oxide Emissions and Gas Collection System Efficiencies in California Landfills” by the Civil and Environmental Engineering Department at California Polytechnic State University under the sponsorship of the California Department of Resources Recycling and Recovery and the California Air Resources Board. Work was completed as of March 31, 2020.

ABSTRACT

This investigation was conducted to provide detailed assessment of emissions of 82 gases consisting of 4 primary greenhouse gases (methane, nitrous oxide, carbon dioxide, and carbon monoxide) and 78 non-methane volatile organic compounds (categorized under 11 chemical families) from landfills in California. Limited field emissions data are available for these gases for intra- and inter-landfill variations in California or elsewhere. Initially, analysis was conducted to identify and select representative landfills for emissions measurements. In extensive field testing, methane emissions were determined using aerial measurements at 16 selected landfills and emissions of all 82 gases were determined using ground-based static flux chamber measurements at a subset of 5 landfills. Baseline air quality and emissions from the three main categories of covers at active landfills (daily, intermediate, and final) were determined at the five sites over the two main seasons (wet and dry) in California. The minimum and maximum measured fluxes were -3.73×10^{0} to 9.62×10^{1} g/m^2-day for methane. The nitrous oxide and trace non-methane volatile organic compound fluxes were lower and ranged from -4.10×10^{-3} to 1.45×10^{-1} and -1.93×10^{-3} to 1.81×10^{0} g/m^2-day, respectively. The main factor that controlled surface flux was cover characteristics. The fluxes generally decreased with the order daily, intermediate, and final covers; high to low permeability covers; and thin to thick covers. The gas collection system efficiencies were determined to range from 23.2 to 91.4% (aerial measurements), 38.9 to 100% (ground measurements), and 24.5 to 75.9% (LandGEM) Model.

EXECUTIVE SUMMARY

Introduction

This investigation was conducted to provide detailed assessment of emissions of a total of 82 landfill gases (LFGs) that consisted of 4 greenhouse gases (methane, nitrous oxide, carbon dioxide, and carbon monoxide) and 78 non-methane volatile organic compounds (NMVOCs) from California landfills. The NMVOCs were categorized under 11 chemical families: reduced sulfur compounds, fluorinated gases, halogenated hydrocarbons, organic (alkyl) nitrates, alkanes, alkenes, aldehydes/alkynes, aromatic hydrocarbons, monoterpenes, alcohols, and ketones. In addition, efficiencies of gas collection systems in California landfills were assessed. The investigation included experimental analysis (field and laboratory testing) and modeling. More than 65,000 individual gas concentration measurements were used to determine the surface flux of the 82 target gases from 31 individual cover types using testing during both wet and dry seasons. Operational, environmental, and climatological factors that affect emissions and gas collection efficiency were analyzed. Fluxes for a great majority of the NMVOCs included in the study were determined for the first time from daily covers in landfills and flux data were provided for the first time for 8 chemical species. To the Principal Investigators' (PIs) knowledge, this study represents the most comprehensive landfill gas emissions and gas collection analyses conducted to date in California, U.S., and internationally.

Methods

The investigation consisted of four main phases: 1) comprehensive literature review related to landfill gas generation and emissions, 2) California-specific landfill classification scheme, 3) extensive field-testing program at California landfills and supplementary laboratory analysis, and 4) comprehensive analyses of landfill gas generation and collection efficiency. The literature review established the state-of-the-art for landfill gas generation, collection, and emissions as well as provided the basis for categorization of the gas species included in the investigation. A landfill classification scheme was developed first to categorize all active landfills in California and then to identify and select representative landfills for field testing. The classification scheme included criteria for landfill size (waste in place [WIP], disposal area, waste column height, and permitted throughput); proximity to population centers, oil/gas operations, and quaternary faults; climate; presence of a gas collection system; acceptance of waste tires; cover conditions (daily, intermediate, final); waste age; and landfill configuration and operational details.

The field investigation consisted of two types of measurement programs: aerial measurements of only methane and ethane at height above the landfill surfaces and ground-based measurements of all of the 82 landfill gas species included in the study directly on the landfill surfaces (Figure ES.1). The aerial testing was based on a temporally and spatially integrated mass balance measurement approach. The aerial tests were conducted using a single engine Mooney aircraft that was instrumented with

a Picarro G2401-m Analyzer (cavity ring down spectrometer). The ground testing was based on time series gas concentration measurements conducted over a sealed known landfill surface area and gas volume. The ground tests were conducted using large-scale static flux chamber test instrumentation with dimensions of 1 m x 1 m areal extent (1 m^2 measurement area) and 0.4 m height. The aerial tests were conducted at 16 landfills and the static flux chamber tests were conducted at 5 landfills that were a subset of the 16 aerial measurement sites. The 16 aerial testing landfills included small (WIP < 4,000,000 m^3), medium (4,000,000 m^3 < WIP < 40,000,000 m^3), and large sites (WIP > 40,000,000 m^3) and were located at five different climatic zones representing the climate zones with active landfills in the State. The 5 ground testing landfills included medium (Santa Maria Regional, Teapot Dome) and large (Potrero Hills, Site A, Chiquita Canyon) sites and located in three different climatic zones that contain 98.8% of the waste in place in the State. The waste in place at the 16 aerial measurement landfills contained 30% of the total waste in place in landfills in California and the waste in place at the 5 ground measurement landfills contained 13% of the total waste in place in landfills in California. The field emissions tests were supplemented by determination of thicknesses of the cover materials at specific test locations, temperatures of covers, and in-place densities of covers. Extensive laboratory characterization of geotechnical properties of the cover materials was conducted on field samples from each tested cover system to provide mechanistic explanations of the observed flux behavior.

Figure ES.1 Synchronous Ground and Aerial Testing

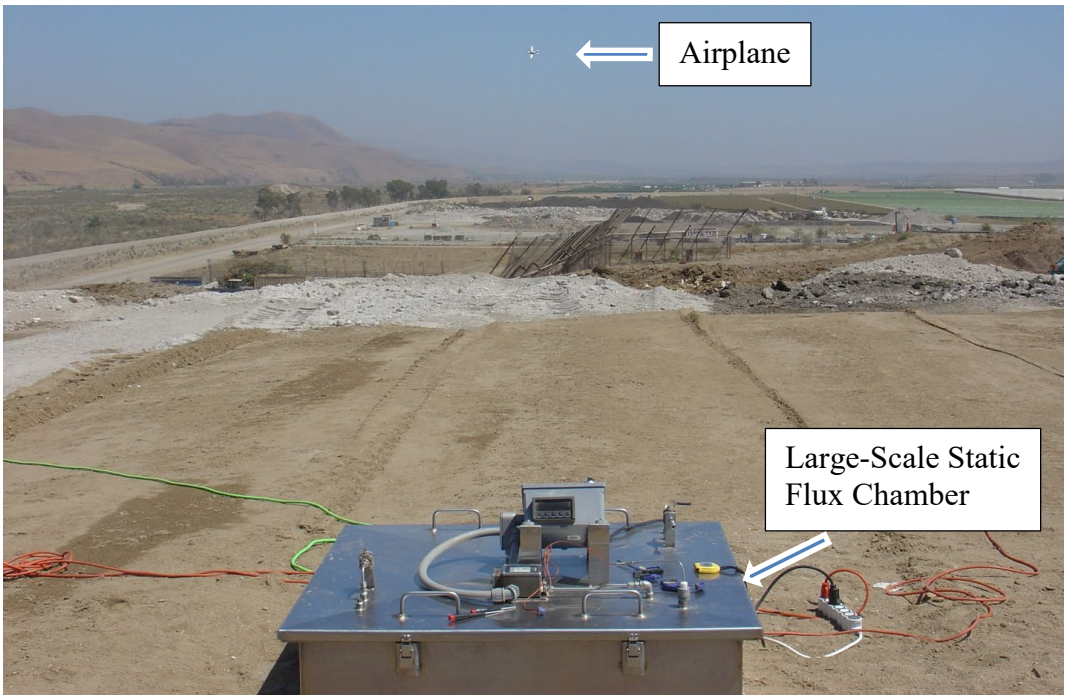

The static flux chamber tests were conducted on all three cover categories (daily, intermediate, and final) used in active landfills. For a given cover category at a given site, all different material types used for that particular cover category were tested. Overall, based on cover categories and cover material types, static flux chamber tests

were conducted at five to seven locations at a given landfill. Testing in the wet and dry seasons was conducted over the project period for both aerial and ground-based measurements. Gas collection efficiencies were determined using two main approaches: i) as a quotient of the reported gas collected at a given site and the summation of gas collected and emissions measured in the field tests and ii) as a quotient of the reported gas collected at a given site and modeled gas generation at the same site. Gas generation was modeled for methane using the LandGEM model specifically developed for this gas (not applicable to NMVOCs). To determine gas generation with LandGEM, two sets of parameters were used: default values provided in the LandGEM model and refined values obtained using an artificial neural network (ANN) modeling process. Gas production and collection efficiency analysis was conducted only for methane as commonly accepted and widely used analysis approaches are not available for trace gases such as nitrous oxide and the NMVOCs included in this investigation. Uncertainty estimates also were provided for both the field measurements as well as modeling analyses.

Results

Surface Gas Flux and Emission Results

The aerial testing program indicated that methane emissions increased from small to medium to large landfills, where the emissions from the small, medium, and large landfills varied from -25 to 11 kg/hr, 90 to 638 kg/hr, and 602 to 3275 kg/hr, respectively. The methane emissions from the large landfills were more than one to two orders of magnitude higher than the emissions from the small landfills, whereas the differences between the medium and large landfills were within the same order of magnitude. Even though the small landfills did not have active gas collection and removal systems, the measured emissions from these sites were very low. While the medium and large landfills had gas collection and removal systems, the emissions from these sites were high. High waste in place, high daily waste throughput, and large working face (i.e., active, uncovered waste placement area during operational hours at a landfill, which ranged between 65 and 12,100 m^2 in the investigation) likely resulted in high emissions.

A summary of the flux data obtained in the ground testing program is provided in Figure ES.2 by landfill site. The highest fluxes at each landfill site were obtained for GHGs, which included methane, nitrous oxide, carbon dioxide, and carbon monoxide. The mean and median GHG fluxes were positive at all sites. The GHG fluxes varied by up to two orders of magnitude between the landfills investigated. The results of this study indicated that NMVOCs are a significant and detectable fraction of the landfill gas emitted from the sites investigated with positive mean and median NMVOC fluxes obtained at all five landfills. The highest NMVOC fluxes were measured for the alcohols, ketones, and monoterpenes chemical families. Based on comparisons to flux data provided in the literature, the ranges of methane and nitrous oxide fluxes were lower (analysis of well-engineered California landfills), while the ranges for NMVOCs were higher (analysis of not previously tested chemicals and covers) in this test program.

Figure ES.2 Inter-landfill Flux Results (open black diamonds, red lines, solid red dots represent means, medians, and outliers, respectively)

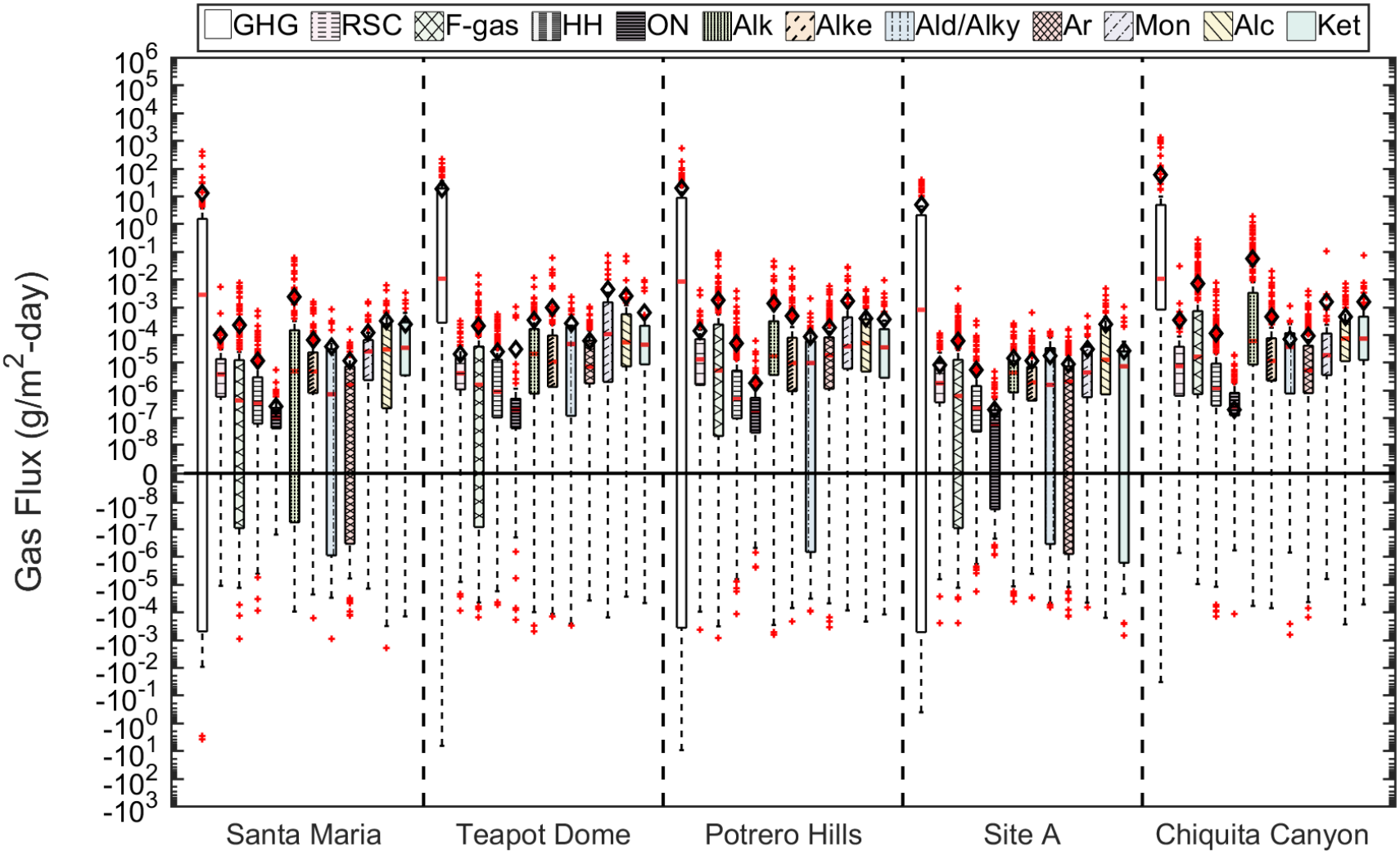

Both positive (emissions to the atmosphere) and negative (uptake from the atmosphere) fluxes were measured. Positive fluxes resulted from higher concentrations in the waste mass than in the ambient air. Negative fluxes resulted from a combination of lower concentrations in the waste mass than in the ambient air and presence of vacuum pressure from gas collection and extraction systems drawing ambient air into the landfill system. A great majority of the measured fluxes were positive indicating net emissions of all of the 82 gases into the atmosphere. The measured flux ranges were -3.73×10^{0} to 9.62×10^{1} g/m^2-day, -4.10×10^{-3} to 1.45×10^{-1} g/m^2-day, and -1.93×10^{-3} to 1.81×10^{0} g/m^2-day for methane, nitrous oxide, and total NMVOCs, respectively. The variations of positive flux of a given chemical at a given landfill was up to 6 orders of magnitude and the variations of a given chemical between landfills was up to 7 orders of magnitude. Seasonal flux variations for a given site were low and generally were within one order of magnitude between the dry and wet seasons.

The overall variation in methane flux in the investigation was from -10^{0} to 10^{1} g/m^2-day (Figure ES.3). Variation by landfill and cover category was comparable and higher than variation by season. The methane fluxes from the medium sized landfills (Santa Maria Regional and Teapot Dome) were comparable to the fluxes from the larger sites (Potrero Hills, Site A, and Chiquita Canyon) indicating that factors other than size and scale of landfill operations contribute to and potentially control methane emissions. The methane fluxes decreased in order of daily to intermediate to final covers with a higher decrease from intermediate to final covers than from daily to intermediate covers. The highest methane fluxes were generally from alternative daily covers and in particular from autofluff. These thin, highly porous daily covers provided low resistance to methane flux. The thick engineered final cover systems with high fine soil content and use of geosynthetics at one site resulted in the lowest fluxes. The seasonal variations generally were within one order of magnitude indicating that landfill and cover conditions influence methane flux more than seasonal variations in California. This study for the first time provided flux data for an alternative cover system and also a comparison between an alternative and a conventional cover (Site A). The data indicated that methane flux from the alternative final cover was significantly higher than the methane flux from the conventional final cover, which may have resulted from a combination of the more interconnected pore structure of the coarser-grained alternative cover compared to the occluded pore structure of the finer-grained conventional cover and the lower thickness of the alternative final cover as compared to the conventional cover.

The overall range in nitrous oxide flux was from -10^{-3} to 10^{-1} (Figure ES.4). Variation by cover category was higher than variation by landfill and season, which were relatively comparable. Nitrous oxide fluxes at the medium-sized landfills were largely positive when compared to the larger landfills, with overall low probability for negative flux (all or most of interquartile ranges above zero in Figure ES.4). Waste composition may have caused these differences, where the amount of incoming wastes with high nitrogen content (i.e., crop wastes/residue, manure) are likely high due to the surrounding agricultural communities of Santa Maria Regional and Teapot Dome Landfills compared to the wastes from mainly urban sources at the large landfills in Northern and Southern California. Similar to methane flux, nitrous oxide fluxes decreased from the daily to

intermediate to final covers with a higher decrease from intermediate to final covers than from daily to intermediate covers. The thin, highly porous daily covers provided low resistance to nitrous oxide flux. The thick engineered final cover systems with high fine soil content and use of geosynthetics at one site resulted in the lowest fluxes. The seasonal variations were generally within one order of magnitude indicating that cover conditions influence nitrous oxide flux more than seasonal variations in California.

Figure ES.3 Tornado Plot of Methane Flux as a Function of Landfill, Cover Type, and Season (open black diamonds, black lines, solid red dots represent means, medians, and outliers, respectively).

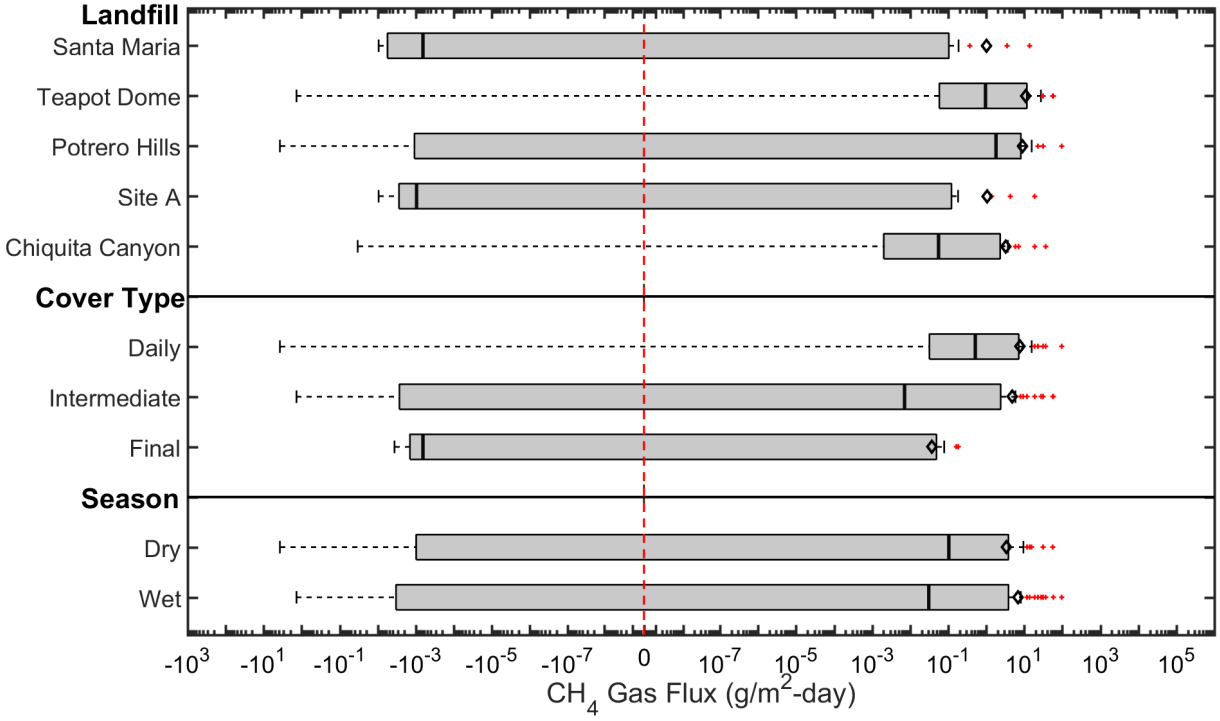

Figure ES.4 Tornado Plot of Nitrous Oxide Flux as a Function of Landfill, Cover Type, and Season (open black diamonds, black lines, solid red dots represent means, medians, and outliers, respectively).

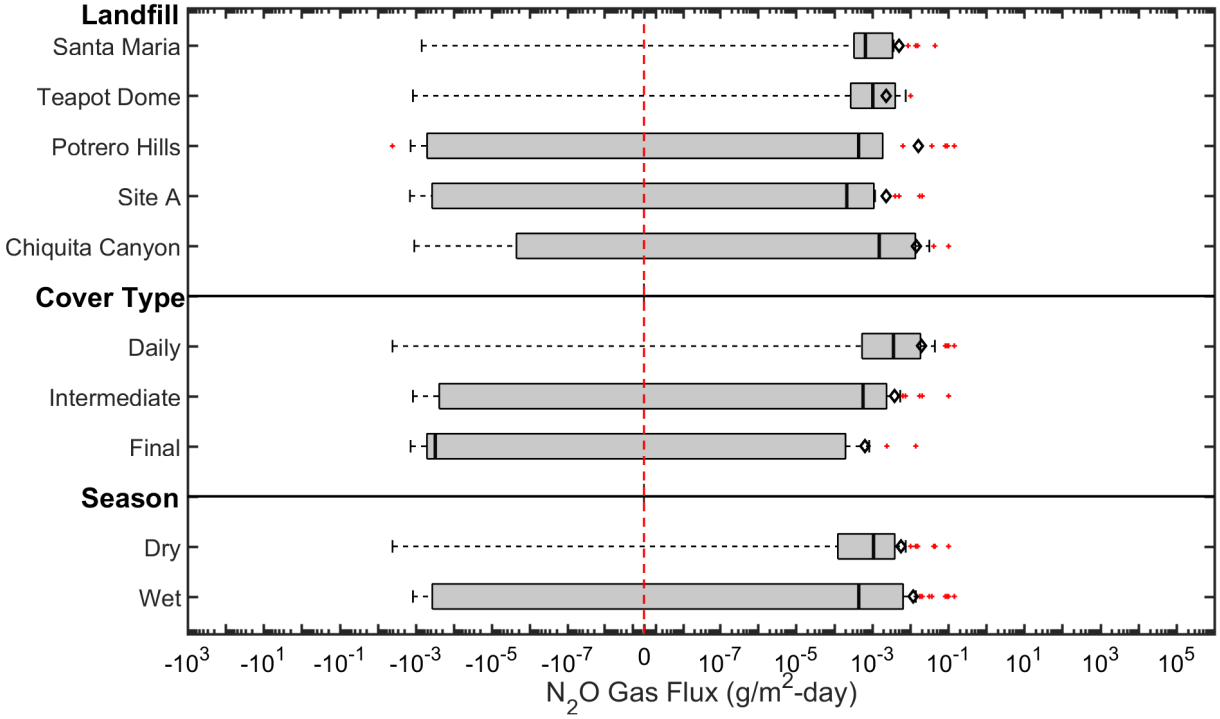

The overall range in NMVOC flux was from -10^{-3} to 10^{0} g/m^2-day (Figure ES.5). Variation in total NMVOC flux was generally comparable across landfills, cover categories, and seasons with less variability compared to methane and nitrous oxide. Positive flux is dominant for the NMVOCs investigated with low probability of uptake (interquartile ranges above zero in Figure ES.5), even though all of the NMVOCs are trace components of landfill gas. Similar to methane and nitrous oxide fluxes, the NMVOC fluxes from the medium sized landfills (Santa Maria Regional and Teapot Dome) were comparable to the fluxes from the larger landfills, indicating that factors other than operational scale contribute to and potentially control NMVOC emissions. Cover category had the most significant effect on NMVOC fluxes, where the fluxes decreased from the daily to intermediate to final covers. In similarity to methane and nitrous oxide flux results, the thin, highly porous daily covers provided low resistance to NMVOC flux. In addition, the daily covers may have been sources of some NMVOCs. NMVOCs such as aromatic hydrocarbons, alkanes, and alkenes may have volatilized from the contaminated soil daily cover. The wood waste and green waste alternative daily covers (ADCs) are potential sources of monoterpenes and the autofluff ADC is a potential source of F-gases. The thick engineered final cover systems with high fine soil content and use of geosynthetics at one test site resulted in the lowest fluxes. The final cover NMVOC fluxes were in one case higher than those for methane and nitrous oxide. The seasonal variations were generally within one order of magnitude indicating the higher influence of the cover conditions on NMVOC flux than seasonal variations in California.

Figure ES.5 Tornado Plot of NMVOC Flux as a Function of Landfill, Cover Type, and Season (open black diamonds, black lines, solid red dots represent means, medians, and outliers, respectively).

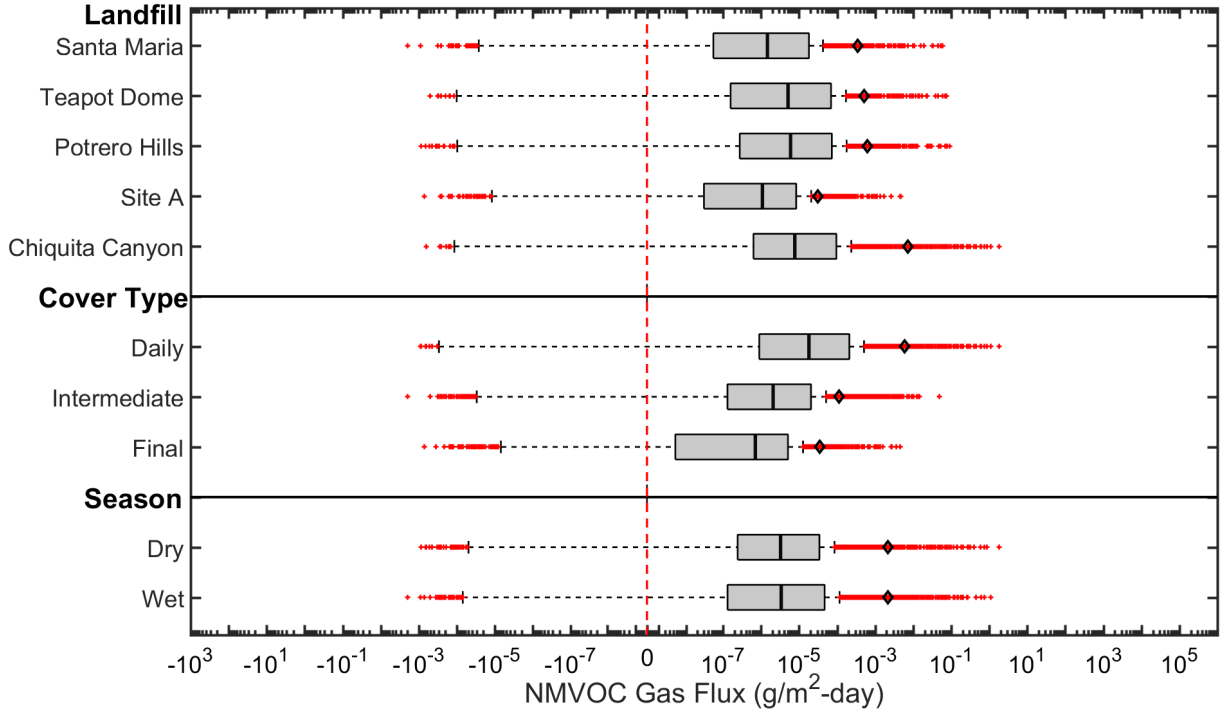

Fluxes of the GHGs and NMVOCs as a function of cover type indicated that for daily covers, locations with autofluff or green wastes had the highest surface fluxes. For intermediate covers, fluxes were generally higher when green wastes were layered or mixed with soils than when soils were used alone for intermediate covers. For final covers, conventional covers were more effective for impeding methane flux compared to the alternative cover. The geosynthetics final cover had the highest nitrous oxide flux with lower flux for both the soil conventional and the soil alternative final covers. The NMVOC fluxes were highly similar through the three final cover types. Overall cover categories and types impacted methane and nitrous oxide fluxes more than NMVOC fluxes. Methane undergoes potential transformations (oxidation, dissolves in soil water, and also attaches to soil solid surfaces) in the cover materials, which affect the surface flux. Similarly, nitrous oxide undergoes transformations in the cover materials as well as is produced through natural biological processes in soil and vegetative covers. Less information is available on potential transformations of the NMVOCs in different landfill covers, which overall may not be significant as observed by the low variation of NMVOC fluxes with cover category and type. Coarser-grained covers with low density, porous structure, interconnected pores, and low thickness promote high fluxes, whereas finer-grained covers with cohesive soils, occluded pores/tortuous flow paths, and high thickness impede flux.

Whole-site emissions from small landfills were negligible even though these sites did not have gas collection and removal systems. Higher emissions were measured at medium and large landfills with gas management systems. Directly calculated and converted to CO_2-eq. emissions were 4.97×10^2 to 1.26×10^5 tonnes/year and 5.16×10^2 to 1.62×10^5 tonnes/year, respectively (1 tonne = 1 metric ton = 1 Mg) (Table ES.1). The difference in weighted emissions was more significant when CO_2 and CO were excluded. This result may be attributed to the high emissions of F-gases, with high global warming potential from Chiquita Canyon Landfill. The highest CO_2-eq. GHG contributions were from Potrero Hills, Teapot Dome, and Site Chiquita Canyon Landfills. NMVOCs contributed appreciably (0.36 to 36% CO_2-eq.) to whole site emissions even though these are trace components in landfill gas.

Table ES.1 – Direct and Weighted Total LFG Emissions with and without CO_2/CO (μ = mean, σ = standard deviation).

Landfill		Direct Emissions (tonnes/yr)		Weighted Emissions (tonnes/yr)	
		With CO_2/CO	Without CO_2/CO	With CO_2/CO	Without CO_2/CO
Santa Maria	μ	4.97E+02	6.85E-03	5.15E+02	1.89E+01
	σ	3.69E+01	1.97E-01	4.50E+01	2.58E+01
Teapot Dome	μ	7.26E+03	1.22E+03	4.06E+04	3.46E+04
	σ	4.28E+03	1.30E+03	3.67E+04	3.65E+04
Potrero Hills	μ	1.26E+05	1.35E+03	1.62E+05	3.80E+04
	σ	2.14E+04	1.11E+03	3.77E+04	3.11E+04
Site A	μ	9.21E+03	9.48E+02	3.55E+04	2.72E+04
	σ	3.19E+03	1.61E+03	4.52E+04	4.52E+04

Landfill		Direct Emissions (tonnes/yr)		Weighted Emissions (tonnes/yr)	
		With CO_2/CO	Without CO_2/CO	With CO_2/CO	Without CO_2/CO
Chiquita Canyon	μ	2.81E+04	4.38E+02	5.21E+04	2.44E+04
	σ	1.06E+04	3.76E+02	1.57E+04	1.16E+04

Acceptance of waste tires likely influenced flux of aromatic compounds with lower fluxes from sites that accepted tires with reduced sizes and large surface areas (e.g., tire chips) compared to the sites that accepted whole tires.

Based on data and analysis conducted at Santa Maria Regional Landfill for the soil intermediate cover: in general, GHG and NMVOC flux did not vary significantly with radial distance from a gas well (from 0.5 to 32 m); GHG flux decreased significantly at a cover thickness above 1.6 m, whereas the NMVOC fluxes were relatively constant (within one order of magnitude), when the cover thickness was varied from 0.4 to 1.9 m; the mean GHG and NMVOC fluxes were relatively constant (within one order of magnitude), whereas the median fluxes varied significantly due to diurnal variations (negative fluxes early morning and overnight, positive fluxes daytime).

Based on all of the data obtained in the test program, landfill gas flux and emissions were correlated to landfill areal coverage, percent area covered by daily and intermediate cover, and waste column height. The methane flux had negative correlation with site age and percent area covered by final cover. Specific correlations were developed to establish thresholds of geotechnical landfill operations for soil covers. Example thresholds include: use long-term cover thickness of at least 150 cm (methane) and 75 cm (NMVOCs); compact soil in cover for maintaining at least 2000 kg of mass in long-term cover systems; and use soil with at least 60% fines content and 12% clay content for long-term covers.

The ground-based methane emissions were generally close, yet consistently lower in magnitude compared to the aerial methane emissions estimates. A comparison of the results from the two measurement approaches is presented in Figure ES.6. The uncertainties in the aerial measurements were higher than the uncertainties in the ground-based measurements in the investigation as indicated by the larger 95% confidence intervals along the x-axis compared to the confidence intervals along the y-axis as presented in Figure ES.6. The average ground-based methane emissions estimates for Santa Maria Regional Landfill (not depicted in Figure ES.6) were -0.122 tonnes/year with 95% confidence intervals ranging from -0.201 to -0.043 tonnes/year and aerial estimates were 1684 tonnes/year with 95% confidence intervals ranging from -221 to 3589 tonnes/year. The aerial methane measurements were mainly sensitive to landfill size characteristics, whereas ground methane measurements were strongly correlated to areal extent of individual cover categories and also correlated to collection efficiencies.

Figure ES.6 Comparison of Ground- and Aerial-Based Methane Emissions Estimates (dashed line indicates 1:1 reference, error bars represent 95% confidence intervals of overall estimates).

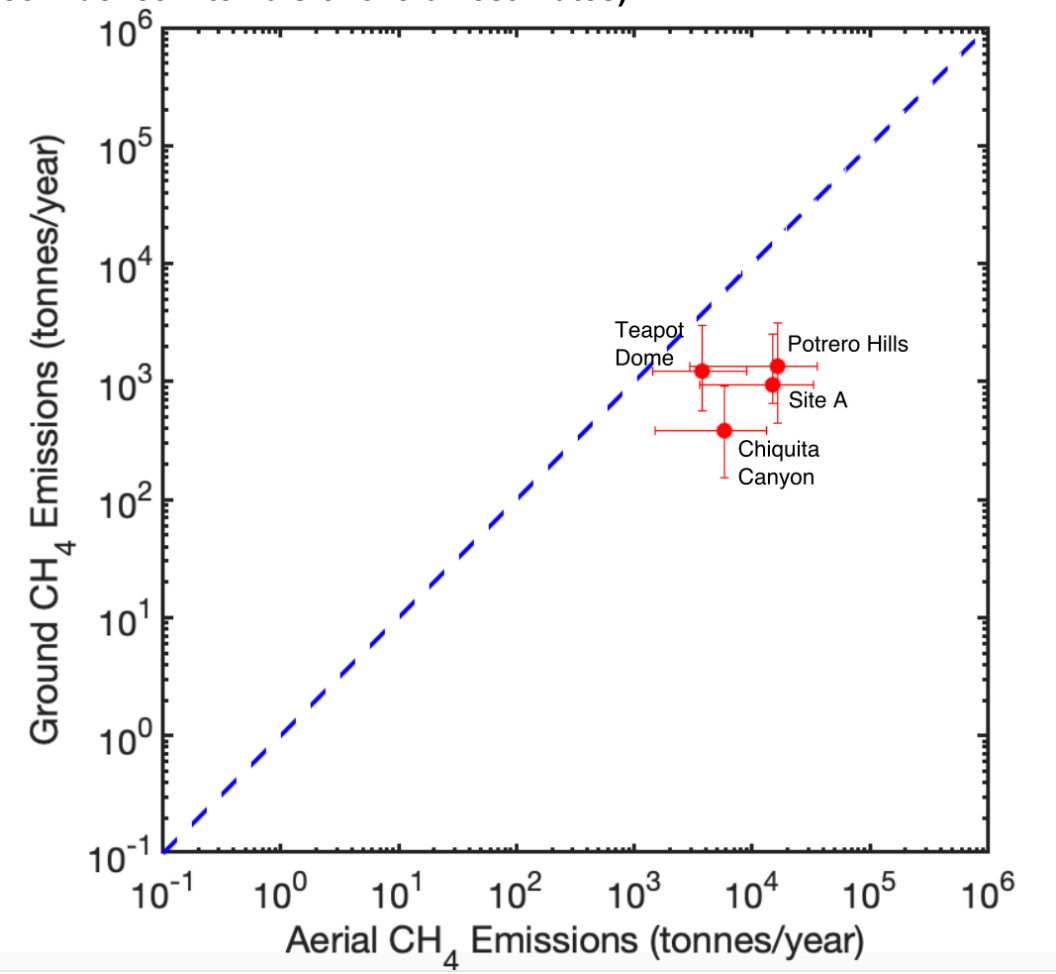

Gas Collection Efficiency Results

Gas collection efficiencies were determined for a subset of the 16 landfills included in the investigation with active gas collection and removal systems. A total of 10 landfills were included in the determination of the collection efficiencies. Two approaches were used for determining collection efficiencies: measured and modeled analyses (Table ES.2). The measured collection efficiencies were determined using the methane recovery data reported by landfills and emissions calculated in the investigation. The methane recovery rates reported by the landfills varied between 7.77×10^2 and 4.15×10^4 tonnes/year. For the 10 sites, emissions data from the aerial measurements were used. The methane emissions determined in the aerial tests varied between 1,684 and 16,402 tonnes/year. Also, analysis was conducted for the 5 ground-testing sites using whole-site emissions determined from flux chamber tests. The methane emissions determined in the ground-based tests varied between -0.122 and 1,345 tonnes/year. The modeled efficiencies were determined using the methane recovery data reported by landfills (range of values provided above) and gas generation estimated using LandGEM model

(using baseline default values). The LandGEM gas generation rates ranged between $3.91x10^4$ to $1.41x10^8$ m^3/year.

The measured and modeled gas collection efficiencies ranged from 23.2 to 91.4%, 38.9 to 100, and 24.5 to 75.9%, respectively (Table ES.2). The average efficiency was 54% for modeled collection efficiency analysis and lower than the average efficiency for the measured collection efficiency analysis (65% for aerial, 85% ground). Significant uncertainty was present for all of the collection efficiency determinations with higher uncertainties for the baseline and refined modeled collection efficiency analyses than the measured efficiency analysis. The measured efficiency analysis potentially overestimates the collection efficiency as only emissions are considered for mass balance and not other methane transport/transformation pathways (oxidation in covers, lateral migration). The high uncertainty in the modeled generation rates results from the uncertainty in the characteristics of the waste mass, environmental conditions, and gas generation mechanisms. A strong negative correlation was observed between measured collection efficiency and ground-based methane emissions. However, these trends were not fully confirmed when using modeled gas collection efficiencies. The high uncertainty in the predicted gas generation rates resulted in the weak correlations between modeled gas collection efficiencies and calculated emissions.

Table ES.2 – Summary of Measured and Modeled Methane Gas Collection Efficiencies (for year 2018)

Landfill	Measured Aerial Data		Measured Ground Data		Modeled LandGEM	
	$\overline{\alpha}$ (%)	95% C.I.	$\overline{\alpha}$ (%)	95% C.I.	$\overline{\alpha}$ (%)	95% C.I.
Santa Maria Regional	61.1	[42,100]	100	[100, 100]	51.5	[31.9, 82.8]
Teapot Dome	23.2	[18.4, 31.4]	38.9	[30.3, 54.4]	24.5	[14.7, 38.9]
Potrero Hills	47.3	[43.2, 52.3]	91.4	[88.9, 94]	60.2	[34, 93.5]
Site A	62.9	[57.7, 69.0]	96.4	[93.9, 98.9]	39.6	[24.6, 63.8]
Chiquita Canyon	84.1	[80.8, 87.7]	98.8	[98.3, 99.3]	62.5	[36.4, 98.2]
Frank R. Bowerman	58.7	[54.1, 64.1]	N/A	N/A	53	[30.8, 83.2]
Redwood	91.4	[89.2, 93.8]	N/A	N/A	75.9	[53.9, 100]
Simi Valley	78.3	[70.3, 88.5]	N/A	N/A	65.3	[38.9, 100]
Sunshine Canyon	86.8	[84.4, 89.4]	N/A	N/A	63.7	[36.1, 99.1]
Yolo County	57.6	[53.4, 62.4]	N/A	N/A	48	[29.8, 77.2]

Conclusions

Flux and emissions of methane, nitrous oxide, and NMVOCs are highly variable at a given landfill and also between landfills. The highest mean flux at each landfill was obtained for the main LFG, methane. NMVOCs were a significant and detectable fraction of the landfill gas emitted from the landfills investigated. The highest NMVOC fluxes were for alcohols, ketones, and monoterpenes. The NMVOCs had significant contributions to whole-site emissions in particular for CO_2-eq. emissions, even though

these gases are all trace constituents in landfill gas. The high intra- and inter-landfill flux variation resulted from differences in cover characteristics, thickness, configuration, and placement/construction practices. Daily covers resulted in the highest flux measurements for the various gases analyzed in this investigation. Some of the measured emissions from daily and also intermediate covers were attributed to cover materials themselves based on their chemical/biological composition (e.g., auto fluff, green waste, contaminated soil). Soil covers were more effective than non-soil covers for a given cover category. Emissions decreased for all categories of gas species investigated from daily to intermediate to final covers, where the relative fractions of these covers at the study sites were 0.1 to 20% (daily), 25 to 99.8% (intermediate), and 0 to 40.7% (final). The relative proportions of the different cover categories control emissions and provide direct means for management of emissions. Differences were observed between aerial and ground measurements, which may have resulted from emissions from the active waste placement surface at the landfills (not measured in the ground tests) and the high uncertainties in the aerial measurements. Gas flux and emissions were primarily controlled by cover characteristics and landfill operational processes with relatively low secondary effects from seasonal differences. Due to large uncertainty in modeling gas generation, the use of collection efficiency as a measure of emissions may not be reliable.

INTRODUCTION

This investigation was conducted to provide detailed assessment of emissions of 82 gas species (main and trace constituents) from landfills in California. The main gases were methane and carbon dioxide. The trace gases included greenhouse gases and additional volatile organic compounds. The three main components of the study were conducting an extensive literature search; identifying main characteristics of California landfills and selecting specific sites for emissions analysis; and conducting an extensive field-testing program. The results of the project are presented in five distinct sections within this report.

The literature review is presented in Part 1. The review included information on landfill gas generation. Storage, transport, and collection of gas in landfill systems were described. Surface flux and emissions of both main and trace gases from landfills were provided. Characteristics and properties of chemical species included in the study were reviewed. Data on landfill gas composition and transformation pathways are summarized.

Landfill classification analysis is presented in Part 2 of this report. Initially a detailed analysis was conducted to identify the main characteristics of California landfills. This analysis was followed by selection of representative sites using the main factors and criteria established based on the landfill characteristics analysis.

The field test program is presented in Part 3. The field tests included two measurement programs: aerial measurements of methane and ethane above the landfill surfaces and measurements of all of the 82 gases directly on the landfill surfaces. Details of the two measurement programs including methods used and specific test protocols were described. Details of the supplementary field and laboratory tests were provided. Determination of methane generation and collection efficiency were presented.

Results of the investigation are presented in Part 4. Aerial measurement data for methane and ethane were included. Detailed results are presented for each landfill site with flux chamber testing for the two measurement seasons (wet and dry) establishing intra-landfill variations. Inter-landfill variations also were identified. Comparisons were made between seasonal measurements. Flux measurements were extended to whole-site emissions. Correlations between measured flux and emissions and landfill characteristics are presented. Assessment of gas collection efficiency was provided. Potential effects of tire disposal on gas emissions was identified.

Engineering significance of the investigation including main conclusions are provided in Part 5. Aerial and static flux measurements were compared. Perspectives were provided in relation to literature gas emissions data. The main factors that affect emissions were identified. Potential anthropogenic versus biogenic sources of the 82 gas species included in the investigation were assessed. Data and analysis were provided for potential indirect human health and climate change effects of the gases that typically are not considered greenhouse gases.

PART 1 – LITERATURE REVIEW

1.1 Introduction

The annual municipal solid waste (MSW) generation in the U.S. has been on the order of 230 million metric tonnes (Mt) since 2005, with 243 Mt of generation in 2017 (USEPA 2017a). Landfilling constitutes the main means of waste disposal in the U.S. with 127 Mt (52.2% of 243 Mt generated) disposed of in landfills in 2017. Significantly higher rates (on the order of 262 Mt) for landfill disposal also were reported (van Haaren et al. 2010, Powell et al. 2016). For California, the annual MSW disposal amount has been on the order of 35 Mt since 2009, with 37.8 Mt reported for 2017 (CalRecycle 2017). The number of active landfills was reported to be 1,738 in the U.S. (USEPA 2017b) and 133 in California (CalRecycle 2019a).

Landfilling of municipal solid waste (MSW) results in three main byproducts: landfill gas (LFG), leachate, and heat. Landfill gas is a biogas consisting of approximately 45-60% (v/v) methane (CH_4) and 45-60% (v/v) carbon dioxide (CO_2) generated due to anaerobic microbial processes that occur in the landfill (Tchobanoglous et al. 1993). LFG also includes minor amounts of oxygen (0.1 to 1%), hydrogen (0 to 0.2%), and nitrogen (2 to 5%) from the atmosphere, carbon monoxide (0 to 0.2%), sulfides (0 to 1%), and ammonia (0.1 to 1%) as well as a large number of trace components (0.01 to 0.6%), which have been directly volatilized from the waste or generated by biotic or abiotic processes within the landfill (Christensen et al. 1996). More than 200 trace species including alkanes, aromatics, alcohols, aldehydes, reduced S gases, and chlorinated and fluorinated hydrocarbons, with measured concentrations (in gas collection headers) in the range of below detection limit to 57.7 μg/L were reported (Scheutz et al. 2008). Due to the presence of engineered cover and gas extraction systems, concentrations of these trace gas components are much lower in the ambient air as compared to gas collection or passive vent systems. For example, Zou et al. (2003) reported concentrations of 100 NMVOCs in the ambient air at a landfill site, where concentrations across all chemical families ranged from 0.0001 to 1.67 μg/L and are generally higher at the active face of municipal solid waste (MSW) landfills (Saral et al. 2009, Duan et al. 2014). Elevated concentrations of aromatic hydrocarbon hazardous trace gas components have been detected in the vicinity of MSW landfills (Kim et al. 2008).

This literature review provides a summary of landfill gas related processes in landfill environments. Particular emphasis is placed on LFG surface emissions of greenhouse gases and a broad class of organic chemicals. Sections 1.2, 1.3, and 1.4 provide a broad overview of LFG generation, storage within the waste mass, transport mechanisms, collection systems, and emissions. Section 1.5 provides an overview of the specific chemical species and corresponding chemical families included in the current study. Section 1.6 describes the composition of LFG and summarizes the findings from previous studies related to methane, nitrous oxide, and other NMVOC concentrations in landfill gas. Section 1.7 provides concise summaries for results from prior field studies on methane, nitrous oxide, and NMVOC emissions from MSW landfills. Finally, Section 1.8 discusses potential chemical and biological transformation

pathways that may be present both in the waste mass and in the cover systems for the specific chemicals included in this investigation.

1.2 Landfill Gas Generation

The generation of LFG in MSW landfills is affected by various factors, including the quantity, composition and age of the waste materials; pH, moisture content, and temperature of the waste mass; and the ingress of oxygen from the atmosphere as well as site specific landfill design and operational practices (Tchobanoglous et al. 1993, Palmisano and Barlaz 1996, Barlaz et al. 2010). In general, MSW in the U.S. is composed of paper and paperboard (~26%), glass (~4%), metals (~9%), plastics (~13.1%), yard trimmings (~13%), food (~15%), wood (~6%), rubber and leather (~3%), textiles (~6%), and other miscellaneous organic and inorganic wastes (i.e., wastewater sludge, household hazardous wastes, electronic wastes, auto shredder residues, soil, etc.) (USEPA 2017a). These estimates of waste composition are slightly different for California, where the overall waste stream has a high organics composition (37% - mainly food and green waste), followed by inerts and other materials (20% - mainly construction and demolition wastes) and recyclable materials (33% - paper, metals, plastics, glass) (CalRecycle 2017).

The higher quantity and fraction of organic materials in the waste stream reaching MSW landfills, particularly readily biodegradable fractions such as food and green wastes, contribute to greater anaerobic bacterial decomposition and generation of LFG in comparison to national averages. The principal, readily biodegradable components in these wastes are composed of soluble sugars and starches (polysaccharides), cellulose and hemicellulose, whereas the more recalcitrant components include proteins, nucleic acids, lipids, and lignocellulose (lignin present in wood waste does not decompose) (El-Fadel et al. 1997, Barlaz et al. 2010). In addition, the presence of household hazardous wastes such as paints, batteries, or cleaning products leads to volatilization of certain organic chemicals (volatile organic compounds) into LFG (Brosseau and Heitz 1994, Nair et al. 2019). Furthermore, unique chemical or biochemical transformative reactions occurring between different chemicals within the waste mass leads to the generation of various trace gas components (Scheutz and Kjeldsen 2005). In addition to waste composition, age of the waste mass, is a critical factor affecting generation, in which waste that is more recently landfilled (less than 10 years) leads to greater generation of LFG. Peak LFG generation generally ranges from within 5 to 7 years of waste disposal in MSW landfills (Tchobanoglous et al. 1993, Palmisano and Barlaz 1996, Barlaz et al. 2010). Waste age also influences trace gases as reported for F-gases by Yesiller et al. (2018), where the distribution of the F-gases within a landfill varied by historical replacement trends. Newer F-gas species were concentrated in new cells with relatively younger wastes in the landfill with older species uniformly distributed across the entire site.

Landfill gas generation is primarily a biologically mediated process, in which the multifaceted consortium of microorganisms (bacteria) in the waste mass decompose the organic materials in the presence of an electron acceptor (i.e., oxygen, nitrate, etc.), forming new biomass, heat, extracellular byproducts (i.e., polymeric substances), and

biogas (methane and carbon dioxide) (Tchobanoglous et al. 1993, Palmisano and Barlaz 1996). Depending on the presence of oxygen, waste biodegradation can either be classified as an aerobic (with oxygen) or an anaerobic (without oxygen) process. The biological decomposition of MSW has been classified into five successive stages (Tchobanoglous et al. 1993, Palmisano and Barlaz 1996), including an initial adjustment phase (Stage I), a transition phase (Stage II), an anaerobic acid phase (Stage III), an accelerated methane production phase (Stage IV), and a decelerated methane production phase (Stage V) as presented in Figure 1.1. Anaerobic waste decomposition in MSW landfills relies on the symbiotic relationship formed among three primary bacterial groups, all with a specific function, including the hydrolytic/fermentative bacteria, the acetogens, and the methanogens (Barlaz et al. 2010).

Figure 1.1 Stages of Landfill Gas Generation in MSW Landfills (Hofstetter 2014)

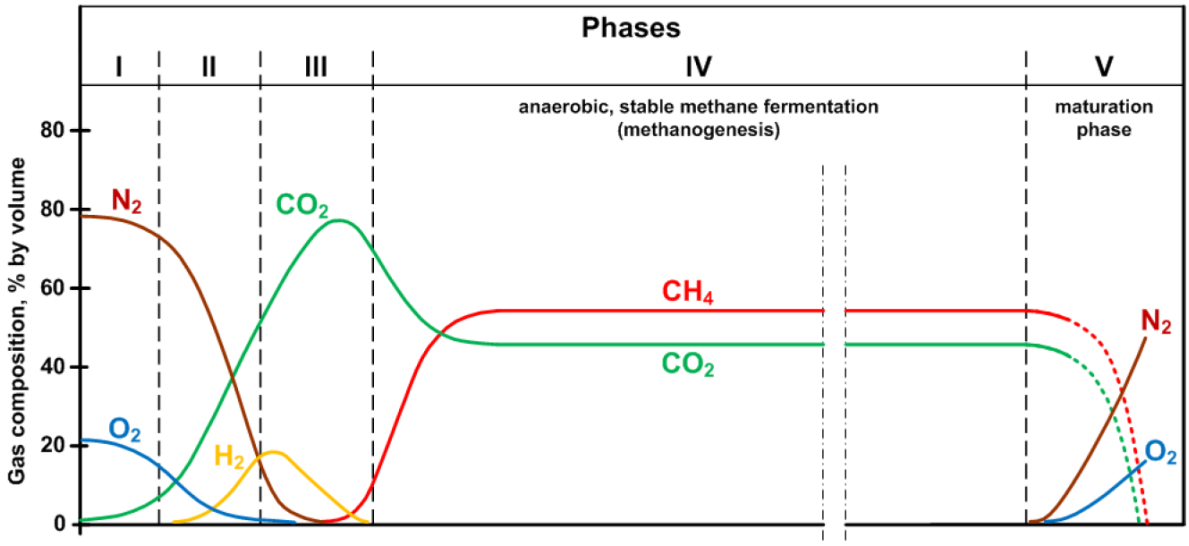

During Stage I of landfill gas generation, oxygen present in voids of the waste mass and in moisture within the waste mass fuels the aerobic decomposition of the organic fraction of MSW. In this phase (lasting on the order of days), both oxygen and nitrate are consumed by aerobic bacteria, along with soluble sugars to form carbon dioxide (100% v/v) (Figure 1.1). The transition phase (Stage II) refers to the time period when oxygen becomes depleted and anaerobic conditions begin to develop. Throughout the early periods of anaerobic decomposition in MSW landfills, complex particulate matter is broken down to proteins, carbohydrates, and lipids, which are then further hydrolyzed to biomonomers such as amino acids, sugars, and high molecular weight fatty acids (El-Fadel et al. 1997). After oxygen is nearly depleted within the waste mass, Stage III (the acidic phase, time frame of months to years) of decomposition begins, where carboxylic acids begin to accumulate as a byproduct of anaerobic soluble sugar fermentation (i.e., organic alcohol production). As more and more acids accumulate, the pH of the waste mass drops considerably (inhibiting methanogenesis, or the production of methane) and due to the fermentative activity, large volumes of carbon dioxide and hydrogen are produced (Palmisano and Barlaz 1996, Barlaz et al. 2010) (Figure 1.1). The fourth stage of decomposition and LFG production denotes the onset of the methane generation

phase, where accumulation of carboxylic acids ceases as they are consumed faster by the acetogens than they are produced by the fermentative and hydrolytic bacteria. At this stage, the pH of the waste mass begins to stabilize (between 6.8 and 8) and acetate, carbon dioxide, and hydrogen produced by the acetogens is consumed anaerobically by the methanogens, thereby producing methane (~60% v/v) and carbon dioxide (~40% v/v) as the primary byproducts. The time period required to reach this stage varies significantly by climate, where peak generation may be reached after only 2 years in a temperate climate, whereas decades may be required in low temperature or arid conditions (Tchobanoglous et al. 1993). Finally, after the onset of methanogenesis, the production of LFG begins to decline as both the available nutrients in the waste mass decline and the substrates that remain in the waste mass are more difficult to biodegrade (Stage V). This phase continues to produce LFG for upwards of 50 years, and LFG will start to include more atmospheric components (i.e., oxygen and nitrogen) as the LFG becomes diluted.

Generation of landfill gas by the microbial populations is highly moisture, pH, and temperature sensitive; therefore, the climate zone in which the landfill resides plays a significant role in LFG generation. The moisture content of fresh waste ranges from 15 to 45% and is generally 20% on a wet weight basis, which is considered low in comparison to optimum conditions for anaerobic microbial decomposition (Farquhar and Rovers 1973, Barlaz et al. 1990). Multiple studies have indicated that moisture content is one of the foremost limiting factors of methane generation, where methane production exhibited an upward trend with increasing moisture content, up to an optimum of 50-60% (w/w, wet basis) (Farquhar and Rovers 1973, Barlaz et al. 1990). Thus, climate zones with high net annual precipitation, and higher probability of infiltration, are favorable for LFG generation. pH is another important factor regulating methanogenesis and LFG generation, where methanogenic bacteria exhibit a narrow range in pH tolerance (6.8 to 7.4) (Tchobanoglous et al. 1993). Even though MSW is typically alkaline in nature (7-8), the fermentative bacteria are largely responsible for lowering the pH and inhibiting LFG generation in the landfill environment. Temperature effects on MSW decomposition is summarized in Yesiller et al. (2015). Biologically mediated decomposition of MSW occurs through two distinct pathways: short-term effects on reaction rates and long-term effects on microbial population balance (Hartz et al. 1982). In general, waste decomposition increases with increasing temperatures up to limiting values. In laboratory studies, optimum temperature ranges for the growth of mesophilic and thermophilic bacteria responsible for waste decomposition were identified to be 35 to 40°C and 50 to 60°C, respectively (Cecchi et al. 1993, Tchobanoglous et al. 1993). Maximum gas production from waste decomposition was identified to occur at temperature ranges between 34 and 41°C based on laboratory analysis representing the landfill environment with a mixture of these two types of microorganisms (Merz and Stone 1964 and Ramaswamy 1970 as reported in DeWalle 1978, Hartz et al. 1982, Mata-Alvarez and Martinez-Viturtia 1986). A temperature range of 40 to 45°C was identified as the optimum range for gas production at a landfill in England (Rees 1980a, b) with highly inhibited and delayed gas generation observed at low waste temperatures (Hanson et al. 2006). Biomass transfer was reported to occur with landfill gas, where the cell counts in the gas were correlated to temperature (Barry 2008). Spatially unique

microbial communities, as influenced by waste temperature among other factors, were reported in landfill environments (Sawamura et al. 2010). Other than climatic factors, the temperature of the waste mass is greatly influenced by heat generation during anaerobic decomposition and other chemical transformations occurring within the waste mass (Yesiller et al. 2005).

As MSW landfills in the U.S. are highly engineered systems, the site-specific landfill design and management of waste materials also influences the generation of landfill gas and subsequent emissions (Section 1.3) from MSW landfills (Tchobanoglous et al. 1993). Regarding landfill design, application of engineered final cover barrier systems affects LFG generation by significantly lowering water and atmospheric air intrusion through the use of the barrier layers with low hydraulic and gas conductivity. Given that the presence of moisture facilitates LFG production, inclusion of a cover system may offset LFG production. However, cover systems also limit oxygen availability in the waste mass, which facilitates biologically mediated anaerobic conversion processes, thereby producing more LFG. Final cover systems range from a thick (~ 1 m) layer of compacted clay overlain by native topsoil to more advanced, composite barrier systems, consisting of a combination of clayey soils, geosynthetic clay liners, or geomembranes ranging up to 1.5 m in thickness (Yesiller and Shackelford 2011). Cover systems typically are equipped with a drainage layer to collect and remove water that collects on the surface of the covers (Yesiller and Shackelford 2011).

Site-specific operational practices, such as the placement and composition of daily and intermediate covers, further affect landfill gas generation and subsequent emissions (Section 1.3) (Tchobanoglous et al. 1993). Daily covers are temporary cover systems used to isolate recently placed waste from the surrounding environment to prevent spread of the waste materials and associated harmful vectors. In the U.S., daily covers are mandated to have a minimum thickness equivalent to the performance of 150 mm of soil, where the composition of materials used in these covers may vary significantly from site to site (USEPA 1993, USEPA 2012). For example, in California, daily covers may consist of soil, wood wastes, green wastes, construction and demolition (C&D) wastes, autofluff, or wastewater biosolids (CalRecycle 2018). The non-soil daily cover materials including natural and synthetic materials are collectively termed alternative daily covers (ADCs). Intermediate covers (also termed interim covers) represent a more permanent barrier system in that they are placed over completed lifts for an extended period of time (ranging from months to a few years). Intermediate cover systems are required to have a minimum thickness equivalent to the performance of 300 mm of soil (USEPA 1993, USEPA 2014). Even though materials similar to ADCs can be used in interim covers, the use of materials other than soils in interim cover systems is generally limited in California (CalRecycle 2018). Similar to final cover systems, the presence of both daily and interim covers limits, to some extent, the ingression of moisture and air into the waste mass, thereby affecting LFG generation. Other operational practices related to placement efficiency of waste materials, such as the degree of compaction and compression of wastes over time, as well as specific waste placement locations and sequence affect LFG production. Higher compaction efforts and compression of the waste mass over time serve to limit atmospheric air intrusion and pore space available

for moisture transport within the waste mass as well as LFG production and transport within the waste mass (Tchobanoglous et al. 1993). Yesiller et al. (2005) reported that waste temperatures increase with increasing waste placement rates and thus lead to rapidly reaching optimum decomposition conditions for landfill gas generation. Winter only placement areas set aside at California landfills contain waste masses at moisture contents above average values and affect LFG generation, potentially increasing gas generation rates due to increased moisture levels.

1.3 LFG Storage, Transport, and Collection

Temporary landfill gas storage within the landfill system has been identified as a significant phenomenon to consider when investigating the complete LFG lifecycle (Bogner and Spokas 1993, Scheutz et al. 2009a). Landfill gas pressures have been observed to vary due to temporal changes in the cover system permeability as a function of precipitation and moisture content. For example, during periods of high precipitation, LFG can be stored temporarily inside the upper portion of waste mass/bottom portion of the soil cover and then subsequently released during follow up dry weather periods. Changes in barometric pressures also can trigger this phenomenon, albeit on much smaller time scales (hours versus days) (Bogner and Spokas, 1993, Scheutz et al. 2009a).

Landfill gas generation throughout the waste mass tends to be heterogenous, producing localized differences in LFG pressure. Therefore, the bulk transport of LFG throughout the waste mass is highly pressure driven (advective) over concentration driven (diffusive), always moving in the direction of least resistance (i.e., areas of higher permeability), across gradients from high to low pressure or concentration (Scheutz et al. 2009a). In addition to advective and diffusive transport, some trace components are highly adsorptive or are likely to partition within different phases of the waste materials. Adsorption entails physico-chemical bonding of a given chemical to a solid present in the waste mass, whereas phase partitioning involves apportionment of a given chemical into another phase (i.e., gas phase dissolving in water, polar versus non-polar) (McCarthy and Zachara 1989). Moreover, many trace components are affected by different chemical and biological reactions while they are transported throughout the waste mass, which either increase or decrease their respective concentrations (Molins et al. 2008). Depending on these differences in local pressures, along with differences in ambient barometric pressure and the physical-chemical nature of the bulk LFG (i.e., molecular weight, densities of different chemicals), LFG is able to migrate in many different directions, including upward, downward, and laterally (Scheutz et al. 2009a). Lateral migration of LFG has been widely reported and is generally enhanced when soil covers are saturated, which drives advective flux of LFG laterally (Christophersen et al. 2001, Christophersen and Kjeldsen 2001).

The installation of passive or active gas extraction wells and a passive or an active gas extraction system are primary measures that help control and stabilize the undesirable migration of LFG. In addition, the presence of a landfill bottom liner and final cover systems both limits the extent of migration of LFG and offsets potential environmental impacts, to some extent. Landfill gas recovery studies with data from Swedish landfills

reported gas collection efficiencies for MSW landfills on the order of 50 to 60% (Borjesson et al. 2007, 2009), where the remaining fraction of LFG escapes into the atmosphere. Studies conducted in the U.S. and France indicated that gas extraction efficiencies can be as high as 97% if state-of-the-art liners, covers, and extraction systems are in place (Spokas et al. 2006). Results reported from a methane mass balance for nine landfill cells at three landfill sites determined that LFG collection efficiencies from the field ranged from 92% to 97% for cover systems incorporating clay covers (Spokas et al. 2006). Recovery results were lower for several cells with geosynthetic covers in place of clay soil covers, ranging from 40.9 to 84% (Spokas et al. 2006). Use of a temporally weighted gas collection efficiency was proposed as an appropriate means for assessing landfill gas recovery over the entire lifetime of a given landfill site (Barlaz et al. 2009). The USEPA has recommended a default value of 75% LFG collection efficiency for performing LandGEM simulations (US EPA 2008).

1.4 Landfill Gas Emissions

Even with engineered protective measures in place, fugitive emissions of LFG through landfill covers remains a significant issue (Bogner et al. 1997a). Similar to the underlying principles governing LFG generation, LFG emissions from landfill covers depend on various interrelated factors. Three general classes of factors affecting LFG migration and subsequent emissions were identified to be meteorological conditions (barometric pressure, precipitation, temperature, wind), soil/cover conditions (cracks, permeability, diffusivity, porosity, moisture content, methane oxidation), and the landfill conditions (LFG production rate, internal barriers, gas vents, extraction system) (Scheutz et al. 2009a). As most single and composite final covers have intrinsically low gas permeability, the primary transport mechanism of bulk LFG from the landfill surface in the presence of final covers is primarily through molecular diffusion, with some contributions from advective transport reported for different cover systems, including highly porous, alternative cover materials (i.e., auto fluff), as well as from wind induced advection (Scheutz et al. 2009a). The pressure differential across the cover systems generated due to the negative pressures (i.e., vacuum) in the waste mass during active gas collection system operation in comparison to the positive outside atmospheric pressure also contributes to potential emissions by creating advective transfer conditions. Pressure gradients between the waste mass and landfill surface can be introduced by wind, variation in barometric pressure, or by pressure build up in the underlying wastes. An increase in barometric pressure often times resulted in reduced advective and/or diffusive transport through landfill covers and frequently ended in a flux reversal (net uptake over net emissions), as reported by several studies (Latham and Young 1993, Kjeldsen and Fisher 1995, Nastev et al. 2001, Christophersen and Kjeldsen 2001, Christophersen et al. 2001, Czepiel et al. 2003, Franzidis et al. 2008, Gebert and Groengroeft 2006). Kjeldsen (1996) and Thorstenson and Pollock (1989) reported that only very low pressure gradients, on the order of 1 Pa/m) are required for LFG transport from advective flux to dominate diffusive flux, where pressure gradients of this magnitude can actually be generated by diffusive processes.

In addition to the meteorological and landfill conditions, the cover conditions, including the degree of LFG (methane, trace gases) oxidation occurring within the cover is a

significant factor influencing LFG emissions. Scheutz et al. (2009a) described methane oxidation as "…a secondary biological treatment process to control methane emissions." Similar to microbial processes occurring within the waste mass, some bacteria (known as the methanotrophs) are responsible for oxidizing (under aerobic conditions only) certain components of LFG (i.e., methane) to produce new biomass, other extracellular byproducts, and biogas (100% carbon dioxide v/v). Most methanotrophic bacterial species are strict aerobes in that they depend on a steady supply of both oxygen and carbon dioxide within the soil cover, confining their distribution to around 15-20 cm below the surface (Scheutz et al. 2009a). Methanotrophs have also been associated with the oxidation of some NMVOC compounds, including F-gases, alkanes, aromatics, and some halogenated hydrocarbons (Kjeldsen et al. 1997, Scheutz and Kjeldsen 2004).

Both methane and NMVOC oxidation are affected by many environmental factors, including soil type, temperature, moisture content, methane/oxygen concentrations, pH, as well as the presence of certain limiting nutrients (i.e., inorganic nitrogen, phosphorus, trace heavy metals, etc.) (Börjesson and Svensson 1997a, Stern et al. 2007, Bogner et al. 1997a). Oxidation of methane, including the relative rates and conversion efficiency, is also affected by the presence of other NMVOC substrates, demonstrating that these methanotrophic communities may show some degree of substrate preference or inhibition through toxicity (Scheutz and Kjeldsen 2004). For example, methane oxidation was demonstrated to be inhibited in the presence of HCFCs, which was likely due to enzyme-substrate competition and accumulation of toxic intermediates during oxidation of the HCFCs (Scheutz and Kjeldsen 2004). Regarding temperature, most methanotrophs cultured in isolation are mesophiles, with optimal temperatures for oxidation in soil environments ranging from 25 to 35°C (oxidation at lower temperatures has been reported for type I methanotrophs at 10°C, albeit at a slower rate) (Hanson and Hanson 1996, Scheutz et al. 2009a).

Soil moisture content is another critical factor affecting oxidation rates, in which the optimal conditions promoting methane oxidation are much more complex than temperature. The soil moisture content must not be too high as to limit diffusion of oxygen or methane into or out of the soil cover, yet not too dry to avoid desiccation of the cells. Reported soil moisture contents that were optimal for methane oxidation ranged from 10 to 20% (w/w), where some studies have reported even higher values (Boeckx et al. 1996, Scheutz et al. 2009a). High air-filled capacity, which defines the share of pores available for gas transport after draining a soil, where the remaining water is bound solely by capillary force, was mentioned as a significant feature of a given cover soil to promote methane oxidation (Scheutz et al. 2009a). Scheutz et al. 2009a identified an air capacity threshold of 50 µm (i.e., 50 x 10^{-6} m) that is necessary for optimal methane oxidation to occur in any cover soil.

Oxygen limitation is another factor that controls methane oxidation. Field studies have reported that oxygen concentrations above 3% are capable of supporting methane oxidation, where lower oxygen mixing ratios have been reported for some methanotrophs in the laboratory setting (0.45%) (Czepiel et al. 2003, Gebert et al.

2003). Oxygen penetration into the soil cover is a factor of both site-specific meteorological conditions, as well as the soil type and geotechnical engineering properties (i.e., particle size distribution, porosity, degree of saturation).

Other important environmental factors affecting methane oxidation include the presence of inorganic nitrogen, production of extracellular polymeric substances, and soil pH (Scheutz et al. 2009a). Several studies have determined that inorganic nitrogen (ammonium/nitrate) may stimulate or inhibit methane oxidation depending on the species of N, the concentration of N, methane concentrations, pH, and the species of methanotrophic bacteria (Boeckx and van Cleemput 1996, Boeckx et al. 1998, Hütsch 1998, Scheutz and Kjeldsen 2004). A majority of studies reviewed have determined that ammonium-based fertilizers stimulate growth and activity of methane oxidizers in landfill cover soils, where the effects of nitrite and nitrate N sources are less understood (Hilger et al. 2000, De Visscher et al. 1999, 2001, De Visscher and van Cleemput 2003, and Bodelier and Laanbroek 2004). Following prolonged exposure to favorable methane oxidizing conditions, the accumulation of EPS as an extracellular byproduct for methanotrophic communities has been shown to decrease the efficiency of methane oxidation. These studies have postulated that EPS either clogs the soil pores, thereby decreasing the gas permeability of the soil or reduces the rate of gaseous diffusive flux of substrate into the bacterial cells (Hilger et al. 1999, Scheutz and Kjeldsen 2003). Optimal soil pH for methanotrophic growth of soils lies between 5.5 and 8.5, which is aligned with expected pH of sandy or loamy soils in the field (4.5-7) (Dunefield et al. 1993, Scheutz and Kjeldsen 2004). Methane and NMVOC oxidation may be significant, however oxidation does not fully attenuate LFG emissions as the conditions in the field typically are not optimal.

Irregularities such as cracks and fissures in landfill cover soils have been reported due to waste settlement or desiccation of the cover soils during dry periods. LFG emissions through these cracks and fissures, termed “hot spots,” can result in high spatial and temporal heterogeneity in LFG emissions. In a study from over two decades earlier more than 50% of the total measured emissions were attributed to less than 5% of the landfill surface with the disproportional emissions indicated to result from hotspots associated with cracks and other heterogeneities in the soil covers Czepiel et al. (1996). As landfill emissions are monitored by landfill owners/operators on a regular basis, such irregularities if present are detected and repaired and do not pose long-term problems. Landfill cover designs have evolved significantly in the last decades with design and analysis used to minimize differential settlement and ascertain structural integrity of the covers. Irregularities are not relevant for conventional final covers as the barrier layers (soil and/or geosynthetics) are placed below ground surface overlain by multiple layers without being exposed to the atmosphere. Geomembranes are not susceptible to cracking and typically have very high tensile strains at break and thus are not susceptible to differential settlement. In general, final covers are placed at areas with old wastes that have completed significant volume change. The PIs during this study or a previous study conducted for CARB, did not observe noticeable cracking on the surface of any of the cover systems installed at the multiple investigated landfills. In the previous study, the void ratio and porosity of the cover soils were determined to be

lower during the dry season indicating shrinkage of the covers. However, cracking was not visually observed and the emissions during the dry season were lower than the emissions in the wet season. The coupled mechanism for the observed behavior is described in detail in Yesiller et al. (2018). High-conductivity, low-fines content, low-cohesion daily and intermediate covers can in themselves constitute hot spots with associated high emissions. The active working face, since there is no cover in place, is also a source of high emissions.

Geotechnical engineering characteristics of cover materials are significant factors for landfill gas emissions. as the particle size of the cover material decreases and soil gradation varies from coarse to fine grained, three distinct phenomena occur: a) the number of pores and amount of pore spaces increase, where the soil pores become more occluded than interconnected; b) tortuosity of the flow paths increases; and c) more water is held (by strong electrochemical forces in addition to gravitational forces and surface tension) and residual state of saturation increases. All three phenomena increase resistance to gas transfer. Yesiller et al. (2018) observed a strong inverse correlation between F-gas emissions and fines content across different soil covers from a landfill site in California. Also, F-gas flux was observed to increase as the degree of saturation of the soil increased, which was attributed to reduced retardation, sorption, and oxidation in cover soils with increasing moisture contents (Yesiller et al. 2018).

Both Bogner et al. (2011) and Yesiller et al. (2018) reported that emissions of methane and F-gases (in Yesiller et al. 2018 only) decreased progressing from daily (thin) to intermediate to final (thick) cover systems, indicating that cover thickness is a significant feature affecting LFG emissions from landfill surfaces. In addition to providing an extra physical barrier to buffer methane or NMVOC emissions (depending of course on the soil properties), extended cover thicknesses also affect the extent and persistence of microbial oxidation of methane or NMVOCs occurring in the cover soils. Cover thickness affects the depth of oxygen penetration and moisture percolation, which highly influences the development, spatial extent, and temporal stability of oxidizing methanotrophic bacterial communities (Scheutz et al. 2009a).

In California and countries with similar climatic attributes, seasonal effects of methane and NMVOC emissions may be less pronounced as compared to the effects of other landfill characteristics such as cover type and site-specific operational practices. For example, mean seasonal fluxes of methane, carbon dioxide, and nitrous oxide rarely exceeded one order of magnitude in difference across a range in daily to intermediate to final covers (Bogner et al. 2011). However, differences between methane fluxes ranged up to four orders of magnitude across daily, intermediate, and final covers at the same landfill sites in California (Bogner et al. 2011). Seasonal differences in LFG emissions can be attributed to the high infiltration of precipitation into the cover soil observed during the winter months, which alters the transport and transformation mechanisms occurring throughout the depth of the soil cover. In some cases, higher moisture contents lead to suboptimal oxidation of methane and other NMVOCs (Scheutz et al. 2009a). During the wet season, higher moisture contents generally reduce the available pore space available for gaseous transport (i.e., volumetric air content), which may have

a stymying effect on transport (Kjeldsen 1996). However, higher soil moisture contents observed in the wet seasons may also facilitate transport of some NMVOCs such as F-gases due to decreased retardation and sorption (Yesiller et al. 2018).

1.5 Chemical Species Included in the Investigation

Information is provided in this section on the potential sources of the chemicals included in the study in the landfill environment, a review of relevant physical-chemical properties affecting fate and transport, and the contribution of these chemicals to air quality on local, to regional, to global scales. The 82 chemical species investigated were categorized into 12 chemical families based on chemical characteristics and atmospheric air impacts. These families include baseline greenhouse gases, reduced sulfur compounds, fluorinated gases (F-gases), halogenated hydrocarbons, organic (alkyl) nitrates, alkanes, alkenes, aldehydes/alkynes aromatic hydrocarbons, monoterpenes, alcohols, and ketones (Table 1.1).

The impact of fugitive LFG emissions emanating from MSW landfills on global climate continues to be a significant issue in both developed and developing countries. In the U.S. and Europe, emissions from MSW landfills constitutes the second largest source of anthropogenic methane emissions, comprising 22 to 23% of the total anthropogenic emissions, respectively (USEPA 2009). In addition to methane, emissions of carbon dioxide, nitrous oxide, and chlorinated and fluorinated gases from MSW landfills have been identified as a direct threat to global climate change. In 2016, the emissions of greenhouse gases (GHGs) including carbon dioxide, methane, nitrous oxide, and F-gases from all global potential sources contributed approximately 72%, 19%, 6%, and 3% of the total global greenhouse gas emissions (49.3 Gt CO_2 equivalents) (Olivier et al. 2017). Emissions from MSW landfills amount to 5% of total global GHG emissions (IPCC 2013).

Table 1.1 – Characteristics of Chemical Species Included in the Investigation

Chemical Family (Abbr.)	Sources	Chemical Species	CAS-#	Chemical Formula	HAP [2]	MIR (g O_3/g species) [3]	FAC (%)[4]	GWP (unitless) [5]	ODP (unitless) [7]
Baseline Greenhouse Gases (GHG)	FW, GW	Methane	74-82-8	CH_4	N	0	0	28	0
		Carbon Dioxide	124-38-9	CO_2	N	0	0	1	0
		Carbon Monoxide	630-08-0	CO	N	0	0	4.4[6]	0
		Nitrous Oxide	10024-97-2	N_2O	N	0	0	265	0
Reduced Sulfur Compounds (RSC)	FW, GW, C&DW	Carbonyl sulfide	463-58-1	COS	Y	0	0	0	0
		Di-methyl sulfide	75-18-3	C_2H_6S	N	0	0	0	0
		Di-methyl disulfide	624-92-0	$C_2H_6S_2$	N	0	0	0	0
		Carbon disulfide	75-15-0	CS_2	Y	0	0	0	0
Fluorinated gases (F-gas)	AppW, C&D, AW	CFC-11	75-69-4	CCl_3F	N	0	0	4660	1
		CFC-12	75-71-8	CCl_2F_2	N	0	0	10200	0.82
		CFC-113	76-13-1	$C_2Cl_3F_3$	N	0	0	5820	0.85
		CFC-114	76-14-2	$C_2Cl_2F_4$	N	0	0	8590	0.58
		HCFC-21	75-43-4	$CHCl_2F$	N	0	0	148	0
		HCFC-22	75-45-6	$CHClF_2$	N	0	0	1760	0.04
		HCFC-141b	1717-00-6	CCl_2FCH_3	N	0	0	782	0.12
		HCFC-142b	75-68-3	$C_2H_3ClF_2$	N	0	0	1980	0.06
		HFC-134a	811-97-2	CH_2FCF_3	N	0	0	1300	0
		HFC-152a	75-37-6	$C_2H_4F_2$	N	0	0	138	0
		HFC-245fa	460-73-1	$CF_3CH_2CHF_2$	N	0	0	858	0
		HFC-365mfc	406-58-6	$C_4H_5F_5$	N	0	0	804	0
		Halon-1211	353-59-3	$CBrClF_2$	N	0	0	1750	7.9
Halogenated Hydrocarbons (HH)	TW, HCW, PW	Chloroform	67-66-3	$CHCl_3$	Y	0.02	0	16	0
		Methyl chloroform	71-55-6	$C_2H_3Cl_3$	Y	0.005	0	160	0.1
		Carbon tetrachloride	56-23-5	CCl_4	Y	0	0	1730	0.82
		Methylene chloride	75-09-2	CH_2Cl_2	Y	0.039	0	9	0
		Trichloroethylene	79-01-6	C_2HCl_3	Y	0.61	0	0	0
		Tetrachloroethylene	127-18-4	C_2Cl_4	Y	0.029	0	0	0
		Methyl chloride	74-87-3	CH_3Cl	Y	0.036	0	12	0.02
		Bromomethane	74-83-9	CH_3Br	Y	0.121	0	0	0.66
		Dibromomethane	74-95-3	CH_2Br_2	N	0	0	0	0
		Bromodichloromethane	75-27-4	$CHBrCl_2$	N	0	0	0	0
		Bromoform	75-25-2	$CHBr_3$	Y	0	0	0	0

Chemical Family (Abbr.)	Sources	Chemical Species	CAS-#	Chemical Formula	HAP [2]	MIR (g O_3/g species) [3]	FAC (%)[4]	GWP (unitless) [5]	ODP (unitless) [7]
		Chloroethane	75-00-3	C_2H_5Cl	N	0.27	0	0	0
		1,2-Dichloroethane	107-06-2	$C_2H_4Cl_2$	Y	1.65	0	0	0
		1,2-Dibromoethane	106-93-04	$C_2H_4Br_2$	Y	0.098	0	0	0
Organic (Alkyl) Nitrates (ON)	OBP	Methyl Nitrate	598-58-3	CH_3NO_3	N	0	0	0	0
		Ethyl Nitrate	625-58-1	$C_2H_5NO_3$	N	0	0	0	0
		Isopropyl nitrate	1712-64-7	$C_3H_7NO_3$	N	0	0	0	0
		N-propyl nitrate	627-13-4	$C_3H_7HO_3$	N	0	0	0	0
		2-butyl nitrate	924-52-7	$C_4H_9NO_3$	N	0	0	0	0
Alkanes (Alk)	PW, HCW, CW, PaW, PapW	Ethane	74-84-0	C_2H_6	N	0.26	0	5.5	0
		Propane	74-98-6	C_3H_8	N	0.46	0	3.3	0
		i-Butane	75-28-5	C_4H_{10}	N	1.17	0	4	0
		n-Butane	106-97-8	C_4H_{10}	N	1.08	0	0	0
		i-Pentane	78-78-4	C_5H_{12}	N	1.36	0	0	0
		n-Pentane	109-66-0	C_5H_{12}	N	1.23	0	0	0
		n-Hexane	110-54-3	C_6H_{14}	Y	1.15	0	0	0
		n-Undecane	1129-21-4	$C_{11}H_{24}$	N	0.55	2.5	0	0
Alkenes (Alke)		Ethene	74-85-1	C_2H_4	N	8.76	0.3	3.7	0
		Propene	115-07-1	C_3H_6	N	11.37	0	1.8	0
		1-Butene	106-98-9	C_4H_8	N	9.42	0	0	0
		i-Butene	115-11-7	C_4H_8	N	6.14	0	0	0
		trans-2-butene	624-64-6	C_4H_8	N	14.79	0	0	0
		cis-2-butene	590-18-1	C_4H_8	N	13.89	0	0	0
		1-Pentene	109-67-1	C_5H_{10}	N	6.97	0	0	0
		Isoprene	78-79-5	C_5H_8	N	10.28	0.6	2.7	0
Aldehydes/Alkynes (Ald/Alky)		Ethyne	74-86-2	C_2H_2	N	0.93	0	0	0
	FW, HCW, CW, PCPW, HSPW, PW, PaW, TW, FuW	Acetaldehyde	75-07-0	C_2H_4O	Y	6.34	0	1.3	0
		Butanal	123-72-8	C_4H_8O	N	5.75	0	0	0
Aromatic Hydrocarbons (Ar)		Benzene	71-43-2	C_6H_6	Y	0.69	2.6	0	0
		Toluene	108-88-3	C_7H_8	Y	3.88	5.4	2.7	0
		Ethylbenzene	100-41-4	C_8H_{10}	Y	2.93	5.4	0	0
		m+p-Xylene	108-38-3/ 106-42-3	C_8H_{10}	Y	7.605	3.15	0	0
		o-Xylene	95-47-6	C_8H_{10}	Y	7.44	5	0	0
		i-Propylbenzene	98-82-8	C_9H_{12}	N	2.43	4	0	0

Chemical Family (Abbr.)	Sources	Chemical Species	CAS-#	Chemical Formula	HAP [2]	MIR (g O_3/g species) [3]	FAC (%)[4]	GWP (unitless) [5]	ODP (unitless) [7]
		n-Propylbenzene	103-65-1	C_9H_{12}	N	1.95	1.6	0	0
		3-Ethyltoluene (M)	620-14-4	C_9H_{12}	N	7.21	6.3	0	0
		4-Ethyltoluene (P)	622-96-8	C_9H_{12}	N	4.32	2.5	0	0
		2-Ethyltoluene (O)	611-14-3	C_9H_{12}	N	5.43	5.6	0	0
		1-3-5-Trimethylbenzene	108-67-8	C_9H_{12}	N	11.44	2.9	0	0
		1,2,3-Trimethylbenzene	526-73-8	C_9H_{12}	N	11.66	3.6	0	0
		1,2,4-Trimethylbenzene	95-63-6	C_9H_{12}	N	8.64	2	0	0
Monoterpenes (Mon)	GW, C&D, HCW, PCPW, HSPW	α-pinene	80-56-8	$C_{10}H_{16}$	N	4.38	30	0	0
		β-pinene	127-91-3	$C_{10}H_{16}$	N	3.38	30	0	0
		Limonene	138-86-3	$C_{10}H_{16}$	N	4.4	0	0	0
Alcohols (Alc)	FW, HCW, PCPW, HSPW	Methanol	67-56-1	CH_4O	Y	0.65	0	2.8	0
		Ethanol	64-17-5	C_2H_6O	N	1.45	0	0	0
		Isopropanol	67-63-0	C_3H_8O	N	0.59	0	0	0
		2-Butanol	78-92-2	$C_4H_{10}O$	N	1.3	0	0	0
Ketones (Ket)		Acetone	67-64-1	C_3H_6O	N	0.35	0	0.5	0
		Butanone	78-93-3	C_4H_8O	N	0.59	0	0	0
		Methylisobutylketone	108-10-1	$C_6H_{12}O$	Y	3.74	0	0	0

[1] Adapted from Nair et al. (2019). FW = food wastes; PapW = paper wastes; GW = green wastes (i.e., yard trimmings); C&D = construction and demolition wastes (e.g., concrete, metal, wood, drywall); AW = auto-wastes; TW = textile wastes (i.e., clothes, carpet); HCW = household cleaning wastes; PW = plastic wastes; OBP = oxidation byproduct of NMVOCs in the landfill environment; CW = cooking wastes (i.e., charcoal, propane fuels); PCPW = personal care product wastes (i.e., shampoo, toothpaste); HSPW = household spray product wastes (i.e., air fresheners); PaW = paint wastes; FuW = furniture wastes; AppW = appliance wastes.
[2]Y(Yes) or N(No) (USEPA 2016b)
[3]Carter (2009)
[4]Grosjean and Seinfeld (1989) and Grosjean (1992)
[5]Indirect GWP values for alkanes, aldehydes, alcohols and ketones obtained from IPCC (2007), all other GWP values obtained from IPCC (2013)
[6]The direct and indirect GWP values based on estimates provided by Daniel and Solomon (1998) (upper range used)
[7]WMO (2014)

Once emitted to the atmosphere, the GHG gases have significant impacts due to their high radiative forcing (RF) and atmospheric lifetimes. RF refers to the relative strength of a given chemical to absorb outgoing thermal (infrared) radiation and thereby alter Earth's energy balance, where larger (positive) values are indicative of a net warming effect on the Earth's average temperature (Scheutz et al. 2009b, IPCC 2013). Chemicals can have both direct and indirect radiative forcing effects on Earth's atmosphere. For example, methane possesses both direct and indirect RF effects as it absorbs outgoing radiation and as the decomposition of methane produces carbon dioxide, water vapor, and ozone, all of which are potent GHGs that affect Earth's energy balance (Scheutz et al. 2009b). The atmospheric lifetime of a given chemical refers to the average time a chemical resides in the atmosphere before being removed or transformed by a chemical reaction or deposition (IPCC 2013). The global warming potential (GWP) is the most widely used metric that integrates both the RF and atmospheric lifetime of a given chemical to measure and compare the net effect of the chemical on global climate change. The mathematical definition of GWP is the time integrated RF resulting from a pulse emission (1 kg) of a given chemical relative to that of carbon dioxide, where a time horizon of 100 years is generally used for calculation (IPCC 2013). Carbon dioxide has a baseline GWP of 1, whereas methane, nitrous oxide, and F-gases have GWP values that range from less than an order to multiple orders of magnitude higher than that of carbon dioxide due to their high infrared absorption properties and atmospheric lifetimes as compared to CO_2. The global warming potentials for the chemical species included in this investigation are presented in Table 1.1.

As compared to impacts on global climate change, the impact of LFG emissions on local to regional atmospheric air quality is a less studied issue. A great majority (95%) of the chemicals included in this investigation are classified as non-methane volatile organic compounds (NMVOCs). NMVOCs constitute a broad class of anthropogenic and biogenic chemical compounds that are chemically distinct, yet have similar fates and transformations once released into the atmosphere (Kansal 2009, Nair et al. 2019). Municipal solid waste landfills represent a small, yet detectable and ongoing source of annual NMVOC emissions in the US. The 2014 USEPA national air emissions inventory (USEPA 2016a) estimated that total landfill NMVOC emissions are 13,741 tonnes per year amounting to 0.024% of the nationwide total. As compared to nationwide results, the California Air Resources Board's (CARB) projected 2015 statewide NMVOC (termed ROG for Reactive Organic Gases) emissions inventory reported estimates of total NMVOCs from MSW landfills of 3,460 tonnes per year, MSW landfill contributions to be an order of magnitude more than national estimates at 0.50% of the statewide total (CARB 2009).

Many NMVOCs are highly reactive compounds, with short to moderate atmospheric half-lives (hours to days), affecting air quality from local to regional scales (Atkinson and Arey 2003). NMVOCs are precursors to tropospheric ozone, photochemical smog, and secondary organic aerosol (SOA) formation in the atmosphere (Kroll and Seinfeld 2008, Ziemann and Atkinson 2012). Due to their active roles in ozone and SOA formation, as well as degradation in the atmosphere, NMVOCs both indirectly and directly contribute

to global climate change (Collins et al. 2002). In addition, some NMVOCs, including benzene and other aromatic or halogenated hydrocarbons, pose acute and/or chronic human health risks, leading to their classification as hazardous air pollutants (HAPs) (Reinhart 1993). Other NMVOC classes, such as reduced sulfur compounds, are olfactory nuisances, presenting aesthetic problems to communities located near emission sources (Ying et al. 2012). Furthermore, in addition to F-gases, some chlorinated and brominated NMVOCs (i.e., chloroform or bromoform) are stratospheric ozone depleting substances (ODSs) (Hodson et al. 2010).

One of the most critical impacts of NMVOC emissions from landfills relates to tropospheric ozone formation. Ozone is a strong chemical oxidant and a GHG, which directly affects human health, environment, and global climate change. The fundamental ozone formation mechanism from NMVOC precursors in the troposphere is as follows: a) OH radicals attack the NMVOCs to produce nitrogen dioxide; b) nitrogen dioxide then dissociates in the presence of sunlight (photolysis) to form nitrogen oxides and oxygen radicals; and c) finally, the oxygen radicals combine with oxygen in the atmosphere forming ozone (Perring et al. 2013). Among many factors, the ozone formation potential ultimately depends on the reactivity of the NMVOC as well as the relative concentrations of NMVOC and nitrogen oxides (NOx) in the atmosphere (Duan et al. 2008, Nair et al. 2019). Depending on these conditions, ozone formation reactions can be either NMVOC or NOx limited, where the former is generally the case in urban environments. Previous field and laboratory studies have determined that aromatics, alkenes, and aldehydes are the main chemical families contributing to tropospheric ozone formation (Duan et al. 2008).

The role of NMVOC emissions in SOA formation also is important, even though this process is more complex and harder to predict in the ambient environment than ozone formation (Hallquist et al. 2009). SOAs are defined as liquid or solid particles suspended in the air that indirectly affect Earth's energy balance through: a) scattering and absorption of incoming solar and outgoing terrestrial radiation, b) influencing cloud formation, and c) being included in chemical reactions that influence the abundance and distribution of atmospheric trace gases (Haywood and Boucher 2000). In addition, SOAs pose a direct threat to human health, where SOA exposure has been linked to damage of respiratory and cardiovascular systems (Harrison and Yin 2000). The fundamental formation of SOA from NMVOC precursors is described as: a) SOA formation is initiated by reaction of NMVOCs with hydroxyl radicals, ozone, or nitrate radicals or via photolysis (the hydroxylation pathway depends on molecular structure of NMVOC and atmospheric conditions); b) the initial oxidation step leads to first generation of polar, fragmented, and oxygenated functional groups (aldehydes, ketones, alcohols, nitrates, carboxylic acids), which either undergo gas to particle transfer, including heterogeneous chemical reactions, condensation, and nucleation (depending on volatility and water solubility), or continue to oxidize to form next generation byproducts in the gas phase; c) the competition between gas-particle transfer and oxidation continues until all fragments have been oxidized to CO_2 or undergo gas-particle transfer (Hallquist et al. 2009). Previous field and laboratory studies have determined that oxygenated compounds, carbonyls, aromatics, alkanes,

and alkenes are the major classes of SOA NMVOC precursors (Ziemann and Atkinson 2012, Guo et al. 2017).

Similar to GWP values used to assess climate change, metrics have been developed to assess and compare the impacts of NMVOC emissions on atmospheric air quality. Common air quality metrics to assess changes in atmospheric air quality used in the current investigation include tropospheric ozone formation, secondary aerosol formation, indirect/direct global warming, and stratospheric ozone depletion potentials. HAP classification can also be used to further evaluate to what extent a chemical emitted from a landfill site impacts human health. The mathematical meaning and calculation of each of these metrics are reviewed in more detail in Section 3.10 of this report.

1.5.1 Baseline Greenhouse Gases

The baseline greenhouse gases included in this investigation consist of the individual chemical species: methane, carbon dioxide, carbon monoxide, and nitrous oxide. Methane, carbon dioxide, and nitrous oxide are well known GHGs that directly affect the radiative forcing of Earth's atmosphere. In addition, carbon monoxide both directly and indirectly affects Earth's radiative forcing through absorption and emission of reflected infrared radiation and by chemically altering the abundances of methane, ozone, and carbon dioxide (Daniel and Solomon 1998). The direct radiative forcing of CO is small (< 1), whereas the indirect forcing is higher at 4.4 (Table 1.1) and results in the production of ozone or oxidation to carbon dioxide as well as the reduction in loss rate of methane (due to a decrease in the hydroxyl mixing ratios) (Daniel and Solomon 1998). Of the baseline GHGs, N_2O has the highest GWP value of 265 (Table 1.1).

The main source of baseline GHGs in the landfill environment is biogenic production during aerobic or anaerobic decomposition of the biodegradable fraction of MSW (Tchobanoglous et al. 1993, Barlaz et al. 2010). Methane is produced during the anaerobic decomposition of waste materials, whereas carbon dioxide and monoxide are both produced during aerobic oxidation and anaerobic decomposition of waste materials. Carbon dioxide and monoxide also are produced as byproducts during methanotrophic oxidation of LFG or oxidation of organic carbon present in soil matter in landfill cover soils (i.e., background soil respiration) (Bogner et al. 1997b). The biological production of CO is not well understood; however, studies have reported that methanogens actively produce CO during exergonic formation of methane from carbon dioxide and hydrogen (Haarstad et al. 2006). Moreover, acetogens and sulfate reducing bacteria also have been observed to produce CO under anaerobic conditions (Haarstad et al. 2006). Aerobic degradation of chlorophyll in leaf waste was identified as another source of CO, which has been observed in composting operations (Haarstad et al. 2006). Depending on the stage of waste decomposition the concentrations of methane, carbon dioxide, and carbon monoxide can vary significantly as described in Section 1.2. While, CO_2 and CO typically are not included in landfill emissions inventories due to the uncertainties in the source of these gases (i.e., waste mass versus cover soils) (USEPA 2008, Henkelman et al. 2016), these gases were measured in this investigation and data and analysis are provided both including and excluding these two gases.

Production of nitrous oxide in the landfill environment is complicated and can be attributed to differences in nitrogen cycling in the waste mass and cover soils. In the waste mass, which is primarily present at anaerobic conditions (depending on the stage of decomposition), denitrification of nitrate producing nitrogen gas releases nitrous oxide as a byproduct through cell leakage (Barton and Atwater 2002). In the top portion of landfill cover soils, which are primarily under aerobic conditions, nitrification of ammonium by resident methanotrophs that co-oxidize methane to nitrate releases nitrous oxide as a byproduct through cell leakage (Mandernack et al. 2000, Barton and Atwater 2002). Moreover, methanotrophs likely compete with indigenous autotrophic and heterotrophic nitrifying bacteria, which naturally oxidize ammonium present in the cover soils and emitted from the waste mass (Mandernack et al. 2000, Barton and Atwater 2002). Emissions of nitrous oxide from landfill leachate is yet another potential nitrous oxide source, as reactive nitrogen tends to dissolve in water percolating through the waste mass (where high total nitrogen concentrations have been reported in the range of 25-1600 mg/L) (Tchobanoglous et al. 1993). Finally, wastewater sludges (biosolids) are another potential source of nitrous oxide emissions (Börjesson and Svensson 1997c). The relative contribution of denitrification and nitrification to nitrous oxide production in MSW landfills depends on MSW age and composition (presence of inorganic and organic nitrogen sources), temperature, pH and moisture content of the waste mass, as well as the presence/absence of oxygen (Barton and Atwater 2002). Similar conditions affect the degree of nitrification in soil covers (i.e. presence of bioavailable ammonium in the soil), soil composition, pH, moisture content, temperature, and presence or absence of oxygen (Barton and Atwater 2002).

Physical and chemical properties of baseline greenhouse gases are presented in Table 1.2. These data are obtained from experimental analysis or predictions compiled in USEPA's CompTox Database (Williams et al. 2017). In this analysis, experimental values are preferred over predicted values. Predicted properties were derived from two quantitative-structure activity modelling suites: TEST and OPERA. Carbon monoxide is the most water-soluble chemical of the baseline GHGs, whereas methane is the least water soluble (Table 1.2). The high vapor pressures, Henry's constants and very low boiling points of all baseline GHG species indicate that these chemicals most likely will be present in the gaseous phase in the landfill environment. Based on octanol-air partition coefficients, nitrous oxide is the most likely to sorb to organic matter in the waste mass or present in cover materials (no experimental or predicted values available for carbon monoxide).

Table 1.2 – Physical and Chemical Properties of Baseline GHGs

Chemical Species	Mol. Weight (g/mol)	Boiling Point (°C)	Log_{10} (Vapor Pressure)	Log_{10} (Octanol-Air)	Log_{10} (Dim. Henry's Constant)	Water Solubility (mg/L)	Log_{10} (Octanol-Water)
Methane	16.04	-163	5.67	-0.38	-0.91	21.97	0.63
Carbon Dioxide	44.01	-78.2	4.68	1.57	-2.88	14699	0.83
Carbon Monoxide	28.01	-192	3.53	-	-1.78	238645	0.07

Chemical Species	Mol. Weight (g/mol)	Boiling Point (°C)	Log_{10} (Vapor Pressure)	Log_{10} (Octanol-Air)	Log_{10} (Dim. Henry's Constant)	Water Solubility (mg/L)	Log_{10} (Octanol-Water)
Nitrous Oxide	44.013	-88.3	4.59	4.13	-3.79	8759	1.38

1.5.2 Reduced Sulfur Compounds

The reduced sulfur compounds included in this investigation consist of the individual chemical species: carbonyl sulfide, dimethyl sulfide, dimethyl disulfide, and carbon disulfide. These chemicals do not affect climate change or impact atmospheric air quality, based on data presented in Table 1.1. However, two of these chemicals, carbon disulfide and carbonyl sulfide are hazardous air pollutants (USEPA 2016b). In addition, these chemical species are largely responsible for olfactory nuisances that have adverse effects on the surrounding communities (Kim 2006, Kim et al. 2006).

The chemical species included under the reduced sulfur compound chemical family are primarily produced from anaerobic biological decomposition of food (dairy and meat products), green wastes, paper, and wastewater sludge materials (Table 1.1) in MSW landfills (Ko et al. 2015). In general, sulfate reducing bacteria are responsible for the generation of the reduced sulfur compounds that use the organic sulfur (sulfate) present in the food or green wastes as terminal electron acceptors (Ko et al. 2015). Amino acids containing sulfur (which are derived from proteins in food/green wastes, including cysteine and methionine) are the principal sources of reduced sulfur compounds in MSW landfills. However, C&D materials containing gypsum (composed of calcium sulfate and water) are also significant sources of sulfate in MSW landfills in the U.S. (Lee et al. 2006).

Physical and chemical properties of reduced sulfur compounds are presented in Table 1.3. The volatility is highest for carbonyl sulfide and lowest for dimethyl disulfide based on the reported median values of vapor pressure and boiling point (in contrast to trends in the dimensionless Henry's Constant). Sorption of carbonyl sulfide to organic matter either in the waste mass or cover soil is least likely for carbonyl sulfide based on octanol-air partition coefficients. Water solubility is highest for carbonyl sulfide and lowest for carbon disulfide, based on data for water solubilities and octanol-water partition coefficients (Table 1.3).

Table 1.3 – Physical and Chemical Properties of Reduced Sulfur Compounds

Chemical Species	Mol. Weight (g/mol)	Boiling Point (°C)	Log_{10} (Vapor Pressure)	Log_{10} (Octanol-Air)	Log_{10} (Dim. Henry's Constant)	Water Solubility (mg/L)	Log_{10} (Octanol-Water)
Carbonyl Sulfide	60.07	-50	3.97	2.18	-4.14	100918	0.39
Dimethyl Sulfide	62.13	38	2.70	2.26	-2.50	20814	1.09
Dimethyl Disulfide	94.19	109	1.46	3.35	-2.62	2995	1.77
Carbon Disulfide	76.131	46	2.56	2.28	-1.55	1180	1.94

1.5.3 Fluorinated Gases (F-gases)

The fluorinated gases included in this investigation consist of chlorofluorocarbons (CFCs), hydrochlorofluorocarbons (HCFCs), hydrofluorocarbons (HFCs), and halons. The CFCs investigated are CFC-11, CFC-12, CFC-113, and CFC-114 The HCFCs investigated are HCFC-21. HCFC-22, HCFC-141b, and HCFC-142b. The HFCs investigated are HFC-134a, HFC-152a, HFC-245fa, and HFC-365mfc. A single species, H-1211, is selected for analysis within the halon category of F-gas chemicals. All chemical species within the F-gas chemical family are high GWP gases, where GWP values are generally highest for the CFCs followed by the HCFCs and HFCs (Table 1.1). The CFCs and HCFCs also are ozone depleting substances, where ODP values are higher for the CFCs than the HCFCs (Table 1.1). H-1211 has the highest ODP value of all species within the F-gas chemical family (Table 1.1).

F-gases are commonly used as blowing agents applied to improve the insulation properties of foam materials as they can absorb large amounts of heat upon vaporization (Kjeldsen and Jensen 2001). The fluorinated gases are alkanes (long groups of single bonded carbon atoms) where all of the hydrogen atoms are replaced by fluorine and chlorine atoms (Vollhardt and Schore 1999). Common sources of the fluorinated gases in the landfill environment include rigid foam insulation materials used in domestic, commercial, and industrial appliances (Fredenslund et al. 2005). Other significant sources of F-gases in the landfill environment include insulation materials used in buildings (C&D wastes) and automobiles (automotive shredder residues) (Scheutz et al. 2010). Due to their negative effects on stratospheric ozone concentrations, CFCs were banned by the Montreal protocol in 1993. After replacement of CFCs with HCFCs (smaller ODP values), HCFCs were eventually phased out by HFCs, which are the latest replacement species (Powell 2002). Halons are commonly used in fire suppressant applications, such as fire extinguishers in residential and commercial settings (McCulloch 1992).

Physical and chemical properties of the CFCs, HCFCs, HFCs, and the halon species are presented in Table 1.4. Due to their relatively low boiling points (in the range of <0 to 100°C) and high vapor pressures and Henry's Constants, CFCs, HCFCs, HFCs, and halon fall within the general classification of NMVOCs. Molecular weights of the CFCs, HCFCs, and HFCs are relatively low, with the lowest values associated with HCFC-22 and HFC-152a (Table 1.4). On average, the HFCs have higher volatility (higher vapor pressure, lower boiling point) and relatively moderate solubility in water as compared to CFCs and HCFCs (HCFCs had the highest water solubility, CFCs the lowest) (Table 1.4). HFCs have the lowest octanol-water and octanol-air partition coefficients, indicating that they are more likely to remain in the water or air phase over organic phases present in the landfill environment (Table 1.4). The CFCs (especially CFC-113 and 114) are most likely to partition to organic phases present in the landfill environment. H-1211 has moderate volatility and moderate-high partitioning potential to the organic matter in the landfill environment.

Table 1.4 – Physical and Chemical Properties of the Fluorinated Gases

Chemical Species	Mol. Weight (g/mol)	Boiling Point (°C)	Log_{10} (Vapor Pressure)	Log_{10} (Octanol-Air)	Log_{10} (Dim. Henry's Constant)	Water Solubility (mg/L)	Log_{10} (Octanol-Water)
CFC-11	137.37	23.8	2.90	2.19	-0.72	1100	2.53
CFC-12	120.91	-29.8	3.69	1.31	-0.17	281	2.16
CFC-113	187.375	47.8	2.56	2.82	-0.79	170	3.16
CFC-114	170.92	3.64	3.30	2.19	0.21	130	2.82
HCFC-21	102.923	8.9	3.13	2.02	-1.46	18835	1.55
HCFC-22	86.47	-40.8	3.86	0.56	-1.10	2767	1.08
HCFC-141b	116.95	32	2.78	2.22	-2.70	420	1.99
HCFC-142b	100.495	-9.52	3.40	1.30	-0.94	1397	1.57
HFC-134a	102.03	-26.5	3.70	0.04	-1.01	2530	1.18
HFC-152a	66.05	-24.9	3.66	0.47	-1.40	3203	0.75
HFC-245fa	134.05	40	3.05	0.44	-0.84	1249	1.43
HFC-365mfc	148	40	3.29	0.97	-0.89	445	2.06
H-1211	165.36	-2.8	3.31	1.78	-0.25	678	2.13

1.5.4 Halogenated Hydrocarbons

The halogenated hydrocarbons included in this investigation consist of the individual chemical species: chloroform, methyl chloroform, carbon tetrachloride, methylene chloride, trichloroethylene, tetrachloroethylene, methyl chloride, bromomethane, dibromomethane, bromodichloromethane, bromoform, chloroethane, 1,2-dichloroethane, and 1,2-dibromoethane. Eleven of the fourteen halogenated hydrocarbons with the exceptions of dibromomethane, bromodichloromethane, and chloroethane are designated as hazardous air pollutants (USEPA 2016b), indicating that the emissions of these chemical species may significantly affect human health. Several of the halogenated hydrocarbon chemical species contribute to tropospheric ozone formation including from most to least active, based on reported MIR values: trichloroethylene, bromomethane, methylene chloride, methyl chloride, tetrachloroethylene, chloroform, and methyl chloroform (Table 1.1). Indirect GWP values are highest for carbon tetrachloride along with methyl chloroform and methyl chloride, indicating that emissions of halogenated hydrocarbons may affect climate change in addition to the well-known GHGs (Table 1.1). Carbon tetrachloride, bromomethane, methyl chloroform, and methyl chloride also are ozone depleting substances, where ODP values are generally less than 1 (Table 1.1).

In this report, halogenated compounds are classified as hydrocarbons (linear or branched, composed of C and H atoms) composed of one or more halogen atoms (i.e., F, Cl, Br, I). Hydrocarbons can be either unsaturated (single bonded) or saturated (double or triple bonded) (Vollhardt and Schore 1999). In this particular inventory of target chemicals, the most common halogen atoms are chlorine and bromine and a majority of chemicals are saturated (i.e., chloroform, bromomethane) as opposed to unsaturated species(methylene chloride, trichloroethylene). Nair et al. (2019) indicated

that halogenated hydrocarbons in the landfill environment are mostly directly volatilized (abiotically) from a variety of waste household consumer products, mainly including cleaning and fragrance-containing products (Table 1.1). Additional sources of halogenated hydrocarbons in the landfill environment are more difficult to define. Methyl chloride has been used as a refrigerant and in the production of synthetic rubber materials. Methylene chloride and chloroform are both commonly used industrial solvents. Carbon tetrachloride and tetrachloroethylene have been used extensively as dry-cleaning solvents, while carbon tetrachloride also has been used in fire extinguishers (Vogel et al. 1987).

Given that there is a general lack of consistent and reliable information on the origin of halogenated hydrocarbons in the landfill environment, CPCat (Chemical/Product Categories) database (Dionisio et al. 2015, 2018) was used to search for specific product use categories for each target chemical. CPCat database contains information on over 75,000 chemical species and 15,000 consumer products which mapped to over 800 terms categorizing their use or function, (Dionisio et al. 2015, Isaacs et al. 2016). Even though this database is not fully representative of the materials that are disposed of in MSW landfills, it provides a general indication of the sources of these chemicals from consumer related products.

For the halogenated hydrocarbons included in this investigation, 175 unique functional use categories were obtained from this database. The fifteen most significant overall categories for this chemical family were determined by summing the number of products linked to each functional use category and then sorting the results in descending order. The relative contribution of each chemical species to products contained within a given functional use category is presented in Table 1.5. This analysis provided several significant functional uses of the halogenated hydrocarbons that have not been identified in the literature including: pesticides (home or lawn/backyard care), adhesives, automotive products, metal, plastic, rubber manufacturing, paints, and other personal care products (i.e., makeup, fragrances, shampoos) (Table 1.5).

The relative contribution of each chemical to different functional uses is also reviewed. Bromomethane is identified as a chemical species present in a large number of products associated with household or commercial pesticide applications. Carbon tetrachloride, methylene chloride, trichloroethylene, and tetrachloroethylene are identified as common chemical ingredients present in products associated with solvent, adhesive, cleaning, and painting applications. Most chemical species were equally distributed among products associated with automotive and personal care products (Table 1.5). Of all chemical species within the halogenated hydrocarbon family, dibromomethane and chloroethane are not associated with any products from the top fifteen functional use categories identified (Table 1.5). The 1,2 dichloro/dibromo ethanes are used in manufacturing chemicals, plastics, and other raw materials intended for a variety of industries.

Physical and chemical properties of the halogenated hydrocarbons are presented in Table 1.6. Of the halogenated hydrocarbons included in this investigation, methyl

chloride and bromoform are the most and least volatile, based on the low and high boiling points and high and low vapor pressures, respectively (Table 1.6). Both of these chemical species are also relatively soluble in water, based on water solubility and octanol-water partition coefficients. Based on Henry's Constant, water solubility, and octanol-water partition coefficients, dibromomethane is the most water-soluble halogenated hydrocarbon included in this study. Tetrachloroethylene and bromoform have high likelihood to partition into organic phases in the landfill environment (based on high octanol-air and octanol-water partition coefficients).

Table 1.5 – Fifteen Most Common Functional Use Categories for Halogenated Hydrocarbons

CPCat Functional Use Category	Definition	Relative Contribution to Each Functional Use Category (%)												
		Chloroform	Methyl Chloroform	Carbon Tetrachloride	Methylene Chloride	Trichloroethylene	Tetrachloroethylene	Methyl Chloride	Bromomethane	Dibromomethane	Bromodichloromethane	Chloroethane	1,2-DCE	1,2-DBE
pesticide	Substances used for preventing, destroying or mitigating pests	5.56	3.33	8.89	1.11	1.11	1.11	1.11	54.4	0	1.11	0	0	6.67
solvent	Paint/graffiti removers, general solvents	17.6	8.82	2.94	26.5	17.6	20.6	0	0	0	0	0	0	5.88
adhesive	General adhesive/binding agents	9.09	6.06	21.2	21.2	24.2	12.1	6.06	0	0	0	0	0	0
manufacturing:chemical	Manufacturing of a given chemical	12.5	0	9.38	12.5	12.5	12.5	15.6	3.13	0	0	0	15.6	6.25
automotive	Related to automobiles or their manufacture	14.3	14.3	14.3	14.3	14.3	14.3	0	14.3	0	0	0	0	0
cleaning_washing	Related to all forms of cleaning/washing including detergents, soaps, de-greasers, spot removers	3.85	15.4	0	23.1	26.9	30.8	0	0	0	0	0	0	0
manufacturing:metals	Manufacturing of metals	0	4.17	12.5	29.2	33.3	20.8	0	0	0	0	0	0	0
chemical:laboratory	Chemical use designated in laboratory	31.8	0	18.2	31.8	9.09	4.55	0	0	0	0	0	0	4.55

CPCat Functional Use Category	Definition	Relative Contribution to Each Functional Use Category (%)												
		Chloroform	Methyl Chloroform	Carbon Tetrachloride	Methylene Chloride	Trichloroethylene	Tetrachloroethylene	Methyl Chloride	Bromomethane	Dibromomethane	Bromodichloromethane	Chloroethane	1,2-DCE	1,2-DBE
personal_care:cosmetics:prohibited_ASEAN	Personal care products: fragrances, shampoos, makeup (banned in ASEAN countries)	10	0	10	10	10	10	10	10	0	0	0	10	10
paint	Various types of paint for various uses	0	0	44.4	38.9	16.7	0	0	0	0	0	0	0	0
manufacturing:machines	Manufacturing of machinery related to production of different products	0	11.8	17.6	35.3	29.4	5.88	0	0	0	0	0	0	0
manufacturing:plastics	Manufacturing of plastics (plastic additives)	0	11.8	17.6	29.4	17.6	17.6	0	0	0	0	0	0	5.88
manufacturing:raw_material	Raw materials used in manufacturing of a variety of products in different industries	5.88	0	17.6	5.88	5.88	5.88	17.6	5.88	5.88	0	0	17.6	11.8
manufacturing:rubber	Manufacturing of rubbers (rubber additives)	0	6.67	26.7	13.3	26.7	26.7	0	0	0	0	0	0	0
pesticide:inert_ingredient	Inert ingredient in a pesticide	7.69	30.8	7.69	7.69	7.69	7.69	7.69	7.69	0	0	0	7.69	7.69

Table 1.6 – Physical and Chemical Properties for the Halogenated Hydrocarbons

Chemical Species	Mol. Weight (g/mol)	Boiling Point (°C)	Log_{10} (Vapor Pressure)	Log_{10} (Octanol-Air)	Log_{10} (Dim. Henry's Constant)	Water Solubility (mg/L)	Log_{10} (Octanol-Water)
Chloroform	119.4	61.2	2.29	2.80	-2.14	7951	1.97
Methyl Chloroform	133.4	96.7	2.09	2.70	-1.47	1494	2.49
Carbon Tetrachloride	153.8	76.8	2.06	2.79	-1.27	794	2.83
Methylene Chloride	84.9	39.8	2.64	2.27	-2.19	12994	1.25
Trichloroethylene	131.4	87	1.84	2.99	-1.71	1100	2.42
Tetrachloroethylene	165.8	121	1.27	3.48	-1.46	201	3.40
Methyl Chloride	50.45	-24.2	3.63	1.39	-1.76	5301	0.91
Bromomethane	109.0	3.6	3.21	2.00	-1.84	17435	1.19
Dibromomethane	173.8	97.3	1.65	3.07	-2.79	11905	1.70
Bromodichloromethane	163.8	88.7	1.97	2.81	-2.38	3031	2.00
Bromoform	252.7	149	0.73	3.98	-2.98	3488	2.40
Chloroethane	64.5	12.3	3.00	2.19	-1.66	5677	1.43
1,2-Dichloroethane	99.0	83	1.90	2.78	-2.63	8520	1.48
1,2-Dibromoethane	187.9	132	1.05	3.65	-2.89	4152	1.96

1.5.5 Organic Alkyl Nitrates

The organic alkyl nitrates included in this investigation consist of the individual chemical species: methyl nitrate, ethyl nitrate, isopropyl nitrate, n-propyl nitrate, and 2-butyl nitrate. These chemical species are relatively reactive, non-hazardous chemicals with moderate-long atmospheric lifetimes compared to other NMVOCs (Muthuramu et al. 1994). Even though the organic alkyl nitrates have not been assigned MIR or FAC values, several studies have identified these species as affecting ozone production/depletion and species involved in SOA formation in the troposphere (Atkinson et al. 1982, Muthuramu et al. 1994, Perring et al. 2015). While these species do not directly affect global climate change, they may have indirect effects by disturbing the balance of ozone in the troposphere (Table 1.1).

The production, fate, and emissions of organic alkyl nitrates in the landfill environment has received little attention in the scientific literature. Alkyl nitrates consist of a nitrate group (negatively charged) bonded to a hydrocarbon chain. Even though the alkyl nitrates in this study are classified as organic, these trace gases generally are not produced as a biogas through aerobic or anaerobic decomposition of waste materials. In contrast, these chemicals are likely produced abiotically through similar transformation pathways as demonstrated in the troposphere involving organic reactants. Perring et al. (2015) summarized two primary pathways for the production of alkyl nitrates in the atmosphere including: 1) hydroxyl radical initiated oxidation of hydrocarbons (alkanes) in the presence of nitrogen oxides (likely occurs in the presence of sunlight), and 2) nitrate radical initiated oxidation of alkenes (occurs in the absence of sunlight). The alkyl nitrate production pathways in the atmosphere may constitute surrogates for the formation of organic alkyl nitrates in the landfill environment. For pathway 1, it is likely that availability of sufficient oxygen is required for transformation reactions to be carried out. In the landfill environment, these reactions may take place and organic alkyl nitrates may be generated in the upper portion of the soil cover where oxygen and radicals are available for the chemical reactions. The second transformation pathway is likely more dominant, as sunlight does not penetrate far into the cover soils or underlying waste layers, and thus alkenes may be precursors for organic alkyl nitrate production in the landfill environment. The sources of alkene precursors are described in Section 1.5.7.

Physical and chemical properties of the halogenated hydrocarbons are presented in Table 1.7. As observed in Table 1.7, as the number of carbons comprising an alkyl nitrate increases, the molecular weights and boiling points also increase. Vapor pressures (and corresponding volatility) are generally higher for methyl nitrate and decrease with increasing number of carbon atoms comprising each chemical species. Both octanol air and octanol water coefficients also increase with an increasing number of carbon atoms, as the chemical species become more non-polar in nature. Thus, 2-butyl nitrate is more likely to partition into organic phases in the landfill environment as compared to all other alkyl nitrates. Water solubility for all alkyl nitrates is generally high (highest for 2-butyl nitrate, which has a relatively low Henry's constant).

Table 1.7 – Physical and Chemical Properties of the Organic Alkyl Nitrates

Chemical Species	Mol. Weight (g/mol)	Boiling Point (°C)	Log_{10} (Vapor Pressure)	Log_{10} (Octanol-Air)	Log_{10} (Dim. Henry's Constant)	Water Solubility (mg/L)	Log_{10} (Octanol-Water)
Methyl Nitrate	77.0	64.6	1.94	2.18	-2.88	150226	0.45
Ethyl Nitrate	91.1	87.2	1.81	2.32	-2.49	34332	0.71
Isopropyl Nitrate	105.1	40	2.29	2.14	-4.59	31318	1.14
N-propyl Nitrate	105.1	110	1.37	2.78	-2.60	3289	1.38
2-butyl Nitrate	119.1	124.3	1.19	3.20	-2.53	1330000	1.97

1.5.6 Alkanes

The alkanes included in this investigation consist of the individual chemical species: ethane, propane, iso-butane, n-butane, iso-pentane, n-pentane, n-hexane, and n-undecane. Most of the alkanes are involved in ozone formation, where reactivity (in terms of ozone production) is generally higher for the pentane isomers and lowest for ethane/n-undecane. Excluding n-undecane, the remaining alkanes are not actively involved in SOA formation (Table 1.1). Indirect GWPs have been reported for ethane and propane. n-hexane is the only alkane that has been identified as a hazardous air pollutant by the USEPA (Table 1.1).

The alkanes are generally straight chain hydrocarbons (composed of carbon and hydrogen) that are saturated (composed of single bonds only) and vary according to the number of carbon atoms comprising each chain (Vollhardt and Schore 1999). Structural isomers (i.e., i/n) of butane and pentane were investigated in this study, where structural isomers refer to the configuration of these molecules in three-dimensional space (iso-variants are branched and not straight-chained). Abiotic sources of alkanes in the landfill environment include household spray products and paints (Nair et al. 2019). Food packaging, cooking oils and fuels (charcoal or vegetable oils), and paper also are indicated as potential sources of alkanes in the landfill environment (Duan et al. 2014). In addition, alkanes are produced during anaerobic decomposition of waste materials (Xie et al. 2013). Although not documented in landfills, methanogens can generate low molecular weight alkanes in the presence of ethylene (i.e., ethylene reduction) (Xie et al. 2013). A similar production and transformation mechanism was suggested by Ikeguchi and Watanabe (1991), where ethane production from ethene was postulated. Ethene can be synthesized by microorganisms in aerobic, upper portions of soil (Primrose 1979), that Ikeguchi and Watanabe (1991) identified as a potential mechanism in landfill cover soils. The biogenic production of longer chain alkanes is possible, but not yet documented in the landfill environment.

Analysis of the top fifteen functional use categories based on the CPCat database indicated more categories related to personal use items for the alkanes as compared to the halogenated hydrocarbons (Table 1.8). Personal care products associated with shaving creams, hair styling, hair spray and deodorant contain alkane chemicals. Paints, lubricants, insecticides, cleaning products, and products associated with automotive care are likely to contain the alkane chemical species included in this report. For personal care products, i-pentane, i-butane, i-butane, and i-butane are the chemical species most likely present in shaving creams, hair-style products, hair sprays, and

deodorants, respectively. Propane and n-butane are most likely present in the paint products identified in Table 1.8. Within the top 15 functional use categories, n-undecane is only present in lubricant products. The functional use categories for ethane are significantly different than the overall functional use categories for the alkane chemical family (Table 1.9). Ethane is present in cooking and camping fuels and also in some paint and lubricant-related products. Household cleaning related products are more likely contain propane, n-butane, i-butane, n-pentane, and n-hexane as compared to the remaining three alkane chemical species included in this investigation (Table 1.8).

Table 1.8 – Fifteen Most Common Functional Use Categories for Alkanes

CPCat Functional Use Category	Definition	Relative Contribution to Each Functional Use Category (%)							
		Ethane	Propane	i-Butane	n-Butane	i-Pentane	n-Pentane	n-Hexane	n-Undecane
personal care: shaving cream	-	0	9.45	23.6	2.55	64	0.36	0	0
personal care: hair styling	-	0	35.5	43.2	19.4	1.47	0.37	0	0
home maintenance: paint	-	0	51	0	49	0	0	0	0
manufacturing:metals	Manufacturing of metals	0	23.3	21.9	23.3	2.74	13.7	15.1	0
pesticides: insecticide	-	0	40.8	33.8	25.4	0	0	0	0
paint	Various types of paint for various uses, modifiers included when more information is known	2.99	23.9	17.9	23.9	4.48	5.97	20.9	0
lubricant	Generic lubricants, lubricants for engines, brake fluids, oils, etc. (does not include personal care lubricants)	3.03	24.2	15.2	22.7	1.52	13.6	15.2	4.55
manufacturing:machines	Manufacturing of machinery related to production of different products	0	26.2	15.4	26.2	1.54	16.9	13.8	0
personal care: hair spray	-	0	22.6	41.9	24.2	3.23	8.06	0	0
surface_treatment	Surface treatments for metals, hardening agents, corrosion inhibitors, polishing agents, rust inhibitors, water repellants, etc. (surfaces to be applied to often not indicated in source description)	0	31.1	18	32.8	0	8.2	9.84	0
auto products: auto paint	-	0	50	0	50	0	0	0	0
cleaning_washing	Related to all forms of cleaning/washing including detergents, soaps, de-greasers, spot removers	0	25	19.6	23.2	1.79	14.3	16.1	0
arts and crafts: arts and crafts paint	-	0	50	0	50	0	0	0	0
personal care: deodorant	-	0	22.4	44.9	30.6	2.04	0	0	0
automotive_care	Related to the maintenance and repair of automobiles, products for cleaning and caring for automobiles (auto shampoo, polish/wax, undercarriage treatment, brake grease)	0	22.9	18.8	20.8	4.17	16.7	16.7	0

Physical and chemical properties of the alkanes are presented in Table 1.9. As molecular weight increase, the boiling points and vapor pressures of the alkanes increase and decrease, respectively with ethane identified as the most and n-undecane as the least volatile species. As the carbon chain length increases, the likelihood of partitioning into organic phases in the landfill environment increases significantly. Water solubility generally decreases from small to long chain lengths, which can be expected as these chemicals become more non-polar and hydrophobic with ethane identified as the most and n-undecane as the least soluble species.

Table 1.9 – Physical and Chemical Properties of the Alkanes

Chemical Species	Mol. Weight (g/mol)	Boiling Point (°C)	Log_{10} (Vapor Pressure)	Log_{10} (Octanol-Air)	Log_{10} (Dim. Henry's Constant)	Water Solubility (mg/L)	Log_{10} (Octanol-Water)
Ethane	30.1	-88.5	4.50	0.42	-0.16	60	1.81
Propane	44.1	-42.2	3.85	0.97	-0.12	63	2.36
i-Butane	58.1	-11.7	3.42	2.00	-0.06	49	2.76
n-Butane	58.1	-2.19	3.26	1.53	-0.04	61	2.89
i-Pentane	72.2	28.6	2.84	2.26	0.06	49	2.99
n-Pentane	72.2	35.9	2.71	1.96	0.39	38	3.39
n-Hexane	86.2	68.6	2.18	2.40	-0.02	9	3.90
n-Undecane	156.3	196	-0.39	5.01	-0.54	0.004	6.06

1.5.7 Alkenes

The alkenes included in this investigation consist of the individual chemical species: ethene, propene, 1-butene, i-butene, trans-2-butene, cis-2-butene, 1-pentene, and isoprene. Comparison of the MIR values indicated that the alkenes are more active in ozone production than the alkanes, in which some chemical species also actively participate in SOA formation (ethene and isoprene) (Table 1.1). Similar to the alkanes, due to their active roles in ozone formation, several alkenes indirectly affect climate change, including ethene, propene, and isoprene. None of the alkenes are recognized hazardous air pollutants as determined by the USEPA (Table 1.1).

The alkenes included in this investigation are acyclic compounds (straight chain and branched) with at least one double bond (unsaturated with respect to hydrogen atoms) (Vollhardt and Schore 1999). For butene, several structural isomers are included and differentiated as iso, trans and cis species. The iso-butene structural isomer has a branched molecular structure, whereas the 1-butene configuration is a straight chain. In the trans isomer, the functional groups reside on opposite sides of the double bond (vertically) and in the cis isomer, the functional groups reside on the same sides of the double bond (vertically) (Vollhardt and Schore 1999). As alkenes are hydrocarbons, major sources identified by Duan et al. (2014) for alkanes also are relevant for the alkene chemical family and include food packaging materials, cooking oils and fuels, as well as paper materials. As presented in the previous section, ethene production in soils (by aerobic bacteria) and from vegetation is a well-known phenomenon and has been postulated to occur in landfill cover soils (Ikeguchi and Watanabe 1991). Production of isobutene and isoprene from bacteria in aerobic environments has also been

documented in the scientific literature (Wilson et al. 2018). Therefore, it is likely that both abiotic and biotic production of alkenes occur in landfill systems.

Analysis of the top fifteen functional use categories based on the CPCat database indicated few categories related to personal use items for the alkenes (Table 1.10). Pesticides, lubricants, adhesives, and paints are the significant functional use categories identified for the alkenes. Fuels, plastics, and food packaging related functional use categories also apply to alkenes. Alkenes also are present in products used in the manufacturing of chemicals, oils, raw materials, and rubber. Ethene and iso-butene are the chemical species that are associated with the greatest number of products under the top fifteen functional use categories (Table 1.10). Ethene is present in products under the lubricants, consumer use products, fuels/fuel additives, plastics and filler functional use categories. Iso-butene is present in rubber manufacturing, pesticides, plastics, and food packaging functional use categories. The cis and trans butene isomers, and 1-pentene are not associated with products under many of the functional use categories prioritized in Table 1.10. Propene is present in products related to lubrication and isoprene in products related to the manufacturing of plastic materials.

Table 1.10 – Fifteen Most Common Functional Use Categories for Alkenes

CPCat Functional Use Category	Definition	Relative Contribution to Each Functional Use Category (%)							
		Ethene	Propene	1-Butene	i-Butene	trans-2-Butene	cis-2-Butene	1-Pentene	Isoprene
pesticide	Substances used for preventing, destroying or mitigating pests	11.1	16.7	16.7	33.3	11.1	11.1	0	0
fuel	General fuels, fuel additives, motor/automotive fuels	35.3	17.6	17.6	11.8	0	0	0	17.6
manufacturing:chemical	Manufacturing of a given chemical	11.8	17.6	17.6	23.5	11.8	5.88	0	11.8
manufacturing:oil	Manufacturing of crude oil, crude petroleum, refined oil products, fuel oils, drilling oils	18.2	18.2	9.09	18.2	18.2	0	9.09	9.09
consumer_use	Consumer product, unspecific	45.5	9.09	9.09	18.2	0	0	0	18.2
manufacturing:plastics	Manufacturing of plastic materials	30	0	10	30	0	0	0	30
adhesive	General adhesive/binding agents	20	30	20	10	10	10	0	0
chemical:laboratory	Chemical use designated in laboratory	10	20	20	10	10	10	0	20
manufacturing:raw_material	Raw materials used in manufacturing of a variety of products in different industries	30	10	10	20	0	10	0	20
manufacturing:rubber	Manufacturing of rubbers (rubber additives)	11.1	11.1	11.1	66.7	0	0	0	0
lubricant	Generic lubricants, lubricants for engines, brake fluids, oils, etc. (does not include personal care lubricants)	66.7	33.3	0	0	0	0	0	0
paint	Various types of paint for various uses, modifiers included when more information is known	25	25	25	12.5	0	0	0	12.5
plastics	Plastic products, industry for plastics, manufacturing of plastics, plastic additives (modifiers included when known)	28.6	14.3	0	28.6	0	0	0	28.6
filler	Fillers for paints, textiles, plastics, etc.	28.6	14.3	14.3	14.3	0	0	14.3	14.3
food_contact	Includes food packaging, paper plates, cutlery, small appliances such as roasters, etc.; does not include facilities that manufacture food	11.1	16.7	16.7	33.3	11.1	11.1	0	0

Physical and chemical properties of the alkenes are presented in Table 1.11. Similar to the alkanes, as the number of carbons in the hydrocarbon chain increases, the boiling point and the vapor pressure increases with ethane identified as the most and isoprene as the least volatile species. Both the octanol-air and octanol-water partition coefficients increase as the chain length increases, indicating that alkene species containing more carbon atoms are more likely to partition into the organic phases in the landfill environment. Differences in water solubility are counterintuitive and with increasing solubility from shorter chain to longer chain alkene chemical species. Solubility may be altered due to different structural conformations, where at least four different structural isomers are included for butene. The low dimensionless Henry's Constants of similar order of magnitude among the alkene species indicate high affinity for the air phase over the aqueous phase for all of the alkene chemical species (Table 1.11).

Table 1.11 – Physical and Chemical Properties of the Alkenes

Chemical Species	Mol. Weight (g/mol)	Boiling Point (°C)	Log_{10} (Vapor Pressure)	Log_{10} (Octanol-Air)	Log_{10} (Dim. Henry's Constant)	Water Solubility (mg/L)	Log_{10} (Octanol-Water)
Ethene	28.05	-104	4.72	0.28	-0.35	131	1.13
Propene	42.08	-47.9	3.94	1.60	-0.41	200	1.77
1-Butene	56.11	-6.3	3.35	2.28	-0.34	221	2.40
i-Butene	56.11	-6.93	3.36	2.28	-0.37	263	2.34
trans-2-butene	56.11	1.42	3.16	2.29	-0.35	578	2.33
cis-2-butene	56.11	2.98	3.17	2.29	-0.35	578	2.33
1-Pentene	70.13	30.2	2.80	1.93	-0.39	148	2.82
Isoprene	68.12	34.3	2.74	2.06	-0.71	636	2.42

1.5.8 Aldehydes/Alkynes

The aldehydes/alkynes included in this investigation consist of the individual chemical species: ethyne, acetaldehyde, and butanal. The aldehydes including acetaldehyde and butanal are significant precursors in tropospheric ozone formation and have high reported MIR values (Table 1.1). An indirect GWP value has been reported for acetaldehyde, indicating potential effects of acetaldehyde on atmospheric chemistry. While aldehydes and alkynes potentially participate as precursors in SOA formation, a FAC value has not been commonly reported for these chemicals. In addition, acetaldehyde has been designated as a hazardous air pollutant by the USEPA (Table 1.1).

Aldehydes are formed from a centralized carbonyl group (carbon atom double bounded to an oxygen atom) that is singly bonded to a hydrogen atom on one side and a variable hydrocarbon chain or functional group on the opposing side. Alkynes are generally straight or branched chain hydrocarbons in which one carbon to carbon bond consists of a triple bond. The potential sources of aldehydes and alkynes in the landfill environment are both abiotically and biotically generated. Potential sources of acetaldehydes in landfills are furniture, cooking charcoals, and textiles, with no chemical sources identified for the alkyne chemical family (Nair et al. 2019). Most oxygenated compounds, including the aldehydes, were indicated to be derived from anaerobic decomposition of food or green wastes in the landfill environment (Duan et al. 2014).

During acidogenesis (the acid phase of LFG production), volatile fatty acids (including carboxylic acids) are produced by fermentative bacteria. Under similar environmental conditions, these volatile fatty acids are building blocks for the anaerobic bacterial synthesis of various organic compounds including aldehydes (Eggeman and Verser, 2005, Singhania et al. 2013). Bacteria also form aldehydes via the oxidation of aliphatic (alkane) hydrocarbons at the methylene carbon alpha to the methyl group (McKenna et al. 1965, Forney and Markovetz 1971, Klug and Markov 1971). Biogenic sources of aldehydes also include emissions from vegetation including plants growing on the cover surface or from decaying green waste materials used as covers or disposed of in a landfill.

Analysis of the top fifteen functional use categories based on the CPCat database indicated that aldehyde containing products are generated in manufacturing operations for chemicals, metals, machines, plastics, raw materials, paints, and paper (Table 1.12). Products related to printing (inks), drugs, and food related additives also are potential sources of the aldehydes. Among the three species within this chemical family, acetaldehyde is present in most of the functional use categories including paints, adhesives, food additives, manufacturing of plastics, printing, and automotive related products. Ethyne is classified as an alkyne with different functional use categories from the aldehydes including metal manufacturing, drugs, plastics, and raw materials (Table 1.12). Butanal is commonly present in paint and the manufacturing of raw materials.

Table 1.12 – Fifteen Most Common Functional Use Categories for Aldehydes/Alkynes

CPCat Functional Use Category	Definition	Relative Contribution to Each Functional Use Category (%)		
		Ethyne	Acetaldehyde	Butanal
manufacturing:chemical	Manufacturing of chemicals	18.8	43.8	37.5
manufacturing:metals	Manufacturing of metals	37.5	25	37.5
paint	Various types of paint for various uses, modifiers included when more information is known	0	53.8	46.2
manufacturing:food	Manufacturing of food for human consumption, does not include food additives (see food_additive)	0	100	0
manufacturing:machines	Manufacturing of machinery related to production of different products	20	40	40
adhesive	General adhesive/binding agents	0	77.8	22.2
food_additive:flavor	Includes spices, extracts, colorings, flavors, etc. added to food for human consumption	0	66.7	33.3
manufacturing:plastics	Manufacturing of plastic materials	14.3	71.4	14.3

CPCat Functional Use Category	Definition	Relative Contribution to Each Functional Use Category (%)		
		Ethyne	Acetaldehyde	Butanal
manufacturing:raw_material	Raw materials used in manufacturing of a variety of products in different industries	14.3	42.9	42.9
printing	Related to the process of printing (newspapers, books media, etc.), printing inks, toners, etc.	0	100	0
building_construction	Related to the building or construction process for buildings or boats (includes activities such as plumbing and electrical work, bricklaying, etc.)	0	80	20
drug	Drug product, or related to the manufacturing of drugs; modified by veterinary, animal, or pet if indicated by source	20	80	0
manufacturing:paint	Manufacturing of paint materials	0	80	20
manufacturing:paper	Manufacturing of paper materials	20	80	0
automotive	Related to automobiles or their manufacture	0	100	0

Physical and chemical properties of the aldehydes/alkynes are presented in Table 1.13. Ethyne and butanal have the lowest and highest molecular weights, respectively. Boiling points and vapor pressures follow the trends in molecular weights, where ethyne and butanal are the most and least volatile chemical species, respectively. Acetaldehyde has the highest water solubility, followed by ethyne and butanal. Butanal is the chemical species most likely to partition into organic phases in the landfill environment due to the high octanol-air and octanol-water coefficients (Table 1.13).

Table 1.13 – Physical and Chemical Properties of the Aldehydes/Alkynes

Chemical Species	Mol. Weight (g/mol)	Boiling Point (°C)	Log_{10} (Vapor Pressure)	Log_{10} (Octanol-Air)	Log_{10} (Dim. Henry's Constant)	Water Solubility (mg/L)	Log_{10} (Octanol-Water)
Ethyne	26.0	-84.3	4.56	0.44	-2.27	1200	0.37
Acetaldehyde	44.1	20.5	2.96	1.79	-3.88	999935	-0.34
Butanal	72.1	75.1	2.05	3.39	-3.65	71028	0.88

1.5.9 Aromatic Hydrocarbons

The aromatic hydrocarbons included in this investigation consist of the individual chemical species: benzene, toluene, ethylbenzne, m/p/o-Xylene, i/n-propylbenzene, 2/3/4-ethyltoluene, as well as 1,3,5-, 1,2,3-, and 1,2,4-trimethylbenzene. Aromatics contribute to tropospheric ozone and secondary aerosol formation (Table 1.1). For ozone formation, trimethyl benzenes are the most reactive compounds with MIR values up to 11.66 g O_3/g VOC. Secondary aerosol formation potentials based on the FAC are highest for the ethyltoluenes (M and O). Benzene, toluene, ethylbenzene, and the

Xylene isomers (collectively termed BTEX) are known human carcinogens that are acutely toxic and are designated as hazardous air pollutants by the USEPA. Toluene is the only species in this chemical family with atmospheric impacts (indirect GWP of 2.7). While the reactivities of other benzene derivatives indicate potential atmospheric effects, GWP values have not been reported for these chemicals (Table 1.1).

Aromatic compounds are unsaturated (alternating single/double bonds) chemical compounds in which the carbon atoms (6) are joined in a hexagonal ring arrangement. The ring-like structure provides chemical stability. These species are not easily broken down or transformed due to physical, chemical, or biological reactions occurring in the landfill environment (Vollhardt and Schore 1999). Benzene is the most commonly used aromatic. Benzene derivatives are formed through substitution or attachment of different functional groups located at various positions of the ring structure. For example, the Xylene isomers differ in the arrangement of the methyl groups attached to the ring structure. Similarly, for ethylbenzene, different isomers vary in the arrangement of the ethyl groups attached to the ring structure.

Similar to the halogenated hydrocarbons, the aromatic hydrocarbons are often termed xenobiotic compounds in that they originate from abiotic sources in the landfill environment. Potential sources of aromatics include household cleaning solvents, personal care products, household spray applications, paints, textiles, cooking fuels, and furniture Nair et al. (2019). Additional potential sources are food packaging and containers and paints (Liu et al. 2016). The ratios of BTEX concentrations (benzene and toluene specifically) in landfill gas have been compared to concentrations in the atmosphere of urban environments to identify different emission sources (Liu et al. 2016). Ratio of benzene to toluene of approximately 0.5 indicate vehicular emissions in the urban environment, with lower values reported for the landfill environment (Liu et al. 2016).

Analysis of the top fifteen functional use categories based on the CPCat database indicate that household and automotive paint products are a potential source of the aromatic hydrocarbons in the landfill environment, (Table 1.14). Solvents, adhesives, manufacturing of plastics, cleaning/washing, and building/construction related materials also are functional use categories for the aromatic hydrocarbons. Toluene, ethylbenzene, and benzene are the three species present in the highest number of products (Table 1.14). Toluene and ethylbenzene are mostly in paint product functional use categories, whereas benzene is in cleaning and washing products and products used in manufacturing of metals and machinery. Trimethyl benzene derivatives are mainly present in paint materials, solvents, and building/construction materials. The remaining chemical species (xylene isomers, propylbenzene, and ethylbenzene derivatives) are present to a lesser extent in products under the top fifteen functional use categories (Table 1.14).

Table 1.14 – Fifteen Most Common Functional Use Categories for Aromatic Hydrocarbons

CPCat Functional Use Category	Definition	Relative Contribution to Each Functional Use Category (%)													
		Benzene	Toluene	Ethylbenzene	m-Xylene	p-Xylene	o-Xylene	i-Propylbenzene	n-Propylbenzene	3-Ethyltoluene	4-Ethyltoluene	2-Ethyltoluene	1,3,5-Trimethylbenzene	1,2,3-Trimethylbenzene	1,2,4-Trimethylbenzene
home maintenance: paint	-	0	44	44	0.5	0	0	0	0	0	0	0	0	0	11
paint	Various types of paint	10	17	15	4.2	4.2	5.5	6.7	9.1	0	1.8	0	12	1.8	12
manufacturing:metal	Manufacturing of metals	21	18	8	1.5	1.5	2.2	8.1	8.1	0	0	0	11	2.2	8.8
manufacturing:mach.	Manufacturing of machinery related to production of different products	23	18	16	1.9	1.9	6.5	7.5	5.6	0	0	0	9.4	0	10
arts and crafts: arts and crafts paint	-	0	26	51	0.9	0	0	0	0	0	0	0	0	0	22
surface treatment	Surface treatments for metals, corrosion inhibitors, etc.	16	20	16	4	0	5.1	5.1	7.1	0	0	0	12	3	11
adhesive	Adhesive/ binding agents	19	25	17	1.3	2.7	5.3	9.3	2.7	0	0	0	8	1.3	8

CPCat Functional Use Category	Definition	Relative Contribution to Each Functional Use Category (%)													
		Benzene	Toluene	Ethylbenzene	m-Xylene	p-Xylene	o-Xylene	i-Propylbenzene	n-Propylbenzene	3-Ethyltoluene	4-Ethyltoluene	2-Ethyltoluene	1,3,5-Trimethylbenzene	1,2,3-Trimethylbenzene	1,2,4-Trimethylbenzene
solvent	Paint/graffiti removers, general solvents	13	16	13	2.8	2.8	5.6	9.9	9.9	0	0	0	13	2.8	13
paint:volatile_ organic	-	10	15	13	0	0	4.4	12	12	0	0	0	15	4.4	15
auto products: auto paint	-	2	48	42	0	0	0	0	0	0	0	0	0	0	7.8
manufacturing: plastics	Manufacturing plastic materials	17	25	19	0	1.6	3.1	11	6.3	0	0	0	7.8	0	9.4
building construction	Related to the building or construction process for buildings or boats	16	15	13	6.5	6.5	6.5	8.1	9.7	0	0	0	9.7	0	9.7
manufacturing: chemical	Manufacturing of chemicals	17	22	12	5.1	5.1	5.1	5.1	3.4	0	1.7	0	8.5	3.4	12

CPCat Functional Use Category	Definition	Relative Contribution to Each Functional Use Category (%)													
		Benzene	Toluene	Ethylbenzene	m-Xylene	p-Xylene	o-Xylene	i-Propylbenzene	n-Propylbenzene	3-Ethyltoluene	4-Ethyltoluene	2-Ethyltoluene	1,3,5-Trimethylbenzene	1,2,3-Trimethylbenzene	1,2,4-Trimethylbenzene
cleaning_ washing	Related to all forms of cleaning/washing including detergents, soaps, de-greasers, spot removers	20	18	14	1.8	3.6	3.6	8.9	7.1	0	0	0	11	0	13
fuel	General fuels, fuel additives, motor/automotive fuels	16	18	13	1.8	1.8	5.4	8.9	5.4	0	0	0	11	3.6	16

Physical and chemical properties of the aromatic compounds are presented in Table 1.15. Benzene has the lowest molecular weight and thee benzene derivatives and isomers have similar molecular weights. The boiling points and vapor pressures increase and decrease, respectively as the number of substituted carbon/hydrogen functional groups increase (Table 1.15). For example, benzene has the lowest boiling point and the highest vapor pressure, whereas the trimethylbenzene groups (with 3 additional functional groups) have higher boiling points and lower vapor pressures. The hydrophobicity, as indicated by the water solubility and octanol-water partition coefficients, increase from benzene to derivatives with increasing carbon/hydrogen atom contents. Thus, the trimethyl benzenes and ethyltoluene derivatives are more likely than benzene and toluene to partition into organic phases in the landfill environment.

Table 1.15 – Physical and Chemical Properties of the Aromatic Hydrocarbons

Chemical Species	Mol. Weight (g/mol)	Boiling Point (°C)	Log_{10} (Vapor Pressure)	Log_{10} (Octanol-Air)	Log_{10} (Dim. Henry's Constant)	Water Solubility (mg/L)	Log_{10} (Octanol-Water)
Benzene	78.1	80	1.98	2.78	-1.96	1789	2.13
Toluene	92.1	111	1.45	3.31	-1.88	526	2.73
Ethylbenzene	106.2	136	0.98	3.74	-1.81	169	3.15
m-Xylene	106.2	139	0.92	3.78	-1.85	161	3.20
p-Xylene	106.2	138	0.95	3.79	-1.87	162	3.15
o-Xylene	106.2	144	0.82	3.91	-1.99	178	3.12
i-Propylbenzene	120.2	152	0.65	3.98	-1.65	61	3.66
n-Propylbenzene	120.2	159	0.53	4.09	-1.68	52	3.71
3-Ethyltoluene	120.2	160	0.48	4.56	-1.79	81	3.98
4-Ethyltoluene	120.2	162	0.48	4.56	-1.78	95	3.63
2-Ethyltoluene	120.2	165	0.42	4.56	-1.81	75	3.53
1,3,5-Trimethylbenzene	120.2	164	0.39	4.54	-1.76	48	3.42
1,2,3-Trimethylbenzene	120.2	176	0.23	4.54	-2.07	75	3.66
1,2,4-Trimethylbenzene	120.2	169	0.32	4.54	-1.92	57	3.63

1.5.10 Monoterpenes

The monoterpenes included in this investigation consist of the individual chemical species: alpha-pinene, beta-pinene, and limonene. The monoterpenes contribute to both ozone and secondary aerosol formation. These chemicals have very short atmospheric lifetimes (on the order of minutes) compared to the other NMVOC chemical families included in this study (Kesselmeier and Staudt 1999). Alpha- and beta-pinene have the highest SOA formation potentials of all of the chemicals included in this investigation (Table 1.1). The monoterpenes are not considered hazardous air pollutants. GWP values have not been assigned to these chemicals, even though the species indirectly contribute to ozone, carbon monoxide, and methane formation in the atmosphere (Perring et al. 2013).

Both isoprene (included under alkenes) and monoterpenes are isoprenoids (terpenoids) with carbon skeletons composed of 5 carbon atoms (termed a unit) that can be arranged in an acyclic, mono-, bi-, or tri- cyclic molecular structure (Kesselmeier and Staudt 1999). The number of carbon units allows terpenes to be classified as either monoterpenes (one unit), di (two units), tri (three units), tetra (four units), or even poly terpenes (> four units), in which the monoterpenes are generally the most volatile out of the existing terpene chemicals. Terpenes generally have strong smells, are not highly water soluble, and ubiquitous in plants, animals, and microorganisms (Kesselmeier and Staudt 1999). Monoterpenes are generated biogenically by plant matter including trees and vegetation. A summary of specific vegetative release characteristics for monoterpenes is provided in Kesselmeier and Staudt (1999).

Monoterpenes also are present in a variety of household consumer products and thus can be released abiotically in the landfill environment. Potential monoterpene sources are household cleaning solvents, personal care products (body wash/air fresheners), and household spray products (Nair et al. 2019). Limonene can be emitted during decomposition of MSW, specifically associated with food wastes (Duan et al. 2014) and may appear as an intermediate byproduct during aerobic oxidation of various compounds (Eitzer 1995, Duan et al. 2014). High concentrations of limonene were reported for LFG in Chinese landfills and attributed to fragrant household detergent and air freshener sources over volatilization from green wastes or emissions from aerobic or anaerobic waste degradation (Duan et al. 2014).

Analysis of the top fifteen functional use categories based on the CPCat database indicate that many of the potential abiotic sources of monoterpenes in the landfill environment are associated with personal hair products (shampoos and conditioners), fragrances, hair styling, air fresheners, deodorants, moisturizers, lotions, hair sprays and color products (Table 1.16). Of the monoterpenes included in this investigation, limonene is present in the highest number of products across all of the functional use categories, with nearly 100% contributions to the functional use categories related to hair styling, shampoos, conditioners, lotions, and moisturizers. Both alpha- and beta-pinene have less presence in the top fifteen functional use categories with presence in cleaning/washing, industrial cleaning/washing, paints, and air fresheners (Table 1.16).

Table 1.16 – Fifteen Most Common Functional Use Categories for Monoterpenes

CPCat Functional Use Category	Definition	Relative Contribution to Each Functional Use Category (%)		
		alpha-Pinene	beta-Pinene	Limonene
personal care: fragrance	-	0	2.22	97.8
personal care: hair styling	-	0	0	100
personal care: shampoo	-	0	0	100

CPCat Functional Use Category	Definition	Relative Contribution to Each Functional Use Category (%)		
		alpha-Pinene	beta-Pinene	Limonene
personal care: hair conditioner	-	0	0	100
inside the home: air freshener	-	0	26	74
personal care: deodorant	-	0	0	100
personal care: face cream/moisturizer	-	0	0	100
personal care: hand/body lotion	-	0	0	100
personal care: hair color	-	0	0	100
cleaning_washing	Related to all consumer forms of cleaning/washing including detergents, soaps, de-greasers, spot removers	25.8	25.8	48.4
personal care: hair spray	-	0	0	100
personal care: hair conditioning treatment	-	0	0	100
industrial:cleaning_washing	Related to all industrial forms of cleaning/washing including detergents, soaps, de-greasers, spot removers	34.8	30.4	34.8
paint	Various types of paint	27.3	13.6	59.1
personal care: body wash	-	0	0	100

Physical and chemical properties of the monoterpenes are presented in Table 1.17. The monoterpenes generally have high volatility (high vapor pressures) and low water solubilities. Alpha-pinene has the highest volatility and the lowest water solubility. All three chemicals in this chemical family are likely to partition into the organic phase in the landfill environment.

Table 1.17 – Physical and Chemical Properties of the Monoterpenes

Chemical Species	Mol. Weight (g/mol)	Boiling Point (°C)	Log_{10} (Vapor Pressure)	Log_{10} (Octanol-Air)	Log_{10} (Dim. Henry's Constant)	Water Solubility (mg/L)	Log_{10} (Octanol-Water)
alpha-Pinene	136.2	155	0.68	4.44	-0.58	2	4.83
beta-Pinene	136.2	165	0.47	4.48	-0.72	8	4.16
Limonene	136.2	175	0.19	4.31	-1.21	11	4.57

1.5.11 Alcohols

The alcohols included in this investigation consist of the individual chemical species: methanol, ethanol, isopropanol, and 2-butanol. The alcohols are relatively reactive compounds in the troposphere, based on the MIR values presented in Table 1.1.

However, these chemical species do not contribute to SOA formation and FAC values have not been reported in the literature. Within this chemical family, only methanol has an assigned GWP. The remaining alcohols are expected to have adverse climate change impacts due to their effects in various atmospheric reactions. However, GWP values have not been reported for these chemicals at the present time. Methanol is considered a hazardous air pollutant by the USEPA.

Alcohols are hydrocarbons (composed of carbon and hydrogen atoms) attached to one or more hydroxyl (OH) groups, where the number of carbon atoms and placement of the hydroxyl group varies with the chemical species (Vollhardt and Schore 1999). Alcohols can be generated both abiotically and biotically in the landfill environment from various sources. Alcohols, similar to monoterpenes, are emitted naturally by vegetation, where emissions likely vary from live plants on the cover soil to green wastes used as covers or disposed of within the waste mass (Kesselmeier and Staudt 1999). Similar to the aldehydes, alcohols are also formed indirectly from carboxylic acids that are produced during acidogenesis (the acid phase) in the anaerobic portions of the waste mass (Barlaz et al. 2010). Some alcohols (including ethanol) are direct products of anaerobic fermentation that occurs during the acid phase of anaerobic waste decomposition (Barlaz et al. 2010). Bacteria also form alcohols via the oxidation of aliphatic (alkane) hydrocarbons by directing their attack between the methylene carbon alpha to the methyl group (McKenna et al. 1965, Forney and Markovetz 1971, Klug and Markov 1971). With these biogenic generation pathways, which occur during preliminary stages of anaerobic waste decomposition, alcohols are associated with fresh as opposed to old waste materials (Allen et al. 1997).

Potential abiotic sources of alcohols in the landfill environment include household cleaning solvents, personal care products, and household spray products (Nair et al. 2019). Analysis of the top fifteen functional use categories based on the CPCat database indicate that many alcohols are present in personal care products such as fragrances, nail polish, hair spray, hair color, shampoo/conditioner, hair styling products, sunscreen, moisturizers, and air fresheners (Table 1.18). Alcohols also are present in laundry detergents, paints, pesticides, and cleaning/washing solvents (Table 1.18). Of the alcohols included in this investigation, ethanol and isopropanol are present in the highest number of products across the functional use categories. Fragrances, hair sprays, hair styling products, hair conditioners, moisturizers, sunscreen, laundry detergents, and air fresheners contain ethanol. Isopropanol is present in nail polish, hair coloring, surface treatments, paints, cleaning/washing materials, and hair conditioners (Table 1.18). The remaining species, methanol and 2-butanol, are least represented under the top 15 functional use categories, where methanol is present in products related to metal manufacturing, surface treatments and paint, whereas 2-butanol is present in paints and cleaning/washing solvent materials.

Table 1.18 – Fifteen Most Common Functional Use Categories for Alcohols

CPCat Functional Use Category	Definition	Relative Contribution to Each Functional Use Category (%)			
		Methanol	Ethanol	Isopropanol	2-Butanol
personal care: fragrance	-	0	99.5	0.48	0
personal care: nail polish	-	0	16.5	83.5	0
personal care: hair spray	-	0	99	0.98	0
personal care: hair color	-	0	6.88	93.1	0
personal care: hair styling	-	0	92.3	7.74	0
inside the home: laundry detergent	-	0	99	1.01	0
manufacturing:metals	Manufacturing of metals	30.1	30.1	33.3	6.45
surface_treatment	Surface treatments for metals, corrosion inhibitors, etc.	29.9	24.1	39.1	6.9
paint	Various types of paint	26.5	27.7	28.9	16.9
personal care: sunscreen	-	0	100	0	0
personal care: face cream/moisturizer	-	0	96.1	3.95	0
pesticide	Substances used for preventing, destroying or mitigating pests	11.1	45.8	41.7	1.39
inside the home: air freshener	-	0	77.5	22.5	0
cleaning_washing	Related to all consumer forms of cleaning/washing including detergents, soaps, de-greasers, spot removers	24.3	30	34.3	11.4
personal care: hair conditioner	-	0	40.3	59.7	0

Physical and chemical properties of the alcohols are presented in Table 1.19. As molecular weights increase from methanol to 2-butanol with increasing number of carbon atoms, the boiling point increases and corresponding vapor pressure decreases. Methanol and 2-butanol are the most and least, respectively volatile alcohols included in this study. Water solubility is relatively similar among the four alcohol species. The likelihood to partition into organic phases in the landfill environment is higher for 2-butanol, which is the most hydrophobic alcohol species based on the high octanol-air and octanol-water partition coefficients.

Table 1.19 – Summary of Relevant Physical and Chemical Properties for the Alcohols

Chemical Species	Mol. Weight (g/mol)	Boiling Point (°C)	Log_{10} (Vapor Pressure)	Log_{10} (Octanol-Air)	Log_{10} (Dim. Henry's Constant)	Water Solubility (mg/L)	Log_{10} (Octanol-Water)
Methanol	32.0	64.5	2.10	2.88	-5.05	999648	-0.77
Ethanol	46.1	78.4	1.77	3.25	-5.01	999719	-0.31
Isopropanol	60.1	82.5	1.66	3.41	-4.80	997660	0.05
2-Butanol	74.1	99.2	1.26	3.85	-4.75	180853	0.61

1.5.12 Ketones

The ketones included in this investigation consist of the individual chemical species: acetone, butanone, and methylisobutylketone. Similar to the aldehydes, the ketones are relatively reactive oxygenated chemical species that readily produce ozone in the troposphere. Among ketones, methylisobutylketone has the highest contribution to ozone production in the troposphere. Ketones are not identified to contribute to SOA formation. However, previous studies indicate potential implications in SOA formation (Perring et al. 2013). Ketones are expected to have adverse climate change impacts due to their effects in various atmospheric reactions. However, GWP values have not been reported for these chemicals at the present time. Methylisobutylketone is considered a hazardous air pollutant by the USEPA (Table 1.1).

Ketones are formed from a centralized carbonyl group (carbon atom double bonded to an oxygen atom) that is singly bonded to a variable hydrocarbon chain or functional group on both sides of the carbonyl group (Vollhardt and Schore 1999). Ketones range from straight chained to branched in configuration (acyclic) with high variation in the functional groups or number of carbons contained in each hydrocarbon chain. Similar to the aldehyde and alcohol chemical families, ketones are generated abiotically and biotically in the landfill environment. Biogenic sources of ketones include emissions from vegetation (similar to monoterpenes aldehydes/alkynes and alcohols) including plants growing on the cover surface or from decaying green waste materials used as covers or disposed of in a landfill. Additional biogenic sources of ketones in the landfill environment include generation from carboxylic and other volatile fatty acids during the acidogenesis phase of anaerobic waste decomposition (Barlaz et al. 2010). Ketones are also potentially produced by fungi through decarboxylation of beta-keto fatty acids and in similarity to alcohols and aldehydes, bacteria also form ketones through oxidation of aliphatic (alkane) hydrocarbons at the methylene carbon alpha to the methyl group (Leadbetter and Foster 1959, Forney and Markovetz 1971). For example, acetone is produced by butyric acid bacteria as a product of butyl alcohol fermentation and further decarboxylation of acetoacetate (Forney and Markovetz 1971). Even though these particular biogenic pathways have not been documented in the landfill environment, these processes are likely for the synthesis of ketones under aerobic and anaerobic conditions present in MSW landfills.

Abiotic production of ketones in the landfill environment is based on volatilization of chemical materials present in the MSW. Potential chemical sources of ketones in the landfill environment are household spray products (Nair et al. 2019). Analysis of the top

fifteen functional use categories based on the CPCat database indicates that ketones are present in paints, adhesives, cleaning/washing materials, and solvents. In addition, ketones are present in products associated with manufacturing of chemicals, plastics, and machinery as well as building/construction functional use categories (Table 1.20). Acetone is the chemical species that is present in the highest number of products within the top 15 functional use categories, followed by butanone and methylisobutylketone. Acetone is common in paints (auto and home), surface treatment products, and nail polish removers. Butanone is present in paints, products used in manufacturing of metal and plastic materials, and cleaning/washing solvents. Methylisobutylketone is present in solvents, paints, products used in manufacturing applications, and building/construction materials (Table 1.20).

Table 1.20 – Fifteen Most Common Functional Use Categories for Ketones

CPCat Functional Use Category	Definition	Relative Contribution to Each Functional Use Category (%)		
		Acetone	Butanone	Methylisobutylketone
home maintenance: paint	-	70.5	13.5	16
auto products: auto paint	-	67.2	23	9.84
paint	Various types of paint	32.8	36.2	31
arts and crafts: arts and crafts paint	-	49.1	23.6	27.3
manufacturing:metals	Manufacturing of metals	32.7	36.5	30.8
adhesive	Adhesive/binding agents	37.5	37.5	25
manufacturing:machines	Manufacturing of machinery related to production of different products	34	36.2	29.8
surface_treatment	Surface treatments for metals, corrosion inhibitors, etc.	50	27.8	22.2
manufacturing:plastics	Manufacturing of plastic materials	33.3	45.5	21.2
cleaning_washing	Related to all consumer forms of cleaning/washing including detergents, soaps, de-greasers, spot removers	36.7	40	23.3
solvent	Paint/graffiti removers, general solvents	33.3	33.3	33.3
manufacturing:chemical	Manufacturing of chemicals	34.5	34.5	31
personal care: nail polish remover	-	100	0	0
paint:volatile_organic	-	35.7	32.1	32.1

CPCat Functional Use Category	Definition	Relative Contribution to Each Functional Use Category (%)		
		Acetone	Butanone	Methylisobutylketone
building_construction	Related to the building or construction process for buildings or boats	36	36	28

Physical and chemical properties of the ketones are presented in Table 1.21. Methylisobutylketone and acetone have the highest and lowest molecular weights, respectively, associated with the lowest and highest volatilities, respectively (based on boiling points and vapor pressures summarized in Table 1.21). Acetone is the ketone with the highest water solubility, whereas methylisobutylketone is the most hydrophobic chemical species. Similarly, methylisobutylketone is most likely to partition into the organic phase in the landfill environment based on the high octanol-air and octanol-water partition coefficients.

Table 1.21 – Physical and Chemical Properties of the Ketones

Chemical Species	Mol. Weight (g/mol)	Boiling Point (°C)	Log_{10} (Vapor Pressure)	Log_{10} (Octanol-Air)	Log_{10} (Dim. Henry's Constant)	Water Solubility (mg/L)	Log_{10} (Octanol-Water)
Acetone	58.1	56	2.37	2.31	-4.16	998976	-0.24
Butanone	70.1	79.7	1.96	2.71	-3.95	216578	0.29
Methylisobutyl-ketone	100.2	117	1.30	3.58	-0.43	19030	1.31

1.6 Landfill Gas Composition

Landfill gas is collected directly from the waste mass and directly represents the gas generated and/or transformed in the waste mass. The source gas composition can provide insight into attenuation processes occurring within the cover systems. A comprehensive review of LFG concentrations of methane, carbon dioxide, nitrous oxide, carbon monoxide, and the trace NMVOCs included in this investigation is provided based on a total of 34, 26, 2, 1, and 33 previously reported studies, respectively. Overall, data from a total of 1109, 497, 59, 8 and 9350 individual summa canister measurements were reviewed herein for methane, carbon dioxide, nitrous oxide, carbon monoxide, and NMVOCs, respectively. The complete summary for the reviewed studies is presented in Table A1 in Appendix A. The studies included were from a wide range of countries, climate zones, and landfill environments. Grab sampling via Summa canister

was used in a majority of the studies. Samples were analyzed by GC-MS typically with low analytical detection limits reported. Samples were taken either from gas headers, wells, or from custom built gas sampling ports that extended beneath the covers to some depth within the wastes. The geographic locations of the LFG composition studies were across multiple continents and included landfill sites in U.S., France, Finland, UK, Japan, Germany, Turkey, South Korea, Spain, Italy, China, and Australia. Four sites were reviewed in California, including Marina landfill, Scholl Canyon landfill, Potrero Hills landfill, and Yolo County landfill (Bogner et al. 2011, Saquing et al. 2014, Sohn 2016, Yesiller et al. 2018).

A summary of the LFG concentrations from literature for the gases included in the investigation is presented in Figure 1.2, organized by chemical family. Overall means and standard deviations for these distributions in LFG concentrations were calculated using the group contribution statistical method (Burton 2016). Methane, carbon dioxide, nitrous oxide, and carbon monoxide are plotted separately for comparison purposes. The diamonds indicate the mean of each distribution, the boxes indicate the 95% confidence intervals surrounding the mean values (assuming normal distributions). The whiskers indicate the maximum and minimum reported values of LFG concentration for each chemical family.

Figure 1.2 LFG Concentrations of Gas Chemical Families Obtained from the Literature

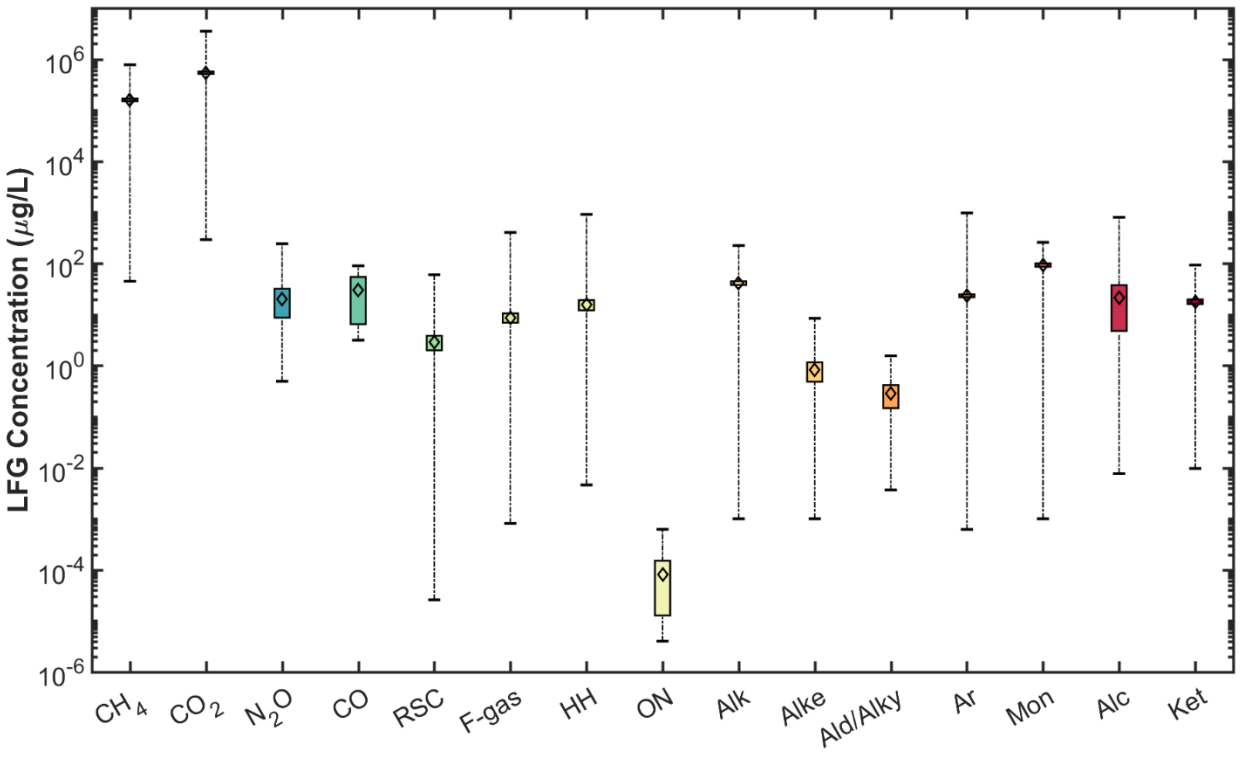

Methane and carbon dioxide were the dominant constituents of LFG across the studies summarized, where the mean values were slightly higher for carbon dioxide

concentrations (on the order of $1x10^6$ μg/L). Concentrations of methane and carbon dioxide in LFG ranged from $1x10^2$ to $1x10^6$ μg/L, or 4 orders of magnitude difference across the landfill sites investigated (Figure 1.2). Mean concentrations of nitrous oxide and carbon monoxide were somewhat higher than all NMVOC chemical families, where the variation was generally higher for carbon monoxide (based on the wide extent of the 95% confidence intervals). For NMVOCs, the monoterpene concentrations were the greatest out of all chemical families included in the analysis (Figure 1.2). Within this family, limonene had the greatest mean LFG concentration of approximately $1.60x10^2$ μg/L. The organic alkyl nitrates demonstrated the smallest mean LFG concentration of approximately $8.2x10^{-5}$ μg/L, while still being detected by GC-MS (Figure 1.2). The alkanes and the aromatics were the chemical families that ranked second and third behind the monoterpenes, with mean LFG concentrations of $4.14x10^1$ and $2.34x10^1$ μg/L, respectively. Within the alkane and aromatic chemical families, ethane and toluene were the individual chemical species that had the highest mean LFG concentrations. The variations in LFG concentrations, as indicated by the width of the boxplots, were generally higher for the alcohol chemical family. Most of the NMVOCs were distributed within a relatively broad range of LFG concentrations (8 orders of magnitude, ranging between $4x10^{-6}$ to $9.71x10^2$ μg/L). In comparison, the baseline GHG LFG concentrations were distributed over 7 orders of magnitude, ranging between $4.92x10^{-1}$ to $3.52x10^6$ μg/L. For a given chemical family, the highest variation in concentrations was 5 orders of magnitude (alcohol family) and the lowest variation was 1 order of magnitude (organic alkyl nitrate family).

1.7 Landfill Gas Surface Flux

An in-depth literature review was conducted on surface flux of the gas species included in this investigation. Data and analysis from studies conducted with the static flux chamber method were included in line with the methodology used in the current investigation. MSW landfill sites included in the review varied from open dumping sites (Malaysia, India) to properly engineered sanitary landfills (U.S., China, Europe). A comprehensive review of surface fluxes of methane, carbon dioxide, nitrous oxide, carbon monoxide, and the trace NMVOCs included in this investigation is provided based on a total of 91, 37, 18, 1, and 14 previously reported studies, respectively. Overall data from a total of 16193, 15613, 2444, 1, 5667 experimental measurements of landfill surface flux were reviewed herein for methane, carbon dioxide, nitrous oxide, carbon monoxide, and NMVOCs, respectively. The complete summary for the reviewed studies is presented in Table A2 in Appendix A. Data provided in Table A2 includes (when available) the location, climate zone, season, waste age, cover material soil index properties, presence of a gas extraction system, cover thickness, cover moisture content and temperature, estimated waste in place, cover category (daily, intermediate, final), air temperature, barometric pressure, and an overview of the waste composition with special emphasis placed on the fraction of organic wastes reported. Table A3 summarizes the overall distributions of methane, carbon dioxide, nitrous oxide, and NMVOC landfill gas surface fluxes from the studies reviewed.

High flux measurements were reported for landfills in Spain, U.S., Italy, China, and Germany. Analysis of the climate zone data indicated that the Csa (29%), Bwk (20.5%),

Cfa (10.5%), Cfb (9.8%), and Dfb (9.1%) zones (based on Koppen-Geiger climate system, Peel at al. (2007)) were dominant in the studies reviewed from the literature. The Csa climate zone was also investigated in the current study. Approximately half of the landfills studied (48%) did not have active gas extraction systems. Presence or absence of extraction systems were not identified in several studies. The types of cover systems tested (daily, intermediate, or final) were not identified in nearly half of the studies (47%) available in the literature. When identified, data were most commonly reported for final cover systems followed by intermediate covers with very limited data provided for daily covers. A large majority of these studies (>99%) were conducted using relatively small static flux chambers with smaller than 1 m^2 in areal coverage.

A summary of the LFG surface fluxes from literature for the gases included in the investigation is presented in Figures 1.3 and 1.4, organized by chemical family and cover category, respectively. Similar to Figure 1.2, overall means and standard deviations for these distributions in LFG concentrations were calculated using the group contribution statistical method (Burton 2016). Methane, carbon dioxide, nitrous oxide, and carbon monoxide are plotted separately for comparison purposes. The diamonds indicate the mean of each distribution, the boxes indicate the 95% confidence intervals surrounding the mean values (assuming normal distributions). The whiskers indicate the maximum and minimum reported values of LFG surface flux for each chemical family.

Figure 1.3 LFG Surface Fluxes of Gas Chemical Families Obtained from the Literature

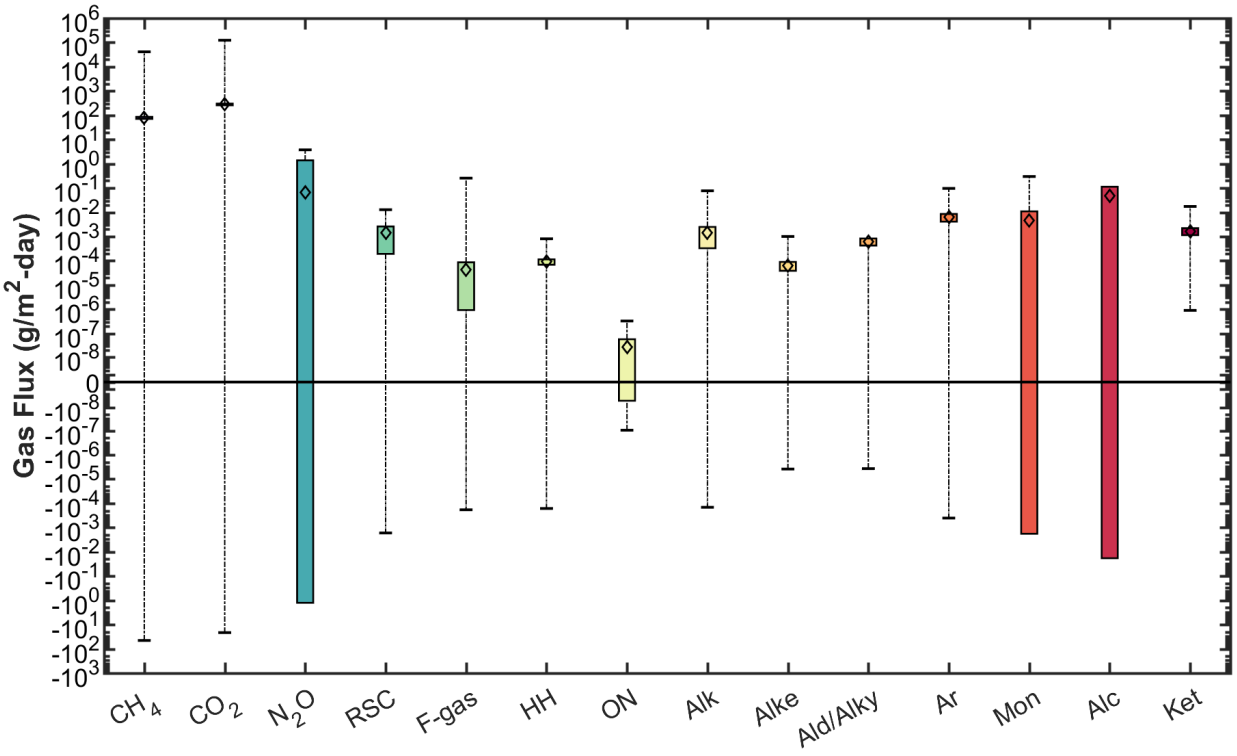

Carbon dioxide fluxes were the greatest among the gases investigated and also had the largest reported range -2.14x10^1 to 1.24x10^5 g/m^2-day (Table A3). Methane fluxes

ranged from -4.50x10^{1} to 4.15x10^{4}. Nitrous oxide emissions were generally greater than the NMVOCs (based on the mean values presented) with high variability (based on the width of the boxplots) and reported net negative emissions, ranging from -2.54x10^{-3} to 3.76x10^{0} g/m^{2}-day. The range in NMVOC emissions obtained from the literature was -1.66x10^{-3} to 3.00x10^{-1} g/m^{2}-day (Table A3). Of the NMVOCs evaluated in this review, the alcohol chemical family was associated with the greatest flux values followed by the aromatics, monoterpenes, and ketones. Within these chemical families, ethanol, m-xylene, alpha-pinene, and acetone were the chemical species associated with the greatest flux measurements. The relative flux values for the NMVOCs were different than the relative concentrations of the same NMVOCs in source landfill gas, which indicated that the monoterpenes (specifically limonene) were the most dominant constituents in raw LFG. As indicated in previous studies, concentrations in LFG do not provide direct indication for flux for a given species and are not recommended to be used as surrogates (Yesiller et al. 2018, Saquing et al. 2014). For a given chemical family, the highest variation in reported flux was observed for the alcohol chemical family, ranging from -1.90x10^{-5} to 5.20x10^{-1} g/m^{2}-day and the lowest variation was observed for the organic alkyl nitrate chemical family, ranging from -9.54x10^{-8} to 3.29x10^{-7} g/m^{2}-day.

Figure 1.4 LFG Surface Fluxes as a Function of Cover Category as Observed from the Literature

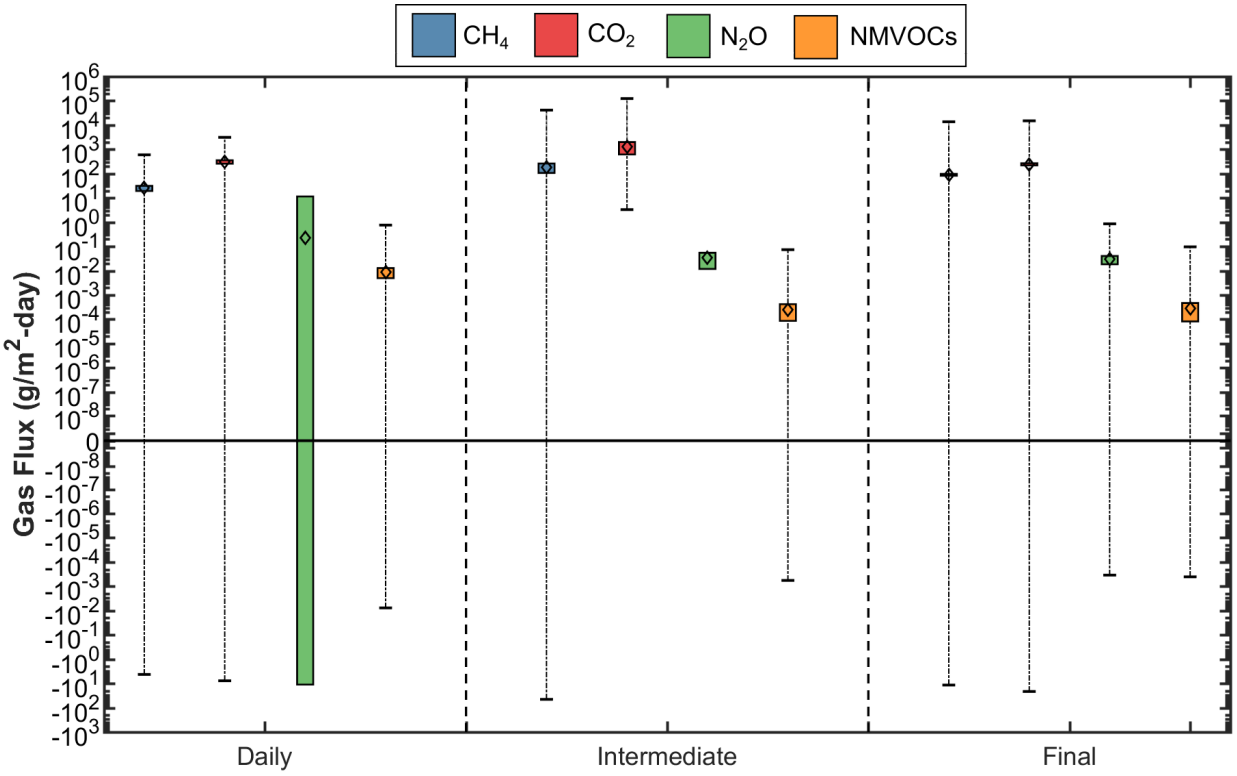

As a function of overall cover category, both methane and carbon dioxide fluxes were observed to increase progressing from daily to intermediate categories. Contrary to what was expected initially, the reported range in methane and carbon dioxide fluxes

were relatively similar between daily and final cover categories. Nitrous oxide fluxes were highly variable for daily cover categories, where the variation tended to decrease progressing to intermediate cover categories (Figure 1.4). The mean and variation in NMVOC fluxes obtained from the literature were relatively similar for the NMVOCs, but tended to decrease slightly progressing from daily, to intermediate, to final cover categories. The overall similarities observed in the central tendencies of the flux distributions obtained from the literature are most likely associated with the wide range and variety of cover types investigated within a given category in addition to the wide international coverage of site specific landfill operational practices and climatic conditions.

1.8 California Specific Inventory of Methane and NMVOC Fluxes and Emissions

California specific methane emissions were obtained from the scientific literature to provide a direct basis for comparison of methane emissions measured in this study. Results from studies conducted using direct (i.e., static flux chambers) and indirect (vertical radial plume mapping, VRPM, and aerial surveys) were summarized in Table 1.22. Data were presented for closed and currently active landfill sites. The WIP at the sites ranged from 6,225,912 to 124,963,317 tons. The reported methane fluxes ranged from -7.77×10^{-4} to 86.3 g/m^2-day, whereas emissions ranged from 355 to 37,600 Mg/year across approximately 50 different landfill sites (Pieschl et al. 2013, Krautwurst et al. 2017, Duren et al. 2019, Thompson et al. 2019, Cusworth et al. 2020). Of all the sites included in the literature review, Puente Hills and Monterey Peninsula Landfills had the highest reported annual net methane emissions and flux, respectively (Table 1.22). Puente Hills had the largest total WIP. The high flux reported from the Monterey Peninsula Landfill was attributed to an interim cover area with sub optimal conditions for methane oxidation (Bogner et al. 2011). Emissions from the active face of Potrero Hills landfill were estimated using remote sensing (Cusworth et al. 2020), where emissions ranged from 1,130 to 1,533 Mg/year which was significantly lower than whole-site emissions reported from larger landfill sites (Table 1.22).

Table 1.22 – Methane Fluxes and Emissions from California Landfills

Reference	Landfill	WIP (tons) (2010 data)	Measurement Methodology	CH_4 Flux (g/m^2-day)	Annual Emissions (Mg/yr)
Spokas et al. (2011), Goldsmith Jr. et al. (2012)	Tri-Cities Recycling and Disposal Facility	10,103,797	Flux Chamber, VRPM	5.6 to 7.1	N/A
Goldsmith Jr. et al. (2012), Green et al. (2009)	Altamont Landfill and Resource Recovery Facility	44,281,078	Flux Chamber, VRPM, CRDS	0.079 to 14.3	N/A
Goldsmith Jr. et al. (2012), Green et al. (2009)	Redwood Landfill	14,143,215	Flux Chamber, VRPM, CRDS	0.018 to 17	N/A
Bogner et al. (2011)	Scholl Canyon Landfill	29,409,357	Flux Chamber	-7.77×10^{-4} to 1.17×10^{-2}	N/A

Reference	Landfill	WIP (tons) (2010 data)	Measurement Methodology	CH_4 Flux (g/m^2-day)	Annual Emissions (Mg/yr)
Spokas et al. (2011)	Lancaster Landfill and Recycling Center	6,225,912	Flux Chamber	0.08 to 2.43	N/A
Pieschl et al. (2013), Shan et al. (2013), Goldsmith Jr. et al. (2012)	Puente Hills Landfill	124,963,317	Aircraft[2], VRPM, Flux Chamber	0.88 to 38.4	36,000 to 37,600
Shan et al. (2013)	Calabasas Landfill	23,441,895	Flux Chamber	0.05	N/A
Bogner et al. (2011)	Monterey Peninsula Landfill	8.388,784	Flux Chamber	0.003 to 86.3[3]	N/A
Pieschl et al. (2013), Shan et al. (2013), Krautwurst et al. (2017)	Olinda Alpha Landfill	52,017,040	Aircraft, VRPM, Flux Chamber	4.3 to 20	9,500 to 24,300
Spokas et al. (2011), Goldsmith Jr. et al. (2012)	Kirby Canyon Recycling and Disposal Facility	7,312,751	Flux Chamber	0.07 to 20.9	N/A
Duren et al. (2019)	28 Different Landfill Facilities	Varies	Aircraft[1]	N/A	355 to 26,359
Thompson et al. (2019)	17 Different Landfill Facilities	Varies	Aircraft[2]	N/A	619 to 28,034
Cusworth et al. (2020)	Portrero Hills LF	11,798,655	Aircraft[1]	19 to 39.2[4]	1,130 to 1,533

N/A Not reported by the study
[1] Anayzed by airborne visible/infrared imaging spectrometer
[2] Analyzed by Picaro cavity ring down spectrometer
[3] A max/min was not given so a range in the mean estimates is provided across different cover categories
[4] Estimated for the active face portion of this landfill only

In addition to methane, California specific emissions estimates of nitrous oxide were obtained from the scientific literature. Nitrous oxide fluxes obtained using static flux chambers were reported in two studies with results summarized in Table 1.23. Data were obtained from daily, intermediate, and final cover systems. The landfills investigated included a large, now closed site (Olinda Alpha Landfill) with high WIP and medium and small landfills with significantly lower WIP (Monterey Peninsula and San Joaquin Landfills). Bogner et al. (2011) conducted flux measurements in both wet and dry seasons. Overall nitrous oxide fluxes ranged from 0.0 (non-detect) to 2.5×10^{-1} g/m^2-day. The range in flux values reported by Bogner et al. (2011) were average flux ranges across daily, intermediate, and final cover categories, whereas the flux values reported by Mandernack et al. (2000) were minimum and maximum ranges for a specific cover category. Annual nitrous oxide emission estimates were not reported for California landfills in the literature.

Table 1.23 – Nitrous Oxide Fluxes from California's Landfills

Reference	Landfill	WIP (tons) (2010 data)	Measurement Methodology	N_2O Flux (g/m^2-day)
Mandernack et al. (2000)	Olinda Alpha Landfill	52,017,040	Flux Chamber	0.0 to $7.9x10^{-3}$
	UCI Landfill	N/A	Flux Chamber	$4x10^{-4}$ to $4.5x10^{-3}$
	San Joaquin Landfill	N/A	Flux Chamber	$4x10^{-4}$ to $4.0x10^{-3}$
Bogner et al. (2011)	Scholl Canyon Landfill	29,409,357	Flux Chamber	$2.3x10^{-3}$ to $2.5x10^{-1}$
	Monterey Peninsula Landfill	8.388,784	Flux Chamber	$1.28x10^{-2}$ to $9.15x10^{-2}$

Yesiller et al. (2017) was the only study in the literature that reported a large number of NMVOC surface fluxes from a landfill in California (Table 1.24). In this study, NMVOC fluxes from Potrero Hills Landfill were measured for daily (soil, green waste, autofluff), intermediate (soil), and final (conventional compacted clay) cover categories over the wet and dry seasons. Static flux chambers were used to measure NMVOC fluxes of halogenated hydrocarbon, alkane, alkene, aldehyde/alkyne, monoterpene, aromatic, reduced sulfur compound, alcohol, ketone, and F-gas chemical families. A total of 53 chemical species within the 10 chemical families identified above were quantified in this investigation. The overall NMVOC fluxes from Potrero Hills landfill ranged from $-7.71x10^{-3}$ to $7.64x10^{-1}$ g/m^2-day across both wet and dry seasons as well as the variety of cover categories investigated. Annual emissions of NMVOCs were not reported by this study.

Table 1.24 – NMVOC Fluxes and Emissions from California's Landfills

Reference	Landfill	WIP (tons) (2010 data)	Measurement Methodology	NMVOC Flux (g/m^2-day)	Annual Emissions (Mg/yr)
Yesiller et al. (2017)	Potrero Hills Landfill	11,798,655	Flux Chamber	$-7.71x10^{-3}$ to $-7.64x10^{-1}$	N/A

1.9 Landfill Gas Transformation Pathways

Once landfill gas is generated in and transported throughout the landfill environment, the gas goes through several potential transformation pathways before being emitted to the atmosphere. In general, transformation pathways can be categorized as biological or physical/chemical in that biological pathways are mediated by microorganisms, whereas physical/chemical pathways are mediated by physical/chemical conditions in the landfill environment (Table 1.22). Transformation can occur within the waste mass as well as through the soil or alternative covers. The processes can take place in the solid, liquid, or gas phases in the wastes or cover materials. Biological transformation pathways can include both aerobic oxidation and anaerobic decomposition in the waste mass or cover materials. Physical/chemical transformation pathways primarily include,

but are not limited to, dissolution of gas into landfill leachate or moisture present in the waste mass/cover materials; phase partitioning of a given gas into organic phases present in the waste mass or organic matter present in the cover materials; and chemical sorption or physical attachment of the gases to solid matter in the waste mass or in the cover materials (Kjeldsen and Christensen 2001, Lowry et al. 2008).

Deipser and Stegmann (1997) studied the anaerobic transformation of select trace NMVOCs simulating conditions in the waste mass. Landfill lysimeters were set up with MSW sampled from the field (in different stages of waste decomposition) and combined with digester sludge and compost. In general, reductive dichlorination of the halogenated hydrocarbons was observed. For example, carbon tetrachloride was degraded to tri/di/chloromethane under the anaerobic conditions studied. Tetrachloroethylene was reduced to trichloroethylene (TCE), 1-1-dichloroethylene (1,1-DCE), cis and trans-1,2-dichloroethylene (1,2-DCE), and vinyl chloride. Methyl chloroform was reduced to chloroethane, whereas methylene chloride was reduced to methyl chloroform (Deipser and Stegmann 1997). HCFC-21 and HCFC-22 are were reported to be significant products of transformation of CFC-11 and CFC-12, respectively in the waste mass (Scheutz et al. 2007). HFCs were reported not to degrade within wastes based on laboratory tests (Scheutz et al. 2007).

For biological transformation pathways, studies were conducted on attenuation of different trace gas constituents in landfill cover soils (Table 1.22) (Kjeldsen et al. 1997, Scheutz and Kjeldsen 2003, Scheutz and Kjeldsen 2004, Scheutz and Kjeldsen 2005, Scheutz et al. 2007). These studies included assessment of landfill cover soils. The soils were sampled from several locations at a landfill and laboratory tests were conducted to assess the biological attenuation of the NMVOCs through these soils. Three modes of testing were used: batch testing, where target gases were added to a container, along with cover soils with bacteria present (in the presence/absence of

Table 1.25 – Summary of Landfill Gas Transformation Pathways

Classification	Transformation Pathway	Location	Chemical Species/Family	Transformed	Documented in Landfill	Reference	Notes
Biological	Aerobic Oxidation	Cover Soil, Waste Mass	Benzene	Yes	Yes	Kjeldsen et al. 1997, Scheutz and Kjeldsen 2003, Scheutz and Kjeldsen 2004, Scheutz and Kjeldsen 2005, Scheutz et al. 2007,	Oxidation byproducts not monitored or reported
			Toluene	Yes	Yes		
			Ethylbenzene	Yes	Yes		
			Xylene	Yes	Yes		
			Trichloroethylene	Yes	Yes		
			Tetrachloroethylene	No	No		
			Carbon tetrachloride	No	No		
			Chloroform	Yes	Yes		
			Methyl chloroform	Yes	Yes		
			Methylene chloride	No	No		
			CFC-11	No	No		
			CFC-12	No	No		
			CFC-113	No	No		
			HCFC-141b	No	No		
			HCFC-142b	-	-		
			HCFC-21	Yes	Yes		
			HCFC-22	Yes	Yes		
			HFC-134a	No	No		
			HFC-245fa	No	No		
			Alkanes	Yes	Yes	Tassi et al. 2009	Alkanes and aromatics oxidized=>ketones, aldehydes produced
			Alkenes	-	-		
			Aldehydes/Alkynes	No	No		
			Monoterpenes	-	-		
			Alcohols	-	-		
			Ketones	No	No		
	Anaerobic Decomposition	Cover soil, Waste mass	Benzene	Yes	Yes	Deipser and Stegmann 1997, Kjeldsen et al. 1997, Balsiger et al. 2002, Scheutz and Kjeldsen 2003, Scheutz	Oxidation byproducts monitored for F-gases only
			Toluene	Yes	Yes		
			Ethylbenzene	-	-		
			Xylene	-	-		
			Trichloroethylene	Yes	Yes		
			Tetrachloroethylene	-	-		
			Carbon tetrachloride	Yes	Yes		

Classification	Transformation Pathway	Location	Chemical Species/Family	Transformed	Documented in Landfill	Reference	Notes
			Chloroform	Yes	Yes	et al. 2004, Scheutz and Kjeldsen 2005, Scheutz et al. 2007, Grossi et al. 2008. Musat 2015	
			Methyl chloroform	-	-		
			Methylene chloride	No	No		
			CFC-11	Yes	Yes		
			CFC-12	Yes	Yes		
			CFC-113	Yes	Yes		
			HCFC-141b	No	No		
			HCFC-142b	No	No		
			HCFC-21	Yes	Yes		
			HCFC-22	Yes	Yes		
			HFC-134a	No	No		
			HFC-245fa	-	-		
			Alkanes	Yes	Yes		
			Alkenes	Yes	Yes		
			Aldehydes/Alkynes	-	-		
			Monoterpenes	-	-		
			Alcohols	-	-		
			Ketones	-	-		
			Benzene	-	-		
Physical-Chemical	Dissolution	Cover Soil	Alcohols, aldehydes, ketones	Yes	Yes	-	-
	Phase Partitioning		Aromatics, long chain alkanes, monoterpenes	Yes	Yes	-	-
	Chemical Sorption		Alcohols, aldehydes, ketones	Yes	Yes	-	-

oxygen), and the headspace monitored over time; soil column testing, where landfill soils were packed in a column and artificial landfill gas was passed through the system and the concentrations at inlet/outlet monitored over time; and a more complex counter gradient system where both oxygen and artificial LFG were injected at opposing sides of the column and the inlet/outlet monitored over time. Similar transformations reported for the waste mass for the CFCs were observed in the cover soil experiments. Many CFCs and highly chlorinated organics (i.e., carbon tetrachloride, tetrachloroethylene) were not aerobically oxidized, whereas some of the HCFCs (21/22) and most of the aromatics (benzene/ toluene/ethylbenzene/xylene) were rapidly oxidized. Some of the more chlorinated organics, such as trichloroethylene and methyl chloroform, were only co-oxidized in the presence of methane by the methanotrophic populations present in the cover soils (and not oxidized alone in batch experiments) (Kjeldsen et al. 1997). In the absence of oxygen, the CFCs and HCFCs (21 and 22) were readily biodegraded in the simulated cover soil environments (Scheutz and Kjeldsen 2003, Scheutz and Kjeldsen 2005, Schuetz et al. 2007). Carbon tetrachloride, which was not biodegraded during the oxygenated experiments, was observed to be degraded in the anaerobic experiments (Table 1.22). HCFC 141b, HCFC-142b, HFC-134a, and HFC-245fa were recalcitrant to biodegradation in all experiments performed, whether aerobic or anaerobic in nature. Balsiger et al. (2002) and Scheutz et al. (2007) identified the degradation byproducts of CFC-11, CFC-12, and CFC-113 under anaerobic conditions. CFC-11 was transformed to HCFC-21 and the further transformed to HCFC-31. CFC-12 was degraded to HCFC-22 and then further degraded to HFC-32 or HFC-41. Finally, CFC-113 was degraded to HCFC-123a, then further degraded to HCFC-133b or HCFC-133.

A single study was identified in the literature (Tassi et al. 009) on oxidation of NMVOCs in a soil cover directly in the field. In this study, soil gas probes were installed and monitored in a final cover system of a closed landfill over an extended time period. Tassi et al. (2009) reported that the C_2-C_{15} alkanes (ethane, propane, butane, undecane) and aromatics were oxidized by resident methanotrophs in the cover soils, where the alkanes were reduced from 11.6% total composition at the deepest measurement location in the cover to 0.45% in the shallowest depth monitored. The ketones, esters, aldehydes, and organic acids were observed to be the most stable and common byproducts of oxidation reactions involving the aromatics or alkanes out of all chemical families in the cover system studied (enriched close to the air-soil surface). Relatively little biotransformation of the halogenated hydrocarbons was observed. Results of this study demonstrated that biological transformations of NMVOCs within the cover soil can be significant factors affecting emissions.

Dissolution, phase partitioning, and sorption, among many competing factors are the main potential physical and chemical transformation reactions for NMVOCs. Dissolution depends on the relative affinity for a chemical species for the aqueous phase. Such affinity depends on the physico-chemical characteristics of the chemical, including water solubility and volatility properties. NMVOC chemicals with low boiling points, high vapor pressures, high Henry’s constants and low water solubilities are more likely to remain in the gaseous phase in wastes and covers within the landfill

environment. Based on these criteria, the physical and chemical properties of the gases included in the investigation were ranked from most to least soluble using the following parameters (in order of most to least significant): water solubility (high values desired), vapor pressure (low values desired), boiling point (high values desired), and Henry's constant (low values desired). The analysis indicated that the alcohols (i.e., methanol), aldehydes, ketones, and some monoterpenes were most likely to dissolve into the aqueous phase in the landfill environment. These gases are oxygenated species (leading to potential hydrogen bonds) and small in molecular weight (limited number of carbon atoms) supporting the high potential for dissolution in the liquid phase (Table 1.22).

A similar exercise was conducted to assess the extent of organic partitioning in the landfill environment for the target gases included in this study. NMVOC chemicals were ranked from most to least likely to partition based on the octanol-air (most significant) and octanol-water partition coefficients (least significant), where higher values of each parameter were desired. Using the above criteria and ranking schemes, many of the chemicals included in the aromatics, long-chain alkanes, monoterpenes, and some baseline GHGs (carbon monoxide/nitrous oxide) were likely to partition into the organic phases present in the landfill environment. Both aromatic compounds and long-chain alkanes or alkenes are generally more hydrophobic than hydrophilic (and lipophilic) and tend to partition into non-polar solvents (Table 1.22).

Data and analysis on sorption of target gases for chemical or physical attachment to waste materials or soil particles present in the landfill environment have not been studied in great detail. In general, various attachment mechanisms are present for chemicals in the environment. The most predominant type of interaction is that based on charge differences. The relative charge of a given chemical depends on its polarity and ionization potential, where more polar compounds (that exert greater differences in electronegativity through dipole moments) and those with a greater number of ionizable functional groups (at the pH range expected in the landfill environment) are more likely to sorb and interact chemically with different materials present (Vollhardt and Schore 2004). Due to the presence of oxygen and hydroxyl functional groups, the aldehydes, alcohols, and ketones are relatively polar compounds among the target gases included in the investigation and may be more inclined to chemically attach to cover soil particles and organic or inorganic materials present in the waste mass.

PART 2 – LANDFILL CLASSIFICATION

2.1 Introduction

The initial step of the investigation consisted of development of a scheme for classifying landfill sites in California and selecting representative sites for aerial emissions measurements and ground-based static flux chamber tests. The main factors and associated expected variations in the main factors used for categorization of the sites are listed in Table 2.1. The categorization scheme was used for active landfill sites in California.

Table 2.1 – General California Landfill Classification Scheme

Main Factor		Variation
Facility Size	Waste in place	Amount of waste disposed at the site
	Disposal area	Permitted waste footprint area
	Waste column height	Average depth of waste at the site
	Permitted throughput	Annual waste intake
Climate		Classification designation by Köppen Geiger System
Oil and Gas Operations		Oil and gas operation sites in California and proximity of the landfill to these sites
Fault Lines		California quaternary faults and proximity of the landfill to the faults
Population Density		Urban and rural areas
Gas System		Yes, no
Tire Disposal		Yes, no

The classification scheme identified in Table 2.1 was used for all of the active landfill sites in California. Further detailed analysis was conducted for finalizing the sites selected for the experimental program by incorporating additional criteria. The detailed classification scheme used in the investigation is provided in Table 2.2. Categories from Table 2.1 are included in Table 2.2 for completeness of the analysis.

Table 2.2 – Detailed California Landfill Classification Scheme

Main Factor		Variation
Facility Size	Waste in place	Amount of waste disposed at the site
	Disposal area	Permitted waste footprint area
	Waste column height	Average depth of waste at the site
	Permitted throughput	Annual waste intake
Climate		Classification designation by Köppen Geiger System
Oil and Gas Operations		Oil and gas operation sites in California and proximity of the landfill to these sites
Fault Lines		California quaternary faults and proximity of the landfill to the faults
Population Density		Urban and rural areas
Gas System		Yes, no

Main Factor		Variation
Tire Disposal		Yes, no
Cover Conditions	Daily	Conventional-soil type and thickness Alternative daily covers (ADCs) including green waste, construction & demolition, biosolids, tarp, spray-on products, other
	Intermediate	Soil type and thickness
	Final	Presence of final cover: Yes, no Type and thickness of final cover - Traditional: single covers [compacted clay (CCL), geosynthetic clay liner (GCL), geomembrane (GM)]; composite covers [GM-CCL, GM-GCL] - Alternative: monolithic or capillary break
Relative Fraction of Cover Categories		Relative areas of daily, intermediate, and final covers (% of waste footprint)
Working Face		Size of active waste disposal area
Range for Age of Waste		Age of wastes
Landfill Configuration		Canyon, area
Operational Conditions		Particularly in relation to N_2O emissions including leachate recirculation, biosolids disposal, etc.

2.2 California Landfill Site Characteristics

The active landfill sites in California were first categorized using the criteria in Table 2.1. The information used for the categorization mainly was obtained from the SWIS database (CalRecycle 2017, data from July 2017) and Landfill Data Compilation provided by Walker (2010). A total of 133 active landfill sites was identified for inclusion in the analysis. A summary of data for all 133 active landfills is presented in Appendix B1. The geographical distribution of these sites is presented in Figure 2.1.

The facility size analysis included waste in place, disposal area, waste column height, and permitted throughput categories. The waste in place (WIP) data were obtained from the SWIS database by calculating the difference between the reported “capacity” and “remaining capacity” data. These data were reported in volume units. In addition, waste in place was calculated by using data obtained from ARB in relation to methane reporting requirements. These data were provided in mass units and converted to volume using a waste density of 1300 lbs/yd^3 (771 kg/m^3) provided by ARB. The WIP data obtained using the two approaches are compared in Figure 2.2 and were determined to be in good agreement. The volumetric WIP data obtained from the SWIS database were selected to be used herein as the data directly represent the amount of waste disposed of at a landfill i) due to no conversions required using assumed parameters (i.e., density) and ii) as the loss in mass due to decomposition/degradation of older wastes is accounted for with periodic surveys that provide the volumetric data.

Figure 2.1 Active California Landfill Sites

Figure 2.2 Waste in Place Determined Using Two Approaches

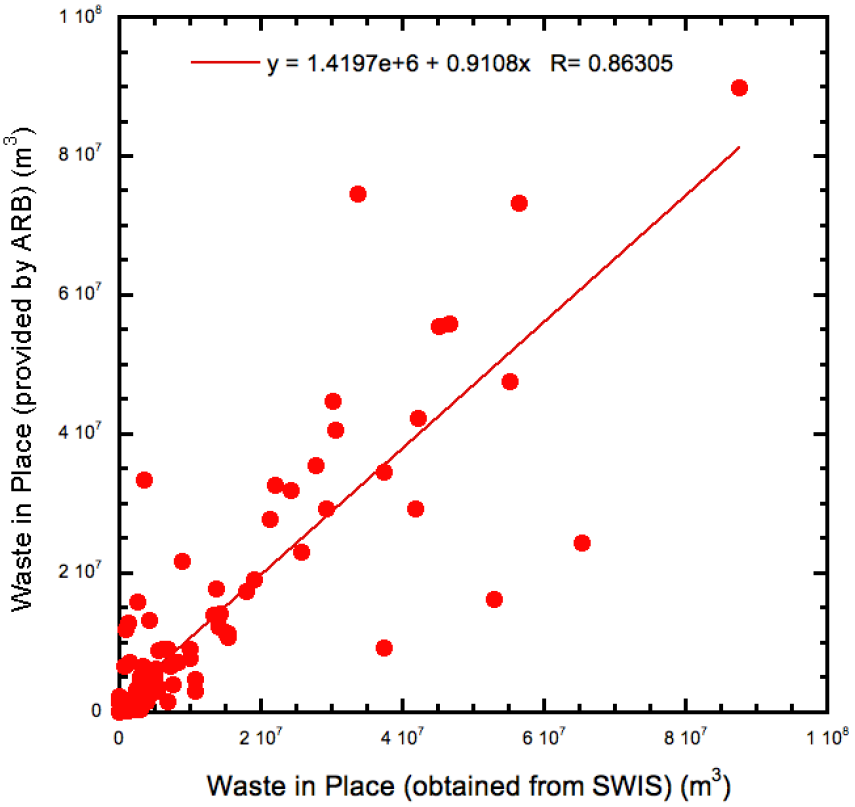

The variation of waste in place with number of landfills is presented in Figure 2.3. The landfills were categorized as small, medium, and large using major breaks in WIP data (analysis performed on large graphical representations of the data) and also presented in Figure 2.3. The limiting WIP values for the cutoffs between the categories were 4,000,000 m^3 and 40,000,000 m^3 based on large breaks in the histogram data. This approach was used for all of the histograms in Part 2. All histograms in Part 2 were presented without and with limiting thresholds to clearly present overall data and delineate categories identified in this investigation. The disposal area was obtained from the "Disposal Acreage" category in the SWIS database. The variation of disposal area with number of landfills is presented in Figure 2.4. The landfills were categorized into small, medium, and large sites using large breaks in area data (analysis performed on large graphical representations of the data) and also presented in Figure 2.4. The limiting disposal area values for the cutoffs between the categories were 1,000,000 m^2 and 2,000,000 m^2. The average waste column height was determined by dividing the WIP with disposal area. The variation of waste column height with number of landfills is presented in Figure 2.5. The landfills were categorized into short, moderate, and tall landfills using large breaks in waste column height data as presented in Figure 2.5. The limiting waste height values for the cutoffs between the categories were 14 m and 30 m. The variation of waste throughput with number of landfills is presented in Figure 2.6. The data were obtained from the SWIS database. The landfills were categorized into low, medium, and large landfills using large breaks in throughput data with limiting values for the cutoffs between the categories as 1500 tons/day and 7000 tons/day.

Figure 2.3 Variation of Waste in Place with Number of Landfills

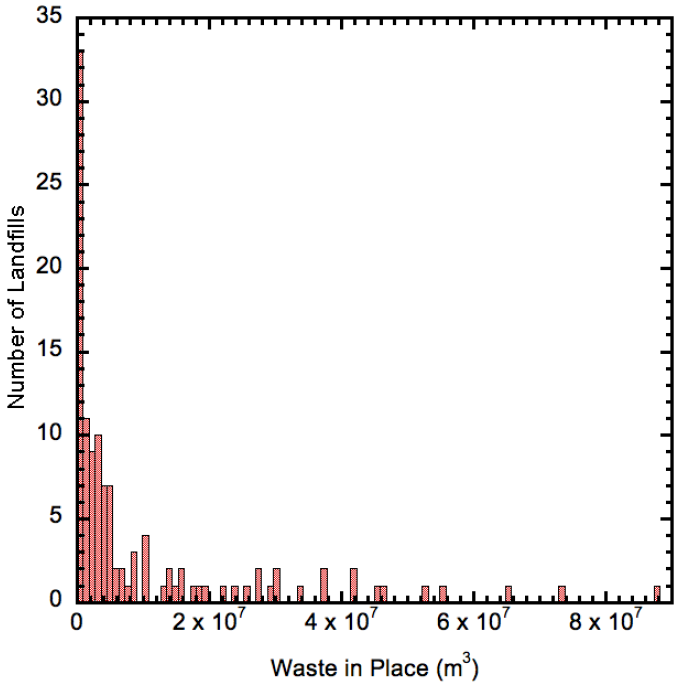

a) Distribution without Thresholds

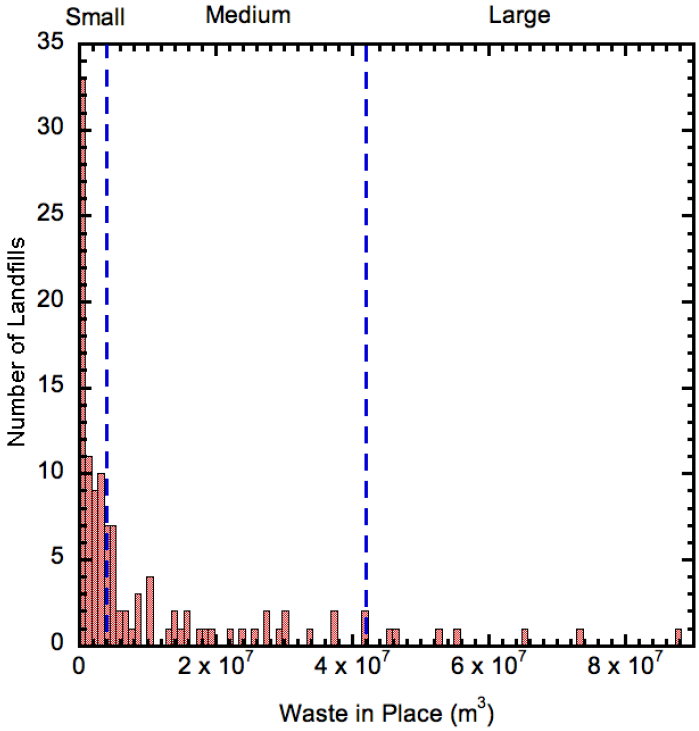

b) Distribution with Thresholds

Figure 2.4 Variation of Disposal Area with Number of Landfills

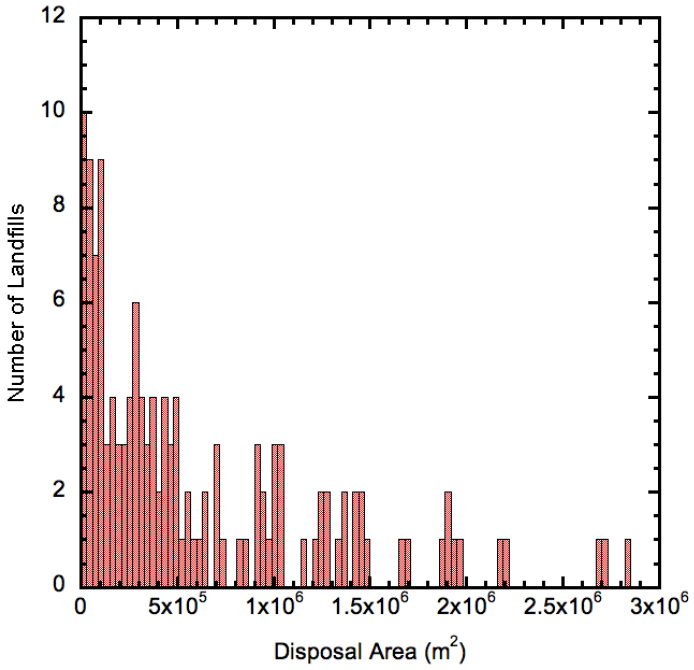

a) Distribution without Thresholds

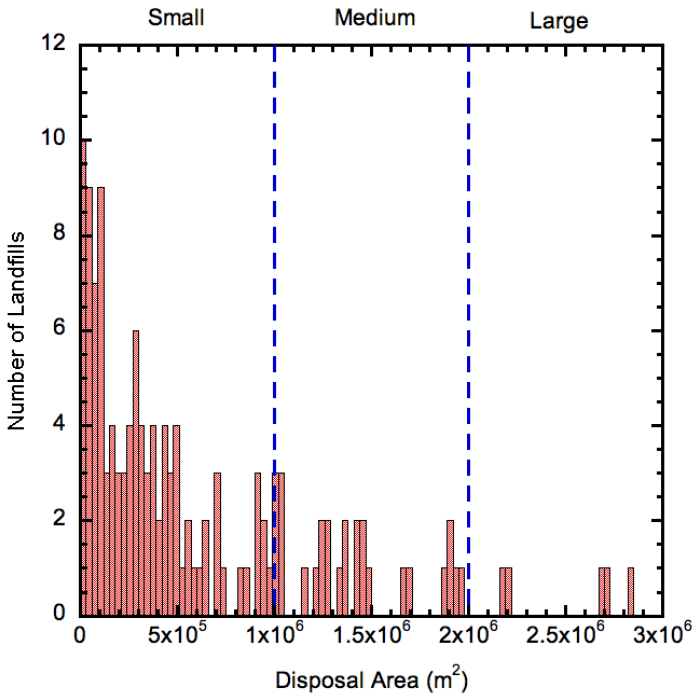

b) Distribution with Thresholds

Figure 2.5 Variation of Average Waste Column Height with Number of Landfills

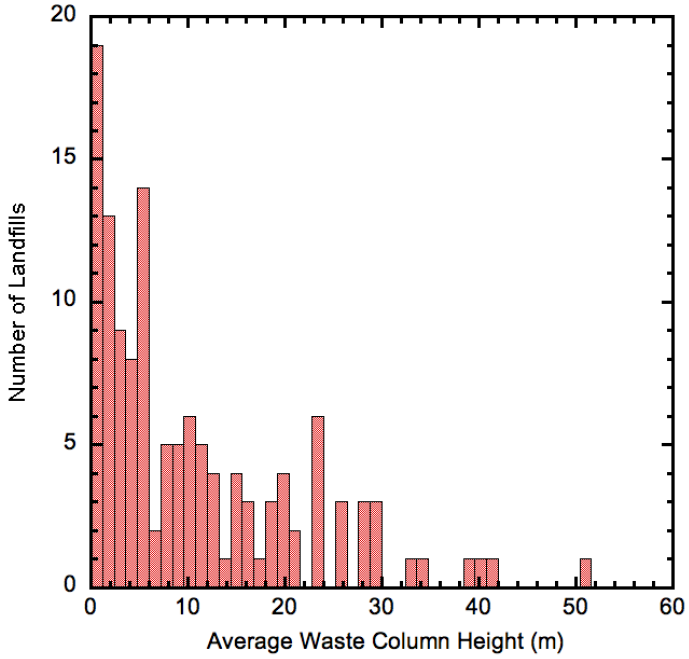

a) Distribution without Thresholds

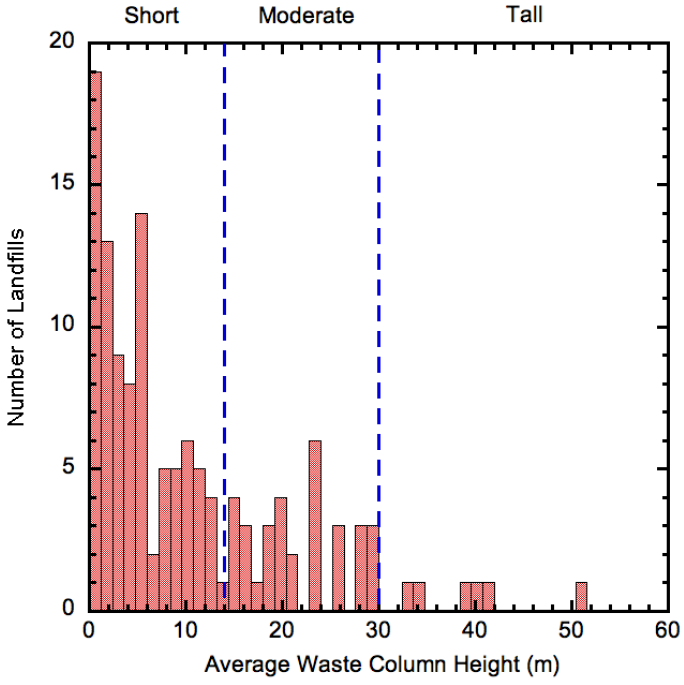

b) Distribution with Thresholds

Figure 2.6 Variation of Waste Throughput with Number of Landfills

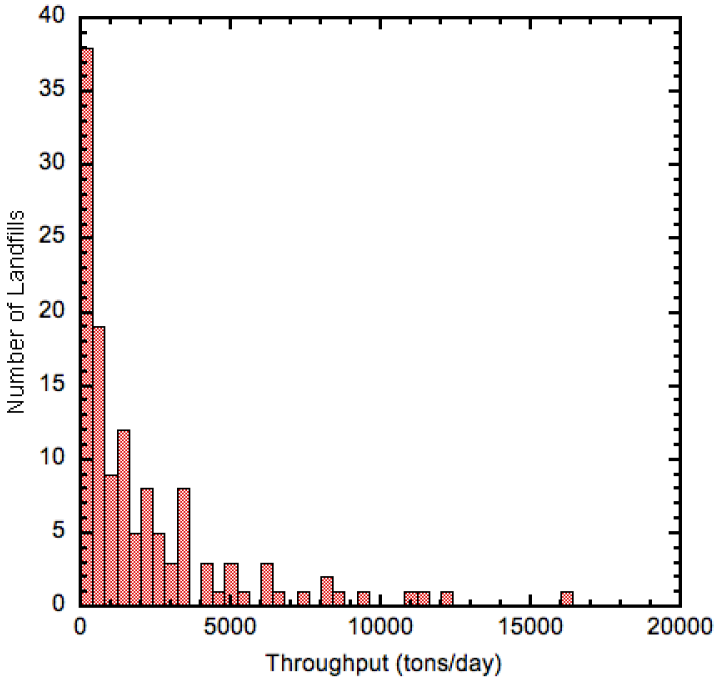

a) Distribution without Thresholds

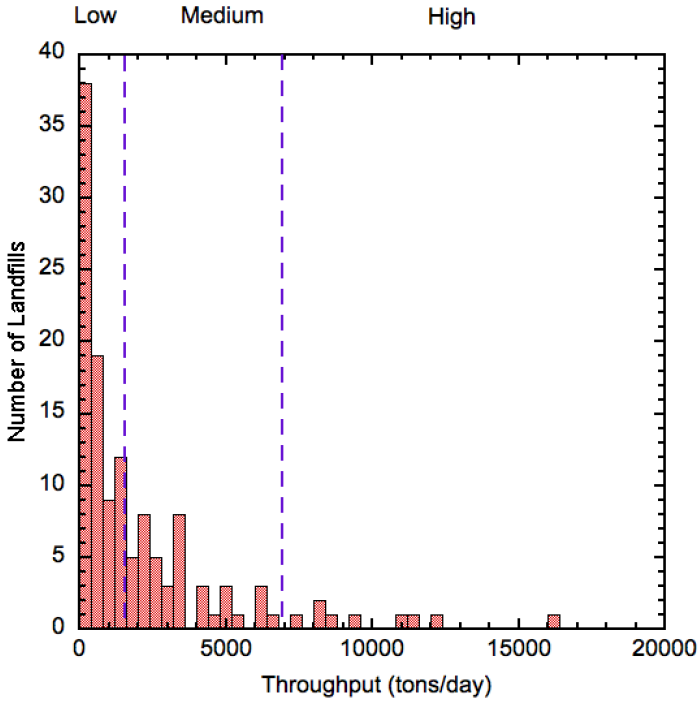

b) Distribution with Thresholds

Positive correlations between waste in place and annual landfill gas recovery were demonstrated for California landfills with increasing gas recovery with increasing WIP (Spokas et al. 2015). Therefore, landfill facility size quantified using the waste in place parameter was identified to be a significant factor for the current emissions study and further analysis was conducted using the waste in place data. Relative distribution of WIP in small, medium, and large landfills is presented in Figure 2.7 for the total WIP amount of 1,237,674,433 m^3 in California. While the highest number of landfills (80) was in the small landfill category (Figure 2.3), the relative amount of WIP in these landfills amounted to only 8.2% (99,347,605 m^3) of the total WIP in California. The majority of the WIP, 50.9% (627,991,773 m^3), was in the 44 medium landfills. With only 9 facilities, the WIP in large landfills was significant at 40.8% of total WIP and equaled to 510,335,055 m^3 of waste.

Figure 2.7 Relative Distribution of Waste in Place in California Landfills

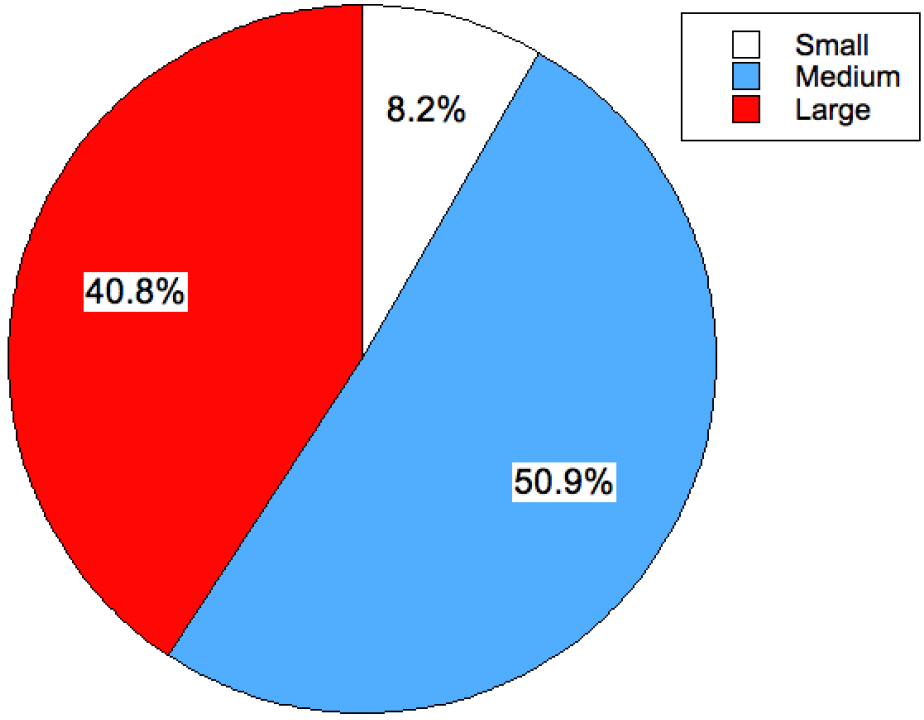

Waste in place data was added to the location data and active California landfills by WIP amount are presented in Figure 2.8. The six main climatic zones in California (Figure 2.9) according to the Köppen Geiger System (Peel et al. 2007) were added to the data in Figure 2.8 and a composite plot of landfill location, size, and climatic zone is presented in Figure 2.10. The majority of California landfills (77 landfills) were located in the Csb (temperate, dry summer, warm summer) climate zone (Figure 2.11). The relative fraction of these 77 facilities was 57.9% (Figure 2.12). The number of landfills in the Csa (temperate, dry summer, hot summer) and BSk (arid, steppe, cold) climate zones were similar and equal to 20 and 22, respectively (Figure 2.11. The majority of the WIP in California was also located in the Csb climate zone (Figure 2.13), which amounted to 77.5% of the total WIP in the state (Figure 2.14). This was

followed by 14% and 7.3% WIP present at the landfills in Csa and BSk climate zones, respectively (Figure 2.14. No landfills were located in the Dsc (cold, dry summer, cold summer) climate zone; only small landfills were located in the BWh (arid, desert, hot) climate zone, and a total of only two landfills (one small, one medium) were located in the BWk (arid, desert, cold) climate zone (Figures 2.11 and 2.13). The WIP in these three climate zones was minimal (Figure 2.14).

Figure 2.8 Active California Landfills with Waste in Place Data

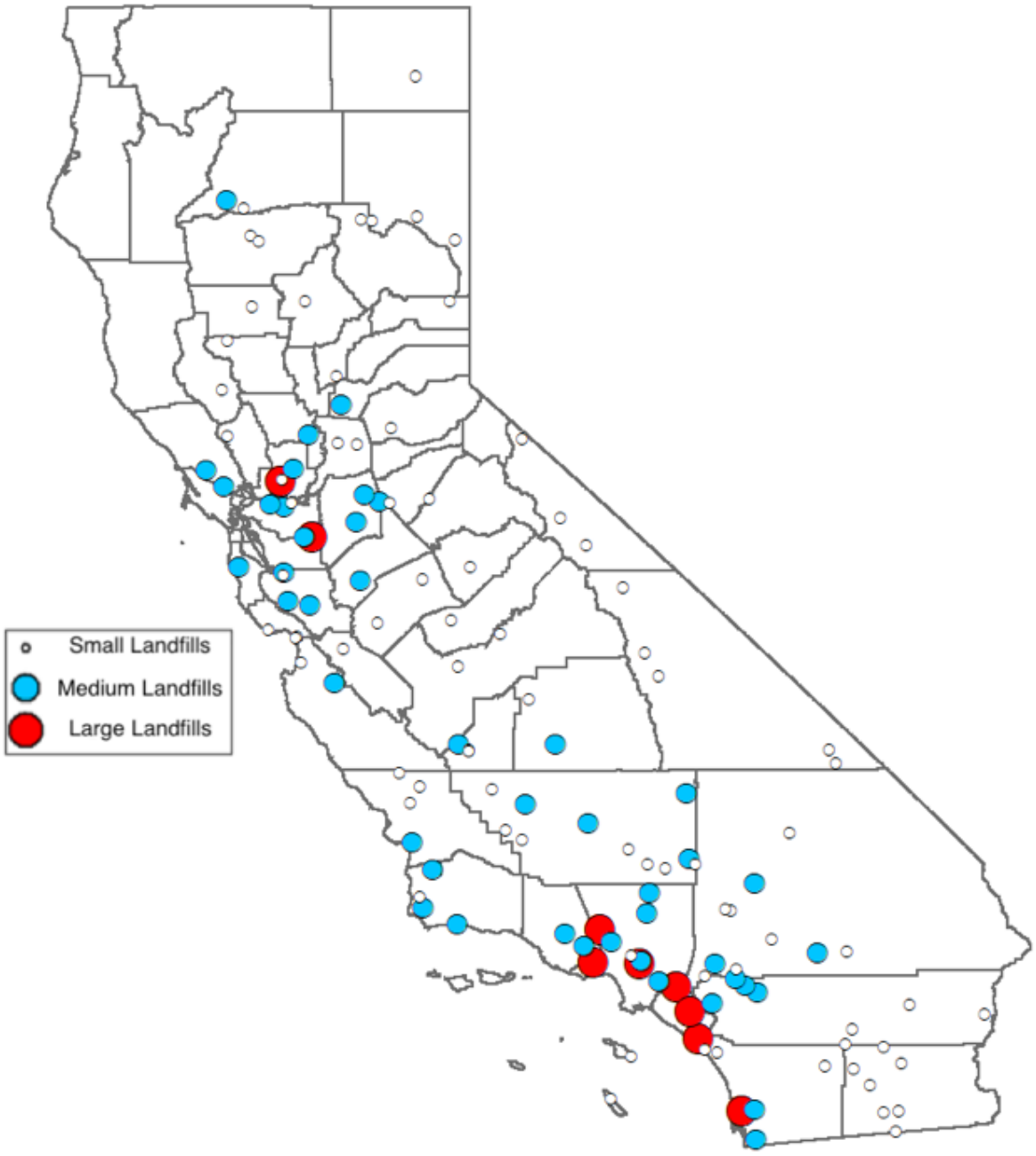

Figure 2.9 Main Climate Zones in California

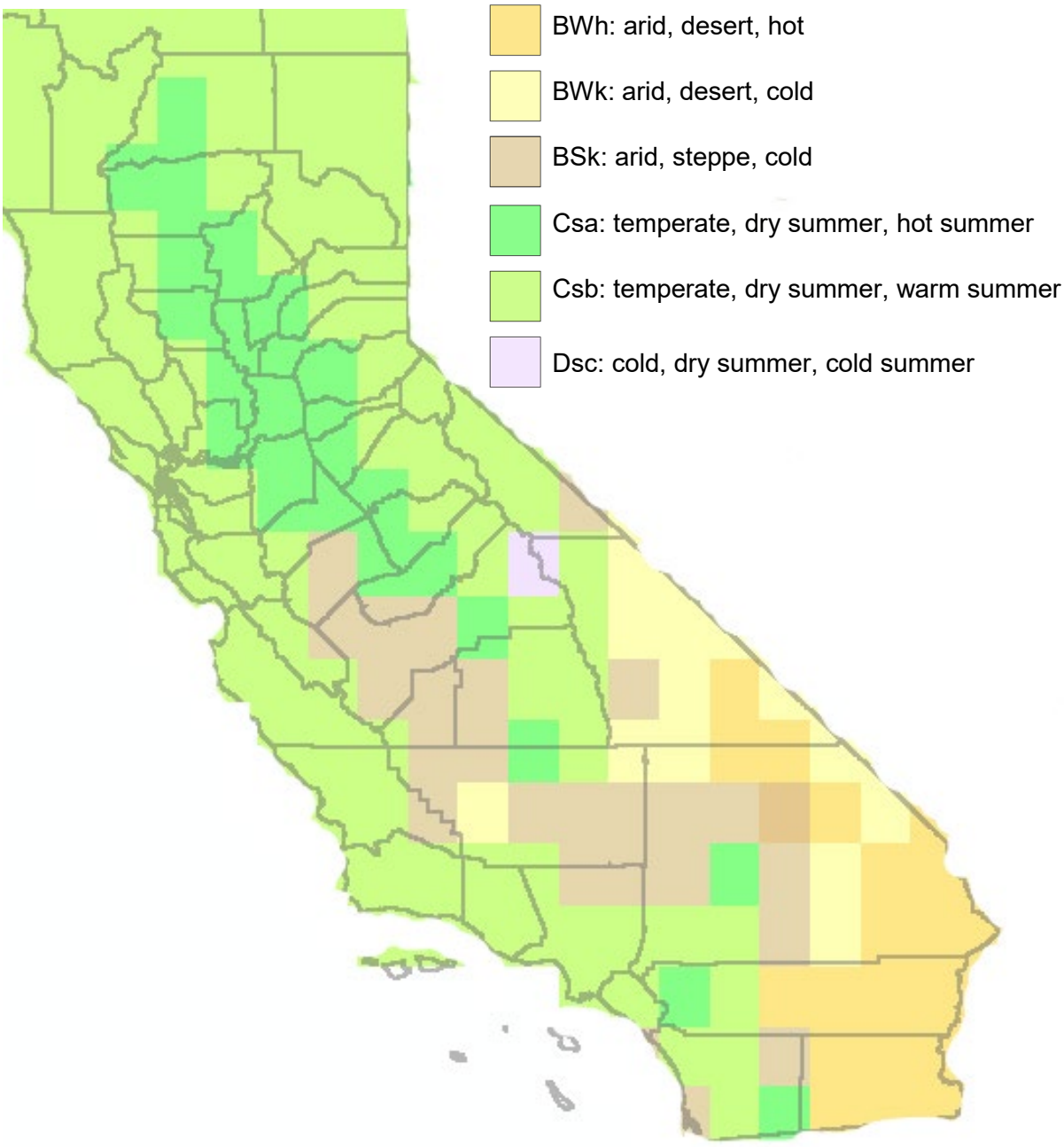

Figure 2.10 Active California Landfills with Waste in Place Data Across Climate Zones

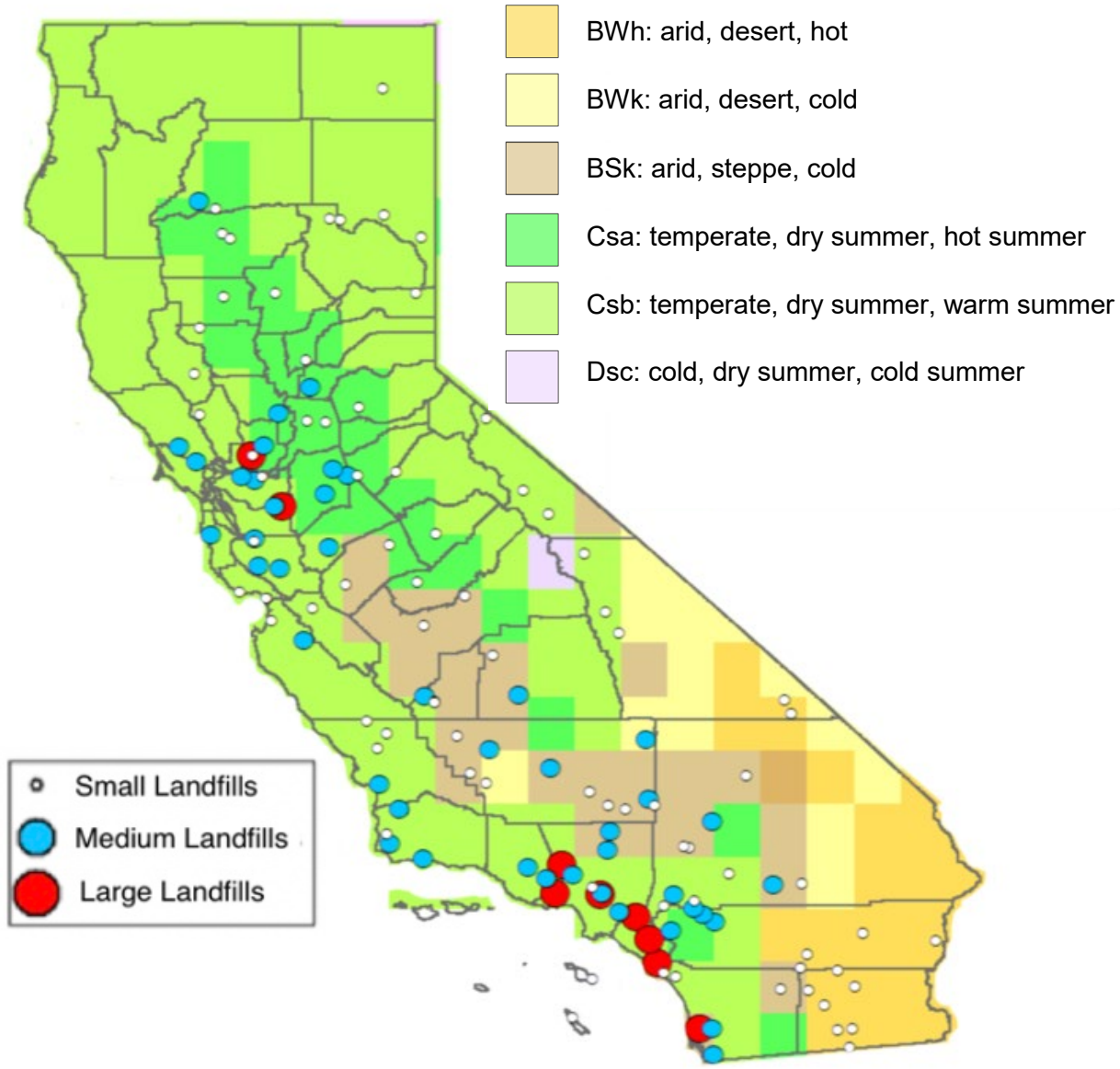

Figure 2.11 Histogram of Number of Landfills with Climate Zone

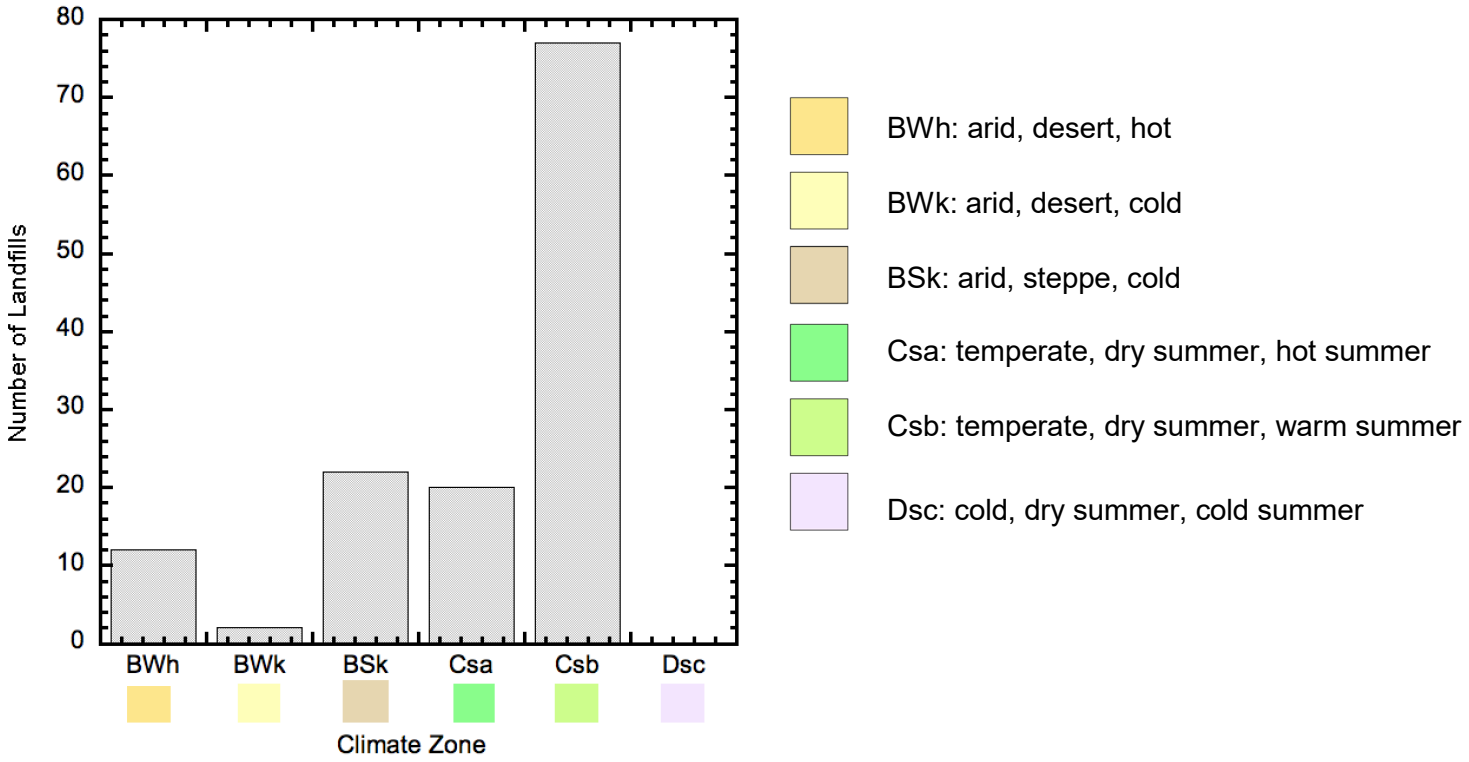

Figure 2.12 Relative Distribution of Number of California Landfills with Climate Zone

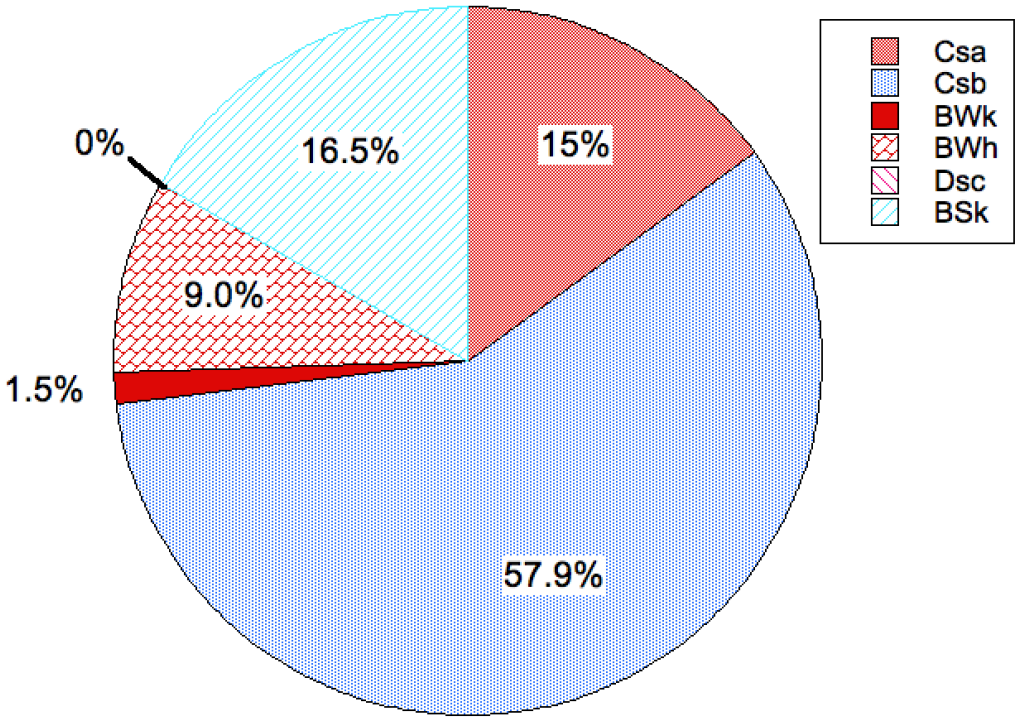

Figure 2.13 Histogram of Number of Landfills and WIP in the Landfills with Climate Zone

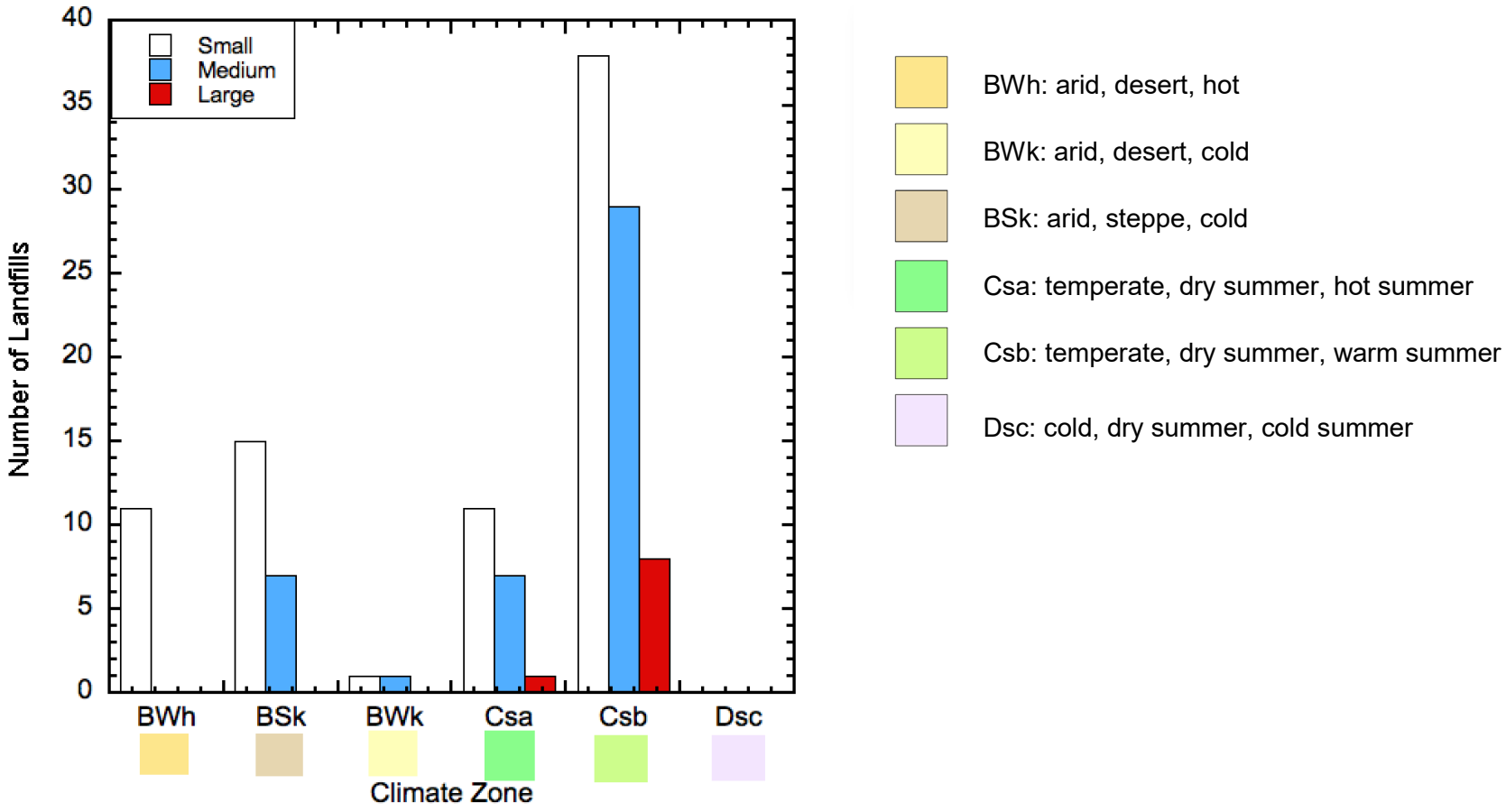

Figure 2.14 Relative Distribution of WIP with Climate Zone

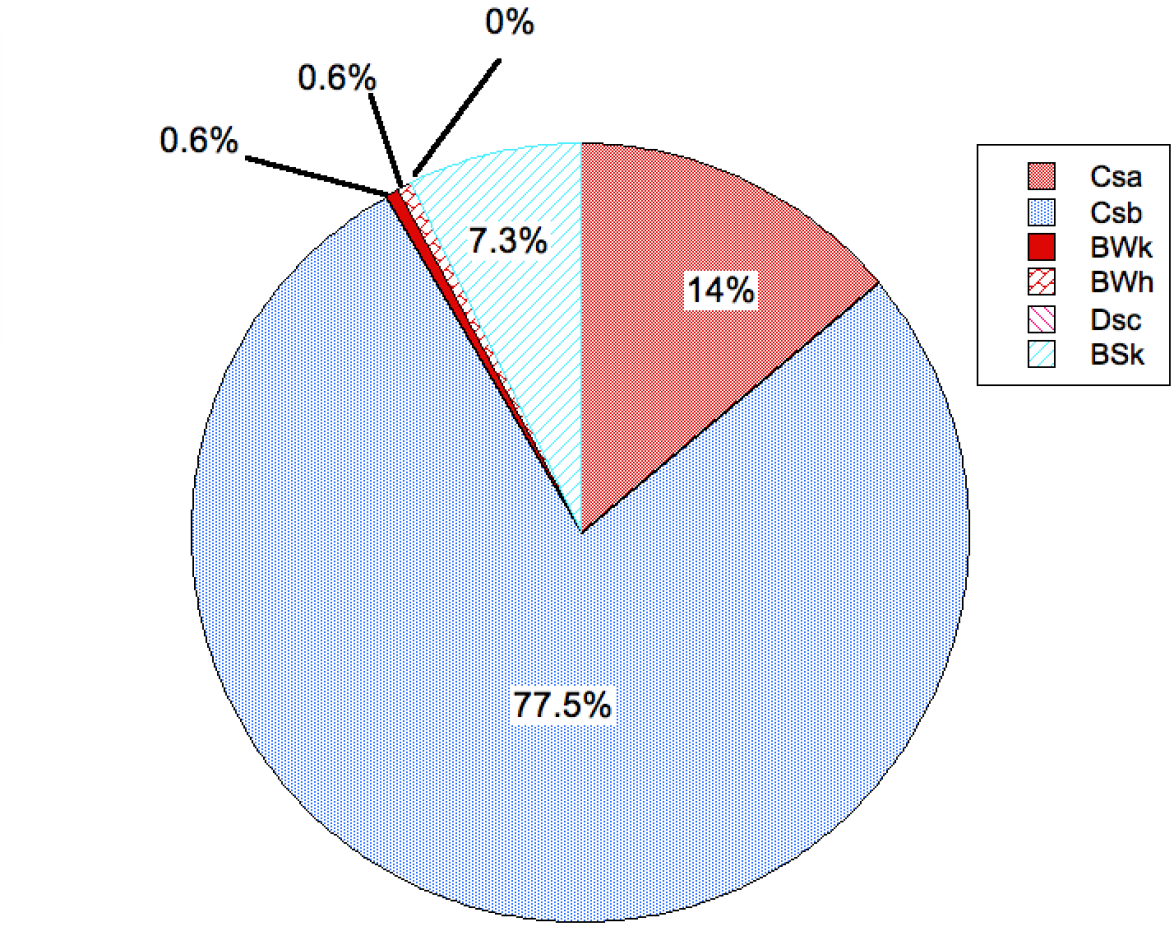

Landfill size classified in accordance with WIP and locations of oil and gas operations and fault lines in the state (that may have emissions/emissions pathways, which may affect landfill emissions measurements) are presented in Figures 2.15 and 2.16, respectively. A composite plot of landfill location, size, oil and gas operations, and fault lines is presented in Figure 2.17. The data in Figure 2.17 indicated that the majority of the landfill sites in California were in close proximity of oil and gas operations and fault lines. Oil and gas operations and landfills typically were located in central to western California. The extent of both oil and gas operations and landfill facilities were very low in eastern California. Fault lines are prevalent throughout the landmass of the state and also were in proximity of landfill facilities. Due to the prevalent extent of nearby oil and gas operations and fault lines, proximity to such features was not considered as a direct selection criterion.

Figure 2.15 Location of California Landfills in relation to Oil and Gas Operations

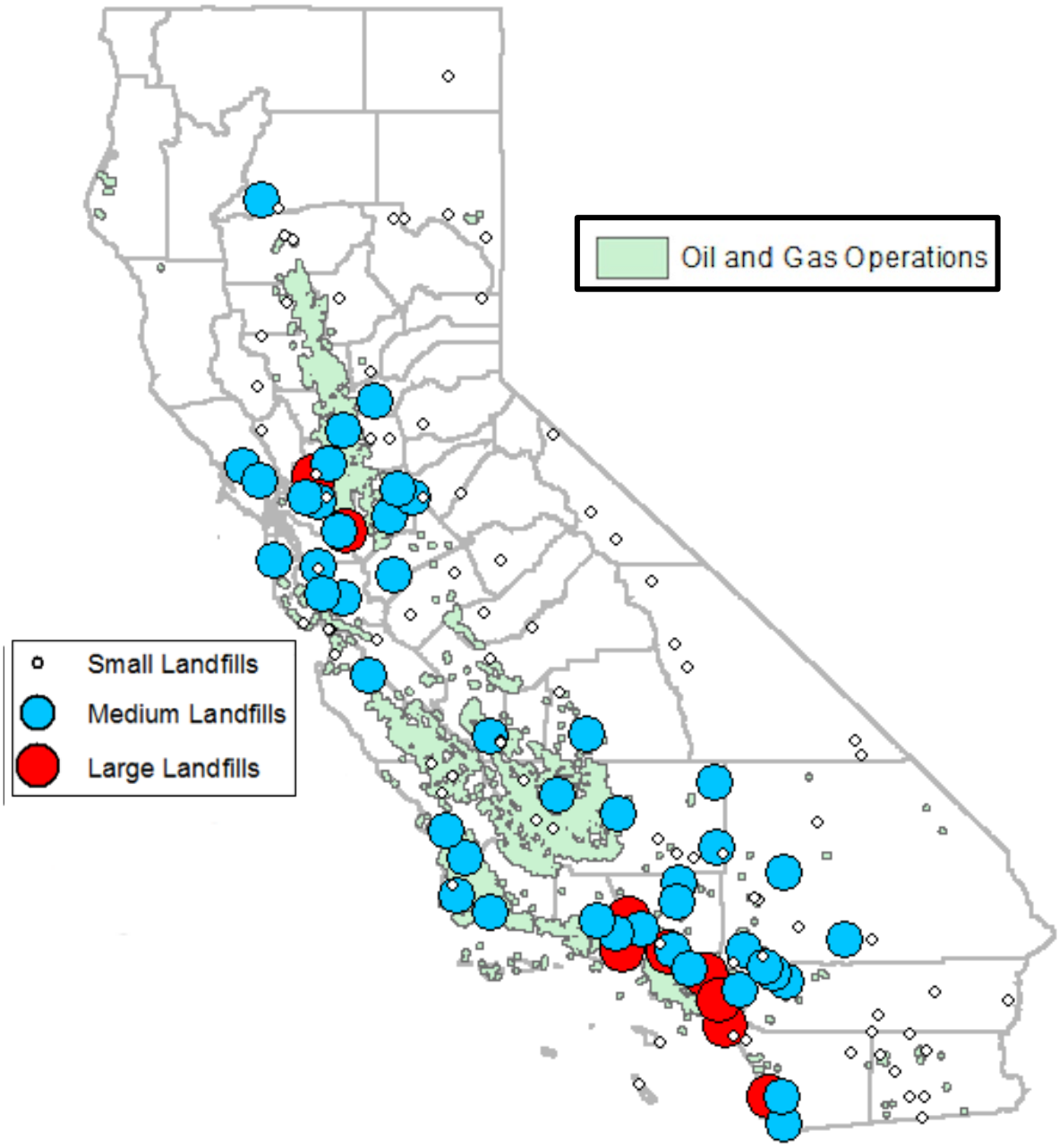

Figure 2.16 Location of California Landfills in relation to Fault Lines

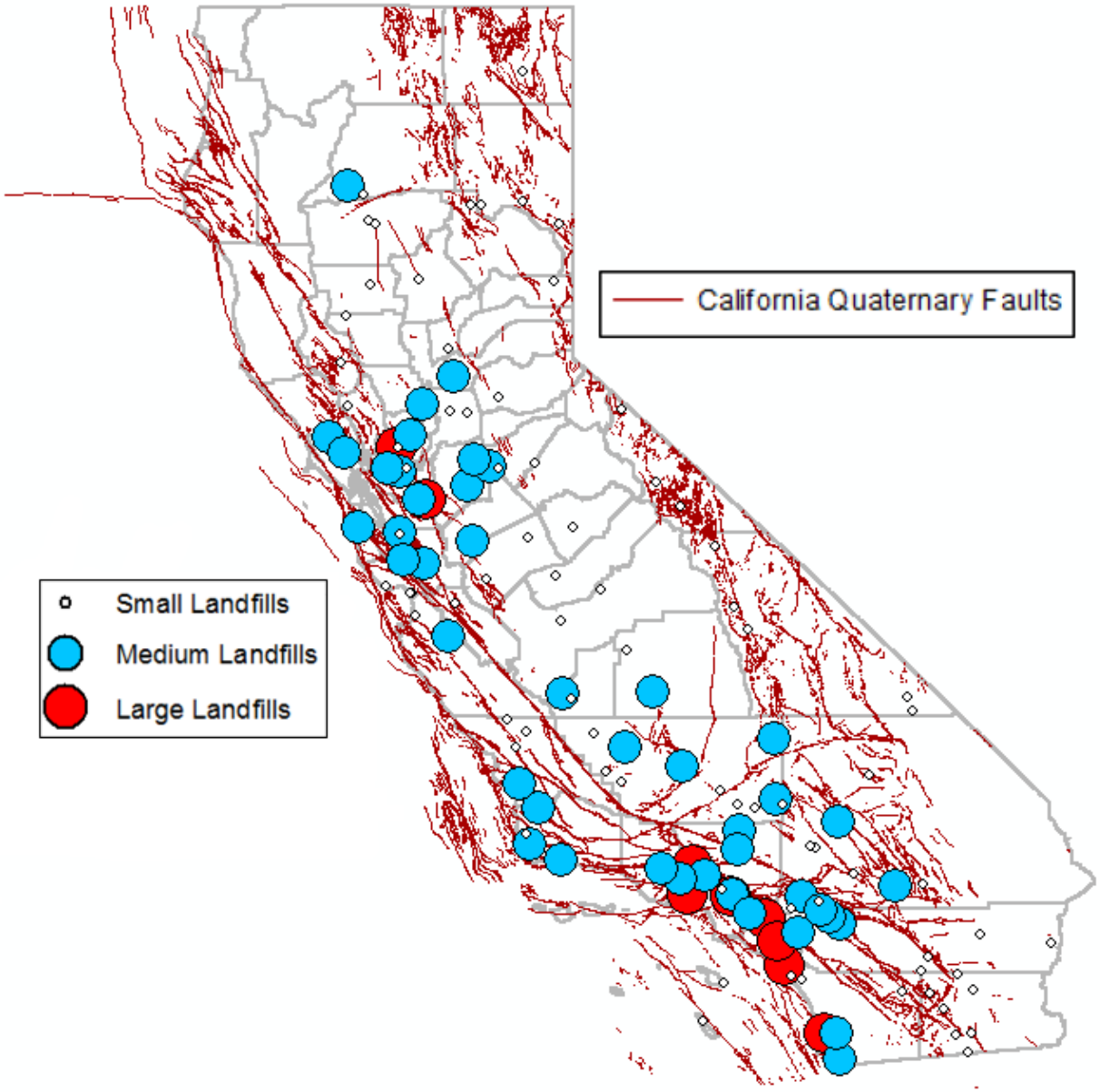

Figure 2.17 Location of California Landfills in relation to Oil and Gas Operations and Fault Lines

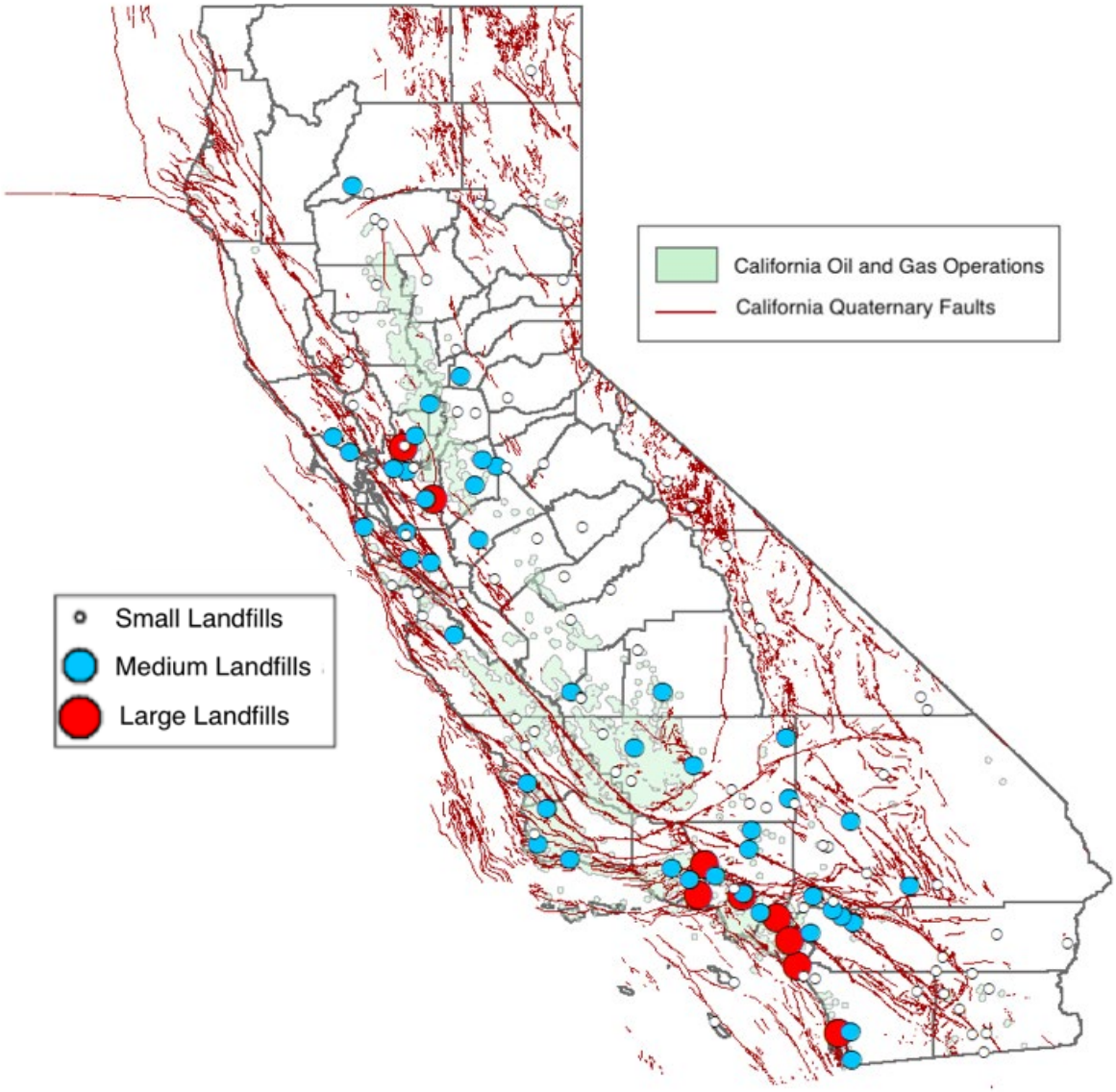

A map of California with population density is presented in Figure 2.18. Location of California landfills with WIP data and variation of population density in the state is presented in Figure 2.19. Landfills are typically located near population centers and were clustered around large metro areas including Bay Area and Sacramento in northern California and Los Angeles and San Diego in southern California.

Figure 2.18 Population Density in California

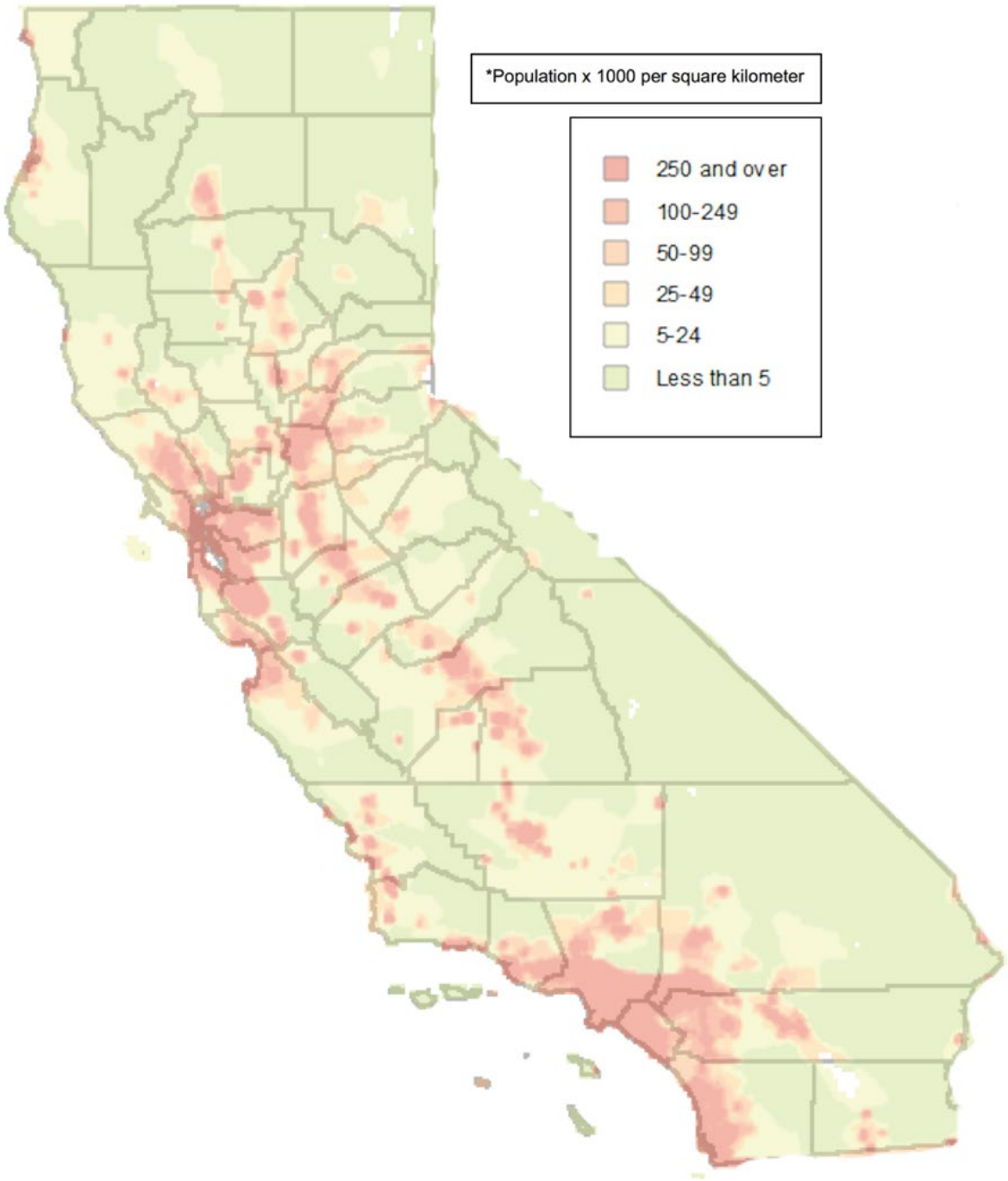

Figure 2.19 Location of California Landfills in relation to Population Density

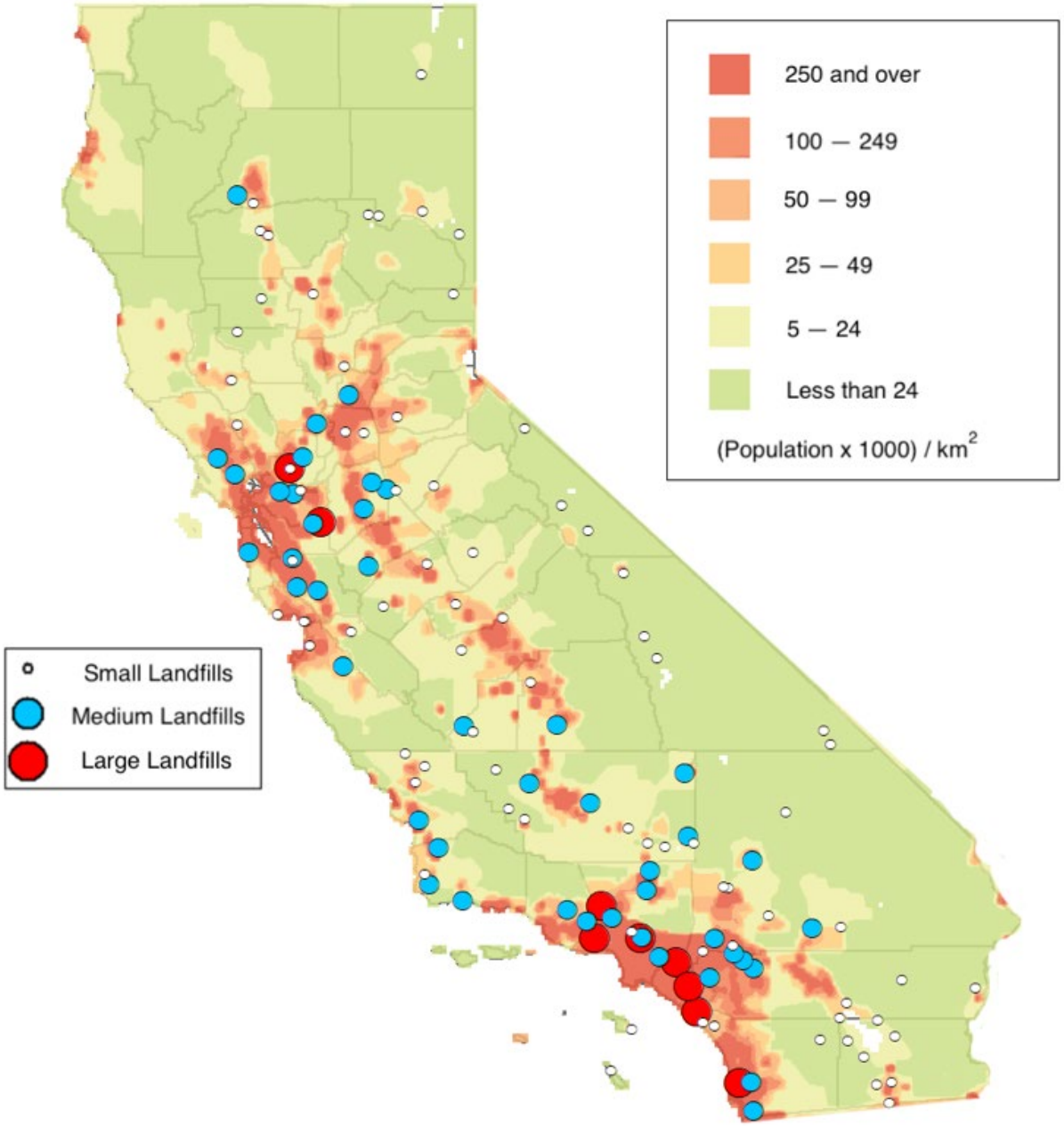

Landfills with active gas collection systems are presented in Figure 2.20. Gas collection systems were identified to have been installed at 74 landfills in the state. Landfills that accept tires are presented in Figure 2.21. A total of 63 landfills were identified as facilities with tires in the disposed waste stream. The landfills without gas collection systems and facilities that do not accept tires also are shown in the plots for reference.

Figure 2.20 California Landfills with Gas Collection Systems

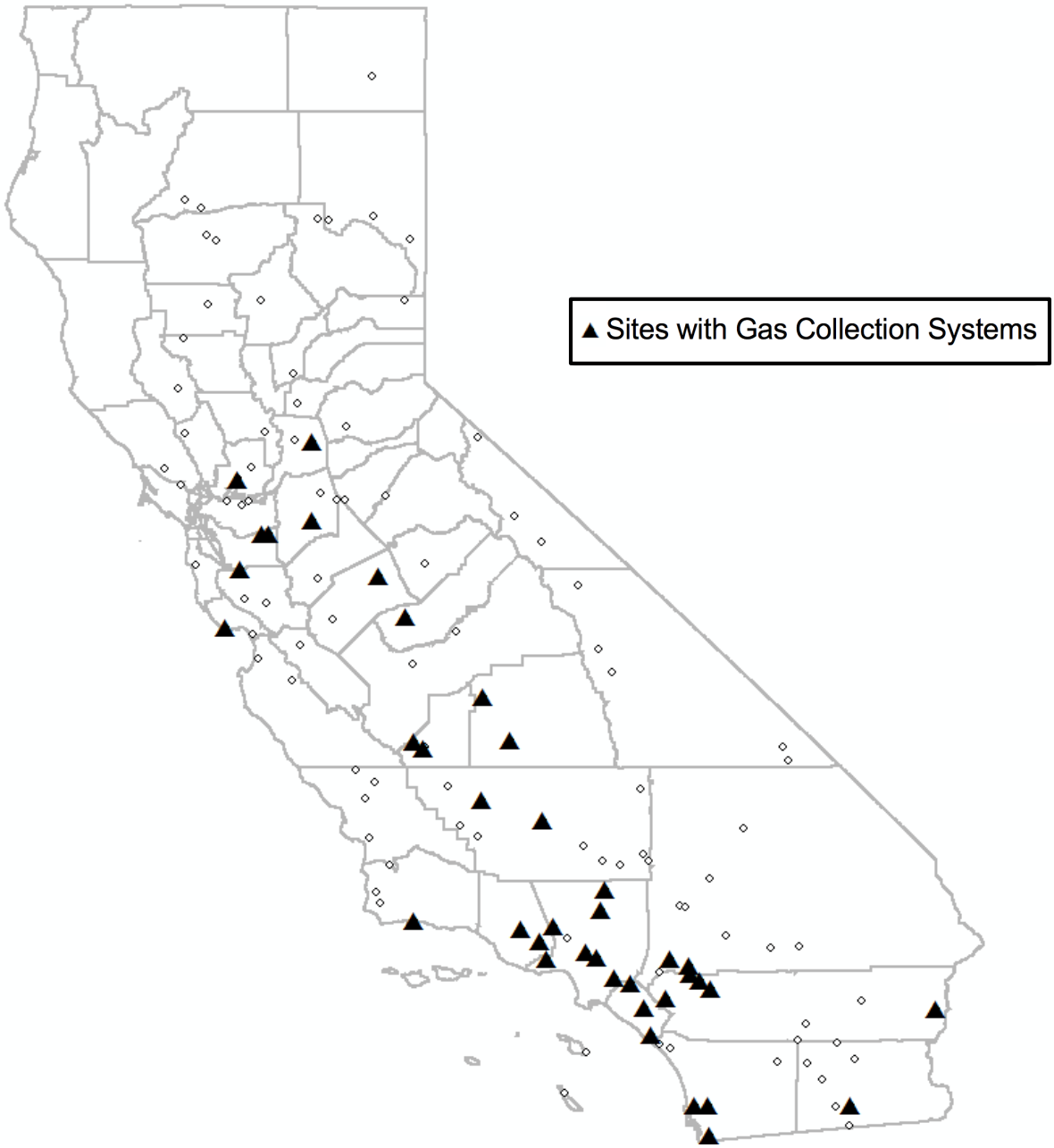

Figure 2.21 California Landfills that Accept Waste Tires

2.3 Landfill Site Selection

The landfill site selection protocol included a two-step process, first identifying a larger subset of landfills for aerial gas emissions measurements and then second identifying a smaller subset of the landfills included in the aerial measurements for land-based static flux chamber measurements. A total of 15 landfills was selected in the first step and then 5 of these landfills were further selected for chamber testing.

The majority of the criteria described in Table 2.2 was used for the first step of the selection process to identify the 15 landfill sites. The main facility size factor used in the analysis was waste in place. Facilities from all three WIP categories including small, medium, and large, were included in the analysis. Climatic conditions also were considered. Sites from all 5 climatic zones with landfills in California were targeted. Proximity to oil and gas operations and proximity to fault lines were not significant selection criteria as the landfill sites throughout the state was demonstrated to be in proximity to these sites (Figure 2.15) with no significant differences between the majority of the landfills in the state based on these criteria. Sites near population density centers and low-population rural areas were targeted. Sites with and without gas collection systems and with and without tire disposal was targeted. In general, sites with all three types of cover systems, including daily, intermediate, and final covers, were considered in the selection process. Relative fraction of the three cover categories and size of the working face at the landfill facilities also were included in the selection process. Landfills representing both areal and canyon facilities were selected. Landfills with wastes with different ages and varying operational conditions in particular in terms of waste types were included in the site identification process.

The 15 sites selected for the aerial measurements are presented in Table 2.3. The sites are listed in order of increasing WIP. The distribution of the sites across the state is presented in Figure 2.22. The small sites were selected to include all five climatic zones with landfills in California (Figure 2.10) in the aerial emissions analysis as medium- and large-size landfills are not located in all five climatic zones. The number of small sites selected for the analysis was higher than the number of medium landfills and also higher than the number of large landfills. The rationale for this choice was to include a high number of landfills without gas collection systems in the analysis recognizing the fact that the medium and large landfills have gas collection systems unless this is a facility that has become operational very recently and sufficient amount of waste placement that requires installation of a gas collection system has not yet occurred. The potential for high emissions from landfill facilities without gas collection systems was evaluated with the selection of these sites. The medium sites were selected in the three climatic zones with the highest amount of waste in place in the state including Csb, Csa, and Bsk climate zones (Figure 2.14). The large landfills are located in Csb and Csa climate zones and four landfills from these climate zones are included in the analysis. The small landfills are located in rural areas, the medium landfills also are located mainly in rural areas, whereas the large landfills are located in close proximity to major urban centers in northern and southern California (Figure 2.22). The active face at the facilities ranged from 65 to 12,100 m^2. The relative fractions of the daily, intermediate, and final covers were 0.1 to 20%, 25 to 99.8%, and 0 to 40.7%, respectively.

Table 2.3 – Landfills Selected for Aerial and Ground Testing (Bold Font for Ground Testing Sites)

No.	Landfill Name	Size	WIP* (m^3)	Permitted Throughput (tons/day)	Climate Zone	Gas Collection System	Tires	Active Face (m^2)	Cover Fraction[a] (%)		
									D	I	F
1	Stonyford Disposal Site	S	71,513	10	Csb	No	Yes	65	1.7	96.5	1.8
2	Salton City Solid Waste Site	S	152,082	6,000	BWh	No	No	NR	NR	NR	NR
3	Borrego Landfill	S	278,752	50	Bsk	No	Yes	NR	NR	NR	NR
4	Pumice Valley Landfill	S	292,496	110	Csb	No	No	1200	NA	25	0
5	Mariposa County Sanitary Landfill	S	594,757	100	Csa	No	Yes	200	20	80	0
6	Taft Recycling and Sanitary Landfill	S	2,767,148	800	BWk	No	Yes	NR	NR	NR	NR
7	**Teapot Dome Disposal Site**	M	5,369,126	800	BSk	Yes	No	1200	15.5	84.5	0
8	**Santa Maria Regional Landfill**	M	8,385,395	858	Csb	Yes	Yes	700	0.1	69.3	30.6
9	Redwood Landfill	M	17,643,577	2,300	Csb	Yes	Yes	2000	0.2	99.8	0
10	Simi Valley Landfill and Recycling Center	M	27,697,889	9,250	Csb	Yes	No	12100	0.7	99.3	0
11	Yolo County Central Landfill	M	37,490,107	1,800	Csa	Yes	Yes	11800	1.4	57.9	40.7
12	**Chiquita Canyon Sanitary Landfill**	L	42,266,798	6,000	Csb	Yes	No	5600	8.3	63.8	27.8
13	**Site A**	L	45,108,745	11,150	Csb	Yes	Yes	6100	0.6	89.5	9.9
14	Frank R. Bowerman Sanitary Landfill	L	46,637,855	11,500	Csb	Yes	No	NR	NR	NR	NR

No.	Landfill Name	Size	WIP* (m^3)	Permitted Throughput (tons/day)	Climate Zone	Gas Collection System	Tires	Active Face (m^2)	Cover Fraction[a] (%)		
									D	I	F
15	**Potrero Hills Landfill**	L	52,928,614	4,330	Csa	Yes	Yes	3000	3	91	6

*Sites listed in order of WIP; Data from SWIS database (2017)
NR – Not Reported
[a]D = daily, I = Intermediate, F = Final

Figure 2.22 Landfills Selected for Aerial and Flux Chamber Testing

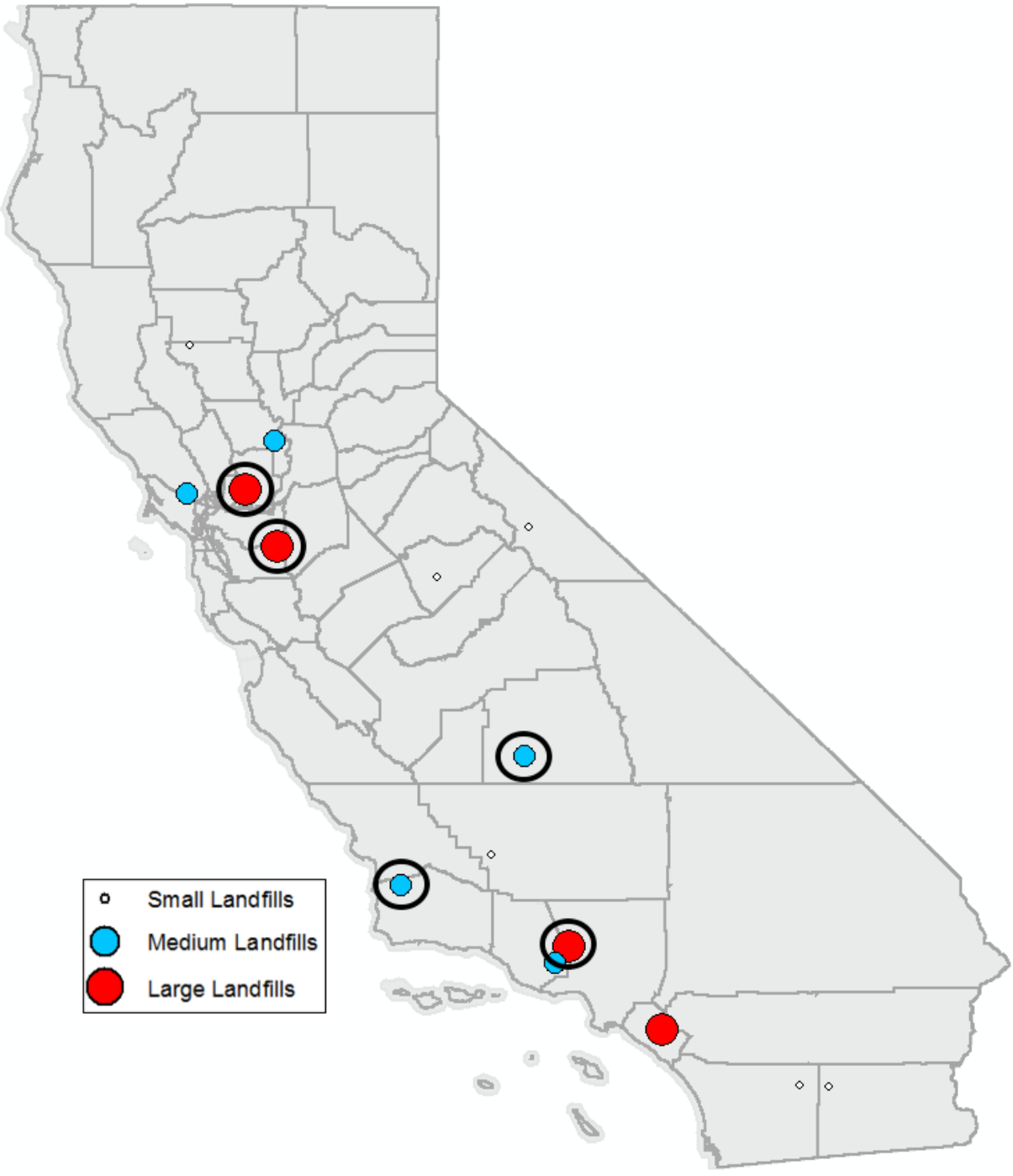

The five sites selected for static flux chamber testing are presented in bold in Table 2.3 and also marked in Figure 2.22. The emissions from the small landfills were low even though these sites did not have gas collection systems and thus small sites were not selected for further testing for static chamber analysis. The five selected sites included two medium-size facilities and three large landfills. The sites were located in the three climatic zones with the highest amount of waste in place in California including Csb, Csa, and Bsk climate zones (Figure 2.14). The total amount of waste in place at the five and fifteen selected sites was 154 million m^3 and 288 million m^3 and represented 13% and 24% of the total amount of WIP in California, respectively. All three large sites and one of the medium sites had all three cover systems, whereas the second medium site had only daily and intermediate covers (Table 2.3). The active face size and the relative areal extent of the three cover systems at the sites were variable and representative of the cover conditions in the state. The medium sites are areal landfills, whereas two of the large landfills (Altamont Landfill and Chiquita Canyon Landfill) are canyon landfills. The third large site (Potrero Hills Landfill) is located in a hilly area. Cooperation of sites was an essential component of selection for participation in the investigation.

PART 3 – FIELD INVESTIGATION, EXPERIMENTAL METHODOLOGY, AND NUMERICAL MODELING

3.1 Introduction

The field-testing program was designed with six specific objectives to obtain representative landfill surface gas flux and emissions data as a function of the main factors that control gas emissions from landfill sites:

- Obtain data and identify emissions trends for a large variety of landfill gas species ranging from the main landfill gases to various classes of trace gases with potential greenhouse gas, human health, and environmental impacts
- Obtain data from multiple landfills to assess the inter-landfill variability of gas emissions
- Obtain data over different seasons to assess effects of climatic conditions on inter- and intra-landfill gas emission variations
- Obtain data from all cover categories at a given landfill including daily, interim, and final covers to assess effects of cover category on intra-landfill gas emission variations
- Obtain data from locations underlain with wastes of varying ages to assess effects of waste age on intra-landfill gas emission variations
- Obtain data gas flux data at one landfill as a function of location away from a gas well, time of day of measurement, changes in gas extraction rates, and thickness of one soil cover material

The field testing included two types of measurement programs (October 2017 to November 2019): aerial measurements of methane and ethane at height above the landfill surfaces and measurements of all of the 82 landfill gas species included in the investigation directly on the landfill surfaces. Testing in the wet and dry seasons was conducted over the project period for both aerial measurements and ground-based measurements. Based on precipitation averages at the ground-based test sites, the wet season was defined as October 15 to April 30, and the dry season as May 1 to October 14.

3.2 Aerial Measurements of Gas Emissions

Aerial testing was completed at 16 sites during the project by Scientific Aviation to measure methane emissions. The test sites included the 15 landfills identified in Section 2 (Table 2.3) and one additional landfill (Sunshine Canyon Landfill) that provided opportunity for comparison of two similar, nearby landfills (Chiquita Canyon Landfill and Sunshine Canyon Landfill) that have different operational practices in regards to stripping of intermediate cover prior to placing overlying wastes (Chiquita Canyon Landfill strips the cover, Sunshine Canyon Landfill does not). When possible, ground testing and aerial testing were aligned to provide synchronous measurements of emissions.

Aerial surveys were conducted using a single engine Mooney aircraft that was instrumented with a Picarro G2401-m Analyzer (cavity ring down spectrometer). Ambient air is collected through tubes protruding from the right wing (Kynar, Teflon, and stainless steel). The Picarro instrumentation can analyze samples in-flight, allowing for almost instantaneous emissions results (Picarro, Inc. 2018). Methane and carbon

dioxide measurements are made with a Picarro 2301f cavity ring down spectrometer as described in Crosson (2008). Ethane measurements are made with an Aerodyne Methane/Ethane tunable diode infrared laser direct absorption spectrometer (Yacovitch et al. 2014). The plane flies in circles at various elevations around the site capturing both the up- and down-wind air concentrations. Assuming a Gaussian plume distribution, an emissions value can be determined in terms of mass per time (i.e., kg/hr). Emissions values have an accompanying uncertainty value, corresponding to a calculated uncertainty for each lap flown and then all uncertainties are summed, leading to generally higher values than expected for a typical standard deviation or similar value (Conley et al. 2017).

Aircraft have been used extensively to estimate surface emissions of pollutants and greenhouse gases (Karion et al. 2013, Caulton et al. 2014, Chang et al. 2014, Conley et al. 2016). Two sampling methods are routinely employed to estimate surface fluxes from aircraft, straight line transects and elliptical flight loops. All else being equal, the ellipse method is preferred because there are as many measurements of the upwind flux as there are the downwind. However, the ellipse method is not always practical, owing to complex terrain, air traffic restrictions, or other obstacles, which precludes creating a reasonable closed flight path around the site. Both methods have been demonstrated to be effective. Each of the methods has an uncertainty that can be determined from a theoretical analysis of the terms in the scalar budget of interest.

For the closed-path method (elliptical method) the flight path is chosen to build a virtual cylinder around the source, as presented in Figure 3.1. The flight path begins approximately 150 m above the ground level (AGL), depending on the site-specific terrain, which is aligned with the lowest safe flight level designated by the FAA, and ends at a higher altitude when enough laps have been conducted to reach a reliable measurement (Conley et al. 2017). At each point along the cylinder, the flux normal to the cylinder is calculated, thus providing the total amount of gas entering and leaving the cylinder. The difference between the two (assuming no other sources or sinks) is the surface emission rate.

Figure 3.1 Schematic of Flight Path around Unknown Source

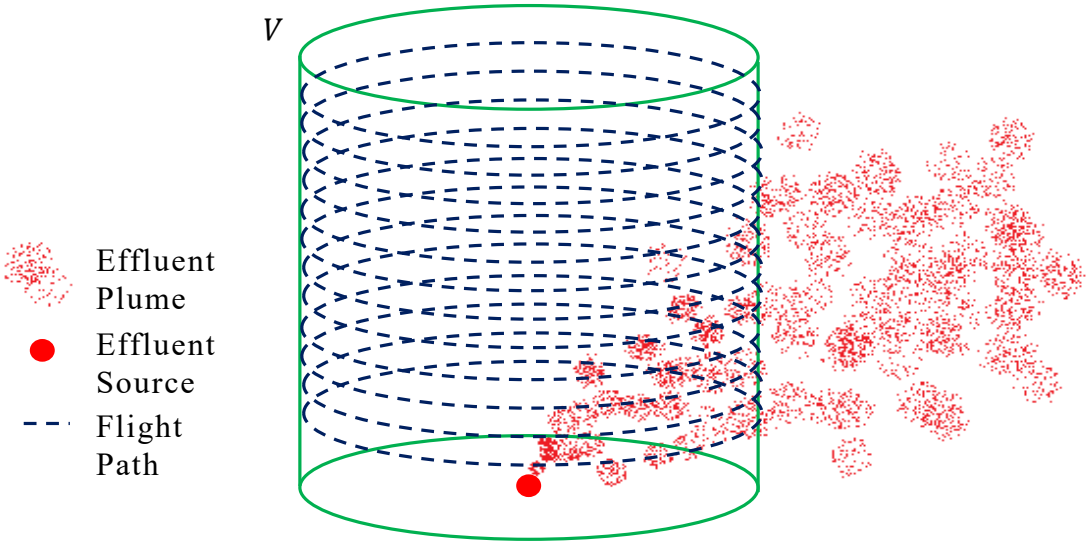

Mathematically, the method is straightforward and begins with the integrated form of the scalar continuity equation.

$$\langle \frac{\partial m}{\partial t} \rangle + \iiint \nabla \cdot \boldsymbol{F}_c dV = Q_c \tag{3.1}$$

Where, m is mass, t is time, F_c is flux, V is volume, Q_c is gas emission rate. The integrand in Equation 1 is the divergence of the flux and is summed (integrated) over the entire volume surrounding the source. The brackets in Equation 1 indicate a volumetrically averaged quantity, such as the time rate of change (or storage). Gauss's theorem is used to establish that the total divergence within a closed path is equal to the line integral (around the closed path) of the flux normal to the path.

$$Q_c = \langle \frac{\partial m}{\partial t} \rangle + \iiint \nabla \cdot \boldsymbol{F}_c dV = \left\langle \frac{\partial m}{\partial t} \right\rangle + \oint \boldsymbol{F}_c \cdot \hat{\boldsymbol{n}}\, dS \tag{3.2}$$

At any point along the path, the gas concentration is multiplied by the component of the wind vector normal to the path to yield the flux normal. Those fluxes are then summed over the closed path, and the result is the total divergence at that altitude. Next the divergences of all the circles at altitudes ranging from near the surface to the top of the plume are added together to yield the total surface source strength. The three main assumptions used in the analysis are: i) no vertical flux across the top of the virtual cylinder, ii) the virtual cylinder encompasses all of the plume from the ground source, and iii) all of the emissions are contributed by the ground source encompassed by the virtual cylinder formed by the flight path.

3.3 Ground-Based Measurements of Gas Emissions

Information for the landfills included in the ground-based testing program of the field investigation is summarized in Table 3.1. The table includes landfill name, landfill

location, size (provided in terms of waste in place), climate zone, annual precipitation, average daily temperature, and number of test locations at each landfill. A period of 30 years is commonly used for analyzing near-surface ground temperatures (e.g., Andersland and Ladanyi 1994) and was selected for this investigation of landfill cover systems. The climate zones for the selected landfills represented the zones with the highest amount of waste in place in the state (Figures 2.13 and 2.14).

Static flux chambers were used to directly evaluate the surface flux of all of the 82 gases included in the investigation. All of the available cover categories and all of the cover types under a given cover category were tested at the ground-testing sites. These locations also had different underlying waste ages, waste column heights, and waste characteristics. Subsequent to completion of the tests, cover temperatures at the test locations were obtained as well as densities of the covers were determined. When the flux tests were completed, cover material samples were collected to determine the geotechnical properties of the cover materials. Source gas (i.e., raw gas) from the landfill gas collection systems, was collected during each field campaign.

Table 3.1 – Ground Testing Landfill Sites

Landfill Name	Landfill Location	Waste in Place[a] (m^3)	Waste in Place[b] (m^3)	Landfill Climate Zone	Annual Ppt. (mm)[c]	Avg. Daily Temp (°C)[c]	Test Locations per Season
Santa Maria Regional Landfill	Santa Maria	1,360,577	8,385,395	Csb	462	14.9	5
Teapot Dome Disposal Site	Porterville	3,038,622	5,369,126	Bsk	278	17.4	5
Potrero Hills Landfill	Suisun City	26,454,935	52,928,614	Csa	462	18.2	7
Site A	Livermore	44,173,397	45,108,745	Csb	387	15.8	6
Chiquita Canyon Sanitary Landfill	Castaic	55,227,178	42,266,798	Csb	630	16.1	7

[a] WIP values reported by sites

[b] WIP values obtained from SWIS (2017)

[c] NOAA 30-year average for 1981-2010 (https://www.ncdc.noaa.gov/cdo-web/datasets)

3.4 Test Sites

Summaries of the ground testing sites are presented in the subsequent sections. The landfills are organized in order of smallest to largest WIP, as classified in SWIS. Thirty-year average weather data (1981 to 2010) for each site was obtained from NOAA (2019). All sites had active gas collection systems in place at the time of testing.

3.4.1 Teapot Dome Disposal Site

Teapot Dome Disposal Site (Teapot Dome Landfill) is a medium-size landfill (Section 2.2, Table 2.3) located in Porterville, California, approximately 115 km south of Fresno. The site is in an arid, steppe, and cold climate (Peel et al. 2007). Average weather data over a 30-year period indicate a daily average temperature of 17.4°C and average annual precipitation of 27.8 cm. The reported disposal area is 287,317 m^2 and the reported design capacity is 6,024,927 m^3 (SWIS 2017). The site is an areal site. The estimated closure date is 2022. The permitted throughput is 381 tonnes/day and the waste in place as of 2018 is 3,038,621 m^3 based on site records. Teapot Dome Landfill does not accept waste tires. The site has a specifically designated winter waste placement area used during the wet season. The site has daily and intermediate covers with no final cover present. Daily cover consists of processed green waste of approximately 4 cm (ranging from 2 to 8 cm) in thickness over 23 cm of soil at tested locations in the dry season, and a soil cover with a depth of 19 cm in the wet season at the tested locations. Intermediate cover consisted primarily of soils ranging in thickness from 34 to 78 cm at tested locations and in one case was 33 cm of soil overlying 9 cm of processed green waste. The cover types, designations, and thicknesses are presented in Table 3.2. A site map with testing locations is presented in Figure 3.2.

Table 3.2 – Teapot Dome Landfill Cover Characteristics

Cover Type Designation	Cover Type Description	Thickness (cm)
DC-GW	Daily Cover - Green Waste	27 (Dry Season)
DC-S	Daily Cover – Soil	19 (Wet Season)
IC-S+GW	Interim Cover - Soil + Green Waste	42
IC-N	Interim Cover - New (Waste)	35
IC-O	Interim Cover - Old (Waste)	78
IC-W	Interim Cover - Winter (Winter Waste Placement Area)	34

Figure 3.2 Teapot Dome Landfill with Test Locations (Google Maps 2019)

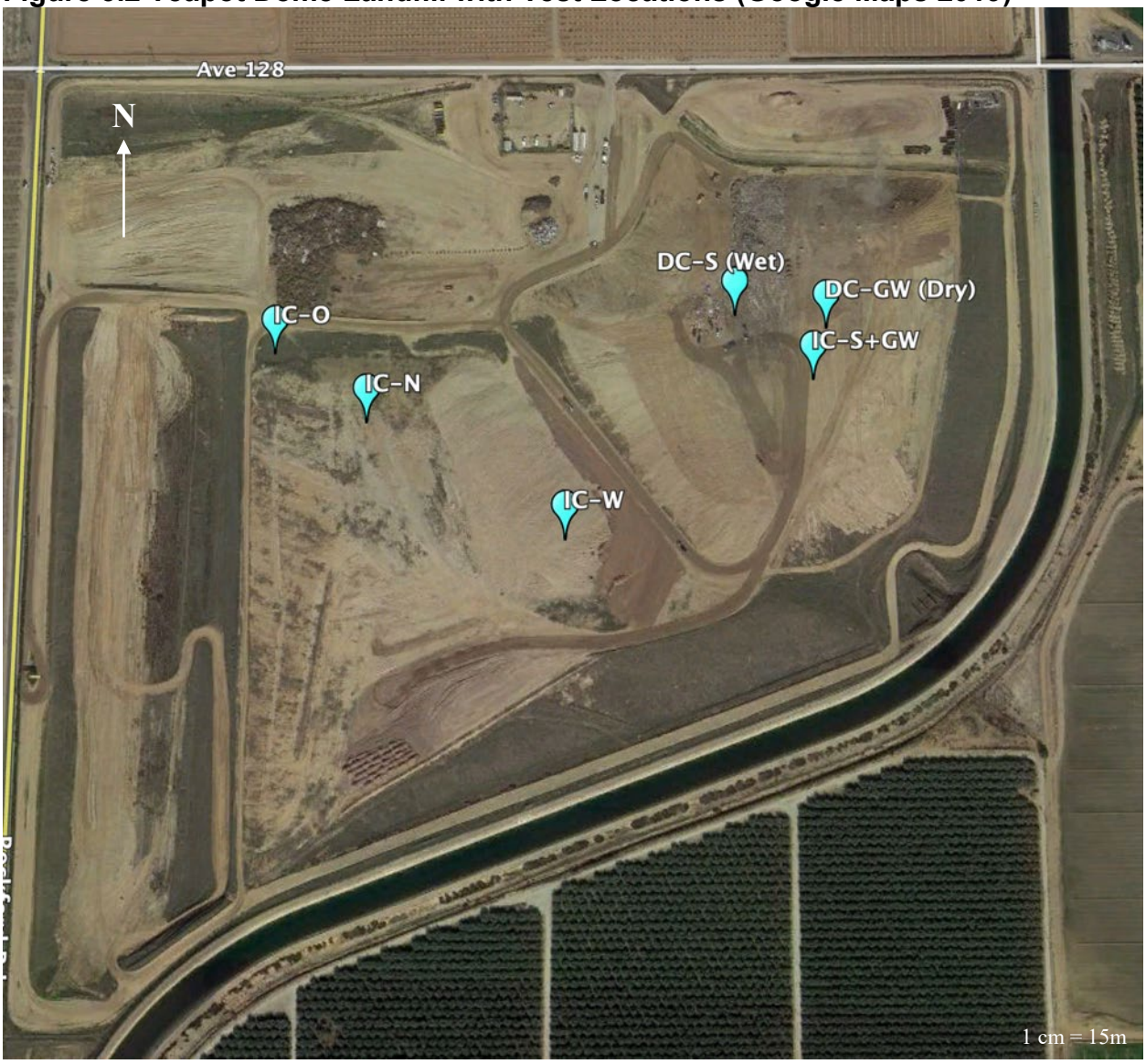

3.4.2 Santa Maria Regional Landfill

Santa Maria Regional Landfill is a medium-size landfill (Section 2.2, Table 2.3) located in Santa Maria, California. The site is in a temperate, dry summer and warm summer climate (Peel et al. 2007). Average weather data over a 30-year period indicate a daily average temperature of 14.9°C and average annual precipitation of 46.2 cm. The reported disposal area is 999,946 m^2 and the reported design capacity is 10,702,545 m^3 (SWIS 2017). The site is an areal site. The estimated closure date is 2020. The permitted throughput is 778 tonnes/day and the waste in place as of 2018 is 1,360,577 m^3, based on site records. Santa Maria Regional Landfill does not accept waste tires. The site has daily, intermediate, and final cover areas. Daily cover consists of wood waste received at the site with an approximate depth of 28 cm at tested locations. This daily cover is overlain with concrete fines with an approximate depth of 50 cm to

construct an interim cover. Other tested locations for interim cover consisted of soil with a thickness of approximately 68 cm. Final cover is present over an older cell of the site and consists of 100 cm of soil underlain by a GCL and 61 cm of interim cover material below the GCL over the waste mass. The landfill's gas-to-energy system is connected to a nearby hospital facility. The site operators indicated that large fluctuation in the gas draw from the landfill occurs due to the variations in hospital electricity use. During the field investigation, the gas-to-energy system was temporarily shut down to simulate of the high and low demand gas draw periods at the hospital. The cover types, designations, and thicknesses are presented in Table 3.3. A site map with testing locations is presented in Figure 3.3.

Table 3.3 – Santa Maria Regional Landfill Cover Characteristics

Cover Type Designation	Cover Type Description	Thickness (cm)
DC-WW	Daily Cover - Wood Waste	28
DC+IC	Daily Cover + Interim Cover	79
IC-H	Interim Cover - High Draw	68
IC-L	Interim Cover - Low Draw	68
FC	Final Cover	100

Figure 3.3 Santa Maria Regional Landfill with Test Locations (Google Maps 2019)

3.4.3 Chiquita Canyon Sanitary Landfill

Chiquita Canyon Sanitary Landfill (Chiquita Canyon Landfill) is a large-size landfill (Section 2.2, Table 2.3) located in Castaic, California, approximately 65 miles northwest of Los Angeles, California. The site is in a temperate, dry summer and warm summer climate (Peel et al. 2007). Average weather data over a 30-year period indicate a daily average temperature of 18.2°C and average annual precipitation of 46.2 cm. The reported disposal area is 1,040,008 m^2 and the reported design capacity is 48,885,055 m^3 (SWIS 2017). The site is a canyon site. The estimated closure date is 2019. The permitted throughput is 5443 tonnes/day and the waste in place as of 2018 is 55,227,178 m^3, based on site records. Chiquita Canyon Landfill accepts waste tires. The site has a specifically designated winter waste placement area used during the wet season. The site has daily, intermediate, and final cover areas. Daily cover consists of soil material disposed of at the site, with both uncontaminated (i.e., clean) and contaminated soils used, with thicknesses ranging from 34-50 cm at tested locations. Intermediate cover consists of soils ranging in thickness between 30 and 68 cm at tested locations. An overlying layer of green waste was used on slopes to aid with erosion control, ranging in thickness from 10 cm (old green waste, approximately 1-2 years old, visibly degraded, and gray) to 30 cm (new green waste, approximately 6 months old, and brown) at tested locations. Final cover consists of soil cover approximately 150 cm in thickness including 60 cm of foundation soil, 30 cm of compacted low hydraulic conductivity soil, and 60 cm of vegetative soil layer. The cover types, designations, and thicknesses are presented in Table 3.4. A site map with testing locations is presented in Figure 3.4.

Table 3.4 – Chiquita Canyon Landfill Cover Characteristics

Cover Type Abbreviation	Cover Type Description	Thickness (cm)
DC-Cl	Daily Cover - Clean Soil	34
DC-Co	Daily Cover - Contaminated Soil	50
IC-S	Interim Cover - Soil	30
IC-W	Interim Cover - Winter (Placement of Waste)	40
IC-OGW	Interim Cover - Old Green Waste	65
IC-NGW	Interim Cover - New Green Waste	98
FC	Final Cover	150

Figure 3.4 Chiquita Canyon Landfill with Test Locations (Google Maps 2019)

3.4.4 Site A

Site A is a large-size landfill (Section 2.2, Table 2.3) located in Livermore, California, approximately 55 km northeast of San Jose, California. The site is in a temperate, dry summer and warm summer climate (Peel et al. 2007). Average weather data over a 30-year period indicate a daily average temperature of 15.8°C and average annual precipitation of 38.7 cm. The reported disposal area is 1,910,054 m^2 and the reported design capacity is 95,110,624 m^3 (SWIS 2017). The site is a canyon site. The estimated closure date is 2025. The permitted throughput is 10,115 tonnes/day and the waste in place as of 2018 is 44,173,397 m^3, based on site records. Site A accepts waste tires. The site accepts both Class II (designated waste) (only site included in the analysis with Class II waste) and Class III (nonhazardous solid waste) waste. These wastes are disposed of at different areas at the landfill. Surface flux tests were conducted at both areas of the landfill to capture potential variations in surface gas flux between due to the different waste types. The site has daily, intermediate, and final cover areas. Daily cover consists of auto shredder waste that is covered with soil, ranging in thickness from

approximately 32 to100 cm at tested locations. Intermediate cover consists of different soils ranging in thickness from 40-150 cm at tested locations. Final cover at the site consists of two different types: a traditional final cover and an alternative final cover. The traditional final cover consists of a foundation soil layer, compacted clay layer, and a vegetative soil layer totaling 210 cm thickness. The alternative cover consists of a monolithic evapotranspirative (ET) cover system with an approximate thickness of 90 cm overlying existing interim cover of at least 30 cm. The cover types, designations, and thicknesses are presented in Table 3.5. A site map with testing locations is presented in Figure 3.5.

Table 3.5 – Site A Cover Characteristics

Cover Type Designation	Cover Type Description	Thickness (cm)
ED-II	Extended Daily - Class II (Waste)	100 (Dry Season); 230 (Wet Season)
ED-III	Extended Daily - Class III (Waste)	32 (Dry Season); 139 (Wet Season)
IC-II	Interim Cover - Class II (Waste)	39
IC-III	Interim Cover - Class III (Waste)	151
FC	Final Cover – Class III (Waste)	210
AFC	Alternative Final Cover – Class III (Waste)	120

Figure 3.5 Site A with Test Locations (Google Maps 2019)

3.4.5 Potrero Hills Landfill

Potrero Hills Landfill is a large-size landfill (Section 2.2, Table 2.3) located in Suisun City, California, approximately 72 km southwest of Sacramento, California. The site is in a temperate, dry summer and hot summer climate (Peel et al. 2007). Average weather data over a 30-year period indicate a daily average temperature of 16.1°C and average annual precipitation of 63.0 cm. The reported disposal area is 1,375,886 m^2 and the reported design capacity is 63,534,509 m^3 (SWIS 2017). The site is a canyon site. The estimated closure date is 2048. The permitted throughput is 3,928 tonnes/day and the waste in place as of 2018 is 26,454,935 m^3, based on site records. Potrero Hills Landfill accepts waste tires. In addition to regular daytime testing, nighttime testing was conducted at the site to capture diurnal differences in surface flux. The site has daily, intermediate, and final covers. The daily cover consists of auto shredder and green waste disposed of at the site, ranging in thickness from 31-76 cm at the tested locations. In the wet season, an additional daily cover of construction and demolition waste was tested, with a thickness of 21 cm at the tested location. The nighttime testing

was conducted at the auto fluff daily cover location during the dry season. The intermediate cover consists of different types of soil disposed of at the site, ranging in thickness from 84-290 cm. The high thickness (i.e., 290 cm) location for the upper bound of the interim covers was associated with soil material left in place from a former stockpile area at the site tested during the dry season. The final cover consists of 30 cm of topsoil overlying 60 cm of compacted clay overlying 30 cm of foundation soil overlying existing interim cover. The cover types, designations, and thicknesses are presented in Table 3.6. A site map with testing locations is presented in Figure 3.6.

Table 3.6 – Potrero Hills Landfill Cover Characteristics

Cover Type Designation	Cover Type Description	Thickness (cm)
DC-AF	Daily Cover - Auto Fluff	76 (Dry Season); 44 (Wet Season)
DC-GW	Daily Cover - Green Waste	31 (Dry Season); 52 (Wet Season)
DC-C+D	Daily Cover - Construction and Demolition Waste	21
IC-S	Interim Cover - Soil	290 (Dry Season)
IC-BM	Interim Cover - Bay Mud	130
IC-C1	Interim Cover - Cell 1	84
FC	Final Cover	120

Figure 3.6 Potrero Hills Landfill with Test Locations

3.5 Static Flux Chamber Testing

Surface gas emissions from landfills can be determined using small to large-scale direct and indirect measurement approaches applied on a continuous or discrete basis. Point, line, and areal measurements can be made. The test methods can be used to estimate flux and/or concentration of target gases. The majority of the testing techniques provide direct measurement of or estimation of concentration data and require the use of analytical or numerical models to estimate flux. The only method that can be used to directly determine concentrations and thereby flux (negative or positive) is the flux chamber method (Rolston 1986, Livingston and Hutchinson 1995). The static chamber technique is based on establishing a sealed volume above the measurement surface where gas is emitted through (or gas is absorbed through) such that the gas cannot escape and its accumulation (or depletion) in the volume can be monitored. The method allows for determination of flux from specific individual cover materials and types and has long been used for methane as well as trace gases at landfills to identify variability of surface flux across cover types and conditions (e.g., Bogner et al. 1995, Bogner et al. 1997c, Borjesson and Svensson 1997, Scheutz and Kjeldsen 2003, Barlaz et al. 2004, Scheutz et al. 2003, Abichou et al. 2006a). This method was selected for the project to obtain representative estimates of the gas emissions.

3.5.1 Static Flux Chamber Specifications

For this test program, custom-built large-scale stainless-steel chambers with lateral dimensions of 1 x 1 m (1 m^2 measurement area) and 0.4 m height were used. At each test location, two chamber tests were conducted to provide duplicate testing using nearby chamber placements. This provides measurement of variability and increases statistical significance of data obtained. Two different sampling intervals were used for the static flux chamber measurements. These were selected to provide different sampling rates. The sampling intervals, including logarithmic and linear time increments, were selected to account for different types of gas accumulation. Some gases accumulate and volatilize quickly, whereas other gas species accumulate more slowly and constantly, requiring the different sampling intervals for each chamber. The testing schedules are summarized in Table 3.7. At each cover type location, a total of 10 gas samples were collected consisting of 5 samples collected from Chamber A and 5 samples collected from Chamber B. The two chambers were placed at randomly selected locations within a given cover type ensuring safe distance from operations, level ground, and proximity of the two chambers.

Table 3.7 – Flux Chamber Testing Schedules

Sample Number	Chamber A Elapsed Time (min)	Chamber B Elapsed Time (min)
1	0	0
2	7	30
3	15	60
4	30	90
5	60	120

3.5.2 Protocol for Testing

For conducting a measurement: first the collar was inserted into the landfill surface to a depth of approximately 50 to 100 mm (Figure 3.7). Then a bentonite-water paste was applied around the perimeter of the collar at the soil-collar interface to seal the interface against gas leakage (Figure 3.8). Next the lid was placed and secured over the collar to form an air-tight seal. Finally, a fan installed on the underside of the lid, installed to circulate the gas collected to ensure uniform distribution prior to sampling, was turned on to start mixing the gas accumulating in the chamber. A generator, which was placed 30 m downwind from the chambers, was used to power the fan. A photograph of an assembled flux chamber is presented in Figure 3.9.

Figure 3.7 Installation of Chamber Collar

Figure 3.8 Placement of Bentonite around Perimeter of Collar

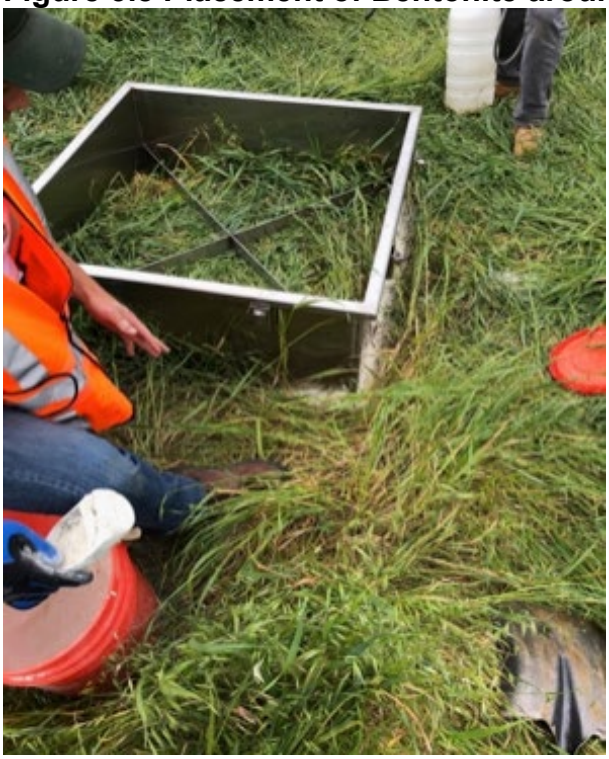

Figure 3.9 Assembled Flux Chamber

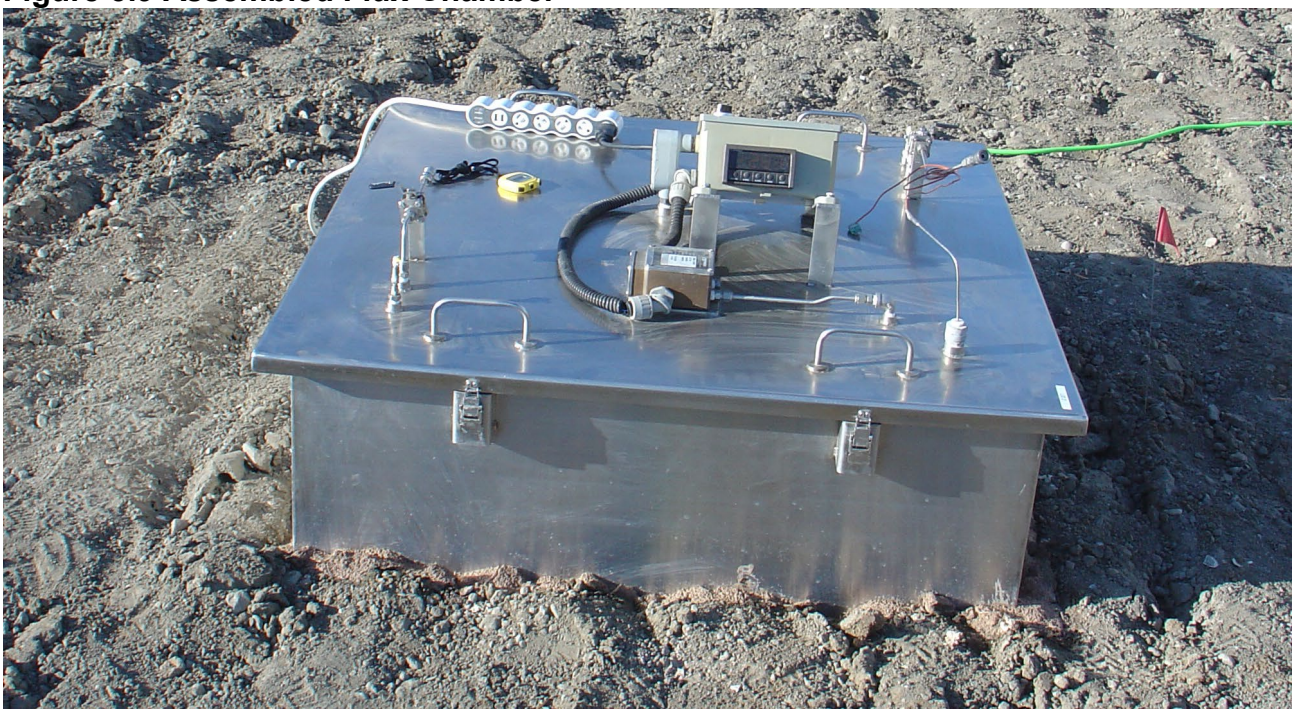

To prepare for the flux chamber testing, the Swagelok hardware on the chamber (Figure 3.10a) is baked at 225°C in an oven in the laboratory to volatilize any chemical residue

from previous use or storage. The hardware is installed on the chamber prior to each field campaign. Gas samples were obtained from the chamber during a sampling event by connecting gas canisters to sampling ports installed on the lid of the chambers (Figure 3.10b). The gas samples were obtained using 2-L evacuated stainless steel canisters equipped with bellow valves. The sampling ports consisted of ball valves, stainless steel tubing, and a Swagelok stainless steel Ultra-Torr vacuum fitting. For sampling, the valves were opened in the following order: the ball valve then the bellow valve. The valves were left open for approximately 10 seconds until the canister was full. The Rowland Blake Laboratory recommends opening the bellow valve on the canister a quarter turn only to ensure the canister is completely closed upon collection of the sample. Then, the valves were closed in the reverse order they were opened. This order was followed for opening and closing the valves to minimize contamination of the gas samples. The canister was then removed from the sampling port and was stored in a weather-proof box. The gas samples were collected using the pre-established schedule of sampling intervals (Table 3.7). The start time of an individual sampling event was established as the time of the sealing of the lid/starting of the fan on the lid.

Figure 3.10 Gas Sample Collection

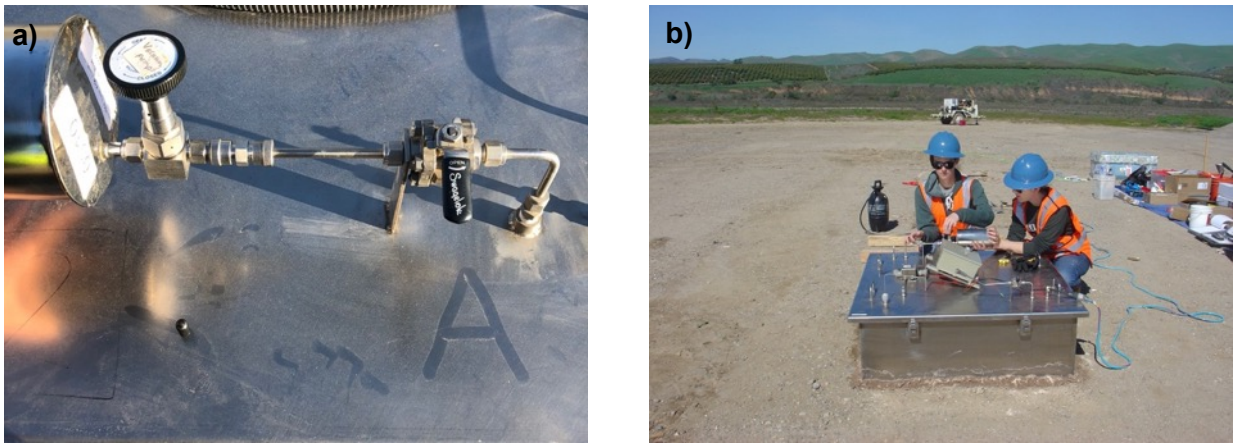

3.6 Complementary Field Tests

Field tests, in addition to surface flux tests were conducted to supplement interpretation of the results of the main test program and provide mechanistic explanations for the observed behavior. These additional tests included gas management system sampling, determination of cover temperatures, determination of in-situ cover properties, and collection of cover material samples for laboratory analysis.

Raw gas, which is the gas collected from the site prior to inflowing to the gas management system (flare or gas-to-energy facility) was sampled during each individual field campaign at a given site. This gas provides a composite gas concentration distribution for the given site at the time of sampling. Raw LFG samples were obtained from the flare system or gas-to-energy facility header at a location near the inlet to the system. The raw gas samples also were collected using the 2-L capacity, custom-built evacuated stainless steel canisters. The canister was directly connected to the sampling

port using a flexible PVC tube of minimal length. When all the connections were secured, the ball valve on the sampling port was opened to purge any ambient air present in the sampling connection. Subsequently, the bellow valve on the canister was opened for only 3-4 seconds until the canister was full to minimize the potential for gas escaping the canister back into the flare system. A total of two raw LFG samples was taken during each field campaign. An example of raw gas sampling is presented in Figure 3.11.

Figure 3.11 Raw Gas Sampling

After the last scheduled sample was retrieved from a given chamber, the lid was removed and the height of the collars was measured at midpoint along each side for use in calculation of the chamber volume (Figure 3.12a). In addition, the temperature of the tested cover material was measured at three different points within the perimeter of the chamber using a rigid thermocouple probe that was inserted approximately 50-150 mm into the cover material (Figure 3.12b). An attempt was made to insert the thermocouple probe to the maximum depth of 150 mm for each temperature measurement. However, this was not possible when the cover materials were exceedingly hard and stiff, in particular during the dry season.

Figure 3.12 Post-Flux Tests Prior to Removal of Chamber Collar

Further cover temperature analysis was conducted by using permanently installed thermocouple arrays. Temperature measurement arrays were installed within the intermediate covers at each of the five landfill sites at positions near the flux chamber test locations. The temperatures were measured using Type K thermocouples. The arrays each contained 4 thermocouple sensors that extended between 10 and 100 cm beneath the ground surface into the covers. Photographs of power augering to install a temperature array and retrieval of temperature data from datalogger are presented in Figure 3.13.

Figure 3.13 Installation of Thermocouple Array and Field Temperature Measurement

In addition, sand cone tests in accordance with ASTM D1556 were conducted at each chamber location to determine density of the cover materials (Figure 3.14). Certain cover systems, such as green waste, were not conducive to sand cone testing due to large particle size and void space. Finally, cover samples were obtained from each chamber location for laboratory analysis with the mass of samples ranging from 100 to 2000 g depending on the cover material. A surface sample was taken from each chamber (A and B). A sample also was taken as part of the sand cone test. Therefore, a total of 4 samples were collected per cover type.

Figure 3.14 Sand Cone Testing

Furthermore, the cover thickness was evaluated at each test location. A backhoe or excavator was typically provided by the landfill personnel and the cover material was excavated to determine the cover thickness after all of the measurements (i.e., flux chamber, collar depth, cover temperature, cover sample collection, and sand cone) were made at a test location. The excavation was made until the boundary between the cover system and underlying waste layers was delineated and the thickness of the cover system was measured using a measuring tape. If heavy construction equipment were not available, a shovel was used in relatively loose covers or thin covers. The cover thicknesses were measured experimentally in daily and intermediate cover systems. Excavations were not conducted in final covers in order not to disturb the integrity of these cover systems. Examples of cover thickness characterization is presented in Figure 3.15.

Figure 3.15 Cover Thickness Characterization

3.7 Laboratory Investigation

The main categories of laboratory analyses conducted in the investigation were analytical testing and geotechnical testing. The analytical testing was conducted to determine the concentrations of the chemical species included in the study. The geotechnical testing was conducted to determine index properties and engineering behavior of the cover materials.

Laboratory investigations were conducted to determine the concentrations of methane and nitrous oxide and to characterize the cover materials at each landfill. The gas concentrations were determined by the Rowland-Blake Laboratory at the University of California at Irvine. Geotechnical characterizations tests, including moisture content and density, particle size distribution and specific gravity were conducted at California Polytechnic University at San Luis Obispo to enable interpretation of the gas flux data.

3.7.1 Analytical Testing

The gas samples obtained in the field tests were analyzed at Rowland-Blake Laboratory in the Chemistry Department at the University of California-Irvine. The laboratory has high-resolution analysis systems capable of identifying and quantifying over 100 non-methane hydrocarbons and halocarbons including the (hydro)chlorofluorocarbons investigated in the current study. The laboratory is equipped with two VOC analytical systems, each of which consists of 3 Agilent 6890 gas chromatographs that house 2 electron capture detectors, 3 flame ionization detectors, and a quadrupole mass spectrometer.

For analysis of gas samples obtained in the study for VOCs, the amount of gas trapped from the canisters ranged between 10-1000 cm^3 (at standard temperature and pressure). This gas was introduced into the analytical system's manifold and then passed over glass beads contained in a loop and maintained at liquid nitrogen temperature. The flow was regulated by a Brooks Instrument mass flow controller (model 5850E), and was kept below 500 cm^3/min to ensure complete trapping of the

relevant components. This procedure pre-concentrated the relatively less volatile components of the sample (such as halocarbons and hydrocarbons) while allowing more volatile components (such as N_2, O_2, and Ar) to be pumped away. The less volatile compounds were next re-volatilized by immersing the loop containing the beads in hot water (80°C), and then flushed into a helium carrier flow (head pressure 330 kPa). This sample flow was then split into six streams. Each stream was chromatographically separated on an individual column and sensed by a single detector. Three GCs (each HP 6890) form the core of the analytical system. The research group uses two ECDs (sensitive to halocarbons and alkyl nitrates), two FIDs (sensitive to hydrocarbons), and one quadrupole MSD (for unambiguous compound identification and selected ion monitoring). The output signal was captured using Dionex software. Each resulting chromatogram was inspected, and each peak shape individually checked. This type of quality control is very important for datasets of large sizes, because a slight change in retention time or peak shape can cause problems for automated quantification.

Calibration and measurement intercomparisons are conducted on a continuous basis. Calibration is an ongoing process, whereby new standards are referenced to older certified standards, with appropriate checks for stability, and also with occasional inter-laboratory comparisons. Multiple standards are employed, including working standards that are analyzed every four samples and absolute standards that are analyzed twice daily. The UCI research group regularly collects and calibrates pressurized cylinders of air from different environments for use as working standards. The primary reference standard for halocarbons was previously calibrated from static dilutions of standards prepared in the laboratory. Its absolute accuracy is tied to a manometer measurement and how accurately the appropriate volume ratios for the dilution line used are known. For hydrocarbons, the research group uses a National Bureau of Standards propane standard (SRM 1660A) to calculate a Per-Carbon-Response-Factor (PCRF) for the FIDs. This is compared to PCRFs calculated from more readily available commercial standards to check the absolute accuracy of the commercial standard, as well as the appropriateness of using the same PCRF for different compounds. The research group had cross-checked their calibration scheme against absolute standards from other groups for both hydrocarbons and halocarbons. In addition, the group has participated in the Non-Methane Hydrocarbon Intercomparison Experiment (NOMHICE). The results of this experiment demonstrate that the group's analytical procedures consistently yield accurate identification of a wide range of unknown hydrocarbons and produce excellent quantitative results. The typical absolute accuracy is estimated to be 2-10%, and up to 30% for some compounds, increasing as the detection limits are approached (Colman et al. 2001). The researchers impose a conservative limit of detection (LOD) of 3 pptv on the NMHCs. The halocarbon LOD varies by compound, from 0.01 pptv for chlorobrominated species (e.g., $CHBrCl_2$, $CHBr_2Cl$, CH_2BrCl) to 10 pptv for CFC-12. Once the samples are assayed, the stored chromatograms are individually inspected and the reports from these are then summarized in spreadsheet format and checked for inconsistencies. A summary of the LODs for all chemicals included in this study is presented in Appendix B (Table B2).

3.7.2 Geotechnical Testing

The cover material index properties and engineering behavior were determined at the geotechnical/geoenvironmental testing laboratories in the Civil and Environmental Engineering Department at Cal Poly. Geotechnical tests were conducted to determine moisture content, specific gravity, particle size distribution, and Atterberg limits of the cover materials to supplement the interpretation of the surface flux data.

A total of 232 samples were collected from the five landfill sites during the course of dry and wet season testing, consisting of daily, intermediate and final covers from both the surface and the sand cone depth, when applicable. Moisture content tests were conducted on all samples, and specific gravity tests were conducted on samples from each cover type. Particle size analysis was only conducted on soil samples. Atterberg limits were performed only on plastic soils when applicable. If a sand cone test could not be conducted in the field, a density range estimate was made in the laboratory to complete phase relations for each cover type.

The moisture contents of the cover materials were determined using procedures described in ASTM D2216. For each material, samples with masses in the range of 200 to 600 g were used. Larger quantities of samples were required for materials with larger particle sizes to obtain representative measurements.

The specific gravity of the landfill covers composed of soil was determined using the standardized procedure described in ASTM D854. A modified version of the same test was used for non-soil cover materials with relatively large particle sizes based on the methodology outlined in Yesiller et al. (2014). A 1900-mL mason jar was used to accommodate larger particle diameters of materials such as green waste or auto-shredder waste. To avoid floating particles, the samples were placed in a mesh bag (191 x 356 mm) with a lead weight. An example specific gravity test setup is presented in Figure 3.16.

Figure 3.16 Modified Specific Gravity Testing for Large Particle Cover Materials

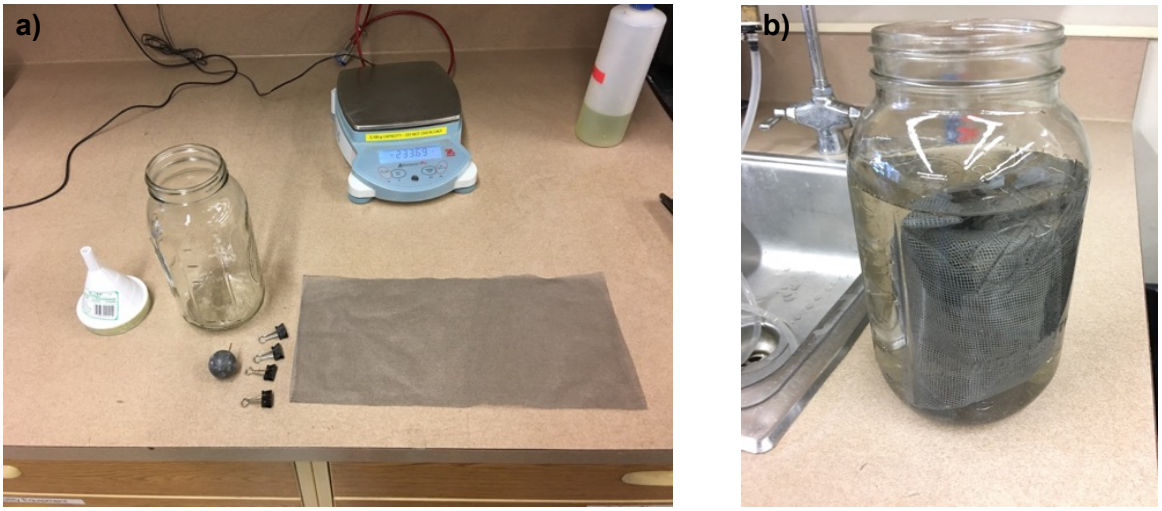

The particle size distribution tests for the soil samples were conducted using ASTM D422. The analysis consisted of first a hydrometer test to determine the distribution of fine-grained particles, followed by a dry sieve to determine the composition of the coarse-grained fraction. The particle size analysis results were used to classify the soils based on the United Soil Classification System (USCS) and also the United States Department of Agriculture (USDA) Method. On fine-grained soils with plastic characteristics, Atterberg Limits tests were performed according to ASTM 4318.

Density was estimated in the laboratory for cover materials where sand cone tests could not be determined in the field. The density was obtained either using a vessel of known volume filled to an approximated representative field density and then determining the mass of the material in the vessel or using a water submersion method similar to the bulk density method (ASTM D7263).

3.8 Determination of Surface Flux

In order to quantify gas emissions from the numerous cover materials, surface flux specific to each location and constituent was determined. The surface flux of the 82 chemicals was determined by converting the concentration datasets obtained from the field investigation to surface flux using Equation 3.3.

$$F = \frac{dC}{dt} * \frac{V}{A} \tag{3.3}$$

Where, F is the surface flux (expressed in units of mass per area-time.), dC/dt is the concentration gradient, (the rate of change of concentration over time within the flux chamber), V is the volume within the static flux chamber (units of volume), and A is the area of the landfill surface enclosed by the chamber (units of area). To determine the concentration gradient, plots of the concentration versus sampling time were constructed for each location, constituent, and chamber. Prior to calculating the surface flux, a linear regression analysis was performed to evaluate the fit of each concentration versus time dataset to obtain gradient data.

The fit of each linear regression model was evaluated using coefficient of determination (R^2), which indicates how well the regression models the data (Devore 2008). The analysis started with generating the concentration versus time data for each chamber measurement. R^2 acceptance and rejection criteria were used to determine the number of points that may need to be removed to potentially reach a predetermined threshold. Point removals were performed from data points obtained later in time to earlier points in order to give higher weight to the earlier points. The earlier data points were assigned higher weight in the analysis due to the potential decrease in the concentration gradient over the duration of the sampling event, which can be caused by the accumulation of the chemical that may occur after extended run time of the chamber. The target threshold R^2 value was established as 0.9.

For determination of flux, first, a regression line was fit to all five datapoints from a given chamber. If the fit resulted in a linear relationship with R^2>0.9, all data points were used. If R^2<0.9, data points were systematically removed from the curve fit starting with the last point until a fit with R^2>0.9 was attained (Yeşiller et al. 2018). Up to 2 data points are removed from a given chamber test, leaving three data points for determining the R^2 value. (An example of the regression evaluation process is presented in Figure 3.17.

Figure 3.17 Regression Evaluation Process with 3, 4, and 5 Points

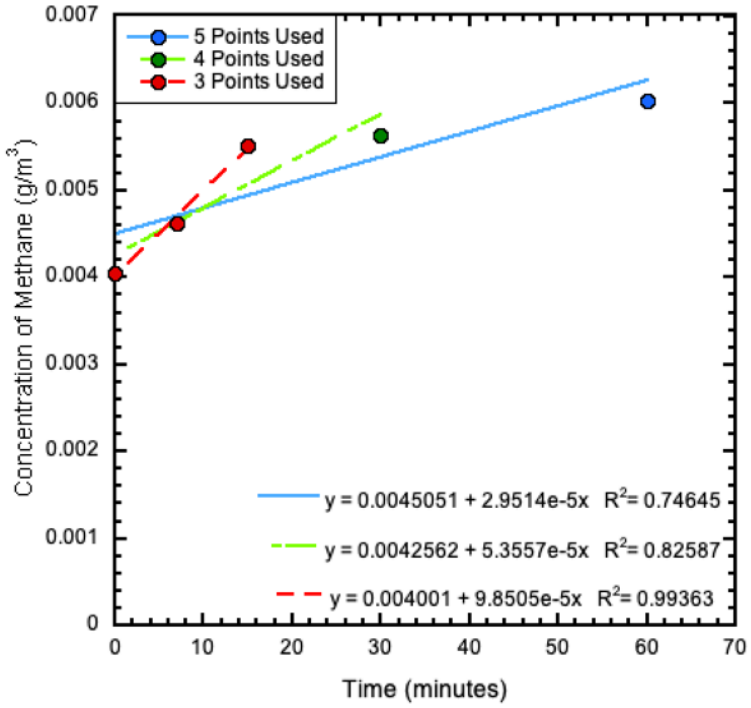

For cases when R^2 was not greater than or equal to 0.9 for both chambers at a given test location, a secondary threshold of R^2 greater than or equal to 0.7 was used and for these cases based on engineering judgement, the R^2 value is reported in parentheses after the calculated flux value to indicate the relative confidence in the regression fit. When the alternate method to determine flux was used, only one value per cover type was calculated. For tests conducted during excessively windy conditions and for some highly porous covers (i.e., auto fluff) with R^2<0.7, the first two data points were used in the analysis when flux could not be calculated otherwise for either chamber. In these cases, the data points indicated concentrations increasing with time and then quickly decreasing starting with the third data point. This trend indicated that dilution of the accumulated chemicals in the chamber was present.

The concentration values for the gases included in the analysis were provided in units of ppmv and ppbv, respectively by the Rowland Blake Laboratory. Using temperature and barometric pressure data recorded during the field campaigns, the concentration was converted from volumetric-based to mass-based units, as shown in Equation 3.4.

$$C_{(\frac{g}{m^3})} = \frac{C_{(ppmv)} * P * MM * 1e3}{1e6 * R * T} \quad (3.4)$$

Where, C (g/m^3) is the concentration expressed in mass-based units, C (ppmv) is the concentration expressed in volume-based units, P is atmospheric pressure in kPa, MM is molar mass in g/mol, R is the ideal gas constant expressed in units of J/mol*K, and T is soil temperature in Kelvin.

3.9 Methane Generation and Gas Collection Efficiency

Moisture content, temperature, pH, presence of oxygen, and waste age/composition significantly affect methane generation. In general, high methane generation is associated with fresh, high moisture content MSW in a warm environment under anaerobic conditions and a stable, slightly acidic pH ((Tchobanoglous et al. 1993, Christensen et al. 1996).). MSW with a high fraction of biodegradable organic matter has high methane generation potential. Site specific climatic conditions (i.e., precipitation/average temperatures) and operational practices (i.e., waste depth, degree of compaction, waste in place) affect the MSW state and associated LFG generation rate.

Given that in-situ methane generation rates in full scale, MSW landfills are difficult to measure, various kinetic models have been developed to estimate generation rates. USEPA's Landfill Gas Emissions Model (LandGEM) is the most widely applied kinetic model to estimate LFG generation rates from MSW landfills. LandGEM is based on a first order MSW decomposition rate analysis for quantifying methane generation rates (Equation 3.5). The site-specific inputs to the LandGEM model include the landfill open and expected closure dates (or waste design capacity) and the past and projected annual waste acceptance rates (Mg or short tons/year). The first order decomposition rate and methane generation potential are singular values for a given site at a given climatic region using LandGEM analysis, whereas variations in these parameters occur potentially over time, space, and between sites at a given climatic region.

$$Q_n = kL_0 \sum_{i=0}^{n} \sum_{j=0}^{0.9} \frac{M_i}{10} e^{-kt_{i,j}} \quad (3.5)$$

Where, Q_n is the methane generation rate in year n (m^3/year), M_i is the waste mass placement in the ith year, j is an intra-annual time increment, t is time (years), k is the first order decay rate (year^{-1}), and L_0 is the methane generation potential (m^3/Mg wet waste).

LandGEM predictions are based on two parameters: first order MSW decay rate (k, year^{-1}) and methane generation potential (L_0). The first order decomposition rate k is a site-specific parameter that depends on the moisture content, availability of nutrients, pH, and temperature of the waste mass, among many potential factors. Higher k values used in LandGEM simulations result in both a faster increase in methane generation and a faster decay in methane generation over time (USEPA 2005). First order decomposition rates have been reported to range from 0.003 to 0.21 year^{-1}, where

higher values have been determined for bioreactor landfills up to 2.2 $year^{-1}$ (Tolaymat et al. 2010, Kim and Townsend 2012). L_0 represents the maximum volume of methane that can be generated per unit input of MSW and is based on the composition of the incoming and previously placed MSW (Krause et al. 2016). High L_0 values are associated with wastes with high cellulose content, equivalent to a high fraction of biodegradable organic carbon. L_0 values typically range between 6.2 to 270 m^3/Mg wet waste, where higher and lower values have been reported for individual waste components (i.e., paper or food waste alone) (US EPA 2005, Krause et al. 2016). Based on field data collected in the early 1990's, the USEPA recommends several default parameter sets of both k and L_0 based on the climatic conditions (i.e., precipitation) at a given landfill site.

As input, LandGEM requires waste acceptance data for the entire operational lifespan of a landfill. Insufficient records for multiple study landfills and unknown waste generation rates in the future required both a back and forward projection in the waste acceptance rates over time. Various mathematical models were tested and compared to fit the trends in overall waste generation data from open to closure.

Waste generation data used as the basis for curve fitting was obtained from two sources including CARB compiled data (1996 to 2019) and data (1991 to 2012) compiled by Scott Walker (2012). The generation data from these sources were combined, where Walker's data was used pre-2012 and CARB's data was used for 2013-2019 resulting in final datasets for each landfill for the period 1991-2019. Open and closure dates for each landfill were obtained from the Walker (2012) and SWIS databases, respectively.

MATLAB's (r2017a) built in curve fitting toolbox (i.e., the "fit" function) was used for computing back and forward trends in waste generation rates. The trust region algorithm (based on non-linear minimization of sum of squared residuals) and all default optimization settings were used for each curve fit. Values of the parameters were routinely initialized at the same starting points for each curve fitting run (at 0.01). Each of the curve fits were passed through the origin (i.e., zero WIP in the first year) by modifying the mathematical functions and/or corresponding optimization routine. Waste in place as a function of time was used as the dependent variable for curve fitting. For each landfill, time dependent WIP values from 1990 to 2019 were obtained from the 2012 WIP estimate from the Walker dataset and by adding or subtracting the respective generation values. The mathematical model functions investigated for curve fitting ranged from exponential, to polynomial and power functions of different orders (Table 3.8). In addition, hyperbolic and single and double logistic equations were investigated as they replicated the trends in WIP for multiple landfills. Model performance was assessed using two quantitative criteria: coefficient of determination (R^2) and the root mean squared error. Qualitative performance of each model was evaluated by assessing whether the curve fits over or underpredicted past or future WIP values. Based on these performance criteria, an acceptable mathematical model was selected for each site. For Santa Maria Regional Landfill, all curve fits led to equally poor

predictions; therefore, linear interpolation was used to estimate back and forward trends in waste generation rates over time.

Table 3.8 – Mathematical Models Used to Predict Back/Forward Trends in Waste Generation Over Time (*t* represents time)

Model Name	Mathematical Formulation	Model Parameters
Exponential-1	$WIP = Ae^{Bt}$	A, B
Exponetnial-2	$WIP = Ae^{Bt} + Ce^{Dt}$	A, B, C, D
Polynomial-1	$WIP = At^2 + Bt$	A, B
Polynomial-2	$WIP = At^3 + Bt^2 + Ct$	A, B, C
Polynomial-3	$WIP = At^4 + Bt^3 + Ct^2 + Dt$	A, B, C, D
Power-1	$WIP = At^B$	A, B
Power-2	$WIP = At^B + C$	A, B, C
Hyperbolic	$WIP = \frac{At}{(B+t)}$	A, B
Logistic	$WIP = \frac{A}{(1+e^{(-Bt+C)})}$	A, B, C
Double Logistic	$WIP = \frac{A}{(1+e^{(-Bt+C)})} + \frac{D}{(1+e^{(-Et+F)})}$	A, B, C, D, E, F

Full methane mass balance in a landfill (Equation 3.6) has the methane generated for the *n*th year (Q_n) equivalent to the summation of that collected by the gas extraction system ($Q_{co,n}$), emitted through the cover ($Q_{em,n}$), oxidized in the cover ($Q_{ox,n}$), stored in the landfill ($Q_{st,n}$), or migrated through the sides or bottom of the landfill ($Q_{mi,n}$) (Barlaz et al. 2009).

$$Q_n = Q_{co,n} + Q_{em,n} + Q_{ox,n} + Q_{st,n} + Q_{mi,n} \quad (3.6)$$

While gas collection efficiency can be determined using the full mass balance, the efficiency typically is calculated considering the emissions and collection data (e.g., Barlaz et al. 2009) (Equation 3.7) due to the lack of specific data for gas oxidation in covers, gas stored in the waste mass or migrated through the liner systems. The gas emissions measured in the field campaigns and gas extraction data obtained from the landfills as reported to CARB were used to estimate the collection efficiencies in this study.

$$\alpha_n = \frac{Q_{co,n}}{Q_{co,n} + Q_{em,n}} \quad (3.7)$$

A baseline analysis using default LandGEM parameters and a more refined approach using modeled parameters were included to provide a potential range of values for gas generation. The refined approach included data from studies more recent than the 1990s. A methane mass balance was used to assess the effectiveness of the refined approach.

3.9.1 Default LandGEM Analysis

Baseline estimates of methane generation were obtained by varying the LandGEM default parameter values. LandGEM includes two default parameter sets (Table 3.9). The first set is used to determine the applicability of the Clean Air Act (CAA) regulations for MSW emissions, relating to New Source Performance Standards for new MSW landfills and Emissions Guidelines for existing MSW landfills (US EPA 2005). The second set is based on emissions factors from the USEPA's AP-42 report summarizing air pollutant emissions factors for MSW landfills and is used in the absence of site-specific data for methane or NMVOC concentrations (US EPA 2005, 2008).

Table 3.9 – Default LandGEM Parameters

Default Parameter Set	Landfill Type	L_0 (m^3/Mg wet waste)	k ($year^{-1}$)
CAA	Conventional	170	0.05
	Arid Area	170	0.02
Inventory	Conventional	100	0.04
	Arid Area	100	0.02

Conventional and arid are used for landfills in areas with rainfall exceeding or less than 635 mm/year, respectively (Wang et al. 2013, 2015). The landfills in the study were located in areas with 278 to 630 mm/year precipitation. Four simulations, as listed above in Table 3.9, were run for each landfill and then averaged to determine the baseline methane generation and corresponding collection efficiency values for 2018. To assess uncertainty in these predictions, 95% prediction intervals were calculated assuming the error residuals were normally distributed with a mean of 0 and standard deviation equal to the standard deviation of methane generation for 2018-2019.

3.9.2 Refined LandGEM Analysis

The refined analysis was based on the improved determination of both L_0 and k using two novel, yet independent approaches.

3.9.2.1 Determination of Waste-Specific L_0 Parameter

A waste component specific methane generation potential model, similar to that proposed by Machado et al. (2009) and Cho et al. (2012), was adopted to predict overall L_0 values for each landfill. This model assumes that methane is generated from the biodegradable MSW components only and that an aggregate, whole-site methane generation potential can be calculated based on the weighted average of the individual methane generation potentials ($L_{0,i}$) of the n waste components. The individual methane generation potentials are multiplied by the weight fraction of the ith component in the waste stream and summed to determine the overall L_0 value (Equation 3.8). In the model, F is a correction factor (ranging from 0 to 1) that scales down the L_0 values predicted in the laboratory assays to that expected under field conditions. Typically, the specific methane generation potential for each waste component is measured independently in the laboratory using biochemical methane potential assays which are representative of the maximum methane that can be generated under optimal conditions.

$$L_0 = F * \sum_{i=1}^{n} L_{0,i} * WF_i \quad (3.8)$$

A comprehensive Monte Carlo analysis was conducted to provide whole-site methane generation potentials for each landfill. Monte Carlo analyses evaluate the uncertainty of model predictions due to the uncertainty in methane generation potentials and the correction factor. First, probability distributions of uncertain model inputs are assigned or developed, based on prior knowledge or expert judgement. Next, the model is run for thousands of iterations, where each model run randomly samples the input probability distributions, and the model predictions are stored. After a large number of iterations has been reached, the distribution of model predictions (and hence the predictive certainty) was analyzed and compared with a parametric statistical model.

To develop the sampling distributions, a large number of waste component specific methane generation potentials were obtained from the literature for a variety of biodegradable wastes: food, paper, green (yard), wood, and textiles. All other constituents of MSW were considered inert and non-biodegradable. Only studies that had explicitly stated that a laboratory BMP assay was conducted were included. Based on the pervasiveness of certain components within these general categories, specific sampling distributions of $L_{0,i}$ values were developed for cardboard, office paper, newspaper, magazines/coated paper/junk mail, other miscellaneous paper, mixed food waste, mixed yard waste, manure, mixed textile, and mixed wood waste. The cardboard component comprised $L_{0,i}$ values ranging from un-corrugated/corrugated cardboard to paperboard products. The office paper component comprised $L_{0,i}$ values ranging from printer paper to recycled office paper of varying degrees. The coated paper component comprised $L_{0,i}$ values ranging from magazines, brochures, phone books, to junk mail products. The miscellaneous paper component comprised remaining paper materials, including soiled paper. Food waste components included $L_{0,i}$ values calculated for mixed food wastes separated to individual fruits and vegetables. Similarly, green waste components included $L_{0,i}$ values calculated for mixed yard wastes separated to individual branches, grasses, and leaves/stems. Textile waste components included $L_{0,i}$ values calculated for mixed textile wastes separated to individual products containing leather, rubber, cotton, and cloth diapers. Finally, wood waste components included $L_{0,i}$ values ranging from mixed wood wastes (C&D materials) to individual wood obtained from different tree specimens. The values for each of these distributions are presented in Appendix B (Table B3).

Non-parametric statistical distributions were developed for waste components with a sufficient number of samples (N > 20). A non-parametric kernel density estimator (KDE) tool based on the kd-trees algorithm (MATLAB version) was used to develop the non-parametric probability distributions for sampling. A Gaussian kernel was used along with a rule of thumb estimator for determining the bandwidth of each kernel center. An example KDE distribution is developed for the cardboard waste component (Figure 3.18). The probability density estimate of the KDE model is overlain on an empirical histogram of the $L_{0,i}$ values obtained from the literature. The KDE model matched the general trend in the empirical probability density estimates of the data obtained from the

literature. Methane generation potential values around 230 m^3/Mg have a higher probability of selection in the MC simulations, based on the bell shape of the KDE curve. Similar bell-shaped KDE distributions were obtained for office paper, newspaper, coated paper, miscellaneous paper, food wastes, yard wastes, textile wastes, and wood wastes.

Figure 3.18 Empirical (Blue Histogram) and Modeled (Red Line, KDE) Probability Density Estimates for the Methane Generation Potential of Cardboard Waste

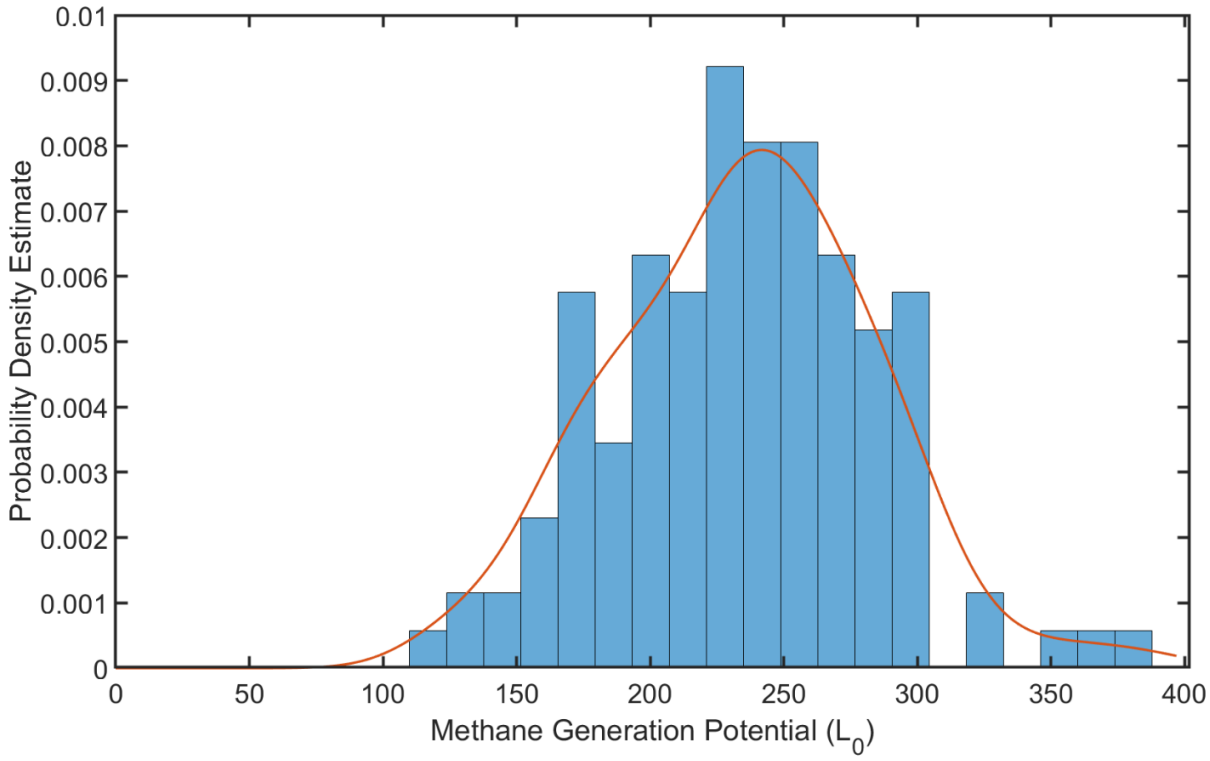

Model inputs that lacked sufficient data (N <20) to estimate kernel density distributions were assigned uniform probability densities. The ranges of the uniform distributions covered the minimum and maximum values expected based on the values obtained from the literature. $L_{0,i}$ values for manure and values of the correction factor (F) were designated as uniform input distributions.

Table 3.10 summarizes all input sampling distributions for the MC analysis and the corresponding references from which the values of $L_{0,i}$ were obtained. A majority of the input distributions was developed using the KDE tool. The number of data points used in the construction of each kernel distribution ranged from 31-125. Office paper had the highest methane generation potential. Food wastes had the highest range in $L_{0,i}$ values, based on the median of the $L_{0,i}$ values obtained from the literature. $L_{0,i}$ values were low for both wood waste and green waste, which contain higher amounts of lignin (non-biodegradable) compared to cellulosic matter (biodegradable).

Table 3.10 – Input Sampling Distributions Constructed for the MC Analysis

Model Input	Distribution Type	N	Min.	Median	Max.	Reference
Cardboard	KDE	125	119	236	387	1-8
Office Paper	KDE	49	115	293	369	1-3, 5-10
News-Paper	KDE	39	18	75	322	1,2,3,7,8
Coated Paper	KDE	38	84.4	289	366	1,2,3,8
Misc. Paper	KDE	43	106	279	367	1,2,8,13
Food Wastes	KDE	68	11	272	538	6, 8-11, 12-20
Green(Yard) Wastes	KDE	31	30.6	124	345	3, 6, 8, 13, 16, 21
Manure	Uniform	-	2	-	99	20
Textile Wastes	KDE	43	3	207	365	4, 6-8,10, 11, 13
Wood Wastes	KDE	49	0	41.2	310	6-8, 10, 11, 19, 22
Correction Factor, F	Uniform	-	0	-	1	12
Weight Fractions (WF)	Point	-	0	-	100	-

[1]Vermuelen et al. 1993, [2]Owens and Chynoweth 1993, [3]Eleazer et al. 1997, [4]Jokela et al. 2005, [5]Qu et al. 2009, [6]Machado et al. 2009, [7]Krause et al. 2018a, [8]Krause et al. 2018b, Chickering et al. 2018, [9]Ishii and Furuichi 2013, [10]Wangyao et al. 2010, [11]Jeon et al. 2007, [12]Cho et al. 2012, [13]Karanjekar et al. 2015, [14]Zhang et al. 2007, [15]Lee et al. 2009, [16]Buffiere et al. 2006, [17]Cho et al. 1995, [18]Nieto et al. 2012, [19]Manfredi et al. 2010, [20]Moody et al. 2011, [21]Yazdani et al. 2012, [22]Wang et al. 2011

Site specific waste characterization data was obtained from CalRecycle (2019b). The web tool integrates the 2016 Statewide Waste Characterization study data with local employment and population data to provide both commercial and residential waste disposal estimates and composition for different counties and specific jurisdictions. For each landfill, commercial and residential disposal and composition data from the nearest jurisdiction was downloaded and used to determine the weights required in Equation 3.8. The data from the commercial and residential sectors were filtered to only include biodegradable waste components resulting in 22 distinct material types: various types of cardboard, paper waste, food waste, yard waste, textile waste, manure, and other wood wastes such as clean dimensional lumber. The commercial and residential sectors for each material type were then summed, and a general weight fraction for each material type was determined using the total amount of disposed biodegradable waste.

For each landfill, L_0 values were predicted a high number of times using Equation 3.8 and random sampling of the model inputs/distributions presented in Table 3.10. Preliminary analysis varying the number of simulations from 10K to 50K indicated that 50,000 model simulations was sufficient to reach a stable output parametric distribution. A logarithmic (base 10) transformation of the predicted L_0 values was required to improve the parametric distribution model fit. The empirical histogram of the output L_0 values predicted for Santa Maria Regional Landfill overlain with the parametric model fit

is presented in Figure 3.19. The extreme value parametric distribution demonstrated the best fit to the histograms summarizing the empirical probability density estimate for all L_0 predictions. This result was confirmed by comparing the maximum likelihood estimate of all parametric model fits from the parametric models available in MATLAB's statistics toolbox. The uncertainty of L_0 values was summarized using the 95% confidence intervals derived from the 5% and 97.5% quantiles of the fitted extreme value distribution. For this particular output distribution, the mean value of L_0 was 79.3 m^3/Mg with a variance of 1.43 m^3/Mg.

Figure 3.19 Empirical (Blue Histogram) and Modeled (Red Dash Line, Using a Parametric Model) Probability Density Estimates for the Methane Generation Potential of Santa Maria Regional Landfill

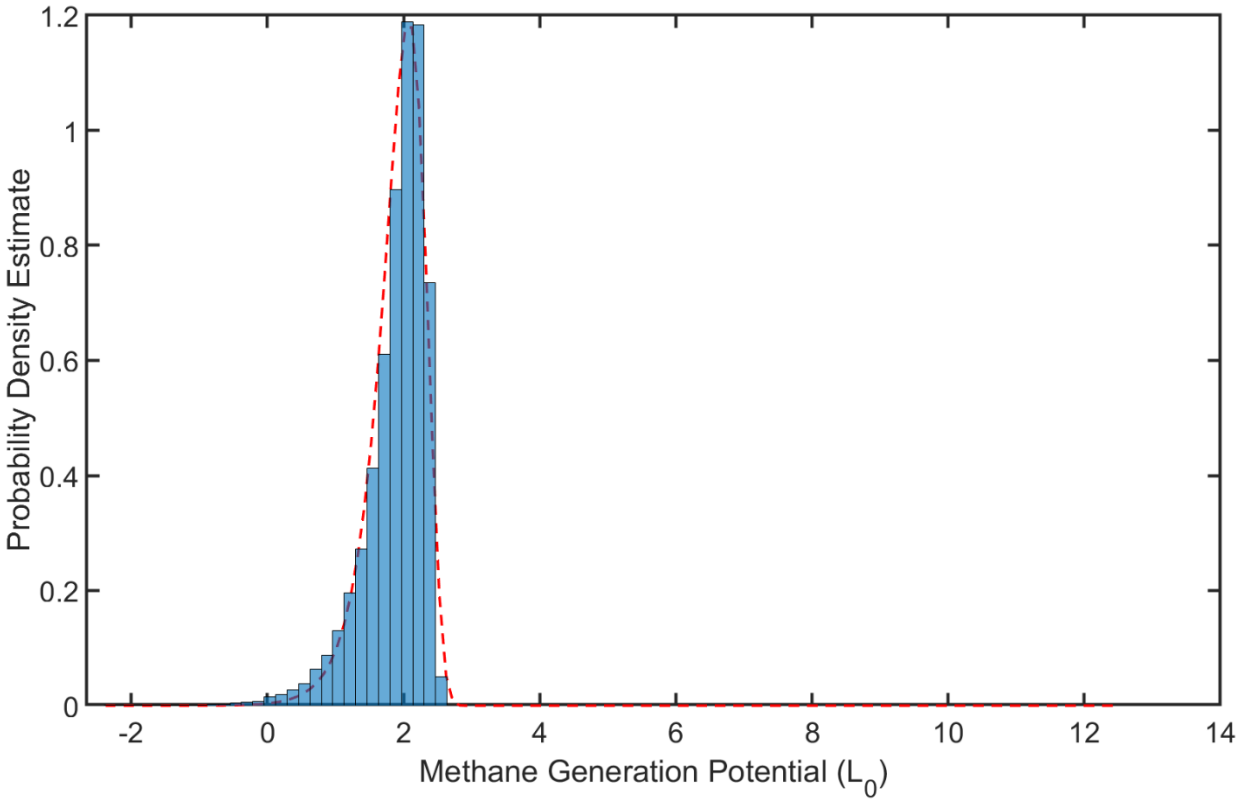

3.9.2.2 Determination of Site-Specific *k* Parameter

Site-specific *k*-values conventionally have been determined through fitting LandGEM against time-variable gas recovery data (not representative of gas generation). While this approach is effective, large datasets (time and recovery rate) are required to obtain reliable statistically significant results. For the sites investigated in this study, extensive historical data were not available for an effective model calibration. Thus, a regression analysis was used herein. Several previous studies indicated that correlations exist between site-specific climatic/ operational conditions and field calibrated first order decay values and simple linear regression models were developed for predicting site-specific values of the first order decay rate (Garg et al. 2006, Thompson et al. 2009, Fei et al. 2016). Garg et al. (2006) identified four key parameters for predicting k-values using a fuzzy synthetic evaluation methodology including annual precipitation rates,

average daily temperature, biodegradable fraction of the MSW, and landfill depth. Through a multiple-linear regression analysis using site specific data from 57 landfills, Fei et al. (2014) indicated that waste in place, the fraction of biodegradable waste, and waste temperature, were correlated to *k*-values. Thompson et al. (2009) developed a linear regression between annual precipitation rates and *k*-values for Canadian landfills. For predicting *k*-values, a major limitation of previously developed regression models is that these are unable to describe potential complex, non-linear relationships between the model inputs and outputs. Moreover, uncertainty in the model predictions typically were not assessed in the previous studies. An artificial neural network (ANN) model was developed in this study to predict k-values for all landfill sites.

In baseline analysis, the architecture of a neural network contains 3 layers: an input, hidden, and output layer (Figure 3.19). Within each layer are nodes (also termed neurons) that connect the input layer to the output layer. In general, the number of nodes in the input and output layers is equal to the number of input and output variables, respectively. The number of nodes in the hidden layer is set to vary. The mathematical connection between the input and hidden layers is similar to a multiple linear regression model (Equation 3.9). As input, the ANN model receives the independent variables used for prediction (i.e., precipitation, daily average temperature, etc.) and the necessary parameters required to run the model (i.e., weights and biases) and outputs a prediction ($\hat{Y}$) that is different than the true target output (Y) by some error (e). The n values in Figure 3.20 are a linear combination of the input weights (IW) multiplied by the inputs themselves with an added bias (b^1) value to account for noise.

Figure 3.20 Architecture of an Artificial Neural Network (adapted from MATLAB 2019)

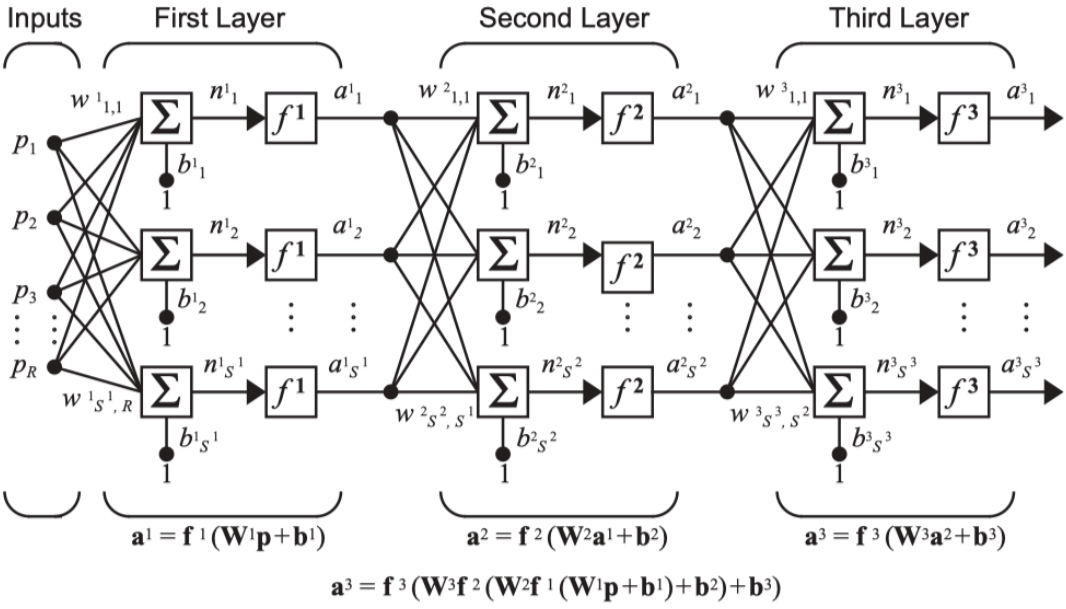

Optimization of the input/output layer weights and biases was performed backpropagation. A loss function (Equation 3.10) that measures the discrepancy

between the input and output target values from the model (the mean squared error, *MSE*) is minimized by iteratively running the forward model using a random initialization of the weights and biases. This process continues until an optimal value of the loss function is reached.

$$Y = f(X_i, IW, b^1, LW, b^2) + e \tag{3.9}$$

$$MSE = \frac{1}{N} \sum_{k=1}^{N} (Y - \hat{Y})^2 \tag{3.10}$$

The overall fit and predictive accuracy of a neural network is highly dependent on the quality of the input data and the potential relationships linking the input and output variables. The eight inputs selected in this study included annual precipitation (mm), daily average temperature (°C), waste in place (tons), waste throughput (tons/day), landfill depth (m), landfill areal coverage (m^2), fraction of biodegradable waste (%), and relative waste age (years) (the difference between the year in which the landfill opened and the year of analysis). Studies with the inputs identified above and k-values that had been predicted using calibration of landfill gas collection data with modeled generation data from LandGEM. A total of 23 studies from MSW landfills worldwide (Finland, Netherlands, Mexico, U.S., Canada) were found in the literature with the necessary data to populate the regression model (Garg et al. 2006, Barlaz e al. 2010a, Zhao et al. 2013, El-Fadel et al. 1996, Faour et al. 2007, Tolaymat et al. 2010, Wang et al. 2013, 2015, Bentley et al. 2005, Karanjekar et al. 2015, Sormunen et al. 2013, Oonk et al. 2013, Wangyao et al. 2010, Machado et al. 2009, Lamborn et al. 2012, Vu et al. 2017, Nwaokorie et al. 2018, Willumsen and Terraza 2007, Amini et al. 2012, 2013, Lagos et al. 2017, Budka et al. 2007). Individual values are presented in Appendix B, Table B4. While the majority of the landfills were located in cold, wet regions, landfill data also were used from dry temperate regions including California, Mexico, and South America.

The ANN models were configured, trained, and tested using MATLAB's built in neural network toolbox. A feed forward neural network with one hidden layer was used for the primary ANN architecture (similar to Figure 3.20). The ANN was trained using the standard Levenberg Marquart backpropagation technique, with all of the default settings for learning of the weights and biases applied. These settings included normalization of the input data and minimization of *MSE* during training. The dataset of 53 individual data points was randomly divided into training, testing, and validation data sets at a set ratio of 70%, 15%, and 15%. One of the most critical parameters of any ANN architecture is the number of hidden layers and number of nodes within the hidden layer(s). In general, one layer is sufficient for learning low dimensional problems and was adopted herein (Hagan et al. 2014). The number of nodes within the hidden layer was optimized using a novel evolutionary, global single objective optimizer (detailed settings of the optimization runs are similar to those described in Awad et al. 2016). The objective function of this optimization routine was set to equally weigh the errors obtained from the training, test, and validation sets to avoid overfitting of the network. The *MSE* of the training, test, and validation sets were normalized by the total expected variance of the model (*VAR*) (Equation 3.11, where $\bar{Y}$ is the mean of the *j* measured values of the target variable, *Y*). The optimizer was set to run for a limited number of

generations and was run for ten independent realizations. The best run (lowest objective function) from these realizations was used as the final ANN architecture for the prediction of *k*-values based on site specific climatic/ operational conditions. The uncertainty of *k* values (95% confidence interval) was calculated assuming the residuals from the ANN model were normally distributed with zero mean and standard deviation equal to the square root of the overall *MSE* of the ANN model.

$$VAR = \frac{1}{N} \sum_{j=1}^{N} (Y_j - \bar{Y})^2 \tag{3.11}$$

3.9.3 Methane Mass Balance Model

According to Equation 3.6, the methane generation predicted by LandGEM should be equal to the sum of the methane outputs, transformations, and inputs from, within, and to the landfill, respectively. In Equation 3.6, the methane mass balance outputs include emissions, gas collection, storage, and migration. Transformations in the methane mass balance model include methane oxidation in the soil covers, resulting in a net loss of methane. Potential inputs to the mass balance model included negative emissions, or net uptake of methane from the atmosphere. Predicted methane generation was subtracted from the sum of the methane collected and emitted to determine net surplus or deficit of methane, which were indications of the importance of transformation or output/input pathways other than collection/emission pathways measured herein. In this model, outputs/transformations and inputs are designated as positive and negative values, respectively.

The time frame considered (2018-2019) for the mass balance was associated with the field campaigns and was the most recent year from which methane collection data was available. Mass balances were conducted using the refined LandGEM predictions. Results are presented for both the mean and 95% confidence intervals of methane flows expected for each pathway to capture the full variation expected at each site.

Gas collection typically is calculated using the sum of the average daily flows recorded at the entrance to the flare or main header of the gas collection system. To estimate total methane volume, the net LFG collection is multiplied by the average inlet volumetric methane composition. To investigate the potential uncertainty in methane collection measurements resulting from these two steps, LFG flow and methane composition data were analyzed from four landfills in the U.S. (Santa Maria Regional and Crazy Horse Landfills in California; Loudoun County Solid Waste Management Facility in Virginia; and Franklin County Landfill in Ohio) from which data were available. These landfills represent a range in operational scale (small to large) and climate (dry, temperate to cold, wet). An MC prediction framework was run to simulate the total methane collection volume (m^3) at each of these sites for the time periods in which data was available. Similar to the L_0 MC predictive framework, non-parametric KDE distributions were fitted to the time varying LFG flow rate and, if available, the time varying volumetric methane composition. If the volumetric methane composition was not available, it was assumed that this input distribution to the MC simulations was uniform, ranging from 40 to 60% (vol/vol). Predictions of methane composition were made for the same time periods/intervals. To arrive at a stable output distribution in total methane

volume, 50,000 simulations were conducted. The resulting distributions in total methane volume predicted from these simulations appeared normal (Figure 3.21). After fitting a normal distribution to each output distribution, the mean and standard deviation were used to build 95% confidence intervals representing the overall uncertainty in gas collection measurements.

To extrapolate the estimated uncertainty in gas collection from the four landfills to the landfill sites in this study, several assumptions were made. First, it was assumed that the percent difference between the mean value and the lower or upper tail of the 95% confidence interval was representative of the overall measurement uncertainty in gas collection. This calculation was performed using the log (base 10) values of the mean and 95% confidence bound to reduce potential scaling effects of total methane collection between landfills of different size. Next, as a conservative measure, the median of the overall uncertainty calculated for the four representative landfills (44.1%) was applied to each of the landfill sites in this study to arrive at an overall 95% confidence interval.

Figure 3.21 Total Methane Collection Predicted for the Loudoun County Solid Waste Management Facility in Virginia using the New MC Simulation Framework

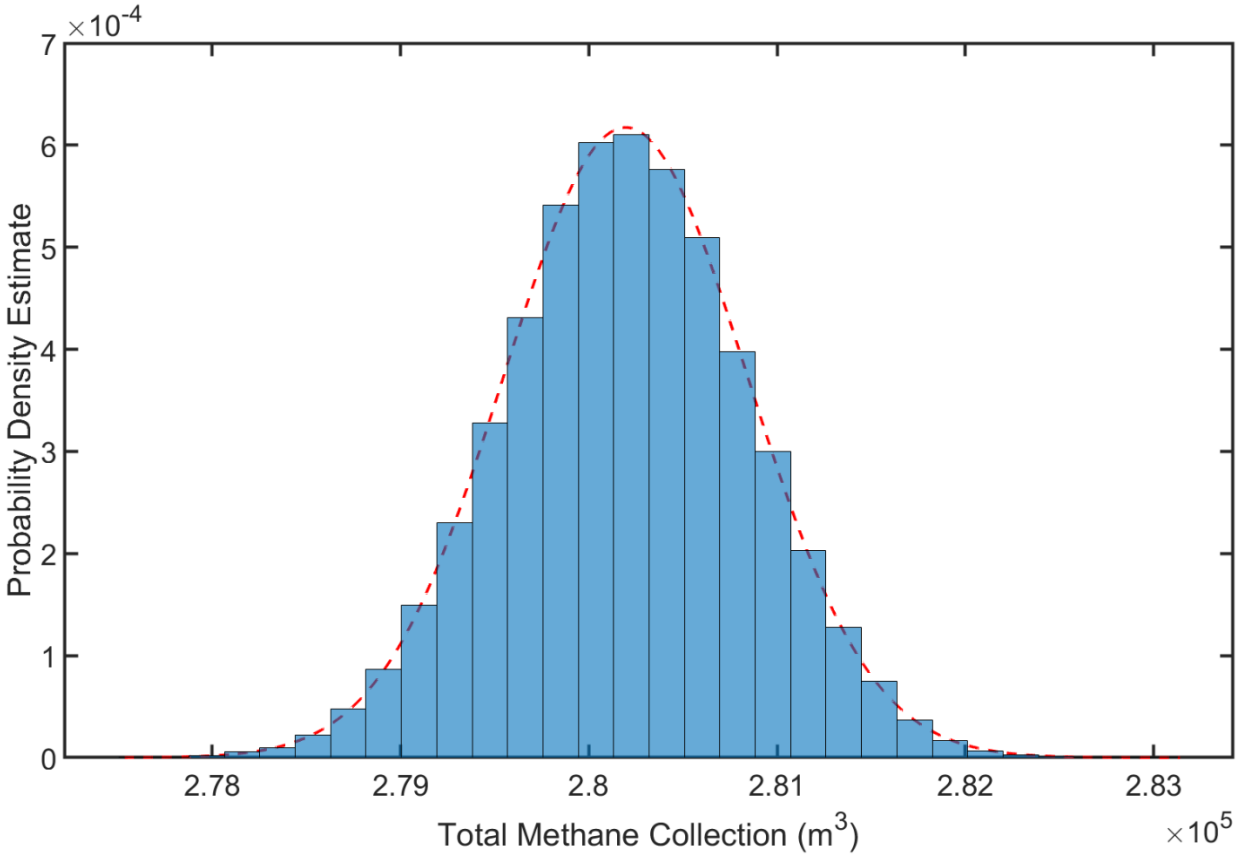

The uncertainty in the LandGEM methane generation predictions was assessed using the refined parameter approach. For ground-based measurements, the distribution in methane whole-site emissions from daily, intermediate, and final covers was assumed

to be normal (for each season). These normal distributions were then combined across cover categories and then across seasons, resulting in a composite normal distribution, with mean, standard deviation, and associated 95% confidence intervals. For aerial-based measurements, the reported uncertainty was not assumed to be the overall standard deviation, as recommended by Bromley (2017). Instead, the uncertainty was assumed to be representative of the 95% confidence bounds of the reported mean in emissions estimates obtained from the aerial testing investigations.

3.10 Calculation of the Indirect Effects of LFG Emissions

The metrics applied to assess the indirect effects of LFG emissions on public health, air quality, and climate change included tropospheric ozone formation, secondary aerosol formation, indirect/direct global warming, and stratospheric ozone depletion potentials. HAP classification was also used to further evaluate to what extent a chemical emitted from a landfill site impacted human health. Tropospheric ozone formation potentials (OFPs) for each site were quantified using the MIR scale, which is determined through modeling of the change in peak ozone concentration when an individual chemical species is released into the troposphere, assuming high concentrations of NOx (i.e., in an urban environment) (Carter 2009). The OFP (g O_3/yr) for the *i*th NMVOC species was calculated using Equation 3.12 below, using the MIR_i (g O_3/g NMVOC) value in Table 1.1:

$$OFP_i = E_{LF,i} * MIR_i \quad (3.12)$$

Where, $E_{LF,i}$ represents the annual net surface emissions of the *i*th NMVOC for a given landfill (g/yr). In this report, whole site, annual emissions were calculated using the fluxes measured for the different cover categories at a given landfill. For each landfill, the relative areas of the different cover categories and the area of the landfill are used together with the specific fluxes for the covers to calculate annual emissions for the entire landfill site, where calculated fluxes for each NMVOC species were averaged from both chamber estimates.

Secondary organic aerosol formation potentials (SOAFPs) were calculated through application of the FAC, which represents the fraction of a given NMVOC that is converted into an organic aerosol, as measured through laboratory-based smog chamber experiments (Grosjean and Seinfeld 1989, Grosjean 1992). The SOAFP for the *i*th NMVOC is simply the product of the net surface emissions from a given landfill site and the given FAC_i value presented in Table 1.1 (Equation 3.13):

$$SOAFP_i = E_{LF,i} * FAC_i \quad (3.13)$$

Other than carbon tetrachloride (CCl_4, which is a high GWP gas), certain NMVOC species surveyed in this study also exert an indirect and direct effect on global climate change. Indirect effects on global climate change associated with NMVOCs can be attributed to formation of secondary organic aerosols (thereby increasing cloud albedo), increase in O_3 formation and depletion of hydroxyl radicals (thereby increasing the atmospheric lifetime of CH_4), where indirect GWP values have been previously reported

and are summarized in Table 1.2 (Collins et al. 2002). In this way, the indirect effect on global climate change (in terms of carbon dioxide equivalents, CO_2-eq) was calculated for the *i*th NMVOC as the product of the indirect GWP_i and the net surface emissions from a given landfill site (Equation 3.14). Direct effects of NMVOC degradation products on climate change (i.e., an increase in carbon dioxide from NMVOC oxidation) were calculated based on the molecular weight (MW_i) and number of carbon atoms ($N_{c,i}$) for the *i*th NMVOC, based on a simple molar conversion (Equation 3.14) (IPCC). Thus, the total combined CO_2-eqs was calculated in this study by summing the indirect (IGW_i, Eq. 3) and direct radiative forcing effects (DGW_i, Equation 3.15) (Majumdar and Srivastava 2012, Majumdar et al. 2014).

$$IGW_i = E_{LF,i} * GWP_i \tag{3.14}$$

$$DGW_i = \frac{E_{LF,i}}{MW_i} * N_{c,i} * (44) \tag{3.15}$$

The stratospheric ozone depletion potential (ODP) weighted emissions was further computed to compare the effect of NMVOC emissions on air quality across different landfill sites. This metric was relevant for the halogenated hydrocarbons chemical family as well as the CFCs and HCFCs belonging to the F-gas classification, where, depending on the extent of vertical mixing in the atmosphere, the presence of chlorine or bromine atoms significantly contributes to a reduction in the stratospheric ozone layer. The ODP weighted emissions for the *i*th NMVOC was calculated as the product of the ODP value (Table 1.1) and the net surface emissions for a given landfill site (Equation 3.16).

$$WODP_i = E_{LF,i} * ODP_i \tag{3.16}$$

Finally, the cumulative surface emissions from all HAPs identified in Table 1.1 were obtained to compare the human health impacts of net NMVOC surface emissions on surrounding communities and workers present at each site.

3.11 Additional Static Flux Chamber Investigations

Additional tests were conducted in the dry season at Santa Maria Regional Landfill and Teapot Dome Landfill. The tests at SMRL were conducted to investigate the influence of various landfill operational conditions on flux. The testing program at Teapot Dome Landfill was conducted to evaluate the effects of the specific operational practice of designated winter waste placement at California landfills on LFG surface flux.

3.11.1 Radial Gas Extraction Well Testing at SMRL

Additional static flux chamber testing was conducted at Santa Maria Regional Landfill to experimentally ascertain the radius of influence of a typical gas extraction well. A well located at a central location of the waste mass away from other gas extraction wells was selected to minimize the potential influence of nearby gas extraction wells on the flux tests. The tests were conducted on the interim cover composed of native soil materials near testing locations that were previously investigated (e.g., the same cell of

the landfill). Flux chamber testing was conducted on two separate days (1 week apart) during the dry weather season to obtain replicate results (October 4, 2019 and October 11, 2019). The gas well investigated had had two nested casings with shallow and deep active extraction zones, where each zone was representative of younger and older waste conditions, respectively. The waste depths contributing LFG to each screened zone was 6.1-9.1 m and 21.3 m for the shallow and deep casings, respectively. During both testing periods, flux chambers were placed at logarithmically spaced intervals (i.e., 0.5, 1, 2, 4, 8, 16, and 32 m) to capture both the magnitude and variation in fluxes extending radially from the gas extraction well (Figure 3.22). The number on the chamber locations depicted in Figure 3.22 corresponds with the raw concentration and flux chamber data tabulated in the spreadsheets provided as supplemental information to this report. Photographs of the tests are presented in Figure 3.23. The chamber testing locations were selected to avoid interference between tests (Figure 3.23b). For the second day of testing, it was difficult to find a location placed 1 m away from the extraction well that was not infringing on existing or upcoming chamber footprints; therefore, this location was offset by approximately 0.5 m.

Figure 3.22 Flux Chamber Locations at SMRL: a) Testing Day 1, b) Testing Day 2.

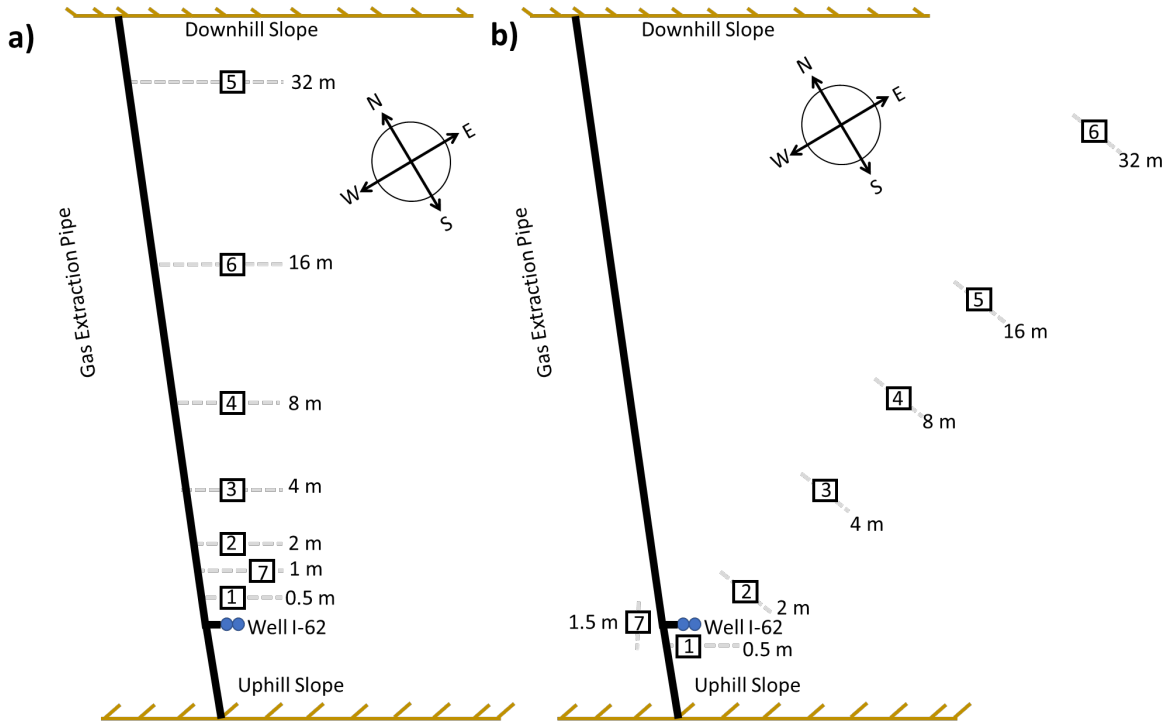

Gas extraction vacuum pressures and LFG composition were monitored throughout the entire duration of both field-testing days using a GEM5000. At least one GEM measurement was made at each extraction casing (shallow and deep) during each individual flux chamber test. The flux tests were conducted using logarithmic sampling (1 hr total duration) to be able to finish all of the radial testing in a given test day and not have any influence from potential variations in weather conditions. The 1-hr test

duration was determined to be effective for obtaining reliable flux measurements in terms of tests passing the R^2 threshold based on the previous flux chamber tests at the landfill.

After the flux chamber measurements, the cover was excavated near the vicinity of the specific testing locations to determine the thickness of the interim covers as a function of radial distance from the well. A photograph of determination of cover thickness is presented in Figure 3.24.

Figure 3.23 a) Radial Gas Well Static Flux Chamber Testing at SMRL (0.5 and 2 m distance) and b) Chamber Footprints and Spacing from the Gas Extraction Well.

Figure 3.24 Excavation Results adjacent to Chambers Placed at a) 32 m versus b) 1 m from the Gas Collection Well.

3.11.2 Cover Thickness Testing at SMRL

To ascertain the effects of cover thickness on GHG and NMVOC fluxes, an experimental test program was carried out on October 18, 2019 at Santa Maria Regional Landfill. A rectangular testing plot with dimensions of 4.7 m width, 4 m length, and 1.1 m height was constructed by the landfill operators over the existing intermediate cover with an approximate thickness of 0.45 m (Figure 3.25a). The test plot was constructed over the same intermediate cover as the cover investigated in the radial gas extraction well tests. The test plot was constructed at a central location in the cell to minimize the potential effects of the gas wells on the landfill gas emissions. Flux measurements were made at approximately 0.31 m depth intervals over the course of the one-day testing campaign, where an excavator was used to carefully remove each layer of the test plot to progressively reduce the thickness of the cover (Figure 3.25b). Overall, a total of 6 flux chamber measurements were made at varying heights above or below the existing intermediate cover level including: 1.12 m, 0.90 m, 0.61 m, 0.32 m, 0.02 m, and -0.31 m (i.e., below the top of the existing intermediate cover). Gas extraction vacuum pressures and LFG composition were monitored during each test using a GEM5000. Similar to the radial well testing experiments, the flux tests were conducted using a logarithmic sampling frequency (i.e., Chamber A, sampling at 0, 7, 15, 30, and 60 minutes) as this method resulted in reliable results at this landfill as verified using the results from previous tests.

Figure 3.25 a) Static Flux Chamber Testing on the Test Plot Constructed at SMRL, b) Removal of 0.3 m-thick Soil Layer for Testing the Next Cover Thickness.

3.11.3 Temporal Surface Flux Testing at SMRL

Testing was conducted at Santa Maria Regional Landfill to evaluate the temporal variability in landfill gas flux. As flux chamber tests represent a single snapshot in time, conducting chamber measurements over a weeklong period provides variation expected as a function of time. For the temporal tests, a was placed at a central location within the well-field at the same landfill cell used for both the radial testing and cover thickness testing (soil intermediate cover). This chamber was not moved or disturbed in any way throughout the duration of this field-testing program. A series of flux tests were conducted on October 21, 2019, October 25, 2019, and October 26, 2019 at different times throughout each testing day. On October 21, 2019, one flux chamber test was conducted at 1:13 PM. On October 25, 2019 and October 26, 2019, 4 consecutive flux

chamber tests were conducted at 8:00 AM, 1:30 PM, 6:30 PM, and 1:15 AM. For each of these chamber tests, a logarithmic sampling frequency was selected, similar to the testing programs for radial well distance and cover thickness tests. A final sampling time of 2 hours was added to improve the resolution of the flux measurements. Gas extraction vacuum pressures and LFG composition were monitored during each test using a GEM5000. After each test was performed, both the air and soil temperatures (in triplicate locations) were measured in the vicinity of the chamber location.

3.11.4 Contaminated, Non-Hazardous Soils Testing at SMRL

The fourth additional field-testing program conducted at SMRL focused on quantification of both GHG and NMVOC fluxes from an inactive cell and an active cell containing non-hazardous hydrocarbon impacted soil (NHIS). Even though NHIS is deemed non-hazardous by state and federal regulations (due to concentrations below regulatory limits), NHIS still contains detectable amounts of crude oil, where the variety of chemical compounds composing crude oil is generally referred to as total petroleum hydrocarbons (TPH). All of the chemicals within the aromatic family under investigation in this study (i.e., BTEX), as well as longer chain alkanes, alkenes, and alkynes are expected to constitute some fraction of TPH in the contaminated soil. These compounds are expected to be readily volatilized from the contaminated sediment or easily dissolved/transported via the aqueous phase during precipitation events, which may pose a significant threat to the environment as these materials are generally left uncovered during filling of the NHIS cells at SMRL.

The NHIS facility at the SMRL contains two active cells: one that has portions of final cover and been filled (Cell 2) and the other that does not yet have final cover in place (Cell 1). Historically, the landfill has accepted contaminated soils from large and small projects. Both cells were constructed over 15-21-m-thick MSW that was placed prior to 1970 through to 2001. A bottom geomembrane liner system was placed over the existing MSW at both cells prior to placement of the NHIS wastes. In addition, Cell 2 has a final cover in place that consists of either GCL or geomembrane liner system overlain by 0.9 m of vegetative soil cover. NHIS Cell 2 has an active gas recovery system in place that extends into both shallow and deep MSW layers at the cell. NHIS Cell 1 has an active gas recovery system in place that extends into the deep MSW layers at the cell. Cell 1 was filled in various stages and includes an active face (which remains uncovered from day to day operations) and an extended daily cover area where clean soil is placed over the contaminated soil until filling restarts.

For the NHIS field-testing campaign, two distinct testing locations were selected for flux chamber measurements. The first site was selected and tested in Cell 2 to represent final cover conditions. The cover topsoil at the first testing location was sandy, not well compacted, and highly vegetated. The second site was selected at an extended daily cover area in Cell 1, where clean soil had been placed to a relatively shallow thickness for an extended period of time. The cover soil was sandy, not well vegetated, and very dry compared to the final cover testing location. At both sites, flux chamber tests were conducted using the two primary sampling frequencies (logarithmic and linear) to

ensure that a broad spectrum of fluxes could be reliably predicted for the NMVOCs surveyed. The field campaign was conducted on October 7, 2019.

3.11.5 Wet Waste Placement Testing at Teapot Dome Landfill

Wet and dry season field campaigns ascertained that the interim cover location at Teapot Dome landfill that was designated as a wet waste placement area was associated with some of the highest fluxes of GHGs and NMVOCs measured throughout the entire field-testing program in this investigation. An additional field-testing program was conducted at this landfill to further investigate the effects of dedicated wet waste placement on LFG flux. The tests were conducted on November 18, 2019. While the tests were conducted at the same cell and approximate location in November 2019 as the previous wet and dry season tests, the cell had been filled with 3 to 4.5 m of fresh wastes. The wastes were covered with an intermediate cover (thickness of approximately 0.45 m) similar to the cover that was present during the previous wet and dry season tests. Similar to previous field-testing methodology, two chambers with different sampling frequencies (logarithmic and linear) were placed and tested at the same site that was associated with wet waste placement that was identified during previous campaigns. Raw gas samples were also collected to determine the LFG composition and concentration during the site visit.

PART 4 – RESULTS

4.1 Introduction

This section of the report is provided to summarize and interpret the main findings from the flux and cover material measurements conducted in the study. In addition, results are provided for the gas collection efficiency analysis conducted in the study. The results are organized into twelve main sections: i) aerial measurements for 16 landfills; ii) site-specific (intra-landfill) flux analysis for 5 landfills; iii) between site (inter-landfill) flux analysis for 5 landfills; iv) seasonal comparison of flux; v) whole-site landfill emissions; vi) geotechnical properties of cover systems; vii) correlations between flux and cover/landfill characteristics; viii) gas collection efficiency calculations; ix) effect of waste tires on LFG emissions; x) characterization of raw gas; xi) temperature conditions in covers; xii) additional static flux chamber analysis-radial distance, cover thickness, temporal variation, contaminated soil waste, wet waste placement.

The results related to the flux measurements are grouped into twelve distinct chemical families (Section 1.5) and data are presented mostly for these grouped chemicals in this part of the report. These twelve individual chemical families are: baseline greenhouse gases (i.e., methane, nitrous oxide, carbon dioxide, carbon monoxide) referred to as GHGs, reduced sulfur compounds (RSC), fluorinated gases (F-gas), halogenated hydrocarbons (HH), organic alkyl nitrates (ON), alkanes (Alk), alkenes (Alke), aldehydes/alkynes (Ald/Alky), aromatic hydrocarbons (Ar), monoterpenes (Mon), alcohols (Alc), and ketones (Ket).

A complete summary of the baseline site properties (including an overview of testing locations and weather conditions), raw concentration data, and flux data is provided in Appendix files C1, C2, and C3, respectively.

4.2 Aerial Measurements

The determination of landfill gas emissions from flyover surveys included testing at 16 different landfills. The test sites included the 15 landfills identified through the site selection process (Section 2.3) and one additional site – Sunshine Canyon Landfill. The Sunshine Canyon Landfill was included to provide direct comparison between similar nearby landfills (Chiquita Canyon Landfill and Sunshine Canyon Landfill) that differ in their operational practices for stripping intermediate covers prior to placing overlying waste (Chiquita Canyon Landfill strips intermediate cover whereas Sunshine Canyon does not strip intermediate covers). The descriptions of the aerial testing results are provided on a site-by-site basis in chronological order of the flights. A summary of the results is provided subsequent to the descriptions in Table 4.1. In all of the photos depicting the flight paths in Sections 4.2.1 through 4.2.23, the white arrows indicate the main wind direction. For the five small landfills, emissions were very low and below the detection limit of the aerial measurement system and for the sixth small landfill, the measurements were just over the detection limit. Emissions values are provided in Table 4.1 in the report for reference for the five small landfills even though the measurements were below detection limit based on the common calculation algorithm used in the test program.

4.2.1 Mariposa County Sanitary Landfill -- October 18, 2017

A total of 10 laps were flown around Mariposa County Sanitary Landfill as shown in Figure 4.1. The aircraft completed circles between 170 meters above ground level (AGL) and 495 meters AGL. Winds were out of the southwest, averaging 2.3 m s^{-1}, but changed substantially from the lower laps to the higher laps (direction of 240 at 150 m and 120 at 800 m). The wind variability resulted in a large uncertainty with the total methane emissions below the detection limit of the aerial measurement system for these conditions. The full flight path is presented in Figure 4.1.

Figure 4.1 Flight Path around Mariposa County Sanitary Landfill on October 18, 2017

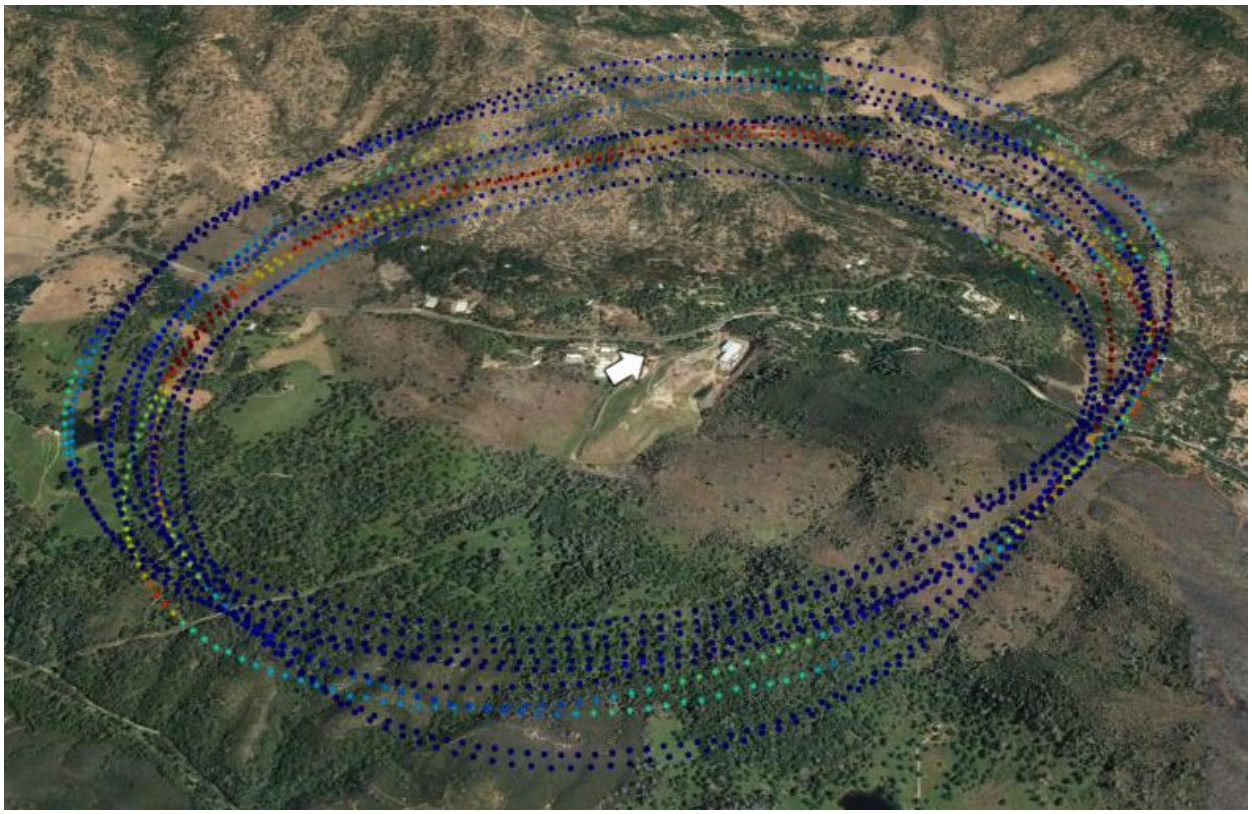

4.2.2 Teapot Dome Landfill -- October 18, 2017

A total of 10 laps were flown around Teapot Dome Landfill, as shown in Figure 4.2. The aircraft completed circles between 112 meters AGL and 435 meters AGL. Winds were out of the southwest, averaging 1.1 m s^{-1}. Total methane emission is estimated at 294 ± 100 kg hr^{-1}. The full flight path is presented in Figure 4.2.

Figure 4.2 Flight Path around Teapot Dome Landfill on October 18, 2017

4.2.3 Taft Recycling Center -- October 18, 2017

A total of 6 laps (4 useable) were flown around Taft Recycling Center, as shown in Figure 4.3. The aircraft completed circles between 144 meters AGL and 543 meters AGL. Winds were out of the north, averaging 1.6 m s^{-1}. The total methane emission was below the detection limit of the aerial measurement system for these wind conditions (very low winds). This measurement was also complicated by the mountains on the downwind side (south) of the landfill. The full flight path is presented in Figure 4.3.

Figure 4.3 Flight Path around Taft Recycling Center on October 18, 2017

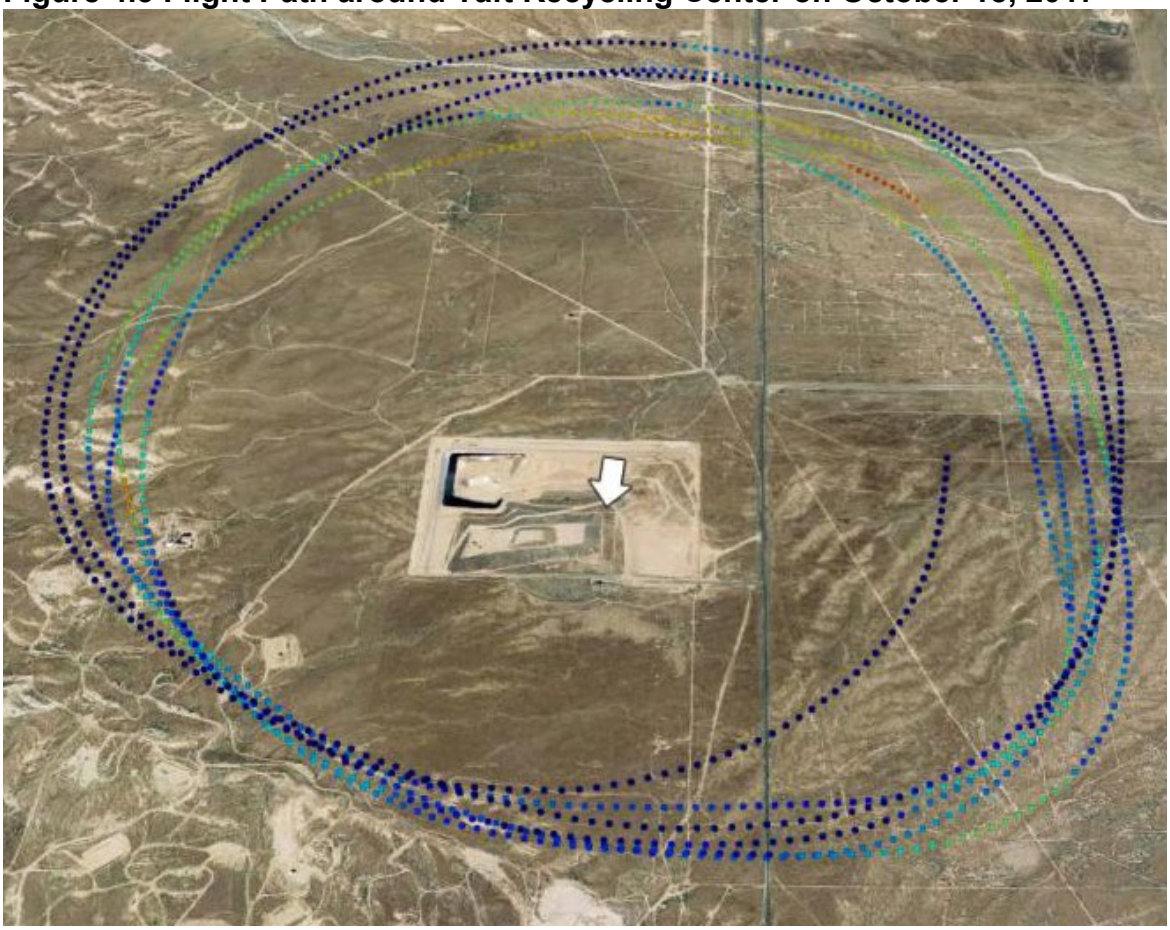

4.2.4 Frank R. Bowerman Sanitary Landfill -- November 10, 2017

A total of 16 laps (15 useable) were flown around the Frank R. Bowerman Sanitary Landfill, as shown in Figure 4.4. The aircraft completed circles between 80 meters AGL and 876 meters AGL. Winds were out of the southwest, averaging 1.7 m s^{-1}. Total methane emission is estimated at 3275 ± 669 kg hr^{-1}. The full flight path is presented in Figure 4.4.

Figure 4.4 Flight Path around Frank R. Bowerman Landfill on November 10th, 2017

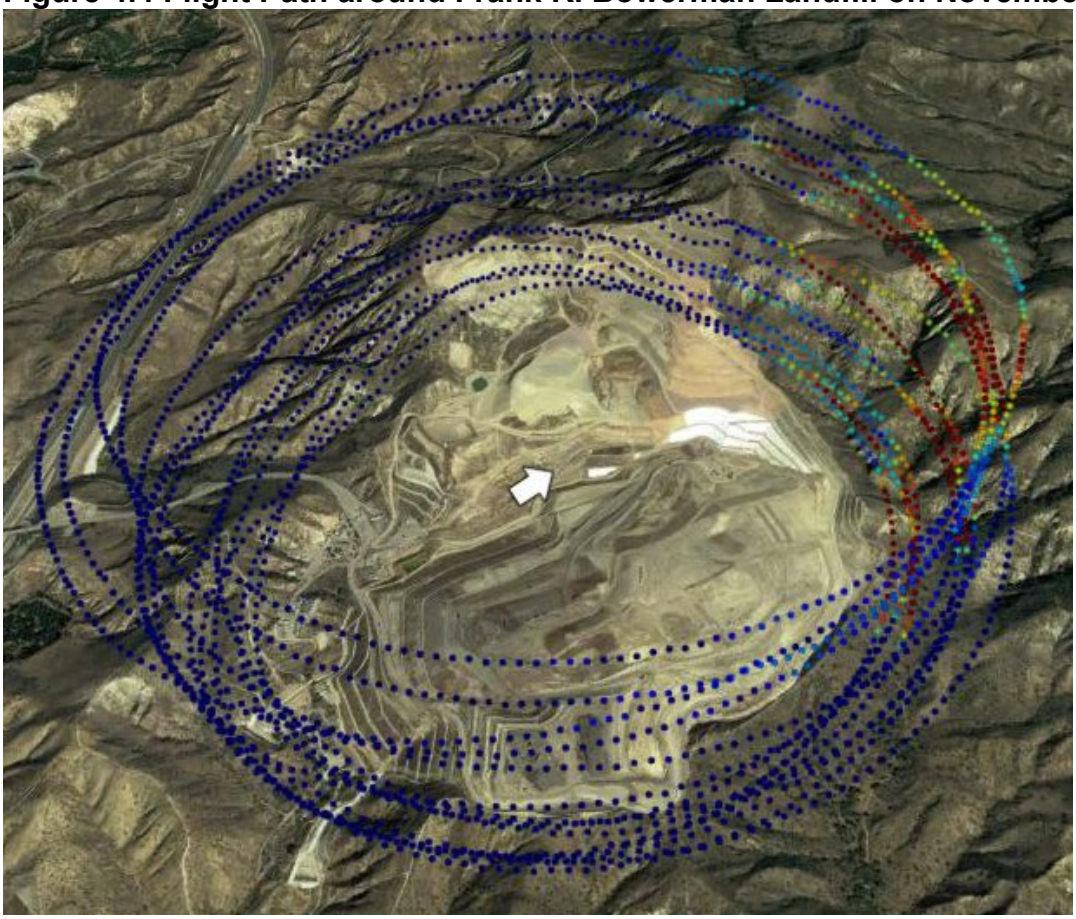

4.2.5 Chiquita Canyon Sanitary Landfill -- November 10, 2017

A total of 17 laps (15 useable) were flown around Chiquita Canyon Sanitary Landfill, as shown in Figure 4.5. The aircraft completed circles between 167 meters AGL and 475 meters AGL. Winds were out of the southwest, averaging 4.9 m s^{-1}. Total methane emission is estimated at 1306 ± 207 kg hr^{-1}. The full flight path is presented in Figure 4.5.

Figure 4.5 Flight Path around Chiquita Canyon Sanitary Landfill on November 10, 2017

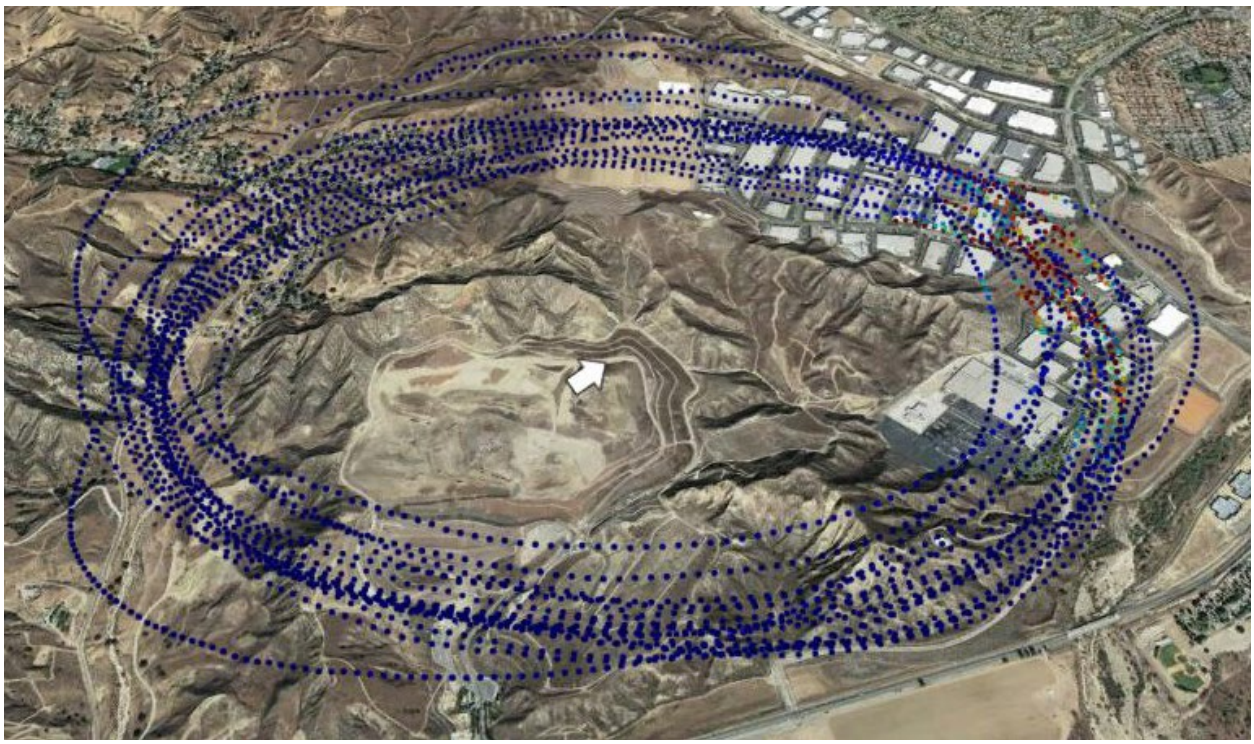

4.2.6 Santa Maria Regional Landfill -- November 10, 2017

A total of 18 laps (14 useable) were flown around Santa Maria Regional Landfill, as shown in Figure 4.6. The aircraft completed circles between 105 meters AGL and 491 meters AGL. Winds were out of the west/northwest, averaging 10.4 m s^{-1}. Total methane emission is estimated at 90 ± 39 kg hr^{-1}. The largest enhancement was seen on the lowest leg, and that enhancement was several times more than the next largest enhancement. This implies that the estimate of 90 kg hr^{-1} methane emitted is most likely an underestimate of the true emissions- due to the high wind speeds, it is possible emissions below the lowest flight altitude were not captured. The full flight path is presented in Figure 4.6. A profile of flux with elevation is presented in Figure 4.7.

Figure 4.6 Flight Path around Santa Maria Regional Landfill on November 10, 2017

Figure 4.7 Flux Profile of Santa Maria Regional Landfill

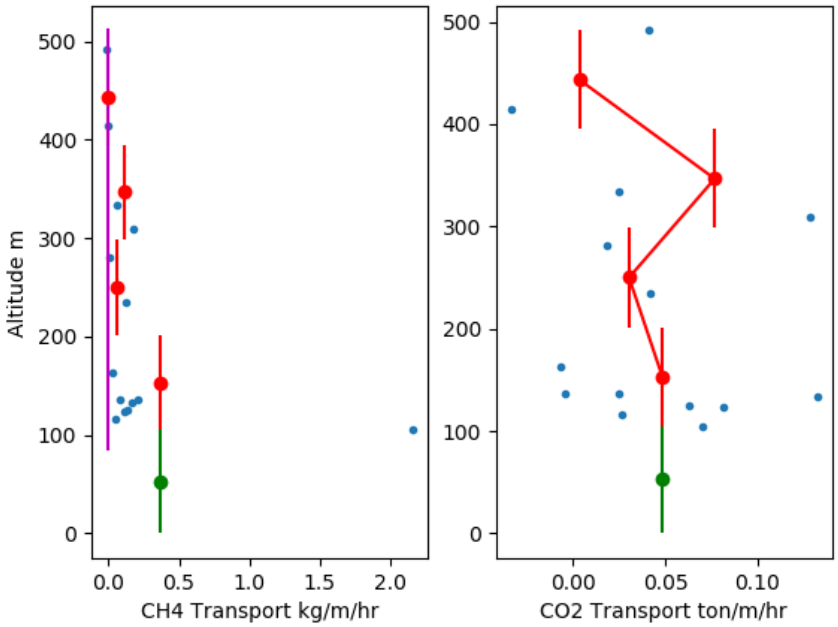

4.2.7 Redwood Landfill -- November 17, 2017

A total of 8 laps were flown around Redwood Landfill, as shown in Figure 4.8. The aircraft completed circles between 64 meters AGL and 208 meters AGL. Winds were out of the north, averaging 4.8 m s^{-1}. Total methane emission is estimated at 140 ± 42 kg hr^{-1}. The full flight path is presented in Figure 4.8.

Figure 4.8 Flight Path around Redwood Landfill on November 17, 2017

4.2.8 Yolo County Central Landfill -- November 17, 2017

A total of 11 laps were flown around Yolo County Central Landfill, as shown in Figure 4.9. The aircraft completed circles between 61 meters AGL and 306 meters AGL. Winds were out of the north/northwest, averaging 7.4 m s^{-1}. Total methane emission is estimated at 376 ± 68 kg hr^{-1}. The full flight path is presented in Figure 4.9.

Figure 4.9 Flight Path around Yolo County Central Landfill on November 17, 2017

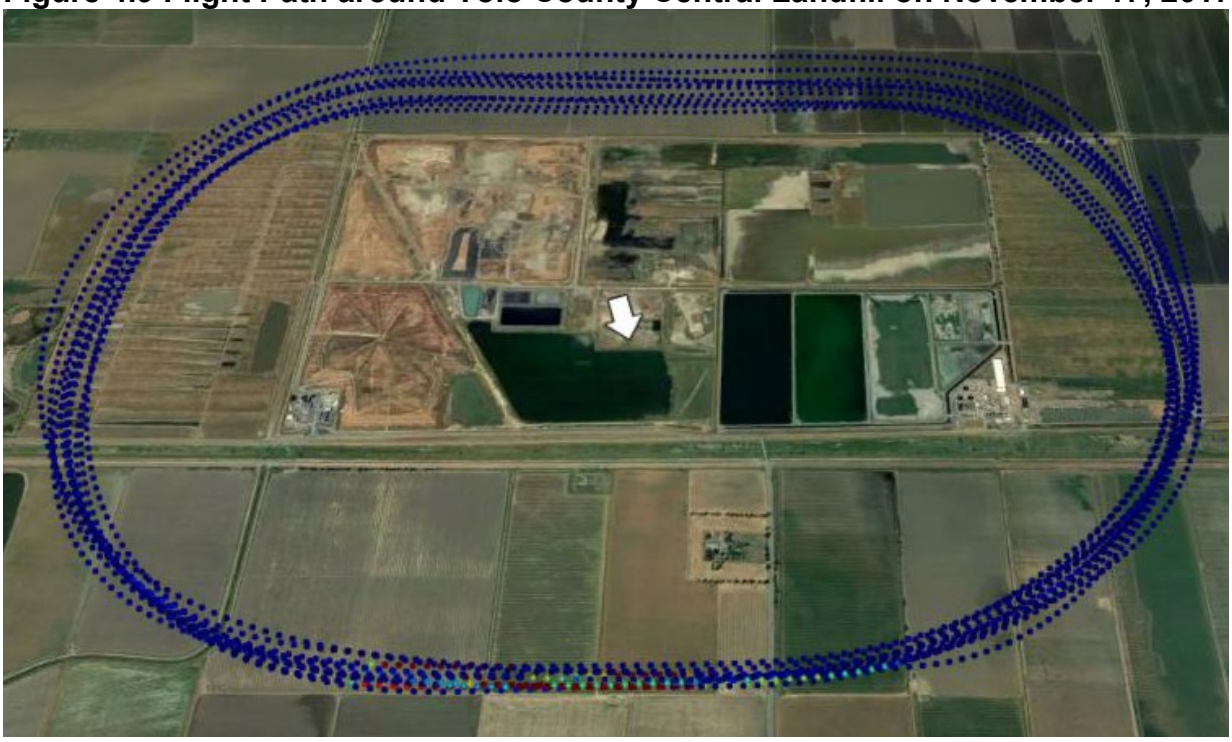

4.2.9 Stonyford Disposal Site -- November 17, 2017

A total of 11 laps were flown around the Stonyford Disposal Site, as shown in Figure 4.10. The aircraft completed circles between 62 meters AGL and 334 meters AGL. Winds were out of the north, averaging 4.4 m s^{-1}. No significant downwind enhancements were observed, and the total methane emission was below the detection limit of the aerial measurement system. The full flight path is presented in Figure 4.10.

Figure 4.10 Flight Path around Stonyford Disposal Site on November 17, 2017

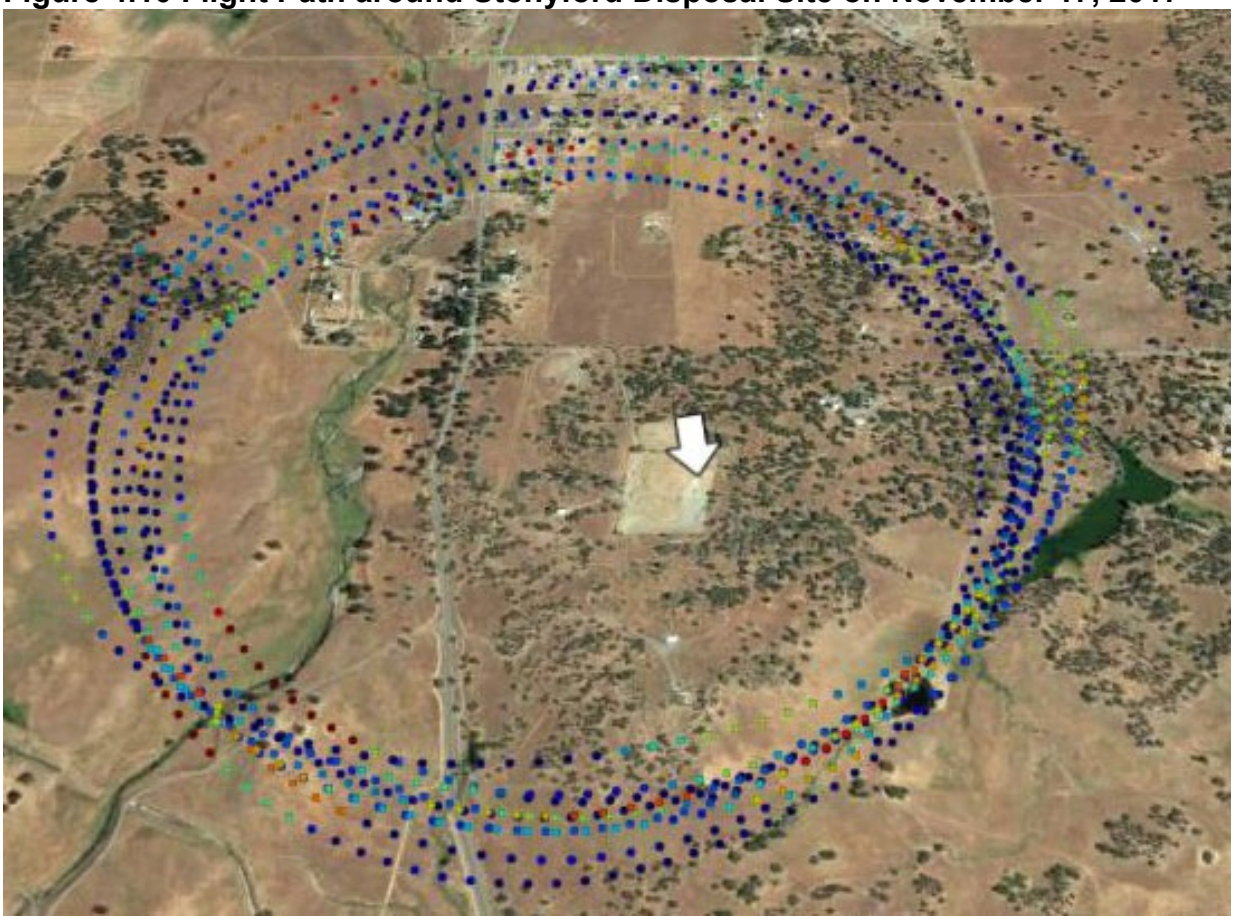

4.2.10 Salton City Landfill -- December 4, 2017

A total of 12 useable laps were flown around the Salton City Landfill, as shown in Figure 4.11. The aircraft completed circles between 46 meters AGL and 305 meters AGL. Winds were out of the north, averaging 9.6 m s^{-1}. Total methane emission is estimated at 11 ± 3 kg hr^{-1}. The full flight path is presented in Figure 4.11.

Figure 4.11 Flight Path around Salton City Landfill on December 4, 2017

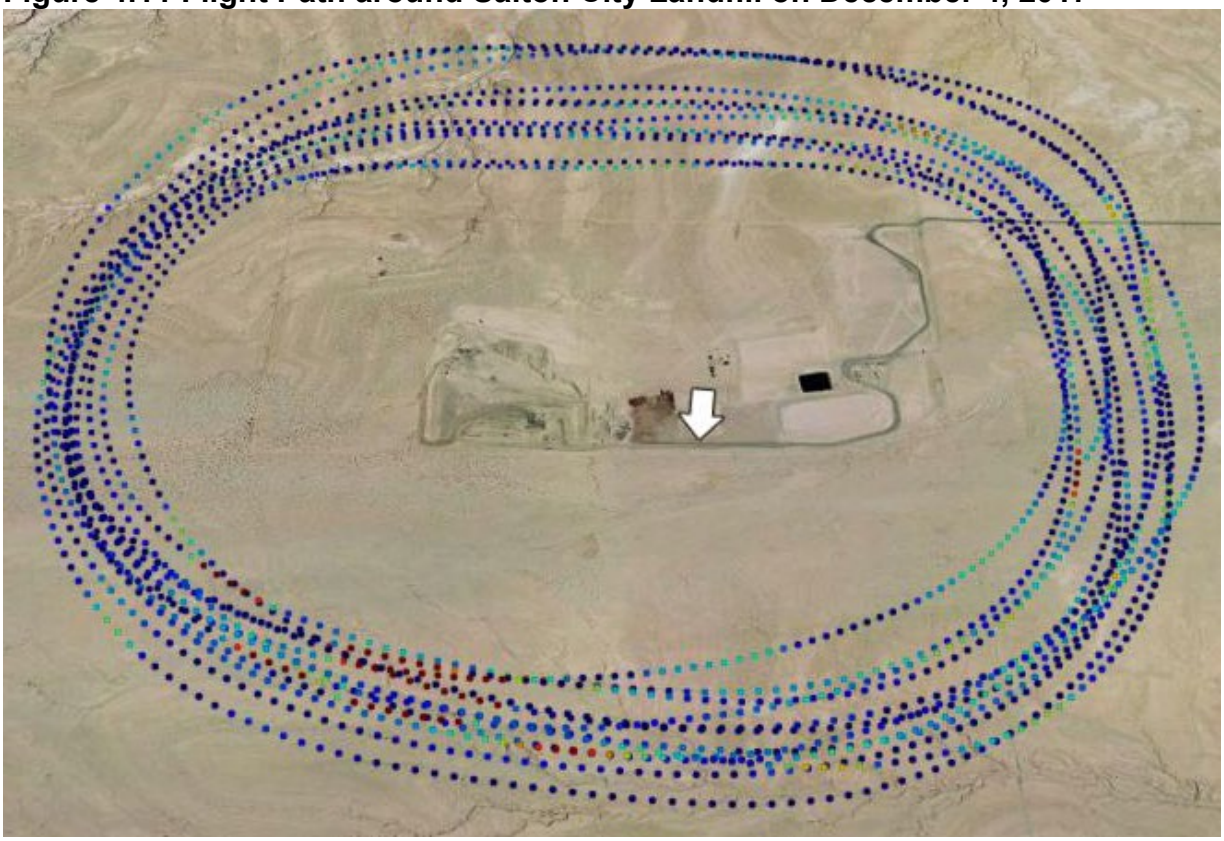

4.2.11 Borrego Landfill -- December 4, 2017

A total of 17 useable laps were flown around Borrego Landfill, as shown on Figure 4.12. The aircraft completed circles between 48 meters AGL and 458 meters AGL. Winds were out of the east/southeast, averaging 2.1 m s^{-1}. Total methane emission was below the detection limit of the aerial measurement system. The full flight path is presented in Figure 4.12.

Figure 4.12 Flight Path around Borrego Landfill on December 4, 2017

4.2.12 Simi Valley Landfill -- December 4, 2017

A total of 9 laps (8 useable) were flown around Simi Valley Landfill, as shown in Figure 4.13. The aircraft completed circles between 264 meters AGL and 518 meters AGL. Winds were out of the northeast, averaging 16.2 m s^{-1}. Total methane emission is estimated at 638 ± 337 kg hr^{-1}. The full flight path is presented in Figure 4.13.

Figure 4.13 Flight Path around Simi Valley Landfill on December 4, 2017

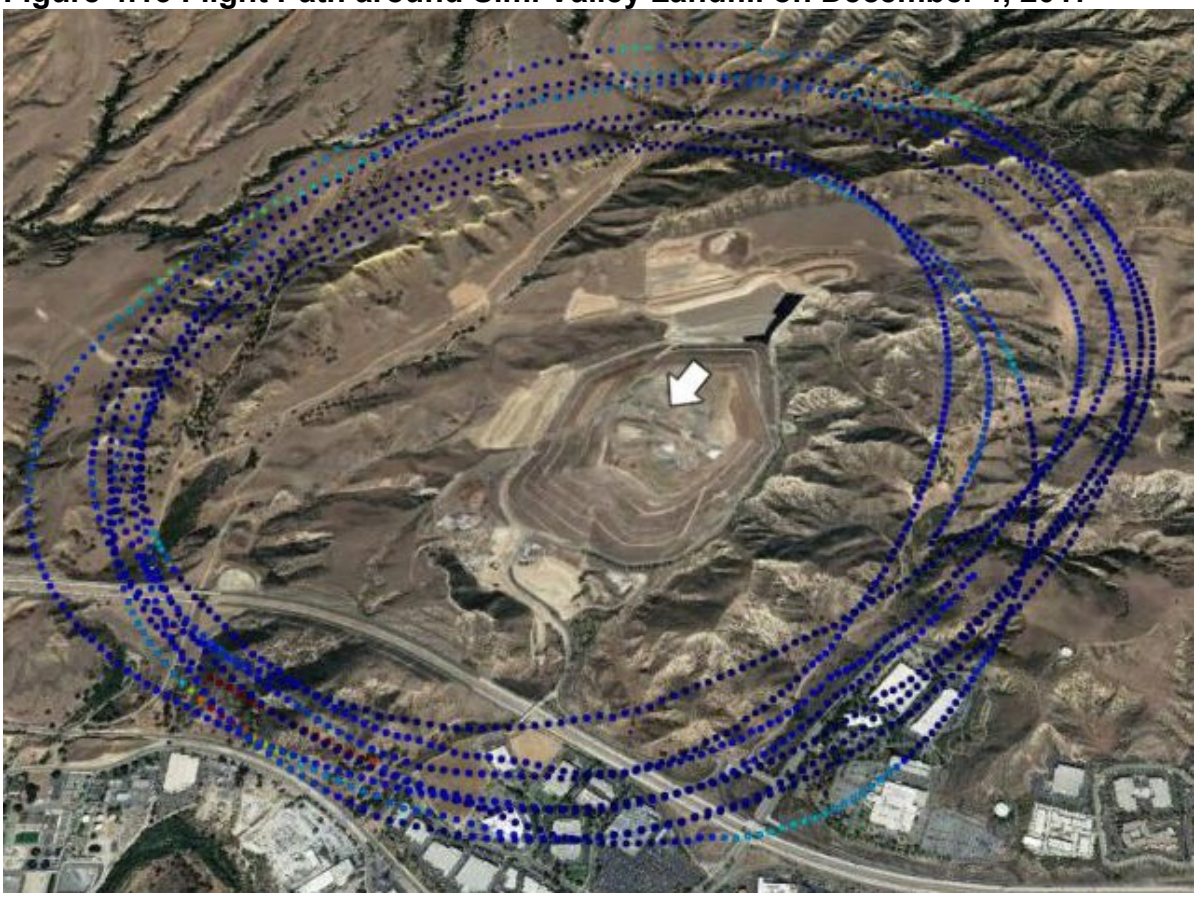

4.2.13 Stonyford Disposal Site -- December 6, 2017

A total of 20 useable laps were flown around Stonyford Disposal Site, as shown in Figure 4.14. The aircraft completed circles between 61 meters AGL and 620 meters AGL. Winds were out of the north, at 9.6 m s^{-1}. Total methane emission is estimated at 6 ± 1 kg hr^{-1}, which is below the detection limit of 10 kg hr^{-1}. The full flight path is presented in Figure 4.14.

Figure 4.14 Flight Path around Stonyford Disposal Site on December 6, 2017

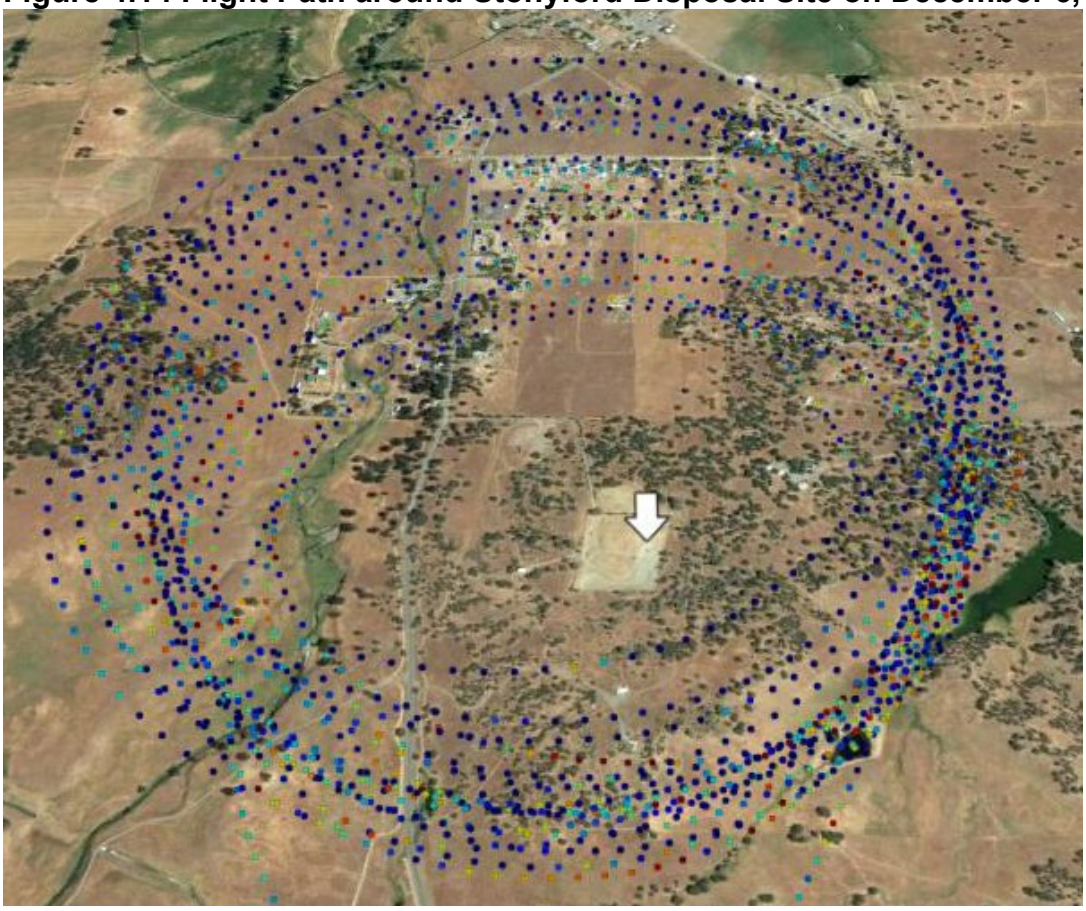

4.2.14 Pumice Valley Landfill -- December 6, 2017

A total of 16 useable laps were flown around Pumice Valley Landfill, as shown in Figure 4.15. The aircraft completed circles between 37 meters AGL and 620 meters AGL. Winds were out of the north/northeast, averaging 2 m s^{-1}. Total methane emission was below the detection limit of the aerial measurement system. The full flight path is presented in Figure 4.15.

Figure 4.15 Flight Path around Pumice Valley Landfill on December 6, 2017

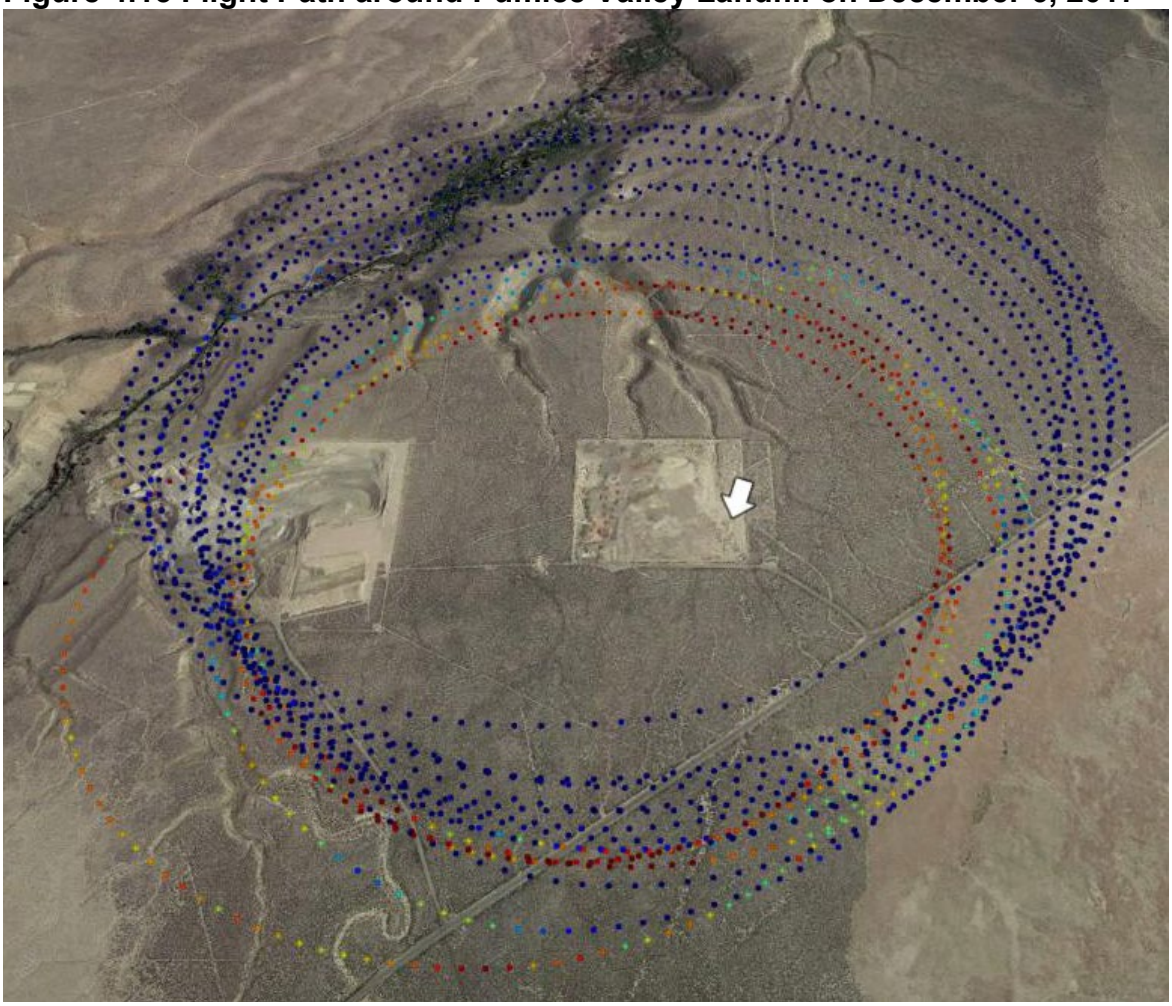

4.2.15 Site A -- December 7, 2017

A total of 11 useable laps were flown around Site A Landfill, as shown in Figure 4.16. The aircraft completed circles between 122 meters AGL and 409 meters AGL. Winds were out of the east, averaging 3.4m s^{-1}. Total methane emission is estimated at 1358 ± 547 kg hr^{-1}. The full flight path is presented in Figure 4.16. A profile of flux with elevation is presented in Figure 4.17.

Figure 4.16 Flight Path around Site A on December 7, 2017

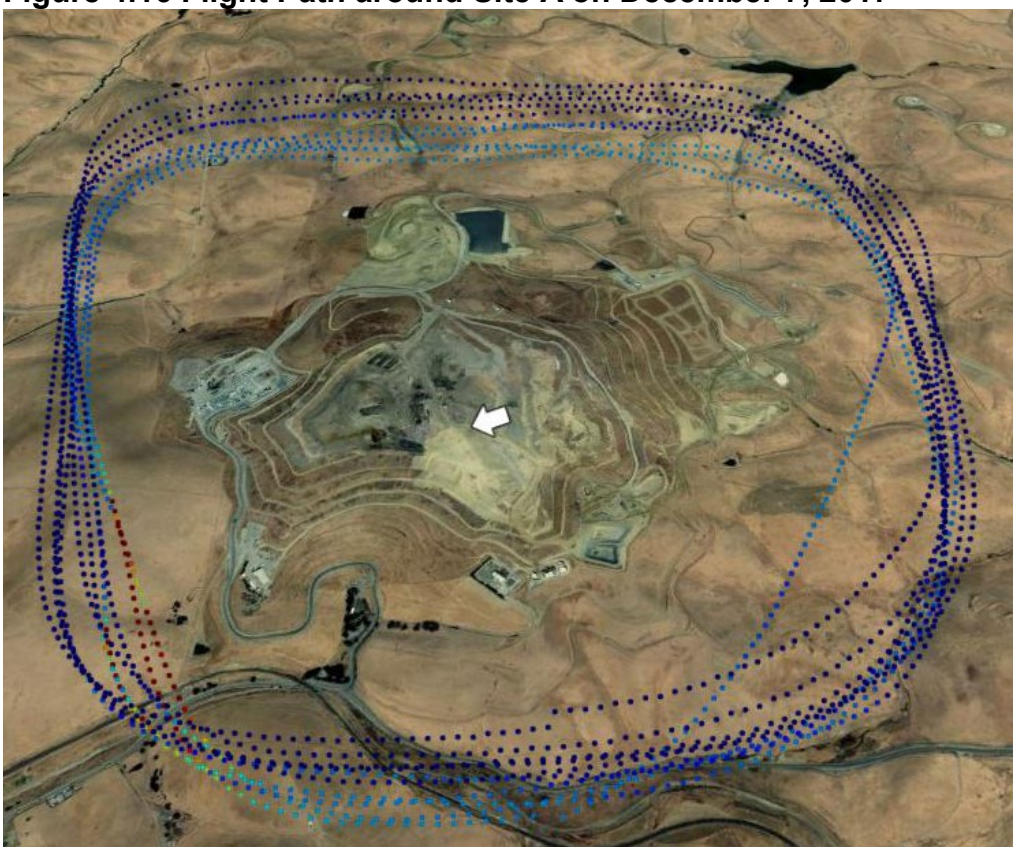

Figure 4.17 Flux Profile of Site A

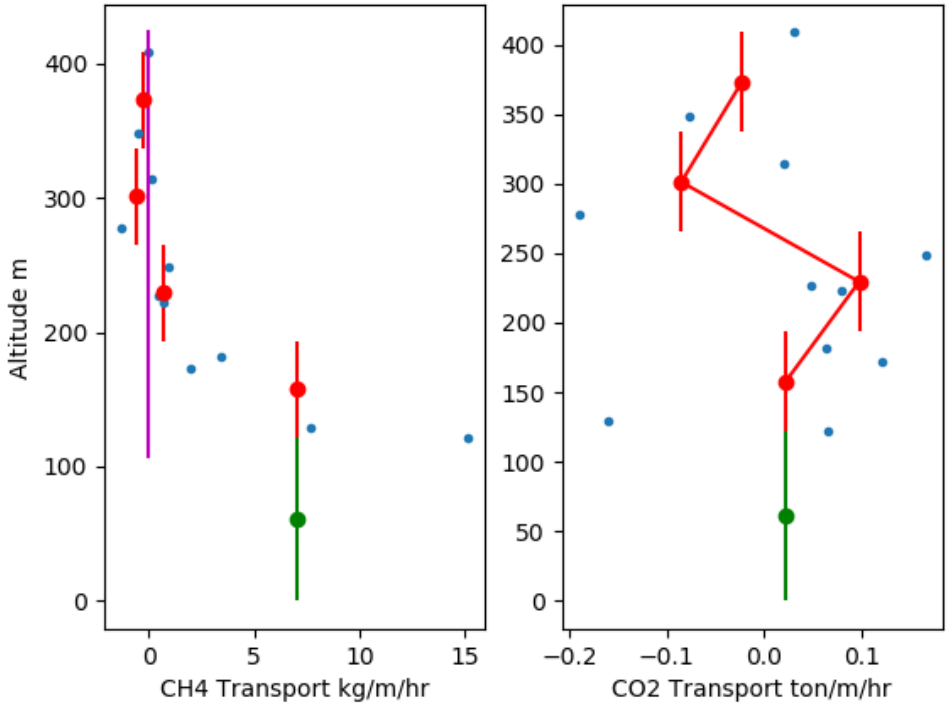

4.2.16 Potrero Hills Landfill -- December 7, 2017

At total of 12 useable laps were flown around Potrero Hills Landfill, as shown in Figure 4.18. The aircraft completed circles between 59 meters AGL and 364 meters AGL. Winds were out of the northeast, averaging 8.6 m s^{-1}. Total methane emission is estimated at 2004 ± 417 kg hr^{-1}. The full flight path is presented in Figure 4.18. A profile of flux with elevation is presented in Figure 4.19.

Figure 4.18 Flight Path around Potrero Hills Landfill on December 7, 2017

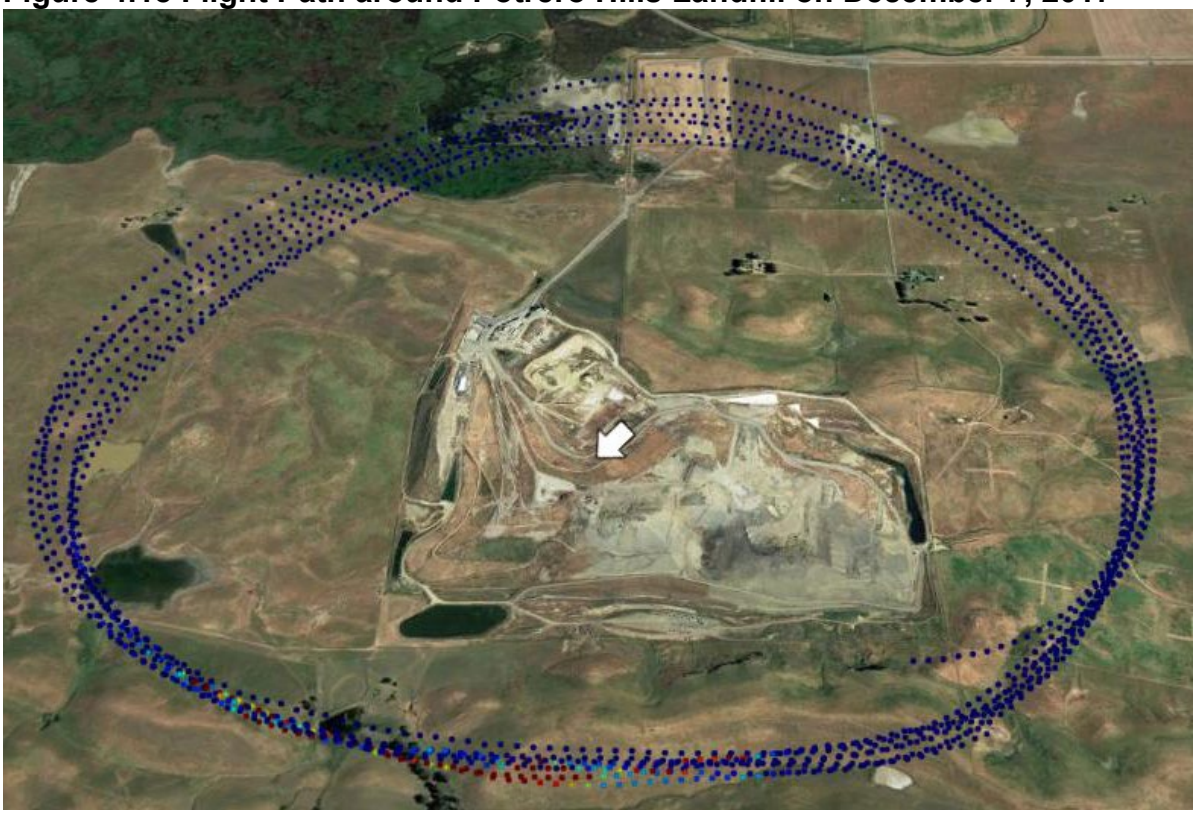

Figure 4.19 Flux Profile of Potrero Hills Landfill

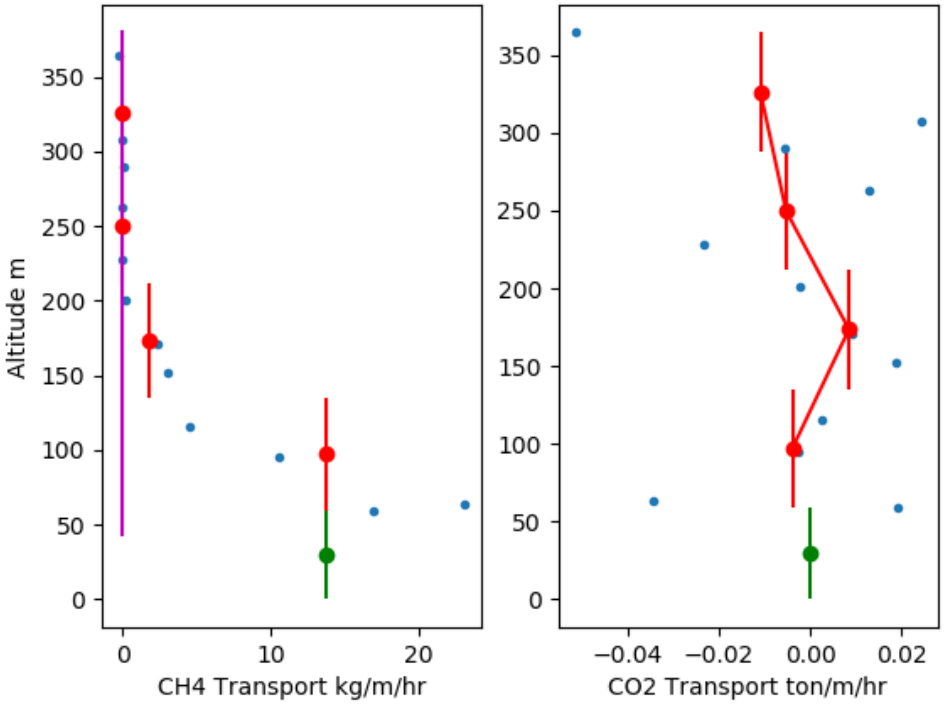

4.2.17 Chiquita Canyon Sanitary Landfill -- April 19, 2018

Twenty-seven laps were flown around the site at altitudes between 81 and 589 meters AGL (Figure 4.20). Winds were from the southwest at 5 m s^{-1}. Total methane emission is estimated at 602 ± 79 kg hr^{-1}. The full flight path is presented in Figure 4.20.

Figure 4.20 Flight Path around Chiquita Canyon Landfill on April 19, 2018

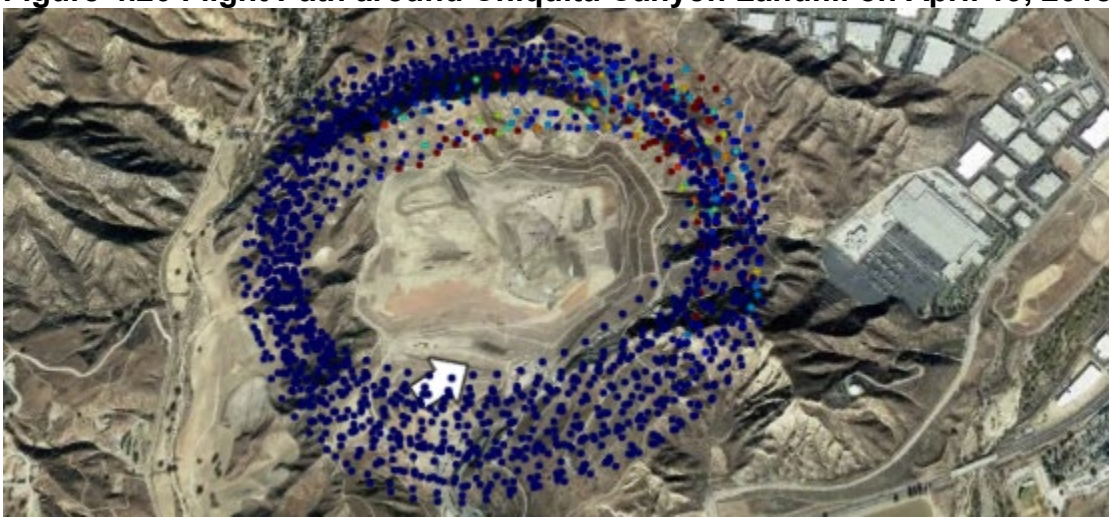

4.2.18 Sunshine Canyon Landfill -- April 19, 2018

A total of 28 laps were flown around Sunshine Canyon at altitudes of 81 to 871 meters AGL (Figure 4.21). Winds were from the south at 3.5 m s^{-1}. Total methane emission is estimated at 719 ± 155 kg hr^{-1}. The full flight path is presented in Figure 4.21.

Figure 4.21 Flight Path around Sunshine Canyon Landfill on April 19, 2018

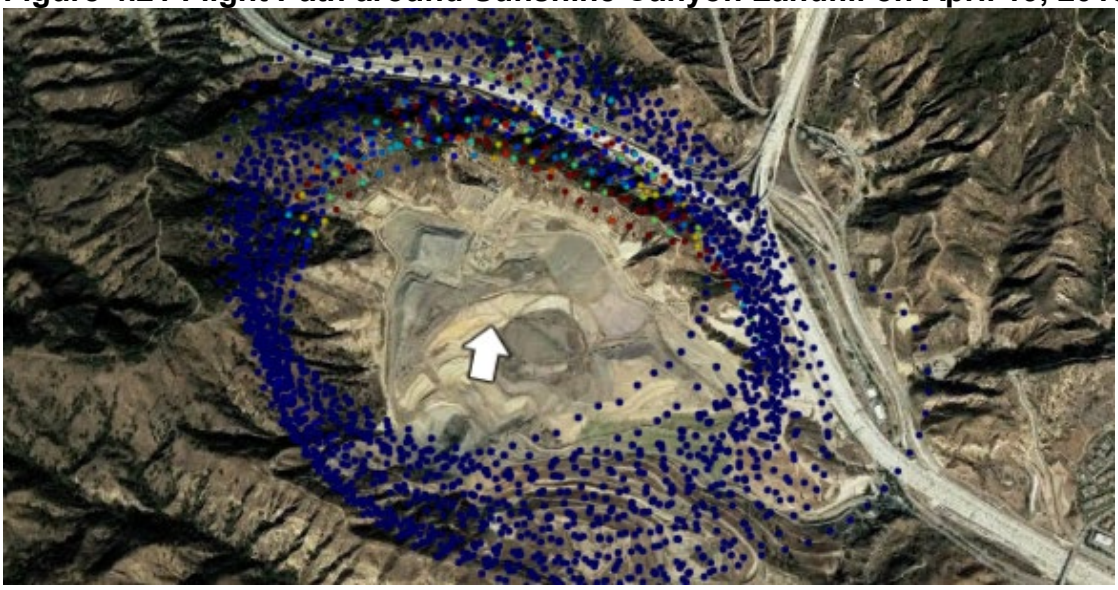

4.2.19 Sunshine Canyon Landfill -- July 24, 2018

Sixteen laps were flown around Sunshine Canyon at altitudes of 108 to 512 meters AGL (Figure 4.22). Winds were from the south at 4.9 m s^{-1}. Total methane emission is estimated at 712 ± 114 kg hr^{-1}. The full flight path is presented in Figure 4.22.

Figure 4.22 Flight Path around Sunshine Canyon Landfill on July 24, 2018

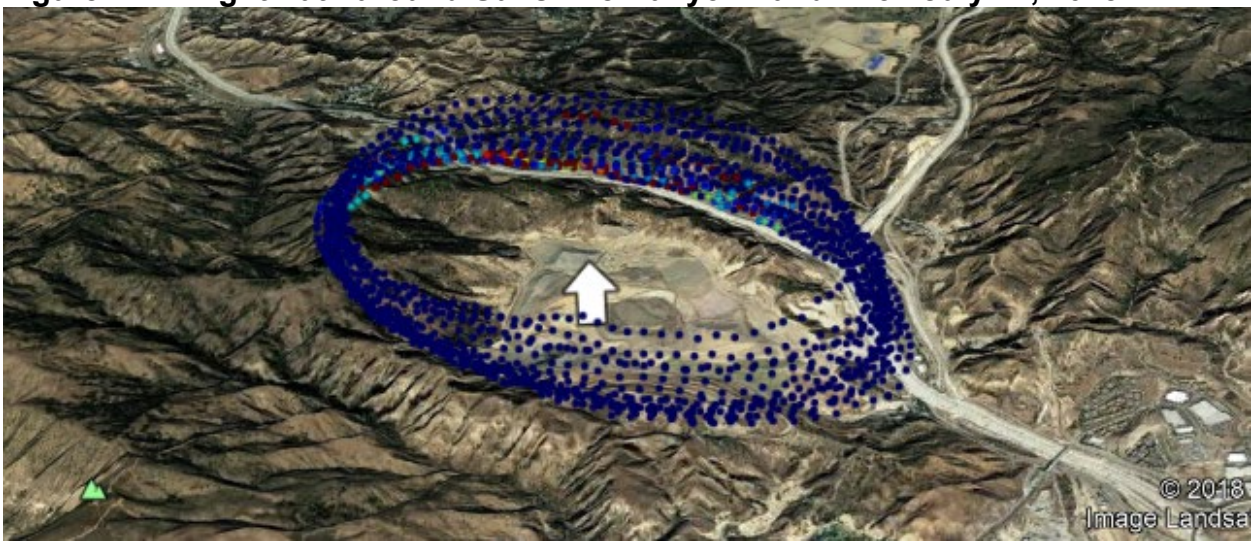

4.2.20 Chiquita Canyon Sanitary Landfill -- July 24, 2018

Seventeen laps were flown around Chiquita Canyon Landfill at altitudes of 166 to 617 meters AGL (Figure 4.23). Winds were from the southwest at 6.8 m s^{-1}. Total methane emission is estimated at 734 ± 128 kg hr^{-1}. The full flight path is presented in Figure 4.23.

Figure 4.23 Flight Path around Chiquita Canyon Landfill on July 24, 2018

4.2.21 Santa Maria Regional Landfill -- July 24, 2018

Seventeen laps were flown around Santa Maria Regional Landfill at altitudes of 61 to 374 meters AGL (Figure 4.24). Winds were from the west at 4.0 m s^{-1}. Total methane emission is estimated at 312±77 kg hr^{-1}. The full flight path is presented in Figure 4.24.

Figure 4.24 Flight Path around Santa Maria Regional Landfill on July 24, 2018

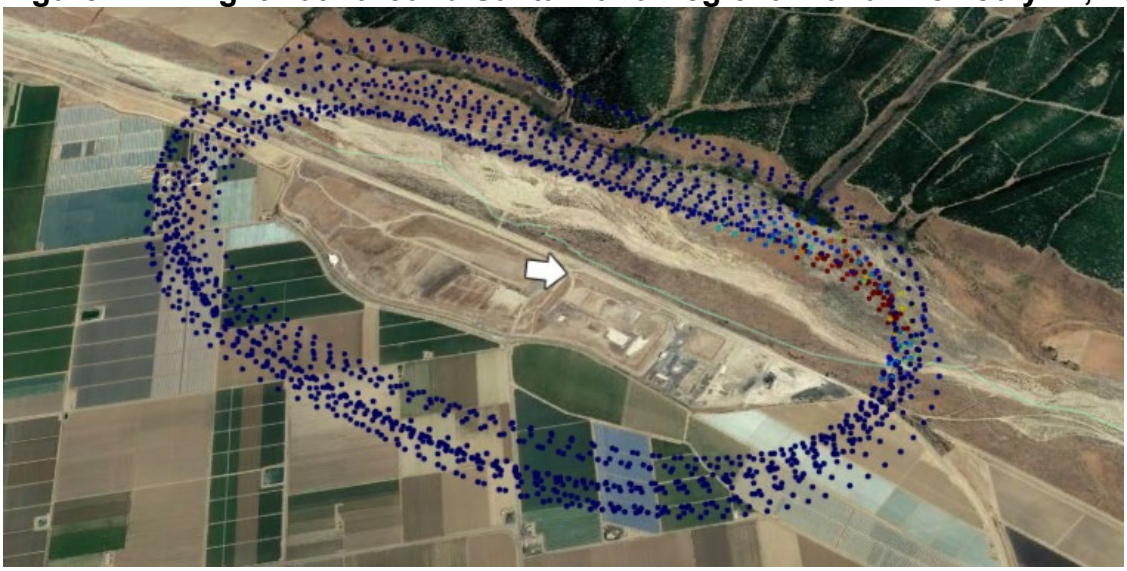

4.2.22 Potrero Hills Landfill -- August 23, 2018

Fourteen useable laps were flown around Potrero Hills Landfill at altitudes of 81 to 459 meters AGL (Figure 4.25). Winds were from the west/southwest at 8.7 m s^{-1}. Total methane emission is estimated at 1718 ± 252 kg hr^{-1}. The full flight path is presented in Figure 4.25.

Figure 4.25 Flight Path around Potrero Hills Landfill on August 23, 2018

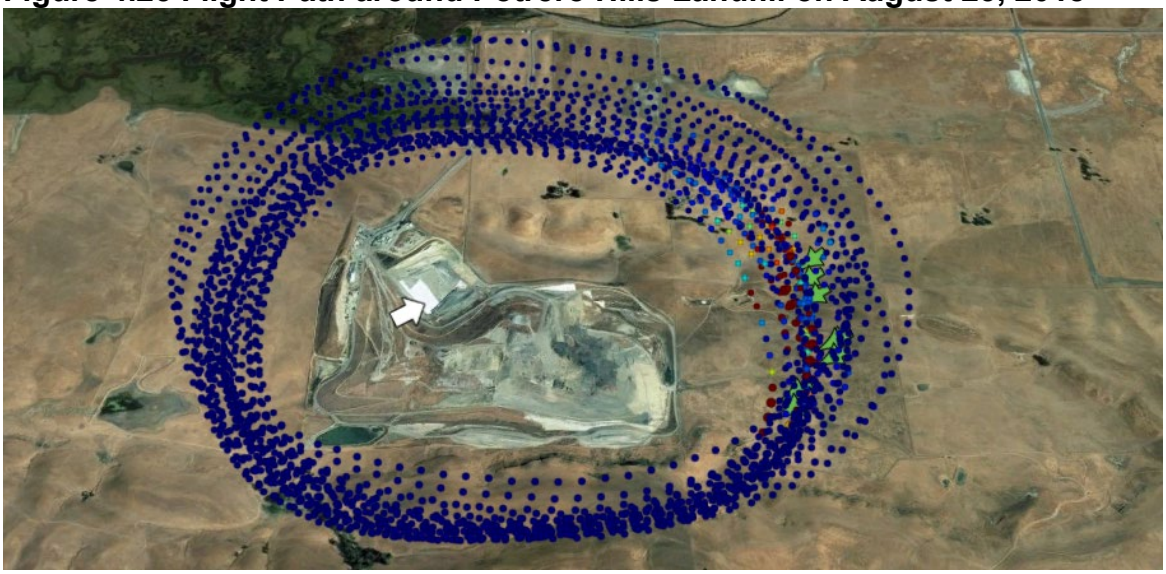

4.2.23 Site A -- August 27, 2018

Twenty-six laps were flown around Site A at altitudes of 111 to 843 meters AGL (Figure 4.26). Winds were from the southwest at 3.9 m/s. Total methane emission is estimated at 2077 ± 240 kg/hr. The flight path is presented in Figure 4.26.

Figure 4.26 Flight Path around Site A on August 27, 2018

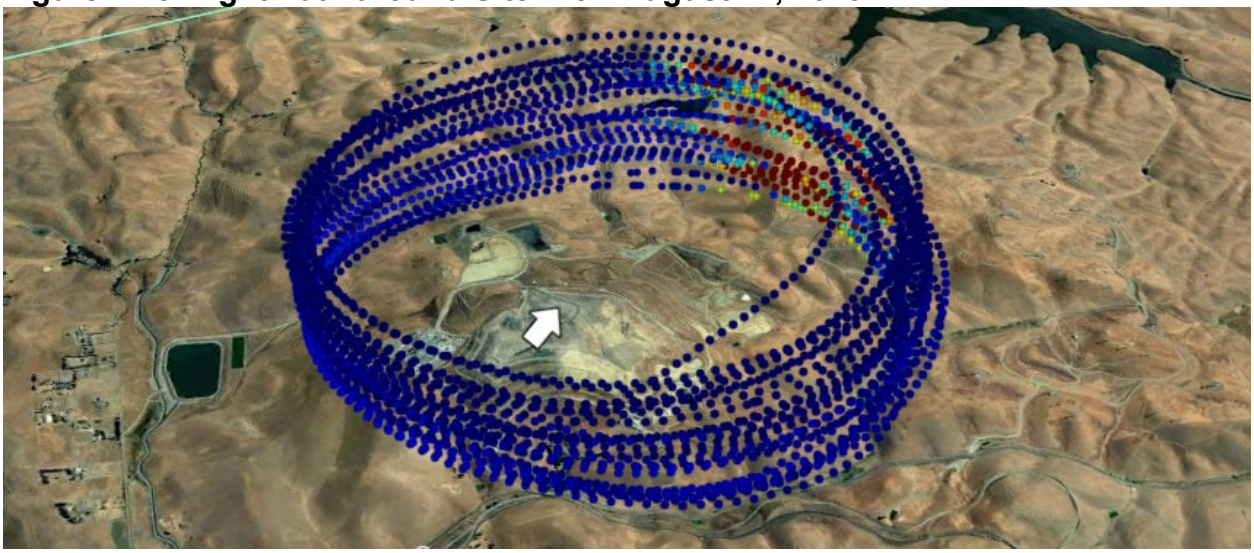

4.2.24 Teapot Dome Landfill – January 11, 2020

Fourteen laps were flown around Teapot Dome Landfill at altitudes of 117 to 424 meters AGL (Figure 4.27). Winds were from the west at 2.3 m/s. Total methane emission is estimated at 283.8 ± 131.5 kg/hr. The flight path is presented in Figure 4.27.

Figure 4.27 Flight Path around Teapot Dome Landfill on January 11, 2020

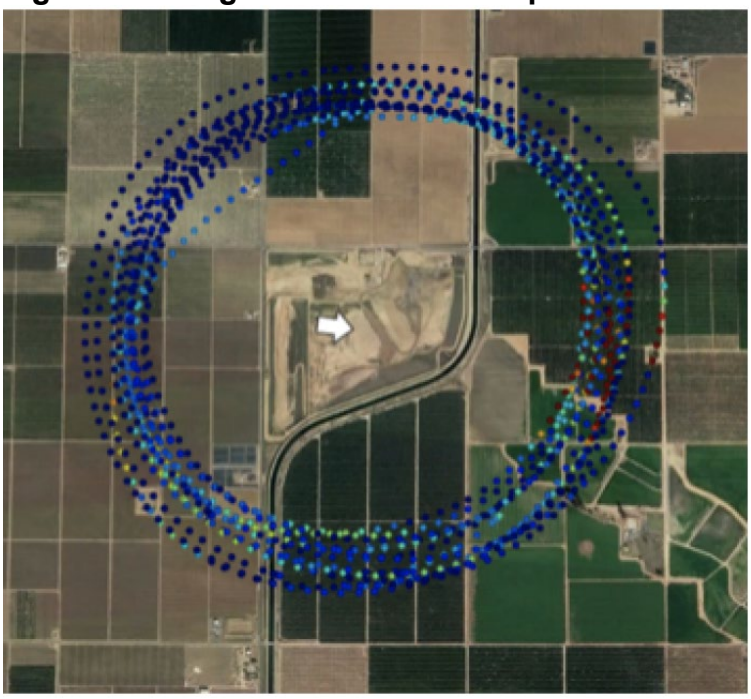

4.2.25 Summary of Aerial Measurements

A summary of the aerial measurements is presented for each landfill in ascending order in terms of waste in place and time (Table 4.1). The methane emissions increased from small to medium to large landfills where the emissions from the small, medium, and large landfills varied from -25 to 11, 90 to 638, and 602 to 3275 kg/hr, respectively. The methane emissions from the large landfills were more than one to more than two orders of magnitude higher than the emissions from the small landfills, whereas the differences between the medium and large landfills were within the same order of magnitude. While the tested small landfills did not have active gas collection and removal systems, the small size including the low waste in place and low daily throughput at these sites did not lead to generation/emission of methane. The medium and large landfills had gas collection and removal systems, yet the high waste in place and high throughput at these sites resulted in high gas generation and emissions.

The methane emissions from the two large nearby landfills, Chiquita Landfill and Sunshine Canyon Landfill, were relatively similar on the measurement days: 602 kg/hr-Chiquita and 719 kg/hr-Sunshine Canyon (4/19/2018) and 734 kg/hr-Chiquita and 712 kg/hr-Sunshine Canyon (7/24/2018). For the three large sites that were also included in the ground-based static flux chamber measurements, consistent differences were not observed between the dry and wet season measurements. At Chiquita Canyon and Potrero Hills Landfills, dry season measurements were lower than wet season measurements, whereas at Site A, the dry season measurement was higher than the wet season measurement. The highest differences between the dry and wet seasons were for Site A.

Table 4.1 – Summary of Aerial Test Results

Site	Date	CH_4 Emission (kg/hr)	UC[1] (kg/hr)	Ethane Emission (kg/hr)	UC[1] (kg/hr)	Laps	Wind Direction	Wind Speed (m/s)	Lowest Altitude (m)	Highest Altitude (m)
Stonyford Disposal Site	11/17/17	0.6	0.7	0	0	11	354	4.4	62	334
Stonyford Disposal Site	12/6/17	6.1	1.4	2.4	14.1	20	359	9.6	61	620
Salton City LF	12/4/17	10.8	3	0	0	12	5	9.6	46	305
Borrego LF	12/4/17	4.1	1.2	0	0	17	109	2.1	48	458
Pumice Valley Landfill	12/6/17	-0.2	1.7	1.6	2.6	16	18	2	37	620
Mariposa County LF	10/18/17	9	14.7	0	0	10	239	2.3	171	495
Taft Recycling Center	10/18/17	-24.6	32.8	0	0	4	9	1.6	144	543
Teapot Dome LF	10/18/17	293.7	99.9	0	0	10	250	1.1	112	435
Teapot Dome LF	1/11/20	283.8	131.5	0	0	14	278	2.3	117	424
Santa Maria Regional LF	11/10/17	90.1	39.1	14	15.5	14	289	10.4	105	491
Santa Maria Reginal LF	7/24/18	312	77.1	0	0	17	288	4	61	374
Redwood Landfill	11/17/17	139.8	41.5	0	0	8	12	4.8	64	208
Simi Valley LF	12/4/17	637.7	337.2	0	0	8	39	16.2	264	518
Yolo County Central Landfill	11/17/17	375.6	68.4	0	0	11	344	7.4	61	306
Chiquita Canyon LF	11/10/17	1306.4	207.2	6.1	51.1	15	236	4.9	167	475

Site	Date	CH_4 Emission (kg/hr)	UC[1] (kg/hr)	Ethane Emission (kg/hr)	UC[1] (kg/hr)	Laps	Wind Direction	Wind Speed (m/s)	Lowest Altitude (m)	Highest Altitude (m)
Chiquita Canyon LF	4/19/18	601.9	79.4	2.3	8.5	27	236	5	81	589
Chiquita Canyon LF	7/24/18	733.8	128.4	0	0	17	234	6.8	166	617
Sunshine Canyon LF	4/19/18	718.5	155.4	-5	10.4	28	194	3.5	81	871
Sunshine Canyon LF	7/24/18	712	113.6	0	0	16	177	4.9	108	512
Site A	12/7/17	1357.6	547	-0.8	6.3	11	77	3.4	122	409
Site A	8/27/18	2076.7	239.7	0	0	26	233	3.9	111	843
Frank R Bowerman LF	11/10/17	3275.4	668.5	3.3	9.3	15	234	1.7	80	876
Potrero Hills LF	12/7/17	2004.2	416.6	2.9	8.6	12	40	8.6	59	364
Potrero Hills LF	8/23/18	1717.9	251.6	0	0	14	245	8.7	81	459

[1]Uncertainty

4.3 Static Flux Chamber Measurements – Intra-Landfill Variations

Initially, surface fluxes are presented individually for each of the 5 landfills included in the static flux chamber field campaigns. Results are presented for the two measurement seasons: dry and wet seasons. Variations in flux due to cover locations/types and chemical species are provided. Results are organized from the smallest to largest landfill site tested in terms of waste in place and this order is used throughout the report. Results obtained for the dry season testing campaigns are presented first, followed by the wet season testing campaigns. Results are presented in box plots, which include all of the data obtained in the test program.

4.3.1 Santa Maria Regional Landfill

4.3.1.1 Dry Season Test Results

Figure 4.27 presents box plots summarizing the flux measurements conducted across all testing locations at Santa Maria Regional Landfill during the dry weather season organized by chemical family. Out of the 820 potential measurements that could be obtained at this site, 640 measurements (78%) were viable given the R^2 threshold applied in this study. The remaining 16.5% and 5.5% of flux measurements were not included due to low R^2 value and below detection limit/analytical measurement errors, respectively. Overall, surface fluxes (including all chemical families) for this testing campaign varied from -9.50×10^{-3} to 4.02×10^{2} g/m^2-day. A majority of the measured fluxes were positive (79%), albeit small positive numbers (median flux of 5.95×10^{-6} g/m^2-day). Positive fluxes (out of the cover) and negative fluxes (into the cover) varied by 11 orders of magnitude (from 5.7×10^{-9} to 4.02×10^{2} g/m^2-day) and 6 orders of magnitude -9.50×10^{-3} to -2.57×10^{-8} g/m^2-day), respectively.

Comparison of the median flux values indicated that the greenhouse gas emissions (methane, nitrous oxide, carbon dioxide, and carbon monoxide) were greatest out of all the chemical families included, where fluxes of methane were most dominant. The variation in GHG emissions was also highest out of all chemical families, as indicated by the wide interquartile (IQR) and inter-whisker (IWR) ranges (Figure 4.27). During the dry season, average skewness and kurtosis values were approximately 1 and 3.68, respectively, indicating that the distribution of fluxes was positively skewed and heavy tailed (e.g., high number of potential outliers or anomalies in flux values). The span of the IQR for a majority of the chemical families was greater than zero for all chemical families included, further indicating that emissions were positively skewed. Positive skewness suggests that net emissions were more likely over net uptake for all the gases and high kurtosis is indicative of high variation in the measured fluxes for a given chemical family.

Figure 4.27 Measured Fluxes at Santa Maria Regional Landfill by Chemical Family in the Dry Season (open black diamonds, red lines, and solid red dots represent means, medians, and outliers, respectively).

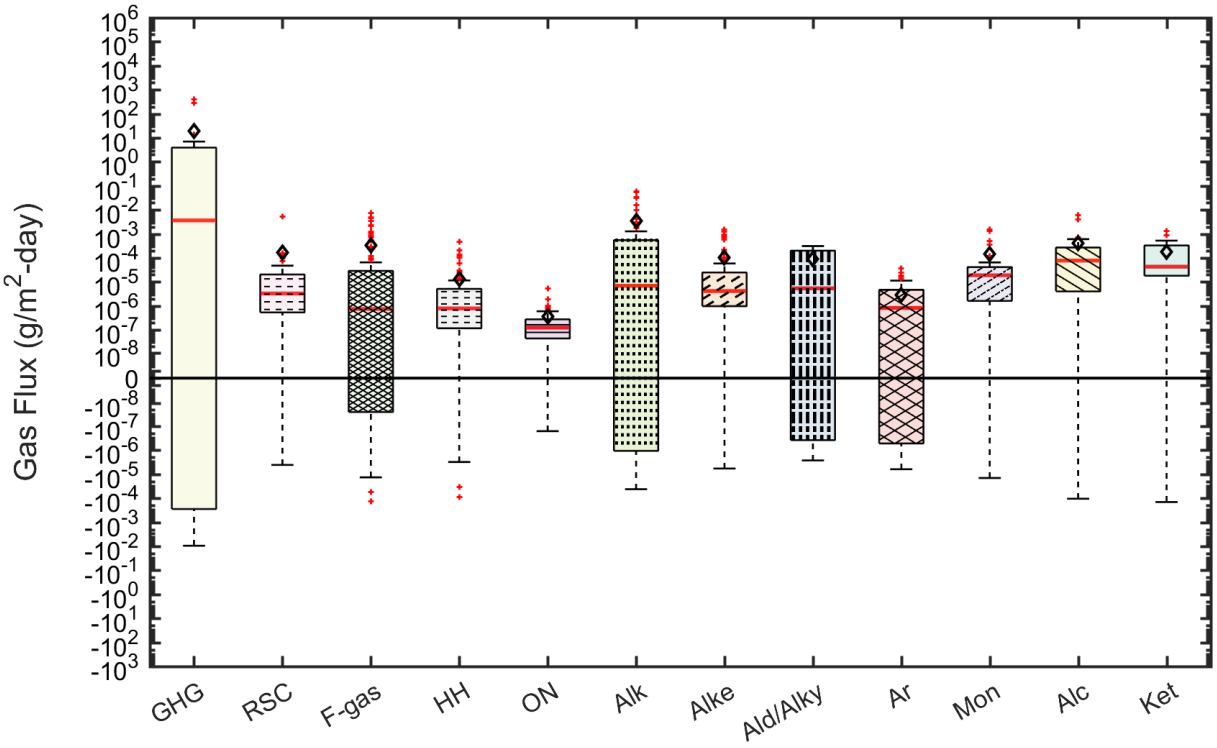

Comparison of median flux values for the NMVOCs indicated that fluxes for the sulfur compounds, F-gases, halogenated hydrocarbons, organic alkyl nitrates, alkanes, alkenes, aldehydes/alkynes, and aromatic hydrocarbon chemical families were relatively low compared to the other chemicals. Based on the median flux values presented, emissions of the alcohols, ketones, and monoterpenes categories were relatively higher than the aforementioned NMVOC families (Figure 4.27). Within each of these chemical families, methanol, acetone, and alpha-pinene demonstrated the highest median flux values. Variation in measured fluxes was highest and lowest for the alkane and organic nitrate chemical families, respectively where variation in fluxes among the remaining families (excluding the aromatics) was relatively similar (Figure 4.27). For this particular site and season, NMVOC fluxes varied from -1.44×10^{-4} to 5.82×10^{-2} g/m^2-day.

Measured fluxes of the project gases at Santa Maria Regional Landfill as a function of overall cover category are presented in Figure 4.28 for the dry season. Generally, the baseline GHGs (specifically carbon dioxide) had the highest maximum and median flux values across all cover categories. For NMVOCs, the highest median flux for daily, intermediate, and final covers were for the alkanes, alcohols, and aldehydes/alkynes, respectively. By individual chemical species, the highest flux for daily, intermediate, and final covers were for n-pentane, beta-pinene, and beta-pinene, respectively. For all gases, the fluxes generally decreased from daily to intermediate to final cover systems. For the daily cover locations, fluxes were generally positive, in particular for

the baseline greenhouse gases. However, net uptake of methane was observed for both the intermediate and final cover testing locations. The carbon dioxide fluxes were highest for all cover categories investigated, reaching up to 4.02×10^2 g/m^2-day. Comparison of median flux values indicated that the flux of nitrous oxide was also greater than the NMVOCs for both the daily and intermediate cover systems investigated.

Figure 4.28 Measured Fluxes at Santa Maria Regional Landfill by Overall Cover Category in the Dry Season (open black diamonds, red lines, and solid red dots represent means, medians, and outliers, respectively).

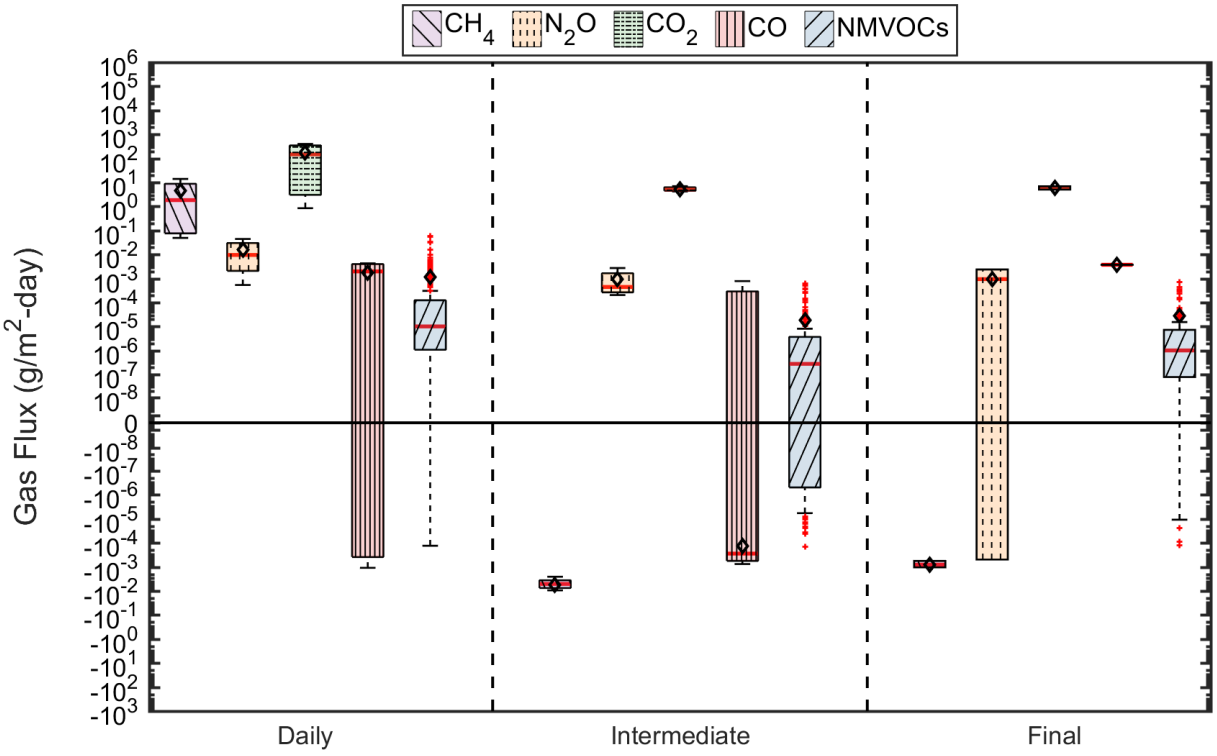

The fluxes for individual cover systems are presented in Figure 4.29. The intermediate-high cover represents the intermediate cover system tested at the normal vacuum pressure level of the gas collection system used at the site and is directly comparable to the daily and final covers. The intermediate-low cover represents the same intermediate cover system tested at a vacuum pressure lower than the normal vacuum pressure level used at the site. Of the cover systems investigated during the dry season field campaign, the daily cover primarily composed of wood waste was associated with the highest fluxes for all gases investigated (Figure 4.29). The presence of soil as an amendment to the wood waste significantly attenuated the fluxes of all gas species in the daily cover that consisted of wood waste and soil. The magnitude of fluxes and flux trends were relatively similar between the interim and final cover systems. The variation and magnitude of fluxes were somewhat higher during the high draw (i.e., high vacuum pressure) of the gas collection system than the low draw (i.e., low vacuum pressure) of the gas collection system for the intermediate cover system (Figure 4.29). The higher flux during high draw may have resulted from

larger concentration differentials across the cover system during operation of the gas collection system at the higher level of vacuum pressure.

Figure 4.29 Measured Fluxes at Santa Maria Regional Landfill by Individual Cover Type in the Dry Season (open black diamonds, red lines, and solid red dots represent means, medians, and outliers, respectively).

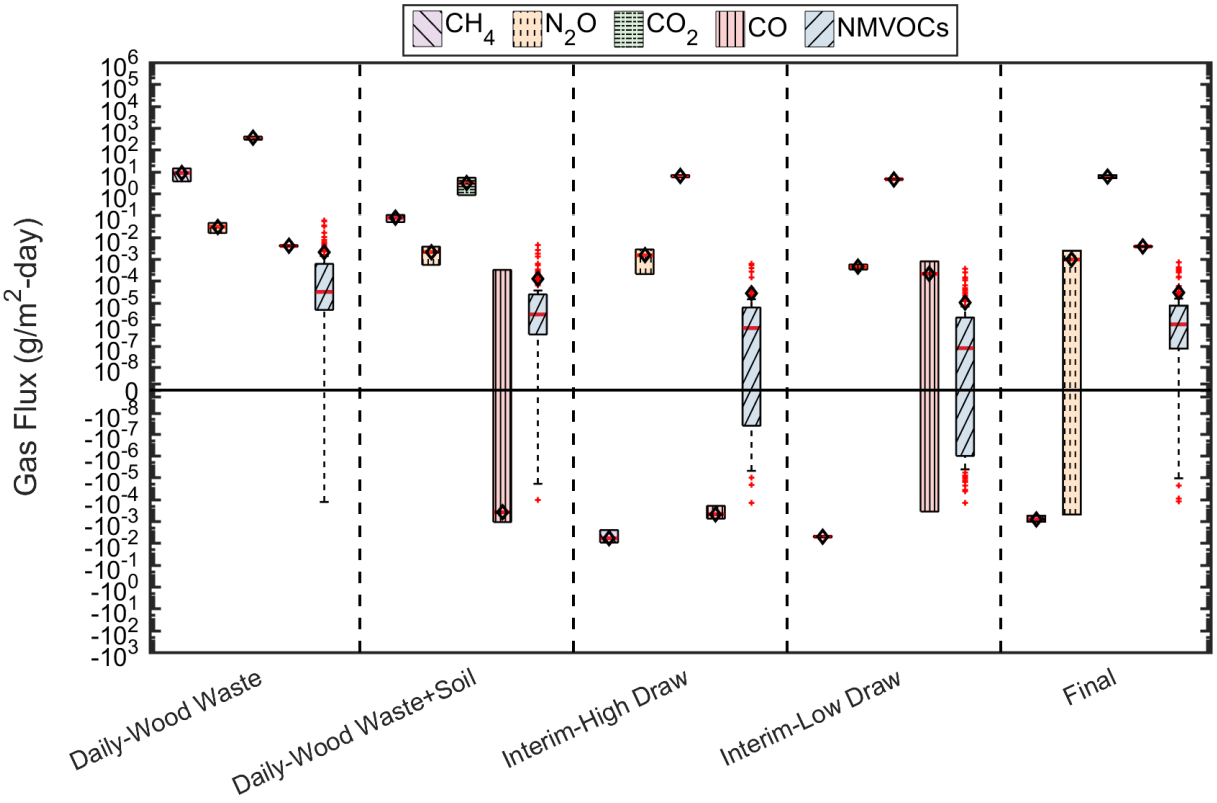

4.3.1.2 Wet Season Test Results

At Santa Maria Regional Landfill, flux testing conducted during the wet season differed from the dry season tests in various aspects. The number of acceptable flux measurements decreased slightly from approximately 78% to approximately 76% (N=623 flux measurements), where the contribution from low R^2 values were on the order of 20% and the below detection limit/analytical measurement error measurements amounted to 3%. Also, the range in baseline GHG emissions was observed to decrease compared to dry season testing program. The overall flux values in wet season testing ranged from -3.95×10^{0} to 1.14×10^{2} g/m^2-day. The percentage of measurements that were positive decreased slightly from 79% in the dry season to 76% in the wet season, where the median value of positive measurements also decreased (5.28×10^{-6} g/m^2-day). Positive fluxes (out of the cover) and negative fluxes (into the cover) varied by 10 (from 4.75×10^{-9} to 1.14×10^{2} g/m^2-day) and 9 (-3.94 to -5.23×10^{-9} g/m^2-day) orders of magnitude, respectively.

Figure 4.30 presents box plots summarizing the flux measurements conducted across all testing locations at Santa Maria Regional Landfill during the wet weather season

organized by chemical family. For the most dominant chemical family (baseline GHGs), median flux values were slightly lower in the wet season as compared to the dry season. Variation in baseline GHG emissions decreased during the wet season, based on the IQRs and IWRs observed (Figure 4.30). Distributions of measured fluxes were still positively skewed (average skewness of approximately 1) and heavy-tailed (average kurtosis approximately 3.9), indicating that net emissions were more likely over net uptake and that variation in the measured fluxes was high for a given chemical family.

Figure 4.30 Measured Fluxes at Santa Maria Regional Landfill by Chemical Family in the Wet Season (open black diamonds, red lines, and solid red dots represent means, medians, and outliers, respectively).

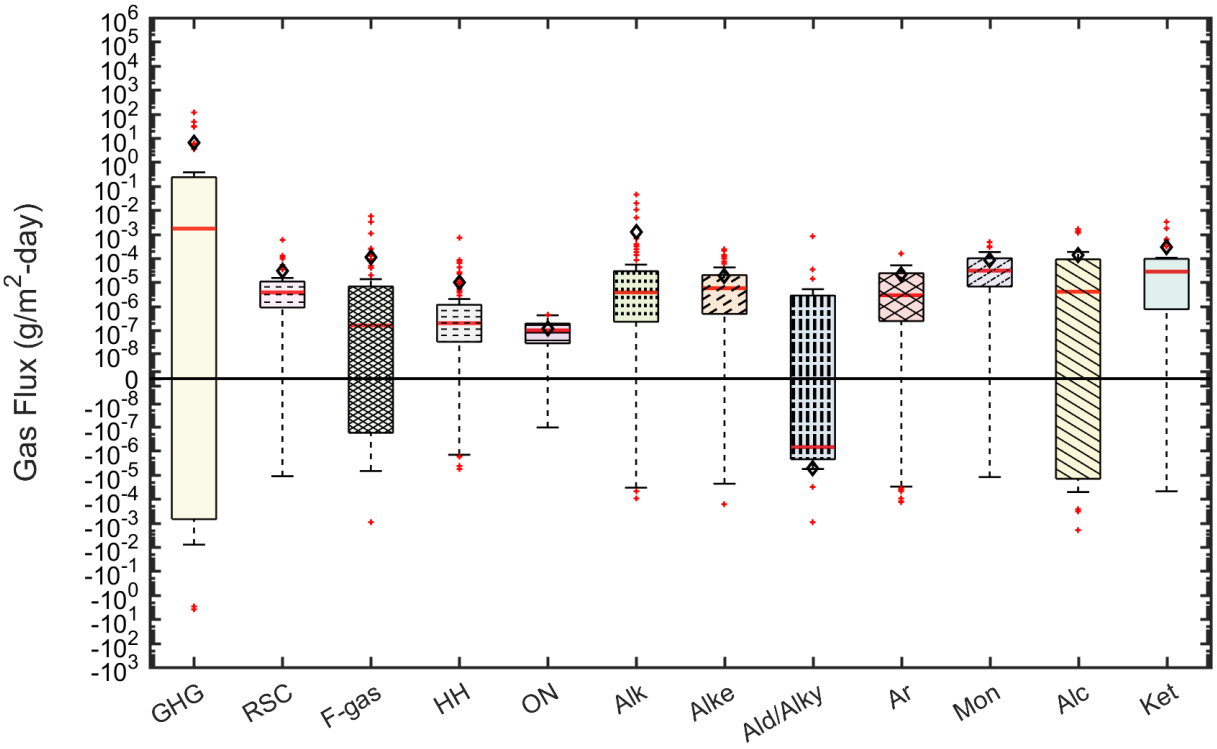

Overall, median NMVOC fluxes generally decreased during the wet season at Santa Maria Regional Landfill as compared to the dry season. In addition, the variation in NMVOC flux measurements, as assessed using the average IQR and IWR across NMVOC families, decreased during the wet season as compared to the dry season (Figure 4.30). Based on the median flux values presented in Figure 4.30, emissions of the monoterpenes, ketones, and alkenes were relatively higher than all of the NMVOC families analyzed. Within each of these chemical families, alpha-pinene, acetone, 1-pentene demonstrated the highest median flux values. Variation in measured fluxes was highest and lowest for the alcohols and organic nitrate chemical families, respectively, where variation in fluxes among the remaining families (excluding the aldehydes/alkynes) was relatively similar (Figure 4.30). For this particular site and season, NMVOC fluxes varied from -1.93×10^{-3} to 4.48×10^{-2} g/m^2-day.

Measured fluxes of the project gases at Santa Maria Regional Landfill as a function of overall cover category are presented in Figure 4.31 for the wet season. Generally, the baseline GHGs (specifically carbon dioxide) had the highest maximum and median flux values across all cover categories. For NMVOCs, the highest median fluxes for daily, intermediate, and final covers were for the monoterpenes in all cases. By individual chemical species, the highest flux for daily, intermediate, and final covers were for i-butene, 1-3-5 trimethylbenzene, and beta-pinene, respectively. During the wet weather season, median NMVOC fluxes generally decreased and the variation within chemical families was reduced as the average IQR and IWRs decreased (Figure 4.31). The monoterpenes and ketone chemical families were still dominant NMVOC families in the wet weather season, even though the emission of alcohols generally decreased as opposed to the alkane chemical family. Similar to the dry season, alpha-pinene and acetone were the NMVOCs with the highest median emissions, along with i-butane within each of these dominant chemical families. Intra-landfill NMVOC fluxes at Santa Maria Regional Landfill ranged from -1.93×10^{-3} to 4.45×10^{-2} g/m^2-day, which is comparable, yet slightly lower than the variation observed in the dry weather season.

During the wet season at Santa Maria Regional Landfill, the effect of overall cover category was somewhat less pronounced on measured surface fluxes for all chemicals investigated compared to the dry season (Figure 4.31). Methane flux generally decreased from the daily to intermediate cover systems tested during the wet season, which was consistent with results obtained during the dry season field campaigns. Both carbon dioxide and nitrous oxide fluxes were highly variable as a function of cover category. In particular, for the daily cover locations tested, the interquartile range of carbon dioxide fluxes ranged from -1 to 1.00×10^2 g/m^2-day. Nitrous oxide fluxes were more variable through the final covers tested during the wet season. In contrast, for the NMVOCs, there was a general decrease in median flux values and interquartile lengths progressing from daily to final cover materials.

Figure 4.31 Measured Fluxes at Santa Maria Regional Landfill by Overall Cover Category in the Wet Season (open black diamonds, red lines, and solid red dots represent means, medians, and outliers, respectively).

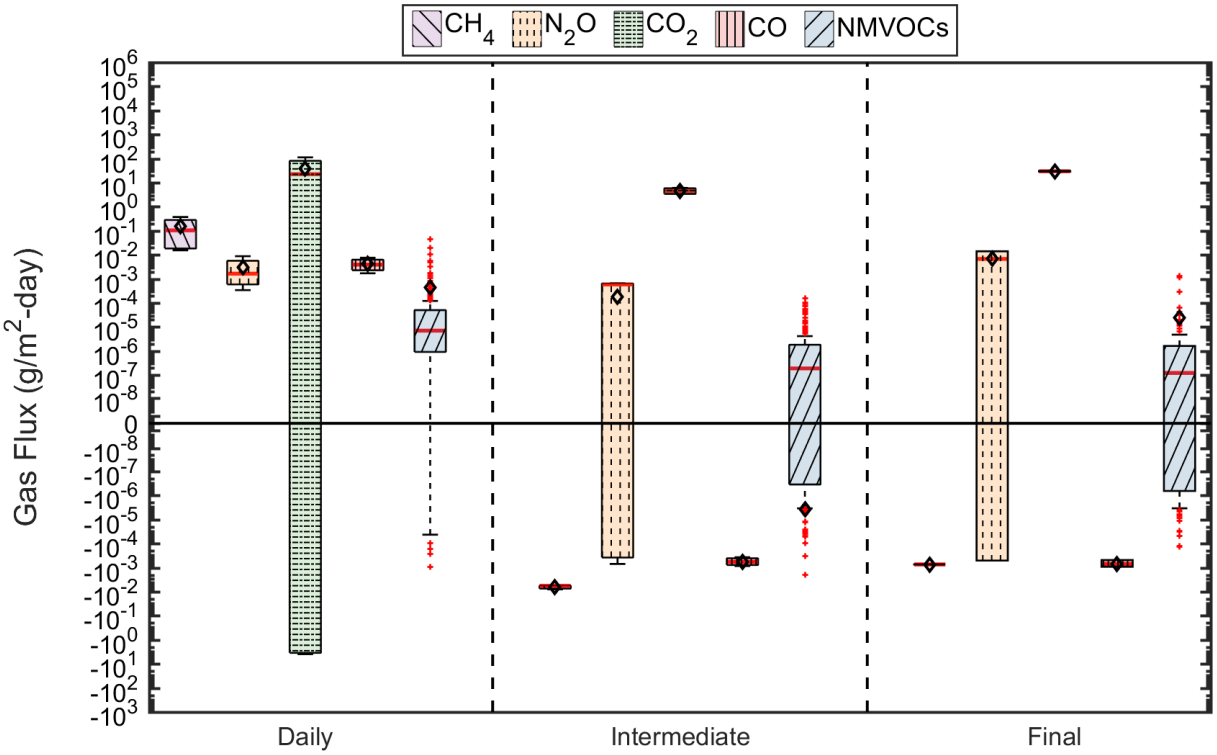

The fluxes from individual cover systems are presented in Figure 4.32 for the wet season. In the wet season differences were observed in the measured fluxes between the wood waste only and wood waste and soil mix daily cover materials in similarity to the dry season (Figure 4.32). The greatest difference between the daily cover materials was observed for the carbon dioxide fluxes, where net emissions (on the order of 1.00×10^{1} g/m^2-day) were observed for the wood waste only daily cover as compared to net uptake (on the order of -5.00×10^{0} g/m2-day) for the wood waste and soil daily cover location. Median flux values also decreased for methane and nitrous oxide from the wood waste to wood waste amended with soil and were relatively constant for the NMVOCs (even though the variability in measured fluxes decreased). Similar to the dry testing season, there was relatively low variation in measured fluxes across the different intermediate and final cover locations for methane, carbon dioxide, and NMVOCs. While median methane, carbon dioxide, and NMVOC fluxes were similar between the intermediate-high and intermediate-low tests, the median nitrous oxide flux increased significantly from intermediate-high to intermediate-low testing conditions. Nitrous oxide fluxes were relatively high for the final cover location in contrast to the dry season tests.

Figure 4.32 Measured Fluxes at Santa Maria Regional Landfill by Individual Cover Type in the Wet Season (open black diamonds, red lines, and solid red dots represent means, medians, and outliers, respectively).

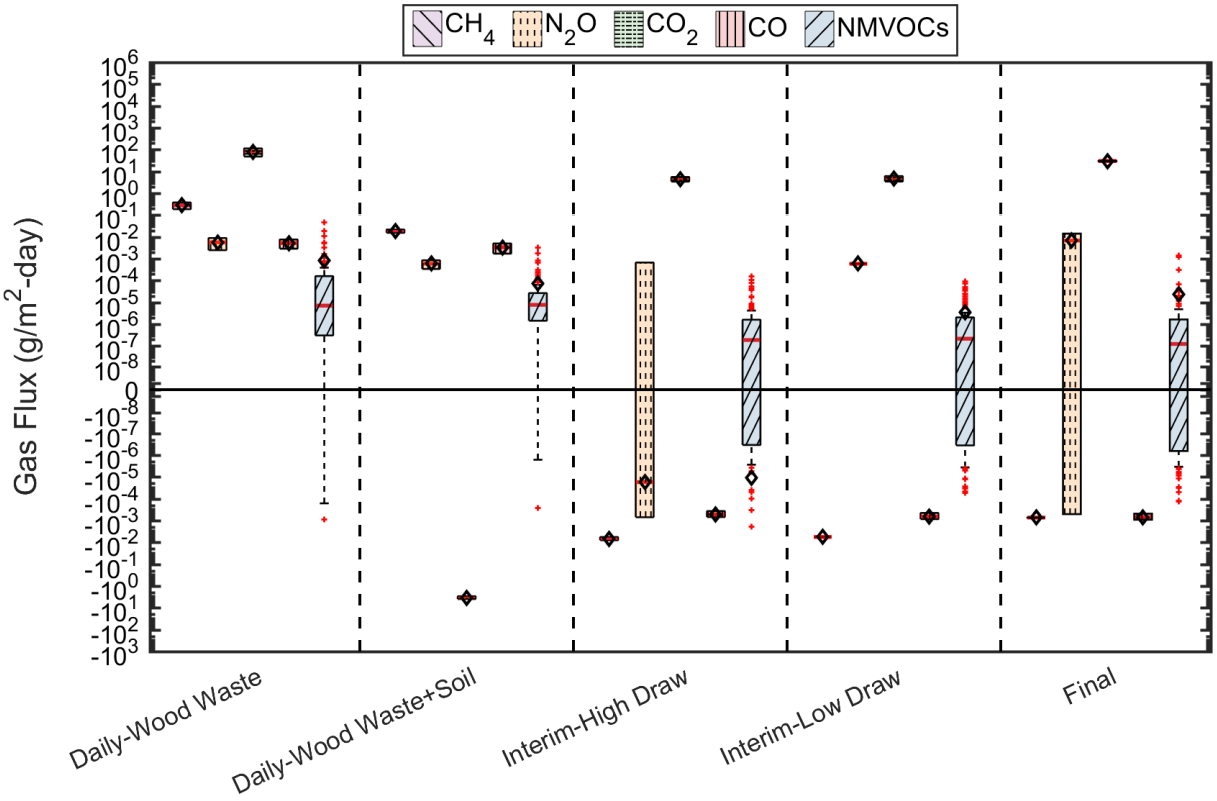

4.3.1.3 Summary of Flux Measurements from Santa Maria Regional Landfill

A comprehensive summary of the flux measurements obtained from the dry and wet season field campaigns at Santa Maria Regional Landfill is presented in Table 4.2. Overall minimum, maximum, and median flux values are organized in Table 4.2 according to chemical family and season. Measurements presented in Table 4.2 are intended to provide supplemental quantitative data to the boxplots included in the previous sections above to facilitate interpretation of the results.

Table 4.2 – Summary of Flux Measurements Obtained from Santa Maria Regional Landfill

Chemical Family	Dry Season (g/m^2-day)			Wet Season (g/m^2-day)		
	Min	Max	Median	Min	Max	Median
GHG	$-9.48x10^{-3}$	$4.02x10^{2}$	$3.66x10^{-3}$	$-3.95X10^{0}$	$1.14x10^{2}$	$1.72x10^{-3}$
RSC	$-4.11x10^{-6}$	$5.30x10^{-3}$	$3.32x10^{-6}$	$-1.14x10^{-5}$	$5.70x10^{-4}$	$3.83x10^{-6}$
F-gases	$-1.31x10^{-4}$	$7.25x10^{-3}$	$7.56x10^{-7}$	$-9.13x10^{-4}$	$5.70x10^{-3}$	$1.61x10^{-7}$
HH	$-8.70x10^{-5}$	$4.78x10^{-4}$	$7.97x10^{-7}$	$-5.48x10^{-6}$	$7.39x10^{-4}$	$2.01x10^{-7}$
ON	$-1.61x10^{-7}$	$5.26x10^{-6}$	$1.25x10^{-7}$	$-1.06x10^{-7}$	$4.50x10^{-7}$	$9.97x10^{-8}$
Alk	$-4.19x10^{-5}$	$5.82x10^{-2}$	$6.97x10^{-6}$	$-9.63x10^{-5}$	$4.48x10^{-2}$	$3.84x10^{-6}$
Alke	$-5.77x10^{-6}$	$1.51x10^{-3}$	$4.19x10^{-7}$	$-1.62x10^{-4}$	$2.40x10^{-4}$	$5.73x10^{-6}$
Ald/Alky	$-2.67x10^{-6}$	$3.14x10^{-4}$	$5.43x10^{-6}$	$-9.13x10^{-4}$	$7.97x10^{-4}$	$-7.00x10^{-7}$
Ar	$-6.21x10^{-6}$	$3.62x10^{-5}$	$8.30x10^{-7}$	$-1.36x10^{-4}$	$1.62x10^{-4}$	$2.91x10^{-6}$
Mon	$-1.44x10^{-5}$	$1.51x10^{-3}$	$1.91x10^{-5}$	$-1.24x10^{-5}$	$4.60x10^{-4}$	$3.08x10^{-5}$
Alc	-1.05x10-4	$6.02x10^{-3}$	$7.81x10^{-5}$	$-1.93x10^{-3}$	$1.61x10^{-3}$	$4.08x10^{-6}$
Ket	$-1.44x10^{-4}$	$1.33x10^{-3}$	$4.34x10^{-5}$	$-4.82x10^{-5}$	$3.17x10^{-3}$	$2.79x10^{-5}$

4.3.2 Teapot Dome Landfill

4.3.2.1 Dry Season Test Results

Figure 4.33 presents box plots summarizing the flux measurements conducted across all testing locations at Teapot Dome Landfill during the dry weather season organized by chemical family. Out of the 820 potential measurements that could be obtained at this site, 665 measurements (81%) were viable given the R^2 threshold applied in this study. The remaining approximately 10% and 9% of flux measurements were not included due to low R^2 value and below detection limit/analytical measurement errors, respectively. Overall, surface fluxes (including all chemical families) for this testing campaign varied from $-2.7x10^{-3}$ to $2.20x10^{2}$ g/m^2-day. A great majority of the measured fluxes were positive (92.6%) with a median flux of $1.59x10^{-5}$ g/m^2-day. Positive fluxes (out of the cover) and negative fluxes (into the cover) varied by 10 orders of magnitude (from $1.95x10^{-8}$ to $2.20x10^{2}$ g/m^2-day) and 5 orders of magnitude ($-2.70x10^{-3}$ to $-1.03x10^{-8}$ g/m^2-day), respectively.

At Teapot Dome Landfill, the baseline greenhouse gas fluxes were dominant, however exhibited a higher variation than the NMVOCs (Figure 4.33). Average skewness and kurtosis were 1.4 and 4, respectively and IQRs were above zero, indicating the higher probability of net emissions over uptake and the high variation in measured fluxes. Low probability of uptake was present for multiple chemical families. The likelihood for uptake over emissions was greatest for the GHGs, and also high for the alkanes, aromatics, and alcohols based on the extent of the lower whiskers below zero.

Figure 4.33 Measured Fluxes at Teapot Dome Landfill by Chemical Family in the Dry Season (open black diamonds, red lines, and solid red dots represent means, medians, and outliers, respectively).

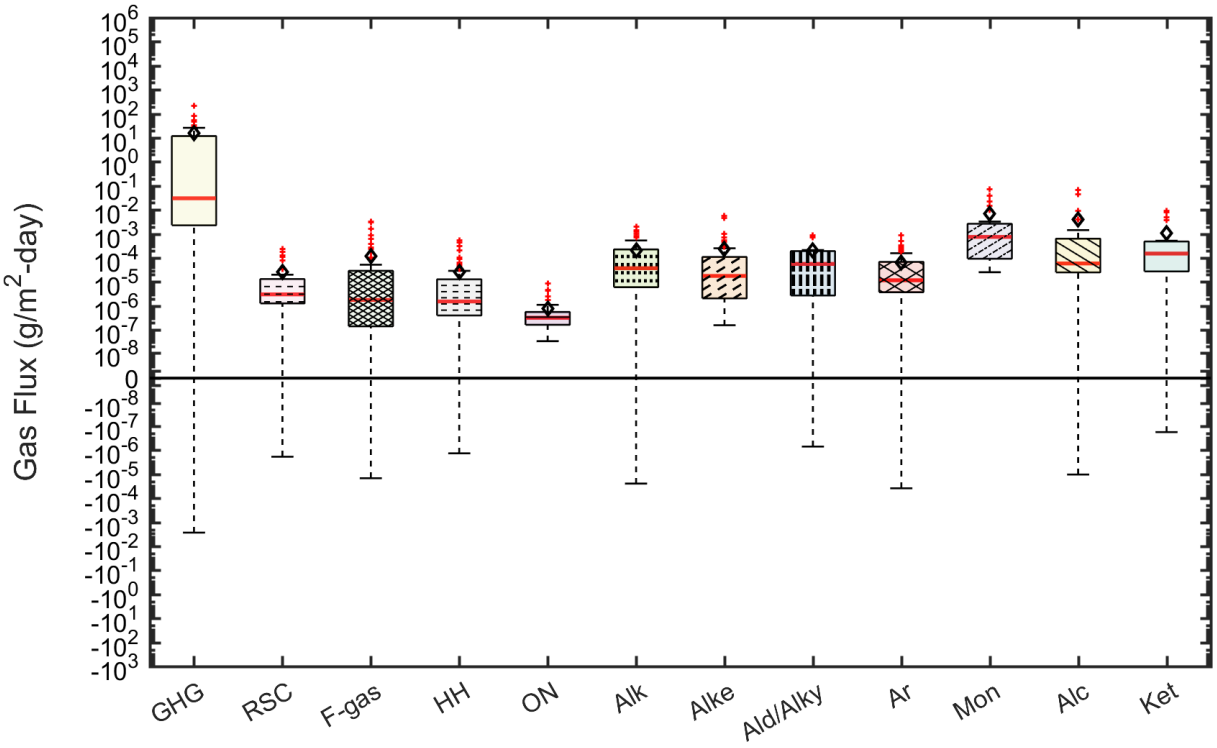

Among the NMVOCs investigated, the monoterpenes, ketones, alcohols, aldehydes/alkynes, and alkanes were associated with the highest fluxes based on the median flux data (Figure 4.33). Within each of these families, alpha pinene, acetone, and methanol demonstrated the highest median flux values. The NMVOC fluxes were comparable (assessed using IQR and IWR) across all NMVOC chemical families with the exception of the organic alkyl nitrates, halogenated hydrocarbons, and reduced sulfur compounds that demonstrated lower variations in measured fluxes (Figure 4.33). Overall NMVOC emissions ranged from -3.86×10^{-5} to 7.44×10^{-2} g/m^2-day.

Measured fluxes of the project gases at Teapot Dome Landfill as a function of overall cover category are presented in Figure 4.34 for the dry season. Generally, the baseline GHGs (specifically carbon dioxide) had the highest median flux values across all cover categories. For NMVOCs, the highest median flux for daily and intermediate covers were for the monoterpenes. By individual chemical species, the highest fluxes observed for both daily and intermediate covers were for 1,2,4-trimethylbenzene. For all gases, the fluxes generally decreased from daily to intermediate cover locations. The decreases in flux were relatively modest and the differences in median fluxes were between 7.69×10^{-5} (NMVOCs) and 4.37×10^{0} (GHGs). For dry weather testing, a high number of uptake measurements were obtained for the intermediate covers at Teapot Dome Landfill, as indicated by the wider interquartile ranges and extent of the whiskers below zero for these locations. For a given GHG, variability in the measured fluxes were higher at the intermediate cover locations compared to the daily cover

locations, whereas the variability in NMVOC measurements decreased progressing from daily to intermediate cover systems.

Figure 4.34 Measured Fluxes at Teapot Dome Landfill by Overall Cover Category in the Dry Season (open black diamonds, red lines, and solid red dots represent means, medians, and outliers, respectively).

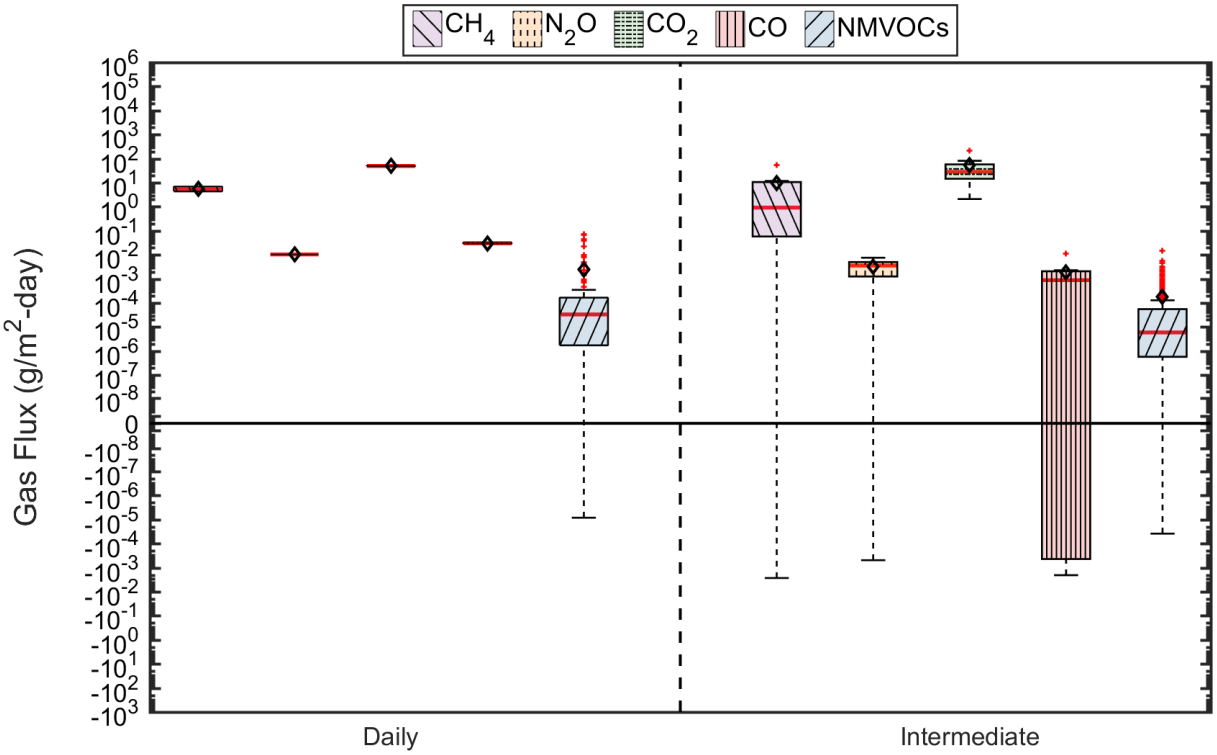

The fluxes from individual cover systems are presented in Figure 4.35. Of the intermediate cover systems investigated, the cover overlying the old waste was generally associated with the lowest emissions for all gases analyzed with significant uptake of methane as indicated by the extent of the interquartile range below zero. Fluxes of methane and carbon dioxide were greatest at the intermediate cover overlying the designated wet waste placement area at the site. At this cover location, nitrous oxide emissions were highly variable. The magnitude and extent of NMVOC emissions were generally comparable across all testing locations, where the daily cover location had the highest fluxes (based on the mean and median values presented in the boxplots) (Figure 4.35).

Figure 4.35 Measured Fluxes at Teapot Dome Landfill by Individual Cover Type in the Dry Season (open black diamonds, red lines, and solid red dots represent means, medians, and outliers, respectively).

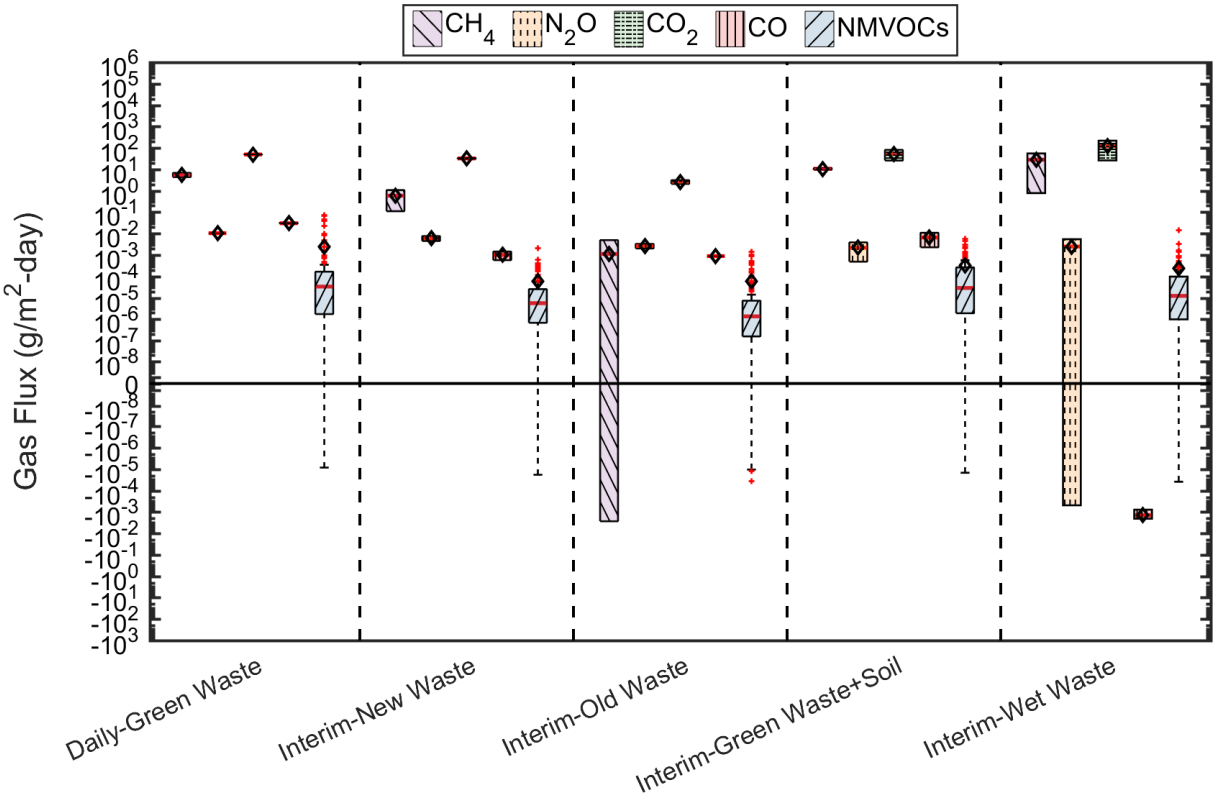

4.3.2.2 Wet Season Test Results

At Teapot Dome Landfill, flux testing conducted during the wet season differed from the dry season tests in various aspects. The number of acceptable flux measurements decreased from 81% to 76% (N=625 flux measurements), where the contribution from low R^2 values were on the order of 18% and the below detection limit measurements amounted to 6%. The overall range (including all chemical families) in measured fluxes changed from -2.7×10^{-3} to 2.20×10^{2} in the dry season to -6.70×10^{0} - 1.52×10^{2} g/m^2-day. The percentage of measurements that were positive decreased significantly from 92.6% in the dry season to 67% in the wet season. However, the median value of positive measurements increased (2.75×10^{-5} g/m^2-day). Positive fluxes (out of the cover) and negative fluxes (into the cover) varied by 11 (from 2.44×10^{-9} to 1.52×10^{2} g/m^2-day) and 10 (-6.70×10^{0} to -1.38×10^{-9} g/m^2-day) orders of magnitude, respectively.

Figure 4.36 presents box plots summarizing the flux measurements conducted across all testing locations at Teapot Dome Landfill during the wet weather season organized by chemical family. The baseline GHG fluxes remained dominant out of all chemical families included in the project. However, the variation in measured fluxes increased during wet season testing. Median flux values for the baseline GHGs decreased by two orders of magnitude. The corresponding IQRs and IWRs increased by a factor of two from the dry to wet season field measurement campaigns (Figure 4.36). Average

skewness and kurtosis values summarizing the overall distributions of flux measurements decreased to 0.9 and 3.52, respectively, during the wet season campaign. The distributions of flux measurements became more symmetric and homogenous (less positively skewed and lighter tailed) as a greater proportion of measurements were observed to be negative. The somewhat lower kurtosis was indicative of a somewhat reduced yet still high variation in the measured fluxes for a given chemical family.

Figure 4.36 Measured Fluxes at Teapot Dome Landfill by Chemical Family in the Wet Season (open black diamonds, red lines, and solid red dots represent means, medians, and outliers, respectively).

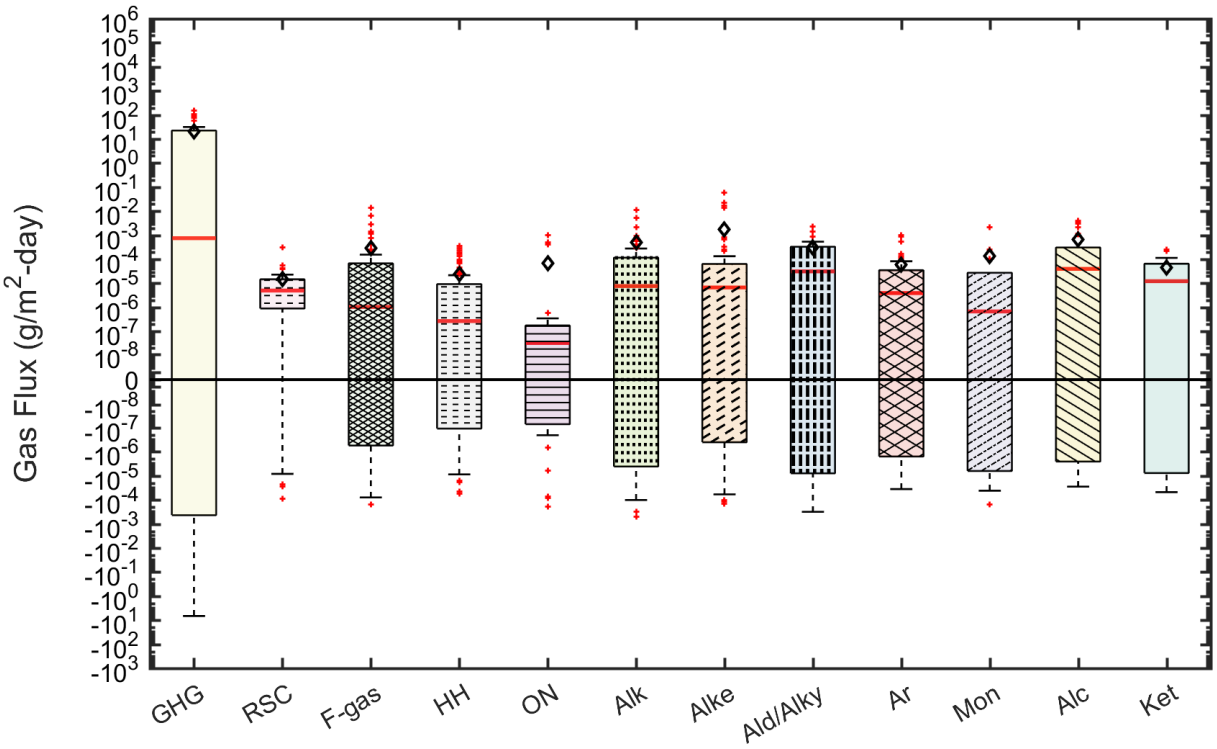

Overall, median NMVOC fluxes generally decreased two orders of magnitude during the wet season at Teapot Dome Landfill. In addition, the variation in NMVOC flux measurements, as assessed using the average IQR and IWR across NMVOC families, decreased by one order of magnitude during the wet season (Figure 4.36). The alcohols, aldehydes/alkynes, and ketones were the NMVOC families with the highest measured fluxes, which were comparable to those observed during the dry season. The highest median fluxes for specific chemical species within each family were measured for 2-butanol, ethyne, and methylisobutylketone. Similar to the baseline GHGs, the range in overall NMVOC emissions decreased during the wet season to -5.11×10^{-4} to 6.04×10^{-2} g/m^2-day.

Measured fluxes of the project gases at Teapot Dome Landfill as a function of overall cover category are presented in Figure 4.37 for the wet season. Generally, the baseline GHGs (specifically carbon dioxide) had the highest median flux values across

all cover categories. For NMVOCs, the highest median flux for daily and intermediate covers were obtained for the aldehydes/alkynes and alcohols, respectively. By individual chemical species, the highest flux observed for daily and intermediate covers were for 1-butene and HCFC-22. The central tendencies of methane, nitrous oxide, and carbon dioxide flux measurements were relatively similar between daily and intermediate cover systems at Teapot Dome Landfill during the wet season. However, the variation in the baseline greenhouse gas emissions increased for the intermediate cover systems, in particular for methane and carbon dioxide, where long lower whisker lengths were observed. Higher variation in flux measurements were observed for intermediate cover systems at Teapot Dome Landfill during the dry season. The variation in intermediate cover flux measurements was generally higher in the wet season than the dry season, given the longer IQR and IWR observed in Figure 4.37 as compared to Figure 4.34. Fluxes of NMVOCs generally decreased from daily to intermediate cover systems at Teapot Dome during the wet season which corresponded with a decrease in the variation of flux measurements (Figure 4.37).

Figure 4.37 Measured Fluxes at Teapot Dome Landfill by Overall Cover Category in the Wet Season (open black diamonds, red lines, and solid red dots represent means, medians, and outliers, respectively).

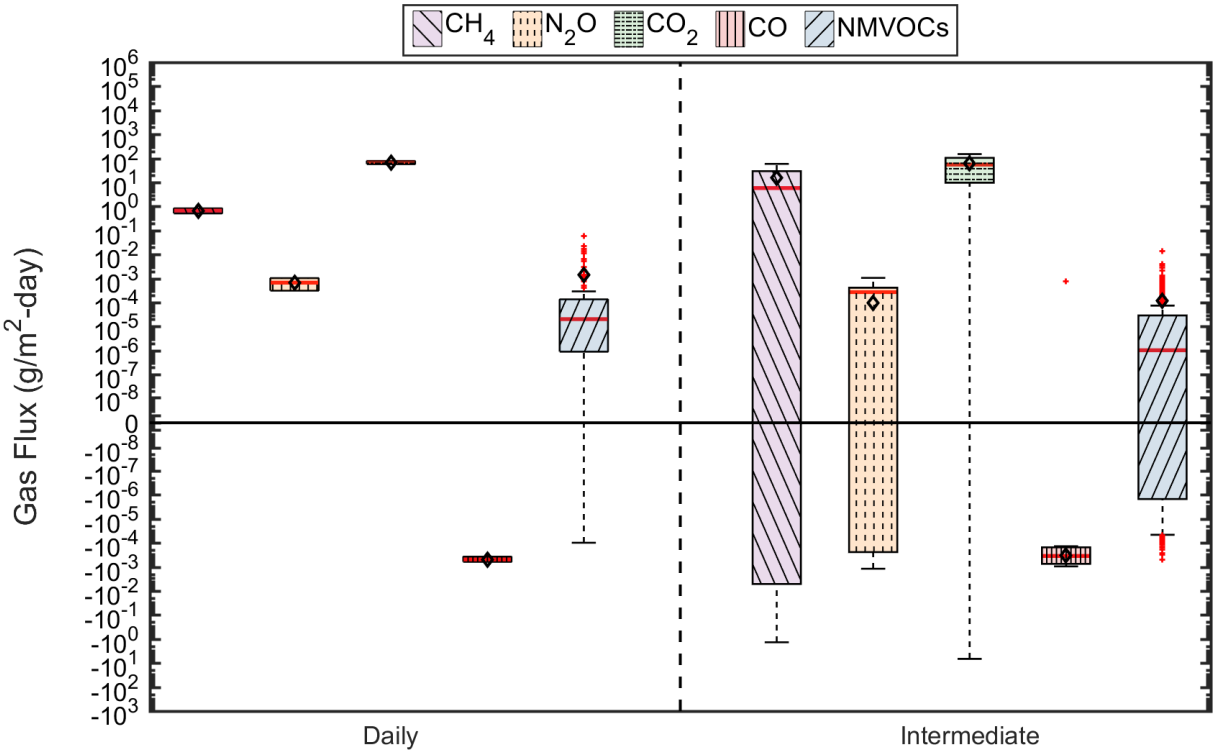

The fluxes from individual cover systems are presented in Figure 4.38 for the wet season. Similar to the dry season testing, the intermediate cover overlaying wet waste was associated with the highest fluxes for all the measured gases in the wet season, even exceeding daily cover emissions (Figure 4.38). The largest variation in flux measurements was observed for the intermediate cover with green waste and soil, particularly for methane and carbon dioxide flux measurements. On average, NMVOC flux measurements at Teapot Dome Landfill were near zero to slightly negative. The intermediate cover overlying older wastes had net uptake of methane and NMVOC fluxes were on the same order of magnitude as the intermediate cover with green waste and soil. The intermediate cover overlying new waste was associated with net uptake of nitrous oxide. NMVOC emissions generally decreased from the daily cover to the intermediate covers overlying new waste and old waste, and to the intermediate cover composed of green waste and soil (Figure 4.38).

Figure 4.38 Measured Fluxes at Teapot Dome Landfill by Individual Cover Type in the Wet Season (open black diamonds, red lines, and solid red dots represent means, medians, and outliers, respectively).

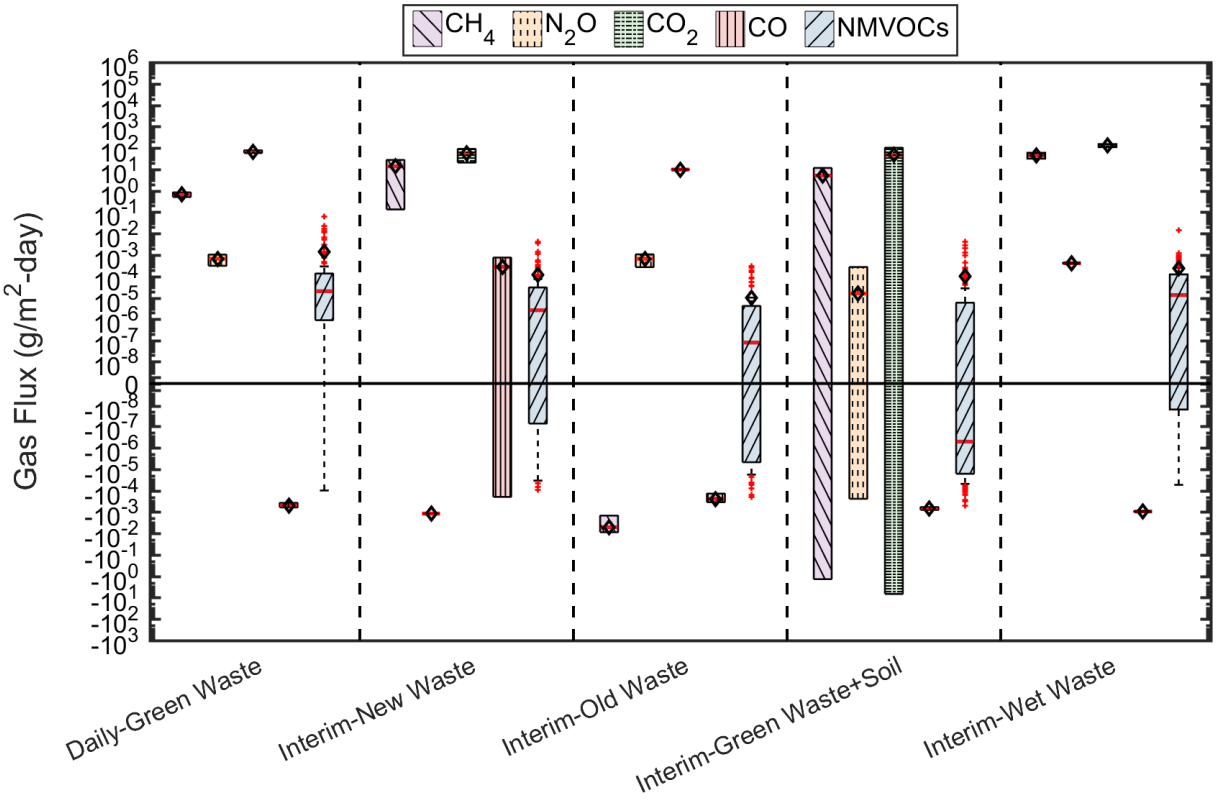

4.3.2.3 Summary of Flux Measurements from Teapot Dome Landfill

A comprehensive summary of the flux measurements obtained from the dry and wet season field campaigns at Teapot Dome Landfill is presented in Table 4.3. Overall minimum, maximum, and median flux values are organized in Table 4.3 according to chemical family and season. Measurements presented in Table 4.3 are intended to provide supplemental quantitative data to the boxplots included in the previous sections above to facilitate interpretation of the results.

Table 4.3 – Summary of Flux Measurements Obtained from Teapot Dome Landfill

Chemical Family	Dry Season (g/m^2-day)			Wet Season (g/m^2-day)		
	Min	Max	Median	Min	Max	Median
GHG	-2.69×10^{-3}	2.20×10^{2}	3.06×10^{-2}	-6.70×10^{0}	1.52×10^{2}	7.58×10^{-4}
RSC	-1.87×10^{-6}	2.42×10^{-4}	3.06×10^{-6}	-8.97×10^{-5}	3.13×10^{-4}	5.03×10^{-6}
F-gases	-1.47×10^{-5}	3.17×10^{-3}	1.79×10^{-6}	-1.59×10^{-4}	1.39×10^{-2}	1.05×10^{-6}
HH	-1.35×10^{-6}	5.50×10^{-4}	1.55×10^{-6}	-5.54×10^{-5}	3.68×10^{-4}	2.71×10^{-7}
ON	3.34×10^{-8}	8.59×10^{-6}	3.23×10^{-7}	-1.96×10^{-4}	1.00×10^{-3}	3.25×10^{-8}
Alk	-2.45×10^{-5}	2.06×10^{-3}	3.74×10^{-5}	-5.11×10^{-4}	1.15×10^{-2}	7.72×10^{-6}
Alke	1.58×10^{-7}	5.57×10^{-3}	1.80×10^{-5}	-1.49×10^{-4}	6.04×10^{-2}	6.77×10^{-6}
Ald/Alky	-7.05×10^{-7}	2.04×10^{-4}	5.67×10^{-5}	-3.13×10^{-4}	2.32×10^{-3}	3.16×10^{-5}
Ar	-3.86×10^{-5}	9.12×10^{-4}	1.18×10^{-5}	-3.55×10^{-5}	9.98×10^{-4}	3.95×10^{-6}
Mon	2.55×10^{-5}	7.44×10^{-2}	7.56×10^{-4}	-1.57×10^{-4}	2.09×10^{-3}	6.83×10^{-7}
Alc	-1.03×10^{-5}	6.84×10^{-2}	5.93×10^{-5}	-2.80×10^{-5}	4.13×10^{-3}	4.02×10^{-5}
Ket	-1.76×10^{-7}	9.15×10^{-3}	1.52×10^{-4}	-4.76×10^{-5}	2.63×10^{-4}	1.23×10^{-5}

4.3.3 Potrero Hills Landfill

4.3.3.1 Dry Season Test Results

Figure 4.39 presents box plots summarizing the flux measurements conducted across all testing locations at Potrero Hills Landfill during the dry weather season organized by chemical family. Out of the 1148 potential measurements that could be obtained at this site, 916 measurements (80%) were viable given the R^2 threshold applied in this study. The remaining approximately 17% and 3% of flux measurements were not included due to low R^2 value and below detection limit/analytical measurement errors, respectively. Overall, surface fluxes (including all chemical families) for this testing campaign varied from -9.6×10^{0} to 9.48×10^{1} g/m^2-day. A high majority of the measured fluxes were positive (82%) with a median flux of 1.17×10^{-5} g/m^2-day. Positive fluxes (out of the cover) and negative fluxes (into the cover) varied by 10 orders of magnitude (from 6.99×10^{-9} to 9.48×10^{1} g/m^2-day) and 10 orders of magnitude (-9.6×10^{0} to -2.10×10^{-9} g/m^2-day), respectively.

At Potrero Hills Landfill, the baseline greenhouse gas fluxes were dominant. The variation in GHG fluxes was higher than the variation in the NMVOCs included in the investigation (Figure 4.39). Average skewness and kurtosis values were 1.6 and 5.4, respectively and IQRs were above zero, demonstrating the higher probability of net emissions over uptake and the high variation in measured fluxes. Low probability of uptake was present for multiple chemical families. The likelihood for uptake over net emissions was greatest for the GHGs, and also observed for the alkanes, aromatics, and alcohols based on the extent of the lower whiskers below zero

Figure 4.39 Measured Fluxes at Potrero Hills Landfill by Chemical Family in the Dry Season (open black diamonds, red lines, and solid red dots represent means, medians, and outliers, respectively).

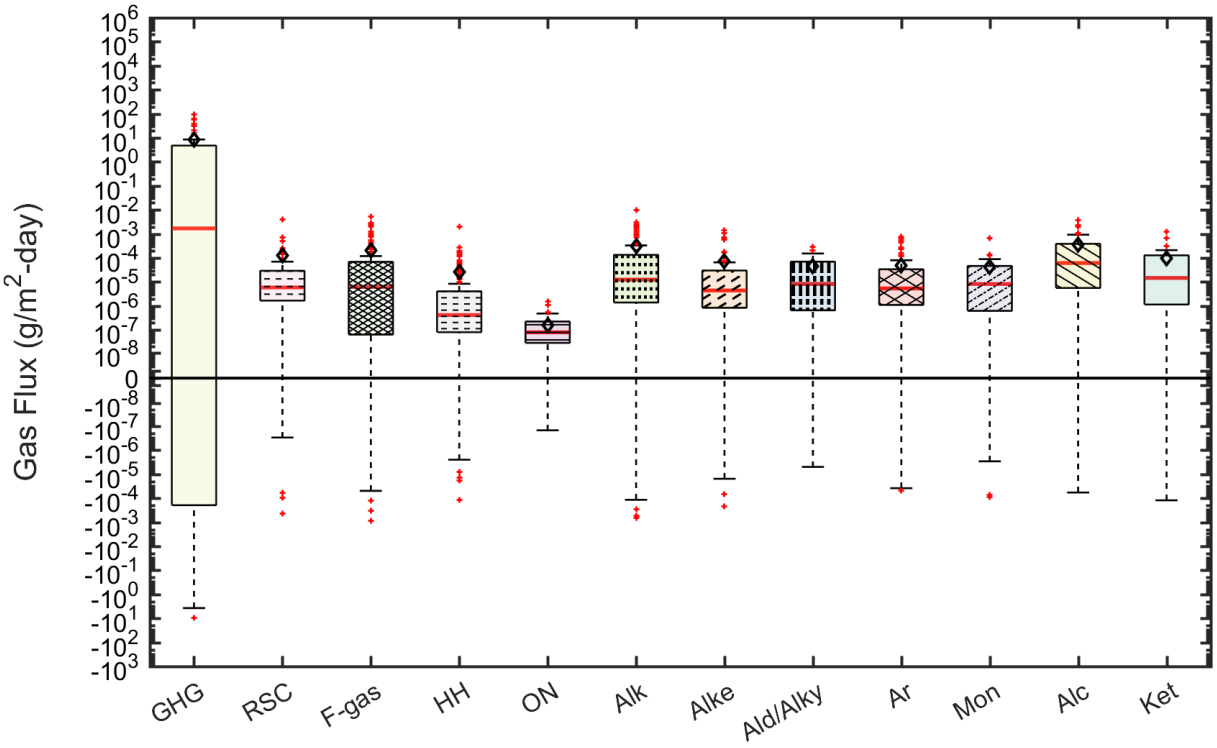

Among the NMVOCs investigated, the alcohols, ketones, and alkanes were associated with the highest fluxes based on the median flux data (Figure 4.39). The highest median fluxes for specific chemical species within each family were measured for methanol, alpha-pinene, and i-butane. The NMVOC fluxes were relatively similar (assessed using IQR and IWR) across all NMVOC chemical families with the exception of the organic alkyl nitrates and reduced sulfur compounds that demonstrated lower variations in measured fluxes (Figure 4.33). Overall NMVOC emissions ranged from -8.64×10^{-4} to 9.96×10^{-3} g/m^2-day.

Measured fluxes of the project gases at Potrero Hills Landfill as a function of overall cover category are presented in Figure 4.40 for the dry season. Generally, the baseline GHGs (specifically carbon dioxide) had the highest maximum and median flux values across all cover categories. For NMVOCs, the highest median flux for daily, intermediate, and final covers were for the alcohols, alcohols, and aldehydes/alkynes, respectively. By individual chemical species, the highest fluxes observed for the daily, intermediate, and final covers were for HCFC-245fa, n-butane, and beta pinene. For all gases, the fluxes generally decreased from daily to intermediate to final cover locations. The decreases in flux were relatively modest from daily to intermediate cover systems, where the differences in median fluxes were between 1.27×10^{-5} (NMVOCs) and 8.30×10^{-3} (GHGs). Decreases in flux were greater from intermediate to final covers, particularly for methane and nitrous oxide (Figure 4.40). For dry season testing, a high number of uptake measurements were obtained for the final cover at

Potrero Hills Landfill, as indicated by the distribution of flux measurements below zero for methane and nitrous oxide. For a given GHG, variability in the measured fluxes were higher at the daily cover locations compared to the intermediate cover locations. The variability in NMVOC measurements decreased from daily to intermediate cover systems.

Figure 4.40 Measured Fluxes at Potrero Hills Landfill by Overall Cover Category in the Dry Season (open black diamonds, red lines, and solid red dots represent means, medians, and outliers, respectively).

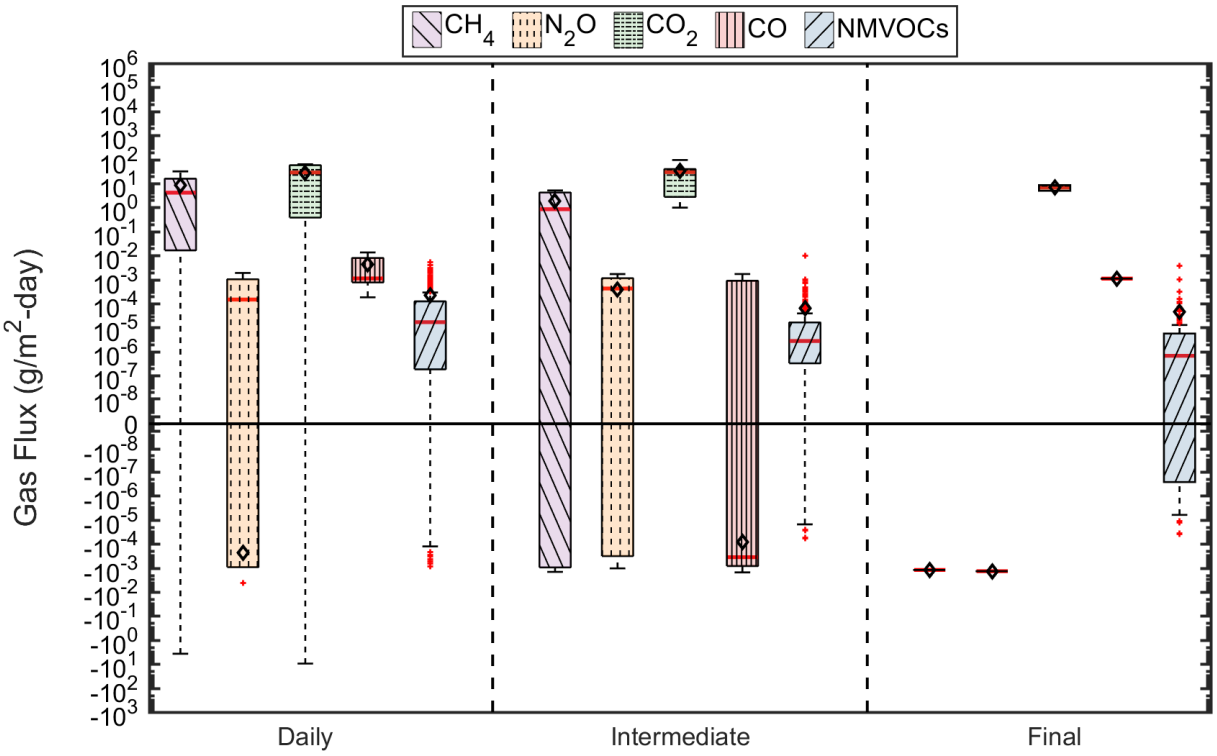

The fluxes for individual cover systems at Potrero Hills Landfill are presented in Figure 4.41 for the dry season. Aside for nitrous oxide, the daily cover system with green waste demonstrated the greatest variability in methane, carbon dioxide, and NMVOC flux measurements. Emissions of NMVOCs (both central tendencies and IQR/IWR) were comparably high at the daily cover location with autofluff during both day and nighttime testing conditions. Of the intermediate cover systems investigated, the interim cover had net uptake of methane, whereas the intermediate covers with Bay Mud and soil had high net emissions of methane. The magnitude and extent of NMVOC emissions were generally comparable for a given cover type. The autofluff daily cover (daytime) had the highest fluxes (based on the mean and median values of the boxplots) (Figure 4.41). The diurnal variations were relatively low except for nitrous oxide flux, where the N_2O flux increased by several orders of magnitude at nighttime.

Figure 4.41 Measured Fluxes at Potrero Hills Landfill by Individual Cover Type in the Dry Season (open black diamonds, red lines, and solid red dots represent means, medians, and outliers, respectively).

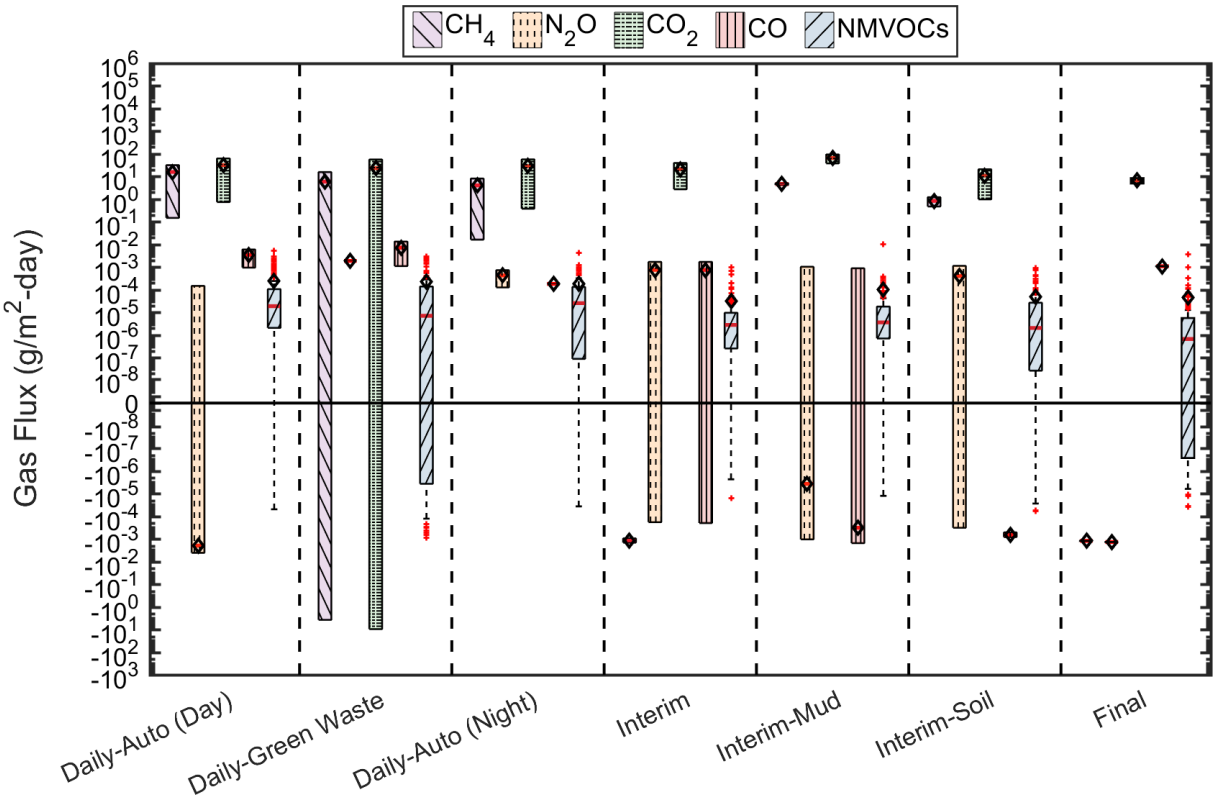

4.3.3.2 Wet Season Test Results

At Potrero Hills Landfill, flux testing conducted during the wet season differed from the dry season in various aspects. The number of acceptable flux measurements decreased from 80% to 77% (N=761 flux measurements, out of 984 potential measurements), where the contribution from low R^2 values were on the order of 22% and the below detection limit measurements amounted to 1%. The overall range (including all chemical families) in measured fluxes changed from -9.6×10^{0} to 9.48×10^{1} g/m^2-day in the dry season to -3.63×10^{-3} to 5.42×10^{2} g/m^2-day in the wet season. The percentage of measurements that were positive increased slightly from 82% in the dry season to 83% in the wet season. The median value of positive measurements also increased (5.62×10^{-5} g/m^2-day). Positive fluxes (out of the cover) and negative fluxes (into the cover) varied by 10 orders of magnitude (from 1.74×10^{-8} to 5.42×10^{2} g/m^2-day) and 6 orders of magnitude (-3.63×10^{-3} to -7.11×10^{-9} g/m^2-day), respectively.

Figure 4.42 presents box plots summarizing the flux measurements conducted across all testing locations at Potrero Hills Landfill during the wet weather season organized by chemical family. The baseline GHG fluxes remained dominant out of all chemical families included in the project. However, the variation in measured fluxes increased during wet season testing. Median flux values of the baseline GHGs increased by

approximately an order of magnitude. The corresponding IQRs and IWRs increased by a factor of six from the dry to wet season field measurement campaigns (Figure 4.42). Average skewness and kurtosis values were 1.7 and 5.3, respectively, and similar to the dry season results. Higher probability of net emissions over uptake and high variation in measured fluxes were observed.

Figure 4.42 Measured Fluxes at Potrero Hills Landfill by Chemical Family in the Wet Season (open black diamonds, red lines, and solid red dots represent means, medians, and outliers, respectively).

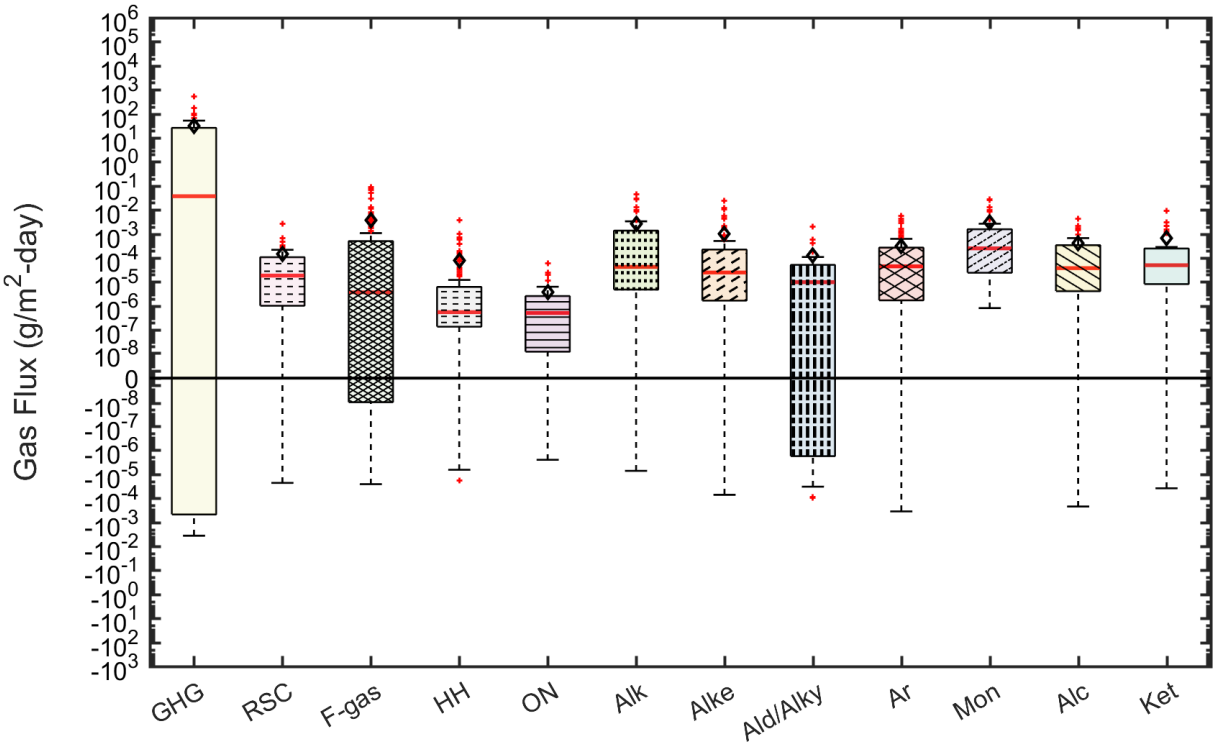

Overall, median NMVOC fluxes generally increased an order of magnitude during the wet season at Potrero Hills Landfill. In addition, the variation in NMVOC flux measurements, as assessed using the average IQR and IWR across NMVOC families, increased during the wet season by approximately an order of magnitude (Figure 4.42). The monoterpenes, ketones, and aromatics were NMVOC families with the highest fluxes, which were slightly different than the observations made for the dry season. The highest median fluxes for specific chemical species within each family were measured for limonene, butanone, and toluene. Similar to the baseline GHGs, the range in overall NMVOC emissions increased during the wet season to -3.53×10^{-4} to 9.00×10^{-2} g/m^2-day.

Measured fluxes of the project gases at Potrero Hills Landfill as a function of overall cover category are presented in Figure 4.43 for the wet season. In general, the baseline GHGs (specifically carbon dioxide) had the highest median flux values across all cover categories. For NMVOCs, the highest maximum and median flux for daily, intermediate, and final covers were for the alkanes, monoterpenes, and

monoterpenes, respectively. By individual chemical species, the highest flux observed for daily, intermediate, and final covers were for HCFC-141b, methanol, and alpha-pinene, respectively. The central tendencies of methane, nitrous oxide, and carbon dioxide flux measurements decreased from daily to intermediate to final cover systems at Potrero Hills Landfill during the wet season. However, the variation in the baseline greenhouse gas emissions increased for the intermediate cover systems, in particular for methane and nitrous oxide, where long interquartile lengths were observed. Higher variation in flux measurements were observed for daily cover systems at Potrero Hills Landfill during the dry season. The variation in final cover flux measurements was generally higher in the wet season than the dry season for methane, given the larger IQR and IWR presented in Figure 4.43 as compared to Figure 4.40 (net emissions over uptake). Fluxes of NMVOCs generally decreased from daily to intermediate to final cover systems at Potrero Hills during the wet season which corresponded with a decrease in the variation of flux measurements (Figure 4.43).

Figure 4.43 Measured Fluxes at Potrero Hills Landfill by Overall Cover Category in the Wet Season (open black diamonds, red lines, and solid red dots represent means, medians, and outliers, respectively).

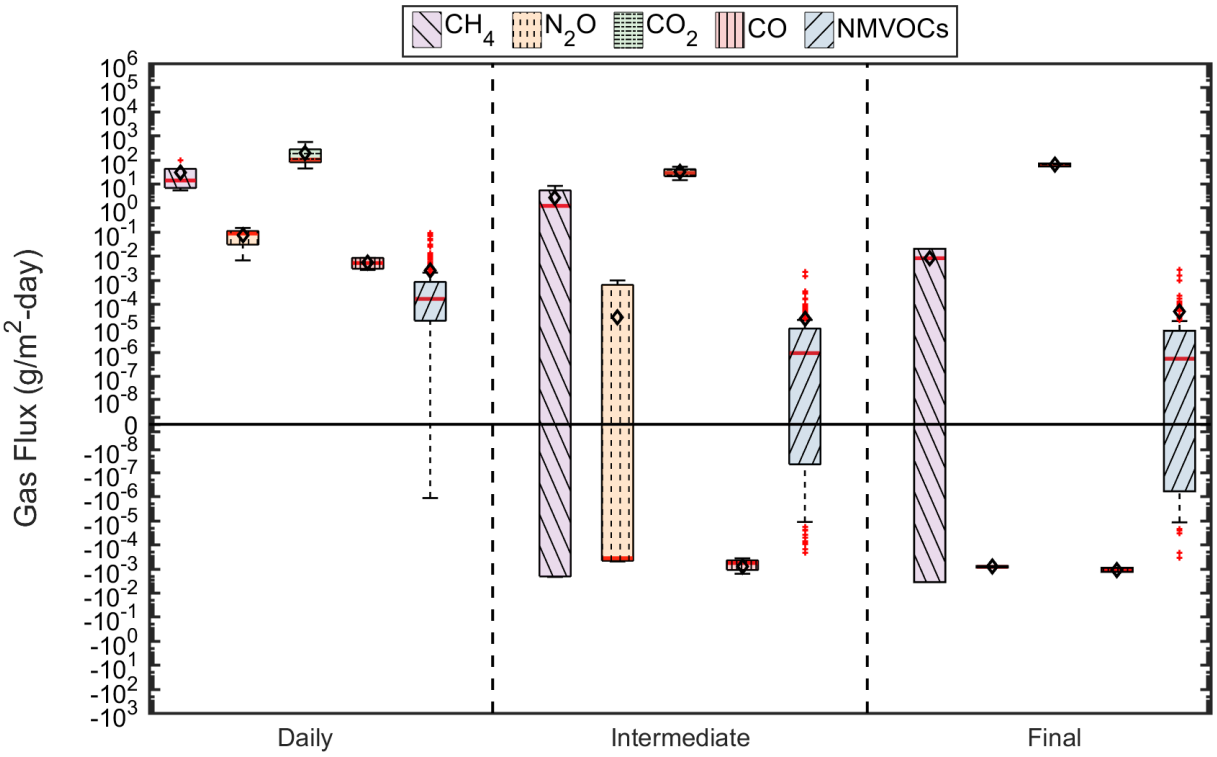

The fluxes from individual cover systems are presented in Figure 4.44 for the wet season. The fluxes from the daily cover with green waste were generally the highest flux data obtained at this site (Figure 4.44). For the wet weather testing campaign, the C+D location also was associated with relatively high emissions of all baseline GHGs and NMVOCs. The variation in flux measurements of all target baseline greenhouse gases decreased in the wet season. The largest variation in methane flux

measurements was observed for the final cover location. On average, NMVOC flux measurements were generally high at the daily cover locations and were significantly reduced at the intermediate and final cover locations. The intermediate cover composed of soil had net uptake of methane and nitrous oxide, similar to results obtained in the dry season (Figure 4.44). Sludge and sludge-derived materials include the residual solids and semi-solids from the treatment of water, wastewater, and other liquids. Concentrated placement of these materials (e.g., use in daily cover without mixing with other materials) is associated with high N_2O emissions. The region beneath Intermediate cover (Bay Mud) at Potrero Hills Landfill was known to have large quantities of sludge wastes and demonstrated higher emissions of N_2O as compared to other intermediate cover systems.

Figure 4.44 Measured Fluxes at Potrero Hills Landfill by Individual Cover Type in the Wet Season (open black diamonds, red lines, and solid red dots represent means, medians, and outliers, respectively).

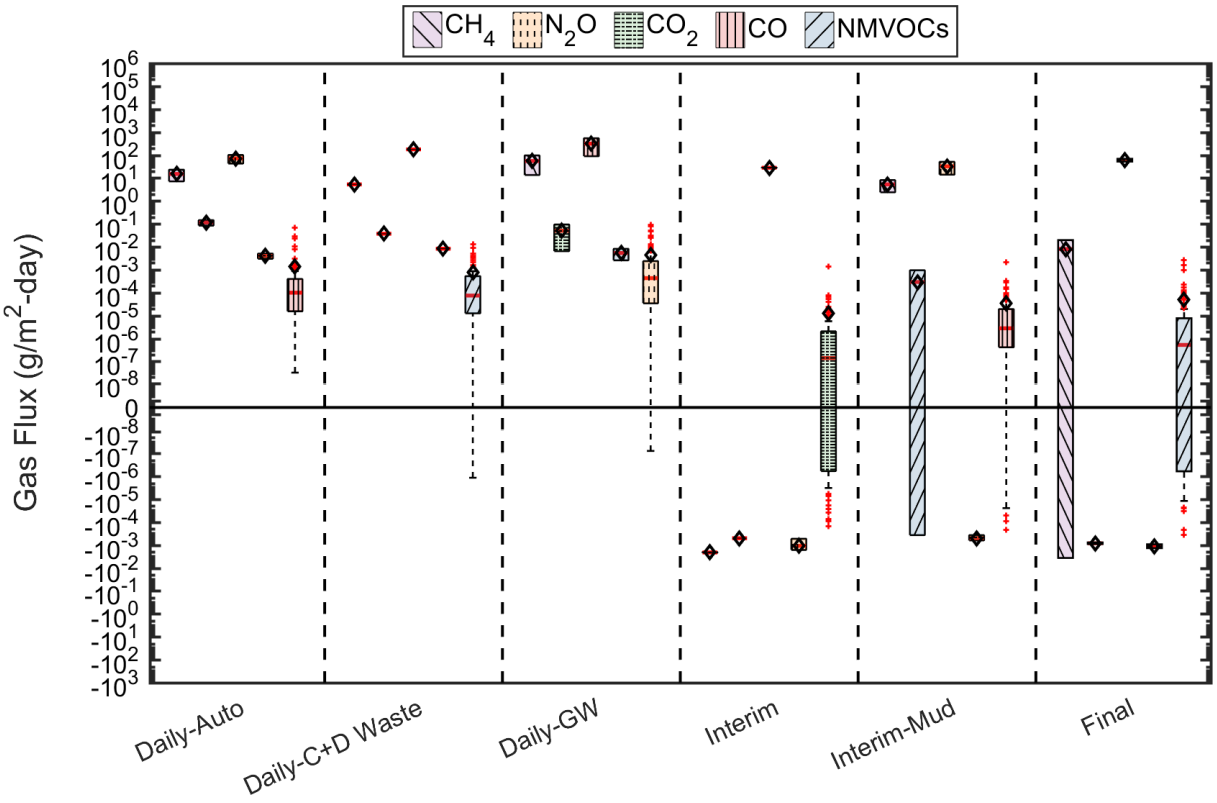

4.3.3.3 Summary of Flux Measurements from Potrero Hills Landfill

A comprehensive summary of the flux measurements obtained from the dry and wet season field campaigns at Potrero Hills Landfill is presented in Table 4.4. Overall minimum, maximum, and median flux values are organized in Table 4.4 according to chemical family and season. Measurements presented in Table 4.4 are intended to provide supplemental quantitative data to the boxplots included in the previous sections above to facilitate interpretation of the results.

Table 4.4 – Summary of Flux Measurements Obtained from Potrero Hills Landfill

Chemical Family	Dry Season (g/m^2-day)			Wet Season (g/m^2-day)		
	Min	Max	Median	Min	Max	Median
GHG	-9.60×10^{0}	9.48×10^{1}	1.70×10^{-3}	-3.63×10^{-3}	5.41×10^{2}	3.73×10^{-2}
RSC	-4.43×10^{-4}	4.12×10^{-3}	5.95×10^{-6}	-2.29×10^{-5}	2.61×10^{-3}	1.85×10^{-5}
F-gases	-8.64×10^{-4}	5.25×10^{-3}	6.25×10^{-6}	-2.59×10^{-5}	9.01×10^{-2}	3.73×10^{-6}
HH	-1.19×10^{-4}	2.03×10^{-3}	4.19×10^{-7}	-1.86×10^{-5}	3.64×10^{-3}	5.53×10^{-7}
ON	-1.48×10^{-7}	1.60×10^{-6}	7.97×10^{-8}	-2.51×10^{-6}	5.89×10^{-5}	5.11×10^{-7}
Alk	-6.54×10^{-4}	9.97×10^{-3}	1.25×10^{-5}	-7.23×10^{-6}	4.61×10^{-2}	4.27×10^{-5}
Alke	-2.21×10^{-4}	1.45×10^{-3}	4.44×10^{-6}	-7.20×10^{-5}	2.33×10^{-2}	2.49×10^{-5}
Ald/Alky	-4.96×10^{-6}	2.84×10^{-4}	8.31×10^{-6}	-9.27×10^{-5}	2.09×10^{-3}	9.87×10^{-6}
Ar	-4.88×10^{-5}	7.75×10^{-4}	5.40×10^{-6}	-3.53×10^{-4}	5.85×10^{-3}	4.48×10^{-5}
Mon	-8.76×10^{-5}	6.65×10^{-4}	8.27×10^{-6}	8.20×10^{-7}	2.83×10^{-2}	2.51×10^{-4}
Alc	-5.78×10^{-5}	3.62×10^{-3}	6.19×10^{-5}	-2.21×10^{-4}	4.23×10^{-3}	3.77×10^{-5}
Ket	-1.22×10^{-4}	1.21×10^{-3}	1.48×10^{-5}	-3.85×10^{-5}	9.00×10^{-3}	5.00×10^{-5}

4.3.4 Landfill Site A

4.3.4.1 Dry Season Test Results

Figure 4.45 presents box plots summarizing the flux measurements conducted across all testing locations at Landfill Site A during the dry weather season organized by chemical family. Out of the 984 potential measurements that could be obtained at this site, 774 measurements (79%) were viable given the R^2 threshold applied in this study. The remaining approximately 19% and 2% of flux measurements were not included due to low R^2 value and below detection limit/analytical measurement errors, respectively. Overall, surface fluxes (including all chemical families) for this testing campaign varied from -2.54×10^{-3} to 3.77×10^{1} g/m^2-day. A high majority of the measured fluxes were positive (83%) with a median flux of 2.50×10^{-6} g/m^2-day. Positive fluxes (out of the cover) and negative fluxes (into the cover) varied by 10 orders of magnitude (from 4.18×10^{-9} to 3.77×10^{1} g/m^2-day) and 6 orders of magnitude (-2.54×10^{-3} to -7.81×10^{-9} g/m^2-day), respectively.

At Landfill Site A, the baseline greenhouse gas fluxes were dominant, however exhibited a higher variation than the NMVOCs included in the investigation (Figure 4.45). Average skewness and kurtosis values were 0.96 and 4.6, respectively and IQRs were above zero, demonstrating the high probability of net emissions over uptake and the high variation in the measured fluxes for a given chemical family. Limited probability of uptake was present for multiple chemical families, as none of the IQR extended below zero. The likelihood for uptake over emissions was greatest for the GHGs, and also observed for the alkanes, aromatics, and alcohols based on the span of the lower whiskers below zero (Figure 4.45).

Figure 4.45 Measured Fluxes at Landfill Site A by Chemical Family in the Dry Season (open black diamonds, red lines, and solid red dots represent means, medians, and outliers, respectively).

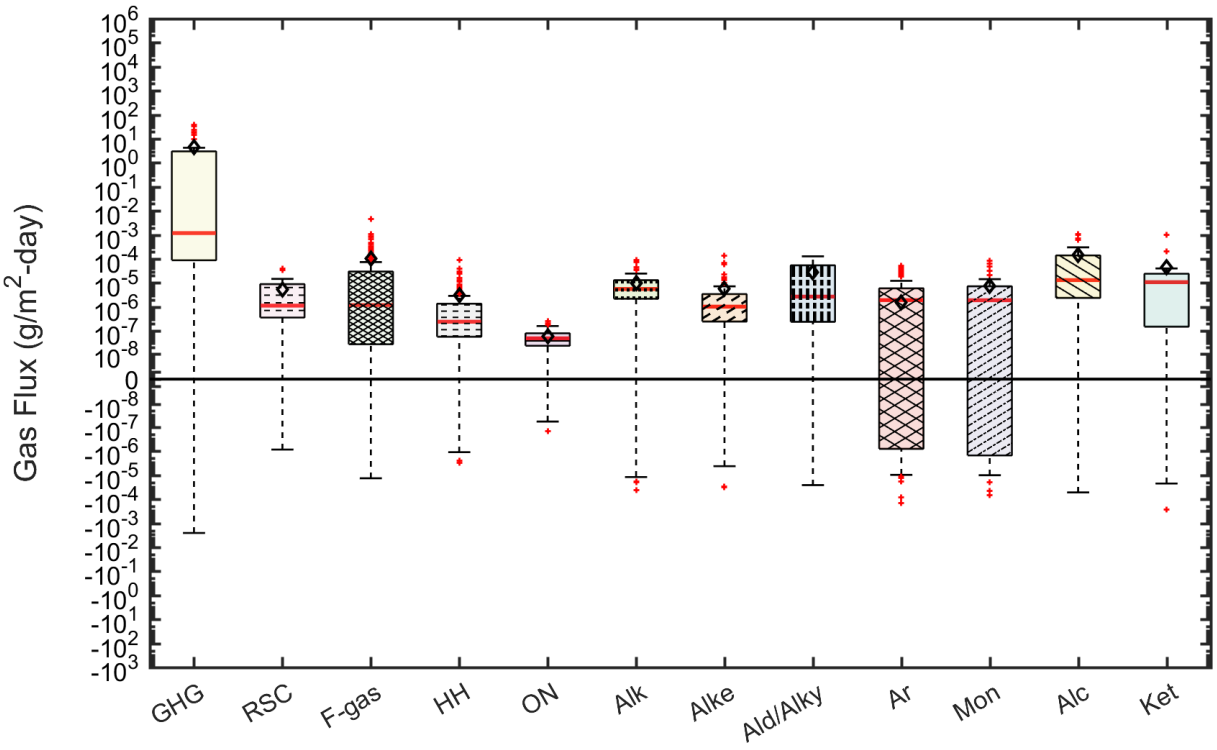

Comparison of median flux values for the NMVOCs indicated that fluxes for the alcohols, ketones, and alkanes were high compared to the other chemical families (Figure 4.45). The highest median fluxes for specific chemical species within each family above were measured for methanol, acetone, and i-pentane. The NMVOC fluxes were relatively similar (assessed using IQR and IWR) across all NMVOC chemical families with the exception of the F-gases, aromatics, alcohols, monoterpenes, and ketones, that demonstrated higher variations in measured fluxes (Figure 4.45). Overall NMVOC emissions ranged from -2.67×10^{-4} to 4.66×10^{-3} g/m^2-day.

Measured fluxes of the project gases at Landfill Site A as a function of overall cover category are presented in Figure 4.46 for the dry season. Generally, the baseline GHGs (specifically carbon dioxide) had the highest maximum and median flux values across all cover categories. For NMVOCs, the highest median flux for extended daily, intermediate, and final covers were for the alcohols, ketones, and alcohols, respectively. By individual chemical species, the highest fluxes observed for the daily, intermediate, and final covers were for HFC-134a, beta pinene, and 2-butanol, respectively. The fluxes generally increased from extended daily to intermediate to final cover locations for the baseline greenhouse gases. The NMVOCs increased with the same order of the cover. The increases in flux were relatively modest from extended daily to intermediate cover systems, where the differences in median fluxes

were between 1.53×10^{-6} g/m^2-day (NMVOCs) and 4.83×10^{-2} g/m^2-day (GHGs). On average, increases in flux were greater from intermediate to final covers, particularly for methane (Figure 4.46). For a given GHG, variability in the measured fluxes was lower and higher at the daily cover locations for nitrous oxide and methane, respectively, compared to the intermediate cover locations, whereas the variability in NMVOC measurements was relatively similar between daily, intermediate, and final cover systems.

Figure 4.46 Measured Fluxes at Landfill Site A by Overall Cover Category in the Dry Season (open black diamonds, red lines, and solid red dots represent means, medians, and outliers, respectively).

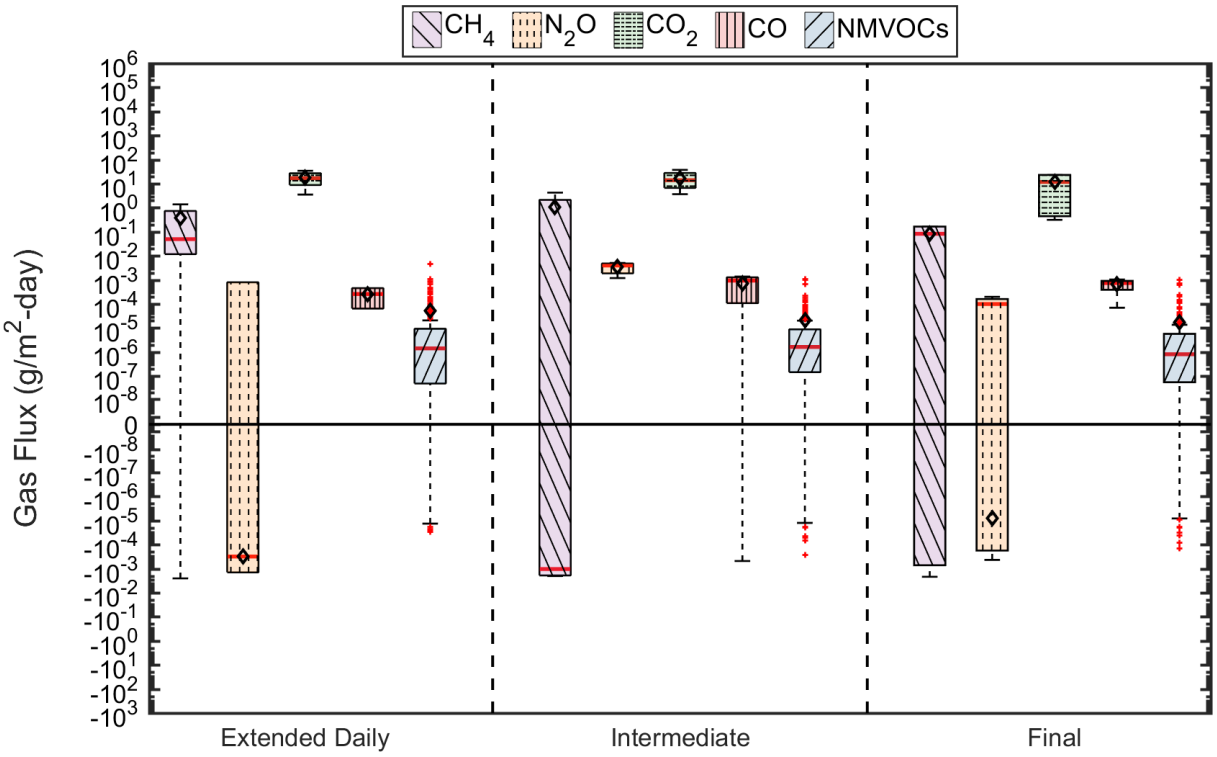

The fluxes for individual cover systems at Landfill Site A are presented in Figure 4.47 for the dry weather season. Waste type (Class II or Class III) is identified as the landfill is permitted for both waste types (the only landfill in this study to have permit for Class II waste). Based on comparison of the median flux values, the Interim-II (Class II MSW) location was associated with the greatest fluxes for all gases analyzed. This location also had the greatest variability in methane emissions. The Daily-Class III cover location had higher fluxes than the Daily-Class II cover location, where the Daily-Class II cover had a higher probability of uptake over emissions (particularly for methane and nitrous oxide). The intermediate cover systems had an opposite trend, in which the Interim-Class III cover had lower emissions of all target gases. Fluxes of all target gases were significantly higher and less variable from the alternative cover system as compared to the conventional final cover system (Figure 4.47). The magnitude and extent of NMVOC fluxes were generally comparable across all testing

locations, where the Interim-Class II cover had the highest fluxes (based on the mean and median values in the boxplots) (Figure 4.47).

Figure 4.47 Measured Fluxes at Landfill Site A by Individual Cover Type in the Dry Season (open black diamonds, red lines, and solid red dots represent means, medians, and outliers, respectively).

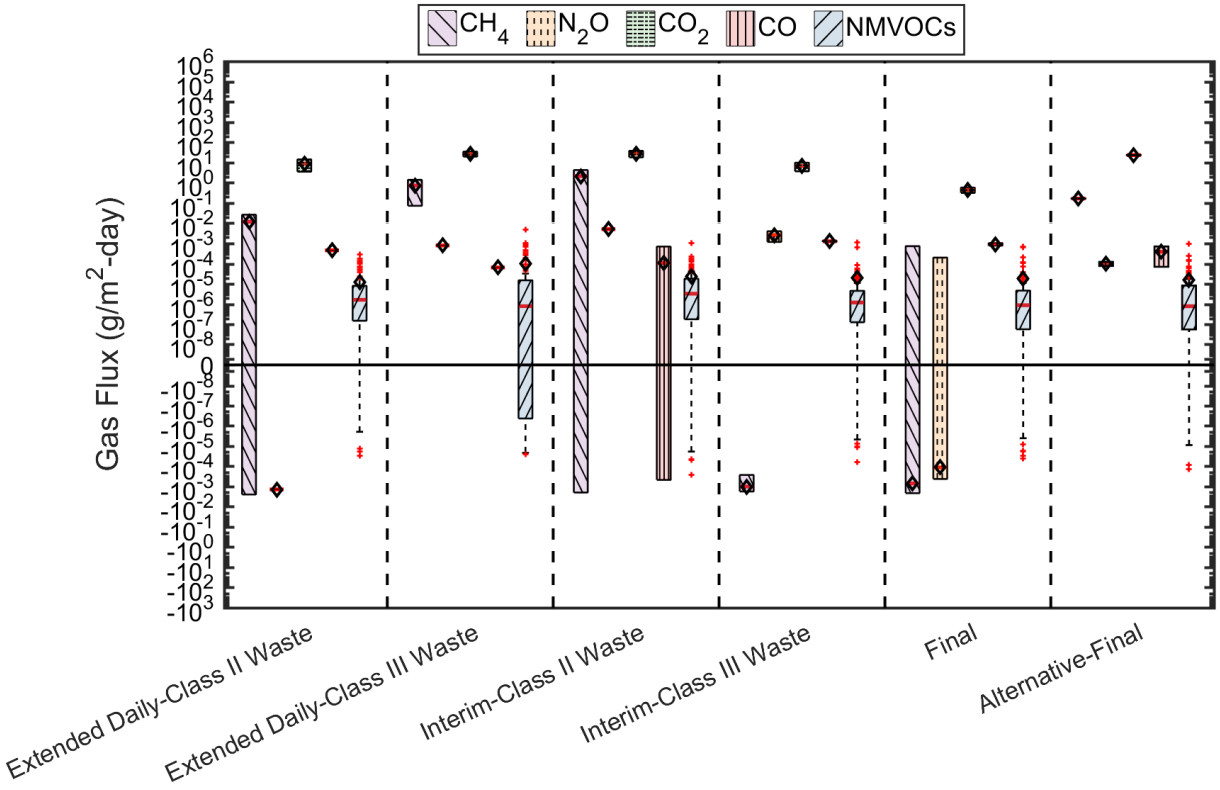

4.3.4.2 Wet Season Test Results

At Landfill Site A, flux testing conducted during the wet season differed from the dry season in several aspects. The number of acceptable flux measurements remained at 78% (N=771 flux measurements), where the contribution from low R^2 values were on the order of 19% and the below detection limit measurements amounted to 3%. The overall range (including all chemical families) in measured fluxes changed from -2.54x10^{-3} to 3.77x10^{1} g/m^2-day in the dry season to -4.15x10^{-1} to 3.97x10^{1} g/m^2-day in the wet season. The percentage of measurements that were positive deceased from 83% in the dry season to 70% in the wet season. The median value of positive measurements increased (4.21x10^{-6} g/m^2-day). Positive fluxes (out of the cover) and negative fluxes (into the cover) varied by 10 (from 1.12x10^{-8} to 3.97x10^{1} g/m^2-day) and 8 (-4.15x10^{-1} to -9.12x10^{-9} g/m^2-day) orders of magnitude, respectively.

Figure 4.48 presents box plots summarizing the flux measurements conducted across all testing locations at Landfill Site A during the wet weather season organized by chemical family. The baseline GHG fluxes remained dominant out of all chemical families included in the project. However, the variation in measured fluxes decreased during wet season testing. Median flux values of the baseline GHGs decreased

approximately an order of magnitude. The corresponding IQRs and IWRs decreased by a factor of three from the dry to wet season field measurement campaigns (Figure 4.48). Average skewness and kurtosis values summarizing the overall distributions of flux measurements increased to 1.1 and 4.5, respectively, during the wet season campaign. This result implied that the distributions of flux measurements became less symmetric and homogenous (more positively skewed and heavier tailed) as a smaller proportion of measurements were observed to be negative. The higher kurtosis value indicated higher variation in the fluxes in the wet than the dry season.

Figure 4.48 Measured Fluxes at Landfill Site A by Chemical Family in the Wet Season (open black diamonds, red lines, and solid red dots represent means, medians, and outliers, respectively).

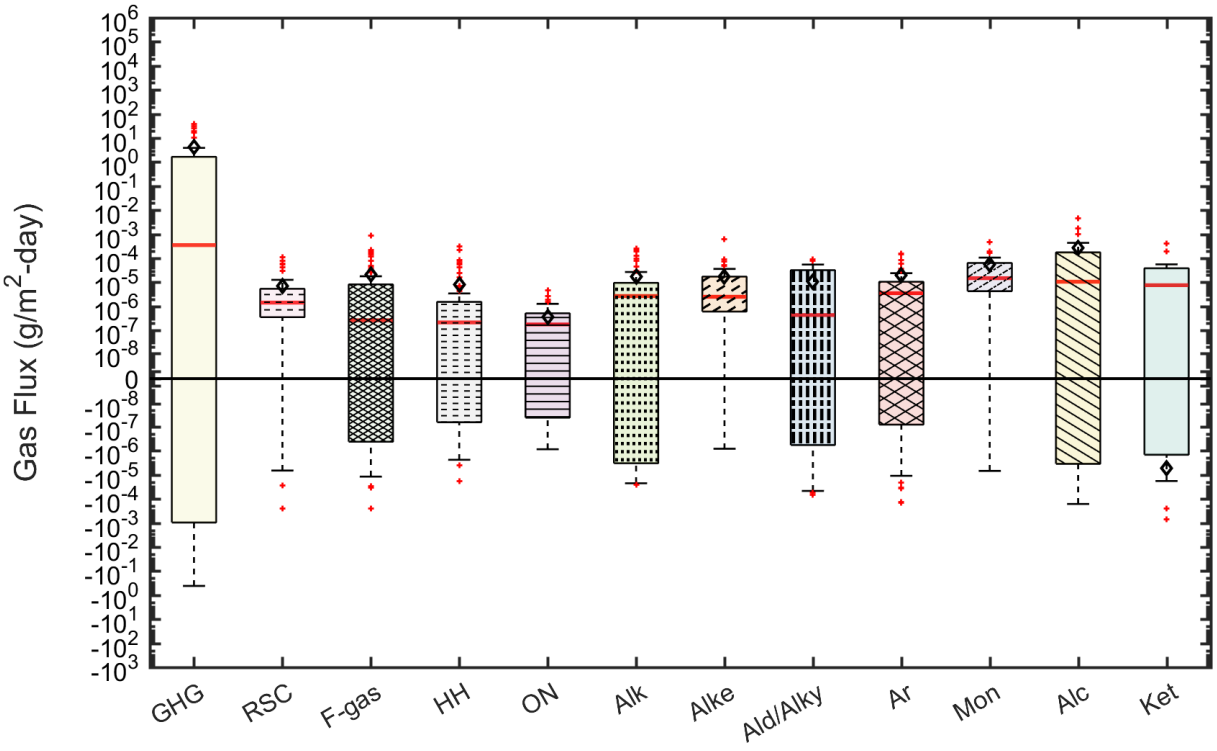

Overall, median NMVOC fluxes decreased by an order of magnitude during the wet season at Landfill Site A. In addition, the variation in NMVOC flux measurements, as assessed using the average IQR and IWR across NMVOC families, slightly increased during the wet season (Figure 4.48). The monoterpenes, alcohols, and ketones were the most highly emitting NMVOC families, which was slightly different than those observed during the dry season. The highest median fluxes for specific chemical species within each family were measured for alpha-Pinene, methanol, and acetone. Unlike the baseline GHGs, the range in overall NMVOC emissions decreased during the wet season to -7.13×10^{-4} to 4.52×10^{-3} g/m^2-day.

Measured fluxes of the project gases at Landfill Site A as a function of overall cover category are presented in Figure 4.49 for the wet season. Generally, the baseline GHGs (specifically carbon dioxide) had the highest median flux values across all cover

categories. For NMVOCs, the highest median fluxes for extended daily, intermediate, and final covers were for the ketones, monoterpenes, and monoterpenes, respectively. By individual chemical species, the highest fluxes observed for extended daily, intermediate, and final covers were all for beta pinene. Based on mean and median data the methane fluxes did not decrease from the daily to intermediate to final covers, with low values measured at the extended daily cover locations in contrast to general trends observed for the different cover systems at the other landfills. The variation in the baseline greenhouse gas emissions increased for the intermediate cover systems, in particular for methane and nitrous oxide, where long interquartile lengths were observed. Higher variation in flux measurements were observed for extended daily cover systems in place at Site A Landfill during the dry season, particularly for methane and nitrous oxide. The variation in final cover flux measurements was generally higher in the wet season than the dry season for methane and similar for nitrous oxide, given the longer IQR and IWR observed in Figure 4.49 as compared to Figure 4.46. The NMVOC fluxes were relatively similar with lower values for the final cover compared to the other cover categories. The variation in the NMVOC flux measurements was generally highest across the intermediate cover sites (Figure 4.49).

Figure 4.49 Measured Fluxes at Landfill Site A by Overall Cover Category in the Wet Season (open black diamonds, red lines, and solid red dots represent means, medians, and outliers, respectively).

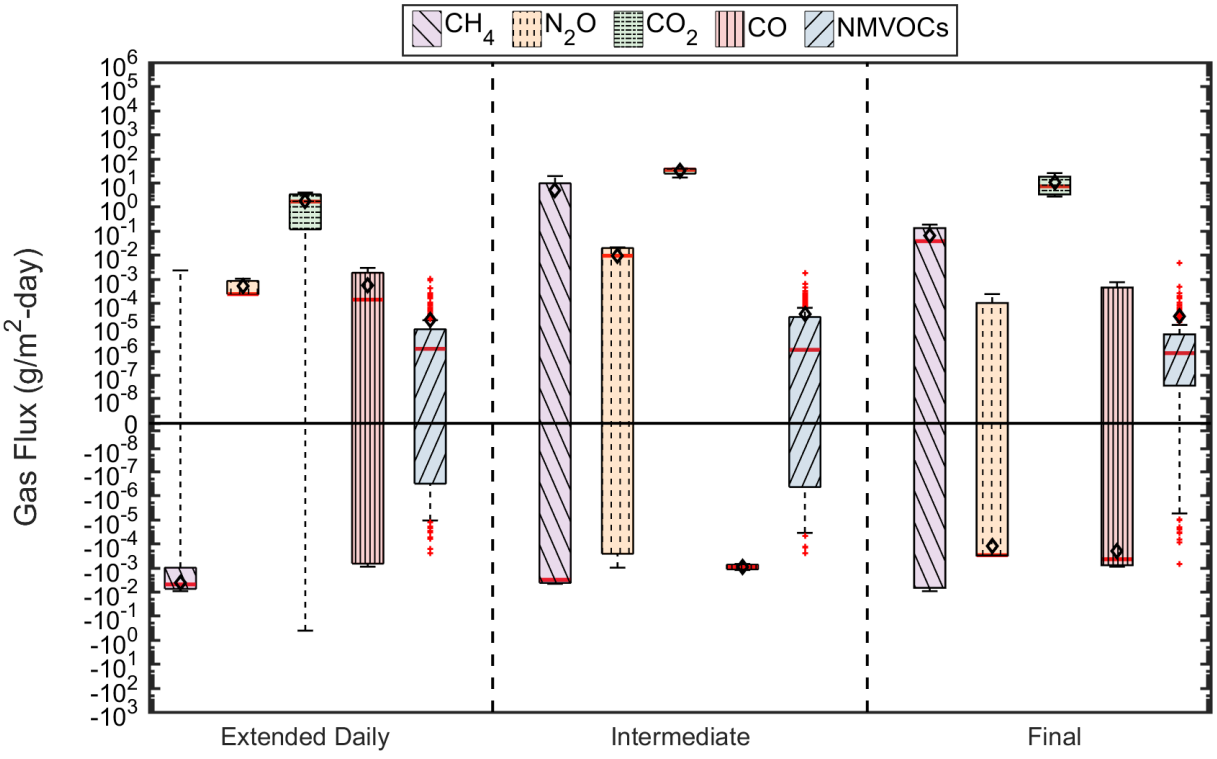

The fluxes from individual cover systems are presented in Figure 4.50 for the wet season. Similar to the dry season, the Interim-II cover location had the largest methane and NMVOC fluxes. Nitrous oxide and carbon dioxide emissions were

highest for the Daily-II and Interim-III cover locations, respectively. More variation in flux measurements were observed for the Daily-II cover location in the wet than the dry season, where the probability of uptake over net emissions increased during the wet season field campaigns. Net uptake of methane over emissions was observed for both daily cover locations, which had the reverse trend during the dry season (net emissions over uptake). Similar to results presented for the dry season, very high methane fluxes (with little variation) were observed from the alternative cover site, whereas net uptake was observed for the conventional cover system for methane and nitrous oxide (Figure 4.50) during the wet season. Moreover, NMVOC flux measurements were higher from the alternative cover as compared to the final cover, consistent with trends observed during the dry season.

Figure 4.50 Measured Fluxes at Landfill Site A by Individual Cover Type in the Wet Season (open black diamonds, red lines, and solid red dots represent means, medians, and outliers, respectively).

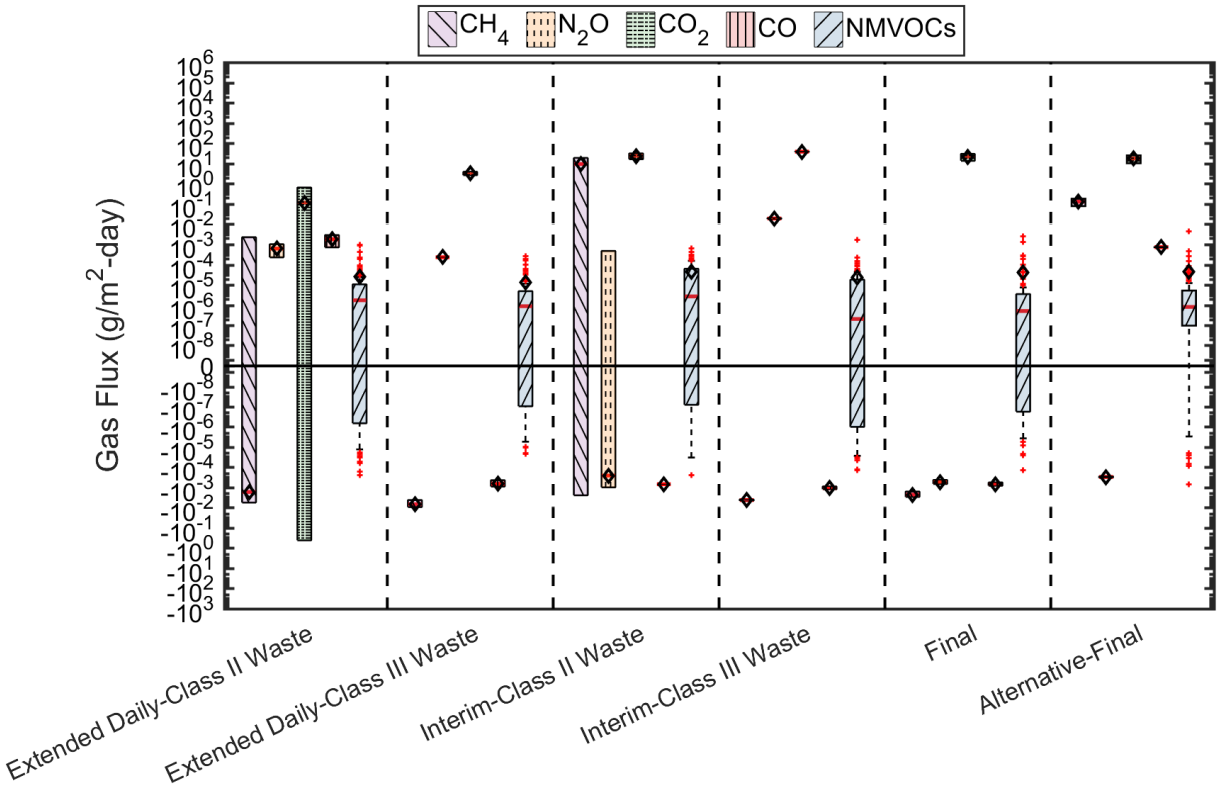

4.3.4.3 Summary of Flux Measurements from Site A Landfill

A comprehensive summary of the flux measurements obtained from the dry and wet season field campaigns at Site A Landfill is presented in Table 4.5. Overall minimum, maximum, and median flux values are organized in Table 4.5 according to chemical family and season. Measurements presented in Table 4.5 are intended to provide supplemental quantitative data to the boxplots included in the previous sections above to facilitate interpretation of the results.

Table 4.5 – Summary of Flux Measurements Obtained from Site A Landfill

Chemical Family	Dry Season (g/m^2-day)			Wet Season (g/m^2-day)		
	Min	Max	Median	Min	Max	Median
GHG	-2.54×10^{-3}	3.77×10^{1}	1.19×10^{-3}	-4.15×10^{-1}	3.97×10^{1}	2.35×10^{-4}
RSC	-8.53×10^{-7}	3.93×10^{-5}	1.14×10^{-6}	-2.48×10^{-4}	1.14×10^{-4}	2.08×10^{-6}
F-gases	-1.34×10^{-5}	4.66×10^{-3}	1.21×10^{-6}	-2.51×10^{-4}	8.92×10^{-4}	2.38×10^{-7}
HH	-3.14×10^{-6}	8.97×10^{-5}	2.44×10^{-7}	-1.78×10^{-5}	3.12×10^{-4}	2.12×10^{-7}
ON	-1.45×10^{-7}	2.64×10^{-7}	4.89×10^{-8}	-8.60×10^{-7}	4.54×10^{-6}	1.45×10^{-7}
Alk	-4.09×10^{-5}	9.36×10^{-5}	5.63×10^{-6}	-2.53×10^{-5}	2.60×10^{-4}	3.76×10^{-6}
Alke	-3.07×10^{-5}	1.40×10^{-4}	1.04×10^{-6}	-8.22×10^{-7}	6.25×10^{-4}	2.27×10^{-6}
Ald/Alky	-2.58×10^{-5}	1.29×10^{-4}	2.72×10^{-6}	-6.98×10^{-5}	9.03×10^{-5}	-1.68×10^{-7}
Ar	-1.47×10^{-4}	5.40×10^{-5}	1.94×10^{-6}	-1.45×10^{-4}	1.60×10^{-4}	2.28×10^{-6}
Mon	-6.58×10^{-5}	8.49×10^{-5}	1.92×10^{-6}	-6.85×10^{-6}	4.76×10^{-4}	1.50×10^{-5}
Alc	-5.18×10^{-5}	1.11×10^{-3}	1.32×10^{-5}	-1.62×10^{-4}	4.52×10^{-3}	1.07×10^{-5}
Ket	-2.67×10^{-4}	9.84×10^{-4}	1.08×10^{-5}	-7.13×10^{-4}	4.20×10^{-4}	4.41×10^{-6}

4.3.5 Chiquita Canyon Landfill

4.3.5.1 Dry Season Test Results

Figure 4.51 presents box plots summarizing the flux measurements conducted across all testing locations at Chiquita Canyon Landfill during the dry weather season organized by chemical family. Out of the 1148 potential measurements that could be obtained at this site, 937 measurements (82%) were viable given the R^2 threshold applied in this study. The remaining approximately 15% and 3% of flux measurements were not included due to low R^2 value and below detection limit/analytical measurement errors, respectively. Overall, surface fluxes (including all chemical families) for this testing campaign varied from -3.37×10^{-2} to 1.07×10^{3} g/m^2-day. A high majority of the measured fluxes were positive (90%) with a median flux of 7.66×10^{-6} g/m^2-day. Positive fluxes (out of the cover) and negative fluxes (into the cover) varied by 11 orders of magnitude (from 7.78×10^{-9} to 1.07×10^{3} g/m^2-day) and 6 orders of magnitude (-3.40×10^{-2} to -1.46×10^{-8} g/m^2-day), respectively.

At Chiquita Canyon Landfill, the baseline greenhouse gas fluxes were dominant. The variation of the GHGs was higher than the variation of the NMVOCs included in the investigation (Figure 4.51). Average skewness and kurtosis values were 2.1 and 6.9, respectively and IQRs were above zero, demonstrating the higher probability of net emissions over uptake and high variation in the measured fluxes for a given chemical family. Limited probability of uptake was present for multiple chemical families, as the IQRs did not extend below zero. The likelihood for uptake over emissions was greatest for the GHGs, and also observed for the alkanes, aromatics, monoterpenes, halogenated hydrocarbons, and alcohols based on the span of the lower whiskers below zero (Figure 4.51).

Figure 4.51 Measured Fluxes at Chiquita Canyon Landfill by Chemical Family in the Dry Season (open black diamonds, red lines, and solid red dots represent means, medians, and outliers, respectively).

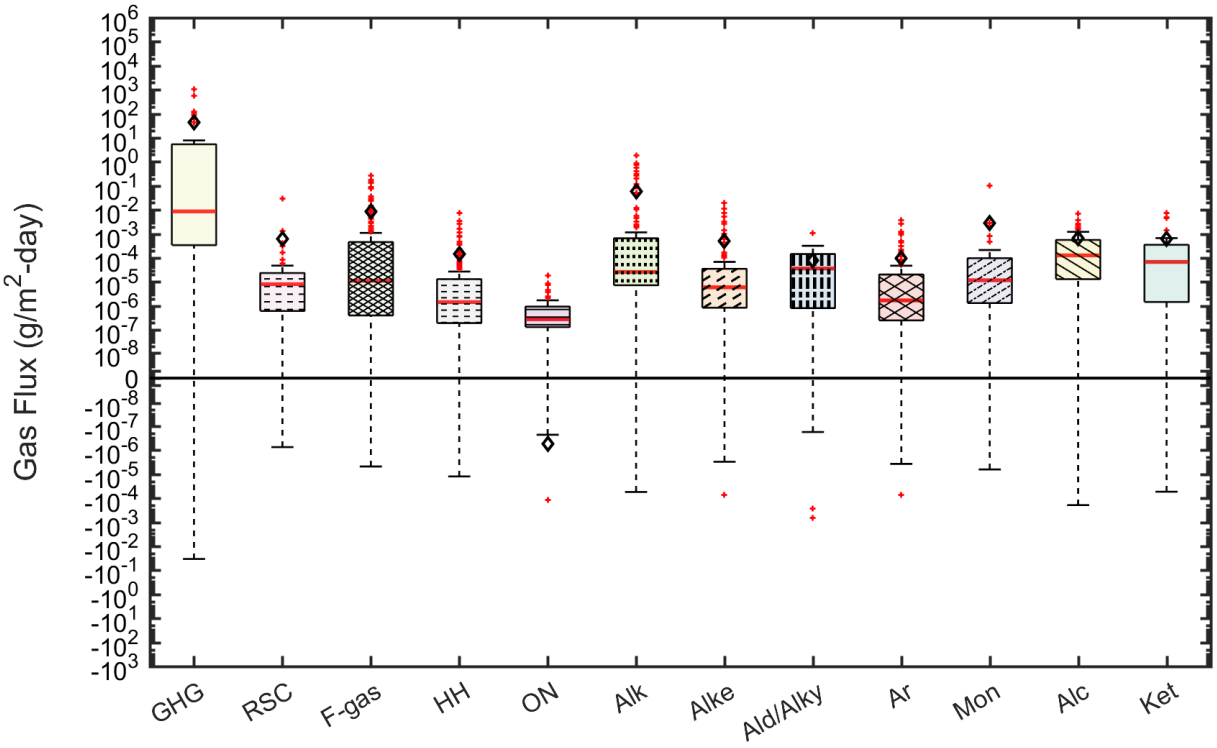

Among the NMVOCs investigated, the alcohols, ketones, and aldehydes/alkynes had the highest median flux values (Figure 4.51). The NMVOC fluxes were relatively similar (assessed using IQR and IWR) across all NMVOC chemical families with the exception of the reduced sulfur compounds, organic alkyl nitrates, and halogenated hydrocarbons, that demonstrated lower variations in measured fluxes (Figure 4.51). Overall NMVOC emissions ranged from -6.39×10^{-4} to 1.81×10^{0} g/m^2-day.

Measured fluxes of the project gases at Chiquita Canyon Landfill as a function of overall cover category are presented in Figure 4.52 for the dry season. Generally, the baseline GHGs (specifically carbon dioxide) had the highest maximum and median flux values across all cover categories. For NMVOCs, the highest median flux for daily, intermediate, and final covers were for the alkanes, alcohols, and ketones, respectively. By individual chemical species, the highest fluxes observed for the daily, intermediate, and final covers were for i-Butene, i-Butene, and limonene, respectively. The fluxes generally decreased from daily to intermediate to final cover locations for all target gases. The decreases in flux were relatively significant from daily to intermediate cover systems, where the differences in median fluxes were between 5.30×10^{-5} (NMVOCs) and 2.24×10^{-1} (GHGs). On average, decreases in flux were smaller from intermediate to final covers, particularly for nitrous oxide (Figure 4.52) For dry weather tests, a high number of uptake measurements were obtained for methane through the final covers at Chiquita Canyon Landfill, as indicated by the median values and distribution of flux measurements below zero. For a given GHG, variability in the

measured fluxes were higher at the intermediate cover locations compared to the daily cover locations, whereas the variability in NMVOC measurements was relatively high at the daily cover locations, and decreased progressing from daily to intermediate to final cover systems (Figure 4.52).

Figure 4.52 Measured Fluxes at Chiquita Canyon Landfill by Overall Cover Category in the Dry Season (open black diamonds, red lines, and solid red dots represent means, medians, and outliers, respectively).

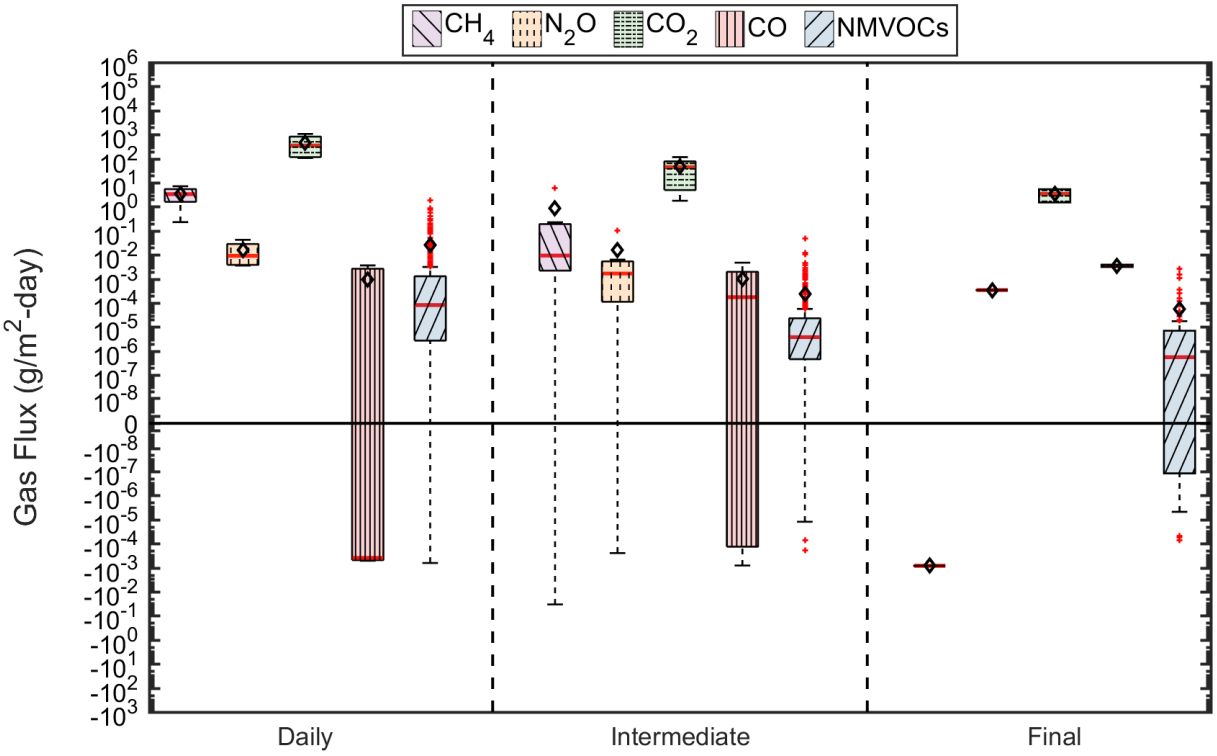

The fluxes for individual cover systems at Chiquita Canyon Landfill are presented in Figure 4.53 for the dry weather season. Flux measurements for all target gases were generally higher at the daily cover location with clean soil than all other testing locations. The Interim-Wet Waste cover location had the highest distribution of flux measurements of all intermediate cover locations for a majority of target gases analyzed (i.e., excluding nitrous oxide). The Interim-Old Green Waste also had relatively high fluxes of methane, carbon dioxide, and nitrous oxide. The methane fluxes were low for the Interim-Fresh Green Waste cover location in comparison to the other intermediate covers (Figure 4.53). The magnitude and extent of NMVOC emissions were generally comparable across all testing locations, where the Daily-Clean Soil location had the highest fluxes (based on the mean and median values of the boxplots) (Figure 4.53).

Figure 4.53 Measured Fluxes at Chiquita Canyon Landfill by Individual Cover Type in the Dry Season (open black diamonds, red lines, and solid red dots represent means, medians, and outliers, respectively).

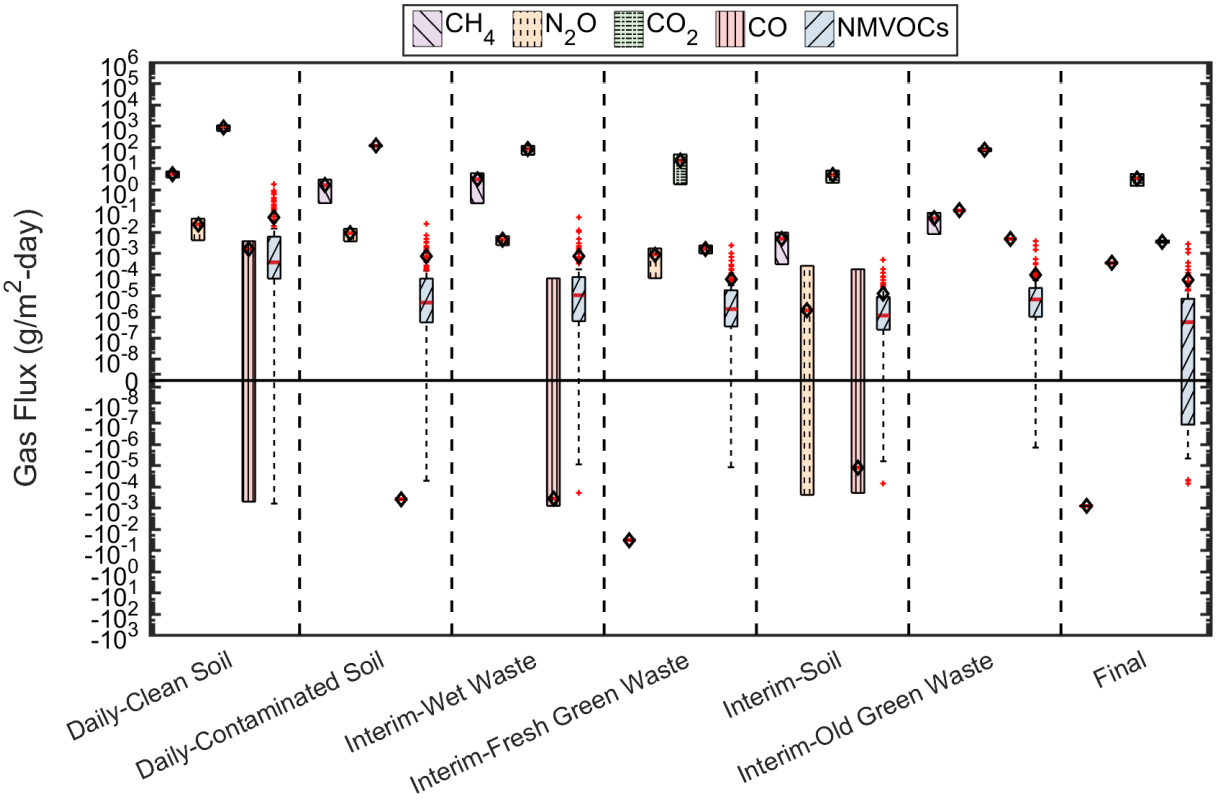

4.3.5.2 Wet Season Test Results

At Chiquita Canyon Landfill, flux testing conducted during the wet season differed from the dry season in various aspects. The number of acceptable flux measurements increased to 86% (N=987 flux measurements), where the contribution from low R^2 values were on the order of 12% and the below detection limit measurements amounted to 2%. The overall range (including all chemical families) in measured fluxes changed from -3.37×10^{-2} to 1.07×10^{3} g/m^2-day in the dry season to -4.91×10^{-3} to 1.31×10^{3} g/m^2-day in the wet season. The percentage of measurements that were positive increased from 90% in the dry season to 93% in the wet season. The median value of positive measurements also increased (1.66×10^{-5} g/m^2-day). Positive fluxes (out of the cover) and negative fluxes (into the cover) varied by 11 (from 1.24×10^{-8} to 1.31×10^{3} g/m^2-day) and 5 (-4.91×10^{-3} to -1.86×10^{-8} g/m^2-day) orders of magnitude, respectively.

Figure 4.54 presents box plots summarizing the flux measurements conducted across all testing locations at Chiquita Canyon Landfill during the wet weather season organized by chemical family. The baseline GHG fluxes remained dominant out of all chemical families included in the project. However, the variation in measured fluxes decreased during wet season testing. Median flux values of the baseline GHGs increased by approximately an order of magnitude. The corresponding IQRs and IWRs

increased when progressing from the dry to wet season field campaigns (Figure 4.54). Average skewness and kurtosis values summarizing the overall distributions of flux measurements decreased to 1.86 and 5.86, respectively, during the wet season. This result implied that the distributions of flux measurements became more symmetric and homogenous (less positively skewed and lighter tailed) as a smaller proportion of measurements were observed to be negative. The higher kurtosis value was indicative of a greater probability of high fluxes for a given chemical family.

Figure 4.54 Measured Fluxes at Chiquita Canyon Landfill by Chemical Family in the Wet Season (open black diamonds, red lines, and solid red dots represent means, medians, and outliers, respectively).

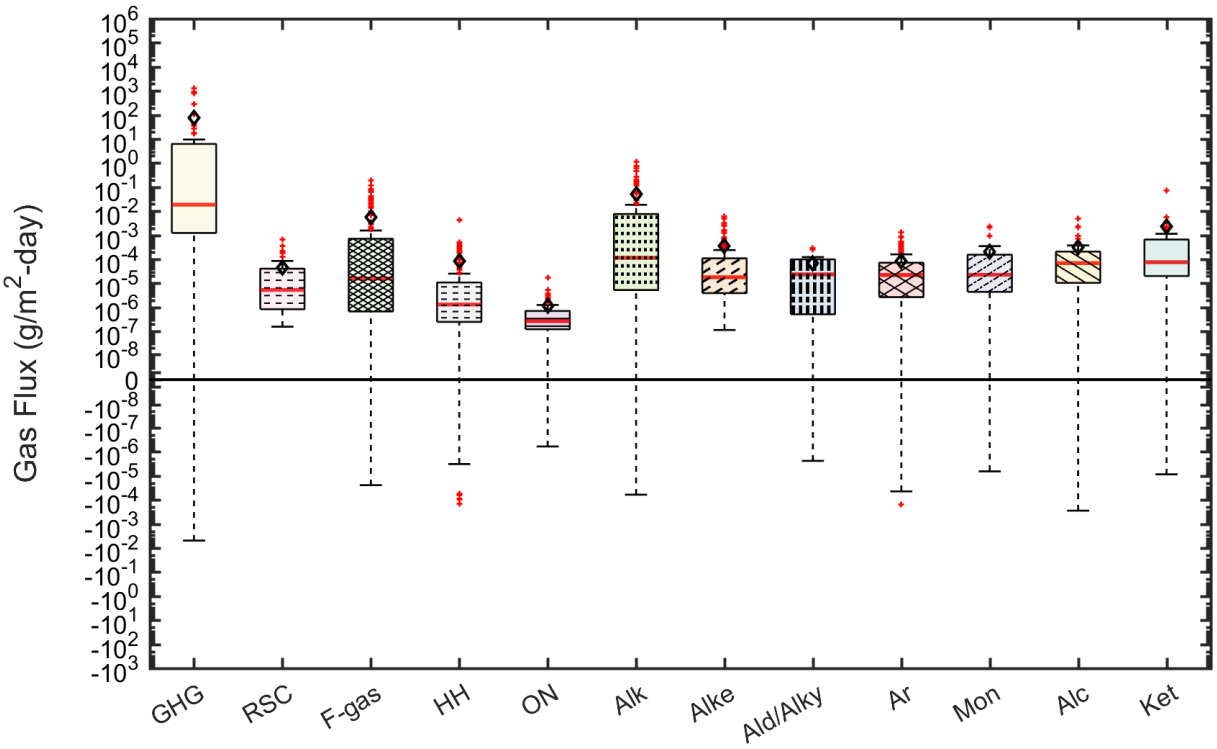

Overall, median NMVOC fluxes slightly increased during the wet season at Chiquita Canyon Landfill. In addition, the variation in NMVOC flux measurements, as assessed using the average IQR and IWR across NMVOC families, slightly increased during the wet season (Figure 4.54). The alkanes, ketones, and alcohols had the highest median fluxes among the NMVOC families, which was slightly different than the observations during the dry season. The highest median fluxes for specific chemical species within each family were measured for i-Pentane, acetone, and methanol. Similar to the baseline GHGs, the range in overall NMVOC emissions decreased during the wet season to -2.80×10^{-4} to 1.12×10^{0} g/m^2-day.

Measured fluxes of the project gases at Chiquita Canyon Landfill as a function of overall cover category are presented in Figure 4.55 for the wet season. Generally, the baseline GHGs (specifically carbon dioxide) had the highest median flux values across all cover categories. For MNVOCs, the highest median fluxes for daily, intermediate,

and final covers were for the alkanes, alkanes, and aldehydes/alkynes, respectively. By individual chemical species, the highest fluxes observed for daily, intermediate, and final covers were for i-Butene, i-butene, and beta-pinene. The central tendencies of methane, nitrous oxide, and carbon dioxide flux measurements generally decreased from daily to intermediate to final cover systems at Chiquita Canyon Landfill during the wet season. However, the variation in the baseline greenhouse gas emissions increased for nitrous oxide and carbon dioxide from the daily to the intermediate cover systems, where long interquartile lengths were observed. Variation in flux measurements were observed to be relatively similar for the daily and intermediate cover systems during the dry and wet seasons. The variation in final cover flux measurements was generally higher in the wet season than the dry season for nitrous oxide, given the longer IQR and IWR observed in Figure 4.55 as compared to Figure 4.52, demonstrating some tendency for net uptake over emissions. Fluxes of NMVOCs generally decreased from daily to intermediate to final cover systems at Chiquita Canyon Landfill during the wet season which corresponded with a decrease in the variation of flux measurements (Figure 4.55).

Figure 4.55 Measured Fluxes at Chiquita Canyon Landfill by Overall Cover Category in the Wet Season (open black diamonds, red lines, and solid red dots represent means, medians, and outliers, respectively).

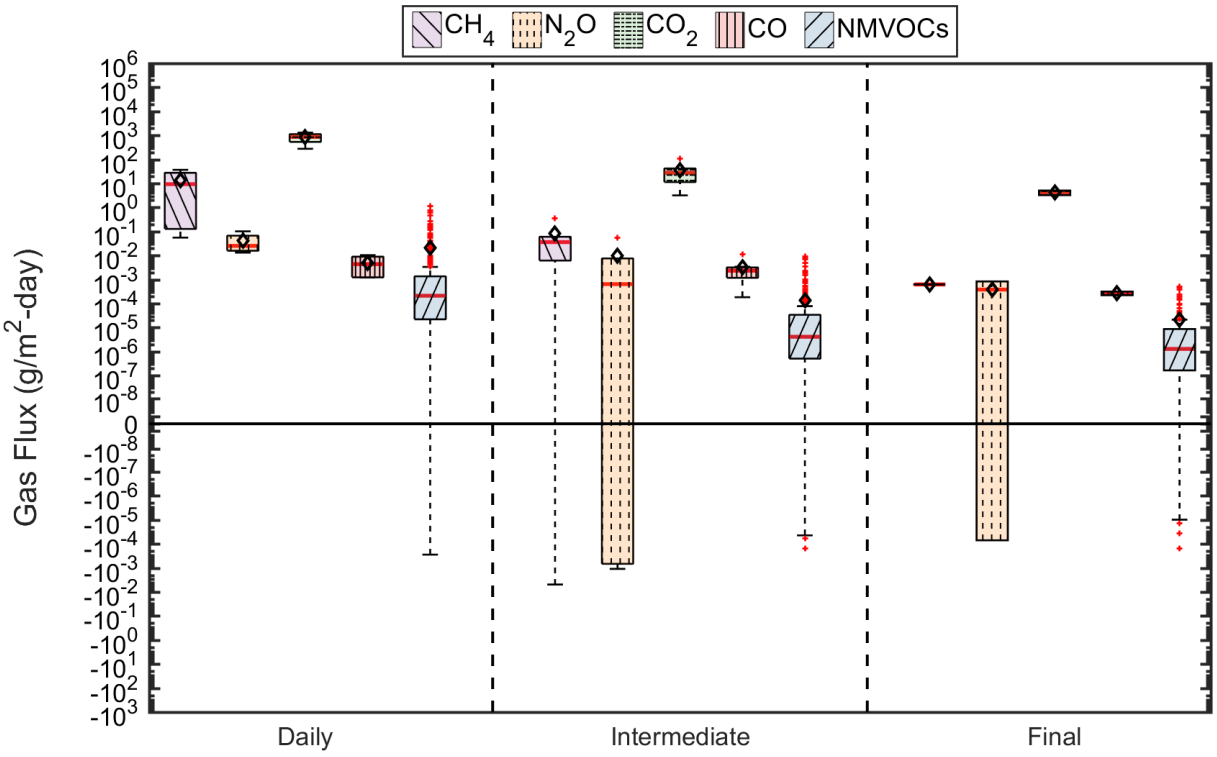

The fluxes from individual cover systems are presented in Figure 4.56 for the wet season. Out of all cover categories investigated, the Interim-Soil cover location had the highest emissions of methane; however, this cover was also associated with the highest uptake of nitrous oxide. In the wet season, NMVOC emissions were greatest for the daily cover with contaminated soil, which contrasted the results obtained during

the dry season. Methane and nitrous oxide emissions were most variable from the Interim-Wet Waste and Interim-Old Green Waste cover locations (Figure 4.56). Net emissions and uptake of methane and nitrous oxide, respectively, were observed from the Interim-Fresh Green Waste cover location in contrast to the observations in the dry season.

Figure 4.56 Measured Fluxes at Chiquita Canyon Landfill by Individual Cover Type in the Wet Season (open black diamonds, red lines, and solid red dots represent means, medians, and outliers, respectively).

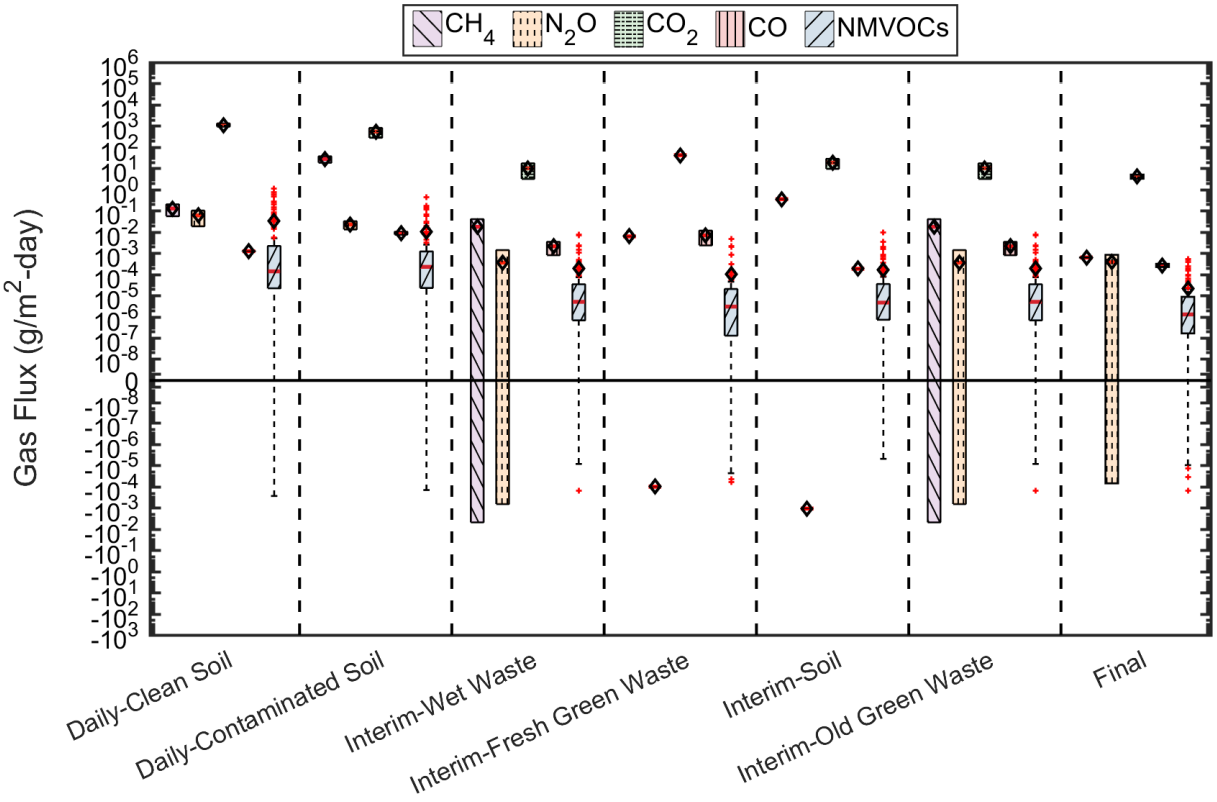

4.3.5.3 Summary of Flux Measurements from Chiquita Canyon Landfill

A comprehensive summary of the flux measurements obtained from the dry and wet season field campaigns at Chiquita Canyon Landfill is presented in Table 4.6. Overall minimum, maximum, and median flux values are organized in Table 4.6 according to chemical family and season. Measurements presented in Table 4.6 are intended to provide supplemental quantitative data to the boxplots included in the previous sections above to facilitate interpretation of the results.

Table 4.6 – Summary of Flux Measurements Obtained from Chiquita Canyon Landfill

Chemical Family	Dry Season (g/m^2-day)			Wet Season (g/m^2-day)		
	Min	Max	Median	Min	Max	Median
GHG	-3.37×10^{-2}	1.07×10^{3}	8.67×10^{-3}	-4.91×10^{-3}	1.31×10^{3}	1.16×10^{-2}
RSC	-7.45×10^{-7}	2.88×10^{-2}	8.12×10^{-6}	1.57×10^{-7}	6.51×10^{-4}	6.18×10^{-6}
F-gases	-4.76×10^{-6}	2.73×10^{-1}	1.12×10^{-5}	-9.84×10^{-6}	1.93×10^{-1}	1.89×10^{-5}
HH	-1.24×10^{-5}	7.29×10^{-3}	1.45×10^{-6}	-1.47×10^{-4}	4.41×10^{-3}	1.17×10^{-6}
ON	-1.16×10^{-4}	1.82×10^{-5}	2.81×10^{-7}	-6.00×10^{-7}	1.72×10^{-5}	2.24×10^{-7}
Alk	-5.48×10^{-5}	1.81×10^{0}	2.61×10^{-5}	-6.06×10^{-5}	1.12×10^{0}	2.60×10^{-4}
Alke	-7.31×10^{-5}	1.90×10^{-2}	6.04×10^{-6}	1.14×10^{-7}	6.26×10^{-3}	1.92×10^{-5}
Ald/Alky	-6.39×10^{-4}	1.06×10^{-3}	3.66×10^{-5}	-7.15×10^{-7}	2.97×10^{-4}	3.24×10^{-5}
Ar	-7.49×10^{-5}	3.66×10^{-3}	1.71×10^{-6}	-1.60×10^{-4}	1.36×10^{-3}	1.63×10^{-5}
Mon	-6.34×10^{-6}	9.91×10^{-2}	1.18×10^{-5}	-6.50×10^{-6}	2.36×10^{-3}	2.14×10^{-5}
Alc	-1.93×10^{-4}	6.89×10^{-3}	1.29×10^{-4}	-2.80×10^{-4}	4.86×10^{-3}	6.99×10^{-5}
Ket	-5.35×10^{-5}	7.28×10^{-3}	6.85×10^{-5}	-8.65×10^{-6}	7.12×10^{-2}	7.59×10^{-5}

4.4 Static Flux Chamber Measurements at 5 Landfills – Inter-Landfill Variations

Surface fluxes are now compared across all of the 5 landfills included in the static flux chamber field campaigns. Results are presented for the two measurement seasons: dry and wet seasons. Variations in flux across different landfills due to cover locations/types and chemical species are investigated. Results are organized from the smallest to largest landfill site tested in terms of waste in place consistent with the order used throughout the report. Results obtained for the dry season testing campaigns are presented first, followed by the wet season testing campaigns.

4.4.1 Dry Season Test Results

During the dry weather season testing campaigns, overall flux values ranged from -9.6×10^{0} to 1.07×10^{3} g/m^2-day across all landfills, with an overall median value of 3.66×10^{-3} g/m^2-day. The composite mean and standard deviation was 1.09 ± 21.2 g/m^2-day (N = 3937 total flux measurements) across all landfills and chemical families. The minimum and maximum fluxes were measured at Potrero Hills and Chiquita Canyon Landfills, respectively.

Median flux values were greatest for Teapot Dome Landfill across all landfills and chemical families during the dry season. The composite means of all distributions of flux measurements across chemical families indicated that Chiquita Canyon was associated with the greatest emissions, contradicting the median results. Based on IQRs and IWRs, the largest variation in flux measurements during the dry season was observed for Teapot Dome Landfill. Both the magnitude and variation in overall fluxes was smallest for Site A Landfill during the dry season. Average skewness (3.74) and kurtosis (24.5) values across all sites and chemical families indicated that the overall distribution in flux measurements was positively skewed and heavy tailed, suggesting greater probability of emissions over uptake and great variation in flux.

Across all landfill sites, positive and negative fluxes varied 11 ($4.18x10^{-9}$ to $1.07x10^{3}$) and 10 ($-9.59x10^{0}$ to $-2.10x10^{-9}$) orders of magnitude, respectively. The inter-site variation in positive fluxes (11 orders of magnitude) was generally greater than the intra-site variation in positive fluxes for all landfills (10 orders of magnitude) excluding Santa Maria and Chiquita Canyon Landfills (11 orders of magnitude) during the dry season. Similarly, the inter-site variation in negative fluxes was generally greater than the intra-site variation in negative fluxes (5-10 orders of magnitude) for all landfills during the dry season.

An inter-landfill comparison of methane, nitrous oxide, carbon dioxide, carbon monoxide, and NMVOC flux measurements obtained during the dry season is presented in Figure 4.57. Median methane and nitrous oxide fluxes were generally highest from Teapot Dome and Chiquita Canyon Landfills during the dry season (Figure 4.57). Carbon dioxide and carbon monoxide fluxes were greatest at Chiquita Canyon and Teapot Dome Landfills, respectively. Analysis of the distributions in overall NMVOC flux values confirmed the trends presented above that Teapot Dome Landfill had the highest measured fluxes. The positive skewness of the distribution in NMVOC fluxes was highest for Chiquita Canyon Landfill, as indicated by the high number of positive outliers and the high mean flux values. The variation in flux measurements (based on IQR/IWR) was highest for Potrero Hills Landfill, especially for methane, nitrous oxide, carbon monoxide, and carbon dioxide gases (Figure 4.57).

Figure 4.57 Inter-Landfill Comparison of GHG and NMVOC fluxes for the Dry Season (open black diamonds, red lines, and solid red dots represent means, medians, and outliers, respectively).

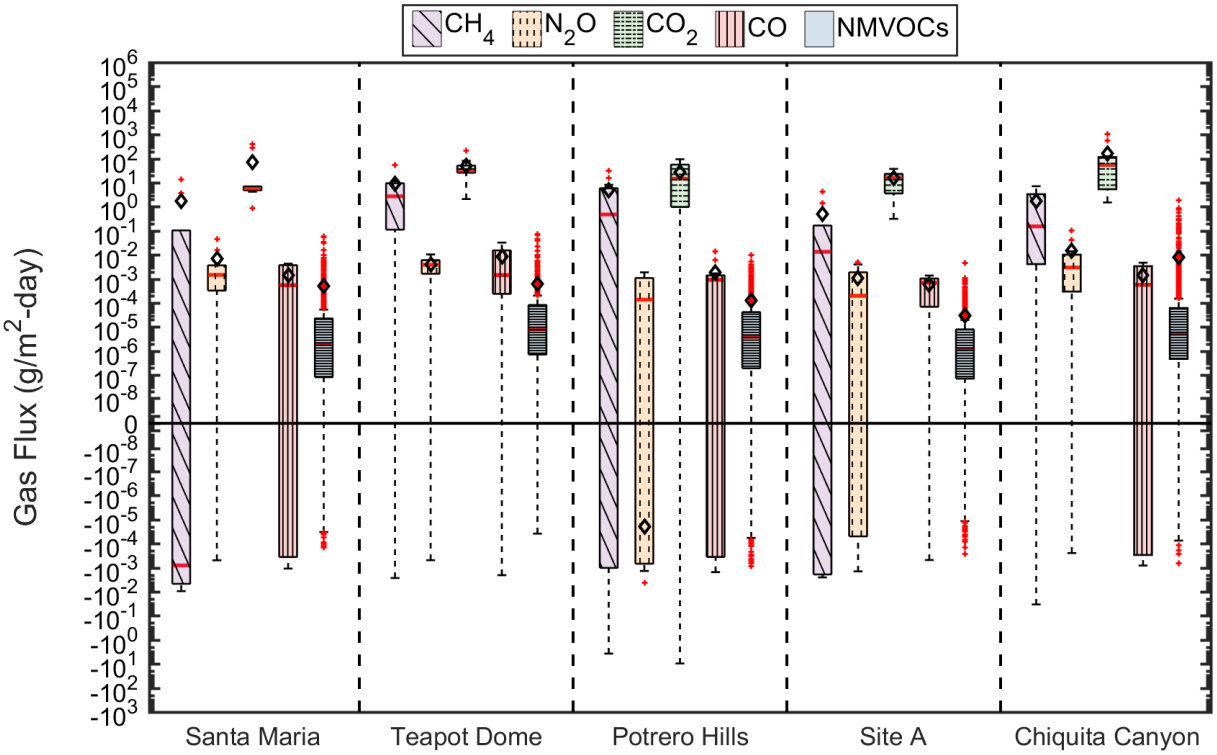

Figures 4.58a and 4.58b compare the overall distributions in flux measurements for each landfill site, categorized by chemical family. Based on median flux values, landfill surface flux measurements of the baseline GHGs were highest from Teapot Dome Landfill (Figure 4.58a), confirming the summary statistics presented above (Figure 4.57). Within the GHGs, methane and nitrous oxide fluxes were greatest at Teapot Dome and Santa Maria Regional Landfills, respectively (Figure 4.58b). Variation in GHG fluxes was highest for Teapot Dome and Santa Maria Regional Landfills, as indicated by the wide IQR and IWR of the boxplots. Relying on median flux values as the basis for inter-site comparison of LFG fluxes, the alcohols, ketones, and monoterpenes were the NMVOC chemical families associated with the highest fluxes across the landfills. Based on this analysis, Chiquita Canyon Landfill, Teapot Dome Landfill, and Teapot Dome Landfill were the sites with the highest median fluxes of the top three NMVOC families identified above, respectively. Considering all NMVOC families, Teapot Dome Landfill was the site with the highest median NMVOC flux value as well as the highest corresponding NMVOC IQR/IWR values during the dry season (Figure 4.58). The range in overall NMVOC fluxes was -8.64×10^{-4} to 1.81×10^{0} g/m^2-day across all landfills during the dry season.

Figure 4.58a Overall Inter-Landfill Flux Measurements in the Dry Season (open black diamonds, red lines, and solid red dots represent means, medians, and outliers, respectively).

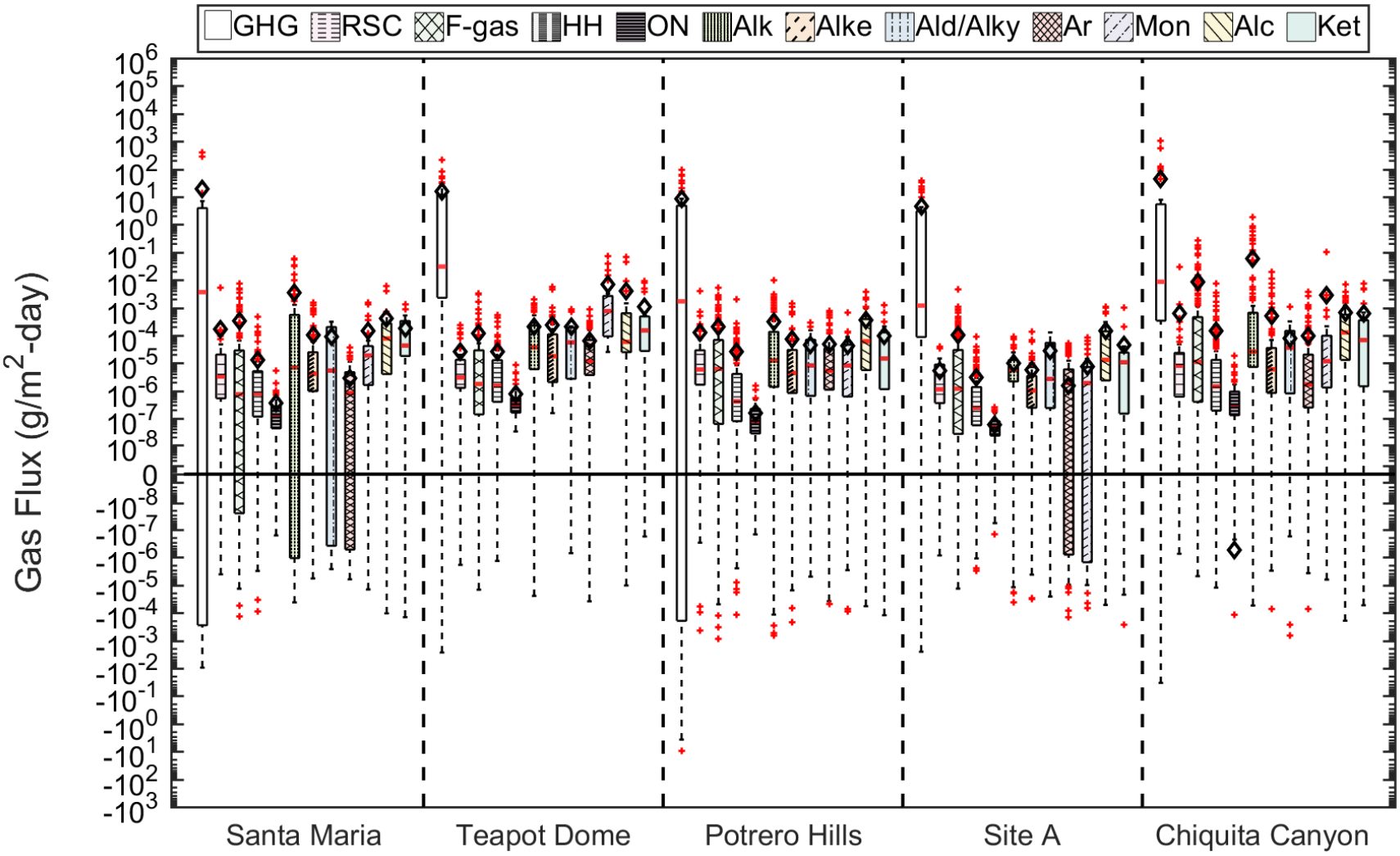

Figure 4.58b Specific GHG and NMVOC Inter-Landfill Flux Measurements in Dry Season (open black diamonds, red lines, and solid red dots represent means, medians, and outliers, respectively).

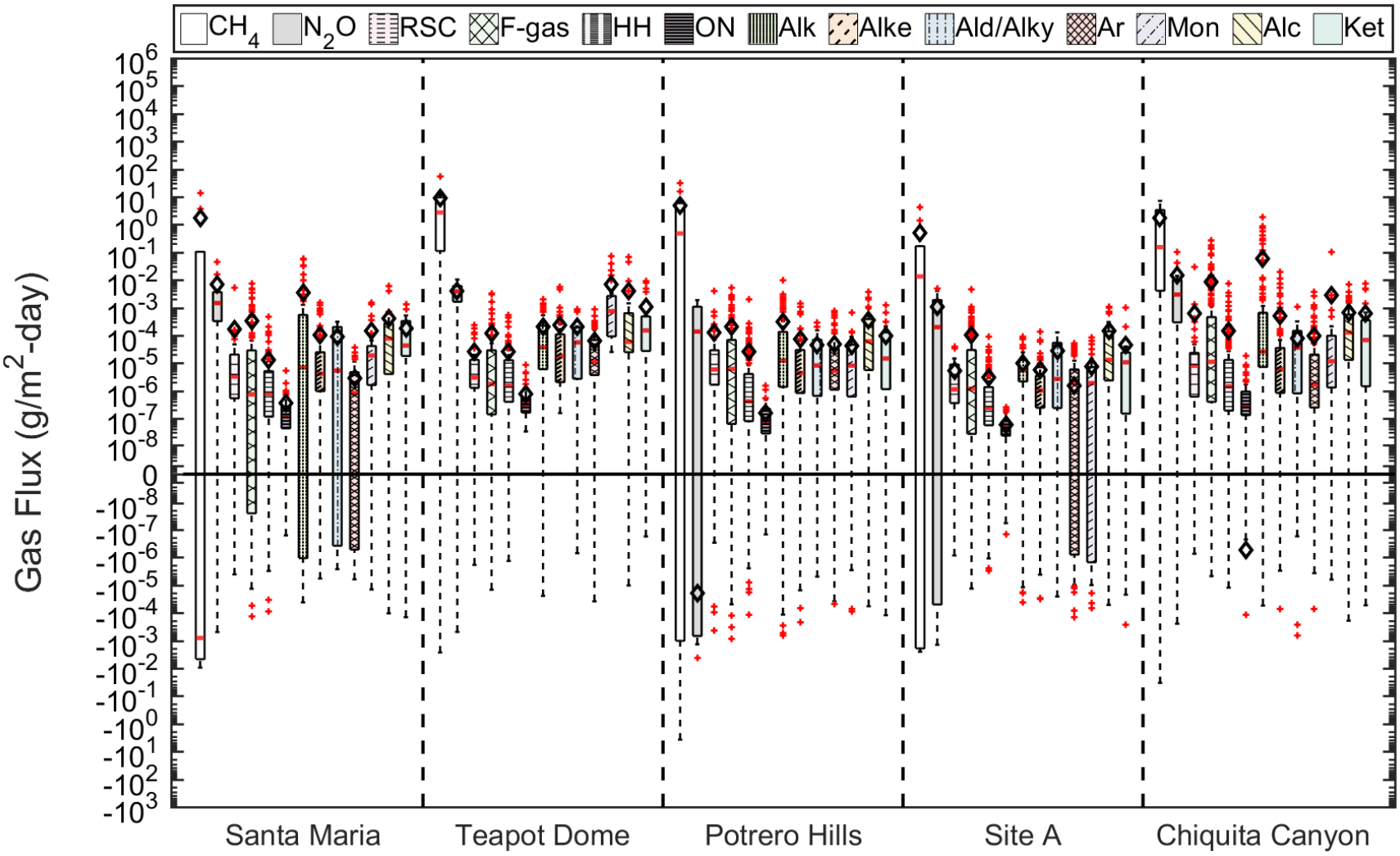

Figure 4.59 compares the GHG and NMVOC flux values collected from all daily, intermediate, and final cover locations at each landfill site during the dry season. As observed in Figure 4.59, GHG and NMVOC fluxes generally decreased progressing from daily to intermediate to final cover systems. GHG and NMVOC fluxes from the final cover of Santa Maria Regional Landfill were slightly higher than those of the intermediate cover. In general, the variation in GHG and NMVOC fluxes (as determined using the IQR/IWR) decreased progressing from daily to intermediate to final cover systems for all target gases analyzed during the dry season (Figure 4.59).

Figure 4.59 Dry Season a) GHG Fluxes and b) NMVOC Fluxes Organized by Site and Cover Category (open black diamonds, red lines, solid red dots represent means, medians, and outliers, respectively).

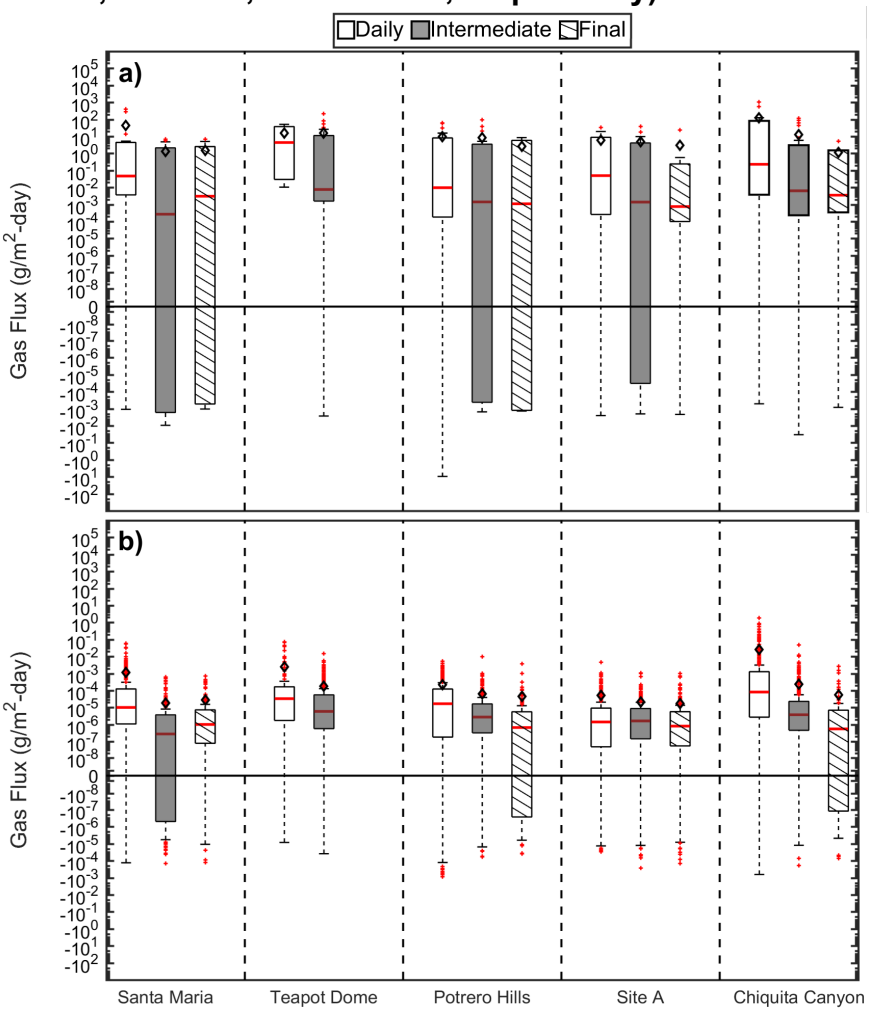

Figure 4.60 provides a detailed comparison of the differences in GHG and NMVOC flux measurements among all landfills as a function of cover category during the dry season. Daily cover flux measurements of GHGs and NMVOCs were highest from Teapot Dome and Chiquita Canyon Landfills, based on median flux values (Figure 4.60). Relying on median flux and the IQR/IWR values, the magnitude and variability of flux measurements from intermediate cover locations were greatest for Teapot

Dome Landfill for both GHGs and NMVOCs. Finally, GHG and NMVOC flux measurements from the final cover systems investigated in this study were generally highest at Santa Maria Reginonal and Chiquita Canyon Landfills, respectively. During the dry season, Chiquita Canyon Landfill had the the highest magnitude and variation of NMVOC fluxes for the final cover system locations. The highest probability of uptake was observed at the intermediate cover locations. Santa Maria Regional Landfill had the largest variation in intermediate-cover NMVOC fluxes based on IQR/IWR values (Figure 4.60).

Figure 4.60 Dry Season a) GHG Fluxes and b) NMVOC Fluxes Organized by Cover Category and Site (open black diamonds, red lines, solid red dots represent means, medians, and outliers, respectively).

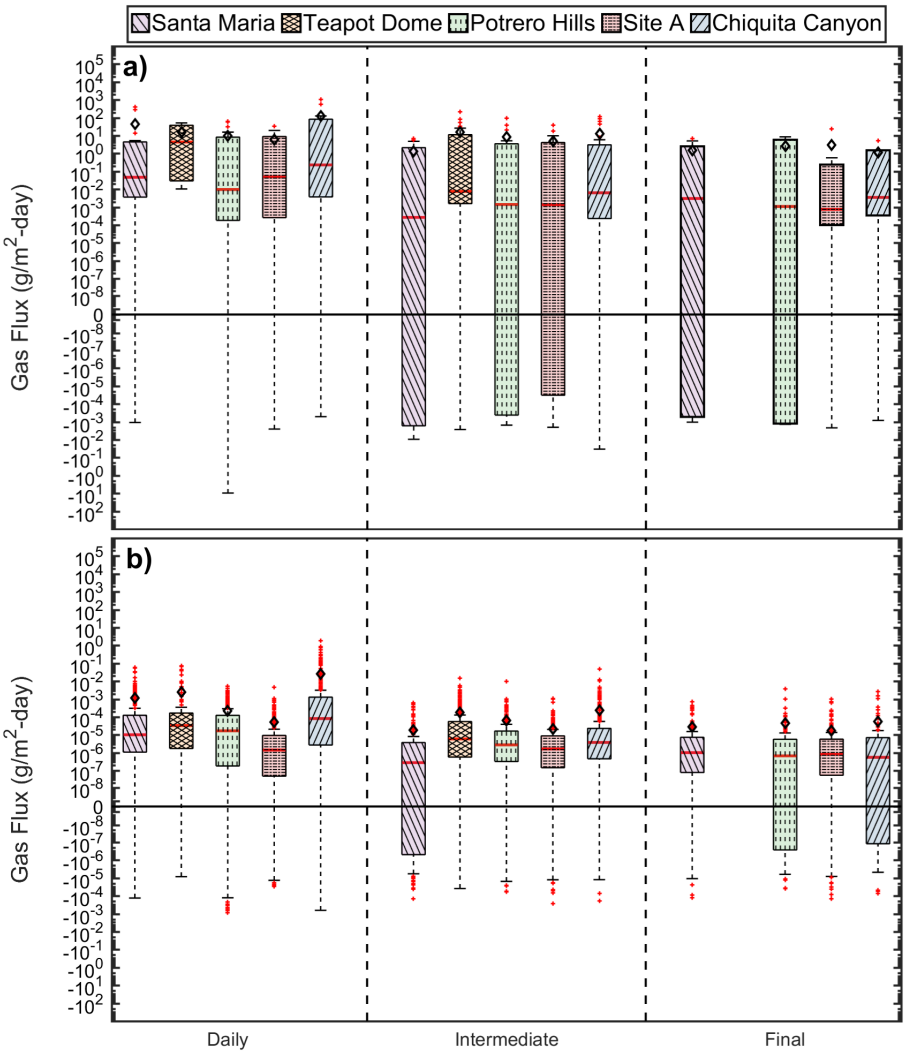

4.4.2 Wet Season Test Results

During the wet weather season testing campaigns, overall flux values across all landfill sites ranged from -6.7×10^{0} to 1.31×10^{3} g/m^2-day, with an overall median value of 7.24×10^{-6} g/m^2-day. Compared to the dry weather season, the overall range in fluxes was relatively similar but shifted in the positive direction, towards net emissions over

net uptake. Based on median values presented, average flux measurements across all sites were higher in the wet season than the dry season. The composite mean and standard deviation across all sites and chemical families was 1.61±31.5 g/m^2-day (N = 3767 total flux measurements). The corresponding minimum and maximum values in reported fluxes corresponded to Teapot Dome and Chiquita Landfill sites, respectively.

Median flux values, across all chemical families and landfill sites, were greatest for Potrero Hills Landfill during the wet season. Based on the IQRs and IWRs, Chiquita Canyon was concluded to have the largest variation in flux measurements during the wet season. The magnitude and variation in overall flux measurements was smallest for the Altamont and Santa Maria landfill sites, respectively. Average skewness (3.77) and kurtosis (24.7) values across all sites and chemical families indicated that the overall distribution in flux measurements was very positively skewed and heavy tailed, suggesting greater probability of emissions over uptake and presence of emission hot spots. Compared to the dry season of testing, the skewness and kurtosis values increased and decreased slightly.

Across all landfill sites, positive and negative emissions varied 12 ($2.44x10^{-9}$ to $1.31x10^{3}$) and 10 ($-6.70x10^{0}$ to $-1.40x10^{-9}$) orders of magnitude, respectively. The inter-site variation in positive emissions was generally greater than the intra-site variation in positive emissions for all landfill sites (ranging from 10-11) during the wet season. Similarly, the inter-site variation in negative emissions was generally greater than the intra-site variation in negative emission for all landfill sites (ranging from 5-10) excluding Teapot Dome during the wet season.

A preliminary inter-landfill comparison of methane, nitrous oxide, carbon dioxide, carbon monoxide, and NMVOC flux measurements obtained from the wet weather season is presented in Figure 4.61. Median methane and nitrous oxide fluxes were generally highest from Potrero Hills Landfill during the wet season (Figure 4.61). Comparably, carbon dioxide and monoxide fluxes were greatest at Chiquita Canyon Landfill. Analysis of the distributions in overall NMVOC flux values indicated that Chiquita Canyon was associated with the greatest emissions of all chemical families (excluding GHGs). The distribution in NMVOC fluxes was most skewed in the positive direction for Chiquita Canyon Landfill, as indicated by the high number of positive outliers and magnitude of the mean flux value. During the wet season, the variation in flux measurements (based on IQR/IWR) was generally highest for Teapot Dome Landfill, especially for methane, carbon dioxide, and total NMVOC gases (Figure 4.57). However, variation in nitrous oxide and carbon monoxide emissions was greatest for Potrero Hills in the wet season.

Figure 4.61 Inter-Landfill Comparison of GHG and NMVOC fluxes for the Wet Season (open black diamonds, red lines, and solid red dots represent means, medians, and outliers, respectively).

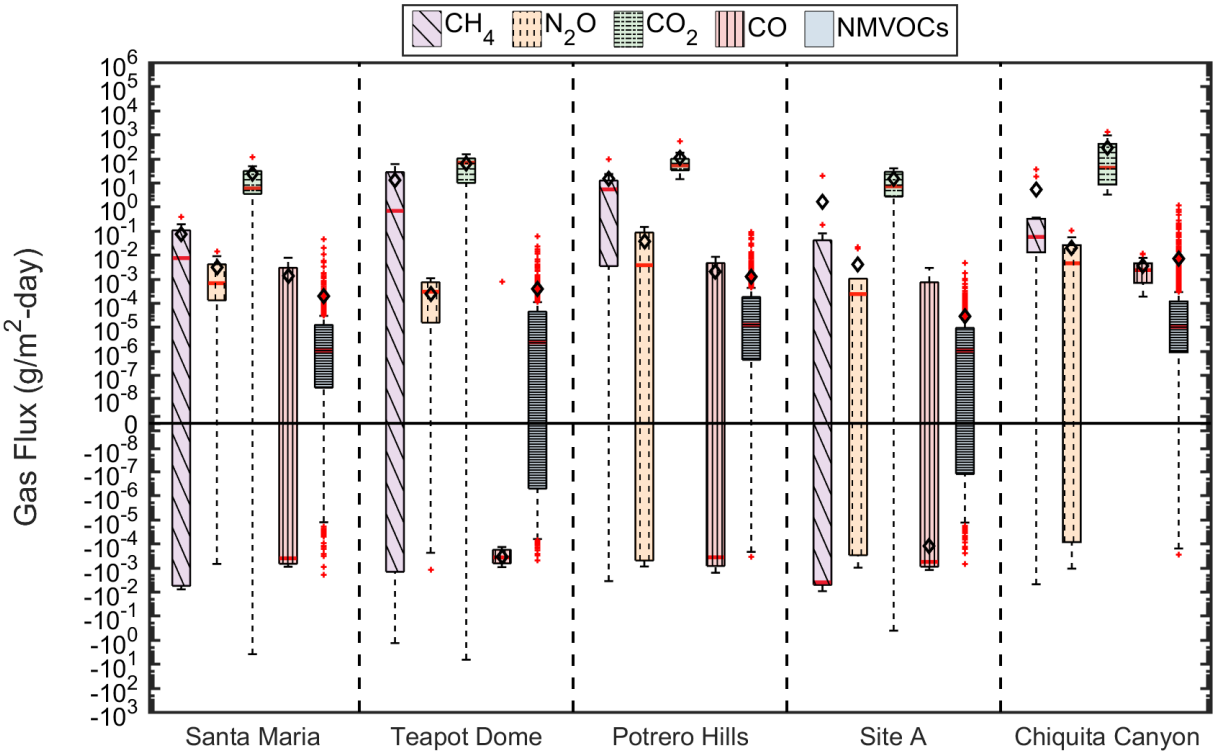

Figure 4.62 compares the overall distributions in flux measurements according to each landfill site, organized by chemical family. Based on median flux values, landfill surface flux measurements of the baseline GHGs were highest from Potrero Hills, confirming the summary statistics presented above (Figure 4.62a). Within the GHGs, methane and nitrous oxide fluxes were greatest at Potrero Hills (Figure 4.62b). Variation in GHG emissions was highest for Potrero Hills, as indicated by the wide IQR and IWR of the boxplots. Relying on median flux values as the basis for inter-site comparison of LFG emissions, the alcohols, monoterpenes, and ketones were the NMVOC chemical families associated with the highest emissions across sites, which is identical to the results obtained for the dry weather season. Based on this analysis, Chiquita Canyon, Potrero Hills, and Chiquita Canyon were the landfills associated with the highest median emissions of the top three NMVOC families identified above. Considering all NMVOC families, Chiquita Canyon was the landfill site with the highest median NMVOC emission value and the highest IQR/IWR values during the wet weather season (Figure 4.62a). The range in overall NMVOC emissions across all testing locations was on the order of -1.93×10^{-3} to 1.12×10^{0} g/m^2-day, which is shifted slightly lower than that of the dry weather season.

Figure 4.62a Overall Inter-Landfill Flux Measurements in the Wet Season (open black diamonds, red lines, and solid red dots represent means, medians, and outliers, respectively).

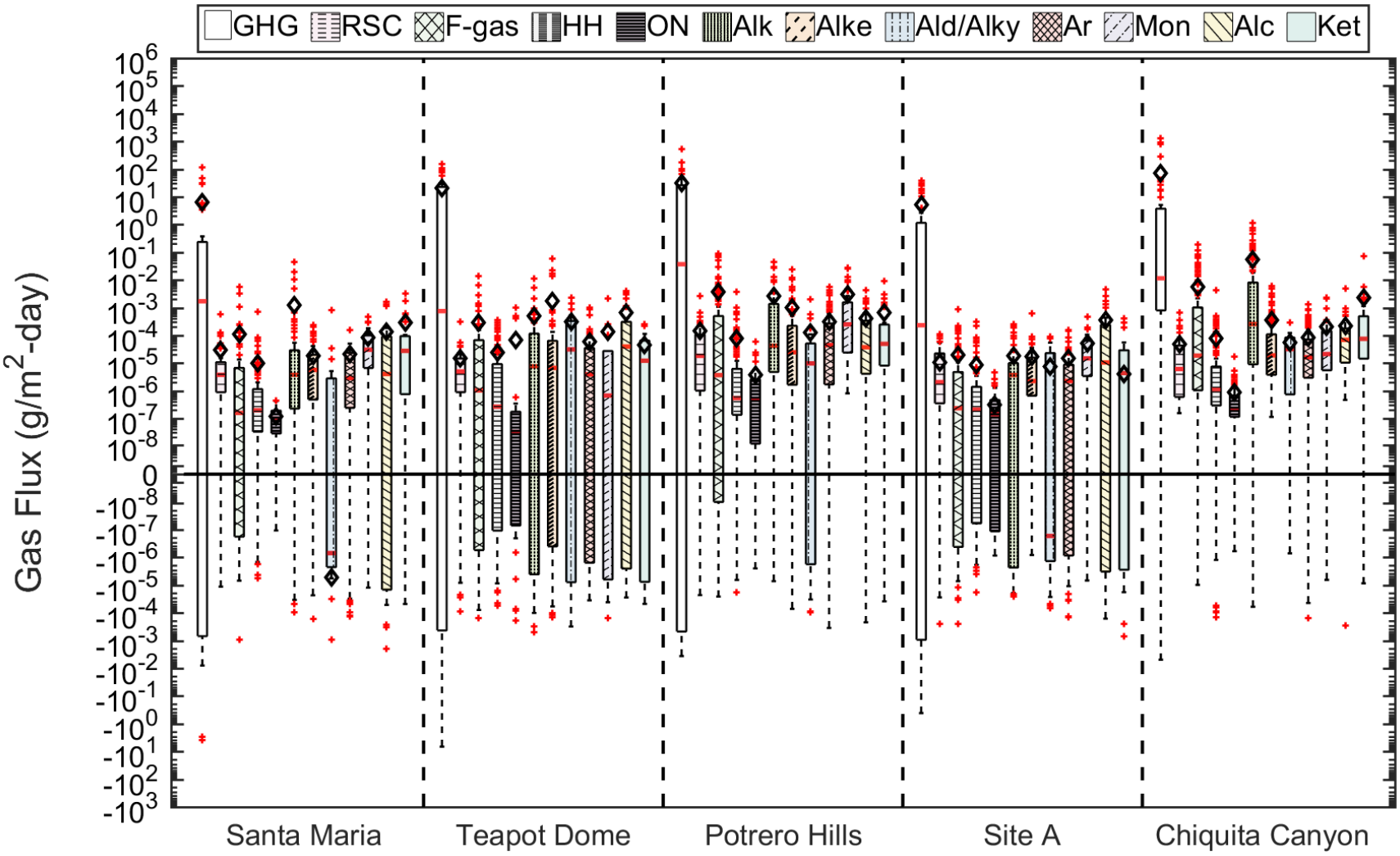

Figure 4.62b Specific GHG and NMVOC Inter-Landfill Flux Measurements in the Wet Season (open black diamonds, red lines, solid red dots represent means, medians, and outliers, respectively).

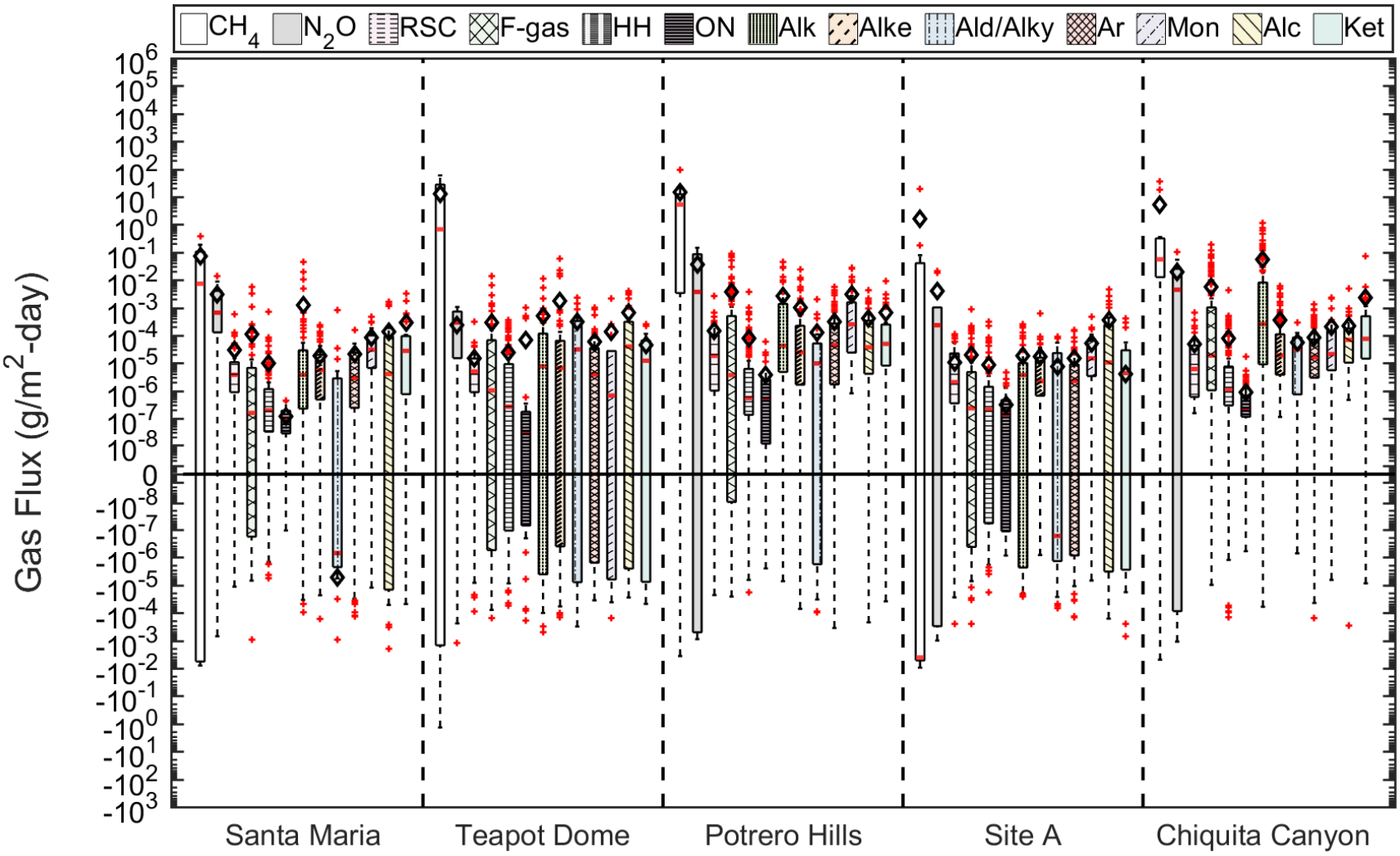

Figure 4.63 compares the GHG (a) and NMVOC (b) flux values collected from all daily, intermediate, and final cover locations at each landfill site during the wet season. As observed in Figure 4.63, GHG and NMVOC emissions generally decreased progressing from daily to intermediate to final cover systems for Teapot Dome, Potrero Hills, and Chiquita Canyon Landfill sites. However, GHG and NMVOC emissions from the final cover of Santa Maria Regional Landfill were slightly higher than those of the intermediate cover. Comparably, the trend among NMVOC emissions at the Altamont site was indicative of increasing, then decreasing flux measurements, similar to that observed in the dry season. In general, the variation in NMVOC emissions (as judged by the IQR/IWR) declined moving from daily to intermediate to final cover systems for all target gases analyzed during the dry season (Figure 4.63).

Figure 4.63 Wet Season a) GHG Fluxes and b) NMVOC Fluxes Organized by Site and Cover Category (open black diamonds, red lines, solid red dots represent means, medians, and outliers, respectively).

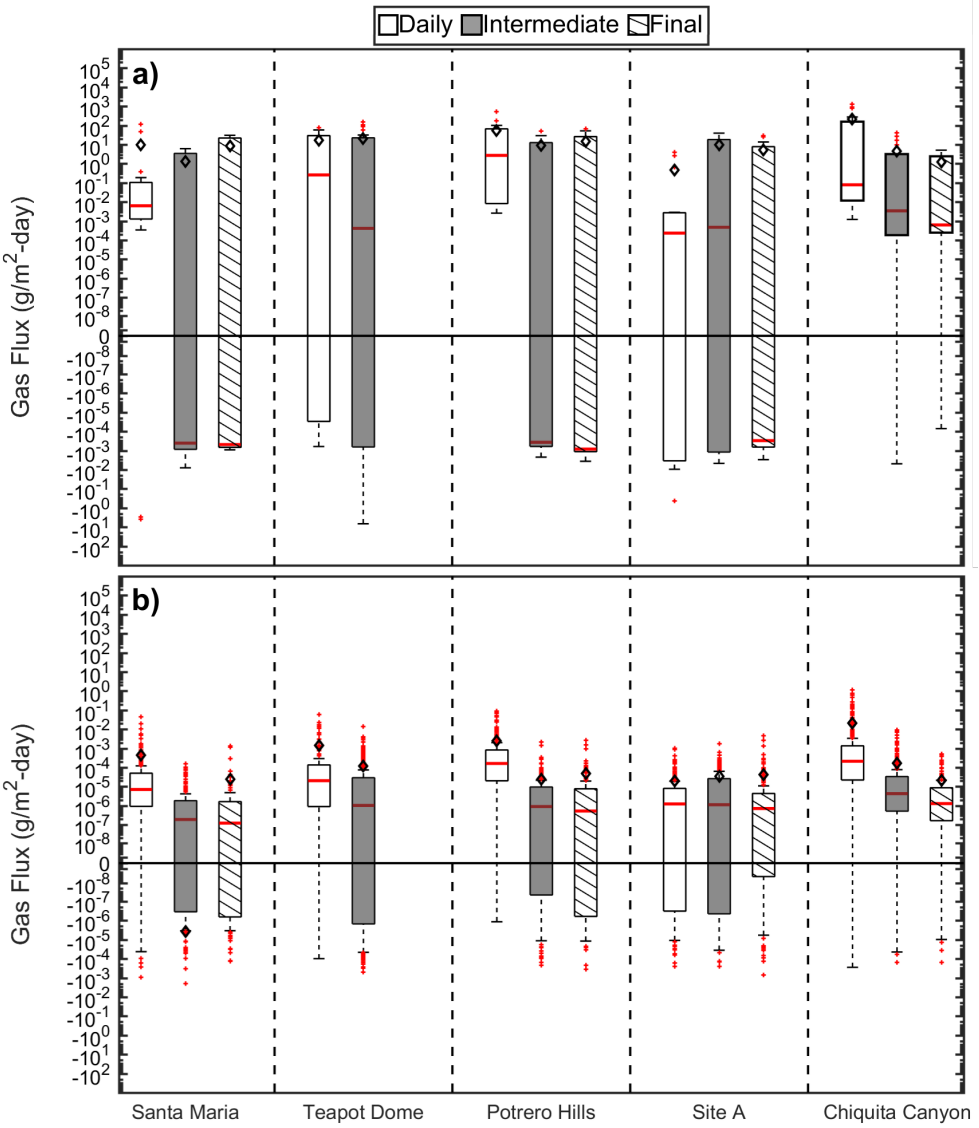

Figure 4.64 compares the differences in GHG and NMVOC flux measurements among all landfill sites as a function of cover category during the wet season. Unlike the dry season, daily cover flux measurements of GHGs and NMVOCs were highest from Potrero Hills and Chiquita Canyon landfills, respectively, based on median flux values (Figure 4.64). Relying on median flux and the IQR/IWR values, the magnitude of GHG and NMVOC flux measurements from intermediate cover locations was greatest for Chiquita Canyon Landfill (Figure 4.64). Among the intermediate cover locations, the variation in GHG and NMVOC flux measurements was generally highest for Teapot Dome Landfill. Finally, GHG and NMVOC flux measurements from the final cover systems investigated in this study were generally highest for Santa Maria and Chiquita Canyon, respectively sites during the wet season, where variation in flux measurements tended to be larger for Santa Maria and Potrero Hills landfills, based on observations of the IQRs and IWRs. In the wet season, the highest probability of uptake was observed at the intermediate cover testing locations, where Teapot Dome Landfill demonstrated the largest variation in GHG and NMVOC flux measurements among landfill sites and locations reviewed for this particular category (Figure 4.61).

Figure 4.64 Wet Season a) GHG Fluxes and b) NMVOC Fluxes Organized by Cover Category and Site (open black diamonds, red lines, solid red dots represent means, medians, and outliers, respectively).

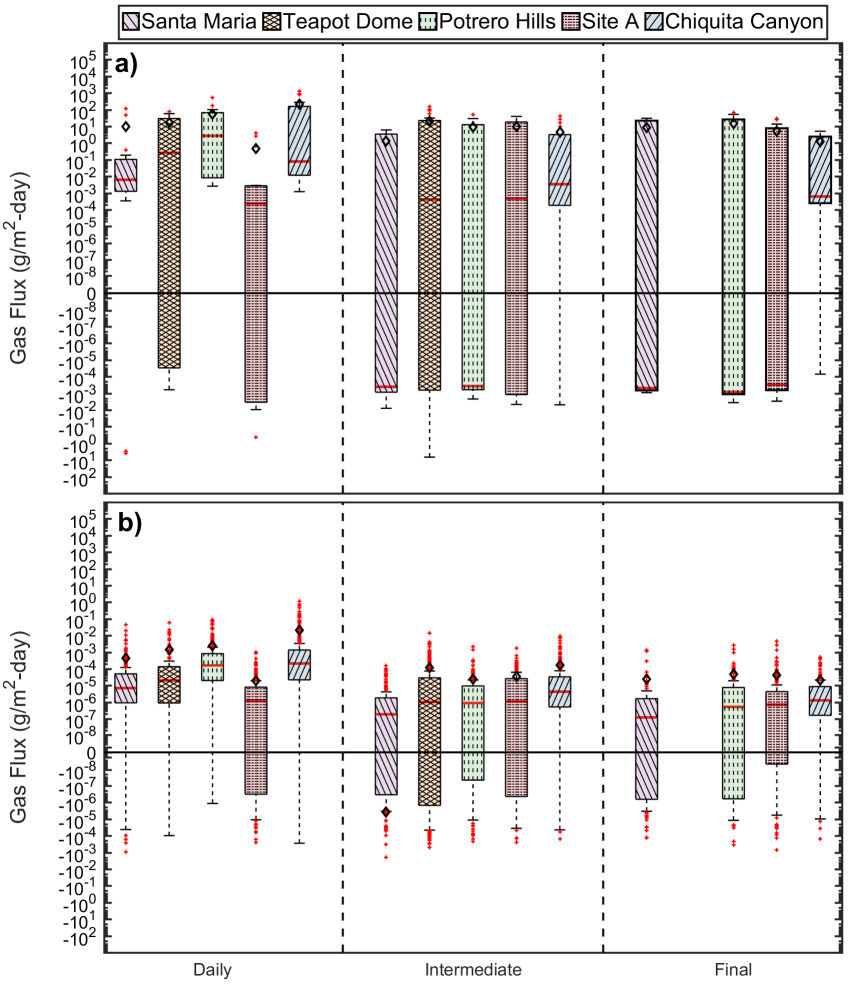

4.5 Seasonal Comparison of Landfill Flux Measurements

The effect of seasonality on flux measurements was investigated for all target gases and landfills. Results presented in Sections 4.3 and 4.4 demonstrated that fluxes were generally higher from the medium (Santa Maria Regional and Teapot Dome Landfills) than the large landfills during the dry season, whereas fluxes were generally higher from the large (Potrero Hills, Site A, and Chiquita Canyon Landfills) than the medium landfills during the wet season.

Figure 4.65 summarizes overall flux measurements for the baseline GHGs and NMVOCs combined from all 5 landfills, presented by cover category and differentiated by season. The results are in agreement with previous observations from intra- and inter-landfill comparisons that overall baseline GHG and NMVOC fluxes decreased progressing from daily to intermediate to final cover systems (Figure 4.65). The central tendencies of fluxes were similar between the two seasons based on the close proximity of both the mean values and the median values (zero to one order of magnitude). For all cover categories, dry season GHG fluxes were slightly higher than wet season fluxes, based on the median values (Figure 4.65). For the NMVOCs, dry season fluxes were slightly higher than wet season fluxes for all intermediate and final cover locations. For both the intermediate and final cover categories, the variation in GHG and NMVOC flux measurements was greater during the wet season, as indicated by the wider IQR and IWR lengths. In addition, there was greater probability of uptake as compared to emissions during the wet season at final and intermediate covers, given that the IQRs extended below zero (for GHGs only).

Figure 4.65 Flux Measurements of a) Baseline Greenhouse Gases and b) NMVOCs According to Cover Category and Season (open black diamonds, red lines, solid red dots represent means, medians, and outliers, respectively).

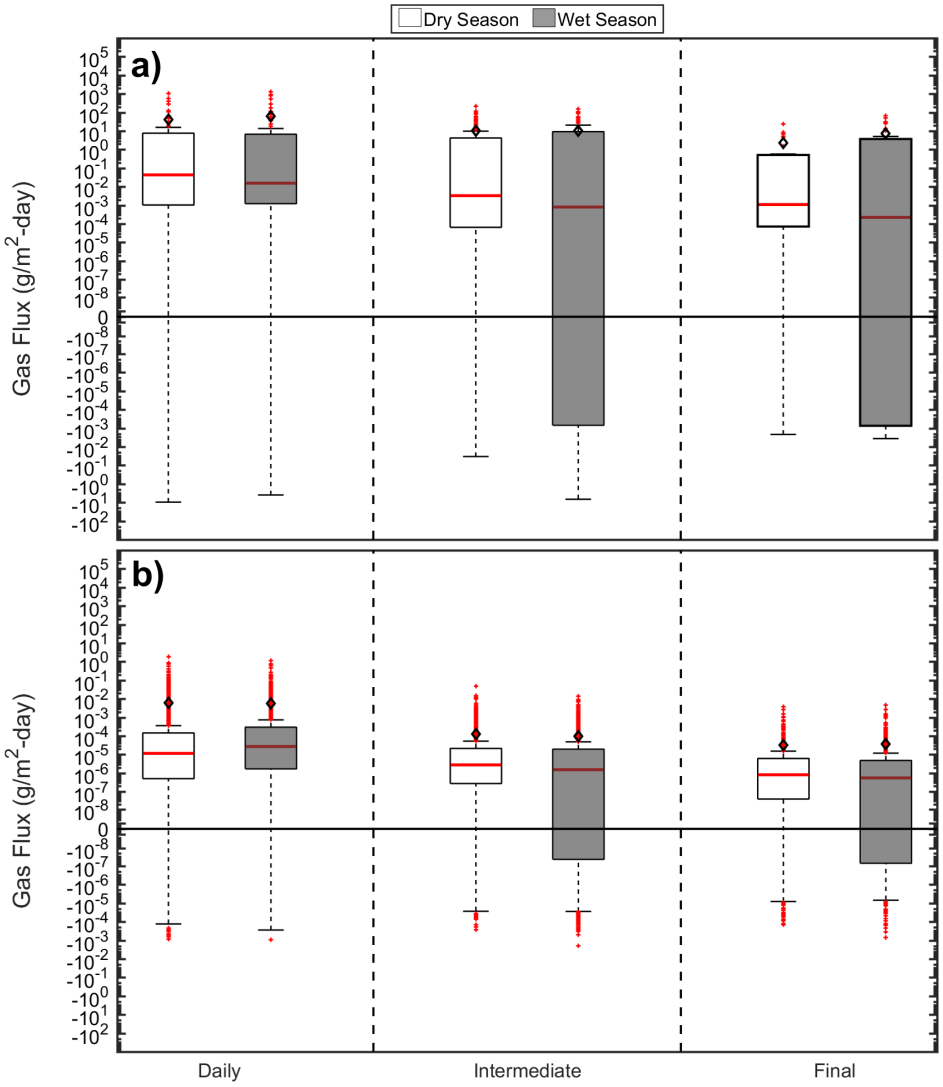

Wet and dry season flux measurements were further investigated as a function of individual GHG and NMVOC chemical families in Figure 4.66. Across all chemical families, the central tendencies of fluxes were similar between the two seasons based on the close proximity of both the mean values and the median values (zero to one order of magnitude). Overall GHG fluxes were somewhat greater in the dry season than the wet season (Figure 4.66a). In addition, dry season methane and nitrous oxide flux measurements were also slightly higher in the dry than the wet season (Figure 4.66b). As indicated by the IQR/IWR values, variation in GHG flux measurements was generally higher in the wet season than the dry season, particularly for nitrous oxide measurements. For the NMVOC families that had high flux in both wet and dry seasons (alcohols, ketones, monoterpenes, and alkanes), there were different trends observed across the landfills investigated. Flux measurements were generally slightly higher for the alcohols, ketones, and alkanes during the dry season, based on comparison of

median values in Figure 4.66. However, flux measurements were somewhat higher for the monoterpenes during the wet season. In general, flux measurements were greater during the dry season for the reduced sulfur compounds, F-gases, halogenated hydrocarbons, and aldehydes/alkynes chemical families. Similar to the monoterpene chemical family, flux measurements of the organic alkyl nitrates, alkenes, and aromatics were greatest during the wet season. For all NMVOC families, the variation in fluxes were similar, but tended to be greater during the wet season (6/11 families), as indicated by the wider IQR and IWRs observed for the sulfur compounds, F-gases, alkanes, alkenes, aromatics, and monoterpenes (Figure 4.66).

Figure 4.66 Flux Measurements of a) Overall and b) Specific Chemical Families Compared Across Seasons (open black diamonds, red lines, solid red dots represent means, medians, and outliers, respectively).

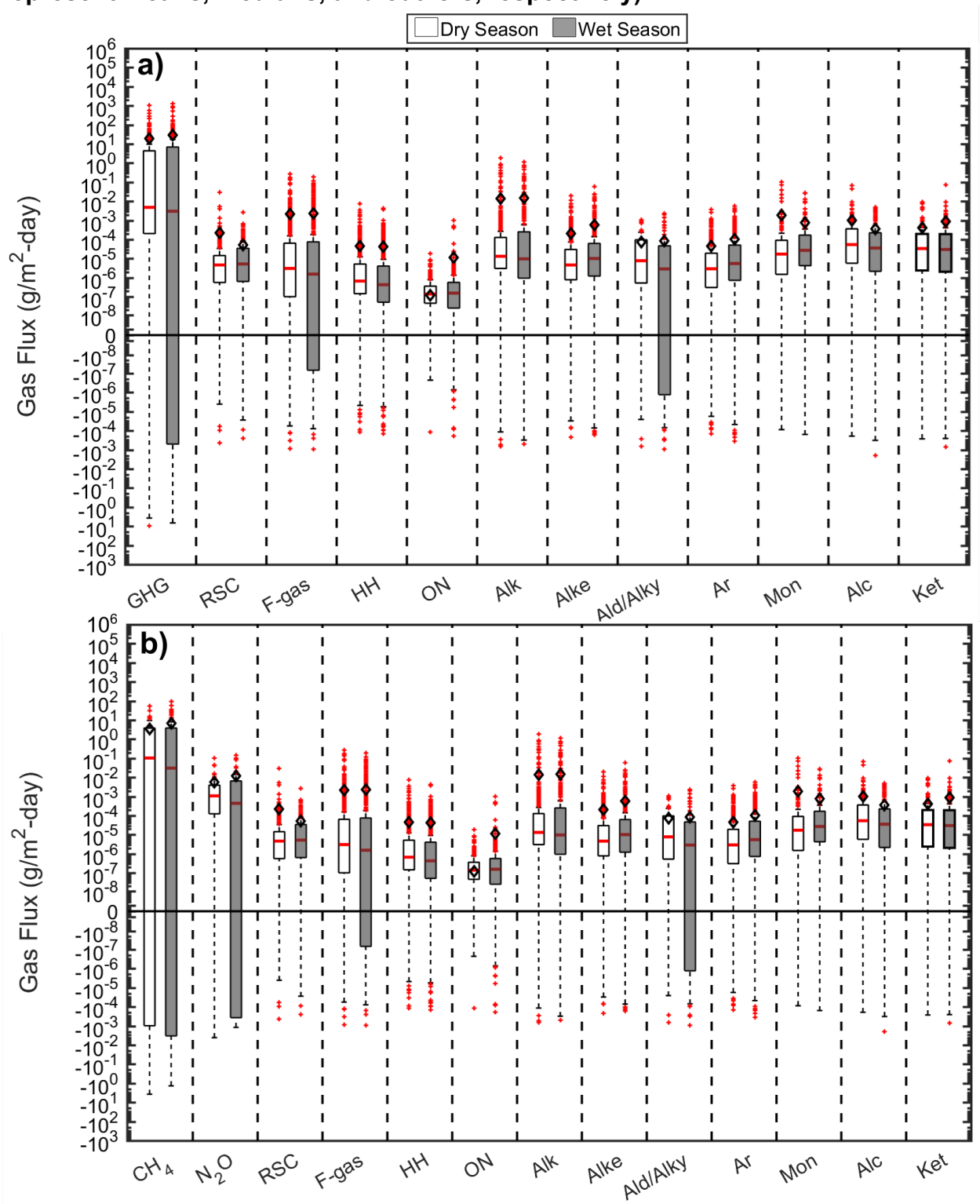

Figure 4.67 further evaluates seasonal differences in flux measurements between baseline GHGs and total NMVOCs as a function of cover category. Comparison of median flux values across the landfills indicated that fluxes of methane generally decreased for daily and intermediate cover categories from the dry to the wet season, whereas methane fluxes increased for final cover systems from the wet to the dry season (Figure 4.67). Nitrous oxide fluxes from both daily and final cover systems were similar during both seasons but tended to be more positively skewed during the dry season at final cover locations. Nitrous oxide fluxes from intermediate covers slightly decreased from dry to wet seasons, where the flux measurements were more negatively skewed during the wet season. Carbon dioxide fluxes decreased to some extent from daily to intermediate to final covers, where seasonal trends were less pronounced than the other baseline GHGs (Figure 4.67). Trends in NMVOCs as a function of cover category and season were already analyzed in Figure 4.65.

Figure 4.67 Baseline Greenhouse Gas and Total NMVOC Flux Measurements as a Function of Cover Category and Season (open black diamonds, red lines, solid red dots represent means, medians, and outliers, respectively). White and grey shading indicate dry and wet seasons, respectively.

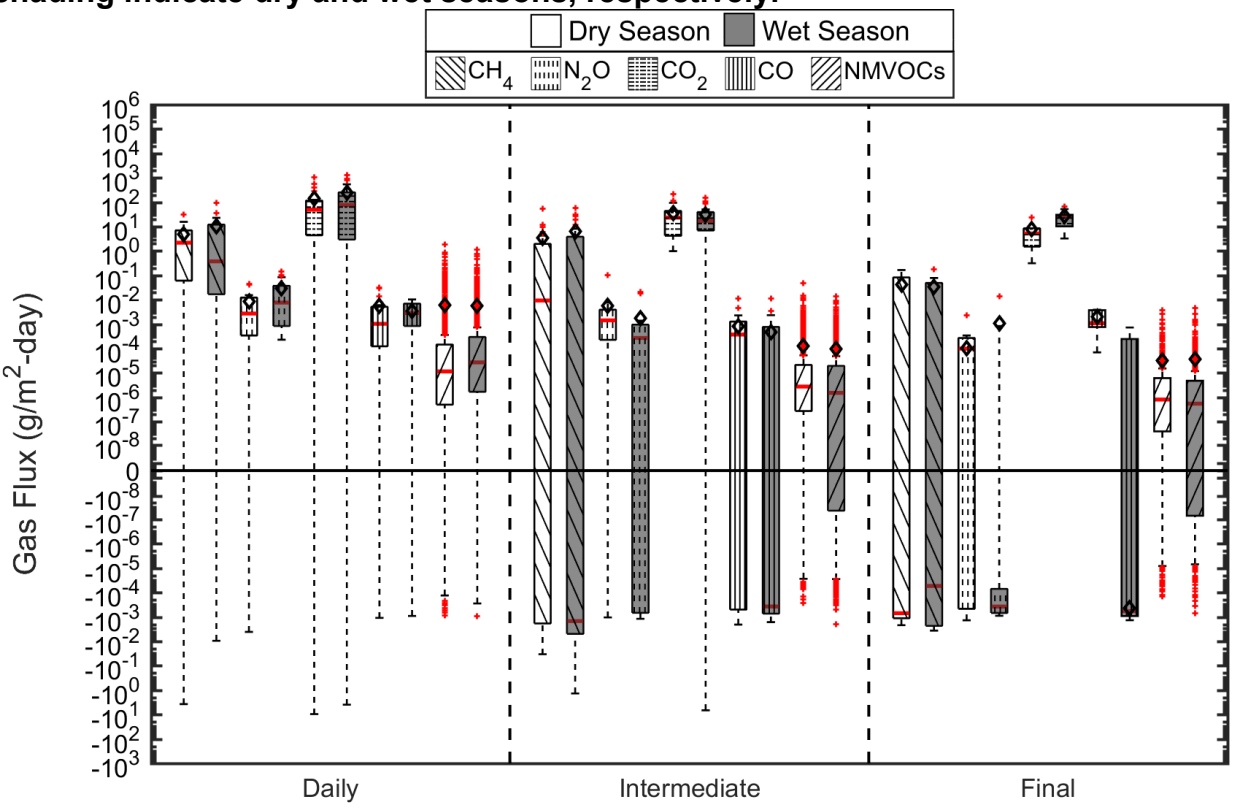

Figure 4.68 provides a final inter-site comparison of the effects of seasonal testing conditions on flux measurements for methane, nitrous oxide, carbon dioxide, carbon monoxide, and total NMVOCs. As previously observed in Figure 4.67, dry season methane fluxes were higher than the wet season fluxes for daily and intermediate cover systems. This trend was observed for flux measurements obtained from Teapot Dome, Site A, and Chiquita Canyon Landfills, where the opposite trend was observed for Santa

Maria Regional and Potrero Hills Landfills (Figure 4.68). Nitrous oxide fluxes were greater in the dry season as compared to the wet season for all landfills investigated, excluding Potrero Hills Landfill (Figure 4.68). As depicted in Figure 4.68, the seasonal effects were less pronounced for carbon dioxide as compared to other target gases. Seasonal effects on NMVOC fluxes also were less pronounced in similarity to carbon dioxide fluxes with slightly higher fluxes in the dry season for Santa Maria Regional and Teapot Dome Landfills, and slightly higher fluxes in the wet season for Potrero Hills and Chiquita Canyon Landfills.

Figure 4.68 Baseline Greenhouse Gas and Total NMVOC Flux Measurements According to Landfill Site and Season (open black diamonds, red lines, solid red dots represent means, medians, and outliers, respectively).

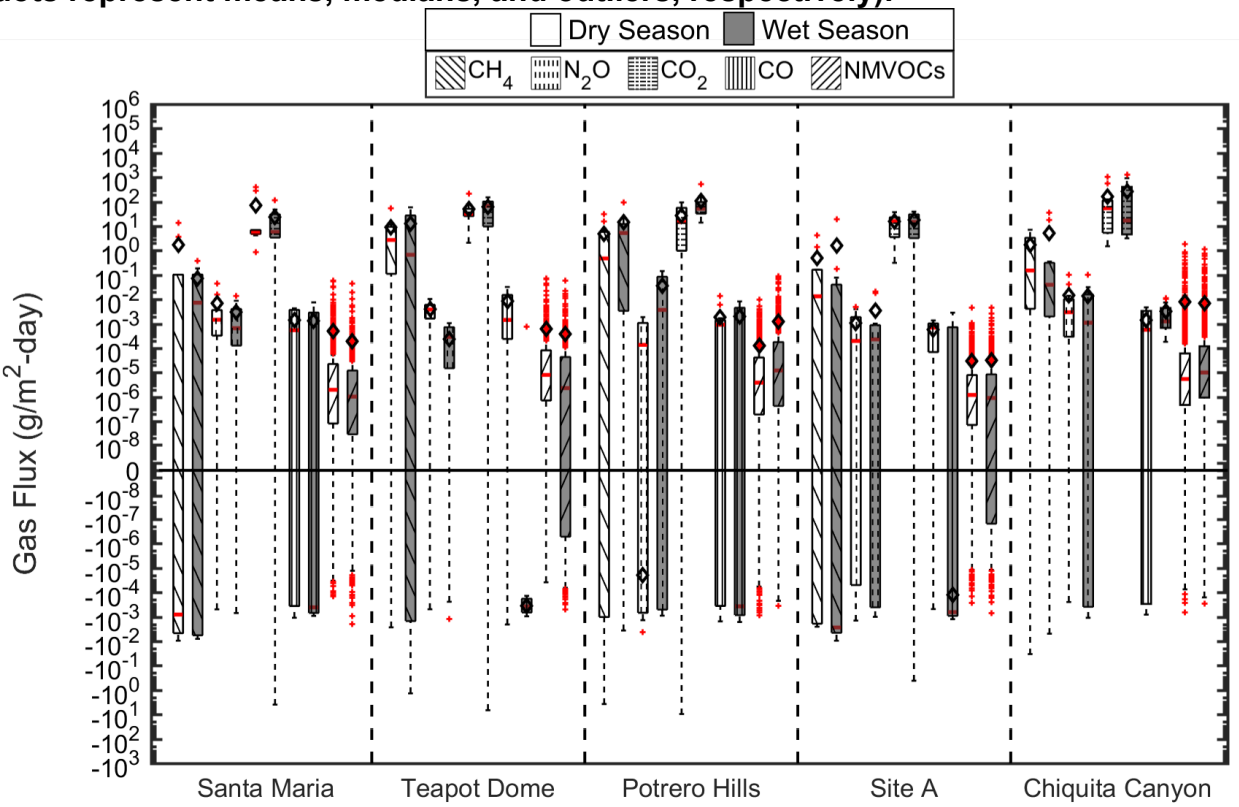

4.6 Whole-Site Landfill Surface Emissions

Whole site, annual emissions were calculated and compared using the fluxes measured for the different cover systems at a given landfill. Measurements from a given cover location, given season, and given chemical were averaged allowing for uncertainty to be determined for the flux measurement. Uncertainty was present due to variation in cover thickness and makeup (minimal for a given pair of chambers), variation in waste present beneath the footprint of the chamber, and potential presence of macrofeatures within the underlying waste or within the cover system below the ground surface. For context, no major cracks or fissures (beyond surficial features extending less than 6 mm depth) were observed in the test program. The uncertainties were carried through the calculations for scaled-up whole site emissions. For each landfill, the relative areas of the different cover categories and the area of the landfill are used together with the

specific fluxes for the covers to calculate annual emissions for the entire landfill. Calculated fluxes for each chemical species were averaged using the two chamber measurements at a given testing location. Results are presented for both direct and weighted greenhouse gas emissions (i.e., in terms of carbon dioxide equivalents), to compare the effect of incorporating chemical-specific GWP values on associated emissions from each site. Results presented in this report combine both seasons to calculate a net annual emission rate for each landfill site. In this calculation, the dry and wet seasons are 168 and 197 days, respectively. In addition, carbon dioxide and carbon monoxide are included in all analyses, even though there is some inherent uncertainty of whether these emissions originate from the landfill or from background soil respiration or other natural processes. Thus, emissions data are provided both with and without these chemicals.

Figure 4.69 and Table 4.7 provides a comparison of the calculated whole-site emissions across the five different landfills investigated in this study both with and without including carbon dioxide and carbon monoxide measurements. The standard deviations were relatively high as the data presented are for all of the measured gases ranging from the main landfill gases methane and carbon dioxide to the remaining 80 trace constituents in landfill gas. As observed in Figure 4.69 and Table 4.7, direct, annual emissions of all target gases were lower than the weighted carbon dioxide equivalent (CO_2-eq.) emissions. Potrero Hills Landfill had the lowest difference in direct versus weighted emissions, whereas Teapot Dome and Chiquita Canyon Landfills had the highest differences in whole-site emissions (Figure 4.69a). Both direct and weighted emissions were highest for Potrero Hills Landfill, on the order of 100,000 tonnes/year, whereas direct and weighted emissions were lowest for Santa Maria Regional Landfill, on the order of 50 tonnes/year (Figure 4.69). When comparing Figure 4.69a and 4.69b, the magnitude of direct and weighted whole-site emissions reduced significantly when carbon dioxide and carbon monoxide were not incorporated into the calculations. At a given landfill, the differences between direct and weighted emissions were significantly more apparent when carbon dioxide and carbon monoxide were excluded from the calculations. Whole-site emissions from large landfills, Site A and Chiquita Canyon, were generally similar to emissions from a medium sized landfill, Teapot Dome. The whole-site emissions from the two medium-size landfills were observed to be significantly different (Figure 4.69).

Table 4.7 – Summary of Direct and Weighted Total LFG Emissions from Each Landfill with and without CO_2/CO (μ = mean, σ = standard deviation).

Landfill		Direct Emissions (tonnes/yr)		Weighted Emissions (tonnes/yr)	
		With CO_2/CO	Without CO_2/CO	With CO_2/CO	Without CO_2/CO
Santa Maria	μ	4.97E+02	6.85E-03	5.15E+02	1.89E+01
	σ	3.69E+01	1.97E-01	4.50E+01	2.58E+01
Teapot Dome	μ	7.26E+03	1.22E+03	4.06E+04	3.46E+04
	σ	4.28E+03	1.30E+03	3.67E+04	3.65E+04
Potrero Hills	μ	1.26E+05	1.35E+03	1.62E+05	3.80E+04
	σ	2.14E+04	1.11E+03	3.77E+04	3.11E+04
Site A	μ	9.21E+03	9.48E+02	3.55E+04	2.72E+04
	σ	3.19E+03	1.61E+03	4.52E+04	4.52E+04
Chiquita Canyon	μ	2.81E+04	4.38E+02	5.21E+04	2.44E+04
	σ	1.06E+04	3.76E+02	1.57E+04	1.16E+04

Figure 4.69 Direct and Weighted Whole-Site Emissions of Total Landfill Gas from 5 Landfills in California a) Including CO_2 and CO and b) Excluding CO_2 and CO. Error bars represent the standard deviation of calculated emissions.

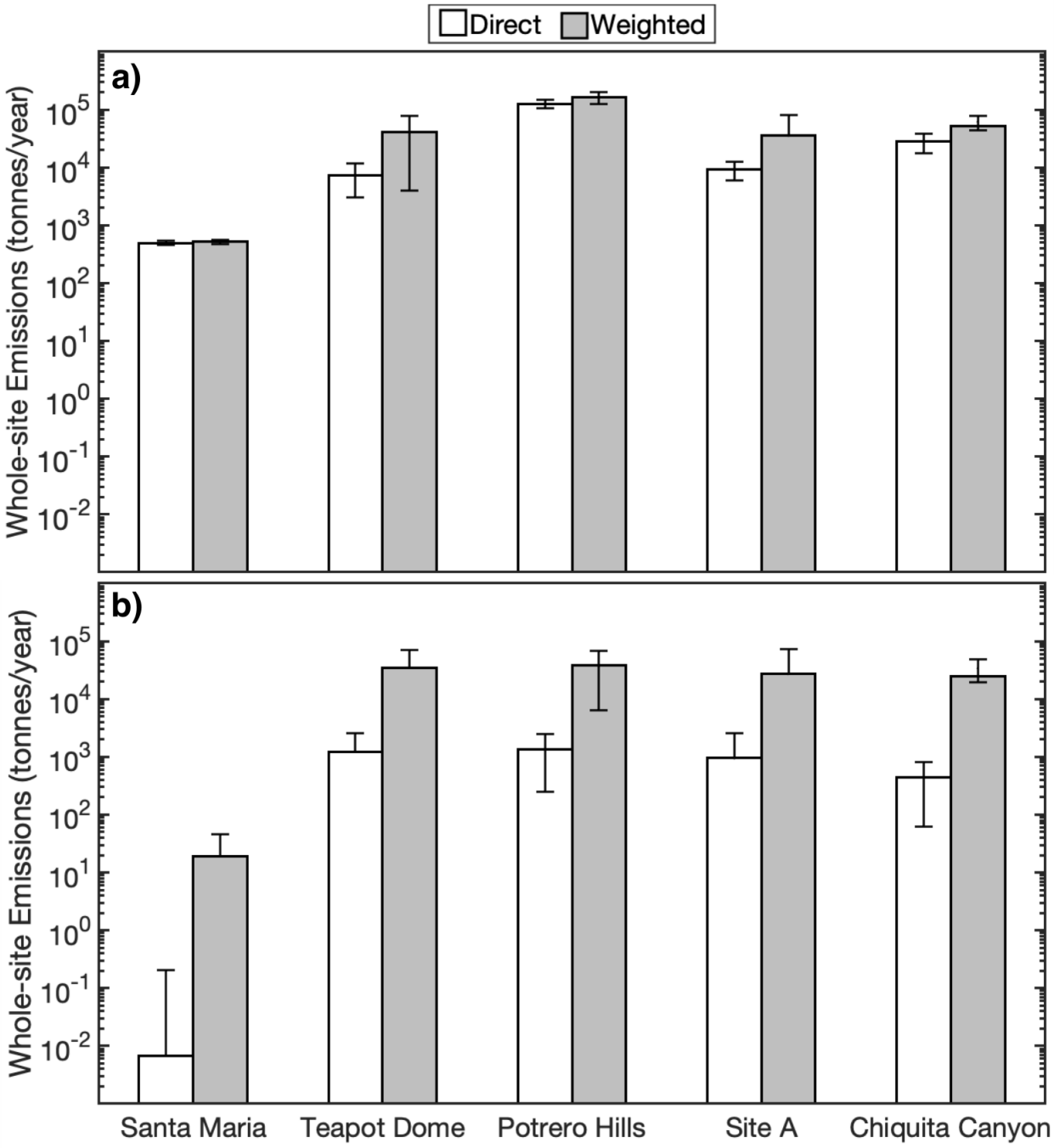

Figure 4.70 further depicts the differences in weighted emissions (i.e., CO_2-eq.) as a function of season both with and without CO_2 and CO. The whole-site emissions were divided into emissions emanating during the wet and dry seasons using the specific time periods assigned to each season. As observed in Figure 4.70, wet season emissions slightly exceeded those from the dry season for each landfill investigated except for Santa Maria Regional Landfill. The greatest differences between dry and wet

seasons were observed for Site A and Potrero Hills Landfills. At these two landfills, wet season fluxes generally exceeded dry season fluxes for all gases analyzed. The lowest differences in emissions between seasons were observed for Chiquita Canyon Landfill. Comparison of Figure 4.70a and 4.70b demonstrates that the seasonal results were affected by the inclusion of CO_2 into the calculation scheme, as affected by the higher CO_2 fluxes in the wet season than the dry season.

Figure 4.70 Comparison of Seasonal Whole-Site Weighted LFG Emissions from 5 Landfills a) Including CO_2 and CO and b) Excluding CO_2 and CO. Error bars represent the standard deviation of calculated emissions.

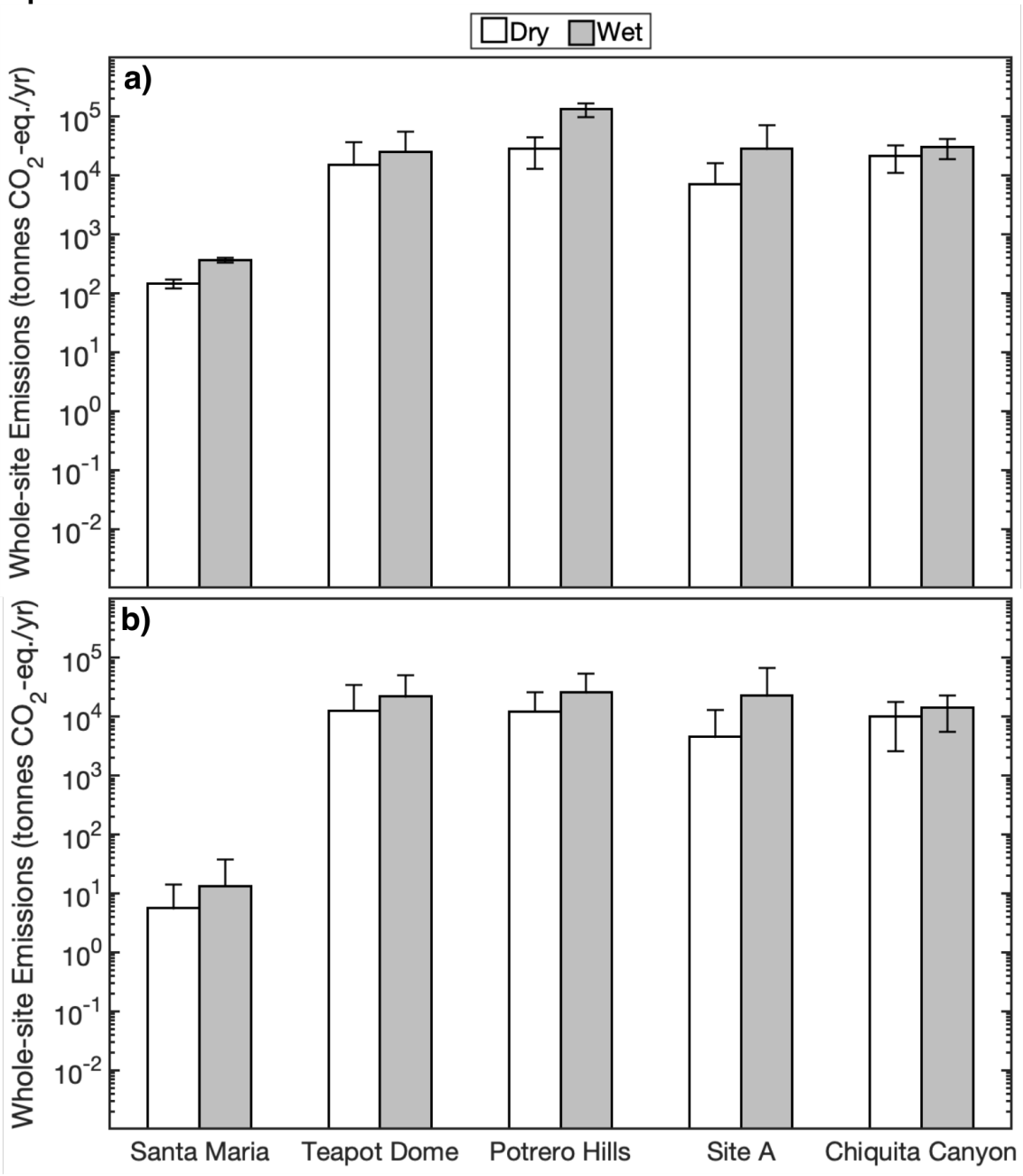

Figure 4.71 and Tables 4.8 and 4.9 provide a comparison of the site-specific weighted emissions of baseline GHGs and NMVOCs. As observed in Figure 4.71 and Tables 4.8 and 4.9, baseline GHG whole-site emissions were typically 2 orders of magnitude higher than NMVOC emissions. At Chiquita Canyon Landfill, weighted whole-site emissions of NMVOCs were comparable or higher than the emissions of the baseline GHGs. At Santa Maria Regional Landfill, net uptake of NMVOCs was observed over emissions (Table 4.9). The difference in weighted emissions was more significant when CO2 and CO were included (Figure 4.71b). The emissions from Santa Maria Regional Landfill were lower than the emissions from the other sites, which had relatively comparable emissions, in particular for GHGs.

Table 4.8 – Summary of Direct and Weighted GHG Emissions from Each Landfill with and without CO_2/CO (μ = mean, σ = standard deviation).

Landfill		Weighted Emissions (tonnes/yr)	
		With CO_2/CO	Without CO_2/CO
Santa Maria	μ	5.16E+02	1.97E+01
	σ	4.50E+01	2.57E+01
Teapot Dome	μ	4.03E+04	3.42E+04
	σ	3.67E+04	3.65E+04
Potrero Hills	μ	1.61E+05	3.70E+04
	σ	3.77E+04	3.10E+04
Site A	μ	3.53E+04	2.70E+04
	σ	4.52E+04	4.52E+04
Chiquita Canyon	μ	3.91E+04	1.14E+04
	σ	1.50E+04	1.06E+04

Table 4.9 – Summary of Weighted NMVOC Emissions from Each Landfill (μ = mean, σ = standard deviation).

Landfill		Weighted Emissions (tonnes/yr)
Santa Maria	μ	-8.35E-01
	σ	1.73E+00
Teapot Dome	μ	3.51E+02
	σ	4.27E+02
Potrero Hills	μ	1.01E+03
	σ	6.96E+02
Site A	μ	1.87E+02
	σ	1.32E+02
Chiquita Canyon	μ	1.30E+04
	σ	4.75E+03

Figure 4.71 Weighted Whole-Site Emissions from 5 Landfills as a Function of Chemical Family a) Including CO_2 and CO and b) Excluding CO_2 and CO. Error bars represent the standard deviation of calculated emissions.

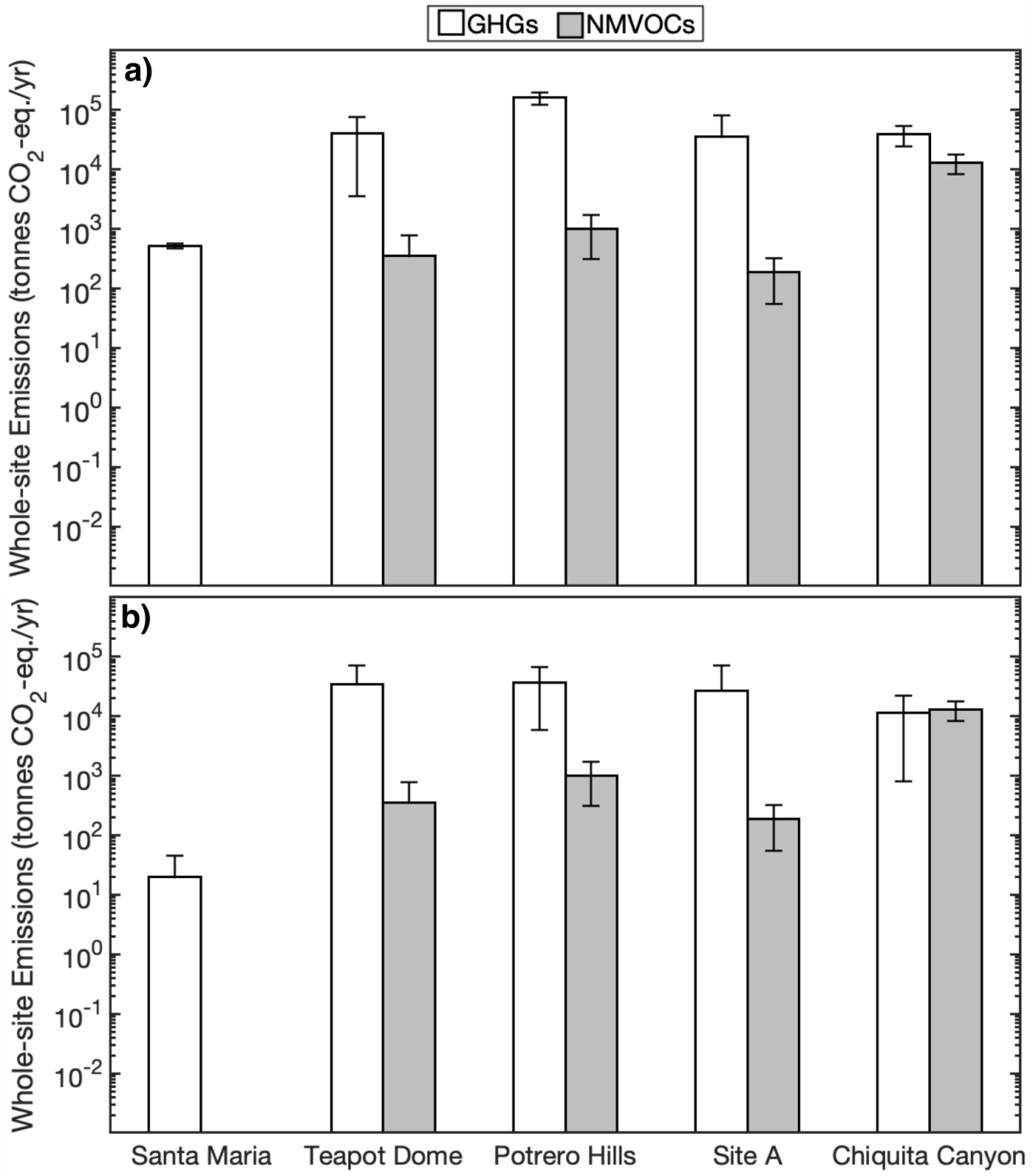

4.7 Geotechnical Properties of Cover Systems

The geotechnical index properties evaluated included specific gravity (G_s), moist and dry densities (ρ_{moist} and ρ_{dry}, respectively), gravimetric moisture content (w), degree of saturation (S), porosity (n), void ratio (e). For cover materials that consisted of soil,

gravel content (USCS classification), sand content (USCS classification), fines content (USCS classification), silt content (USDA classification), and clay content (USDA classification) were also included, respective of season as appropriate. In addition, Atterberg limits (PL, LL, and PI) were determined as appropriate. Cover temperatures measured in-situ during field testing within the chamber footprint were evaluated.

An additional set of geotechnical characteristics (10 total) were further calculated by incorporating the cover thickness, chamber area (1 m^2), and weight-volume relationships of the cover materials to quantify the column of cover material present directly beneath the testing location. These weight-volume characteristics included the mass of solids (M_s), mass of water (M_w), total mass (M_T), volume of solids (V_s), volume of water (V_w), volume of voids (V_v, i.e., volume of air + volume of water), volume of air (V_a). In addition, volumetric solids content (θ_s), volumetric water content (θ_w), and volumetric air content (θ_a) were calculated by dividing the corresponding volume of solids, water or air by the total volume as applicable. Furthermore, waste ages and waste column heights directly beneath the column testing locations were determined through interpretation of historic topographic maps obtained from site records. An average waste age for the entire waste column beneath the testing location was determined.

The geotechnical index properties at Santa Maria Regional Landfill are summarized in Table 4.7. The water content and degree of saturation were higher in the wet season than the dry season across all testing locations. Cover temperatures were generally warmer in the dry season than the wet season, and greater for alternative daily cover materials, such as the wood waste locations than the soil covers (Table 4.7), indicative of biological decay of the wood waste materials. Additional weight-volume properties for the covers at Santa Maria Regional Landfill are presented in Table 4.8.

The geotechnical index properties at Teapot Dome Landfill are summarized in Table 4.9. The water content and degree of saturation were generally higher in the wet season than the dry season across all testing locations. Cover temperatures were generally significantly warmer in the dry season than the wet season. Additional weight-volume properties for the covers at Teapot Dome Landfill are presented in Table 4.10.

The geotechnical index properties at Potrero Hills Landfill are summarized in Table 4.11. The water content and degree of saturation were higher in the wet season than the dry season across all testing locations. Cover temperatures for daily covers were generally significantly higher in the wet season than the dry season. Additional weight-volume properties for the covers at Potrero Hills Landfill are presented in Table 4.12.

The geotechnical index properties at Site A Landfill are summarized in Table 4.13. The water content and degree of saturation were higher in the wet season than the dry season across all testing locations. Cover temperatures of covers were higher in the dry season than the wet season. Additional weight-volume properties for the covers at Potrero Hills Landfill are presented in Table 4.14.

The geotechnical index properties at Chiquita Canyon Landfill are summarized in Table 4.15. The water content and degree of saturation were higher in the wet season than the dry season across all testing locations. With the exception of IC-NGW, cover temperatures of covers were higher in the dry season than the wet season. Additional weight-volume properties for the covers at Chiquita Canyon Landfill are presented in Table 4.16.

Table 4.10 – Baseline Geotechnical Properties for Covers at Santa Maria Regional Landfill

Season	Location	G_s	Moist Density (kg/m^3)	Dry Density (kg/m^3)	w (%)	S (%)	n	e	Gravel (%)[1]	Sand (%)[1]	Fines (%)	Soil Classifcation[1]	Gravel (%)[2]	Sand (%)[2]	Clay (%)[2]	Silt (%)[2]	Soil Classification[2]	LL	PL	PI	D_{10} (mm)	Temperature (°C)
Wet	DC-WW	1.58	342	214	60	15	0.86	6.38	NA	NA	NA	NA	NA	NA	NA	NA	N/A	ND	ND	ND	NA	31.3
	DC+IC	2.62	1672	1512	11	38	0.42	0.73	27.6	62.8	9.6	SM	37.8	52.6	4.7	4.9	GLS	NP	NP	NP	0.087	21.3
	IC-H/ IC-L	2.66	1514	1452	4	14	0.46	0.83	17.9	73.1	9	SM	27.2	61.9	5.5	5.4	GLS	NP	NP	NP	0.026	22.2
	FC	2.6	1384	1291	7	19	0.51	1	4.1	80.3	15.6	SM	8.0	77.1	5.4	9.1	LS	NP	NP	NP	0.013	15.3
	FC-Deep	2.6	1376	1276	8	20	0.51	1	9.2	85.7	5.1	SW-SM	13.4	84.3	0.1	2.2	S	NP	NP	NP	0.297	ND
Dry	DC-WW	1.58	342	300	14	5	0.81	4.25	NA	NA	NA	NA	NA	NA	NA	NA	N/A	ND	ND	ND	NA	51.8
	DC+IC	2.62	1672	1619	3	14	0.39	0.62	15.5	79.3	5.2	SM	25.5	69.0	2.8	2.7	GS	NP	NP	NP	0.184	30.8
	IC-H/ IC-L	2.66	1384	1368	1	3	0.47	0.9	17.9	73.1	9	SM	27.2	61.9	5.5	5.4	GLS	NP	NP	NP	0.026	29.9
	FC	2.6	1513	1490	2	5	0.44	0.79	12.0	82.0	6.0	SM	17.8	79.3	0.4	2.6	GS	NP	NP	NP	0.309	31.8

[NA] Not applicable given cover type was not composed of soil
[ND] Soil temperature not determined at this location
[NP]Non-plastic
[1]USCS classification (4.75 mm > sand > 0.075 mm > fines), SM/SC stands for Silty Sand and Clayey Sand
[2]USDA classification (0.05 mm > silt > 0.002 mm > clay), LS, GLS and GS stand for Loamy Sand, Gravelly Loamy Sand, and Gravelly Sand

Table 4.11 – Composite Geotechnical Properties for Covers at Santa Maria Regional Landfill

Season	Location	M_s (kg)	M_w (kg)	M_T (kg)	V_s (m^3)	V_w (m^3)	V_v (m^3)	V_a (m^3)	θ_s	θ_w	θ_a	Waste Age (years)	Column Height (m)
Wet	DC-WW	59.9	36.0	95.9	0.038	0.036	0.241	0.205	0.135	0.129	0.731	16.9	16.5
	DC+IC	1194.5	131.4	1325.9	0.455	0.126	0.332	0.206	0.575	0.160	0.260	15.7	17.1
	IC-H/IC-L	987.4	39.5	1026.9	0.377	0.044	0.313	0.269	0.554	0.064	0.396	8.28	22.5
	FC	936.4	58.8	995.2	0.353	0.057	0.324	0.267	0.519	0.084	0.393	35	15.9
Dry	DC-WW	84.0	11.8	95.8	0.053	0.011	0.227	0.215	0.191	0.041	0.770	15.0	21.6
	DC+IC	1279.0	38.4	1317.4	0.497	0.043	0.308	0.265	0.629	0.055	0.335	15.7	17.1
	IC-H/IC-L	930.2	9.3	939.5	0.355	0.010	0.320	0.310	0.522	0.014	0.456	8.28	22.5
	FC	930.2	9.3	939.5	0.355	0.010	0.320	0.310	0.522	0.014	0.456	35	15.9

Table 4.12 – Baseline Cover Geotechnical Properties for Teapot Dome Landfill

Season	Location	G_s	Moist Density (kg/m^3)	Dry Density (kg/m^3)	w (%)	S (%)	n	e	Gravel (%)[1]	Sand (%)[1]	Fines (%)[1]	Soil Classification[1]	Gravel (%)[2]	Sand (%)[2]	Clay (%)[2]	Silt (%)[2]	Soil Classification[2]	LL	PL	PI	D_{10} (mm)	Temperature (°C)
Wet	DC-S	2.76	1290	1175	10	19	0.57	1.35	1.9	67.5	30.6	SC-SM	7.8	60.8	7.4	24.0	SL	22	17	5	0.005	15.8
	IC-S+GW	2.72	1230	1065	15	30	0.61	1.57	2.4	37.2	60.4	CL	4.1	51.8	12.3	31.7	SL	28	20	8	0.001	13.2
	IC-N	2.74	1270	1105	15	27	0.6	1.48	0.3	72.0	28.7	SM	2.4	72.3	8.3	17.0	SL	NP	NP	NP	0.004	13.7
	IC-O	2.7	1250	1085	11	27	0.59	1.5	3.7	72.8	23.5	SM	18.2	58.1	8.4	15.3	GSL	25	17	18	0.003	13.7
	IC-W	2.77	1346	1166	15	31	0.58	1.38	0.4	58.8	40.8	SM	2.1	60.5	11.4	26.3	SL	27	22	5	0.002	14.5
Dry	DC-GW	1.8	315	271	16	5	0.85	5.67	NA	NA	NA	NA	NA	NA	NA	NA	NA	NA	NA	NA	NA	29.3
	IC-S+GW	2.72	1440	1339	7	20	0.51	1.05	1.7	58.9	39.4	SC	7.9	67.3	5.1	19.7	SL	23	15	8	0.019	30.9
	IC-N	2.74	1517	1495	2	5	0.45	0.83	16.9	55.1	28	SM	24.1	58.2	6.6	11.1	GSL	NP	NP	NP	0.007	37.2
	IC-O	2.7	1214	1191	2	4	0.56	1.27	2.8	44.6	52.6	CL	12.3	54.1	5.4	28.2	SL	30	15	15	0.011	32.5
	IC-W	2.77	1266	1236	3	5	0.56	1.25	0.1	41.2	58.7	ML	0.7	61.1	6.7	31.5	SL	23	22	1	0.008	34.9

[NA] Not applicable given cover type was not composed of soil

[NP]Non-plastic

[1]USCS classification (4.75 mm > sand > 0.075 mm > fines), SM or SC stand for Silty Sand and Clayey Sand

[2]USDA classification (0.05 mm > silt > 0.002 mm > clay), GSL stands for Gravelly Sandy Loam

Table 4.13 – Composite Geotechnical Properties for Covers at Teapot Dome Landfill

Season	Location	M_s (kg)	M_w (kg)	M_T (kg)	V_s (m^3)	V_w (m^3)	V_v (m^3)	V_a (m^3)	θ_s	θ_w	θ_a	Waste Age (years)	Column Height (m)
Wet	DC-S	223.3	22.3	245.6	0.080	0.021	0.108	0.088	0.422	0.108	0.462	21.4	26.2
	IC-S+GW	447.3	67.1	514.4	0.163	0.077	0.256	0.179	0.389	0.183	0.427	27.1	24.1
	IC-N	386.8	58.0	444.8	0.142	0.057	0.210	0.153	0.405	0.162	0.438	21.7	21
	IC-O	846.3	93.1	939.4	0.307	0.124	0.460	0.336	0.393	0.159	0.431	30.9	4.1
	IC-W	396.4	59.5	455.9	0.143	0.061	0.197	0.136	0.420	0.180	0.400	27.2	27.2
Dry	DC-GW	73.2	11.7	84.9	0.040	0.011	0.230	0.218	0.150	0.043	0.808	26.6	24.4
	IC-S+GW	562.4	39.4	601.7	0.204	0.043	0.214	0.171	0.486	0.102	0.408	27.1	24.1
	IC-N	523.3	10.5	533.7	0.190	0.008	0.158	0.150	0.542	0.023	0.428	21.7	21
	IC-O	929.0	18.6	947.6	0.344	0.017	0.437	0.419	0.441	0.022	0.538	30.9	4.1
	IC-W	420.2	12.6	432.8	0.152	0.010	0.190	0.181	0.448	0.028	0.532	27.2	27.2

Table 4.14 – Baseline Cover Geotechnical Properties for Potrero Hills Landfill

Season	Location	G_s	Moist Density (kg/m^3)	Dry Density (kg/m^3)	w (%)	S (%)	n	e	Gravel (%)[1]	Sand (%)[1]	Fines (%)[1]	Soil Classification[1]	Gravel (%)[2]	Sand (%)[2]	Clay (%)[2]	Silt (%)[2]	Soil Classification[2]	LL	PL	PI	D_{10} (mm)	Temperature (°C)
Wet	DC-AF	1.73	430	337	25	11	0.8	4.14	NA	NA	NA	NA	NA	NA	NA	NA	NA	NA	NA	NA	NA	43.6
	DC-GW	1.35	200	148	37	5	0.89	7.96	NA	NA	NA	NA	NA	NA	NA	NA	NA	NA	NA	NA	NA	55.9
	DC-C+D	1.2	200	146	30	6	0.88	7.25	NA	NA	NA	NA	NA	NA	NA	NA	NA	NA	NA	NA	NA	48.2
	IC-BM	2.75	1735	1525	13	46	0.45	0.8	24.0	31.1	45.0	SC	28.5	42.0	8.6	20.9	GSL	30	18	12	0.005	19.8
	IC-C1	2.65	1341	1074	24	44	0.61	1.53	3.2	29.1	67.7	CH	5.2	49.1	10.1	35.6	L	51	22	29	0.002	16.7
	IC-C1 deep	2.65	1075	840	28	34	0.68	2.16	0.5	15.0	84.5	CH	2.5	27.9	26.1	43.4	CL	51	23	28	<0.001	ND
	FC	2.72	1711	1451	17	55	0.47	0.88	1.1	18.3	80.6	CH	2.0	27.6	36.4	34.0	CL	56	27	29	<0.001	16.4
Dry	DC-AF	1.73	168	161	0.7	0.41	0.75	3.05	NA	NA	NA	NA	NA	NA	NA	NA	NA	NA	NA	NA	NA	38.2
	DC-GW	1.35	170	164	4	0.86	0.86	6.01	NA	NA	NA	NA	NA	NA	NA	NA	NA	NA	NA	NA	NA	31.7
	IC-S	2.73	1711	1602	6	26	0.42	0.71	24.0	31.1	45.0	SC	28.5	33.5	18.9	19.1	GSCL	54	21	33	<0.001	24.9
	IC-BM	2.75	1546	1463	6	17	0.47	0.89	7.1	60.7	32.2	SC	11.9	58.3	12.3	17.5	SL	25	13	12	<0.001	30.6
	IC-C1	2.65	1050	967	8	13	0.64	1.76	3.0	27.2	69.9	CH	5.7	49.6	9.4	35.3	SL	54	21	33	<0.001	26.0
	FC	2.72	1141	1072	7	11	0.61	1.54	2.5	10.9	86.6	CH	3.1	19.7	36.3	41.0	CL	56	27	29	<0.001	24.5

[NA] Not applicable given cover type was not composed of soil
[ND] Sand cone test and analysis not conducted at this location
[1]USCS classification (4.75 mm > sand > 0.075 mm > fines), SM, SC, GM, and GC stand for Silty Sand, Clayey Sand, Silty Gravel, and Clayey Gravel
[2]USDA classification (0.05 mm > silt > 0.002 mm > clay), SL, GC, VGC stand for Silty Loam, Gravelly Clay and Very Gravelly Clay

Table 4.15 – Composite Geotechnical Properties for Covers at Potrero Hills Landfill

Season	Location	M_s (kg)	M_w (kg)	M_T (kg)	V_s (m^3)	V_w (m^3)	V_v (m^3)	V_a (m^3)	θ_s	θ_w	θ_a	Waste Age (years)	Column Height (m)
Wet	DC-AF	148.3	37.1	185.4	0.085	0.039	0.352	0.313	0.193	0.088	0.712	15.1	49.2
	DC-GW	77.0	28.5	105.4	0.058	0.023	0.463	0.440	0.112	0.045	0.846	12.7	50.2
	DC-C+D	30.7	9.2	39.9	0.025	0.011	0.185	0.174	0.121	0.053	0.827	13.3	43.9
	IC-BM	1982.5	257.7	2240.2	0.731	0.269	0.585	0.316	0.563	0.207	0.243	12.7	45.1
	IC-C1	902.2	216.5	1118.7	0.335	0.225	0.512	0.287	0.399	0.268	0.342	19.7	19.4
	FC	1741.2	296.0	2037.2	0.641	0.310	0.564	0.254	0.534	0.259	0.212	18.0	13.7
Dry	DC-AF	122.4	0.9	123.2	0.187	0.002	0.570	0.568	0.246	0.003	0.747	13.5	42.5
	DC-GW	50.8	2.0	52.9	0.044	0.002	0.267	0.264	0.143	0.007	0.853	13.2	41.4
	IC-S	4645.8	278.7	4924.5	1.715	0.317	1.218	0.901	0.592	0.109	0.311	15.1	50.1
	IC-BM	1901.9	114.1	2016.0	0.687	0.104	0.611	0.507	0.528	0.080	0.390	12.7	45.1
	IC-C1	812.3	65.0	877.3	0.305	0.070	0.538	0.468	0.364	0.083	0.557	19.7	19.4
	FC	1286.4	90.0	1376.4	0.475	0.081	0.732	0.651	0.396	0.067	0.543	18.0	13.7

Table 4.16 – Baseline Cover Geotechnical Properties for Site A Landfill

Season		Location	G_s	Moist Density (kg/m^3)	Dry Density (kg/m^3)	w (%)	S (%)	n	e	Gravel (%)[1]	Sand (%)[1]	Fines (%)[1]	Soil Classification[1]	Gravel (%)[2]	Sand (%)[2]	Clay (%)[2]	Silt (%)[2]	Soil Classification[2]	LL	PL	PI	D_{10} (mm)	Temperature (°C)
Wet		ED-II	2.72	1976	1762	12	60	0.36	0.55	20.5	33.2	46.3	SC	27.1	41.6	8.1	23.2	GSL	32	16	16	0.005	20.8
		ED-III	2.76	1980	1801	10	51	0.35	0.53	14.6	32.4	53.1	CL	17.8	44.5	11.9	25.7	GSL	36	16	20	0.001	19.9
		IC-II	2.73	1381	1101	24	45	0.59	1.46	12.7	27.8	59.5	CL	17.8	42.0	10.3	29.8	GL	33	17	16	0.002	10.3
		IC-III	2.73	1055	853	23	29	0.69	2.25	10.6	30.2	59.3	CL	12.8	36.6	32.5	18.0	CL	40	19	21	< 0.001	15.1
		AFC	2.86	1600	1438	8	32	0.50	0.96	5.1	11.3	83.6	CL	3.4	69.7	8.4	18.5	SL	31	15	16	0.003	23.7
		FC	2.78	1618	1415	15	41	0.49	0.98	1.8	15.7	82.4	CL	2.7	27.0	45.2	25.1	CL	49	22	27	< 0.001	16.8
		FC deep	ND	ND	ND	ND	ND	ND	ND	10.4	20.6	69.0	CL	16.0	21.8	24.4	37.9	CL	42	24	18	< 0.001	ND
Dry		ED-II	2.72	1645	1581	4	21	0.42	0.72	19.1	36.8	44.1	CL	28.1	39.3	10.7	21.9	GSL	38	16	22	< 0.001	24.0
		ED-III	2.76	1640	1571	4	16	0.43	0.76	22.1	34.5	43.4	SC	29.1	38.7	11.2	21.0	GSL	38	17	21	< 0.001	23.9
		IC-II	2.73	1535	1468	4	15	0.46	0.86	24.3	13.7	62.0	CL	29.7	24.2	16.3	29.9	GL	36	20	16	0.001	28.9
		IC-III	2.73	1006	963	4	6	0.65	1.85	0.2	28.7	71.1	CL	1.4	38.4	22.1	38.0	L	42	20	22	< 0.001	27.4
		IC-III deep	ND	ND	ND	ND	ND	ND	ND	22.3	34.4	43.3	SC	28.9	36.2	11.3	23.7	GL	38	19	19	0.002	ND
		AFC	2.86	1713	1631	5	19	0.43	0.75	1.4	41.0	57.5	CL	3.7	53.1	15.2	29.6	SL	33	15	18	< 0.001	29.5
		FC	2.78	1206	1155	5	9	0.59	1.41	1.7	9.2	89.1	CL	3.7	19.5	30.9	45.9	GSL	46	26	20	< 0.001	24.8

[ND] Sand cone test and analysis not conducted at this location

[1]USCS classification (4.75 mm > sand > 0.075 mm > fines), SM and SC stand for Silty Sand and Clayey Sand

[2]USDA classification (0.05 mm > silt > 0.002 mm > clay), VGCL, VGSCL, GSCL, and VGL stand for Very Gravelly Clay Loam, Very Gravelly Sandy Clay Loam, Gravelly Sandy Clay Loam, and Very Gravelly Loam

Table 4.17 – Composite Geotechnical Properties for Covers at Site A Landfill

Season	Location	M_s (kg)	M_w (kg)	M_T (kg)	V_s (m^3)	V_w (m^3)	V_v (m^3)	V_a (m^3)	θ_s	θ_w	θ_a	Waste Age (years)	Column Height (m)
Wet	ED-II	4052.6	486.3	4538.9	1.505	0.497	0.828	0.331	0.655	0.216	0.144	28.1	109
	ED-III	2503.4	250.3	2753.7	0.918	0.248	0.487	0.238	0.660	0.179	0.172	27.8	113
	IC-II	429.4	103.1	532.4	0.158	0.104	0.230	0.127	0.404	0.266	0.325	27.3	117
	IC-III	1288.0	296.2	1584.3	0.463	0.302	1.042	0.740	0.307	0.200	0.490	29.0	66.5
	AFC	1725.6	138.0	1863.6	0.625	0.192	0.600	0.408	0.521	0.160	0.340	29.0	108
	FC	2971.5	445.7	3417.2	1.050	0.422	1.029	0.607	0.500	0.201	0.289	29.0	47.6
Dry	ED-II	1581.0	63.2	1644.2	0.806	0.101	0.584	0.482	0.580	0.073	0.347	24.2	110
	ED-III	502.7	20.1	522.8	0.182	0.022	0.138	0.116	0.569	0.069	0.362	29.0	112
	IC-II	572.5	22.9	595.4	0.209	0.027	0.179	0.152	0.535	0.069	0.391	27.3	117
	IC-III	1454.1	58.2	1512.3	0.531	0.059	0.982	0.923	0.351	0.039	0.611	29.0	66.5
	AFC	1988.2	99.4	2087.6	0.695	0.099	0.523	0.425	0.573	0.082	0.348	29.0	108.0
	FC	2425.5	121.3	2546.8	0.879	0.112	1.239	1.127	0.418	0.053	0.537	29.0	47.6

Table 4.18 – Baseline Cover Geotechnical Properties for Chiquita Canyon Landfill

Season	Location	G_s	Moist Density (kg/m^3)	Dry Density (kg/m^3)	w (%)	S (%)	n	e	Gravel (%)[1]	Sand (%)[1]	Fines (%)[1]	Soil Classification[1]	Gravel (%)[2]	Sand (%)[2]	Clay (%)[2]	Silt (%)[2]	Soil Classification[2]	LL	PL	PI	D_{10} (mm)	Temperature (°C)
Wet	DC-Cl	2.44	1116	1069	7	14	0.57	1.3	24.9	50.0	39.8	SC	29.2	54.4	3.6	12.8	GSL	36	21	15	0.047	22.9
	DC-Co	2.69	1671	1515	10	35	0.43	0.78	8.4	57.1	34.5	SC-SM	12.4	65.7	5.1	16.8	LS	25	19	6	0.028	22.8
	IC-S	2.76	1427	1369	4	11	0.51	1	4.0	51.8	44.2	SC	7.6	66.1	6.1	20.2	SL	29	19	10	0.011	18.4
	IC-W	2.72	1500	1415	6	17	0.47	0.93	2.6	44.9	52.5	CL	6.1	58.2	8.6	27.1	SL	31	18	13	0.004	20.4
	IC-OGW	2.12	334	267	27	9	0.87	7	NA	NA	NA	NA	NA	NA	NA	NA	NA	NA	NA	NA	NA	41.6
	IC-NGW	1.65	153	106	62	6	0.95	16	NA	NA	NA	NA	NA	NA	NA	NA	NA	NA	NA	NA	NA	39.6
	FC	2.73	1172	1143	3	5	0.58	1.4	4.2	55.8	40.0	SC	8.6	66.0	5.1	20.4	SL	32	21	11	0.018	23.4
Dry	DC-Cl	2.44	1481	1428	3	13	0.42	0.71	18.3	48.8	32.9	SC	16.2	66.4	1.4	15.9	GLS	27	20	7	0.003	32.5
	DC-Co	2.69	1414	1378	3	7	0.49	0.96	5.1	84.6	10.3	SP-SM	28.0	48.3	9.5	14.2	GSL	NP	NP	NP	0.074	36.4
	IC-S	2.76	1581	1551	3	7	0.46	0.8	10.3	50.3	39.4	SC	13.3	60.5	5.4	20.8	SL	29	18	11	0.011	33.4
	IC-W	2.72	1276	1238	3	7	0.55	1.21	14.0	46.7	39.3	SC	17.4	56.5	5.4	20.7	GSL	28	18	10	0.011	33.0
	IC-OGW	2.12	400	383	4	2	0.82	4.52	NA	NA	NA	NA	NA	NA	NA	NA	NA	NA	NA	NA	NA	45.7
	IC-NGW	1.65	317	307	5	2	0.81	4.47	NA	NA	NA	NA	NA	NA	NA	NA	NA	NA	NA	NA	NA	37.3
	FC	2.73	1432	1414	1	4	0.48	0.93	3.8	57.3	38.9	SC	8.5	66.8	4.9	19.8	SL	27	19	8	0.018	41.1

NA Not applicable given cover type was not composed of soil

[1]USCS classification (4.75 mm > sand > 0.075 mm > fines), SM and SC stand for Silty Sand and Clayey Sand

[2]USDA classification (0.05 mm > silt > 0.002 mm > clay), GSL and VGSL stand for Gravelly Sandy Loam and Very Gravelly Sandy Loam

Table 4.19 – Composite Geotechnical Properties for Covers at Chiquita Canyon Landfill

Season	Location	M_s (kg)	M_w (kg)	M_T (kg)	V_s (m^3)	V_w (m^3)	V_v (m^3)	V_a (m^3)	θ_s	θ_w	θ_a	Waste Age (years)	Column Height (m)
Wet	DC-Cl	363.5	25.4	388.9	0.149	0.027	0.194	0.167	0.438	0.080	0.490	26.3	108
	DC-Co	757.5	75.8	833.3	0.276	0.075	0.215	0.140	0.551	0.151	0.280	24.2	111
	IC-S	410.7	16.4	427.1	0.153	0.017	0.153	0.136	0.510	0.056	0.454	21.6	92
	IC-W	566.0	34.0	600.0	0.202	0.032	0.188	0.156	0.505	0.080	0.390	26.3	105
	IC-OGW	173.6	46.9	220.4	0.081	0.051	0.566	0.515	0.124	0.078	0.792	27.2	79
	IC-NGW	103.9	64.4	168.3	0.058	0.056	0.931	0.875	0.059	0.057	0.893	20.9	97
	FC	1714.5	51.4	1765.9	0.621	0.044	0.870	0.827	0.414	0.029	0.551	27.6	75
Dry	DC-Cl	485.5	14.6	500.1	0.201	0.019	0.143	0.124	0.592	0.055	0.365	23.8	107
	DC-Co	689.0	20.7	709.7	0.255	0.017	0.245	0.228	0.510	0.034	0.456	24.0	109
	IC-S	465.3	14.0	479.3	0.173	0.010	0.138	0.128	0.575	0.032	0.428	21.6	92
	IC-W	495.2	14.9	510.1	0.182	0.015	0.220	0.205	0.455	0.039	0.512	26.3	105
	IC-OGW	249.0	10.0	258.9	0.118	0.011	0.533	0.522	0.181	0.016	0.804	27.2	79
	IC-NGW	300.9	15.0	315.9	0.178	0.016	0.794	0.778	0.181	0.016	0.794	20.9	97
	FC	2121.0	21.2	2142.2	0.774	0.029	0.720	0.691	0.516	0.019	0.461	27.6	75

4.8 Correlation Analyses

The presence of correlations a) between measured geotechnical index properties of covers and LFG fluxes, b) between site-specific operational conditions and whole-site LFG emissions, and c) between gas-specific physico-chemical properties and LFG fluxes were assessed for the 5 selected landfills for ground-based testing. Correlations were quantified through application of Spearman's ρ to describe any monotonic (increasing or decreasing), non-specific relationships between measured LFG fluxes/emissions and associated cover conditions, site operational conditions, and physico-chemical properties. Use of Spearman's ρ makes no assumptions about the linearity of the correlations present and is an appropriate metric to apply in exploratory applications in which the strength of different correlations is relatively unknown. In this section, correlation results are first presented through heatmaps, which combine results from all sites and seasons, where results are separated according to (in cases a and c) soil materials versus non-soil materials. In addition, boxplot summaries of ρ values are provided to compare the strength and directions (i.e., positive or negative) of different correlations developed between LFG fluxes and emissions as well as cover geotechnical properties, site operational conditions, or physical-chemical properties. Finally, individual properties or conditions that are determined to be best correlated with fluxes or emissions are plotted independently to assess the specific correlations.

4.8.1 Correlations Between Site-Specific Cover Geotechnical Properties and Fluxes: Dry Season Results

Figure 4.72 summarizes the distributions in Spearman's ρ differentiating between both positive and negative correlations for all correlations between flux and a) soil and b) alternative cover material geotechnical index properties. Regarding correlations between flux and geotechnical soil properties, the range of median ρ values for positive and negative correlations was 0.09 to 0.32 and -0.09 to -0.29, respectively. On average, positive correlations were greatest for silt content, followed by temperature, and degree of saturation. Similarly, negative correlations were greatest for mass of solids (M_s), followed by total mass (M_T) and the mass of water (M_w). The variation in positive and negative ρ values, as indicated by the IQR and IWR values, was generally highest for temperature and mass of solids, respectively.

The range in median ρ values describing correlations between flux and geotechnical index properties alternative cover material was generally higher than that observed for soil properties, ranging from 0.12 to 0.27 and -0.17 to -0.47 for positive and negative correlations, respectively (Figure 4.72). On average, positive correlations were greatest for volumetric water content, gravimetric water content, and specific gravity of the cover materials. Similarly, negative correlations were greatest for degree of saturation, followed by volumetric water content, and specific gravity of the cover materials. The variation in positive and negative ρ values, as indicated by the IQR and IWR values, was generally highest for gravimetric water content and degree of saturation, respectively.

Figure 4.72 Distributions of Spearman's ρ (both positive and negative correlations) Describing Correlations between Geotechnical a) Soil and b) Alternative Cover Material Properties and Measured Fluxes for the Dry Season across all Landfill Sites and Cover Categories.

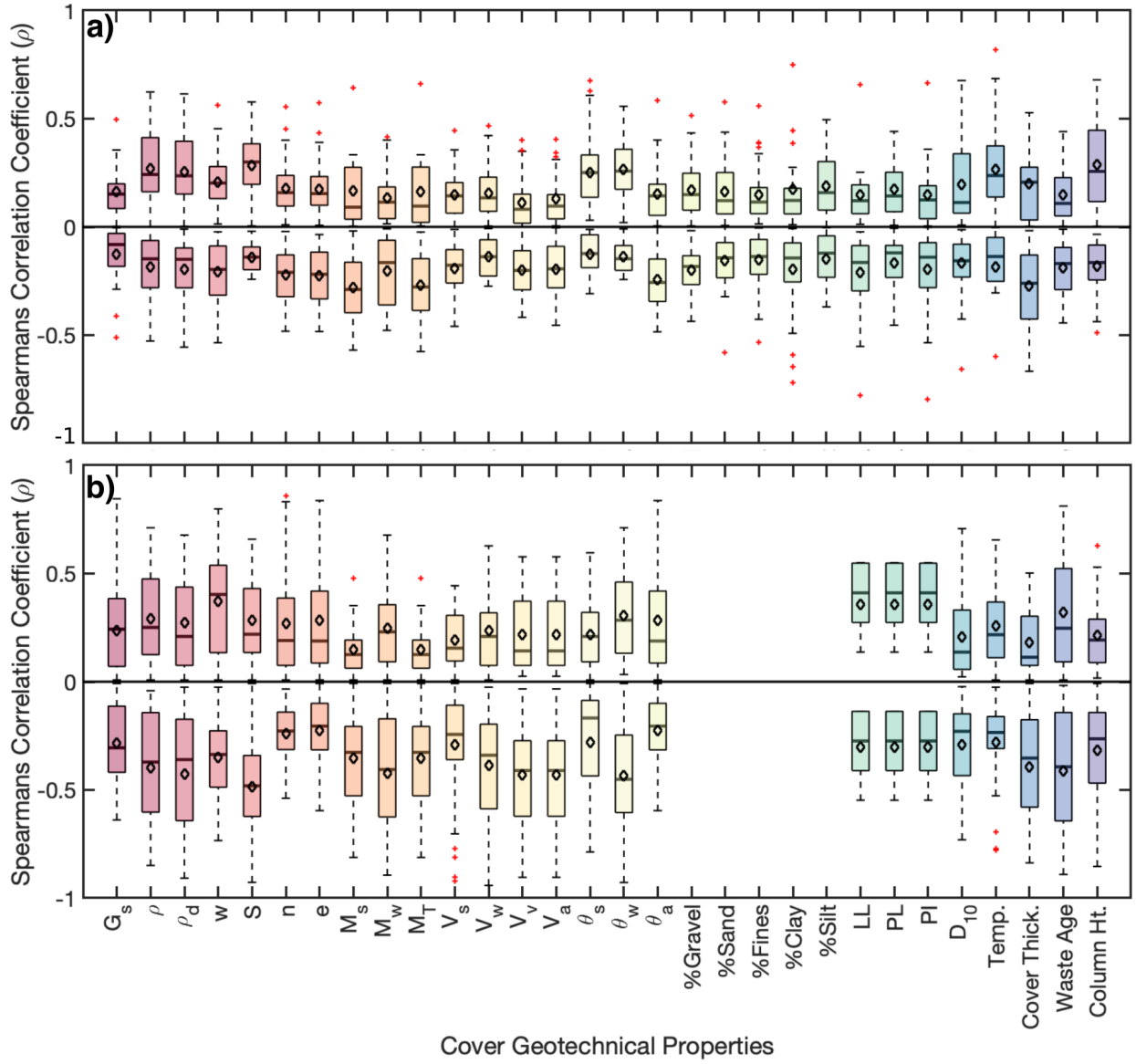

The strength and direction of non-linear correlations evaluated between cover geotechnical index properties and measured fluxes was presented as a function of chemical family in heatmap format (Figures 4.73 and 4.74). Results presented in both figures depict stronger and weaker correlations as darker red/purple and lighter blue shading. The direction of correlations (positive or negative) are indicated by the presence or absence of a down arrow to indicate negative. Correlations between flux and soil or alternative cover materials are presented in Figures 4.73 and 4.74, respectively, where the median of the Spearman's correlation coefficients of all chemicals within a given family is presented. Regarding correlations between flux and

cover geotechnical soil properties, there was a general dearth of strong correlations ($\rho > 0.5$) observed, as indicated by the lack of yellow to red coloring on the heatmap. The majority of the coloring on the heatmap ranges from light blue to dark blue, indicating moderate, non-linear correlations ($0.3 < \rho < 0.5$) were observed between select geotechnical properties and several chemical families. In general, the monoterpenes, ketones, GHGs and organic alkyl nitrates demonstrated the greatest number and magnitude of moderate to strong non-linear correlations out of the chemical families reviewed (Figure 4.73). Based on results presented in the heatmap, correlations were generally strongest for M_s, M_T, V_s, V_v, V_a, silt content, and temperature. In addition, the direction of the correlation for these moderate to strong correlations was mostly negative, with the exception of silt content and temperature of the tested materials.

Results presented in Figure 4.74 indicated that there were more moderate to strong correlations observed between flux and alternative cover material geotechnical index properties as compared to soil geotechnical index properties. In select cases, strong correlations were observed, with median values for certain chemical families on the order of 0.80 (negative direction). The alcohols, monoterpenes, and aromatics were generally associated with the greatest number and magnitude of moderate to strong correlations (Figure 4.74). Specific gravity, dry and wet densities, porosity, void ration, mass of solids, volume of solids, volume of voids, volume of air, and temperature were the geotechnical properties demonstrating the strongest degree of correlation across all chemical families. Similar to results obtained for the soil properties, the majority of these moderate to strong correlations were negative, aside from temperature, porosity, void ratio, and specific gravity (Figure 4.74).

The relative shape and statistical dependency of the strongest non-linear correlations observed between flux and soil/alternative cover geotechnical index properties is examined in further detail in Figures 4.75 and 4.76. In both Figures, the flux is plotted as a function of the cover properties showing the highest a) positive and b) negative strength of correlation. When all of the chemical species within the chemical family associated with the highest mean ρ values are plotted together, a fair amount of scatter was observed (Figures 4.75 and 4.76). However, when flux is plotted on a logarithmic scale, the trends are readily apparent. In general, the negative correlations observed in Figure 4.75b are more discernible than the positive correlations presented in Figure 4.75a.

Figure 4.73 Strength and Direction of Non-linear Correlations between Cover Soil Geotechnical Properties and Measured Fluxes for the Dry Season across all Landfills, Cover Categories, and Cover Soil Types. Median Values of Spearman's Correlation Coefficient are Presented by Chemical Family (black triangle indicates negative correlations and color bar represents the magnitude of Spearman's correlation coefficient).

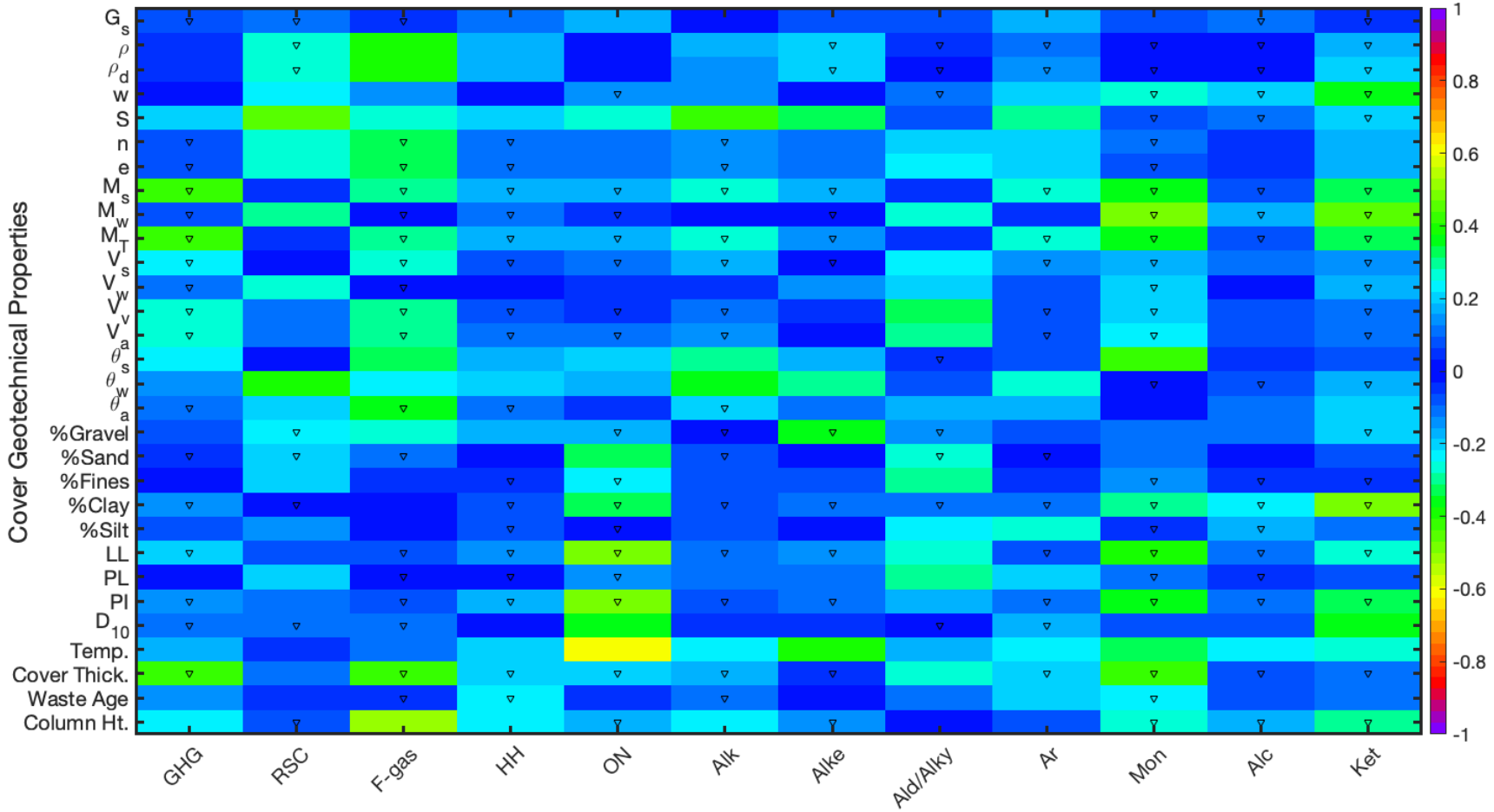

Figure 4.74 Strength and Direction of Non-linear Correlations between Alternative Cover Material Geotechnical Properties and Measured Fluxes for the Dry Season across all Landfills, Cover Categories, and Alternative Cover Types. Median Values of Spearman's Correlation Coefficient are Presented by Chemical Family (black triangle indicates negative correlations and color bar represents the magnitude of Spearman's correlation coefficient).

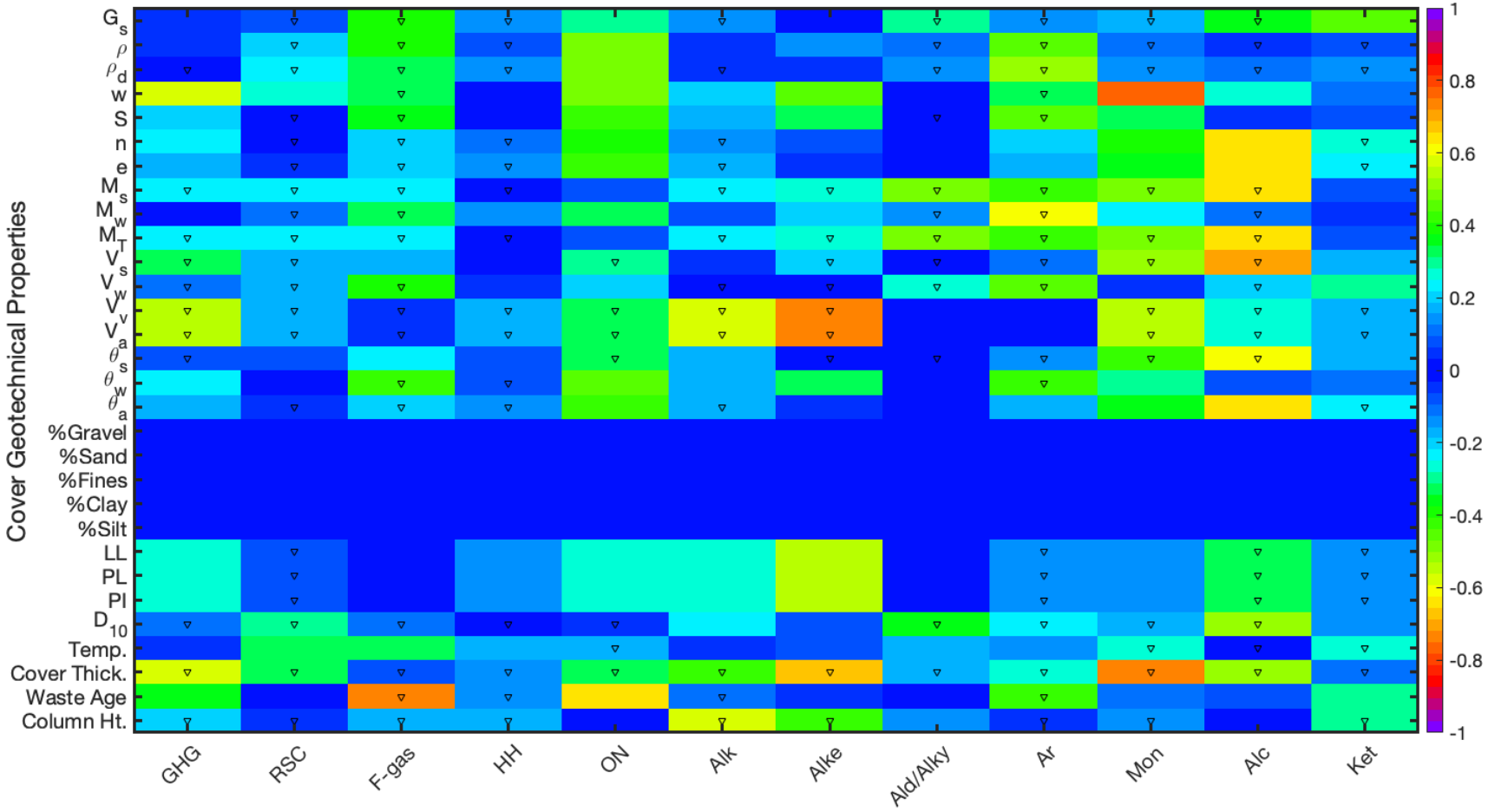

Figure 4.75 Summary of the Strongest Three (from left to right) a) Positive and b) Negative Correlations Observed Between Flux and Cover Soil Geotechnical Properties in the Dry Season. Results are Plotted for all Chemical Species within a Given Family, Differentiated by Color (negative fluxes are omitted since the y-axis is logarithmic scaling).

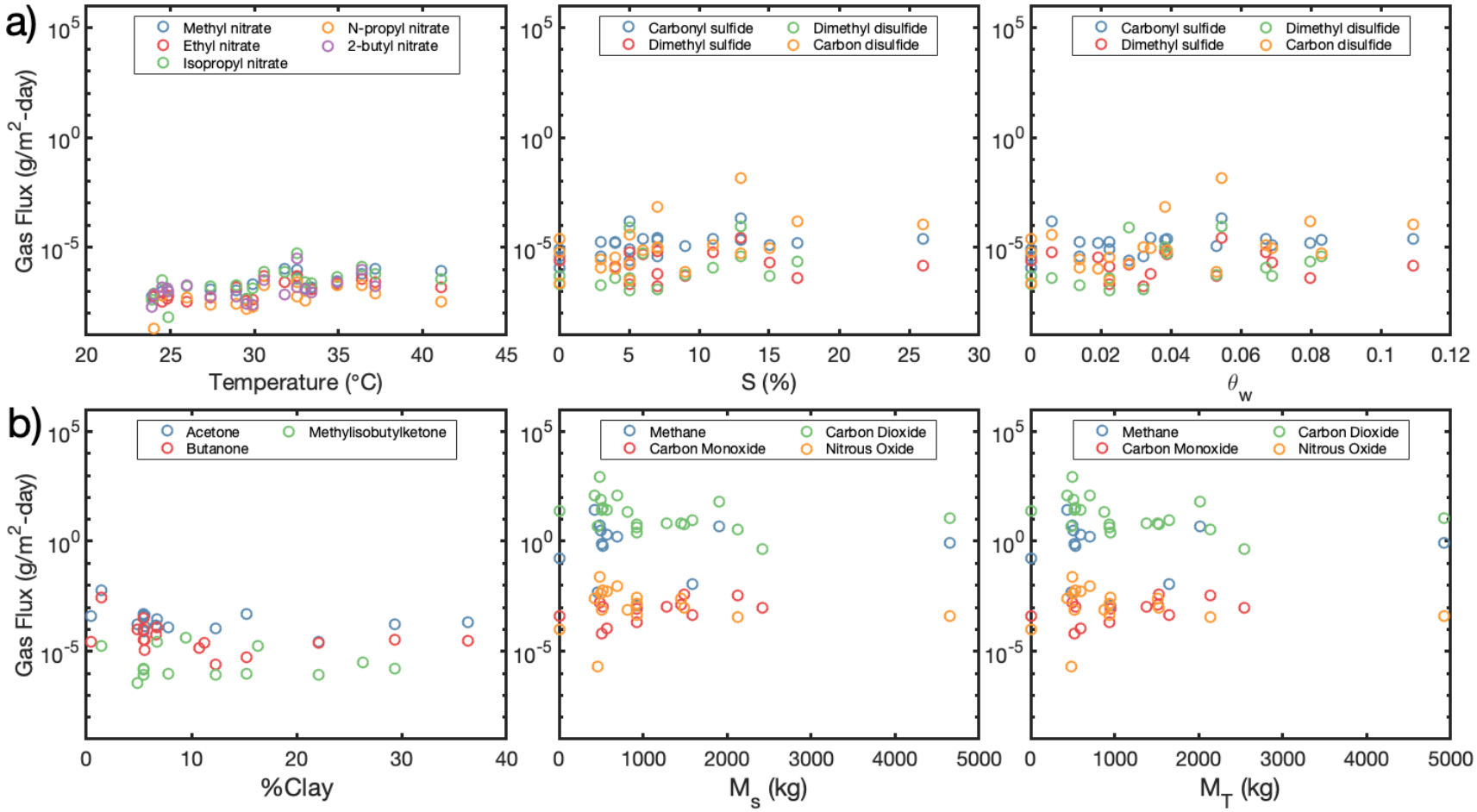

Figure 4.76 Summary of the Strongest Three (from left to right) a) Positive and b) Negative Correlations Observed between Flux and Alternative Cover Material Geotechnical Properties in the Dry Season. Results are Plotted for all Chemical Species within a Given Family, Differentiated by Color (negative fluxes are omitted since the y-axis is logarithmic scaling).

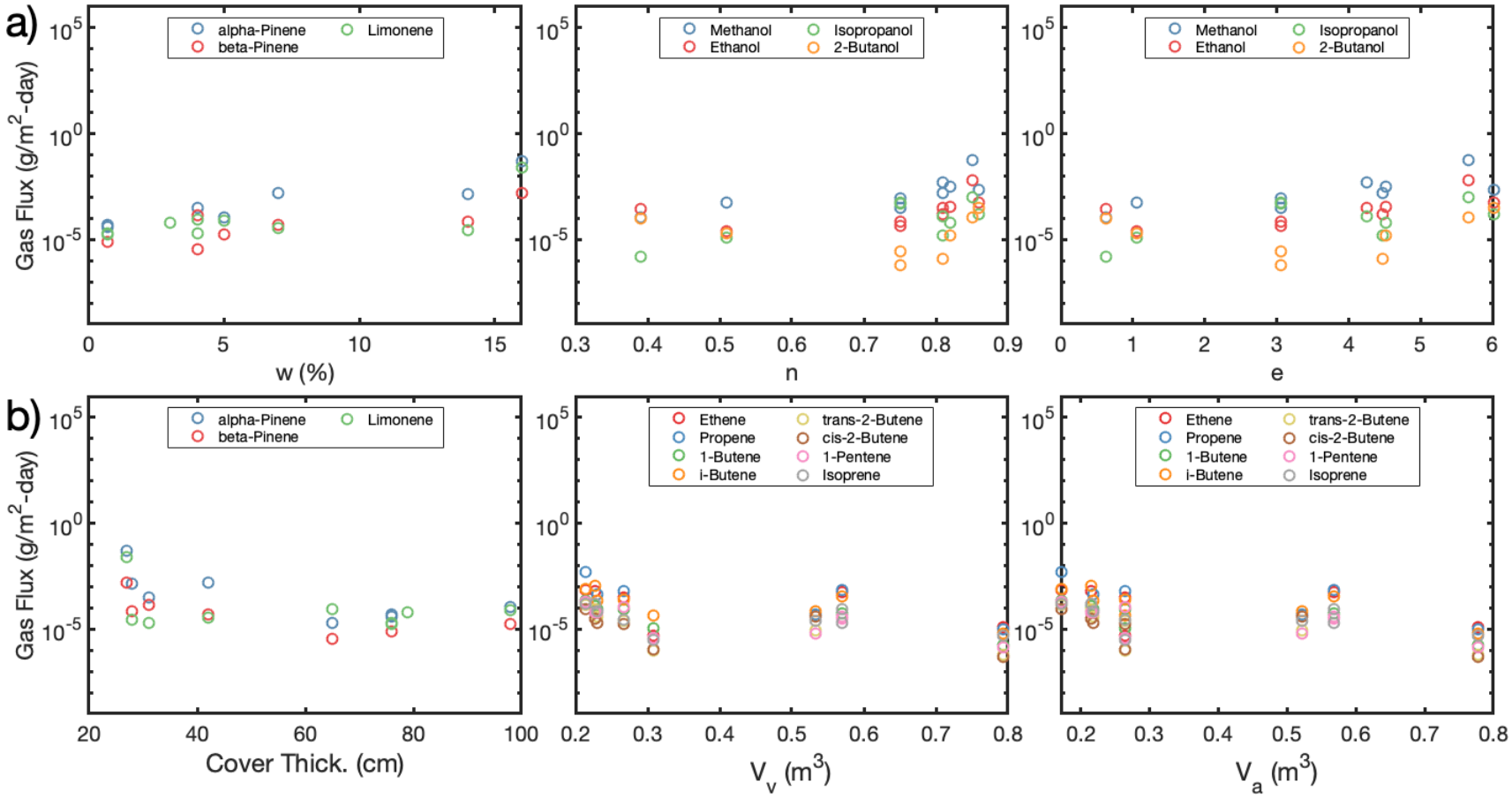

4.8.2 Summary of Correlations Between Site-Specific Cover Geotechnical Properties and Fluxes: Wet Season Results

The distributions in Spearman's ρ for both positive and negative correlations between flux and a) soil and b) alternative cover material geotechnical properties are presented in Figure 4.77. Regarding correlations between flux and soil geotechnical properties, the range in median ρ values for positive and negative correlations was 0.04 to 0.24 and -0.11 to -0.37, respectively. Positive correlations were greatest for silt content, followed by temperature, and dry density (ρ_d). Negative correlations were greatest for mass of solids (M_s), followed by volume of air (V_a) and total mass of solids and water (M_T). The variation in positive and negative ρ values, as indicated by the IQR and IWR values, was generally highest for temperature and water content, respectively.

The range in median ρ values describing correlations between flux and alternative cover geotechnical index properties was generally higher than that observed for soil properties, ranging from 0.15 to 0.60 and -0.20 to -0.55 for positive and negative correlations, respectively (Figure 4.77b). On average, positive correlations were greatest for temperature, specific gravity (G_s), and volumetric air content (θ_a) of the cover materials. In contrast, negative correlations were greatest for mass of solids (M_s), followed by total mass (M_T), and specific gravity (G_s). The variation in positive and negative ρ values, as indicated by the IQR and IWR values, was generally highest for porosity/void ratio and specific gravity, respectively.

For the wet season, the strength and direction of non-linear correlations evaluated between cover geotechnical index properties and measured fluxes was presented as a function of chemical family in heatmap format (Figures 4.78 and 4.79). Similar to dry season, moderate, non-linear correlations ($0.3 < \rho < 0.5$) were observed between select geotechnical index properties and flux for several chemical families, as indicated by the light green to dark green coloring. In general, the F-gases, halogenated hydrocarbons, alkanes, and alkenes demonstrated the greatest number and magnitude of moderate to strong non-linear correlations (Figure 4.78). This result is distinctly different than the dry season, where the alcohols, ketones, and monoterpenes were associated with the highest number and magnitude of correlations. Based on results presented in the heatmap, correlations were generally strongest for the composite properties including M_s, M_T, V_s, V_v, V_a and, in some cases, silt content, and temperature. In addition, the direction of the correlation for these moderate to strong correlations was mostly negative, with the exceptions of silt content and temperature (Figure 4.78).

Figure 4.77 Distributions of Spearman's ρ (both positive and negative correlations) Describing Correlations between Geotechnical a) Soil and b) Alternative Cover Material Properties and Measured Fluxes for the Wet Season across all Landfill Sites and Cover Categories.

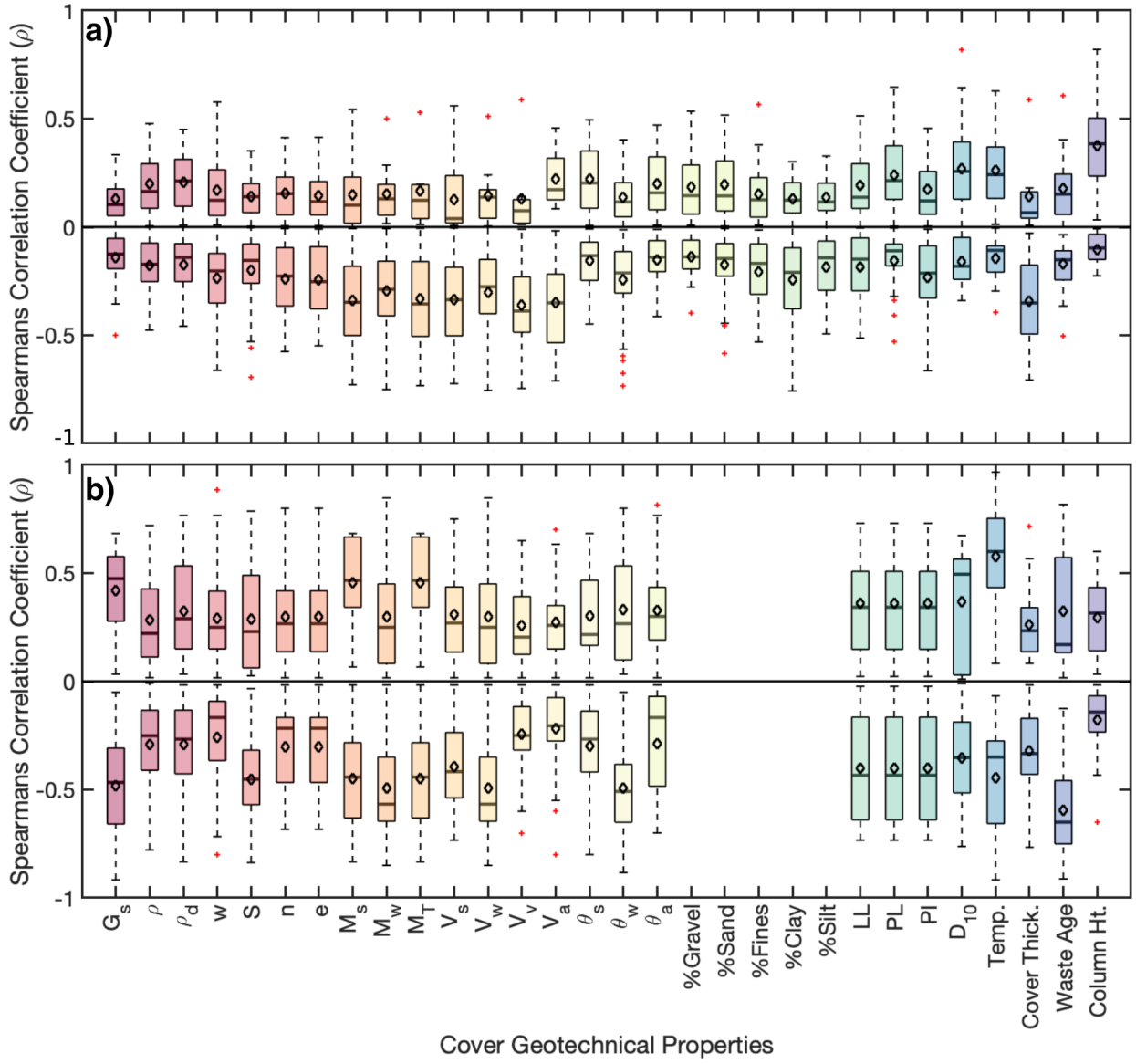

Results presented in Figure 4.79 indicated that there were more moderate to strong correlations observed between flux and alternative cover material geotechnical index properties than for soils , in line with results obtained from the dry season. In select cases, there were very strong correlations observed, with median values for certain chemical families on the order of 0.80-0.90 (G_s and temperature for the monoterpenes). Unlike the soil cover results, the monoterpenes, greenhouse gases, and organic alkyl nitrates were generally associated with the greatest number and magnitude of moderate to strong correlations (Figure 4.79). Specific gravity, dry and moist densities, mass of solids, water-filled porosity, and temperature were the geotechnical properties

demonstrating the strongest degree of correlation across the chemical families reviewed. Similar to results obtained for the soil properties, the majority of these moderate to strong correlations were negative, aside from temperature (Figure 4.79). Compared to the soil properties in Figure 4.78, there were more positive, moderate strength correlations observed across chemical families, particularly for porosity, void ratio, water content, and volumetric air content.

The relative shape and statistical dependency of the strongest non-linear correlations observed between flux and soil/alternative cover geotechnical index properties is examined in further detail in Figures 4.80 and 4.81. In both Figures, the flux is plotted as a function of the cover properties showing the highest a) positive and b) negative strength of correlation. A fair amount of scatter was observed when all of the chemical species within the chemical family associated with the highest mean ρ values are plotted together (Figures 4.80 and 4.81). The alcohol and organic alkyl nitrates were generally associated with the strongest positive median correlation values.

Figure 4.78 Strength and Direction of Non-linear Correlations between Cover Soil Geotechnical Properties and Measured Fluxes for the Wet Season across all Landfills, Cover Categories, and Cover Soil Types. Median values of Spearman's Correlation Coefficient are Presented by Chemical Family (black triangle indicates negative correlations and color bar represents the magnitude of Spearman's correlation coefficient).

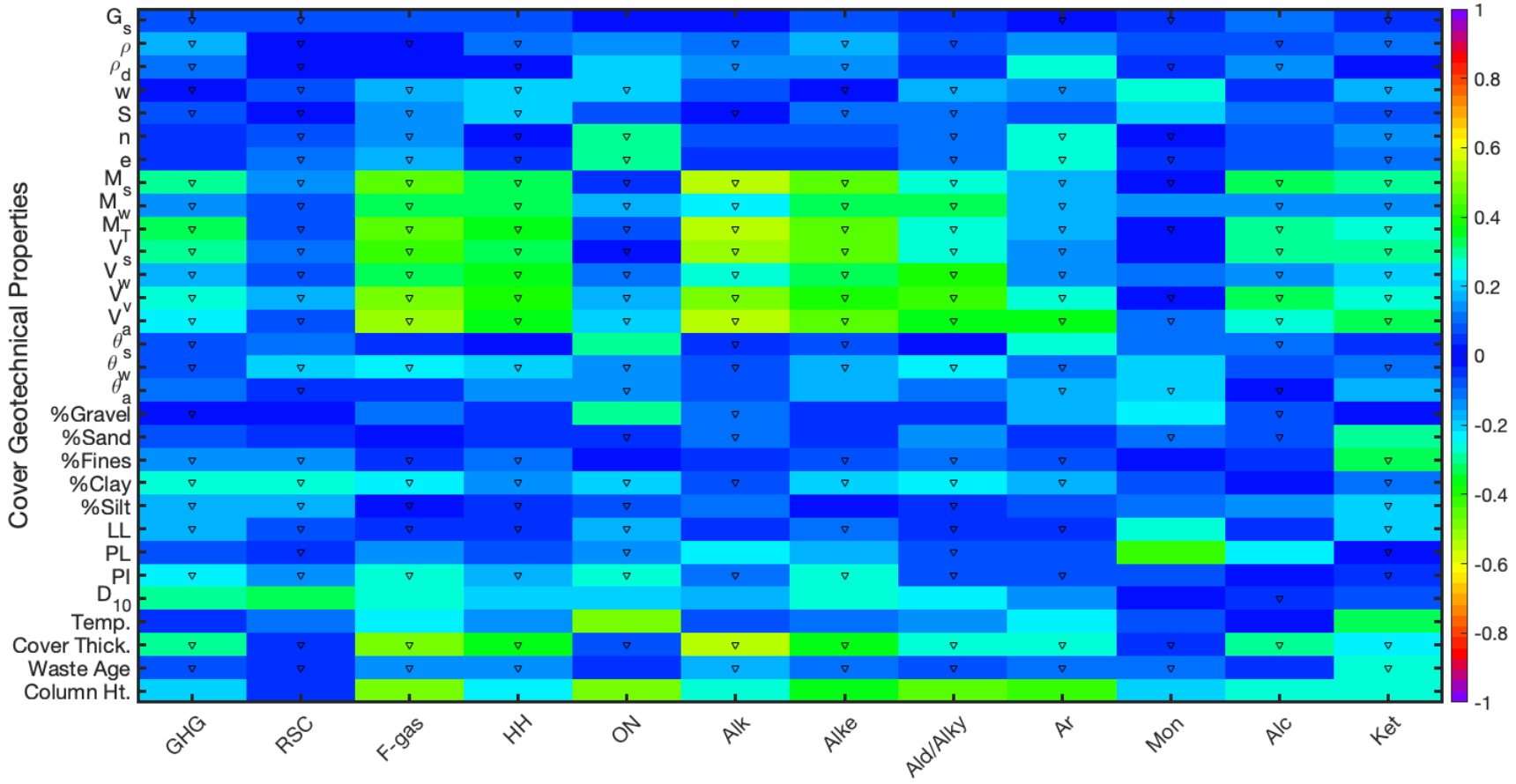

Figure 4.79 Strength and Direction of Non-linear Correlations between Alternative Cover Material Geotechnical Properties and Measured Fluxes for the Wet Season across all Landfills, Cover Categories, and Alternative Cover Types. Median values of Spearman's Correlation Coefficient are Presented by Chemical Family (black triangle indicates negative correlations and color bar represents the magnitude of Spearman's correlation coefficient.

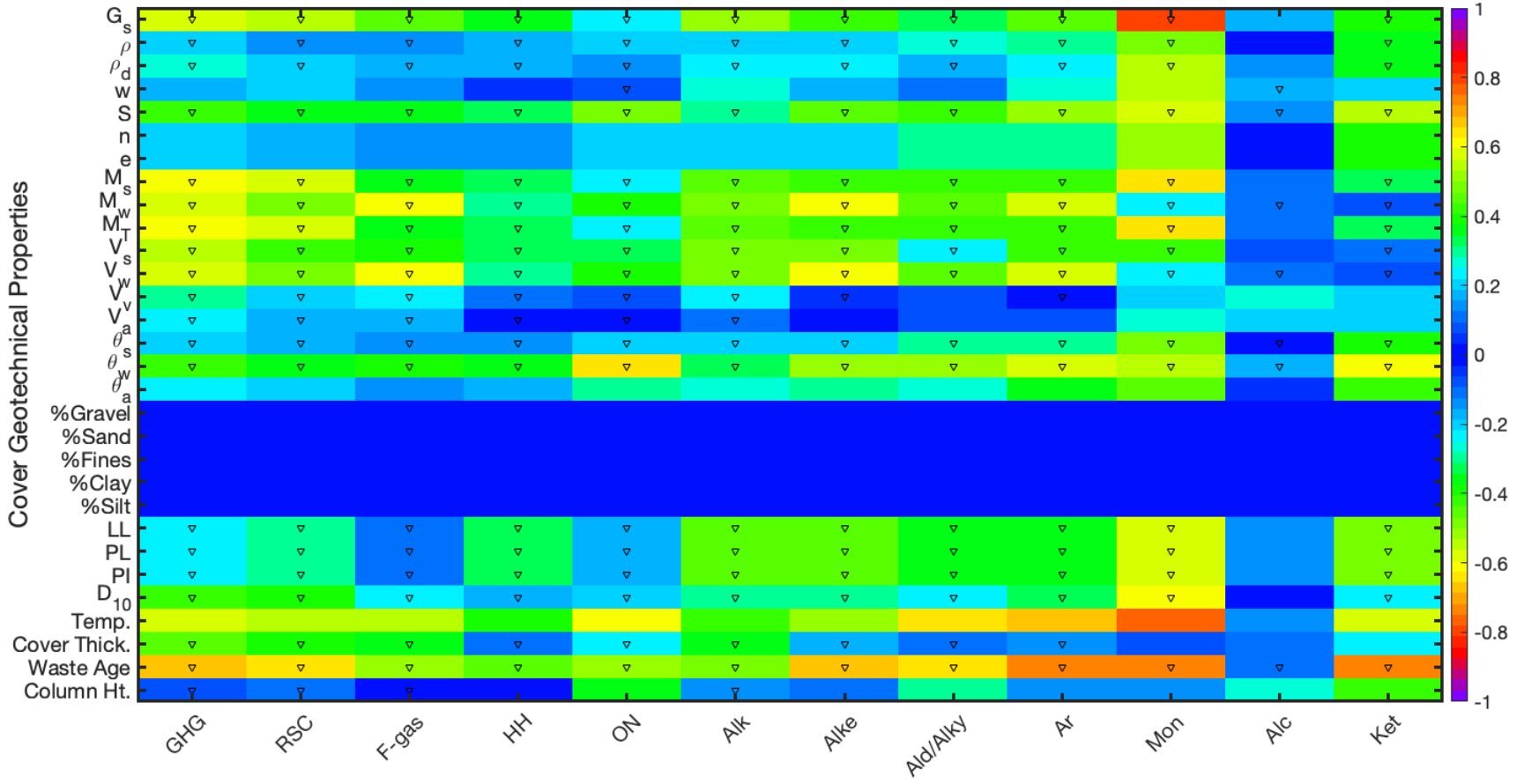

Figure 4.80 Summary of the Three Strongest (from left to right) a) Positive and b) Negative Correlations Observed between Flux and Cover Soil Geotechnical Properties in the Wet Season. Results are Plotted for all Chemical Species within a Given Family, Differentiated by Color (negative fluxes are omitted since the y-axis is logarithmic scaling).

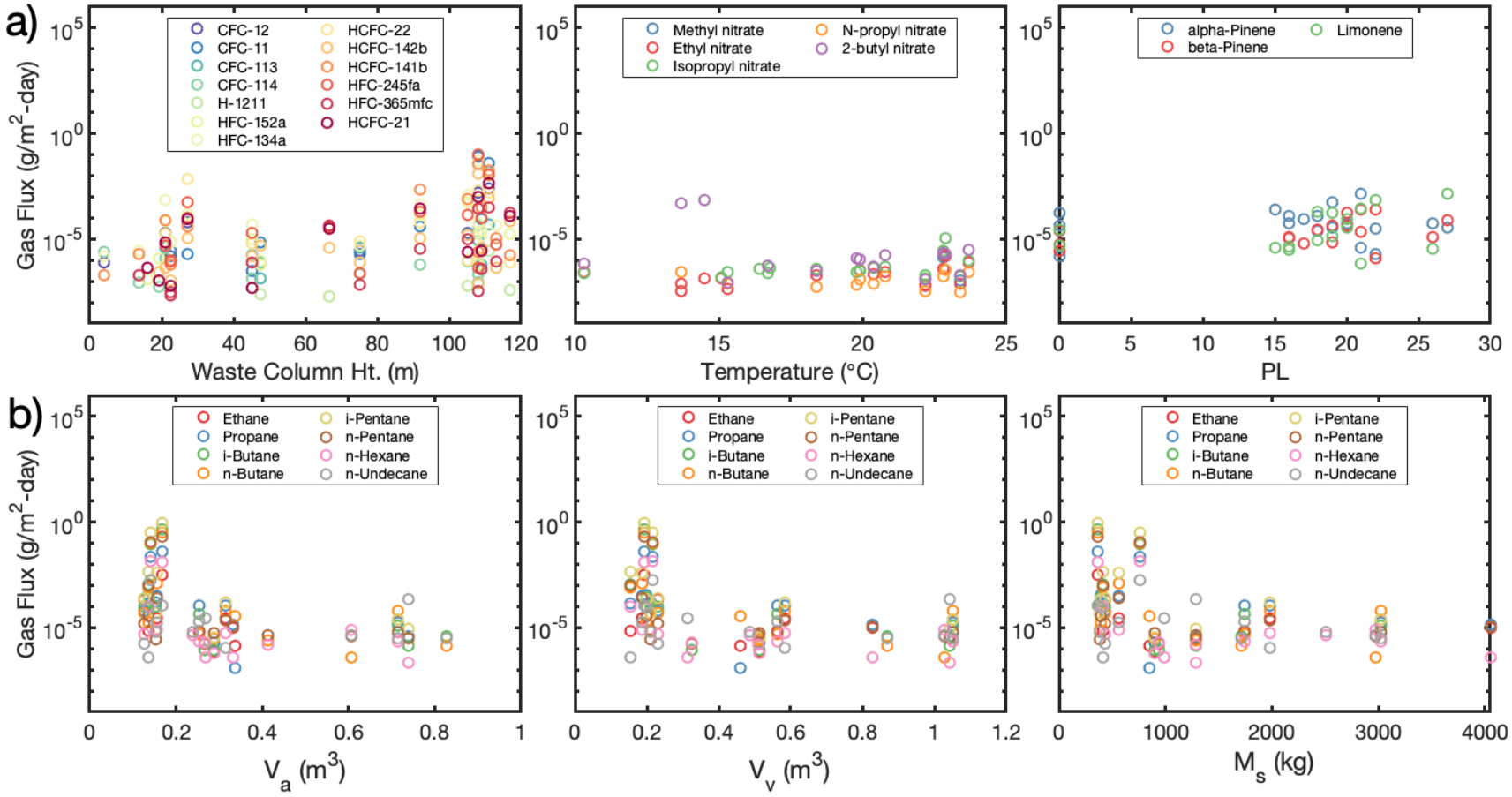

Figure 4.81 Summary of the Three Strongest (from left to right) a) Positive and b) Negative Correlations Observed between Flux and Alternative Cover Material Geotechnical Properties in the Wet Season. Results are Plotted for all Chemical Species within a Given Family, Differentiated by Color (negative fluxes are omitted since the y-axis is logarithmic scaling).

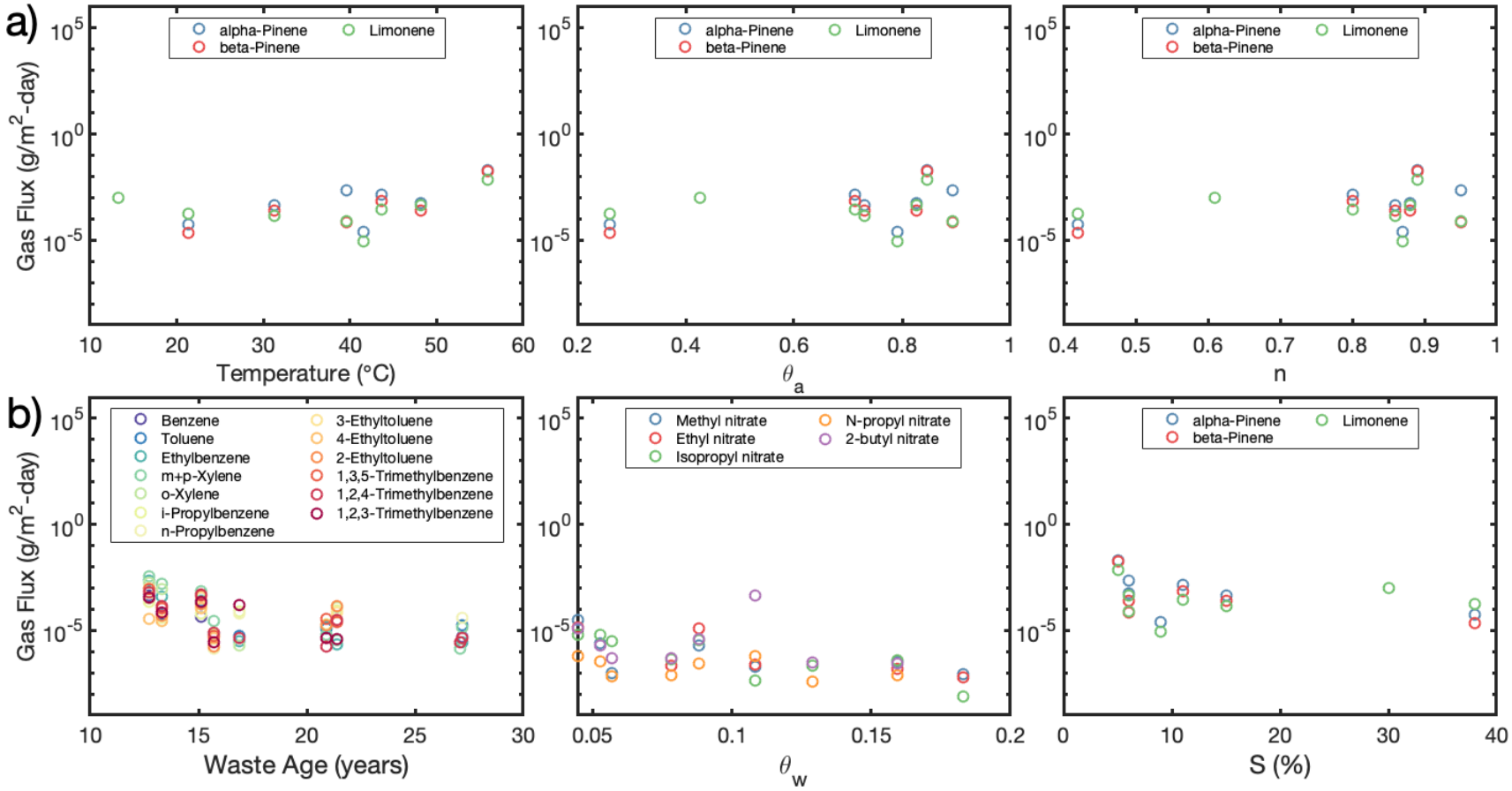

4.8.3 Summary of Correlations Between Site-Specific Operational Conditions and Whole-Site Emissions

Calculated annual whole-site emissions of methane and total LFG (combining all 82 chemicals) were correlated with fourteen different site-specific operational conditions. For sites in which aerial testing was conducted, the most recent average volumetric methane concentration reported in the recent CARB inventory of LFG extraction systems was used to convert methane to LFG. Correlations were conducted using direct whole-site emissions only. The site-specific operational conditions evaluated included total WIP (tonnes), average waste depth for the site (m), waste throughput (tonnes/day), areal coverage (m^2), fractions of daily, intermediate and final cover (%), area of the active face (m^2), annual LFG collected (m^3), average LFG flow rate (m^3/min), measured and modeled collection efficiencies (%), fraction of biodegradable waste materials (%, B_0), and the age of the landfill (years). In addition, site specific climatic conditions including annual precipitation (mm) and daily average temperature (°C) were analyzed.

Waste depth, waste throughput, areal coverage, fractions of daily, intermediate, and final cover, active face area, average LFG flow rate, and site age were reported by landfill operational staff from an initial survey of landfill characteristics, summarized in Section 2, and represent recent site conditions (2017-2019). WIP was determined from site records. The LFG collected (year 2018) was obtained from the latest CARB statewide inventory conducted on LFG collection systems. Modeled LFG collection efficiencies were obtained based on methodology described in Section 3.8, using default and refined estimates of LandGEM parameter values. Climatic data was summarized from 30-year averages (Andersland and Ladanyi 1994) collected from the nearest monitoring station and downloaded from the NOAA online database. Lastly, B_0 values were predicted for each landfill jurisdiction using CalRecycle's online web application, as reviewed in Section 4.8.

Non-linear correlation coefficients determined between landfill characteristics and direct emissions of methane or total LFG are summarized in Table 4.18. In aerial measurements, strong correlations (0.73 to 0.84) were observed between emissions and WIP, waste throughput, areal coverage, and waste depth for methane. The strong correlations were all positive, indicating that emissions are expected to increase with the scale of landfill operations. In ground measurements, strong correlations were observed between emissions and the individual cover areas for methane. The correlations were positive or daily and intermediate covers, indicating increases in methane emissions with increases in the areas of these covers, whereas the highly negative (-0.9) correlation for final covers indicate decreases in methane emissions with increasing final cover area. Final covers are critical for decreasing emissions from landfill facilities over all time frames, with particular significance for the long-term during closure and post closure. In ground measurements, strong negative correlations (-0.9) were observed between emissions and site age and measured collection efficiency and positive correlation (0.7) for waste column height for methane.

The correlations for total LFG (without CO_2 and CO) were controlled by methane and were essentially the same as the data for methane emissions. For total LFG with all four GHGs, the highest correlations were positive and with areal coverage, waste throughput, and waste column height and modest correlations were with WIP, waste depth, site age, precipitation, and modeled collection efficiency. Active face area was moderately correlated to aerial methane and total LFG (with CO_2 and CO) emissions. Both aerial methane and total LFG (with CO_2 and CO) emissions were moderately positively correlated to LFG collected. Measured waste column height was the only parameter that was strongly correlated to all emissions. Graphical representations for the strongly correlated parameters are provided in Figures 4.82 and 4.83.

Aerial methane measurements were mainly sensitive to landfill size characteristics. These measurements did not correlate to specific cover characteristics, climatic conditions, gas collection efficiencies, or landfill organics content or age. Ground methane measurements were strongly correlated to extent of individual cover categories and also correlated to collection efficiencies. These measurements were not highly sensitive to landfill size and climatic conditions. Total LFG emissions were mainly correlated to size parameters and somewhat correlated to collection efficiency. The active face size moderately affected aerial and total LFG emissions.

Table 4.20 – Summary of Correlations between Site-Specific Operational Conditions and Direct Emissions of Methane and Total LFG

Landfill Characteristics and Operational Conditions	Spearman's Correlation Coefficient (ρ) for Methane [Aerial, 15 sites]	Spearman's Correlation Coefficient (ρ) for Methane [Ground, 5 sites]	Spearman's Correlation Coefficient (ρ) for Total LFG [Ground, 5 sites]	
			With CO_2/CO	Without CO_2/CO
WIP (tonnes)	0.838	0.100	0.700	0.100
Waste Depth (m)	0.732	0.200	0.600	0.200
Waste Throughput (tonnes/day)	0.794	0.300	0.900	0.300
Areal Coverage (m^2)	0.753	0.600	1.000	0.600
B_0 (%)	-0.141	-0.600	-0.200	-0.600
Site Age (years)	-0.202	-0.900	-0.700	-0.900
% Daily Cover	-0.100	0.500	0.300	0.500
% Interim Cover	0.291	0.800	0.400	0.800
% Final Cover	-0.350	-0.900	-0.300	-0.900
Active Face (m^2)	0.674	0.200	0.600	0.200
Net Precipitation (mm)	-0.018	0.051	0.564	0.051
Average Daily Temperature (°C)	0.229	0.300	0.500	0.300
LFG Collected (m^3)	0.697	-0.200	0.600	-0.200
LFG Flow Rate (m^3/min)	0.394	-0.100	0.500	-0.100

Landfill Characteristics and Operational Conditions	Spearman's Correlation Coefficient (ρ) for Methane [Aerial, 15 sites]	Spearman's Correlation Coefficient (ρ) for Methane [Ground, 5 sites]	Spearman's Correlation Coefficient (ρ) for Total LFG [Ground, 5 sites]	
			With CO_2/CO	Without CO_2/CO
Measured Collection Efficiency (%)	-0.212	-0.900	-0.300	-0.900
Modeled Collection Efficiency – Default Parameters (%)	-0.103	-0.200	0.600	-0.200
Modeled Collection Efficiency – Refined Parameters (%)	0.067	-0.600	0.200	-0.600
Average Measured Waste Age (years)	0.300	0.500	-0.100	0.500
Average Measured Waste Column Height (m)	1.000	0.700	0.900	0.700

Figure 4.82 Summary of the Strongest Six (from left to right, top to bottom) Correlations Observed between Site-Specific Operational Practices and Direct Methane Emissions Measured from Aerial Testing. Results are Plotted for all Landfills and are Differentiated by Color (dashed line represents 1:1 log scaling and best fit line for positive and negative correlations, respectively).

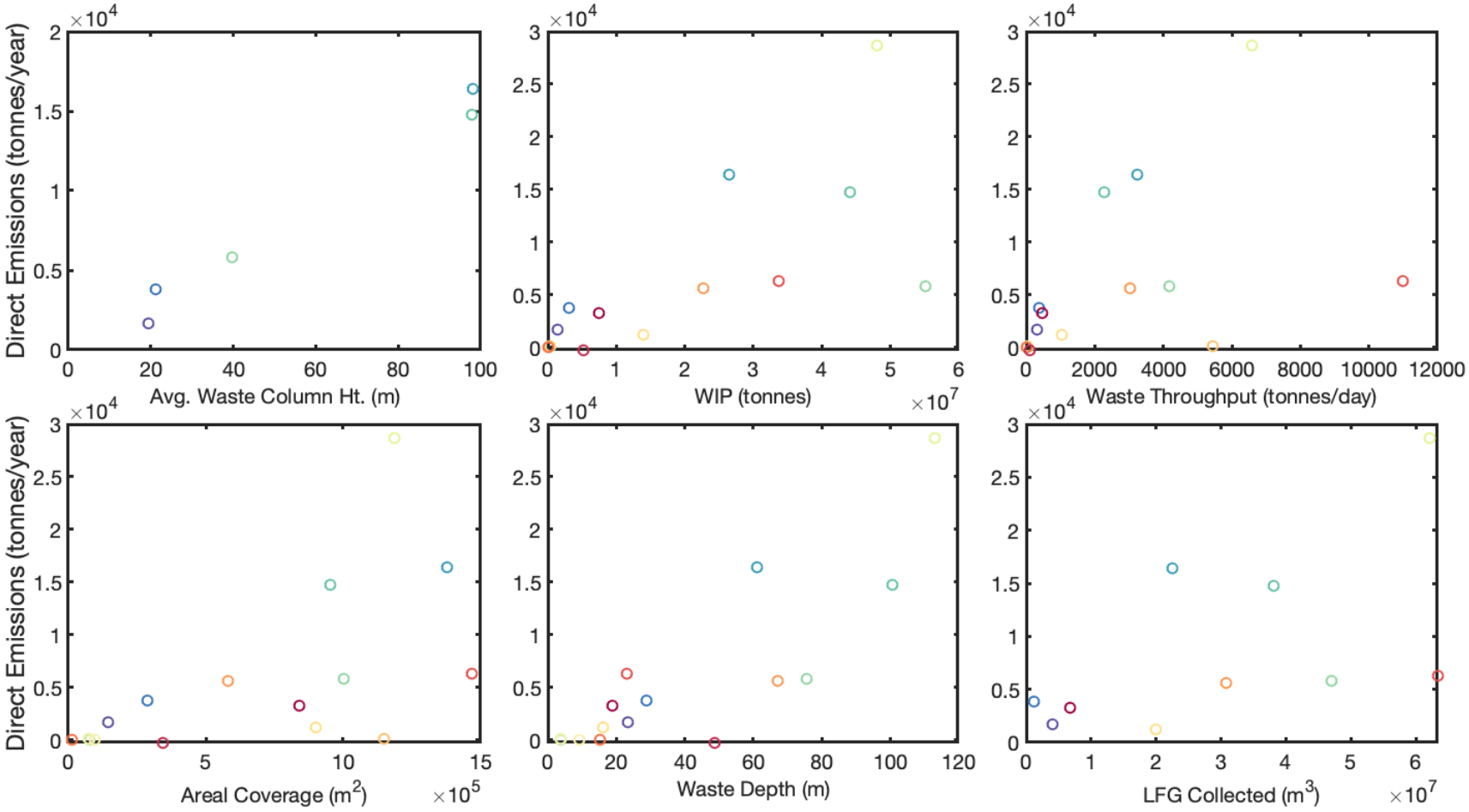

Figure 4.83 Summary of the Strongest Six (from left to right, top to bottom) Correlations Observed between Site-Specific Operational Practices and Direct Methane Emissions Measured from Ground-Based Testing. Results are Plotted for all Landfills and are Differentiated by Color (dashed line represents 1:1 log scaling and best fit line for positive and negative correlations, respectively).

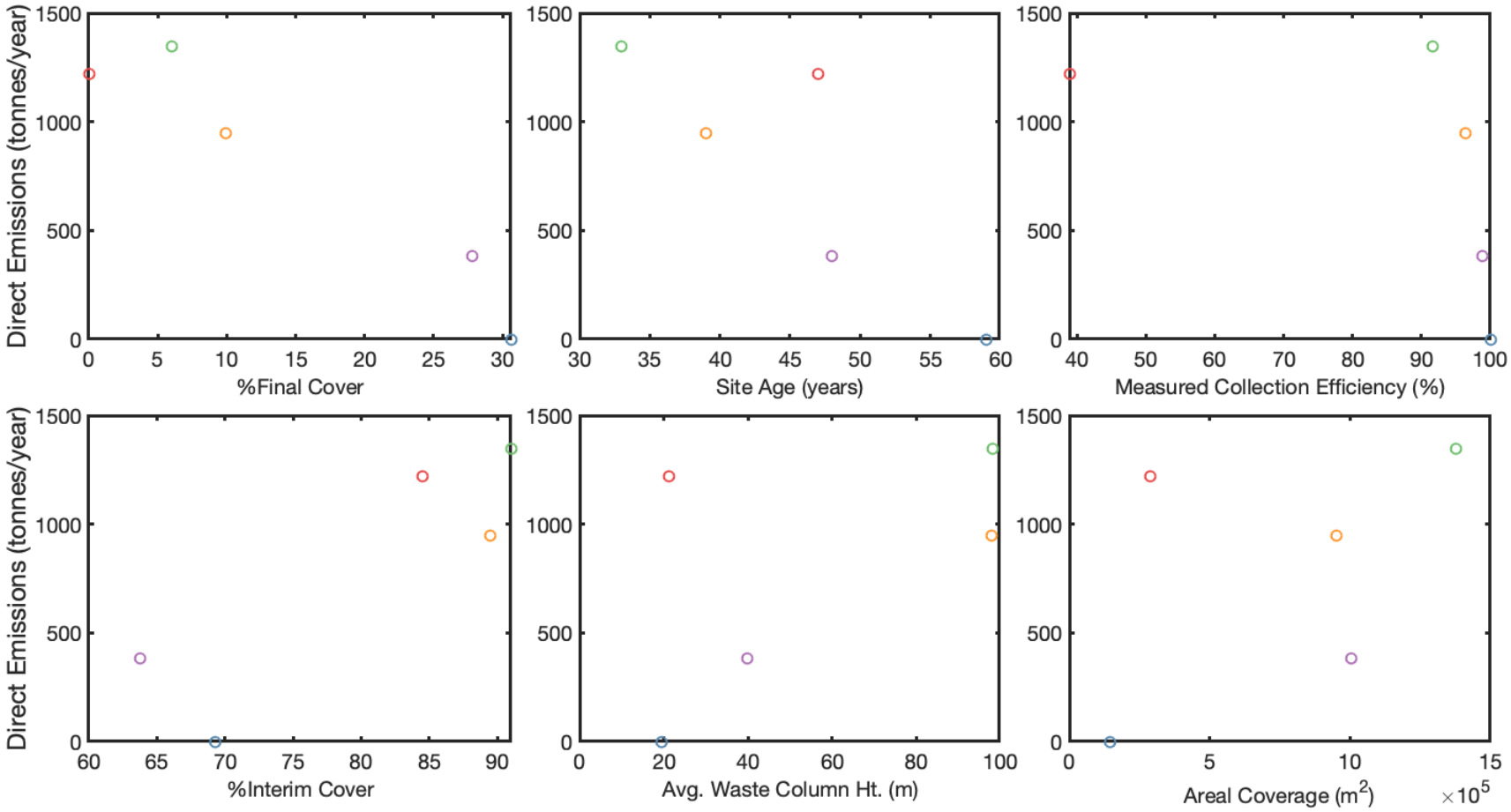

4.8.4 Summary of Correlations Between Physico-Chemical Properties and Measured Fluxes

The presence of non-linear correlations between experimental/predicted physico-chemical properties and measured fluxes were investigated for all landfills and cover categories. Physico-chemical properties for the 82 chemicals were obtained from USEPA's CompTox Chemical Dashboard. The major physico-chemical properties reviewed included molecular weight (g/mol), boiling point (°C), vapor pressure (mmHg), octanol air partition coefficient (dimensionless), Henry's constant (atm*m^3/mol), water solubility (mol/L), and octanol-water solubility (dimensionless). In cases where multiple experimental values of these properties were reported, the median of reported experimental values was used. If experimental values had not been reported, then predictions were obtained from USEPA's OPERA quantitative structure activity relationship modelling tool (Mansouri et al. 2018). The accuracy of such predictions was deemed valid given that the chemicals under investigation in this study were representative of those used in the training, test, and validation sets applied to build the OPERA modelling tool. The physico-chemical properties selected provide baseline indication as to the volatility and partitioning properties of the various chemicals under investigation herein. A chemical was classified as volatile (under environmental conditions similar to those expected in the landfill or soil cover) if it had a low molecular weight, low boiling point, high vapor pressure, low water solubility, and high air over octanol partitioning.

Correlations were assessed by comparing the physico-chemical properties of every gas included under the scope of this study against the mean, ground-based flux measurements for each chemical species within daily, intermediate, and final cover categories at a given landfill. This procedure resulted in 15 overall Spearman's ρ correlation coefficients for a given physico-chemical property (105 correlation coefficients total). Results are presented by season.

Figure 4.84 compares the overall results of the correlation analysis grouping correlation coefficients into positive and negative correlations for both a) dry and b) wet seasons. In general, a much higher number of negative correlations was observed than positive correlations. The strength of the correlations between physico-chemical properties of fluxes was somewhat low for both seasons, where median values rarely exceeded 0.50. In the dry season, median correlation coefficients were highest for vapor pressure, followed by octanol-air partition coefficient and boiling point. The median of negative correlations was greatest for molecular weight followed by boiling point and octanol-air partition coefficient (Figure 4.84). As indicated by the IQR and IWR of the boxplots, the variation was highest for vapor pressures/Henry's constants and boiling points for positive and negative correlations, respectively. In the wet season, median positive correlation coefficients were greatest for vapor pressure, followed by boiling point and Henry's constant. Median values of the negative correlation coefficients were highest for boiling point, water solubility and molecular weight. As indicated by the IQR and IWR of the boxplots, the variation was highest for

Henry's constants and boiling points for positive and negative correlations, respectively (Figure 4.84).

Figure 4.84 Distributions of Spearman's ρ (both positive and negative correlations) Describing Correlations between Physico-Chemical Properties and Measured Fluxes for the a) Dry and b) Wet Seasons across all Landfill Sites and Cover Categories.

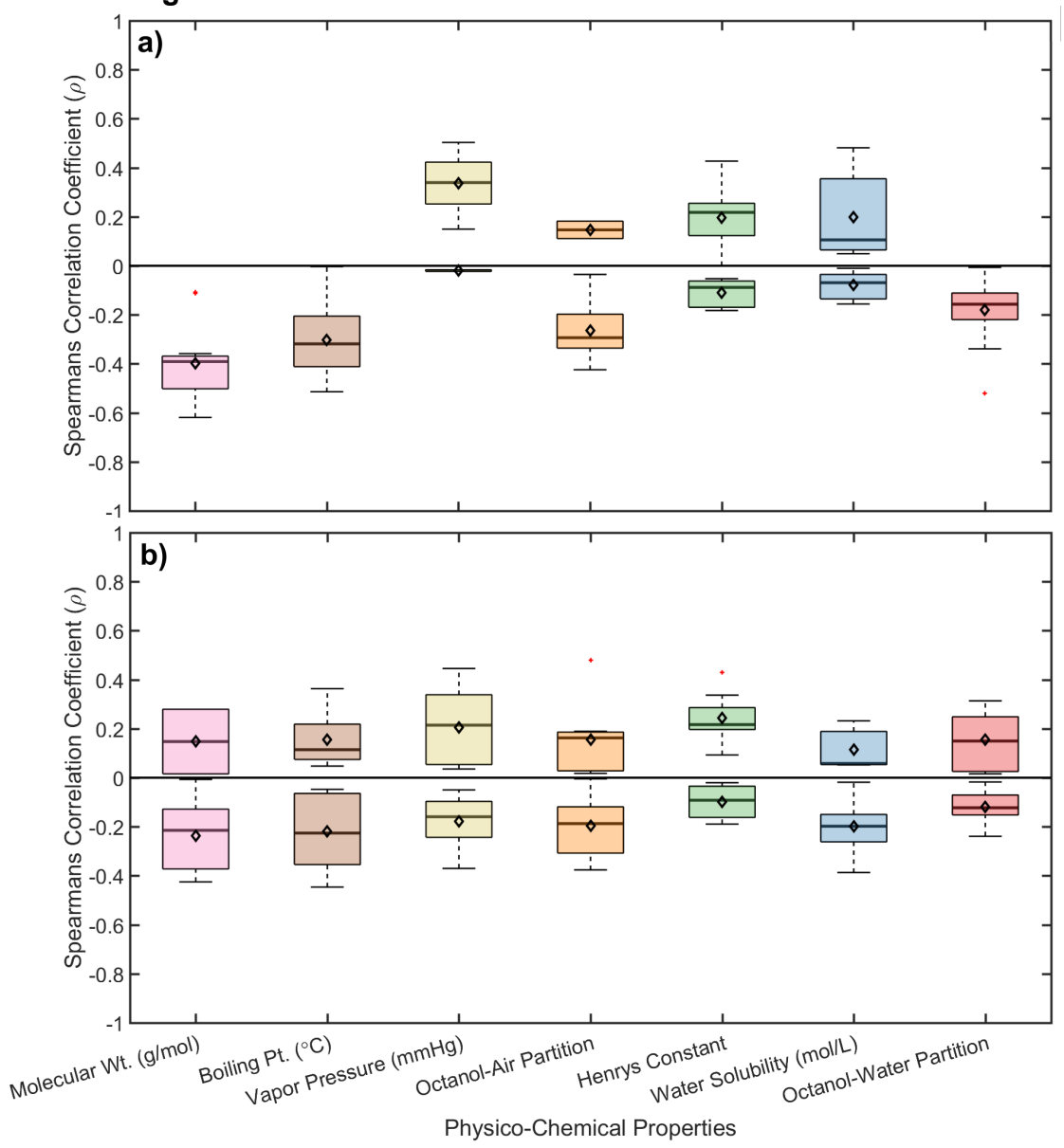

Non-linear correlations were further evaluated as a function of landfill and cover category using bar charts (Figure 4.85). Results are plotted for the three strongest median correlations observed previously in Figure 4.84. In Figure 4.85, the magnitudes of positive and negative correlations are identified as end points of the bars. The analysis demonstrates that the correlations were generally weak to moderate across physico-chemical properties and cover categories.

Figures 4.86 and 4.87 further examine the strongest positive and negative correlations observed between physical-chemical properties and measured flux. Qualitatively, the negative correlations were much more apparent than the positive correlations for both seasons, as there was a sharp decrease in molecular weight, boiling point, water solubility, and octanol-air partition coefficients as gas flux decreased (Figure 4.87b).

Figure 4.85 Mean Values of Spearman's ρ (both positive and negative correlations) Describing Correlations between Physico-Chemical Properties and Measured Fluxes for the a) Dry and b) Wet Seasons as a Function of Cover Category. The X-axis Labels Indicate which Physico-Chemical Property and Flux Correlation is Plotted (positive Correlations/negative Correlations).

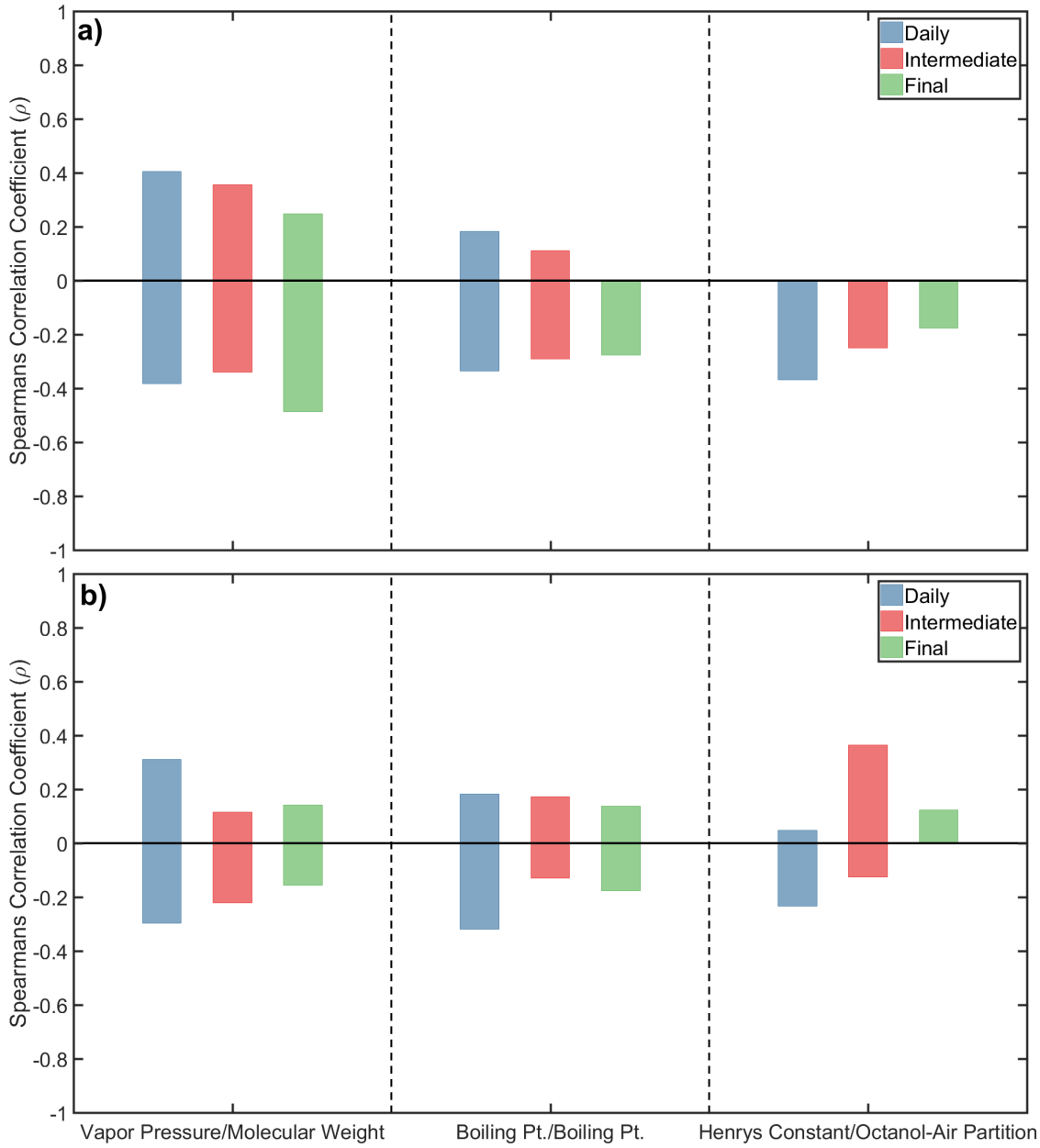

Figure 4.86 Summary of the Three Strongest (from left to right) a) Positive and b) Negative Correlations Observed between Flux and Physical-Chemical Properties in the Dry Season. Results are Plotted for all Chemical Species for a Given Cover Category and Landfill (Gas flux, vapor pressure, and water solubility are scaled logarithmically).

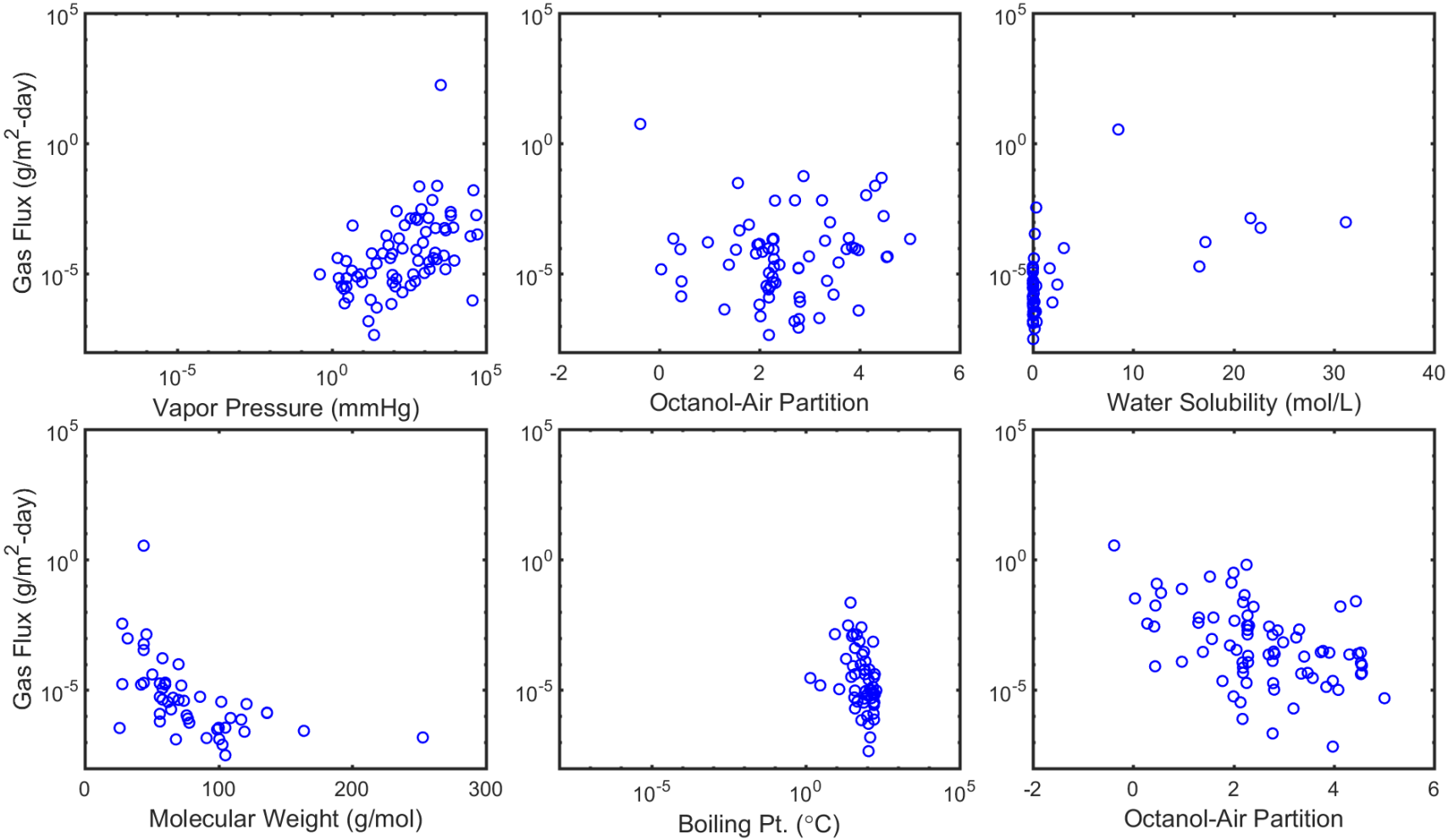

Figure 4.87 Summary of the Three Strongest (from left to right) a) Positive and b) Negative Correlations Observed between Flux and Physical-Chemical Properties in the Wet Season. Results are Plotted for all Chemical Species for a Given Cover Category and Landfill (Gas flux, vapor pressure, and water solubility are scaled logarithmically).

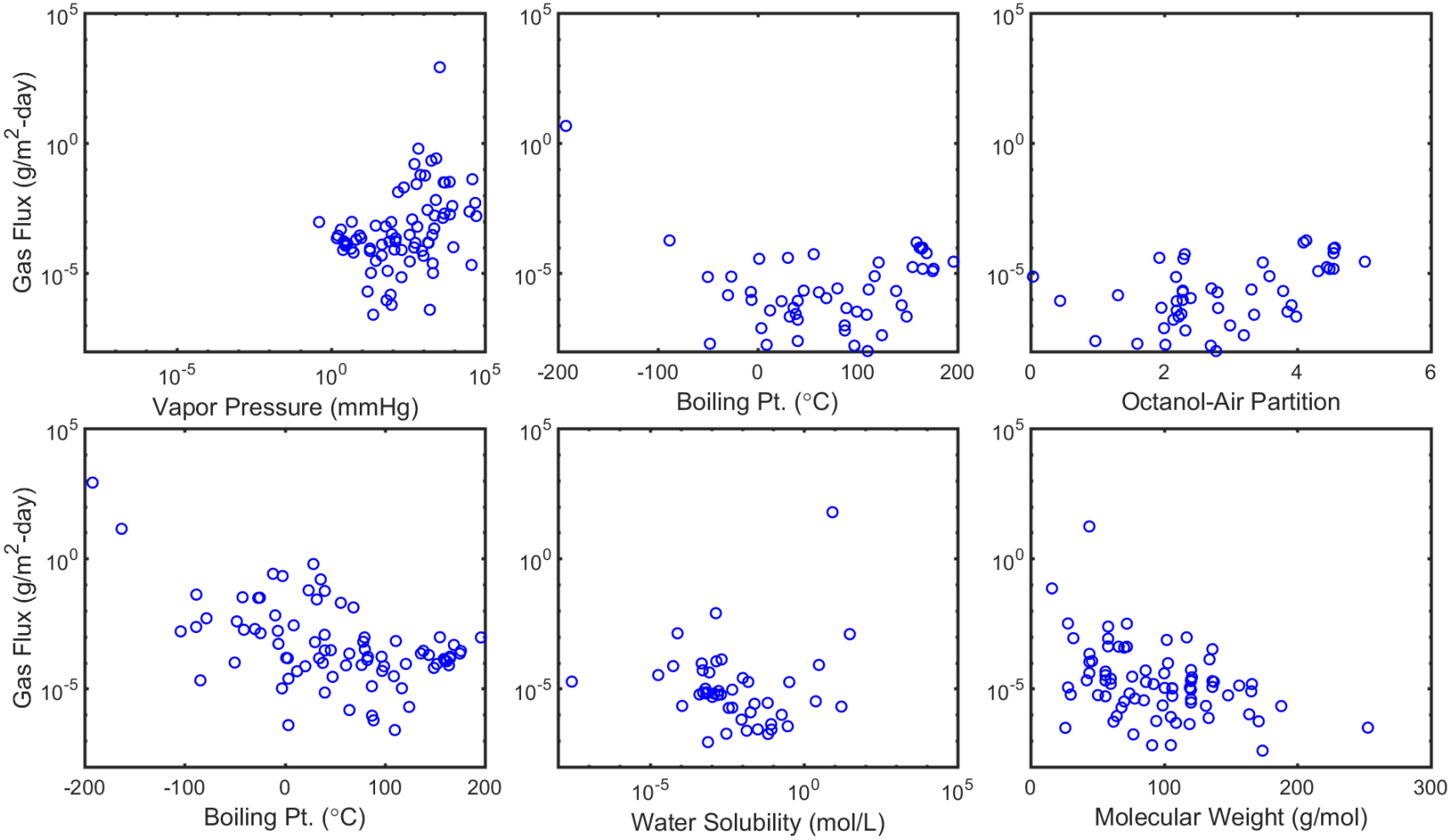

4.9 Methane Generation and Collection Efficiency Results

The results of the LandGEM simulations to predict methane generation rates using both the baseline and refined parameter settings and estimated methane collection efficiencies across landfills is presented in this section of the report. First, the backward and forward prediction of the waste generation trends used as input to the LandGEM model is reviewed (4.9.1). Next, the parameter ranges of L_0 and k predicted by the Monte Carlo simulations and ANN model are summarized in Sections 4.9.2 and 4.9.3, respectively. Comparison of methane generation and collection efficiency using both methods and for all landfills is presented in Section 4.9.4. Lastly, a methane mass balance for all landfills is presented in Section 4.9.5 to compare the agreement between methane collection, emission, and generation data.

4.9.1 Back and Forward Fitting of Waste Generation Trends

Backward and forward trends in WIP were modeled successfully using a combination of second order polynomials (Poly-1) and two parameter power functions (Power-1) (Figure 4.88 and Table 4.18). Using these mathematical models, acceptable fits could not be obtained for Santa Maria Regional, Salton City, and Sunshine Canyon Landfills. Thus, a simple linear interpolation was used to generate the backward and forward trends in WIP for these two sites. The coefficient of determination (R^2) values were greater than 0.97 for the best fitting models (Table 4.18). The magnitude of the scale dependent RMSE was relatively high for all model fits given that the WIP amounts for each site were large (on the order of 10^4 to 10^7 tons) across all landfill sites. The best model-data fits generally were obtained for large landfill sites including Bowerman, Redwood, and Yolo County Landfills, indicating the WIP and corresponding waste generation rates were relatively constant over time (Figure 4.88). Increasing WIP and corresponding waste generation rates were obtained for the landfills where the 2^{nd} order polynomial model fits were best (Teapot Dome, Potrero Hills, Chiquita Canyon, and Simi Valley Landfills), whereas waste generation rates were generally decreasing for landfills where the power model fits were best, as the WIP was observed to tail off over time (i.e., Stonyford, Pumice, Borrego, and Site A Landfills). Some landfill sites, including Sunshine Canyon and Salton City were associated with near constant followed by exponentially increasing WIP trends, indicative of alternative periods of low and high waste throughputs. The mathematical models applied avoided over or under-estimating both past and future trends in WIP; therefore, the corresponding waste generation rates for these past and future time periods were deemed acceptable as input for the LandGEM simulations.

Figure 4.88 Comparison of Qualitative Model Fits Across Landfill Sites from the Time of Open to the Projected Time of Closure

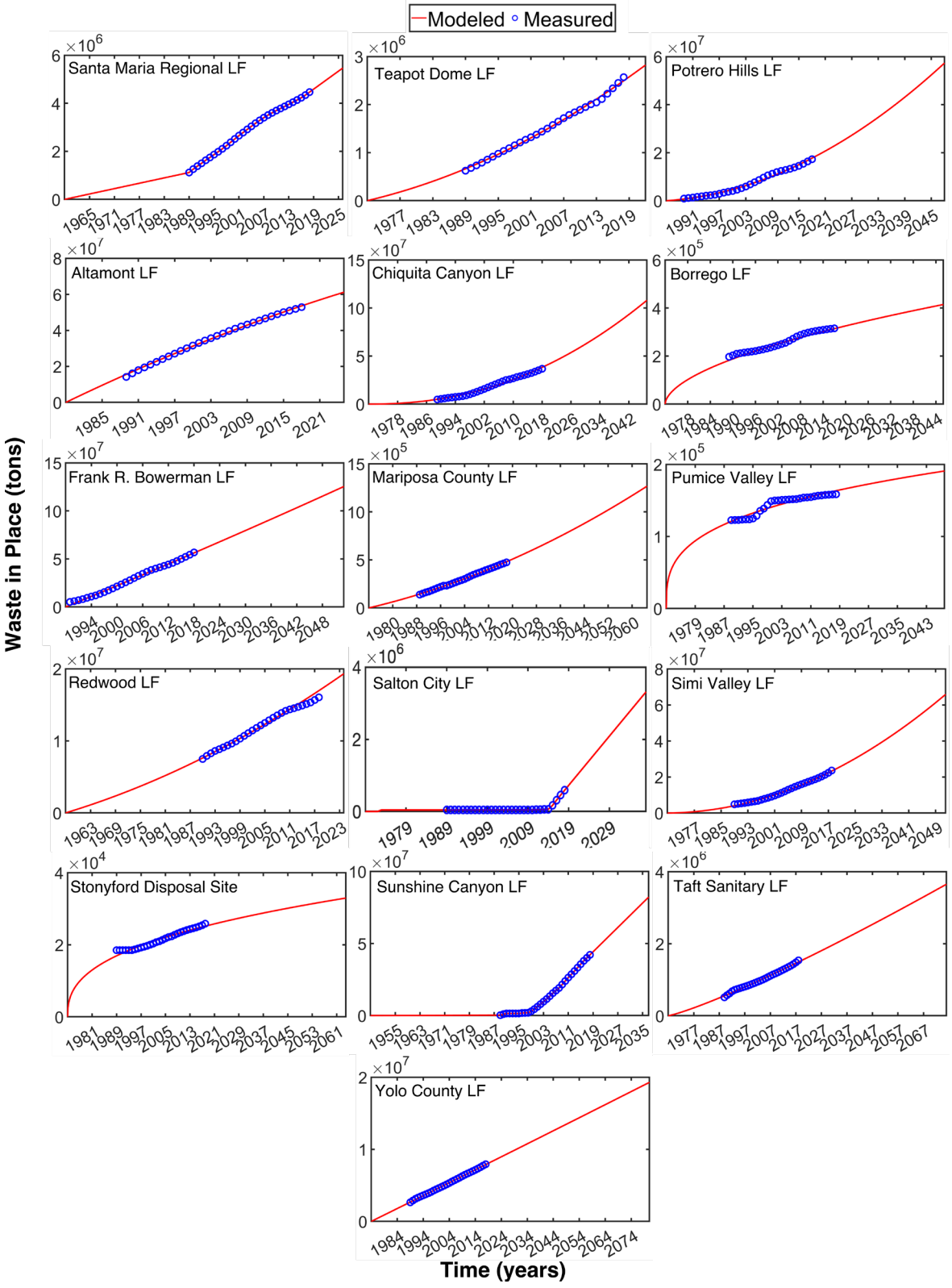

Table 4.21 – Quantitative Model Fitting Metrics for Each Landfill Site

Landfill	Best Fitting Model	R^2	RMSE
Santa Maria Regional Landfill	Linear-Interpolation	N/A	N/A
Teapot Dome	Polynomial-1	0.999	2.46E+04
Potrero Hills	Polynomial-1	0.992	4.93E+05
Altamont Landfill	Polynomial-1	0.999	4.24E+05
Chiquita Canyon	Power-1	0.988	1.78E+06
Borrego Landfill	Power-1	0.988	6.90E+03
Frank R. Bowerman	Polynomial-1	0.996	1.10E+06
Mariposa County LF	Polynomial-1	0.999	3.84E+03
Pumice Valley LF	Power-1	0.979	4.29E+03
Redwood LF	Polynomial-2	0.999	5.56E+07
Salton City LF	Linear-Interpolation	N/A	N/A
Simi Valley	Polynomial-1	0.999	2.72E+05
Stonyford Disposal Site	Power-1	0.971	1.03E+03
Sunshine Canyon	Linear-Interpolation	N/A	N/A
Taft Sanitary Landfill	Power-1	0.991	4.56E+04
Yolo County Landfill	Polynomial-1	0.999	3.07E+04

[N/A] Not applicable since linear interpolation was used

4.9.2 Monte Carlo Simulations: L_0 Results

The Monte Carlo simulations used to predict L_0 values were highly influenced by the landfill specific waste compositions (i.e., weighting factors) obtained from extrapolated data sources (CalRecycle 2019). The outputs predictions were likely more sensitive to the weighting factor inputs given that these values were not allowed to vary in the MC simulations. The differences in the input weighting factors as a function of landfill site are provided in Table 4.19. Food waste comprised a majority of the residential and commercial biodegradable MSW waste streams for all sites, ranging from 35-52% of the total biodegradable waste disposed. Despite recent diversion strategies and legislation, food waste has and continues to be a significant fraction of the total biodegradable component of MSW in California landfills (California SB 1383). In addition, this waste component was generally highest as it also incorporated the remaining unclassified portion of biodegradable organics, which could not be classified into another material type under the “other organic” material category in the CalRecylce waste characterization data. The next most significant waste components were identified as miscellaneous paper (ranging from 21-24%), mixed yard waste (ranging from 6-18%), as well as mixed wood waste (ranging from 6-14%) (Table 4.19). All other waste component categories, including mixed textile wastes, were generally below 6% of the total biodegradable waste disposed for the landfills included in the study. Of the major waste components identified above, Potrero Hills, Sunshine Canyon, Redwood, and Frank Bowerman Landfills had the largest fractions of food waste, miscellaneous paper wastes, yard wastes, and wood wastes disposed, respectively. The variation in

extrapolated waste composition values across landfill sites was generally low (Table 4.19).

Table 4.22 – Landfill Specific Waste Composition Inputs (Weighting Fractions) for the Monte Carlo Simulation Framework

Landfill	Food Waste	.Cardboard/ Paperboard	Newspaper	Office Paper	Coated paper	Phonebooks/ Books	Misc. Paper	Yard Waste	Manure	Textile Waste	Wood Waste
Santa Maria Regional	44.1	3.8	2.7	3.0	1.3	0.1	23.5	6.2	0.1	5.7	9.5
Teapot Dome	46.1	4.0	2.8	2.5	1.1	0.1	22.1	6.6	0.1	7.3	7.3
Potrero Hills	51.8	2.2	2.3	1.8	0.9	0.0	22.5	4.6	0.2	6.8	6.9
Site A	42.0	3.8	2.8	3.7	1.0	0.0	23.3	6.7	0.1	5.1	11.4
Chiquita Canyon	39.5	3.5	3.2	2.9	1.0	0.1	21.1	12.2	0.1	5.5	11.1
Borrego	38.1	3.9	3.6	3.2	1.0	0.1	22.1	11.1	0.1	5.6	11.2
Frank R. Bowerman	35.2	4.5	3.4	4.3	1.1	0.0	22.8	9.7	0.1	4.8	14.1
Mariposa County	48.7	3.7	3.7	2.2	1.1	0.1	21.8	6.3	0.2	6.0	6.1
Pumice Valley	48.2	3.8	3.9	2.5	1.0	0.1	22.1	6.3	0.1	5.5	6.5
Redwood	44.9	3.5	2.9	3.3	1.0	0.0	22.9	6.1	0.1	5.6	9.7
Salton City	32.5	3.1	2.6	2.9	1.2	0.1	21.4	17.6	0.0	5.7	12.9
Simi Valley	37.1	3.5	3.0	3.0	1.0	0.1	21.4	13.4	0.1	5.1	12.5
Stonyford Disposal Site	44.4	4.3	2.7	2.8	1.1	0.1	22.9	7.2	0.1	6.7	7.7
Sunshine Canyon	39.4	3.4	2.7	2.8	0.9	0.1	21.3	12.9	0.1	4.6	11.9
Taft Sanitary	43.0	4.2	2.9	3.2	1.2	0.1	24.2	6.9	0.1	6.8	7.6
Yolo County	44.3	4.3	3.0	2.8	1.0	0.1	22.0	6.7	0.1	6.9	8.8

Table 4.20 summarizes the mean and 95% confidence intervals (C.I.) of the methane generation potential values obtained from the Monte Carlo simulation framework developed in this study. Generally, the mean of the L_0 values was comparable across all landfill sites, ranging from 73 to 81 m^3 methane/Mg wet waste. As the methane generation potential is waste composition specific, the L_0 values were most sensitive to the input weighting factors derived for each site (Tables 4.19 and 4.20). The predicted waste composition data did not vary significantly between the landfills included in the investigation resulting in the relatively similar L_0 values estimated for the different landfills. Landfills associated with greater fractions of food, paper, and yard wastes (with high individual $L_{0,i}$ values) also had higher overall L_0 values. For example, Potrero Hills Landfill had the highest fraction of food waste and one of the highest overall mean L_0 values. Taft Sanitary Landfill, had moderate to high weighting fractions

observed for all waste components, which also resulted in a high predicted L_0 (Table 4.20).

While the variation of L_0 between the landfill sites was not significant, the results of the Monte Carlo simulations indicated a high variation in predicted methane generation potentials for a given landfill (Table 4.20). The high variation in predicted L_0 values was a factor of the high uncertainty of the waste component specific methane generation potentials ($L_{0,i}$) obtained from the literature. Reported values of waste component specific $L_{0,i}$ varied significantly given that the studies from which the $L_{0,i}$ values were derived included different waste materials or mixtures of waste materials in the laboratory scale BMP assays. Moreover, many of these studies did not use consistent BMP protocols (Buffiere et al. 2006, Machado et al. 2009, Krause et al. 2018b). However, the 95% confidence intervals are generally within the range of acceptable values as defined by the USEPA (6.2 to 270 m^3/Mg wet waste), demonstrating that the MC simulations captured the full range in uncertainty of the model inputs.

Table 4.23 – L_0 Values Predicted using the Monte Carlo Simulation Framework Developed in this Study

Landfill	Mean L_0 Value (m^3/Mg wet waste)	95% C.I.
Santa Maria Regional	78.8	[8.61, 302]
Teapot Dome	79.7	[8.62, 308]
Potrero Hills	80.3	[8.30, 319]
Site A	77.6	[8.53, 296]
Chiquita Canyon	76.6	[8.73,286]
Borrego Landfill	76.9	[8.98, 283]
Frank R. Bowerman	76.2	[9.07, 278]
Mariposa County	79.9	[8.46, 313]
Pumice Valley	79.6	[8.40, 312]
Redwood	78.5	[8.55, 302]
Salton City	73.5	[8.66, 269]
Simi Valley	74.2	[8.42, 278]
Stonyford Disposal Site	79.8	[8.77, 305]
Sunshine Canyon	75.4	[8.47, 284]
Taft Sanitary	81.3	[9.21, 305]
Yolo County	78.3	[8.47, 302]

4.9.3 Artificial Neural Network Predictions: *k* Results

Results obtained from the novel, global optimization procedure developed herein indicated that an artificial neural network architecture with three layers (input, 1 hidden layer, output) was sufficient for accurately predicting first-order decay rate values (Table 4.22). From this optimization routine, a total of four neurons within the hidden layer was deemed optimal. The overall predictive performance (sum of the training, testing, and validation performance) of the optimized ANN was excellent, given the

quantitative metrics of goodness of fit summarized in Table 4.22. The MSE and normalized MSE (NMSE) values of the ANN ranged were low and comparable across all divisions of the datasets used. Similarly, the coefficient of determination values were high (0.84-0.903), indicating that the ANN was properly trained and capable of making accurate and reliable predictions of unobserved data. The similarity of the predictive performance metrics (and high validation scores) suggests that the ANN did not overfit the training and/or testing datasets and that proper regularization was carried out during training/optimization of the neural network architecture. Regularization was ensured by explicitly normalizing the MSE values from all datasets by the overall expected variance of the model predictions.

Table 4.24 – Predictive Performance of the Optimized ANN Architecture

Dataset	MSE	NMSE	R^2
Overall	0.000603	0.111	0.889
Training	0.000653	0.111	0.889
Testing	0.000404	0.157	0.843
Validation	0.000573	0.097	0.903

The qualitative fitting performance of the ANN across the different divisions of the dataset is presented in Figure 4.89, where the observed *k* values are plotted against the predicted *k* values by the ANN. A 1:1 line is provided for reference, which delineates a perfect agreement between the observed and predicted *k* values. An empirical 95% prediction interval was determined using a quasi-MC approach by running the ANN model a large number of times (N = 1,000,000) across the full range in the input space (using a Sobol sequence for each input). In this approach, observed values were estimated from the predicted values assuming that the errors were normally distributed with mean 0 and standard deviation equal to the square root of the MSE values. Most of the data points are clustered close to the 1:1 line, indicating good overall agreement between the observed and predicted k-values (Figure 4.89). Only a few data points lie outside the 95% prediction interval, confirming that the ANN model could successfully predict *k* values within an acceptable degree of certainty using the eight distinct inputs of the dataset developed. Several predictions on the unobserved data (validation dataset) lie right on the 1:1 reference line, further confirming that the ANN model can generalize well and was not subject to overfitting during the training process (Figure 4.89). Similar observations can be made regarding the qualitative fitting results of the test set as compared to the validation set.

Figure 4.89 Qualitative Evaluation of ANN Predictive Performance for Overall, Training, Testing, and Validation Datasets.

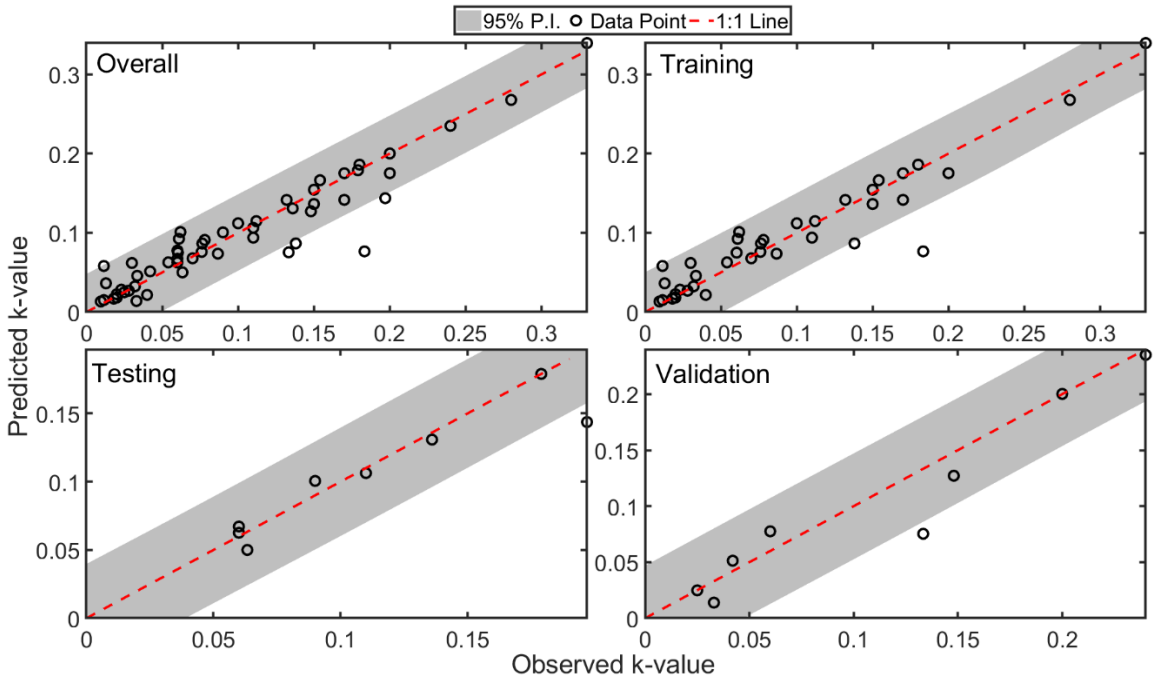

A summary of the input values used to generate k-value predictions is presented in Table 4.22. The WIP values were estimated based on the procedure described in Section 3.8, whereas the throughput, depth, and area were used directly from the most recent estimates provided by the landfills included in the investigation. Normal annual precipitation and average daily temperatures were determined from the most recent 30-year data compiled by the NOAA using the closest weather stations available to each landfill. The total biodegradable waste fraction (B_0) was determined using the data extrapolated from the CalRecycle database and included estimation of site specific L_0 values (total disposed amount of biodegradable waste normalized by the total disposed waste). Relative waste age was defined as the time period spanning from the start of landfill operations (i.e., active waste placement) to 2019.

In addition to B_0 values and relative waste ages, the input factors varied significantly as a function of landfill site. Pumice Valley and Sunshine Canyon landfills were the coldest and warmest sites, respectively. Many sites were located in temperate climate zones (avg. daily temperatures ranging from 16-19°C) differentiated by rainfall received, including Teapot Dome, Potrero Hills, Site A, Chiquita Canyon, Frank R. Bowerman, Simi Valley, Sunshine Canyon, Taft Sanitary, and Yolo County landfills (Table 4.22). Redwood and Salton City landfills received the highest and lowest rainfall per year. Rainfall rates at the landfills in the temperate climates varied from 278 to 630 mm/year. Across all landfills, WIP and landfill area varied by four and three orders of magnitude, respectively. Throughput rates and waste depths generally paralleled trends in WIP/area, as indicated by data presented in Table 4.22.

Table 4.25 – Input Values Used to Generate *k*-values using the Optimized ANN Architecture Developed in this Study

Landfill	Depth (m)	WIP (tons)	Annual Precip. (mm)	Daily Average Temp. (°C)	Throughput (tons/day)	Area (m^2)	B_0 (%)	Relative Waste Age (years)
Santa Maria Regional	23.5	4.46×10^6	462	14.9	347	9.09×10^5	78.2	59
Teapot Dome	28.7	2.57×10^6	278	17.4	420	2.87×10^5	76.9	47
Potrero Hills	61.0	1.73×10^7	630	16.1	3584	1.38×10^6	73.6	33
Site A	101	5.29×10^7	387	15.8	2500	9.52×10^5	73.6	39
Chiquita Canyon	75.6	3.67×10^7	462	18.2	4588	1.00×10^6	79.2	48
Borrego	3.7	3.18×10^5	156	22.4	11	7.69×10^4	78.7	46
Mariposa County	4.1	4.74×10^5	837	15.3	65	1.05×10^5	81.9	46
Frank R. Bowerman	113	5.67×10^7	364	18.5	7250	1.19×10^6	76.9	46
Pumice Valley	9.1	1.58×10^5	546	5.9	11.7	9.55×10^4	83.4	47
Redwood	16.2	1.60×10^7	895	14.7	1150	9.00×10^5	76.3	61
Salton City	32.8	5.90×10^5	74	22.6	127	1.62×10^4	71.2	49
Simi Valley	67.1	2.36×10^7	420	17.0	3353	5.82×10^5	75.3	49
Stonyford	15.2	2.58×10^4	586	15.8	2	1.34×10^4	74.2	45
Sunshine Canyon	61.0	4.21×10^7	372	18.7	6411	1.42×10^6	74.8	71
Taft Sanitary	48.8	1.54×10^6	162	17.9	122	1.80×10^5	73.1	51
Yolo County	18.8	7.92×10^6	542	17.1	500	8.39×10^5	79.1	44

The mean and 95% confidence intervals for the k-values predicted using the ANN developed in this study are summarized in Table 4.23. Of the landfill sites included in this study, Borrego, Mariposa, and Stonyford Landfills had the highest predicted first order decay rates, which were one order of magnitude higher than those for the remaining landfills. The Borrego, Mariposa, and Stonyford landfills are located in warm to cool climates, with limited, to high, to moderate amounts of precipitation per year, respectively. Salton city, which is located in a relatively dry and warm climate zone, also had a relatively high predicted *k* value (0.061). These predictions suggest that both climate and rainfall may not be significant predictors used by the ANN

architecture. Rainfall was more influential than temperature in the ANN model as Mariposa Landfill had a high predicted *k* value. Generally, previous studies have indicated that greater moisture contents, influenced by rainfall received, and higher temperatures are associated with higher *k* values. Other site-specific operational characteristics such as WIP/areal coverage, waste age, and available organic fraction of waste components in the waste mass also were determined to be significant for making reliable predictions.

As compared to predicted L_0 values, the 95% confidence intervals obtained for the ANN predictions were more constrained. This result may be due to several factors, including the fact that *k* values reported in the literature do not span a wide range (i.e., two orders of magnitude, excluding bioreactor landfills) and that the ANN predictions are highly accurate (MSE values below 0.1). Given that the residuals in the loss function were assumed to be Gaussian, white noise, the resulting variation in predicted values was expected to be small.

Table 4.26 – *k* Values Predicted Using the ANN Architecture Optimized in this Study

Landfill	Mean *k* Value (1/year)	95% C.I.
Santa Maria Regional	0.0594	[0.0523, 0.0660]
Teapot Dome	0.0287	[0.0221, 0.0353]
Potrero Hills	0.0928	[0.0862, 0.0994]
Site A	0.0210	[0.0154, 0.0286]
Chiquita Canyon	0.0330	[0.0265,0.0397]
Borrego	0.226	[0.219, 0.232]
Frank R. Bowerman	0.0134	[0.00680, 0.0200]
Mariposa County	0.224	[0.217, 0.230]
Pumice Valley	0.0359	[0.0290, 0.0425]
Redwood	0.0741	[0.0674, 0.0807]
Salton City	0.0610	[0.0539, 0.0672]
Simi Valley	0.0152	[0.00855, 0.0218]
Stonyford	0.119	[0.113, 0.126]
Sunshine Canyon	0.0624	[0.0558, 0.0690]
Taft Sanitary	0.00771	[0.00110, 0.0143]
Yolo County	0.0556	[0.0490, 0.0622]

To evaluate the differences between regression models developed by previous studies to the more advanced architecture herein, several additional factors were investigated. In particular, presence or absence of correlation among inputs, presence or absence of correlation between inputs and targets, and input sensitivity on ANN predictive accuracy were studied. In general, ANN predictions are affected by input correlation, with low predictive significance when input variables are highly correlated to one another. Input variables that are highly correlated with output targets are of high

importance when developing the ANN architecture. Input sensitivity encompasses both factors, indicating how influential the input variables are when the ANN model generates predictions. Both input-input and input-target (output) correlations were assessed using Spearman's non-linear correlation coefficient, ρ. Input sensitivity was evaluated by setting the input variable to zero (keeping all other inputs constant, non-zero values – the modified approach), and calculating the RMSE between the MSE of the non-modified input matrix to that obtained from the modified input matrix (Δ). All of these factors were investigated using the full dataset, including training, testing, and validation data.

Correlations among input variables in the dataset are compared visually in the heatmap presented in Figure 4.90. For correlation among inputs, significant (i.e., ρ > 0.5), positive non-linear correlations were observed between all operational factors, including WIP and depth, WIP and area, and WIP and throughput, with ρ values ranging from 0.5 to 0.75. There was a moderate (0.3<ρ<0.5), positive correlation between annual precipitation and daily average temperature (0.40) and moderate, negative correlations between annual precipitation and waste age and biodegradable fraction of waste components (-0.40 to -0.43). Significant, positive correlations were observed between waste age and depth, WIP, and areal coverage, with ρ ranging from 0.47 to 0.52 (Figure 4.90).The average, absolute ρ values were lowest for B_0 and daily average temperature, suggesting that these inputs were more favorable for making accurate predictions from the ANN model.

Figure 4.90 Correlation Between Input Variables of the Dataset Used for Training, Testing, and Validating the ANN Model (down arrows: negative correlations; color: strength of correlation, where red = strong and blue = weak).

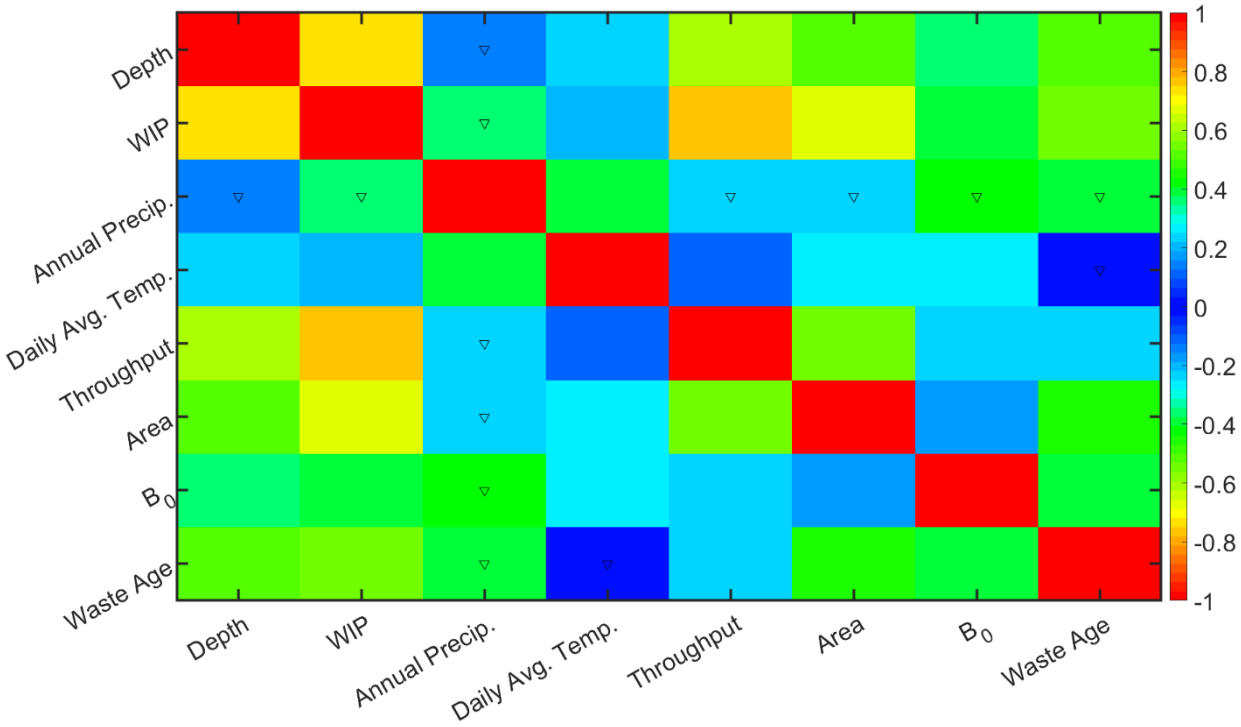

Strong correlations were observed between model inputs and target *k* values (Table 4.24). Input annual precipitation and *k*-values were positively correlated, consistent with correlations observed in previous studies and in agreement with high moisture content of waste masses facilitating decomposition. No correlation was observed between temperature and *k* values. A significant, negative correlation was observed between waste age and *k* values, indicating that fresh waste is degraded faster than older waste (Table 4.24). Moderate, negative correlations were also observed between B_0 and *k*. In addition, moderate, negative correlations were present between WIP, area, throughput and *k*, indicating higher rates of decomposition at smaller landfills (Table 4.24).

Table 4.27 – Summary of Input-Target (Output) Correlations and Overall Sensitivity of ANN Input Variables

Input Variable	Correlation (ρ)	Sensitivity (Δ)
Depth	-0.257	0.0028
WIP	-0.374	0.0024
Annual Precipitation	0.560	0.0084
Daily Average Temperature	-0.021	0.0059
Throughput	-0.312	1.35E-05
Area	-0.361	0.0061
B_0	-0.449	0.0206
Relative Waste Age	-0.556	0.0110

Trends in the nonlinear correlation coefficients were not highly aligned with those obtained from the baseline sensitivity analysis (Table 4.24). The sensitivity results demonstrated that B_0, waste age, and precipitation were the most significant input variables, whereas the ranking based on the input-output correlation analysis indicated that annual precipitation, waste age, then B_0 had the strongest correlations. The reason for the differences between these two methods is that the ANN predictions likely are affected by the presence of correlations among the input variables (Figure 4.90). Compared to both waste age and annual precipitation, B_0, on average, was correlated the least among the input variables assessed. Therefore, the high *k* values predicted for Borrego and Stonyford sites can be partially explained by the relatively high B_0 values and waste ages, as compared to precipitation, observed for these two sites (Table 4.24). Additional factors may affect the ANN model predictions, including similarities between the dataset used to train, test, and validate the model and the landfill sites included in this study. For example, a majority of the site data (75%) used to train, test, and validate the model was obtained from wet climate zones (defined as annual rainfall > 635 mm/year, Wang et al. 2013, 2015), whereas a majority of the sites included in this study are in arid areas. Reliability of ANN predictions can be improved if additional *k* data from sites located in California in similar climate zones become available in future.

4.9.4 Methane Generation and Gas Collection Efficiency: Baseline and Refined LandGEM Predictions

Annual methane generation rates estimated using LandGEM with the L_0 and k parameters from the baseline and refined approaches are presented in Figure 4.91. The trends in methane generation rates over time were in general similar between the two approaches and were affected by trends in estimated waste placement data in both cases. Pronounced peaks in methane production is followed by a quick decline in generation for landfills with high WIP. Landfills with smaller WIP demonstrated a slow increase to peak methane generation followed by a prolonged tail in methane generation beyond site closure. In the baseline approach, for landfills with high WIP, the order of methane generation from highest to lowest was for Chiquita Canyon, Frank R. Bowerman, Sunshine Canyon, Simi Valley, Site A, and Potrero Hills Landfills (Figure 4.91a). This order was modified to Sunshine Canyon, Chiquita Canyon, Potrero Hills, Frank R. Bowerman, Site A, and Simi Valley with the refined approach (Figure 4.91b). The variations in methane generation over time was somewhat more gradual for the refined analysis compared to the baseline analysis. The LandGEM predictions for annual methane generation rates using the baseline parameter values were higher than the predictions obtained using the refined approach ($2x10^8$ compared to $1.5x10^8$ m^3/year). Default methane generation potential values were on the order of 100 to 170 m^3/Mg wet waste, as compared to 70-80 m^3/Mg wet waste used in the refined approach. The higher methane generation potentials in the default LandGEM simulations resulted in the higher rates of methane generation (Figure 4.91). Default first order decay rate values were 0.02, 0.04, or 0.05 $year^{-1}$, whereas refined estimates of k varied by site and ranged from 0.007 to 0.22 $year^{-1}$. The greater variation in the k values in the refined analysis mainly controlled the slopes of the methane generation-time relationships resulting in generally in character with yet more varied slopes compared to the baseline analysis.

Figure 4.91 LandGEM Methane Generation Rates a) Baseline, b) Refined Approach.

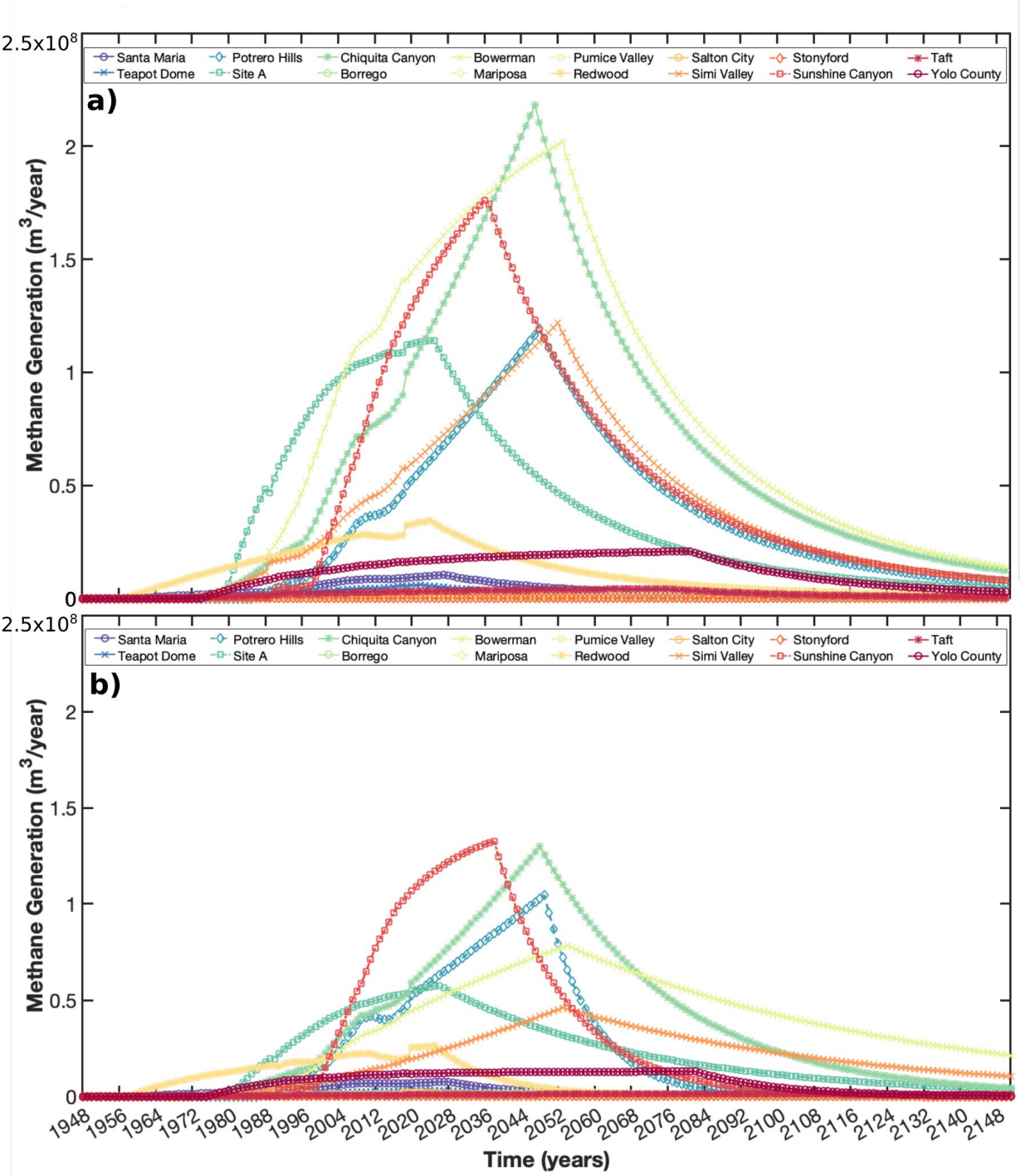

A detailed summary of estimated gas collection efficiencies (for the year 2018, mean and 95% confidence intervals) for both the measured and modeled (baseline and refined) LandGEM approaches is presented in Table 4.26. Mean values of the measured collection efficiencies were generally high, ranging from 38.9 to 99.8%

across landfills. Santa Maria Regional and Teapot Dome Landfills had the highest and lowest measured collection efficiencies, respectively. In addition, the corresponding variation in measured methane collection efficiencies was relatively low, as indicated by the constrained 95% confidence intervals presented in Table 4.26. For modeled methane generation using the baseline approach, the collection efficiencies ranged from 25 to 76% and were highest and lowest for the Redwood and Teapot Dome Landfills, respectively. For modeled methane generation using the refined approach, collection efficiencies ranged from 37.4 to 100% and were highest for the Frank Bowerman, Redwood, and Simi Valley Landfills. In line with the baseline results, Teapot Dome had the lowest methane collection efficiency using the refined approach. The mean α values obtained from the refined approach exceeded 100% for the Frank Bowerman, Redwood, and Simi Valley Landfills. As collection efficiencies higher than 100% are unrealistic; efficiencies were reported as 100% for these sites. Application of the lower 95% range in the parameter estimates for the refined approach generally resulted in an underapproximation of methane generation, and hence collection efficiencies exceeding 100%, even though these were based on realistic values using the full range in uncertainty expected for each prediction method. In general, collection efficiencies were higher using the refined estimates of the parameters compared to the default parameter values. Higher methane generation rates were predicted using the baseline approach as compared to the refined approach resulting in the lower collection efficiencies associated with the baseline approach. The variation in methane collection efficiencies was generally lower for the baseline approach, as indicated by the narrow 95% confidence intervals. The variation in collection efficiencies was higher for the refined approach due to the high uncertainty in the overall methane generation potential for each site, which ranged from 8 to 319 m^3/Mg wet waste (Table 4.20).

Table 4.28 – Summary of Measured and Modeled Methane Gas Collection Efficiencies using the Baseline and Refined LandGEM Parameter Values (for year 2018)

Landfill	Measured-Aerial Data		Measured-Ground Data		Baseline		Refined	
	$\bar{\alpha}$ (%)	95% C.I.	$\bar{\alpha}$ (%)	95% C.I.	$\bar{\alpha}$ (%)	95% C.I.	$\bar{\alpha}$ (%)	95% C.I.
Santa Maria Regional	61.1	[42, 100]	100	[100, 100]	51.5	[31.9, 82.8]	60.3	[15.4, 100*]
Teapot Dome	23.2	[18.4, 31.4]	38.9	[30.3, 54.4]	24.5	[14.7, 38.9]	37.4	[8.8, 100*]
Potrero Hills	47.3	[43.2, 52.3]	91.4	[88.9, 94]	60.2	[34, 93.5]	49.7	[12.3, 100*]
Site A	62.9	[57.7, 69.0]	96.4	[93.9, 98.9]	39.6	[24.6, 63.8]	72	[16.6, 100*]
Chiquita Canyon	84.1	[80.8, 87.7]	98.8	[98.3, 99.3]	62.5	[36.4, 98.2]	90.9	[22.3, 100*]
Frank R. Bowerman	58.7	[54.1, 64.1]	N/A	N/A	53	[30.8, 83.2]	100*	[31.2, 100*]
Redwood	91.4	[89.2, 93.8]	N/A	N/A	75.9	[53.9, 100*]	100*	[26.3, 100*]
Simi Valley	78.3	[70.3, 88.5]	N/A	N/A	65.3	[38.9, 100*]	100*	[36.2, 100*]
Sunshine Canyon	86.8	[84.4, 89.4]	N/A	N/A	63.7	[36.1, 99.1]	62.3	[15.8, 100*]
Yolo County	57.6	[53.4, 62.4]	N/A	N/A	48	[29.8, 77.2]	57.8	[14.6, 100*]

*Indicates that calculated gas collection efficiency exceeded 100%
N/A Not applicable

4.9.5 Methane Mass Balance

The results of the methane mass balance analysis that was conducted for each landfill are presented in Table 4.27. For a majority of the landfills, excess methane is present (77 to 18,820 tonnes) that can be attributed to storage, migration, or oxidation pathways. Most of the excess methane can be attributed to oxidation taking place in the covers as storage and migration are less significant components of the methane balance in the landfill environment (Christophersen and Kjeldsen 2001, Scheutz et al. 2009a). In general, landfills with higher WIP were associated with higher methane collection, emission, and excess amounts. Sites without an active gas extraction system in place generally had small to moderate values of methane stored, migrated, or oxidized, ranging from below 0 to 907 tonnes per year. For some of these sites without an extraction system, net uptake was estimated (Table 4.27). For select landfills with gas extraction systems, including Frank R. Bowerman, Redwood, Yolo, and Simi Valley Landfills, there is a net deficit of methane, indicating that the mean LandGEM simulations using the refined parameter sets did not match measured collection or emissions data. This difference in measured and predicted values most likely resulted from inadequate approximations of site and waste specific k and L_0 values.

The uncertainty in methane flow estimates was generally highest for the LandGEM generation predictions followed by the emissions and collections estimates (Table 4.27). The magnitude of the 95% confidence intervals is high for methane generation (on the order of 10^4 to 10^8), which carries over to the high overall uncertainty of the excess/deficit estimates. The uncertainty in LandGEM predictions was high due to the wide range in methane generation potentials predicted from the MC analysis, which are representative of the highly variable waste compositions at the landfills. The uncertainty of the aerial emission measurements was significantly higher than that for the ground-based measurements, based on the magnitude of the 95% confidence intervals in Table 4.27. Gas collection measurement uncertainty was very low, ranging from 0.5 to 2 tonnes of methane as the LFG flow and methane composition were not observed to vary significantly across the datasets obtained and analyzed from previous studies.

Table 4.29 – Summary of Methane Mass Balance Results (the mean and 95% confidence intervals are presented in the first and second rows, respectively)

Landfill	CH_4 Generated (tonnes)	CH_4 Collected (tonnes)	CH_4 Emitted (tonnes)	ΔCH_4 Excess/Deficit[a] (tonnes)
Santa Maria Regional	4379	2640	-0.1221	1738.8
	$\pm 1.27 \times 10^7$	± 0.536	± 0.079	$\pm 1.27 \times 10^7$
Teapot Dome	2074	777	1220	77.2
	$\pm 6.57 \times 10^6$	± 0.313	± 571	$\pm 6.57 \times 10^6$
Potrero Hills	29629	14732	1391	13506
	$\pm 8.89 \times 10^7$	± 1.14	± 446	$\pm 8.89 \times 10^7$
Site A	34745	25026	945	8774
	$\pm 1.12 \times 10^7$	± 1.45	± 446	$\pm 1.12 \times 10^8$
Chiquita Canyon	33878	30784	381	2713
	$\pm 1.03 \times 10^8$	± 1.58	± 154	$\pm 1.03 \times 10^8$
Borrego	143	0	36	107
	$\pm 3.85 \times 10^5$	0	± 10.5	$\pm 3.85 \times 10^5$
Frank R. Bowerman	27490	40764	28693	-41966
	$\pm 9.80 \times 10^7$	± 1.79	± 5856	$\pm 9.80 \times 10^7$
Mariposa County	567	0	79	489
	$\pm 1.65 \times 10^6$	0	± 129	$\pm 1.65 \times 10^6$
Pumice Valley	82	0	-2	84
	$\pm 2.34 \times 10^5$	0	± 14.9	$\pm 2.34 \times 10^5$
Redwood	12875	13051	1225	-1400
	$\pm 3.68 \times 10^7$	± 1.09	± 364	$\pm 3.68 \times 10^7$
Salton City	1002	0	95	907
	$\pm 2.94 \times 10^6$	0	± 26.3	$\pm 2.94 \times 10^6$
Simi Valley	11875	20213	5586	-13924
	$\pm 4.19 \times 10^7$	± 1.32	± 2954	$\pm 4.19 \times 10^7$
Stonyford	15	0	53	-39
	$\pm 4.15 \times 10^4$	0	± 12.3	$\pm 4.15 \times 10^4$
Sunshine Canyon	66618	41504	6294	18820
	$\pm 1.95 \times 10^8$	± 1.81	± 1361	$\pm 1.95 \times 10^8$
Taft Sanitary	472	0	-215	687
	$\pm 2.04 \times 10^6$	0	± 287	$\pm 2.04 \times 10^6$
Yolo County	7726	4464	3290	-28
	$\pm 2.26 \times 10^7$	± 0.676	± 599	$\pm 2.26 \times 10^7$

[a] Calculated as methane generated minus the sum of methane collected and emitted

4.10 The Effect of Waste Tires on LFG Emissions

4.10.1 LFG Production from Waste Tires

In 2017, the USEPA estimated that 6.5 million tons of waste tires (~290 million tires, cars, trucks, motorcycles) were generated in the US, constituting, 2.4%, of the total MSW generated (USEPA 2017c). In California, CalRecycle estimates that approximately 51.1 million waste tires were generated in 2018 alone, which is 18% of the nationwide total (CalRecycle 2018b). At end of life, three primary pathways for waste tire processing are currently in use: recycling, combustion with energy recovery, and landfilling (USEPA 2017c). USEPA has estimated that, approximately, 40, 40 and 20% of waste tires are recycled, combusted, and landfilled on an annual basis (USEPA 2017c). Due to their size, shape, and physiochemical composition, waste tires typically do not readily degrade in the environment (Conesa et al. 2004, Stevenson et al. 2008). In general, natural (bio) degradation of rubber materials in tires is a slow process (Romine and Romine 1997, Holst et al. 1998). High concentrations of toxic chemicals, such as poly-cyclic aromatic hydrocarbons, phthalates, antioxidants (i.e., zinc oxides), and benzothiazoles have been identified in tires (Menichinni et al. 2011, Llompart et al. 2013). Disposal of waste tires in the landfill environment have high risks, as landfill temperatures, oxygen levels, and leachate are elevated, depleted, and highly acidic, potentially promoting the physical, chemical, and biological transformation or physical and chemical partitioning of these chemicals into more mobile aqueous or gaseous phases (Aydilek et al. 2006, Reddy et al. 2010). The environmental factors governing the decomposition of waste tire materials is complex and primarily depends on the composition of the materials, which vary widely across different manufacturers and automotive classification (car truck, motorcycle) (Aprem et al. 2003). Waste tires consist of vulcanized rubber with steel or fabric belts and reinforcing textile cords (Edil 2008). The tire rubber is a blend of natural and synthetic rubbers. Natural rubber is a biopolymer consisting of repeating poly(cis-1,4-isoprene) units. To improve the durability and elasticity of natural rubber for tire applications, a process termed vulcanization is used. Vulcanization of natural rubber involves covalently bonding the polyisoprene chains with mono, di-, and polysulfide bridges, where the properties of a given rubber material depend on the type and quantity of cross links formed (Aprem et al. 2003). The most commonly used tire rubber (SBR) is a synthetic tire rubber obtained from radiation-based vulcanization of natural rubber latex in the presence of styrene (~25%) and butadiene (~75%) (Dodds et al. 1983, Chaudhari et al. 2005). The radiative based synthetic tires have lower amount of residual toxic chemicals such as zinc oxides or nitrosamines, which improve the biodegradability of the materials (Chaudhari et al. 2005). Waste tire materials also contain carbon black, extender oil, as well as other accelerators such as zinc oxide, stearic acid, and elemental sulfur.

Of the many processes affecting the stability of waste tire composition in the landfill environment, anaerobic/aerobic biological degradation is potentially the most significant transformation pathway. Biodegradation of waste tires consists of three interconnected steps including detoxification, desulfurization, and degradation, all of which are carried out by different microorganisms under varying environmental conditions (summarized in Stevenson et al. 2008). The first step of waste tire

biodegradation, detoxification, involves the removal of chemical compounds that inhibit microbial growth including zinc oxide, salts, aromatic hydrocarbons, and other xenobiotic compounds. Waste tire detoxification is mediated by select species of fungi and bacteria. White rot fungi are xenobiotic degraders that likely metabolize aromatic compounds present in the waste tires under both aerobic and anaerobic conditions (Bredberg et al. 2002). In addition, some bacteria, such as *Rhodococcous rhodochrous*, degrade 2-mercaptobenzothiazole (MBT), a compound commonly used as a vulcanization accelerator (Haroune et al. 2004). Other bacterial genera such as *Corynebacteria*, *Pseudomonas*, and *Escherichia coli* detoxify MBT and other toxic inhibitors (Haroune et al. 2004).

Following detoxification, the elemental sulfur present in the tire waste material is then open to attack by different sulfur oxidizing or reducing bacterial species in a process termed desulfurization (Stevenson et al. 2008). In this stage, the sulfur cross links present in the vulcanized rubber are removed by aerobic oxidizing or anaerobic reducing activity of different sulfur utilizing bacteria (Christiansson et al. 1998). Desulfurization exposes the underlying isoprene polymers that are then available for degradation by other groups of bacteria. In the landfill environment, it is likely that anaerobic conditions persist throughout much of the waste mass, favoring the anaerobic reduction of elemental sulfur to different reduced sulfur compounds (RSC) such as hydrogen sulfide, carbonyl sulfide, carbon disulfide, dimethyl sulfide, and dimethyl disulfide. The reduced forms of elemental sulfur are generally highly volatile and present in the gaseous form, leading to a detectable presence in LFG (Kim 2006).

Polyisoprene polymers composing the initial structure of natural rubber are further broken down during the stage of ultimate degradation of rubber (Rose and Steinbuchel 2005, Stevenson et al. 2008). Two main groups of rubber metabolizing organisms have been identified, including clear zone forming bacteria and adhesively growing bacteria. Clear zone forming bacteria include members of the genera *Streptomyces*, *Xanthomonas*, *Micromonospora*, *Thermomonospora*, and *Actinomyces*, which use latex as a sole carbon and energy source (Rose and Steinbuchel 2005). The other group of bacteria form biofilms (adhesive growth) on the rubber material in order to metabolize rubber and include bacteria from the genera: *Gordonia*, *Corynebacterium*, *Mycobacterium*, *Pseudomonas,* and *Nocardia* (Rose and Steinbuchel 2005, Roy et al. 2006). The intermediate and end products of this metabolism vary from ketones, to aldehydes, to organic acids (i.e., carboxylic acids) (Rose et al. 2005). Considering all of these interconnected stages of biodegradation, the overall rate of anaerobic waste tire decomposition depends on many factors, including the presence of microorganisms specific to each stage and favorable environmental conditions (i.e., moisture, temperature, pH, nutrients, oxygen level) to support the growth of these microorganisms within the landfill environment. It is likely that the level of processing of waste tires prior to landfill disposal (i.e., whole tires, chips, aggregates) highly influences the susceptibly and rate of biological degradation of waste tire materials, where finer materials may improve biodegradation rates. As tires adsorb different toxic chemicals and the organisms that degrade these compounds are rare and potentially

site-specific, detoxification may be the rate limiting step of this multi-stage process (Baykal et al. 1992, Park et al. 1996, Edil et al. 2004).

4.10.2 Potential Impacts on Emissions

The presence of waste tires has potential effects on the physical and mechanical stability of the waste mass and the presence or absence of migration pathways of LFG and moisture throughout the waste in place (Reddy et al. 2010). Depending on the level of pre-processing of incoming tire materials to the landfill, the compressibility of these materials is likely higher than other MSW waste constituents, such as metals, glass, or other hard plastics. Areas with high quantities of these materials are likely to settle faster in the landfill environment (Edil and Bosscher, 1994, Warith and Rao 2006). However, depending on the degree of post-processing, these materials range from relatively impermeable (whole tires) to permeable (aggregates), that will either inhibit or facilitate LFG and moisture transport through the waste mass, thereby serving as both a source and stymy/accelerator of LFG transfer to the gas collection system. While the liquid permeability of these materials has been well studied, gas transport through waste tire materials has received relatively little attention in the scientific literature.

Even though waste tires can leach a variety of contaminants, waste tires are also well-known adsorbents of NMVOCs and other organic contaminants (Baykal et al. 1992, Park et al. 1996, Edil et al. 2004, Edil 2008). Similar to biodegradation, the sorption capacity of tire materials depends on the state of waste tire processing, ranging from whole tires, to chips, to crumb tire particles. As the active surface area for adsorption increases with a decrease in particle size, greater adsorption of organic contaminants has been documented (Kim et al. 1997). Both adsorption (to the surface) and absorption (phase portioning) affect the physico-chemical attachment of organic contaminants to waste tires (Kim et al. 1997, Alamo-Nole et al. 2012, Hüffer et al. 2020). For example, across a range of organic sorbate materials, absorption into the rubber fraction of the SBR was observed to dominate adsorption onto the black carbon component (Alamo-Nole et al. 2012, Hüffer et al. 2020). Regardless of the exact molecular mechanism governing attachment, multiple studies indicated that waste tires can serve as effective sorbents for leachate quality control in the landfill environment, targeting the removal of polar and non-polar organic chemicals such as benzene, toluene, xylene, ethylbenzene, and other harmful petroleum derived contaminants (Baykal et al. 1992, Park et al. 1996, Edil et al. 2004, Edil 2008). Despite the strong coverage of aqueous contaminant removal by waste tires, few studies have directly quantified the effectiveness of waste tire materials in preventing NMVOC emissions from landfill covers; however, waste tires have been considered for enhancing the gas-phase permeability of soil covers to improve methane oxidation (i.e., biocovers) and to facilitate gas collection (Stern et al. 2007, Jung et al. 2011).

4.10.3 Sulfur Compound and Aromatic Hydrocarbon Emissions

Santa Maria Regional Landfill, Teapot Dome Landfill, Site A Landfill, and Chiquita Canyon Landfill accept waste tires, whereas tires were not accepted at Potrero Hills Landfill. Both Santa Maria Regional and Site A Landfills accepted tire chips or

aggregates only, whereas the other two landfills accepted all types of tire wastes, ranging from whole tires to tire chips and aggregates. Figure 4.92 summarizes the RSC flux measurements as a function tire acceptance. Median RSC fluxes were generally highest for the site that did not accept waste tires (Potrero Hills), followed by Chiquita Canyon, Teapot Dome, Santa Maria Regional and Site A Landfills. The whiskers of each boxplot extended below 0, indicating the probability of net uptake over net emissions. However, as there were many positive outliers and the mean was above the median, measurements were positively skewed, indicating greater probability of RSC emissions over uptake. The variation in RSC flux measurements was generally lowest and highest for Chiquita Canyon and Potrero Hills landfills, respectively as indicated by the IQR and IWR values. The magnitude of the median values was relatively similar across all landfill sites, ranging less than 1 order of magnitude (10^{-5} to 10^{-6}). These results indicate that the presence of tires did not have a significant impact on RSC fluxes and that alternative sources, such as organics present in food or yard waste, contribute to RSC emissions.

Figure 4.92 Summary of Reduced Sulfur Compound Emissions from Landfills with and without Waste Tires by Landfill Site (open black diamonds, red lines, solid red dots represent means, medians, and outliers, respectively).

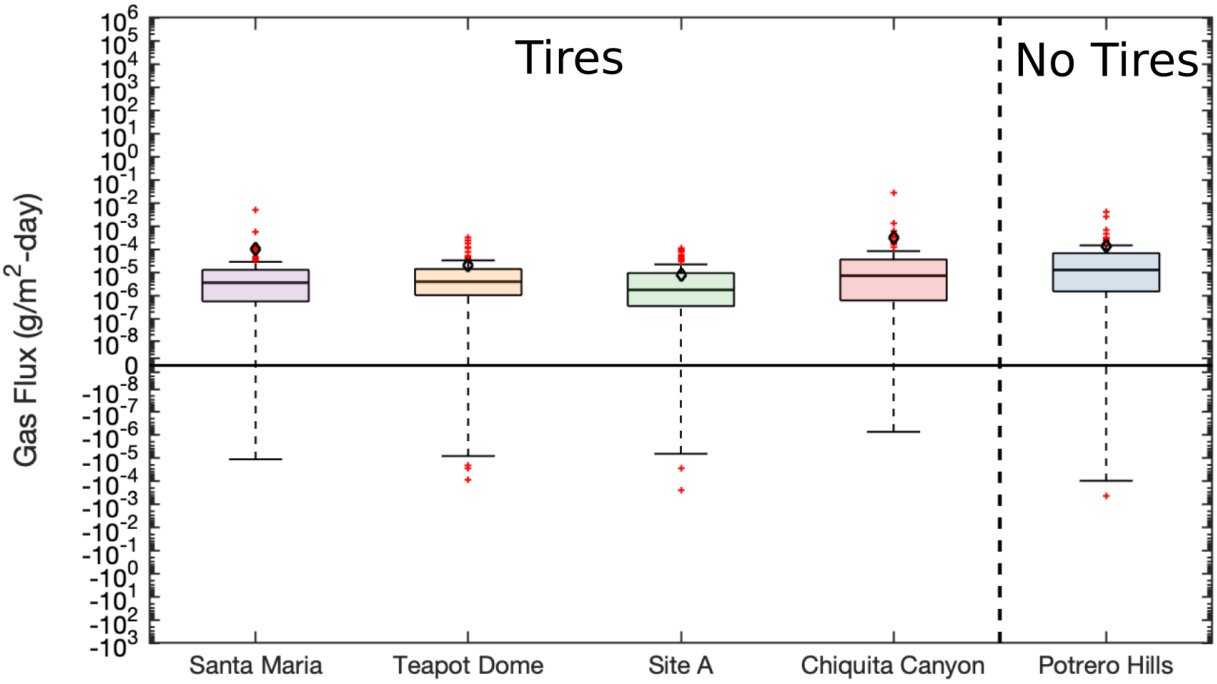

RSC flux measurements are further examined according to cover category for landfills accepting and not accepting waste tires in Figure 4.93. Similar to results presented in Figure 4.92, RSC flux measurements were generally higher for the site that does not accept waste tires based on the median values presented. For both sites accepting and not accepting waste tires, RSC flux measurements were highest from daily cover locations followed by intermediate and final cover locations. Variation in flux measurements as a function of cover category was generally comparable across all cover categories; however, the variation in RSC flux measurements was generally

higher across daily cover locations for sites that did not accept tire wastes (Figure 4.93). The variation in median fluxes between cover categories was within one to two orders of magnitude, indicating that it was difficult to attribute elevated RSC emissions to waste tires alone. Sulfur reducing bacteria may use substrates present in other organic wastes such as food (i.e., decaying meats or dairy products) or green/yard wastes (i.e., fertilizers, manures, treated sewage sludge that lead to the production of RSC.

Figure 4.93 Summary of Reduced Sulfur Compound Emissions from Landfills with and without Waste Tires by Cover Category (open black diamonds, red lines, solid red dots represent means, medians, and outliers, respectively).

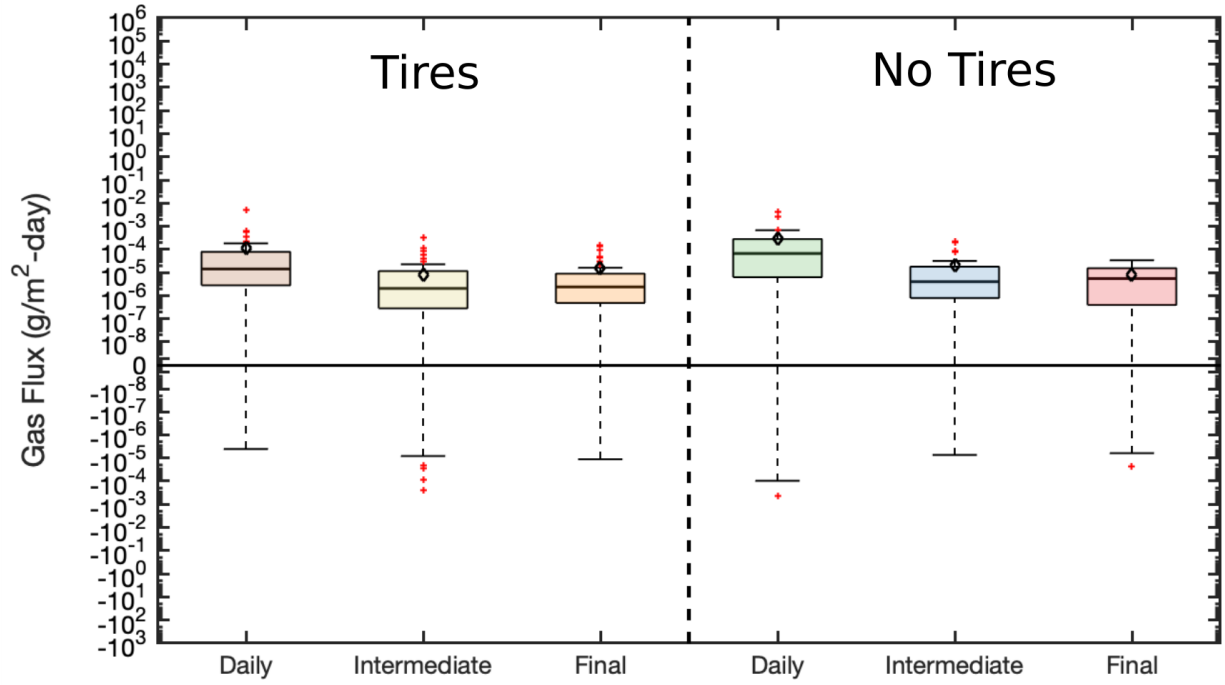

Figure 4.94 summarizes the aromatic compound flux measurements as a function tire acceptance. Aromatic compound fluxes including median flux were generally higher for the site that did not accept waste tires (Potrero Hills). As introduced in 4.10.2 above, waste tires have high sorption potential for aromatic hydrocarbons (i.e., benzene, toluene, xylene, ethylbenzene). Santa Maria Regional Landfill and Site A Landfill had the lowest median Ar fluxes including net uptake at Site A Landfill. These low fluxes likely resulted from the small size and thus large surface area of the form of tires, tire chips and aggregates, accepted at these two sites. The Ar fluxes at Teapot Dome Landfill and Chiquita Canyon Landfill were higher than Santa Maria Regional and Site A Landfills likely due to the large size and thus low surface area of the whole tires accepted at these sites.

Figure 4.95 compares aromatic compound emissions from sites accepting and not accepting waste tires as a function of cover category. In general, Ar fluxes from daily covers at sites not accepting waste tires were greater than fluxes observed from sites accepting waste tires, whereas fluxes from intermediate and final covers were relatively comparable but slightly greater for sites accepting waste tires (Figure 4.95).

These results confirm trends observed above that the presence of waste tires are potentially sorption sites retarding the transport of Ar compounds as they travel through the waste mass.

Figure 4.94 Summary of Aromatic Compound Emissions from Landfills with and without Waste Tires by Landfill Site (open black diamonds, red lines, solid red dots represent means, medians, and outliers, respectively).

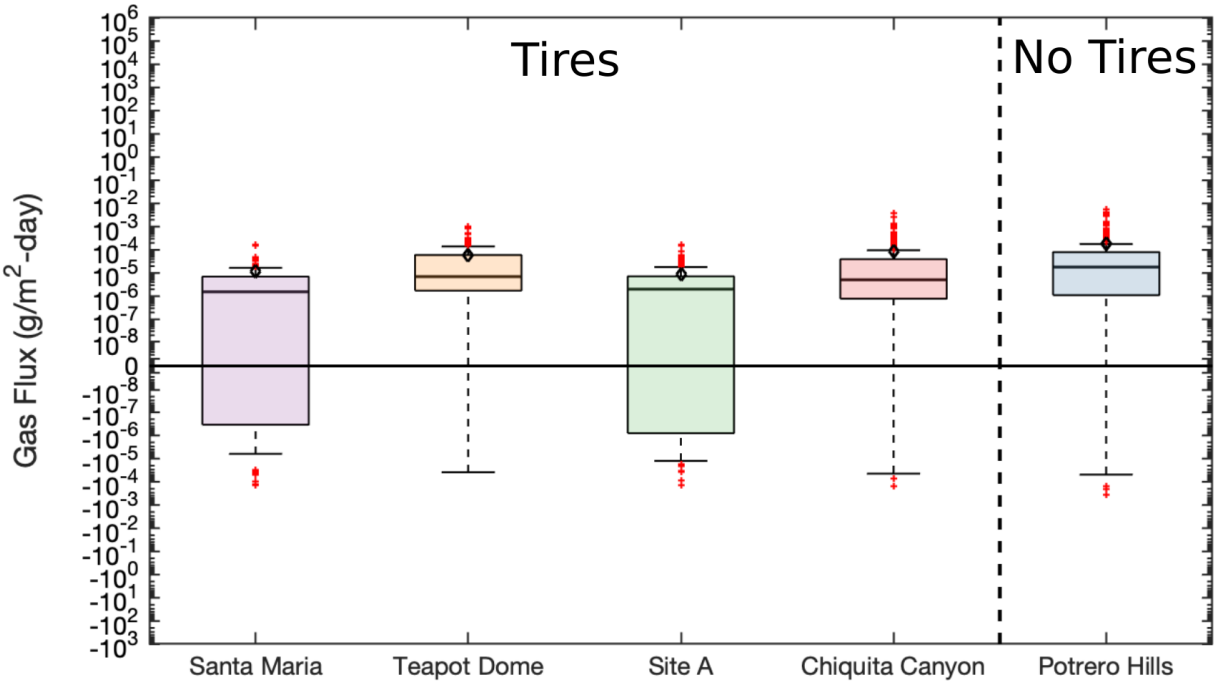

Figure 4.95 Summary of Aromatic Compound Emissions from Landfills with and without Waste Tires by Cover Category (open black diamonds, red lines, solid red dots represent means, medians, and outliers, respectively).

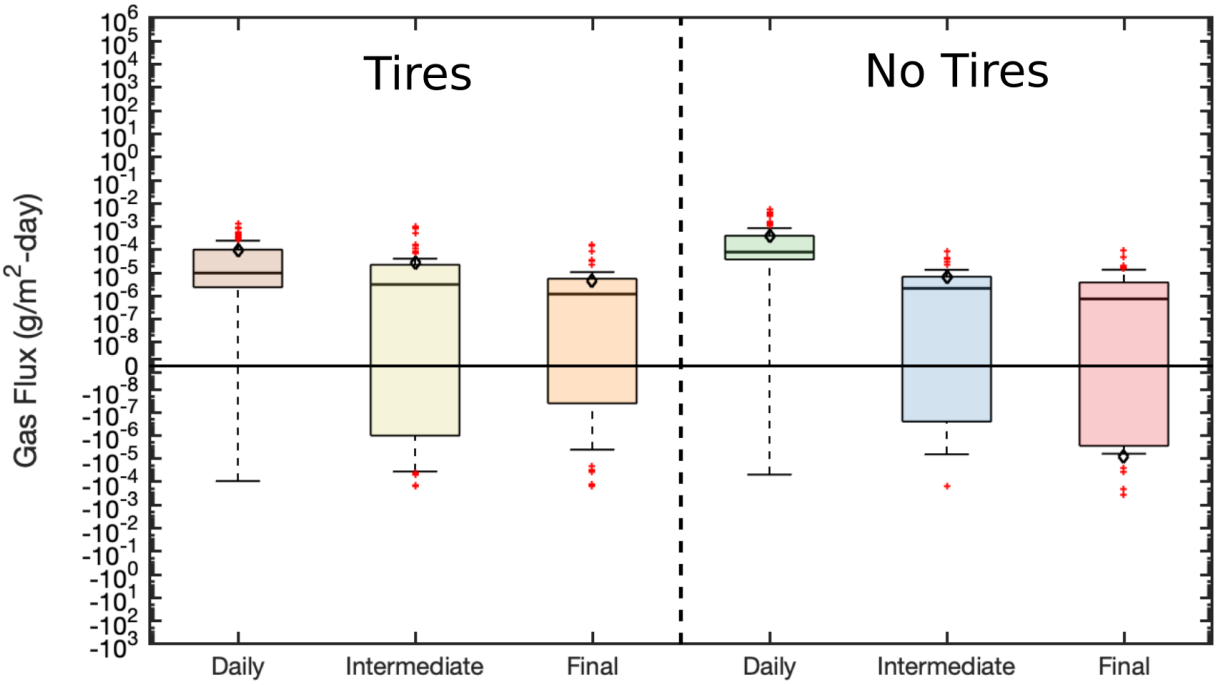

The overall methane, RSC, and Ar fluxes for all sites accepting and not accepting tires are compared in Figure 4.96. Methane fluxes were generally higher from waste sites that do not accept tires, as indicated by the median flux values in the box plots (Figure 4.96). Moreover, RSC and Ar fluxes were slightly higher, on average, for sites not accepting waste tires as compared to sites accepting waste tires (Figure 4.96). There was a higher probability of net uptake over emissions for methane as compared to the RSCs and Ars across all landfills and cover systems investigated (Figure 4.96). The variation in both methane, RSC, and Ar flux measurements was greater for sites not accepting tire wastes given the lengths of the IQR and IWR of the boxplots. Therefore, these results suggest that the presence of tire waste may impede migration of LFG to the base of the cover, thus influencing emissions. However, since there is no way to reliably evaluate both generation and migration of these gases in the landfill environment, it is difficult to make any definitive conclusions about how gas transport is affected in the waste mass by the presence of waste tire materials. Moreover, it is difficult to ascertain the sources of both RSC emissions, as sulfur-reducing bacteria may use substrates present in other organic wastes such as food (i.e., decaying meats or dairy products) or green/yard wastes (i.e., fertilizers, manures, treated sewage sludge). The sources of Ar compounds, however, are primarily anthropogenic, where differences in emissions may be attributed to both generation, sorptive, and perhaps biodegradative processes occurring within the different landfills.

Figure 4.96 Summary of Methane and Reduced Sulfur Compound Emissions from Landfills with and without Waste Tires (open black diamonds, red lines, solid red dots represent means, medians, and outliers, respectively).

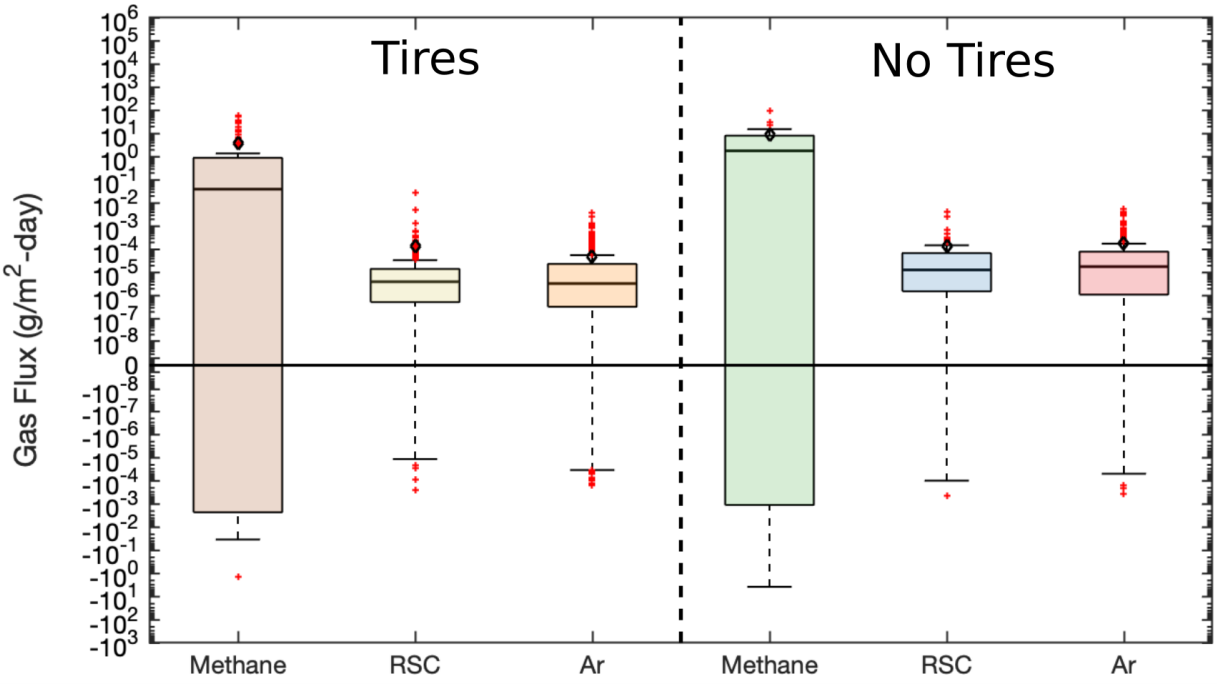

A two-sample t-test (significance level of 0.05, two tails, unequal variance) was conducted to ascertain whether the differences in methane, RSC, and Ar fluxes observed above between sites accepting and not accepting waste tires were in fact statistically significant. A conservative approach using both tails of the normal distributions, unequal variances, and a significance level of 0.05 was applied. Using these assumptions, the null hypothesis is that the distributions of fluxes for a given chemical family between sites accepting/not accepting waste tires come from independent random samples from normal distributions with equal means and unequal but unknown variances. The results of this two-sample t-test are summarized in Table 4.28 below. Statistically significant differences in the fluxes of the aromatic compounds were observed between sites accepting and not accepting waste tires as the p-value was below the significance level of 0.05 (Table 4.28). These results provide further confidence that the presence of waste tires affect the transport and transformation of aromatic compounds in the landfill environment. However, statistically significant differences were not observed for both methane and RSC fluxes between sites accepting and not accepting waste tires, indicating that there is less confidence in the initial presumption that RSC generation and overall LFG transport/transformation are affected by the presence of waste tires. The conclusions presented herein may be affected, to some degree, by differences in the sample sizes of the flux distributions under comparison (4 sites vs. 1 site), where additional data from landfill sites not accepting waste tires would provide a more balanced comparison of the potential effect of waste tires on LFG generation, transport/transformation, and emissions.

Table 4.30 – Summary of t-Test Results for Sites Accepting and Not Accepting Waste Tires

Chemical Family	Accept or Reject?	p-values
Methane	Accept	0.246
RSC	Accept	0.985
Ar	Reject	5.29E-4

4.11 Raw Gas Tests

Concentration data are provided for gases sampled prior to the inlet of the flare and/or gas to energy systems at the five landfills included in the ground-based flux investigation. The composition of these samples represents the composition of gas in the waste mass, unaffected by transformation processes occurring in the cover soils. The concentration data for the raw gas are presented as a function of chemical family and site in Figures 4.97 and 4.98, respectively. Highest LFG concentrations were obtained for the GHGs, with median values ranging from 20,000 to 100,000 μg/L. Concentrations of the remaining NMVOCs were significantly lower, on the order of 10^{-4} to 500 μg/L. Based on median concentration values, the alcohols, ketones, monoterpenes, and alkanes had the highest concentrations. Organic alkyl nitrates (ON) were not detected in LFG. The differences between seasonal results were minimal (Figure 4.97). Among the NMVOC families, the F-gases and the monoterpenes had the highest variation in the dry and wet seasons, respectively.

Figure 4.97 LFG Concentrations Measured in the a) Dry and b) Wet Seasons by Chemical Family (open black diamonds, black lines, solid red dots represent means, medians, and outliers, respectively).

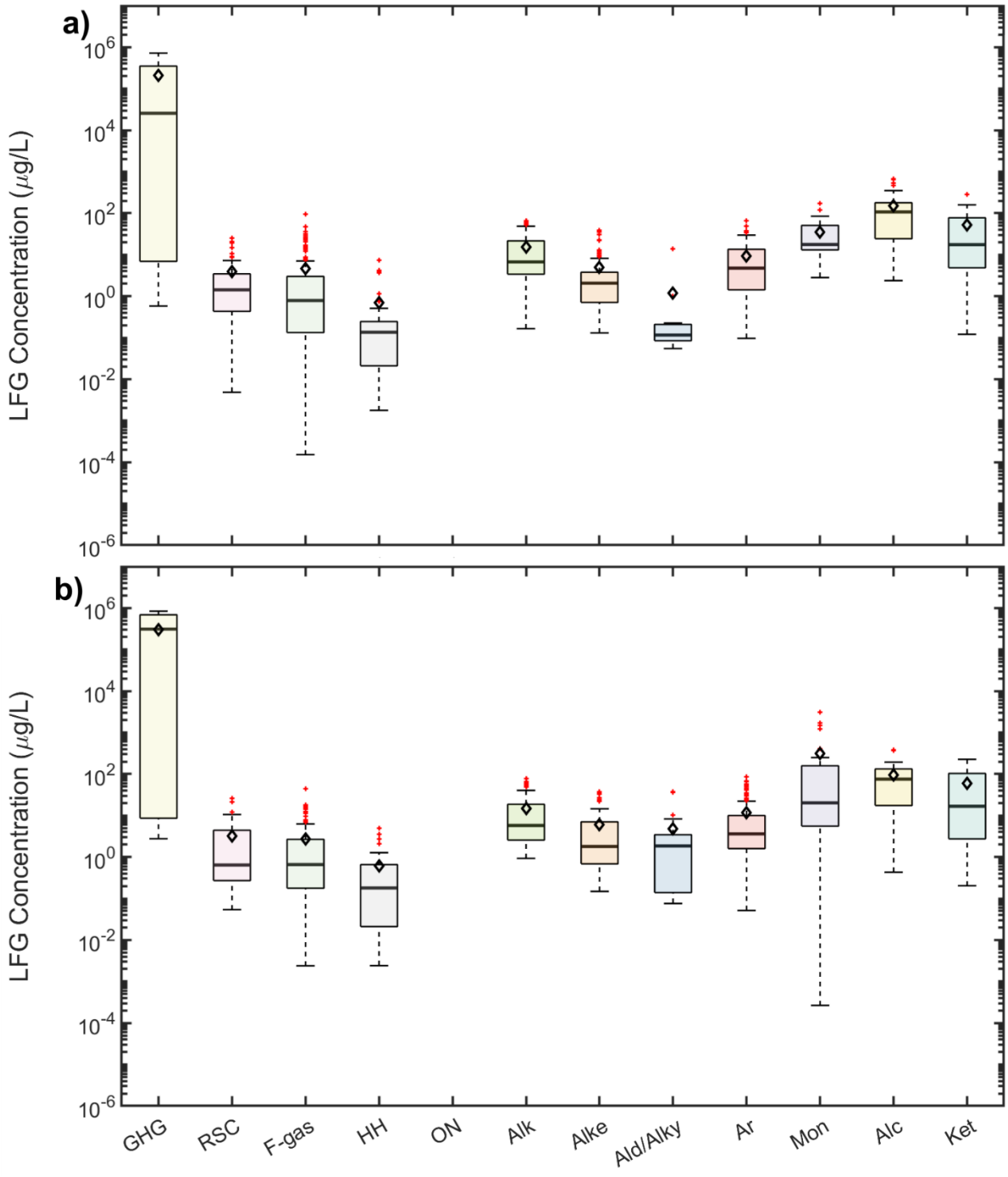

Figure 4.98 summarizes the LFG concentrations as a function of landfill site, where results are presented for methane, nitrous oxide, carbon dioxide, carbon monoxide, and total NMVOCs. LFG concentrations were similar between the sites with the median LFG

concentrations varying less than one to two orders of magnitude. The only exception to this trend was observed for carbon dioxide, where the CO_2 concentrations at Santa Maria Regional Landfill were generally lower than the remaining landfills included in this study (Figure 4.98). Concentrations of the specific gas constituents were generally highest at Site A Landfill and lowest at Santa Maria Regional Landfill. NMVOC concentrations were generally relatively similar across the sites investigated. The mean NMVOC concentrations were higher than the median values calculated. The low differences in LFG concentrations observed between the landfill sites suggest that the waste composition, landfill conditions, and LFG generation mechanisms are relatively similar across the landfills studied, regardless of the differences in operational scale and practice.

Figure 4.98 GHG and NMVOC LFG Concentrations as a Function of Landfill Site (open black diamonds, red lines, solid red dots represent means, medians, and outliers, respectively).

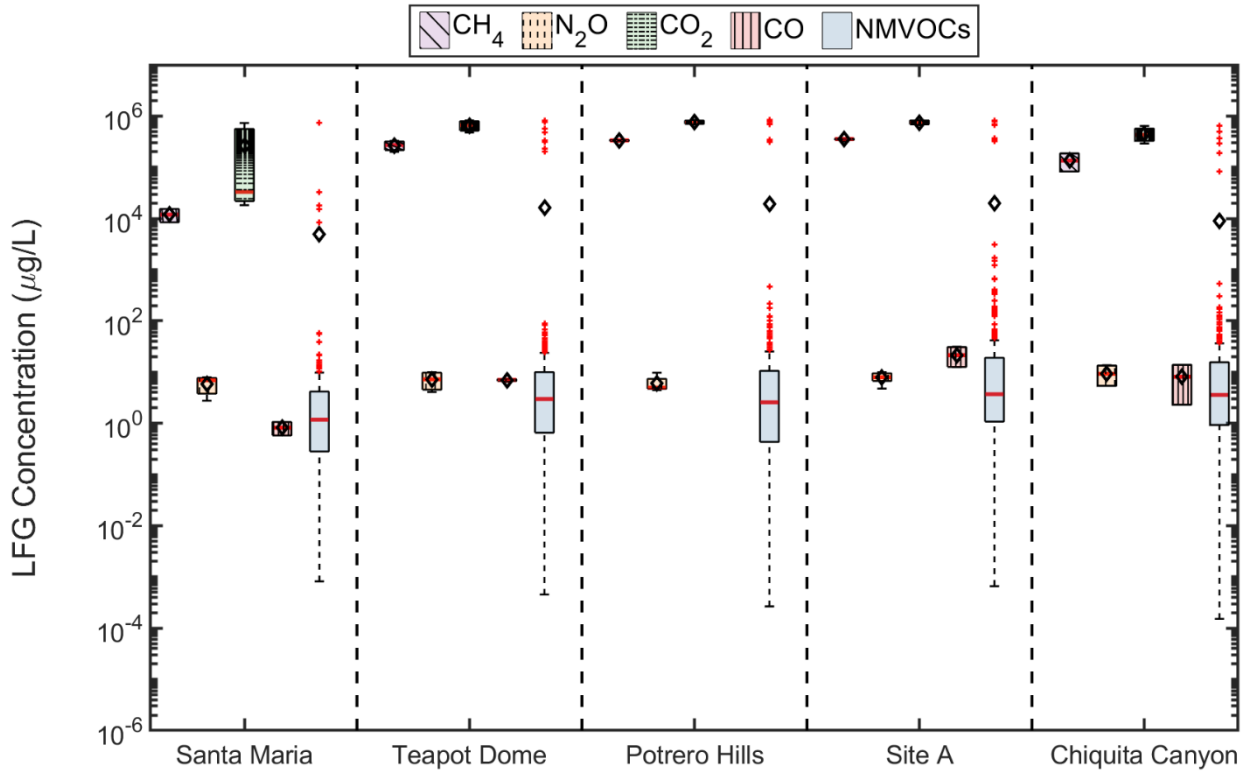

Measured LFG concentrations are compared to ambient LFG concentrations in Figure 4.99. Ambient concentrations were established using the initial (time = 0) concentration datapoints in the flux chamber tests. The raw LFG concentrations were significantly (two to over five orders of magnitude) higher than the ambient concentrations based on differences in median concentrations. The lowest differences were observed for the GHGs. Similar to raw gas data (Figure 4.97), the alcohols, ketones, and alkanes were had the highest ambient concentrations. The organic alkyl nitrates were present in the ambient air at each landfill site (Figure 4.99), yet these chemicals were not detected in

raw gas (Figure 4.97), suggesting potential generation occurring within the cover materials.

Figure 4.99 LFG (darker shading) and Ambient (lighter shading) Concentrations Measured in the a) Dry and b) Wet Seasons by Chemical Family (open black diamonds, black lines, solid red dots represent means, medians, and outliers, respectively).

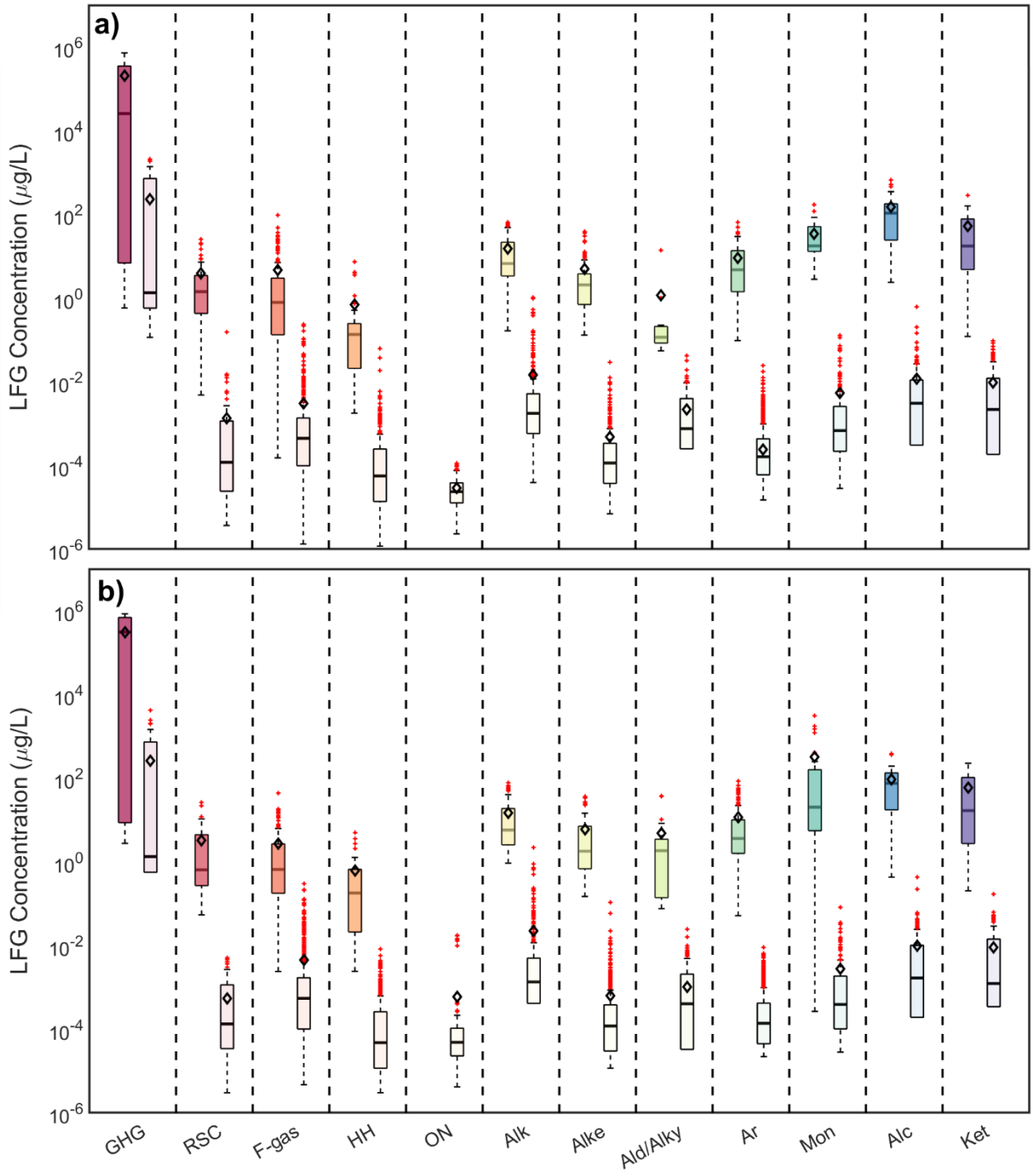

4.12 Temperature Conditions in Covers

Temperatures were measured to determine temperature in tested covers near the ground surface (150 mm depth) at time of testing within each chamber footprint. Also, temperatures were measured with depth at a selected cover location for each of the 5 ground-based testing landfills over seasonal durations. At time of testing, average near-surface temperatures ranged from 10 to 56 °C. Example temperature-time data is presented in Figure 4.100 for Santa Maria Regional Landfill for July 2018 to October 2019. Temperatures are presented for 10, 20, 40, and 80 mm below the ground surface. Maximum and minimum daily air temperatures are also presented. High diurnal variation in temperatures is observed at the shallow depths. This high frequency fluctuation is dampened with depth to where virtually no diurnal fluctuation is present at 40 mm depth. The seasonal variations in temperature are affected by depth with both phase lag (i.e., delay in seasonal peaks) and amplitude decrement (i.e., smaller range of temperatures over seasonal cycles) occurring within the depth of the cover system.

Figure 4.100 Temperature with Time for Various Depths through Interim Cover System at Santa Maria Regional Landfill

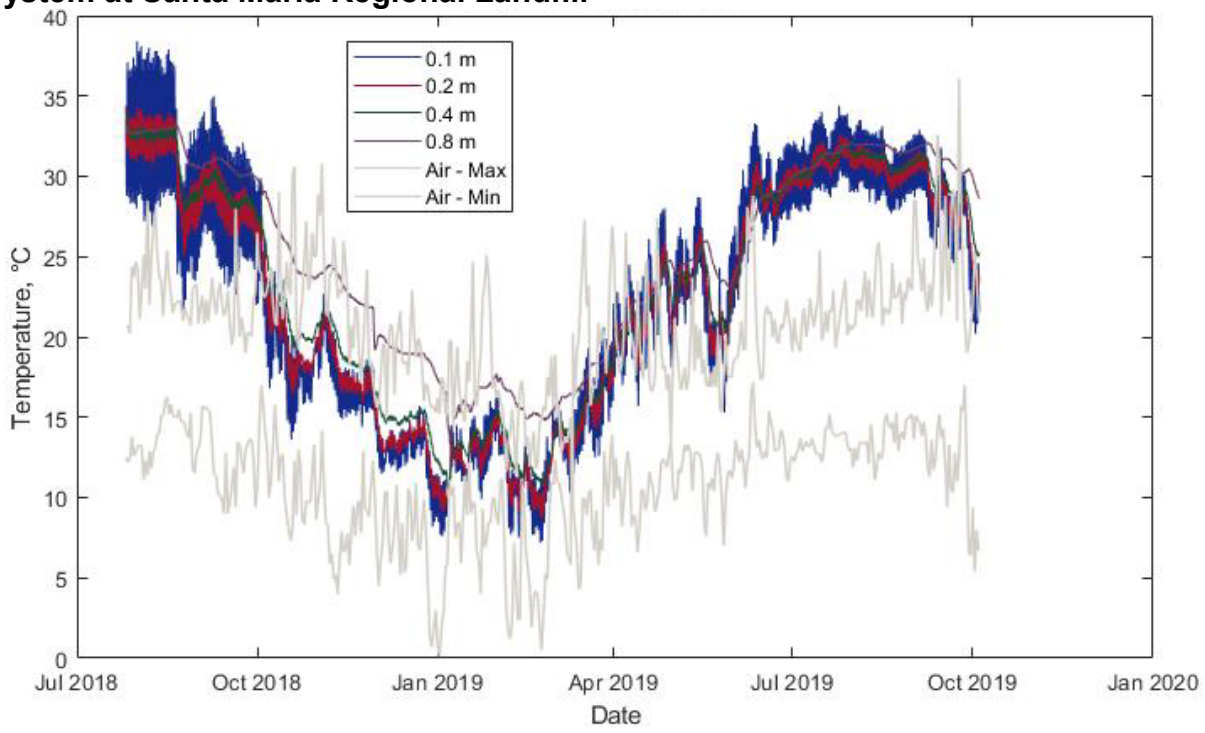

Temperature with depth profiles for the same cover system (and same timeline) are presented in Figure 4.101. All data at each measurement depth are presented to produce an envelope of temperature variation with depth. The seasonal amplitude decrement is present in this plotting domain. Seasonal temperature fluctuation is greatest near the ground surface and decreases with depth. Similar analysis of temperatures was conducted for each of the 5 sites. The range of minimum to maximum temperatures at 10 mm depth over the periods of measurement were 7.2 to

38.4°C for Santa Maria Landfill, 7.6 to 43.4°C for Teapot Dome Landfill, 5.9 to 36.2°C for Potrero Hills Landfill, 7.1 to 39.4°C for Site A Landfill, and 8.3 to 46.3°C for Chiquita Canyon Landfill. The high temperatures in the cover systems (exceeding maximum air temperatures) were partly attributed to warming caused by underlying waste mass (Yesiller et al. 2008). The particularly high temperatures at Chiquita Canyon were attributed to a on old green waste cover (placed for erosion control purposes) overlying interim soil cover.

Figure 4.101 Temperature Variation with Depth for Thermocouple Array within Interim Cover System at Santa Maria Regional Landfill

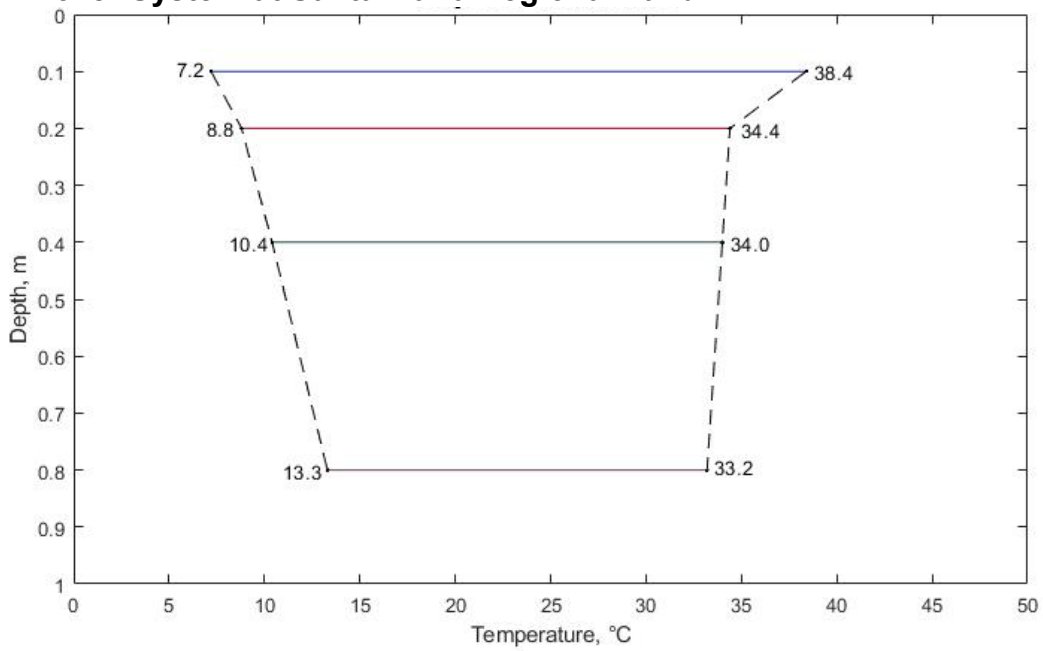

4.13 Additional Static Flux Chamber Investigations

4.13.1 Radial Gas Well Testing Results at SMRL

Figures 4.101 and 4.102 summarize the trends in overall fluxes as a function of the radial distance from the well for both test days. The measured surface flux of the GHGs, both median and mean values, generally increased progressing from near-well locations (0.5 and 1 m radial distance) to the far-field test locations (16 and 32 m radial distance). Negative median GHG fluxes were observed in close proximity of the extraction well on Test Day 1. The variation in GHG fluxes at a given testing location was higher than the variations in NMVOC fluxes at a given location. In general, variations in GHG fluxes with distance from the well was higher than the variations in NMVOC fluxes with distance from the extraction well (Figures 4.101 and 4.102). Overall, the variations in flux with radial distance was detectable, yet relatively low for analysis using directly measured flux data.

Figure 4.102 Influence of Radial Well Distance on a) GHG and b) NMVOC Fluxes at SMRL (Test Day 1).

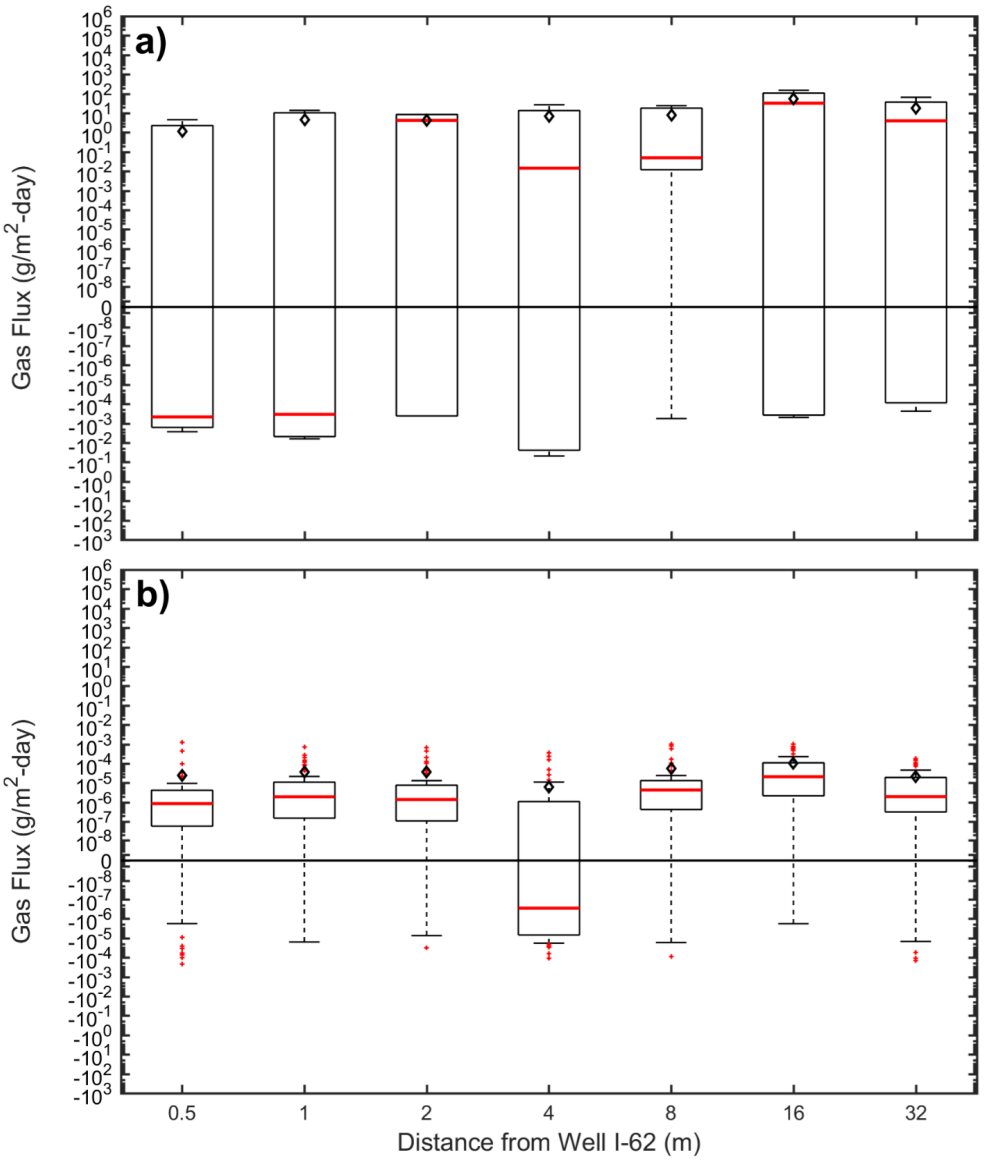

Figure 4.103 Influence of Radial Well Distance on a) GHG and b) NMVOC Fluxes at SMRL (Test Day 2).

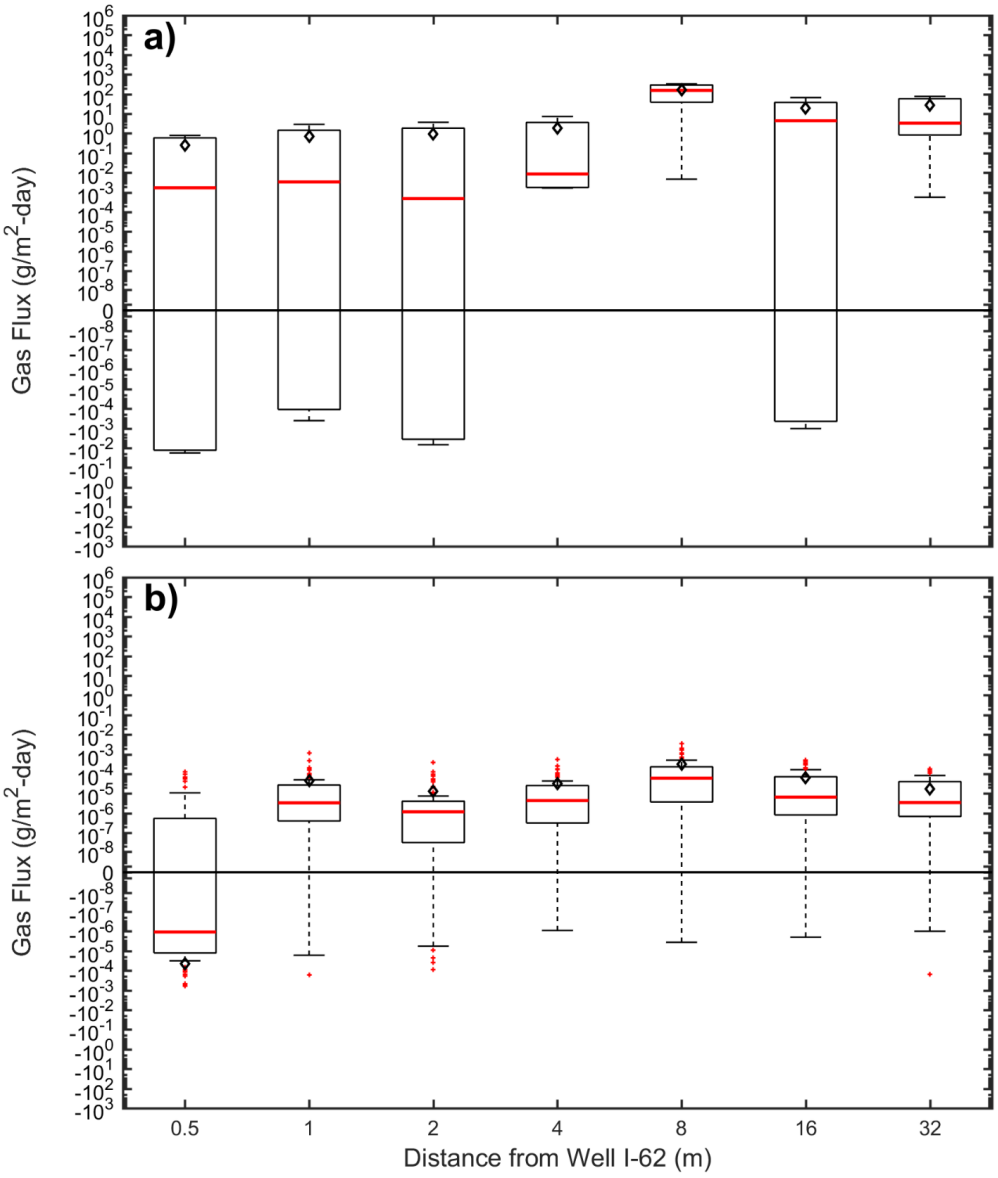

Vacuum pressures of the gas extraction system measured over the two test days are presented in Figure 4.103. During Chamber 3 and 4 tests on both days, the vacuum pressure declined significantly. Variations in cover thickness during the radial well distance tests are presented in Table 4.27. The cover thickness decreased significantly progressing from the near well locations to the farthest test location at 32 m away from the well. High cover thicknesses are used near extraction wells at SMRL to minimize potential intrusion of atmospheric air and fugitive emissions at locations near the annular space of the wells.

Figure 4.104 Variation in Vacuum Pressure Monitored at Well I-62 (shallow) and I-62A (deep) for a) Test Day 1 and b) Test Day 2.

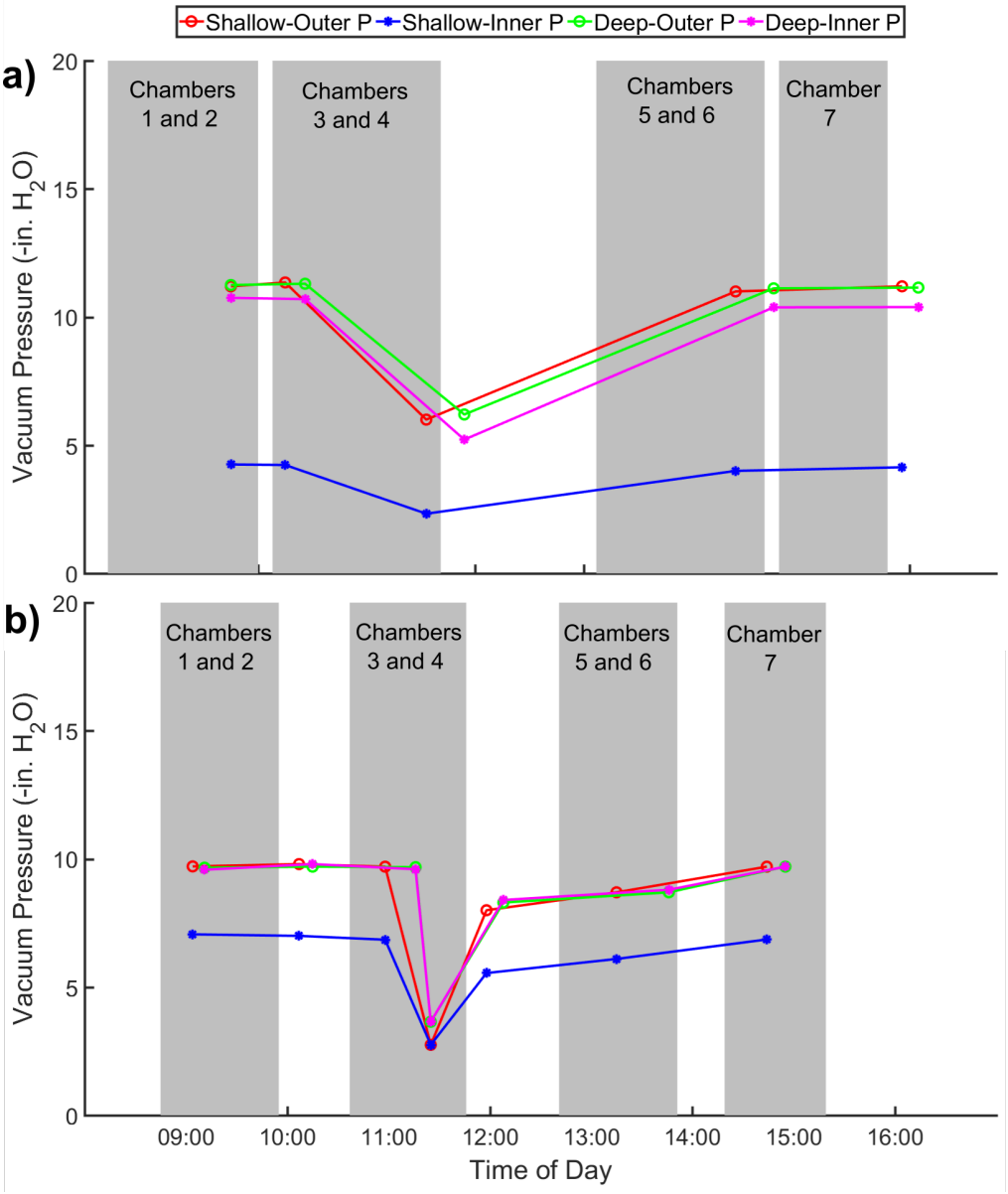

Table 4.31 – Variation in Cover Thickness as a Function of Radial Distance

Chamber Number	Radial Distance (m)	Cover Thickness (cm)
Chamber 1	0.5	125
Chamber 7	1	125
Chamber 2	2	125
Chamber 3	4	109-110
Chamber 4	8	101-102
Chamber 6	16	77-78
Chamber 5	32	61-62

The measured fluxes were adjusted using the vacuum pressure and cover thickness data to analyze variation of flux solely with radial distance without the effects of varying pressure during the tests as well as the varying cover thicknesses at the different measurement locations. Adjustment factors were calculated both for pressure and thickness using the relative ratio of the pressure or thickness at a given location to the maximum pressure and maximum thickness obtained in the investigation, respectively. The measured flux increased with decreasing pressure and decreasing thickness. Measured and adjusted flux data for GHGs and NMVOCs are presented in Tables 4.28 and 4.29, respectively. The adjusted fluxes are presented in Figures 4.104 and 4.105 for Test Days 1 and 2, respectively. The variations between the fluxes with radial distance increased modestly due to the applied adjustment. The adjusted GHG emissions increased from the near-well locations to the far-field test locations with somewhat more variation observed for median fluxes than mean fluxes, in particular for Test Day 1. Similarly, the adjusted NMVOC emissions increased from the near-well locations to the far-field locations with somewhat more variation observed for median fluxes than mean fluxes.

Table 4.32 – Variation in Radial Distance Fluxes for Measured and Adjusted Data (Testing Day 1)

Radial Distance (m)	Measured Mean GHG Flux (g/m^2-day)	ΔP Adjusted Mean GHG Flux (g/m^2-day)	ΔT Adjusted Mean GHG Flux (g/m^2-day)	ΔP+ΔT Adjusted Mean GHG Flux (g/m^2-day)	Measured Median GHG Flux (g/m^2-day)	ΔP Adjusted Median GHG Flux (g/m^2-day)	ΔT Adjusted Median GHG Flux (g/m^2-day)	ΔP+ΔT Adjusted Median GHG Flux (g/m^2-day)
0.5	$1.14x10^{0}$	$1.14x10^{0}$	$1.14x10^{0}$	$-4.68x10^{-4}$	$-4.68x10^{-4}$	$-4.68x10^{-4}$	$-4.68x10^{-4}$	$-4.68x10^{-4}$
1	$4.60x10^{0}$	$4.62x10^{0}$	$4.60x10^{0}$	$-3.42x10^{-4}$	$-3.42x10^{-4}$	$-3.44x10^{-4}$	$-3.42x10^{-4}$	$-3.44x10^{-4}$
2	$4.21x10^{0}$	$4.21x10^{0}$	$4.21x10^{0}$	$4.21x10^{0}$	$4.21x10^{0}$	$4.21x10^{0}$	$4.21 x10^{0}$	$4.21 x10^{0}$
4	$6.72x10^{0}$	$9.79x10^{0}$	$7.55x10^{0}$	$1.61x10^{-2}$	$1.44x10^{-2}$	$2.09x10^{-2}$	$1.61 x10^{-2}$	$2.35 x10^{-2}$
8	$8.03x10^{0}$	$1.17x10^{1}$	$9.54x10^{0}$	$5.87x10^{-2}$	$4.94x10^{-2}$	$7.19x10^{-2}$	$5.87 x10^{-2}$	$8.54 x10^{-2}$
16	$5.38x10^{1}$	$5.46x10^{1}$	$7.43x10^{1}$	$4.48x10^{1}$	$3.25x10^{1}$	$3.30x10^{1}$	$4.48x10^{1}$	$4.55x10^{1}$
32	$1.84x10^{1}$	$1.87x10^{1}$	$2.78x10^{1}$	$6.04x10^{0}$	$4.01x10^{0}$	$4.07x10^{0}$	$6.04x10^{0}$	$6.13x10^{0}$

Table 4.33 – Variation in Radial NMVOC Fluxes for Measured and Adjusted Data (Testing Day 1)

Radial Distance (m)	Measured NMVOC Flux (g/m^2-day)	ΔP Adjusted NMVOC Flux (g/m^2-day)	ΔT Adjusted NMVOC Flux (g/m^2-day)	ΔP+ΔT Adjusted Mean NMVOC Flux (g/m^2-day)	Measured Median NMVOC Flux (g/m^2-day)	ΔP Adjusted Median NMVOC Flux (g/m^2-day)	ΔT Adjusted Median NMVOC Flux (g/m^2-day)	ΔP+ΔT Adjusted Median NMVOC Flux (g/m^2-day)
0.5	$2.39x10^{-5}$	$2.39x10^{-5}$	$2.39x10^{-5}$	$2.39x10^{-5}$	$8.61x10^{-7}$	$8.61x10^{-7}$	$8.61x10^{-7}$	$8.61x10^{-7}$
1	$3.61x10^{-5}$	$3.63x10^{-5}$	$3.61x10^{-5}$	$3.63x10^{-5}$	$1.93x10^{-6}$	$1.94x10^{-6}$	$1.93x10^{-6}$	$1.94x10^{-6}$
2	$3.79x10^{-5}$	$3.79x10^{-5}$	$3.7x10^{-5}$	$3.79x10^{-5}$	$1.39x10^{-6}$	$1.39x10^{-6}$	$1.39x10^{-6}$	$1.39x10^{-6}$
4	$6.24x10^{-6}$	$9.10x10^{-6}$	$7.02 x10^{-6}$	$1.02x10^{-5}$	$-2.84x10^{-7}$	$-4.14x10^{-7}$	$-3.20x10^{-7}$	$-4.66x10^{-7}$
8	$5.64x10^{-5}$	$8.21x10^{-5}$	$6.70x10^{-5}$	$9.75x10^{-5}$	$4.36x10^{-6}$	$6.35x10^{-6}$	$5.18x10^{-6}$	$7.54x10^{-6}$
16	$1.04x10^{-4}$	$1.06x10^{-4}$	$1.44x10^{-4}$	$1.46x10^{-4}$	$2.11x10^{-5}$	$2.14x10^{-5}$	$2.91x10^{-5}$	$2.95x10^{-5}$
32	$2.15x10^{-5}$	$2.18x10^{-5}$	$3.24x10^{-5}$	$3.28x10^{-5}$	$1.97x10^{-6}$	$2.00x10^{-6}$	$2.97x10^{-6}$	$3.01x10^{-6}$

Figure 4.105 Adjusted Radial Flux Data for a) GHG and b) NMVOC Fluxes at SMRL (Test Day 1).

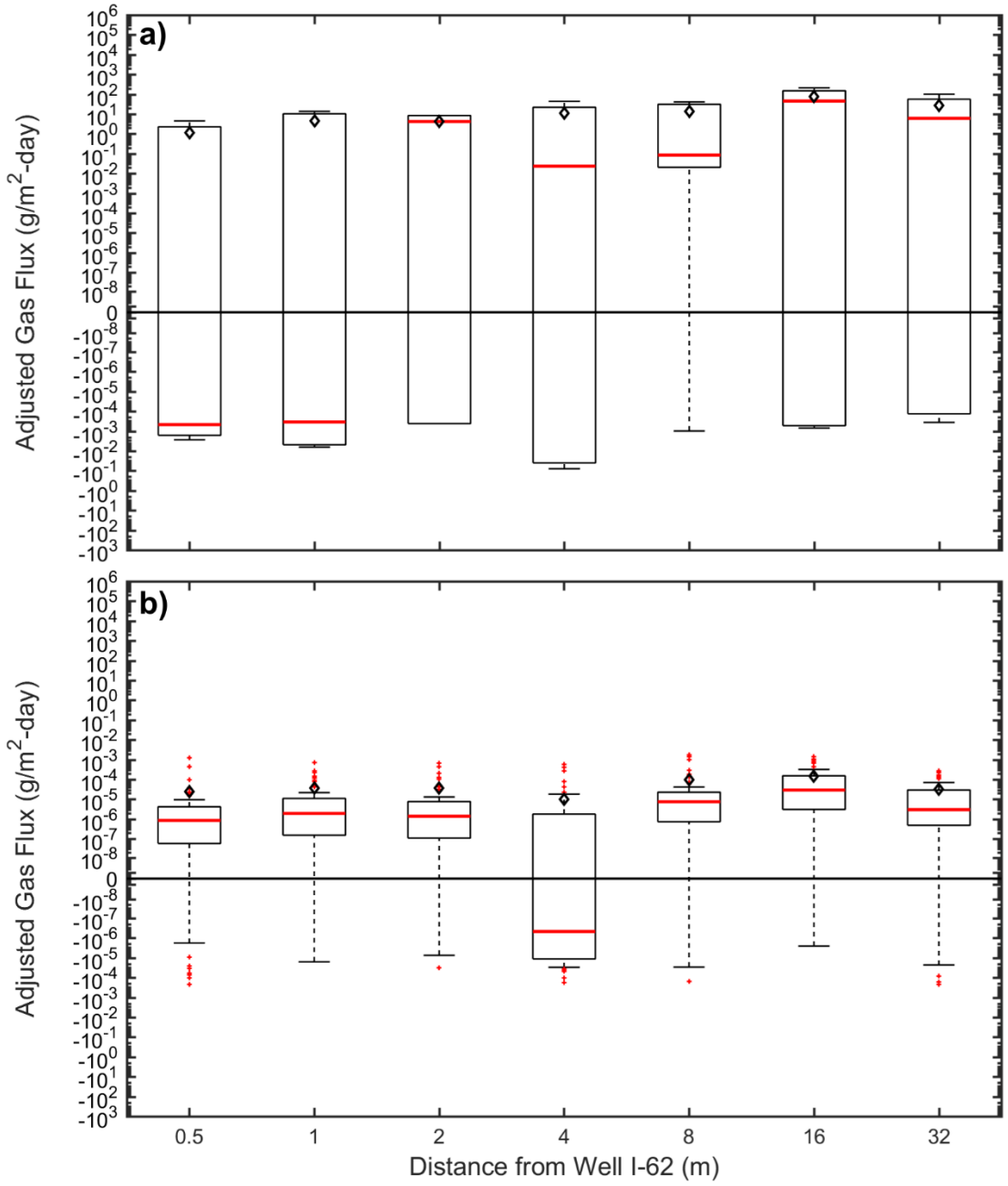

Figure 4.106 Measured and Adjusted Radial Flux Data for a) GHG and b) NMVOC Fluxes at SMRL (Test Day 1).

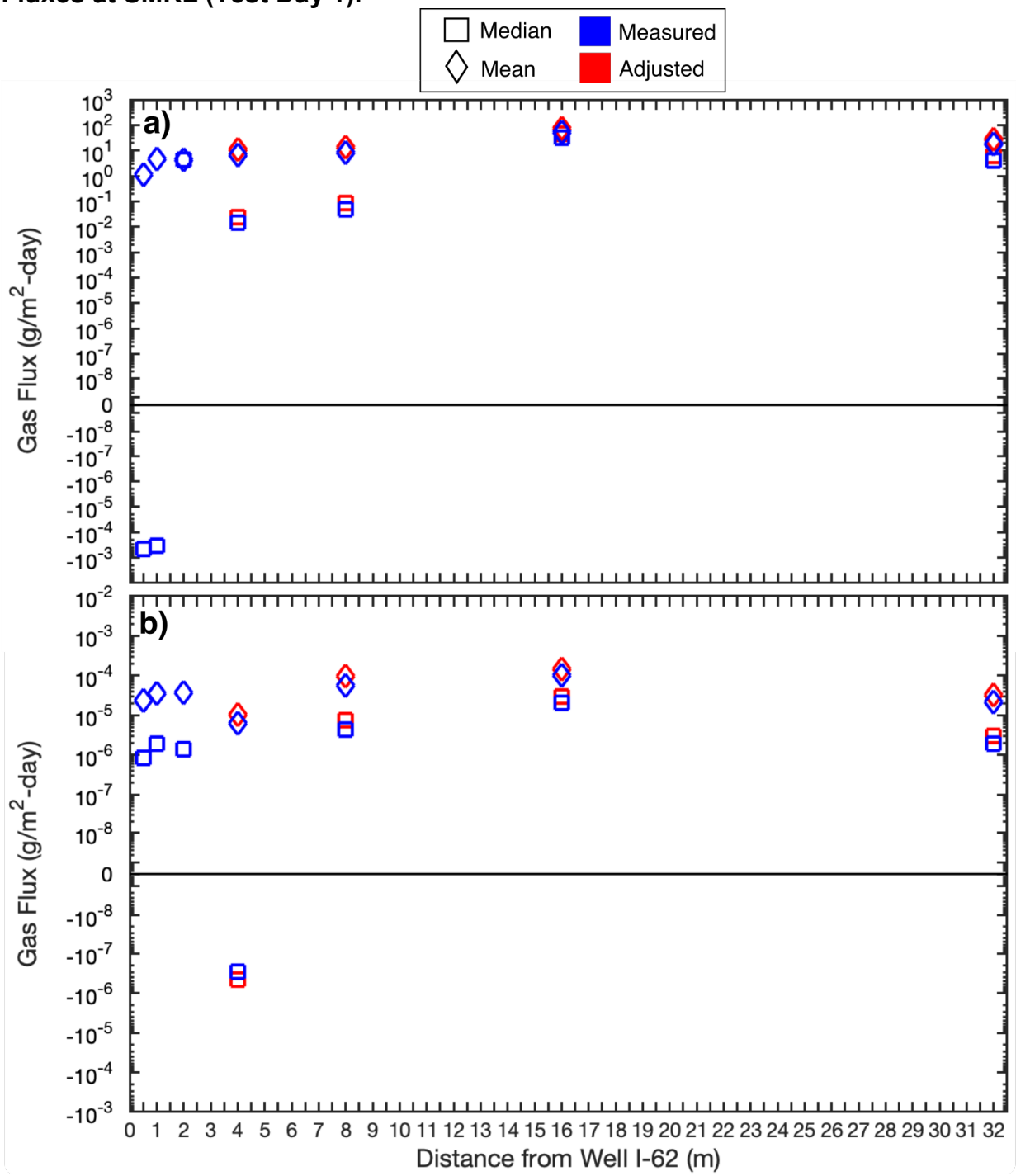

Figure 4.107 Adjusted Radial Flux Data for a) GHG and b) NMVOC Fluxes at SMRL (Test Day 2).

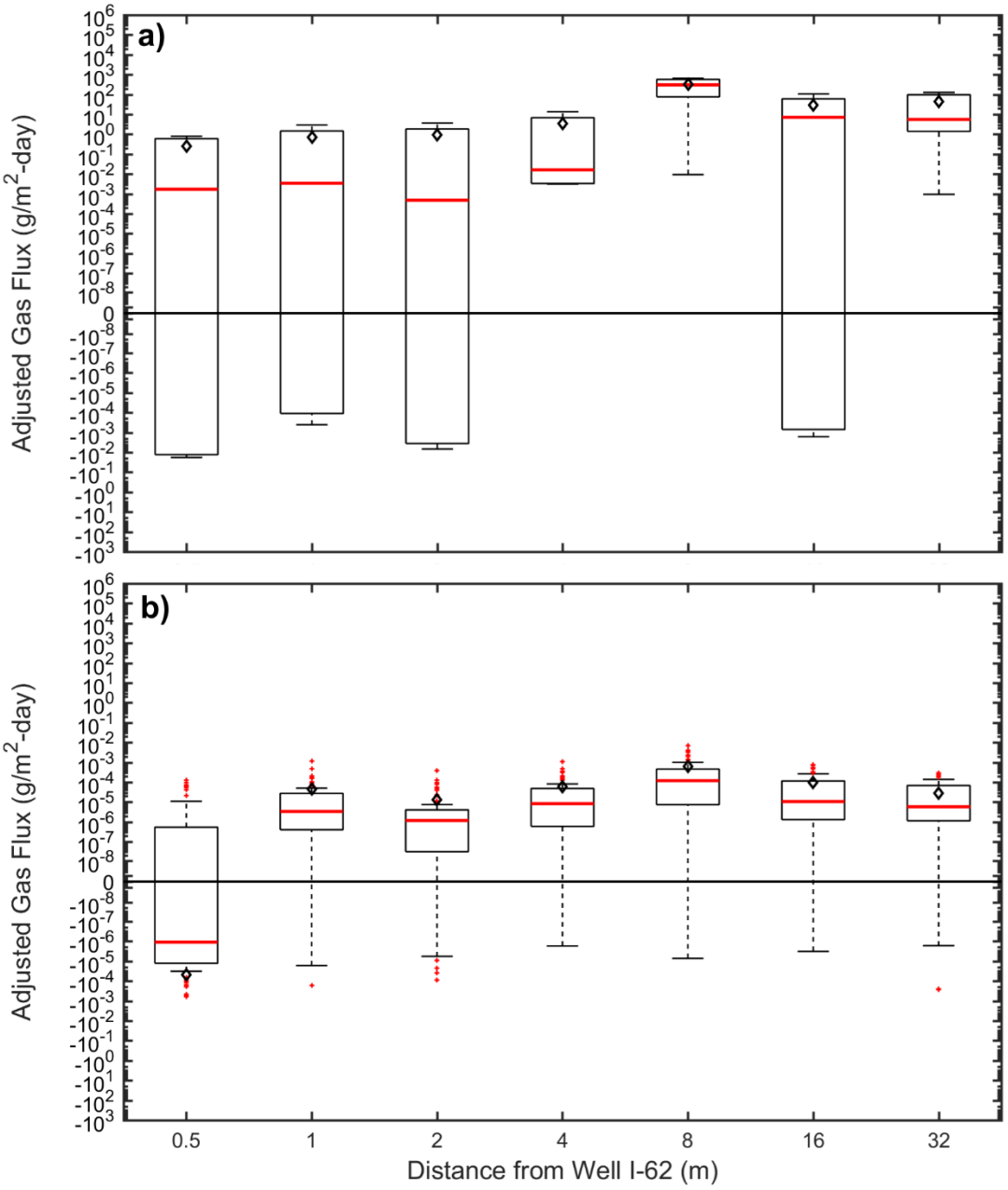

4.13.2 Cover Thickness Testing Results at SMRL

The results of the cover thickness field investigation are presented in Figure 4.107. The median GHG fluxes increased significantly as the intermediate cover thickness decreased from 1.2 m to 0.9 m. For the cover thickness of 1.2 m, the median GHG flux was negative, indicating net uptake from the atmosphere over emissions to the atmosphere, whereas the median GHG fluxes were positive for all lower thicknesses. The average fluxes were all positive and the variation between average GHG fluxes were low between the different thickness measurements. The variation of NMVOC

fluxes was low for a given cover thickness and the variation in NMVOC fluxes between different cover thicknesses also was relatively low, with the lowest NMVOC fluxes observed for the 1.2 m cover thickness.

Figure 4.108 Influence of Cover Thickness on a) GHG and b) NMVOC Fluxes at SMRL.

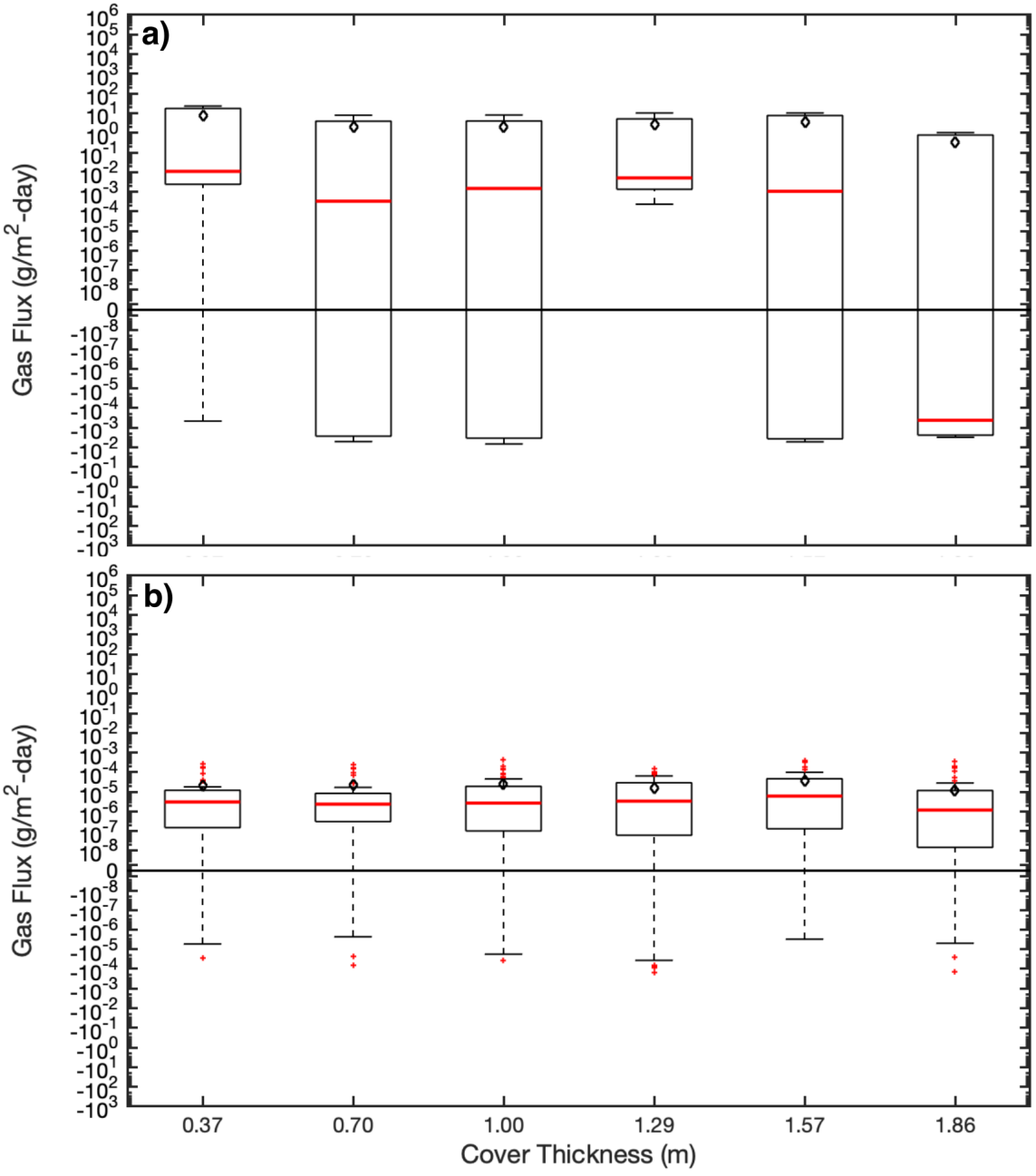

Vacuum pressures of the gas extraction system measured during the thickness tests are presented in Figure 4.108. The pressure was observed to decrease significantly during the 0.61-m cover thickness tests. The pressure was relatively steady during the remaining five thickness tests.

Figure 4.109 Variation in Vacuum Pressure Monitored at Well I-39 (shallow) and I-39A (deep) for the Cover Thickness Testing Program at the SMRL.

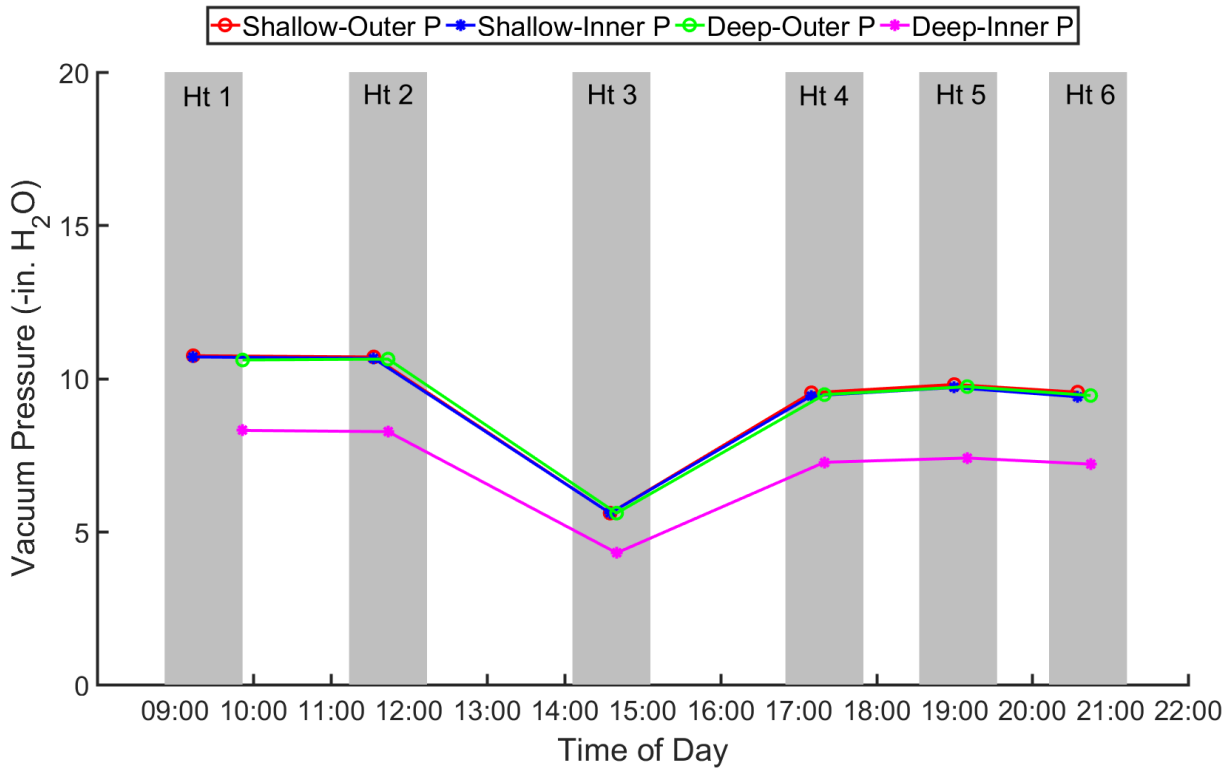

The measured fluxes were adjusted using the vacuum pressure data to analyze variation of flux solely with cover thickness without the effects of varying pressure during the tests. Adjustment factors were calculated for pressure using the relative ratio of the pressure for a given thickness to the maximum pressure obtained in the investigation. The measured flux increased with decreasing pressure from the maximum value. The adjusted fluxes are presented in Table 4.30, Figure 4.109, and Figure 4.110. The adjusted flux data demonstrated modest variations from the measured data with GHG fluxes varying more with cover thickness than NMVOC fluxes.

Table 4.34 – Variation in Cover Thickness Fluxes for Measured and Adjusted GHG and NMVOC Data

Cover Thickness (m)	Measured Mean GHG Flux (g/m^2-day)	ΔP Adjusted Mean GHG Flux (g/m^2-day)	Measured Mean NMVOC Flux (g/m^2-day)	ΔP Adjusted Mean NMVOC Flux (g/m^2-day)	Measured Median GHG Flux (g/m^2-day)	ΔP Adjusted Median GHG Flux (g/m^2-day)	Measured Median NMVOC Flux (g/m^2-day)	ΔP Adjusted Median NMVOC Flux (g/m^2-day)
0.37	$7.74x10^{0}$	$8.59x10^{0}$	$2.08x10^{-5}$	$2.31x10^{-5}$	$1.10x10^{-2}$	$1.23x10^{-2}$	$3.10x10^{-6}$	$3.44x10^{-6}$
0.70	$1.97x10^{0}$	$2.13x10^{0}$	$2.24x10^{-5}$	$2.43x10^{-5}$	$3.32x10^{-4}$	$3.60x10^{-4}$	$2.37x10^{-6}$	$2.57x10^{-6}$
1.00	$2.01x10^{0}$	$2.23x10^{0}$	$2.62x10^{-5}$	$2.91x10^{-5}$	$1.49x10^{-3}$	$1.65x10^{-3}$	$2.70x10^{-6}$	$3.00x10^{-6}$
1.29	$2.57x10^{0}$	$3.79x10^{0}$	$1.59x10^{-5}$	$2.34x10^{-5}$	$5.07x10^{-3}$	$7.48x10^{-3}$	$3.39x10^{-6}$	$5.01x10^{-6}$

Cover Thickness (m)	Measured Mean GHG Flux (g/m^2-day)	ΔP Adjusted Mean GHG Flux (g/m^2-day)	Measured Mean NMVOC Flux (g/m^2-day)	ΔP Adjusted Mean NMVOC Flux (g/m^2-day)	Measured Median GHG Flux (g/m^2-day)	ΔP Adjusted Median GHG Flux (g/m^2-day)	Measured Median NMVOC Flux (g/m^2-day)	ΔP Adjusted Median NMVOC Flux (g/m^2-day)
1.57	$3.39x10^{0}$	$3.39x10^{0}$	$3.58x10^{-5}$	$3.58x10^{-5}$	$1.07x10^{-3}$	$1.07x10^{-3}$	$6.17x10^{-6}$	$6.17x10^{-6}$
1.86	$3.42x10^{-1}$	$3.42x10^{-1}$	$1.22x10^{-5}$	$1.22x10^{-5}$	$-4.18x10^{-4}$	$-4.18x10^{-4}$	$1.19x10^{-6}$	$1.19x10^{-6}$

Figure 4.110 Adjusted Cover Thickness Data for a) GHG and b) NMVOC Fluxes at SMRL.

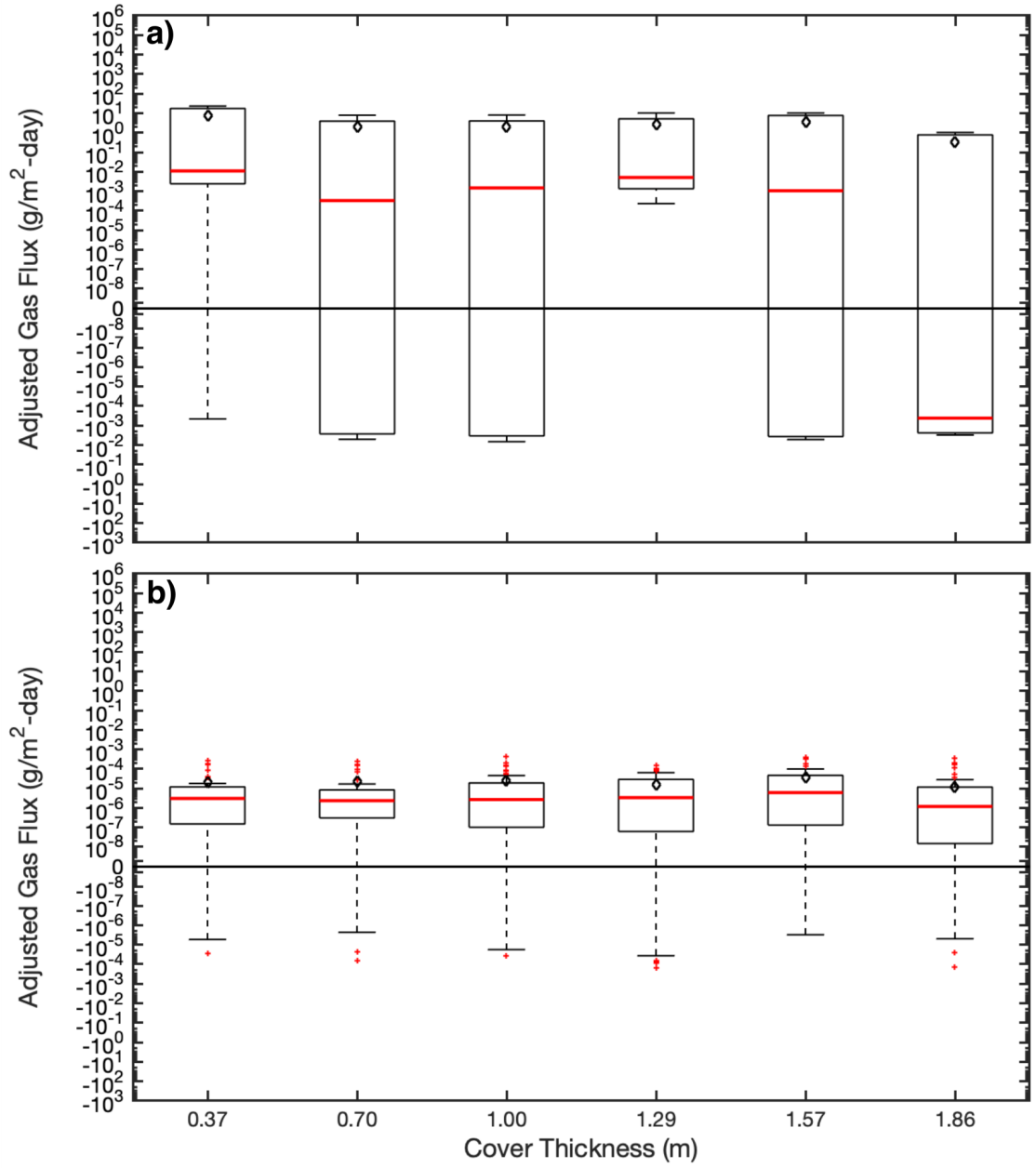

Figure 4.111 Measured and Adjusted Cover Thickness Flux Data for a) GHG and b) NMVOC Fluxes at SMRL.

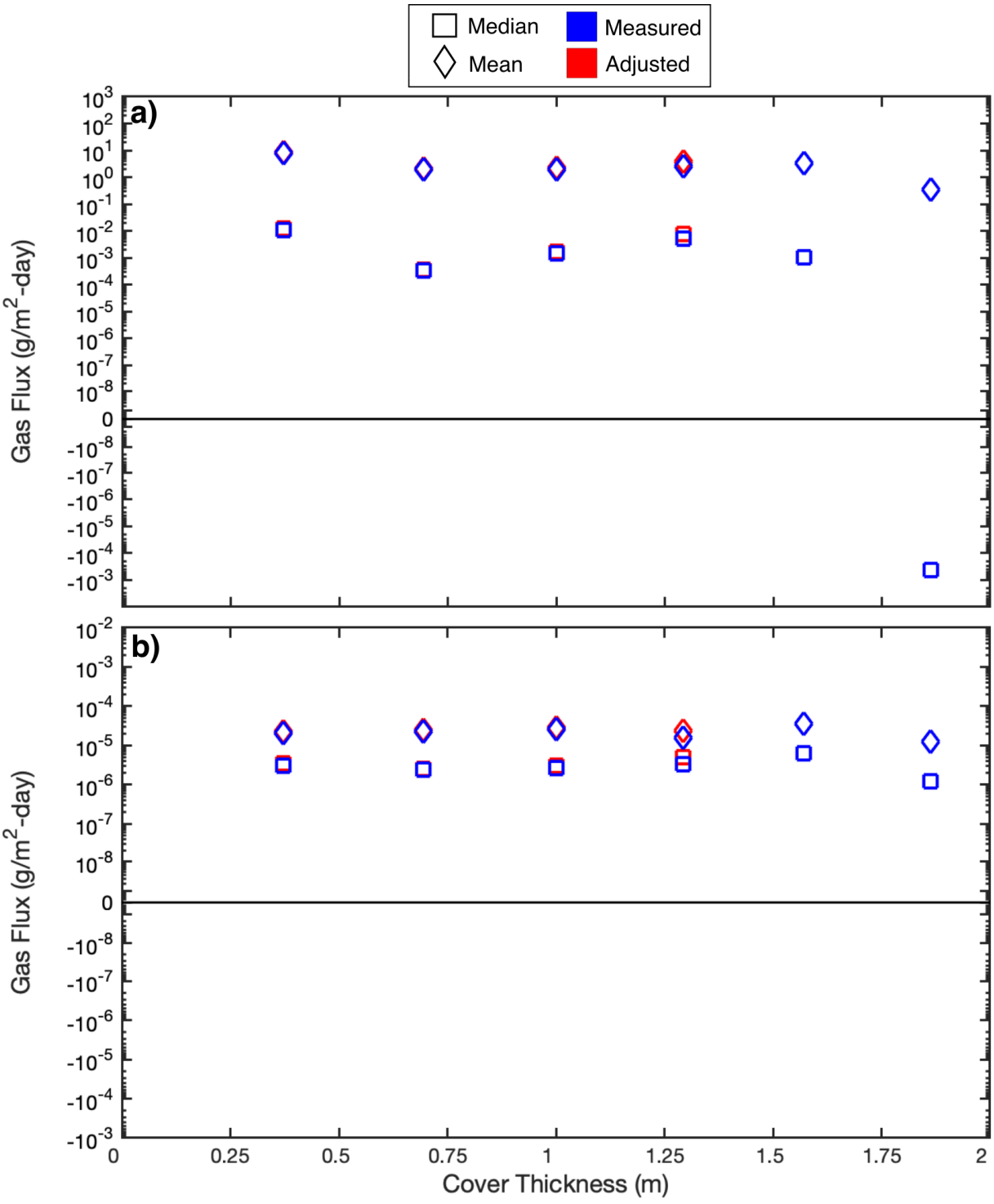

4.13.3 Temporal Surface Flux Variability Testing Results at SMRL

The GHG and NMVOC flux testing results for the temporal testing program are presented in Figure 4.111. For GHGs, based on median values, the daytime

measurements including the 1:15 PM measurement on October 21 and 1:30 PM measurement on October 25 were similar. The 6:30 PM measurement on October 25 also was in line with the midday measurements. The early morning measurement and the overnight measurement were higher than the daytime measurements. The mean fluxes at the different testing times were relatively similar over the five different measurement times. For NMVOCs, based on median values, the measurements were relatively similar except for the 1:30 PM measurement on October 25. The early morning and overnight measurement were somewhat higher than the daytime measurements. The mean NMVOC fluxes at the different testing times were relatively similar over the five different measurement times with slightly higher fluxes for the early morning and overnight measurements.

Figure 4.112 Results of the Temporal Flux Variability Testing for a) GHGs and b) NMVOCs at the SMRL during the Dry Season.

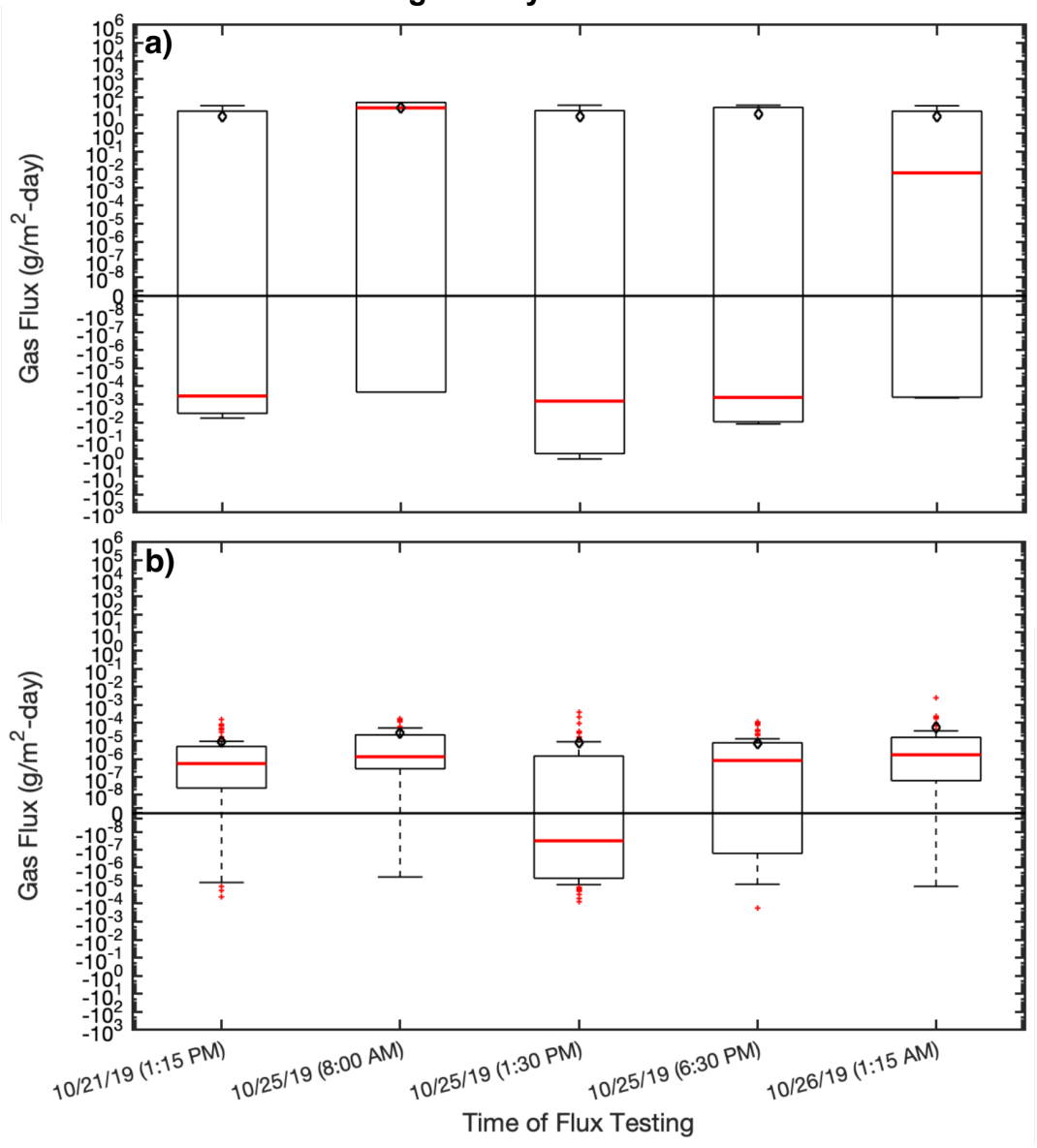

Diurnal variations in flux are assessed using 1:30 PM measurements on October 25 and 1:30 AM measurements on October 26. In line with the overall temporal flux variations described in the previous paragraph, fluxes of both NMVOCs and GHGs increased during the nighttime hours, where a larger difference was observed for the GHGs than the NMVOCs (Figure 4.111). For midday and overnight hours, the median flux for overall GHGs and NMVOCs were -6.73×10^{-4} to 6.44×10^{-3} as well as -3.26x10-8 to 1.73×10^{-6} g/m^2-day, respectively. For midday and overnight hours, the mean flux for overall GHGs and NMVOCs were 8.76×10^{0} to 8.44×10^{0} and 8.38×10^{-6} to 5.39×10^{-5} g/m^2-day, respectively. The variations in flux values likely resulted from a combination of variations in temperature, barometric pressure, and atmospheric chemistry. Optimum methane oxidation rates were associated with temperatures similar to the daytime temperatures (Figure 4.112) observed at the site, with significantly reduced oxidation rates at lower temperatures in line with nighttime temperatures at SMRL (Boeckx and van Cleemput 1996, Börjesson and Svensson 1997b). Barometric pressure was lower during nighttime (99.8 kPa) measurements than the daytime measurements (100.2 kPa) resulting in increased nighttime flux values. Atmospheric mixing is expected to be greater during the daytime, whereas nighttime is generally consistent with atmospheric stability (Yokouchi and Ambe 1988). Atmospheric hydroxylation (by OH radicals primarily) is more prominent in the daytime hours (when OH is produced from sunlight) (Mellouki et al. 2015). Increased transfer of gases from the ground surface to the troposphere and hydroxylation occurring during the daytime may have reduced ambient NMVOC concentrations near the surface of the landfill (depending on the reactivity of the NMVOC family among other factors).

The measured fluxes were adjusted using the vacuum pressure data (Table 4.31 and Figure 4.113) to analyze variation of flux solely with time without the effects of varying pressure during the tests. Adjustment factors were calculated for pressure using the relative ratio of the pressure at a given location to the maximum pressure obtained in the investigation. The measured flux increased with decreasing pressure. Measured and adjusted flux data for median and mean GHGs and NMVOCs are presented in Table 4.31. The trends observed for the measured and adjusted data were similar with somewhat more pronounced variations between flux values for the adjusted data (Table 4.31).

Table 4.35 – Variation in Temporal Fluxes for Measured and Adjusted Data GHG and NMVOC Data

Date and Time	Measured Mean GHG Flux (g/m^2-day)	ΔP Adjusted Mean GHG Flux (g/m^2-day)	Measured Mean NMVOC Flux (g/m^2-day)	ΔP Adjusted Mean NMVOC Flux (g/m^2-day)	Measured Median GHG Flux (g/m^2-day)	ΔP Adjusted Median GHG Flux (g/m^2-day)	Measured Median NMVOC Flux (g/m^2-day)	ΔP Adjusted Median NMVOC Flux (g/m^2-day)
10/21/19 1:13 PM	8.55×10^{0}	9.00×10^{0}	9.12×10^{-6}	9.59×10^{-6}	-3.50×10^{-4}	-3.68×10^{-4}	5.64×10^{-7}	5.93×10^{-7}
10/25/19 7:55 AM	2.58×10^{1}	2.68×10^{1}	2.74×10^{-5}	2.84×10^{-5}	2.58×10^{1}	2.68×10^{1}	1.33×10^{-6}	1.38×10^{-6}
10/25/19 1:34 PM	8.76×10^{0}	9.26×10^{0}	8.38×10^{-6}	8.85×10^{-6}	-6.73×10^{-4}	-7.11×10^{-4}	-3.26×10^{-8}	-3.44×10^{-8}

Date and Time	Measured Mean GHG Flux (g/m^2-day)	ΔP Adjusted Mean GHG Flux (g/m^2-day)	Measured Mean NMVOC Flux (g/m^2-day)	ΔP Adjusted Mean NMVOC Flux (g/m^2-day)	Measured Median GHG Flux (g/m^2-day)	ΔP Adjusted Median GHG Flux (g/m^2-day)	Measured Median NMVOC Flux (g/m^2-day)	ΔP Adjusted Median NMVOC Flux (g/m^2-day)
10/25/19 7:43 PM	$1.20x10^{1}$	$1.20x10^{1}$	$7.05x10^{-6}$	$7.05x10^{-6}$	$-4.20x10^{-4}$	$-4.20x10^{-4}$	$8.35x10^{-7}$	$8.35x10^{-7}$
10/26/19 2:16 AM	$8.44x10^{0}$	$8.65x10^{0}$	$5.39x10^{-5}$	$5.53x10^{-5}$	$6.44x10^{-3}$	$6.60x10^{-3}$	$1.73x10^{-6}$	$1.77x10^{-6}$

Figure 4.113 Variation in a) Vacuum Pressure at Shallow and Deep Waste Layers and b) Soil and Air Temperatures for the Temporal Testing Program at SMRL.

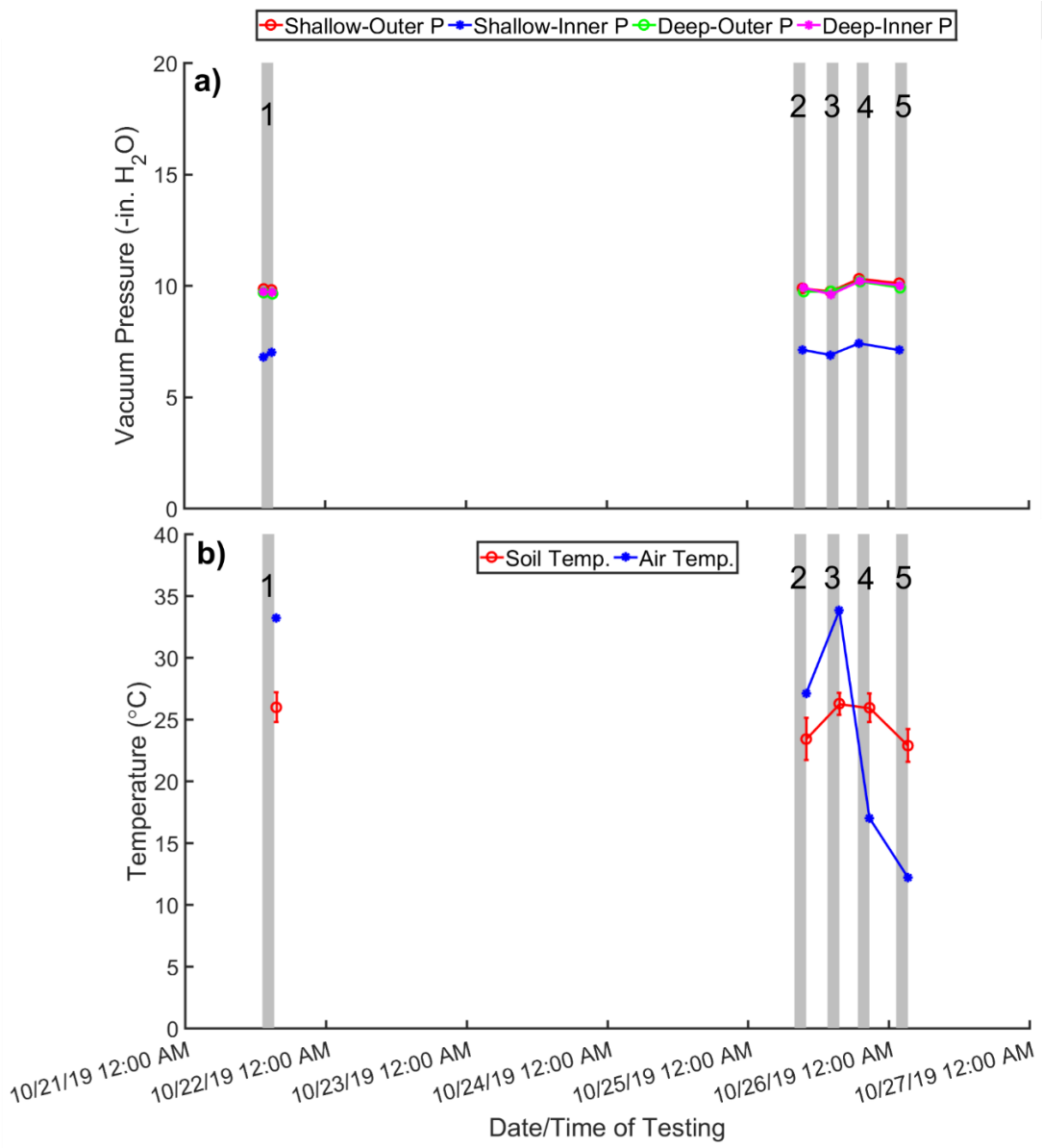

Figure 4.114 Measured and Adjusted Temporal Flux Data for a) GHG and b) NMVOC Fluxes at SMRL.

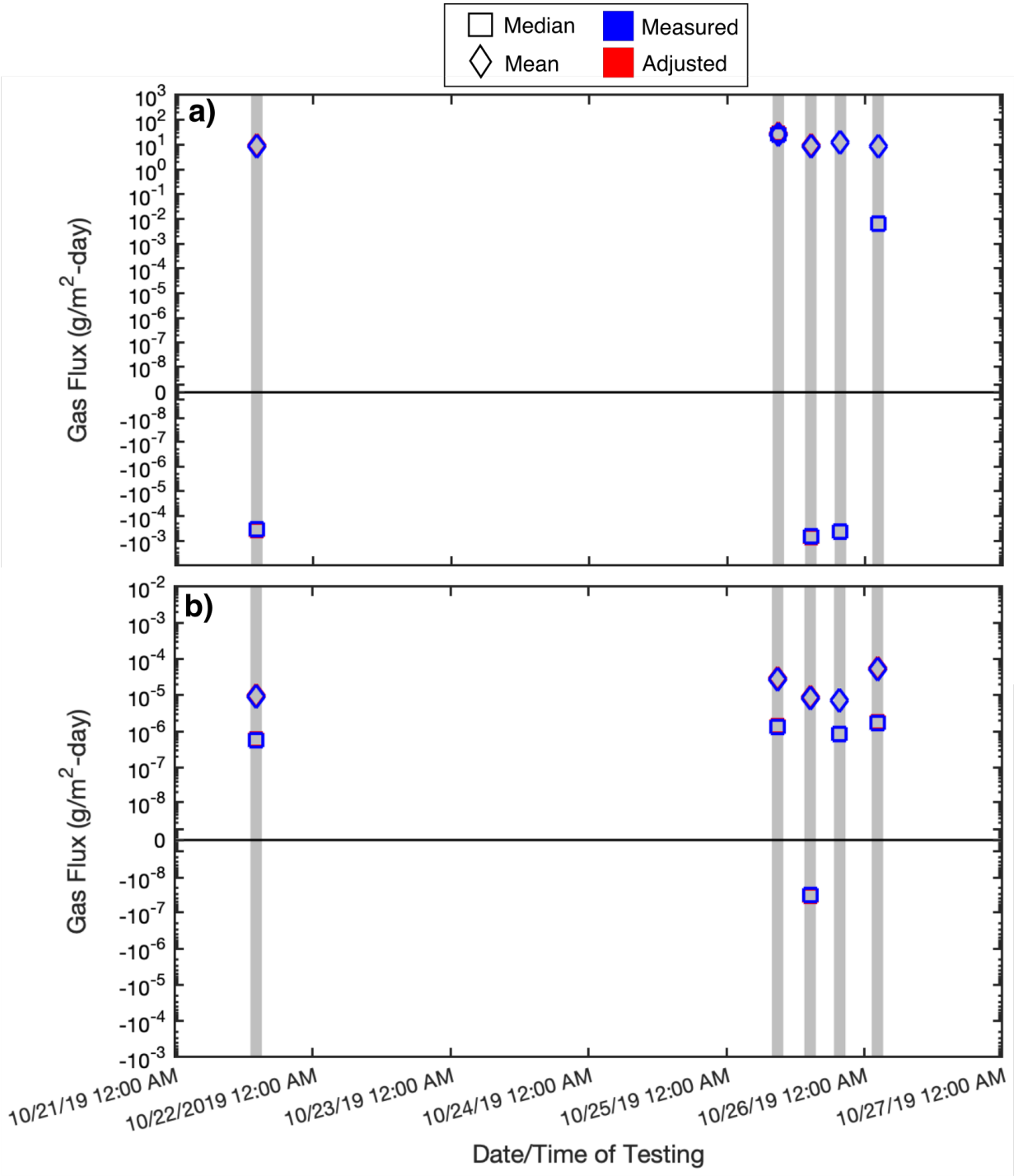

4.13.4 Contaminated, Non-Hazardous Soils Testing Results at SMRL

Figure 4.114 presents box plots by chemical family summarizing the flux measurements conducted across the extended daily and final cover testing locations at the NHIS portion of Santa Maria Regional Landfill during the dry season. Similar to

the MSW testing at SMRL as well as at the other four ground-testing sites, the highest fluxes were observed for GHGs. Following GHG fluxes, the alcohols, ketones, and aldehydes/alkynes had the highest fluxes (Figure 4.114). With the exception of the aldehydes/alkynes, the highly emitting NMVOC chemical families are not directly linked to volatile organic compounds derived from crude oil. The aromatics, alkanes, and alkenes likely were directly related to the petroleum hydrocarbons contained in crude oil. The variability in measured fluxes was generally higher for the aromatics and ketones, which demonstrated some probability of uptake over emissions as the IQR extended below zero.

Figure 4.115 Measured Fluxes at the NHIS Cells at Santa Maria Regional Landfill by Chemical Family in the Dry Season (open black diamonds, red lines, and solid red dots represent means, medians, and outliers, respectively).

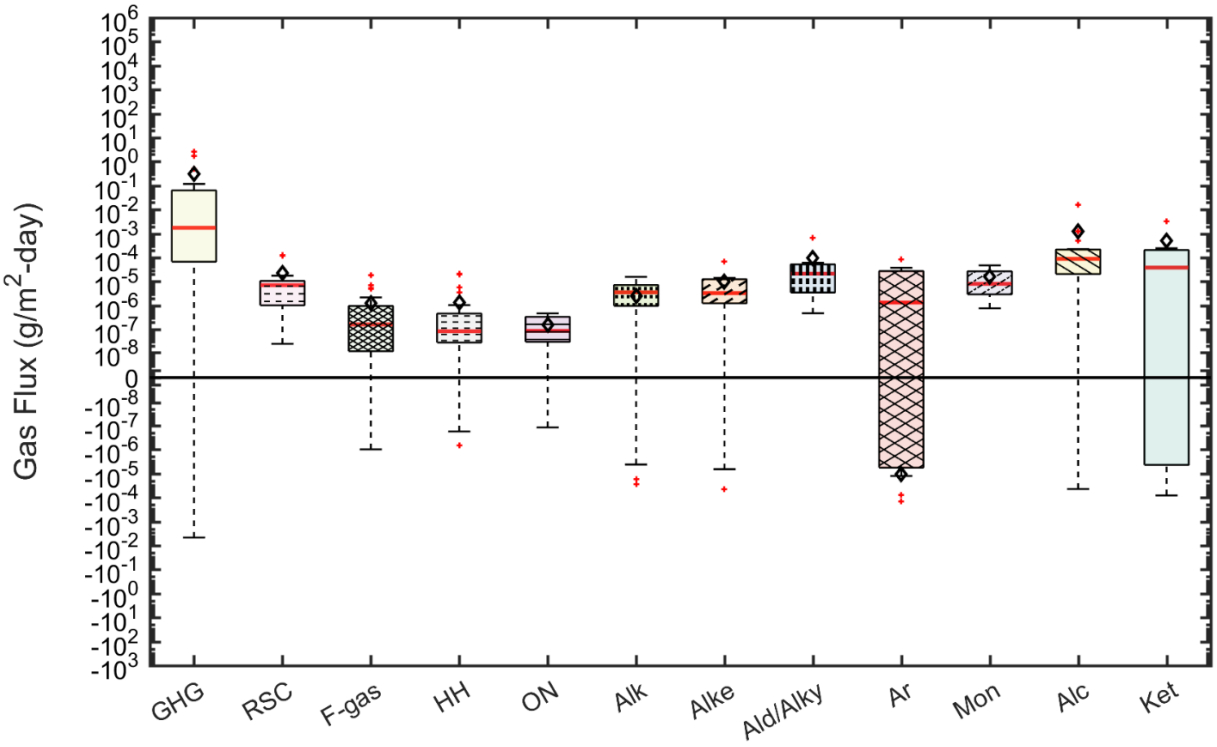

Fluxes by cover category from the NHIS cells are presented in Figure 4.115. Net uptake of methane was more probable over emissions for both of the cover categories tested. Methane and nitrous oxide fluxes were generally higher from the final cover than the extended daily cover. Based on median values presented in Figure 4.115, the NMVOC fluxes were generally higher from the final cover than the extended daily cover.

Figure 4.116 Measured Fluxes by Cover Category at the NHIS Cells at Santa Maria Regional Landfill in the Dry Season (open black diamonds, red lines, and solid red dots represent means, medians, and outliers, respectively).

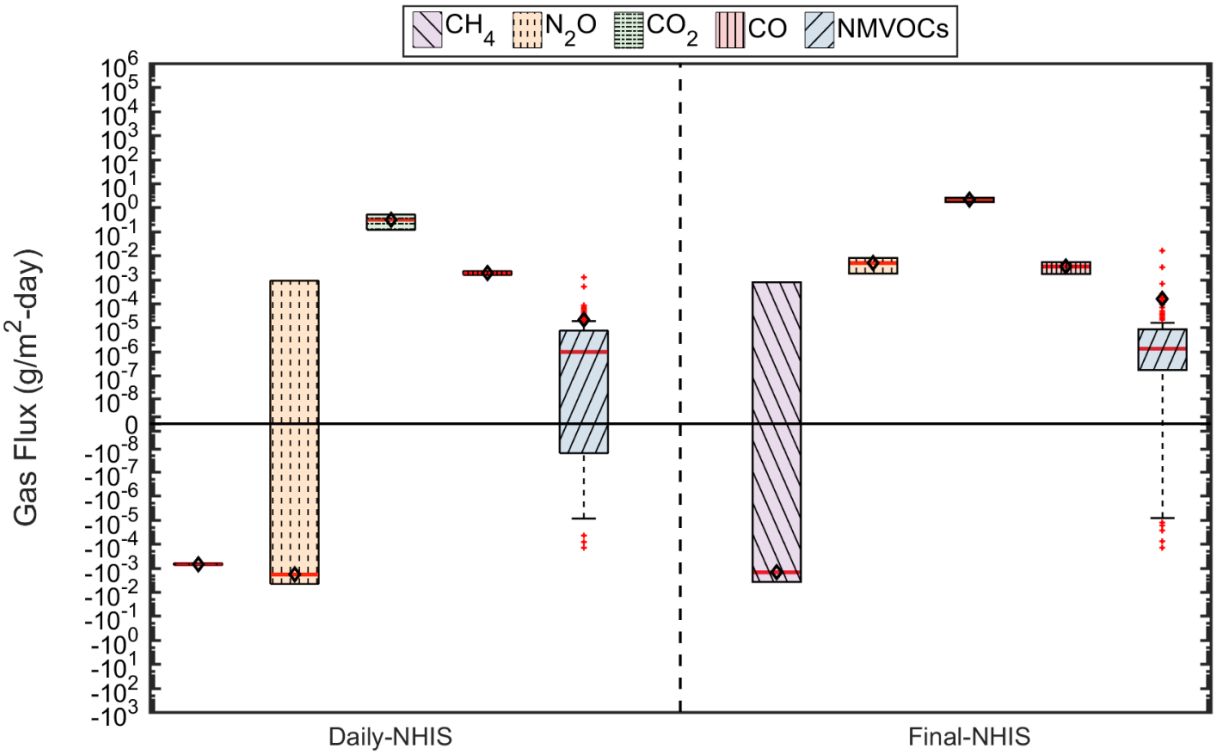

A comparison of daily and final cover flux data for the NHIS and the MSW cells are presented in Figure 4.116. For the daily covers, greenhouse gas fluxes were greatest from the cell receiving MSW. Fluxes of alkanes and alkenes were higher through the daily cover over the MSW compared to the daily cover over NHIS, whereas aldehydes/alkynes and aromatics fluxes were higher for the NHIS cell. For the final covers, GHG fluxes were higher from the NHIS cell than the MSW cell. Also, aromatic fluxes were significantly higher for NHIS than MSW with lower differences for the remaining NMVOCs.

Figure 4.117 Comparison of GHG, Alkane, Alkene, Aldehyde/Alkyne, and Aromatic Hydrocarbon Flux Measurements from a) Daily and b) Final Covers from the NHIS and MSW Cells at SMRL during the Dry Season.

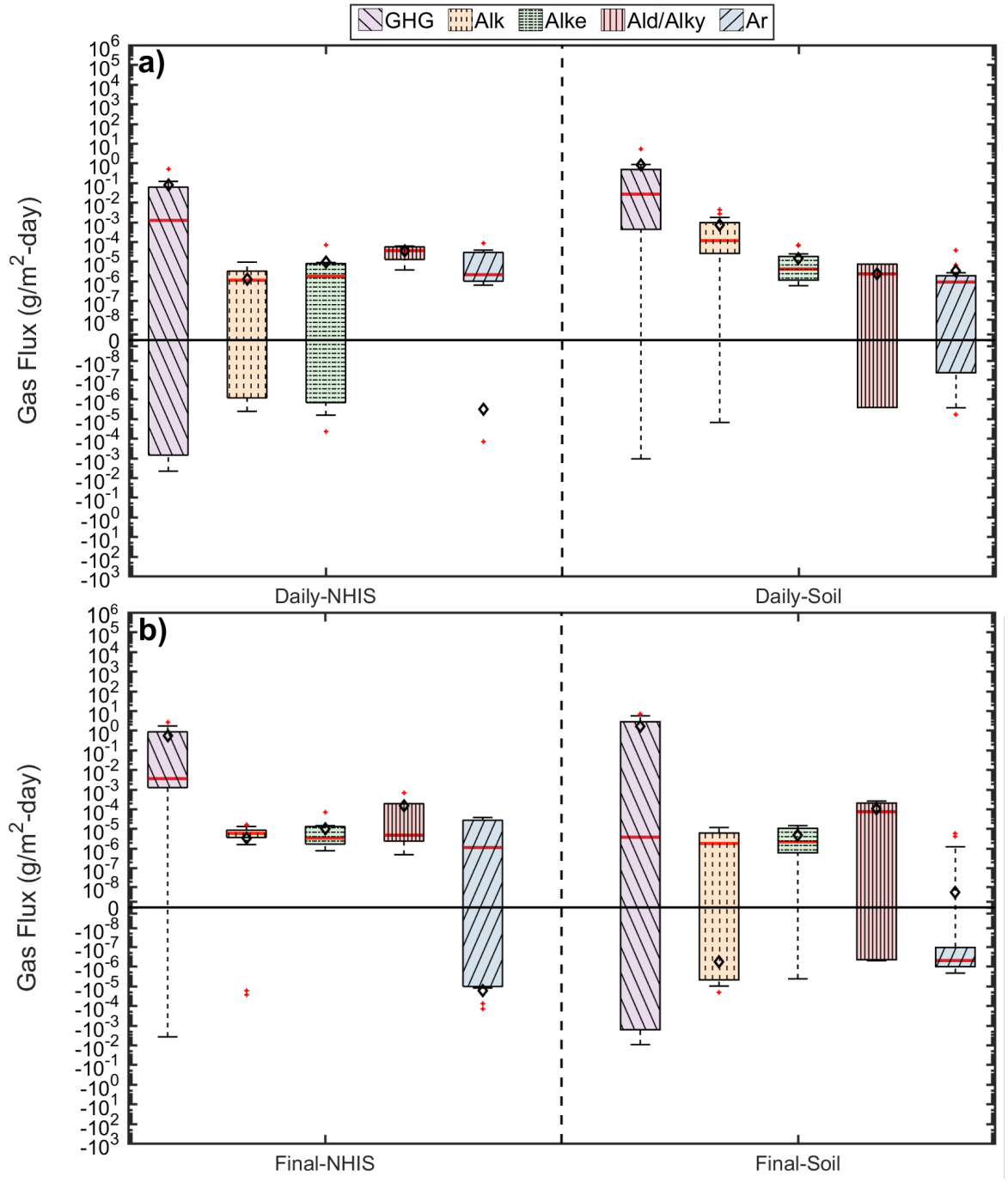

Based on results presented in Figures 4.114-4.116, high GHG fluxes are observed from the NHIS cells at SMRL in line with and even exceeding MSW cells. The high differences resulted from the flux of non-methane GHGs (e.g., nitrous oxide) as the methane fluxes from the NHIS cells were very low (Figure 4.115). Low methane flux is

expected at the NHIS cells as the emissions are mainly coming from the contaminated soils in these cells and not directly from MSW. Surface methane emissions are likely not occurring at the NHIS cells as the MSW at the bottom of these cells are old and also a bottom liner system was installed underneath the contaminated soils separating these from the underlying old MSW. The high GHG fluxes likely resulted from the biological processes naturally occurring in the cover soils at the NHIS cells. The flux of alkanes, alkenes, aldehydes/alkynes, and aromatics, expected to be present in the petroleum contaminated soils, were high from the NHIS cells. The highest differences for these NMVOCs between the NHIS and MSW were for aromatics (higher aromatics fluxes from the NHIS than MSW). The aromatics are the main species present in the petroleum contaminated soils and this is reflected directly in the measured fluxes at the site. The fluxes for alkanes, alkenes, and aldehydes/alkynes were relatively similar for the NHIS and MSW cells (Figure 4.116). Despite these similarities, the sources of these different chemical families, are different between the two areas of the landfill, where the fluxes from the NHIS cells are primarily anthropogenic (contaminated soil) in origin as compared to a mixture of anthropogenic and biogenic sources at the MSW cell. In addition to the four directly petroleum related NMVOCs, positive and high (e.g., alcohols and ketones) fluxes were obtained for the remaining seven NMVOCs investigated in the study (Figure 4.114). Various transformation processes including biological production in the soil cover may have contributed to the production of these chemicals. While the bottom liner system beneath the contaminated soils was likely effective against upward methane migration through the contaminated soils (also potentially the old MSW no longer produces significant methane), the different types of NMVOCs may have moved through the bottom liner materials (example of transport of VOCs through HDPE geomembranes provided above) contributing to the emissions of the NMVOCs from the NHIS cells.

4.13.5 Wet Waste Placement Testing Results at Teapot Dome Landfill

The results from additional tests conducted at the wet (i.e., winter) waste placement area at Teapot Dome Landfill in November 2019 are presented together with the August 2018 data from the same cell (Figure 4.117). Both data sets represent dry season tests at the site. The November 2019 fluxes were also high and in general similar to the data from the August 2018 tests with the exception of the low ketone measurements in November 2019.

Figure 4.118 Fluxes by Chemical Family from the Wet Waste Intermediate Cover at Teapot Dome Landfill in the Dry Season a) August 2018 Tests and b) November 2019 Tests (open black diamonds, red lines, and solid red dots represent means, medians, and outliers, respectively).

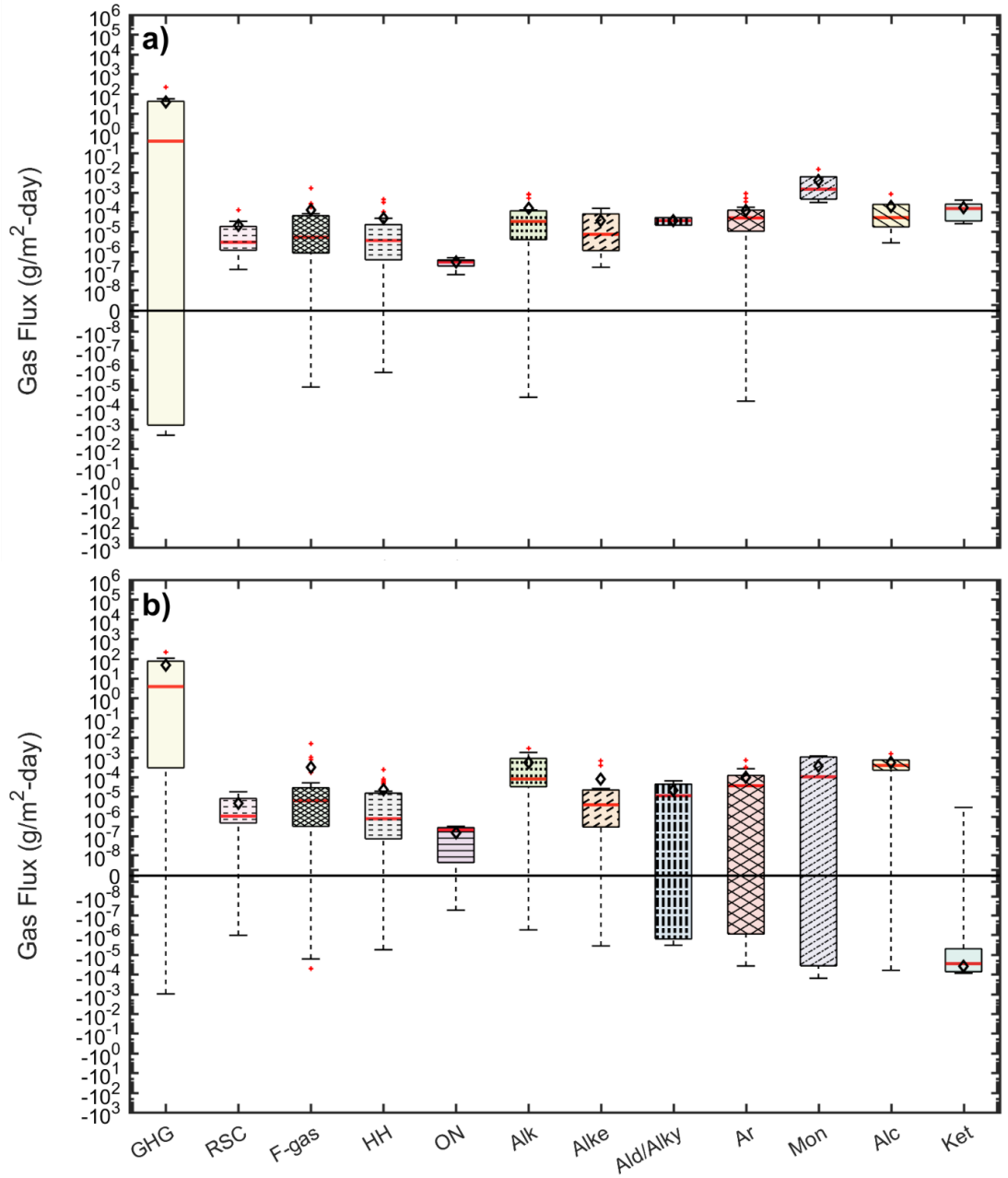

Individual GHG specie and overall NMVOC fluxes for the August 2018 and November 2019 tests are presented in Figure 4.118. The magnitude and variability of the individual GHGs and the overall NMVOCs were also high and in general similar to the August 2018 test results with the exception of the higher variation in nitrous oxide measurements in August 2018 compared to November 2019. Overall, the results presented in Figures 4.117 and 4.118 confirm that high emissions of GHG and

NMVOCs occur through the intermediate cover locations overlying wet waste placement areas at Teapot Dome landfill.

Figure 4.119 Individual GHG and Overall NMVOC Fluxes from the Wet Waste Intermediate Cover at Teapot Dome Landfill in the Dry Season a) August 2018 Tests and b) November 2019 Tests (open black diamonds, red lines, and solid red dots represent means, medians, and outliers, respectively).

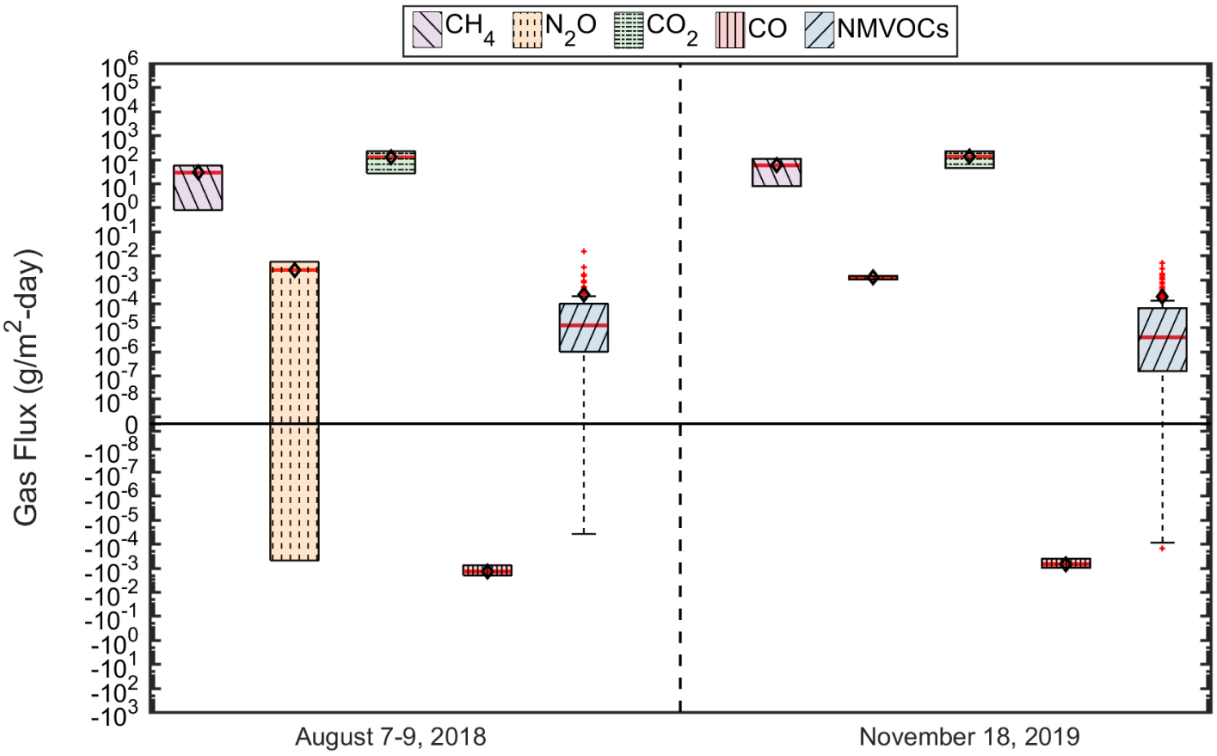

4.14 Comparison to California-Specific Modeling

An overview of methane generation, oxidation, and potential emissions from landfill cover soils in California is presented in Spokas et al. (2015). Spokas et al. (2015) identified a strong, linear relationship between average biogas recovery and WIP for 128 landfill sites in California (using 2010 WIP and reported landfill gas recovery estimates) with the slope of the regression line of 252.24×10^{-6} Nm^3 LFG $hr^{-1} Mg_{waste}^{-1}$. As observed in Figure 4.120, 4 out of the 10 sites from this study are predicted within the 95% confidence intervals of the empirical regression and the remaining 6 sites fall below the prediction zone. A linear regression was fit for the data in this study that resulted in a slope of 9.02×10^{-5} Nm^3 LFG hr^{-1} Mg_{waste}^{-1} (approximately a third of the value reported in Spokas et al. (2015)). While the trend for data from this study indicates positive correlation, the R^2 regression value for this trend was low at 0.36. The average CH_4 flux values from this investigation were 7.68, 4.8, and 0.0373 g/m^2-day for daily, intermediate, and final covers (which were two, one, and one orders of magnitude higher, respectively, than values reported by Spokas et al. (2015)).

Figure 4.120 Comparison of WIP vs. Biogas Recovery for all Landfills Investigated in this Study. The Blue and Red Lines Indicate the Replicated Mean and 95% CIs for the Linear Regression Presented in Spokas et al. (2015) for 128 Landfills in California. The Grey Values Indicate the Sites in this Study and the Green Line Indicates the Best Fitting Linear Regression.

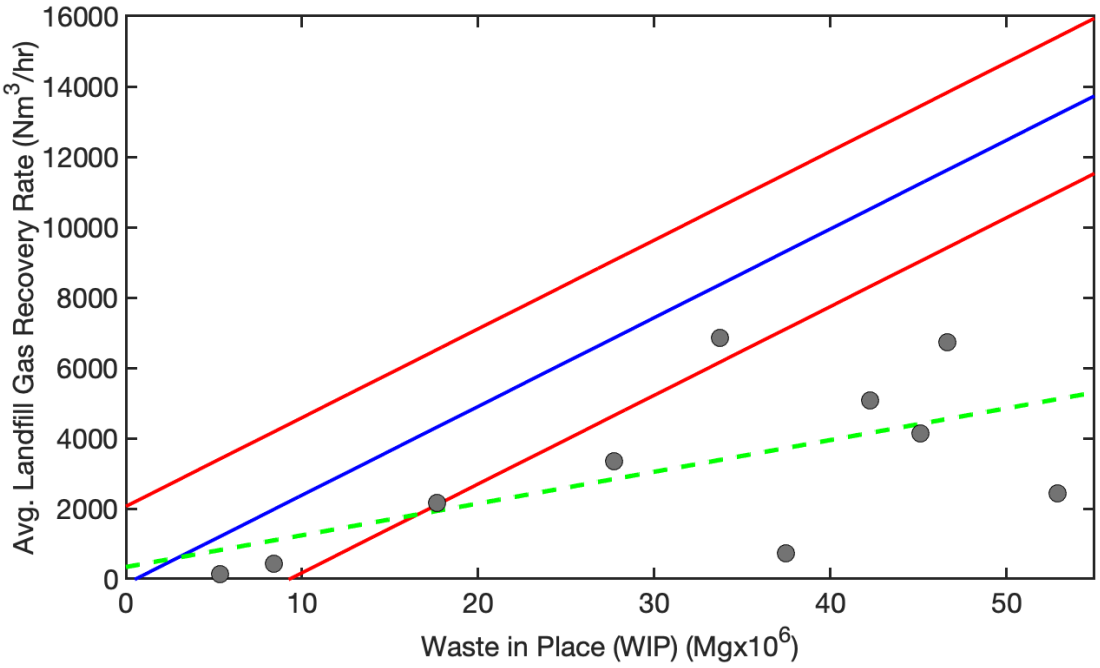

Spokas et al. (2015) further identified, through an intensive modeling effort of 381 landfill sites in California, that climatic variables such as precipitation and temperature were intimately related to methane flux. Regarding precipitation, the modeling results indicated that there was a strong non-linear relationship between methane flux and precipitation, where flux decreased as a function of precipitation. Spokas et al. (2015) also indicated that for sites receiving >500 mm of precipitation annually, the intermediate cover fluxes were all less than 15 g CH_4/m^2-day. As observed in a plot of measured fluxes with precipitation for this current investigation (Figure 4.121), a negative, non-linear correlation was observed for average intermediate cover fluxes, agreeing with results presented by Spokas et al. (2015). In addition, the only site in this study with annual precipitation greater than 500 mm was Potrero Hills landfill, where average methane flux from the intermediate cover was 2.15 g/m^2-day. Spokas et al. (2015) reported an approximately 17-fold difference between seasonal emissions based on monthly analysis. The seasonal variations from this investigation were within one order of magnitude and agreed well with the seasonal difference modeling presented by Spokas et al. (2015).

The differences between results from this study and results presented in Spokas et al. (2015) are attributed to the different approaches used in the studies: this investigation was field-measurement intensive for a limited number of sites and Spokas et al. (2015) was a modeling-intensive study with many sites and site-reported data.

Figure 4.121 Comparison of Annual Normal Precipitation (mm) and Average Flux from Intermediate Cover Locations at all 5 Ground-Based Landfill Sites.

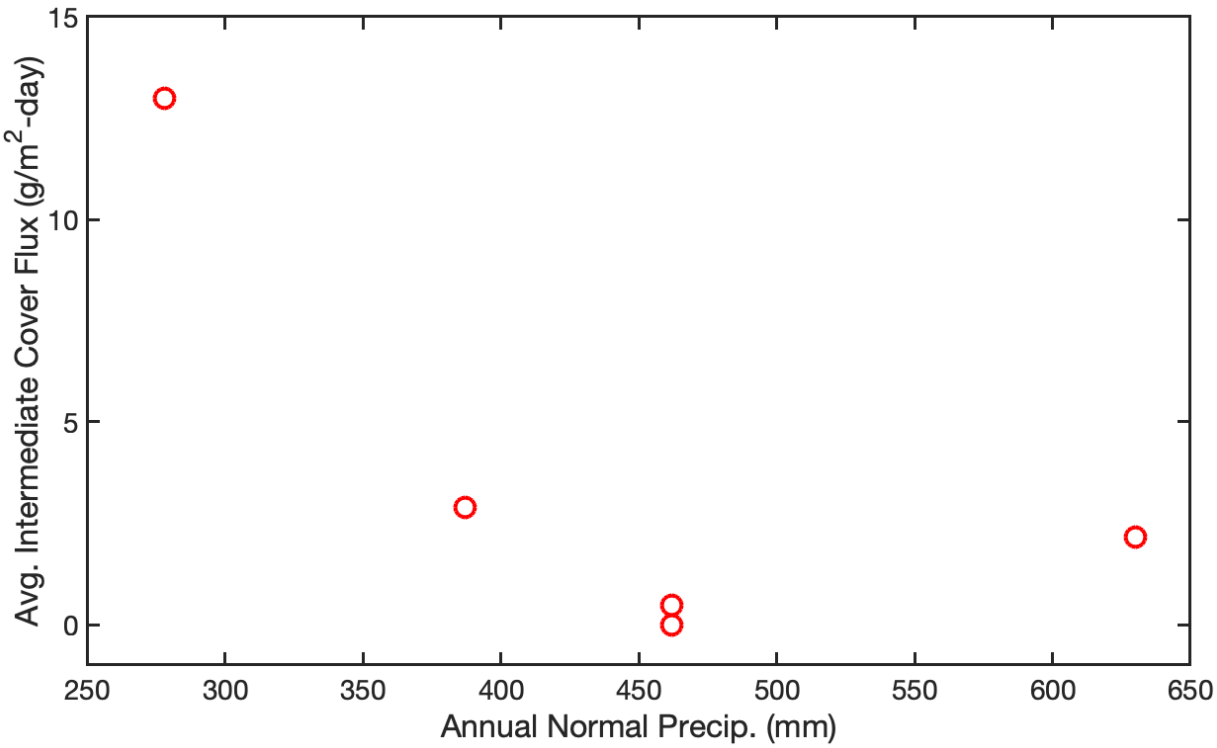

4.15 Presence of Vegetation

Vegetation was present in varying degrees on the covers at the locations selected for testing. A numerical rating scale has been developed to provide context in relation to the test results. Five categories of vegetative cover have been used:

- Woody vegetation (e.g., chipped green waste, construction and demolition waste): designated W;
- No vegetation (bare soil or other material such as auto fluff): designated 0;
- Live vegetation present: rated 1-10 based on areal coverage and growth of vegetation (1 corresponds to nearly bare, 10 corresponds to well vegetated and healthy growth);
- Dried vegetation present: rated 1-10, numerical value as described above for extent of vegetation, halved to reflect dried state of vegetation;
- Partially live, partially dried vegetation: rated using weighted average of numerical methods above.

Example photographs of tested covers with corresponding ratings are provided in Figure 4.122 below. A complete numerical summary of vegetation ratings for the entire test program is presented in Appendix C4.

Figure 4.122 Examples of Vegetation Ratings

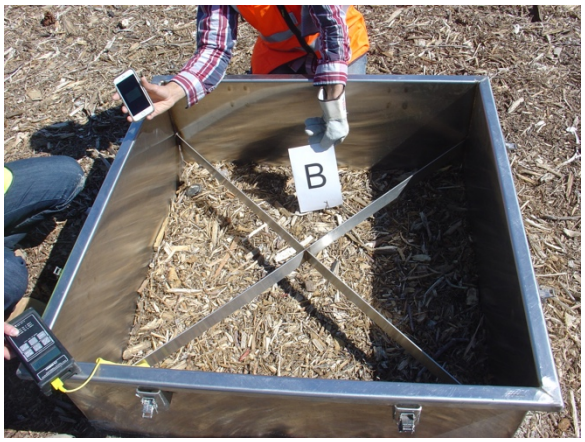

a) Vegetation Rating: W
[Woody Vegetation]

b) Vegetation Rating: W
[Woody Vegetation]

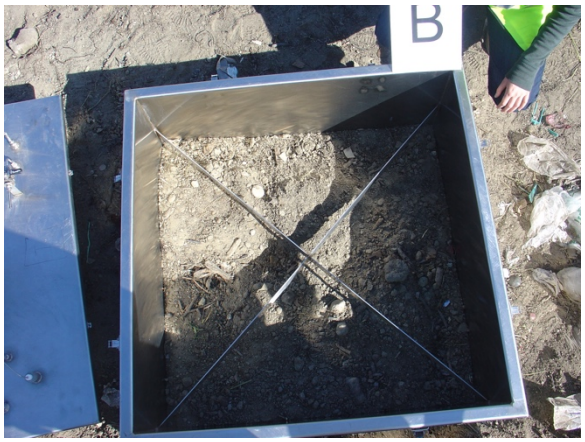

c) Vegetation Rating: 0/10
[No Vegetation]

d) Vegetation Rating: 0/10
[No Vegetation]

e) Vegetation Rating: 2/10
[Live Vegetation]

f) Vegetation Rating: 4/10
[Live Vegetation]

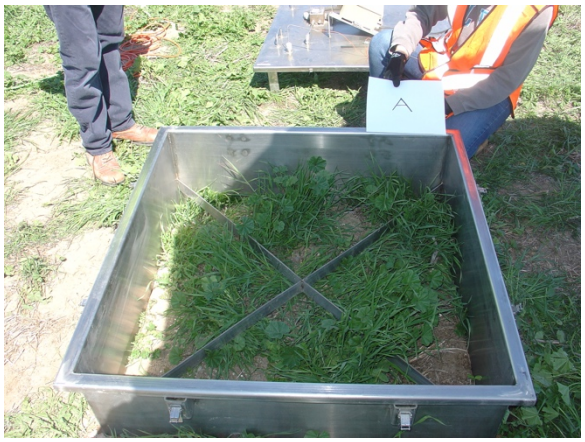

g) Vegetation Rating: 7/10
[Live Vegetation]

h) Vegetation Rating: 10/10
[Live Vegetation]

i) Vegetation Rating: 2/10
[Dried Vegetation]

j) Vegetation Rating: 4/10
[Dried Vegetation]

k) Vegetation Rating: 4.5/10
[Dried Vegetation]

l) Vegetation Rating: 5/10
[Dried Vegetation]

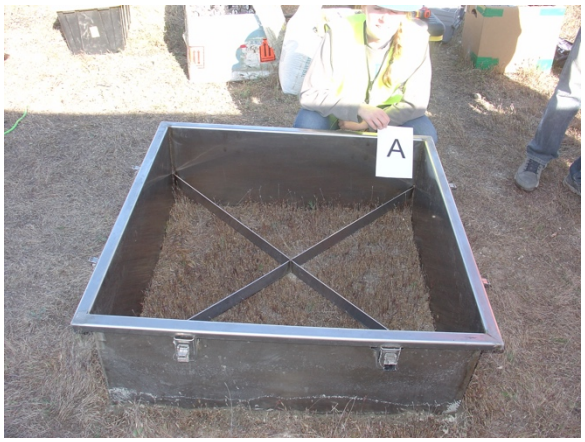

m) Vegetation Rating: 4/10
[Partially Live Vegetation]

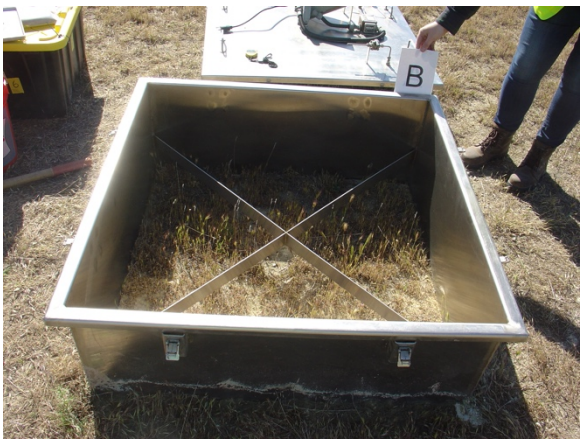

n) Vegetation Rating: 5/10
[Partially Live Vegetation]

Generally, soil and alternative daily covers were bare of vegetation. Interim covers had a mixture of bare condition and some vegetation. Final covers had vegetation present to varying degrees. The presence of vegetation has the potential to influence gas emissions from landfills through numerous mechanisms including disruption of soil structure in the root zone near the ground surface; uptake and production of chemicals through biological processes; uptake of CO_2 and production of O_2 due to photosynthesis; affecting near-surface ground temperatures due to shading, localized wind conditions, and evaporative cooling; modification of moisture conditions near surface due to moisture uptake/transpiration and shading from sun; and modification of air pressure conditions near the surface due to localized wind effects. These mechanisms contribute to differences in soil structure, air pressure conditions for advective flow, and chemical gradient conditions for diffusive flow.

PART 5 – ENGINEERING SIGNIFICANCE

5.1 Gas Flux in California Landfills

This investigation was conducted to determine the flux of main and trace species in landfill gas in California landfills. Over 65,000 individual gas concentration measurements obtained during static flux chamber tests at five landfill sites over the two main seasons (dry and wet) were used to determine flux of a total of 82 individual gases categorized under 12 distinct chemical families. The main landfill gases analyzed were methane and carbon dioxide and the trace components included nitrous oxide, carbon monoxide, and 78 additional NMVOCs.

A summary of the flux data obtained in the investigation is provided in Figure 5.1. The highest fluxes at each landfill site were obtained for GHGs, which included methane, nitrous oxide, carbon dioxide, and carbon monoxide. The GHG fluxes varied by up to two orders of magnitude between the study sites. The results of this study also indicated that NMVOCs are a significant and detectable fraction of the landfill gas emitted from the sites investigated with positive mean and median NMVOC fluxes obtained at all five landfill sites. Highest NMVOC fluxes were measured for the alcohols, ketones, and monoterpenes chemical families. Chiquita Canyon/Teapot Dome Landfills and Site A Landfill were associated with the highest and lowest flux measurements of these chemical families, respectively (Figure 5.1).

Figure 5.1 Inter-landfill Flux Results (open black diamonds, red lines, solid red dots represent means, medians, and outliers, respectively)

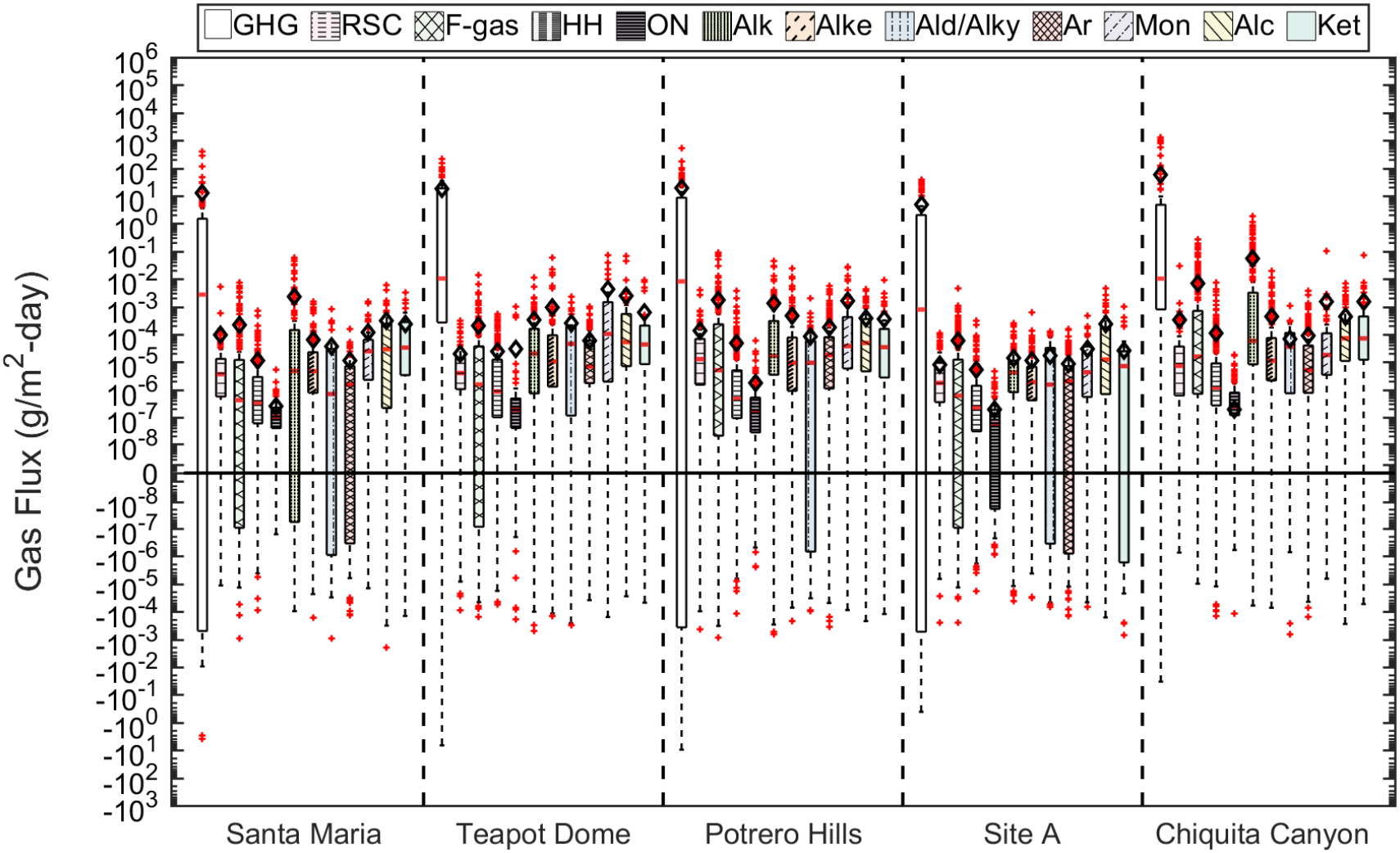

5.2 Variability of Gas Flux in California Landfills

Variation of methane flux as a function of landfill, cover category, and season is presented in a tornado plot in Figure 5.2. The overall range in measured methane flux was from -10^0 to 10^1 g/m^2-day. Variation by landfill and cover category was comparable and more significant than variation by season. The median flux at Site A was low compared to the other sites. The test locations at this site all had thick soil covers consisting of clayey/silty soils with no thin alternative covers such as green waste or autofluff. In addition, the variation in the moisture contents and temperatures of the soils was the lowest at Site A, which may have generated more stable environmental conditions for sustained methane oxidation. The methane fluxes from the medium sized landfills (Santa Maria and Teapot Dome) were comparable to the fluxes from the larger sites (Potrero Hills, Site A, and Chiquita Canyon), indicating the significance of factors other than operational scale on methane emissions. The methane fluxes decreased from the daily to intermediate to final covers with a higher decrease from intermediate to final covers than from daily to intermediate covers. The highest methane fluxes were generally from alternative daily covers and in particular from autofluff. These thin, highly porous daily covers provided low resistance to methane flux. The thick engineered final cover systems with high fine soil content and use of geosynthetics at one site resulted in the lowest fluxes. The seasonal variations were within one order of magnitude indicating the more significant influence of the cover conditions on methane flux than seasonal variations in California.

At Site A, methane flux from the alternative final cover was significantly higher than the flux from the conventional final cover. The large difference may have resulted from the more interconnected pore structure of the coarser-grained alternative cover compared to the occluded pore structure of the finer-grained conventional cover. This study for the first time provided flux data for an alternative cover system and also a comparison between an alternative and a conventional cover. While good hydraulic performance of alternative covers against moisture ingress into landfills have been demonstrated, these covers may not be highly effective as barriers against gas flux.

Figure 5.2 Tornado Plot Summarizing the Variation in Methane Flux as a Function of Landfill, Cover Type, and Season (open black diamonds, black lines, solid red dots represent means, medians, and outliers, respectively).

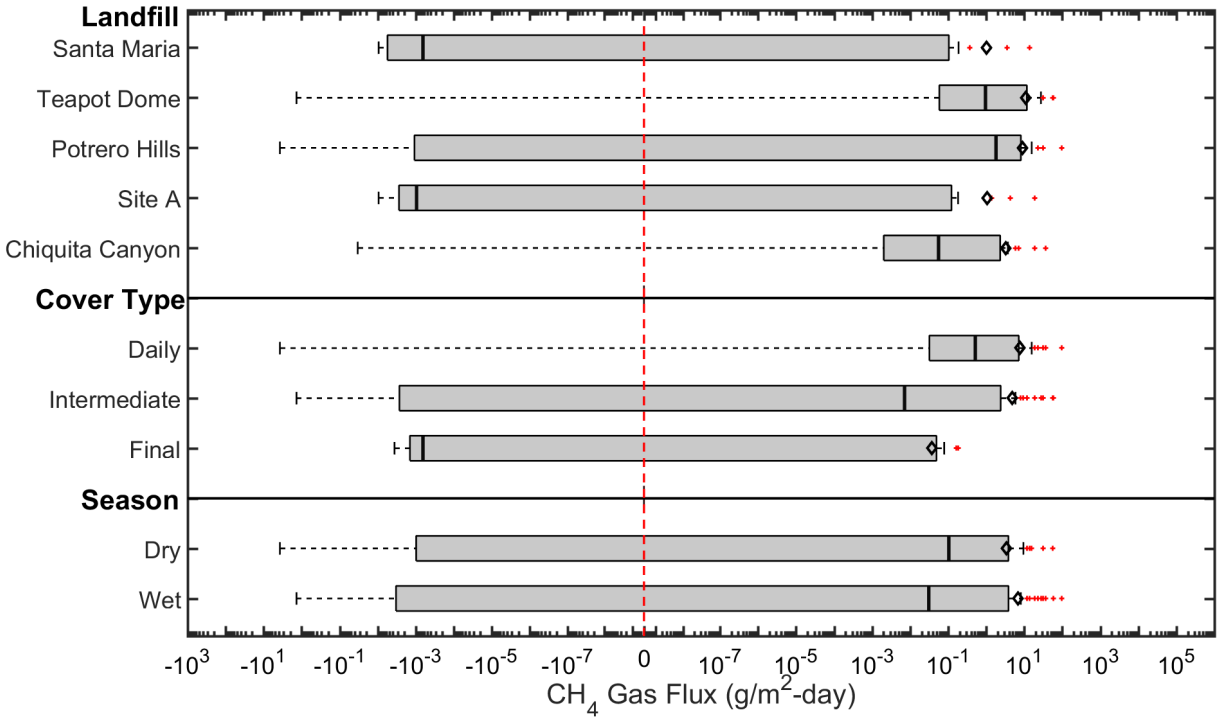

Variation of nitrous oxide flux as a function of landfill, cover category, and season is presented in a tornado plot in Figure 5.3. The overall range in measured nitrous oxide flux was from -10^{-3} to 10^{-1} g/m^2-day. Variation by cover category was more significant than variation by landfill and season, which were relatively comparable. Nitrous oxide fluxes at the medium sized landfills were largely positive (all or most of interquartile ranges above zero in Figure 5.3) with low probability for negative flux compared to the larger landfills. Waste composition may have resulted in these differences, where the amount of incoming wastes with high nitrogen content (i.e., crop wastes/residue, manure) are likely high due to the surrounding agricultural communities of Santa Maria Regional and Porterville Landfills compared to the wastes from mainly urban sources at the large Northern and Southern California landfills. The nitrous oxide fluxes decreased from the daily to intermediate to final covers with a higher decrease from intermediate to final covers than from daily to intermediate covers. In similarity to methane flux results, the thin, highly porous daily covers provided low resistance to nitrous oxide flux. The thick engineered final cover systems with high fine soil content and use of geosynthetics at one landfill resulted in the lowest fluxes. The seasonal variations were within one order of magnitude indicating the more significant influence of the cover conditions on nitrous oxide flux than seasonal variations in California.

Figure 5.3 Tornado Plot Summarizing the Variation in Nitrous Oxide Flux as a Function of Landfill, Cover Type, and Season (open black diamonds, black lines, solid red dots represent means, medians, and outliers, respectively).

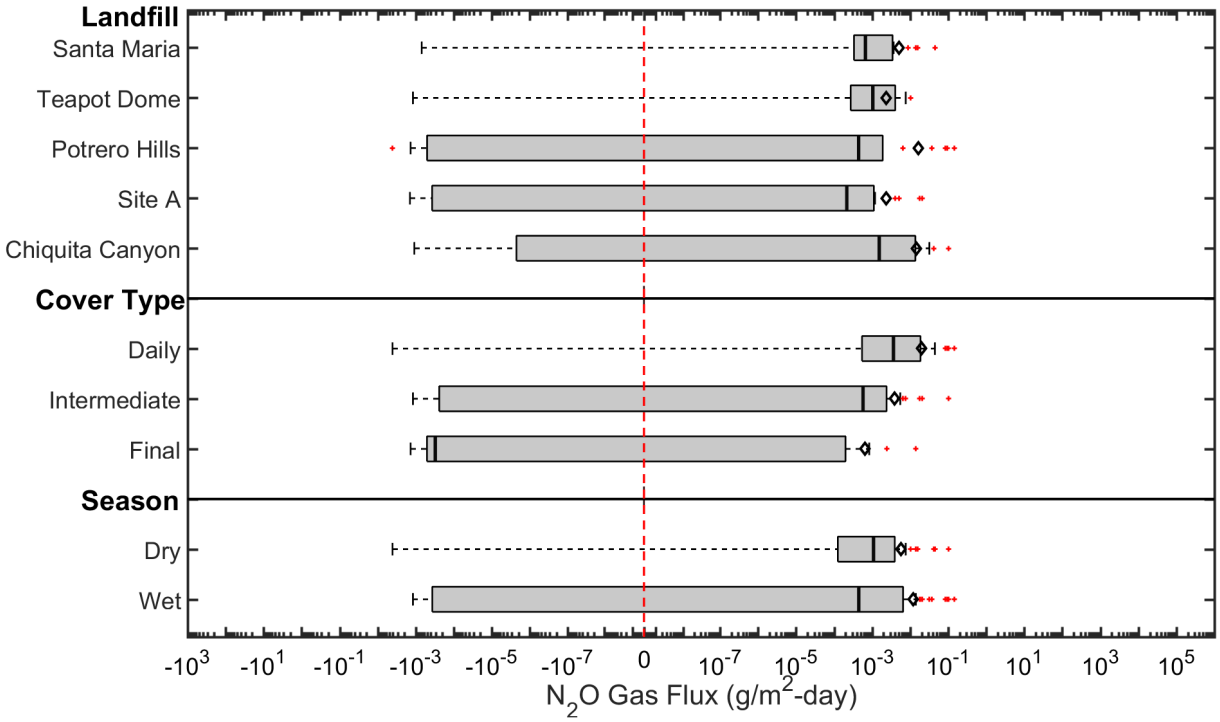

Variation of NMVOC flux as a function of landfill, cover category, and season is presented in a tornado plot in Figure 5.4. The overall variation in NMVOC flux was from -10^{-3} to 10^{0} g/m^2-day. Variation in total NMVOC flux was generally comparable across landfills, cover categories, and seasons and less than variations observed for methane and nitrous oxide. Positive flux is dominant for the NMVOCs investigated with low probability of uptake(interquartile ranges above zero in Figure 5.4), even though all of the NMVOCs are trace components of landfill gas. Similar to methane and nitrous oxide fluxes, the NMVOC fluxes from the medium sized landfills (Santa Maria and Teapot Dome) were comparable to the fluxes from the larger landfills, indicating the significance of factors other than operational scale on NMVOC emissions. Cover category had the most significant effect on NMVOC fluxes, where the fluxes decreased from the daily to intermediate to final covers. In similarity to methane and nitrous oxide flux results, the thin, highly porous daily covers provided low resistance to NMVOC flux. In addition, the daily covers may have been sources of NMVOCs. NMVOCs such as aromatic hydrocarbons, alkanes, and alkenes may have volatilized from the contaminated soil daily cover. The wood waste and green waste ADC materials are potential sources of monoterpenes and the autofluff ADC is a potential source of F-gases. The thick engineered final cover systems with high fine soil content and use of geosynthetics in some cases resulted in the lowest fluxes. The final cover NMVOC fluxes were in some cases higher than those for methane and nitrous oxide. The seasonal variations were within one order of magnitude indicating the more

significant influence of the cover conditions on NMVOC flux than seasonal variations in California.

Figure 5.4 Tornado Plot Summarizing the Variation in NMVOC Flux as a Function of Landfill, Cover Type, and Season (open black diamonds, black lines, solid red dots represent means, medians, and outliers, respectively).

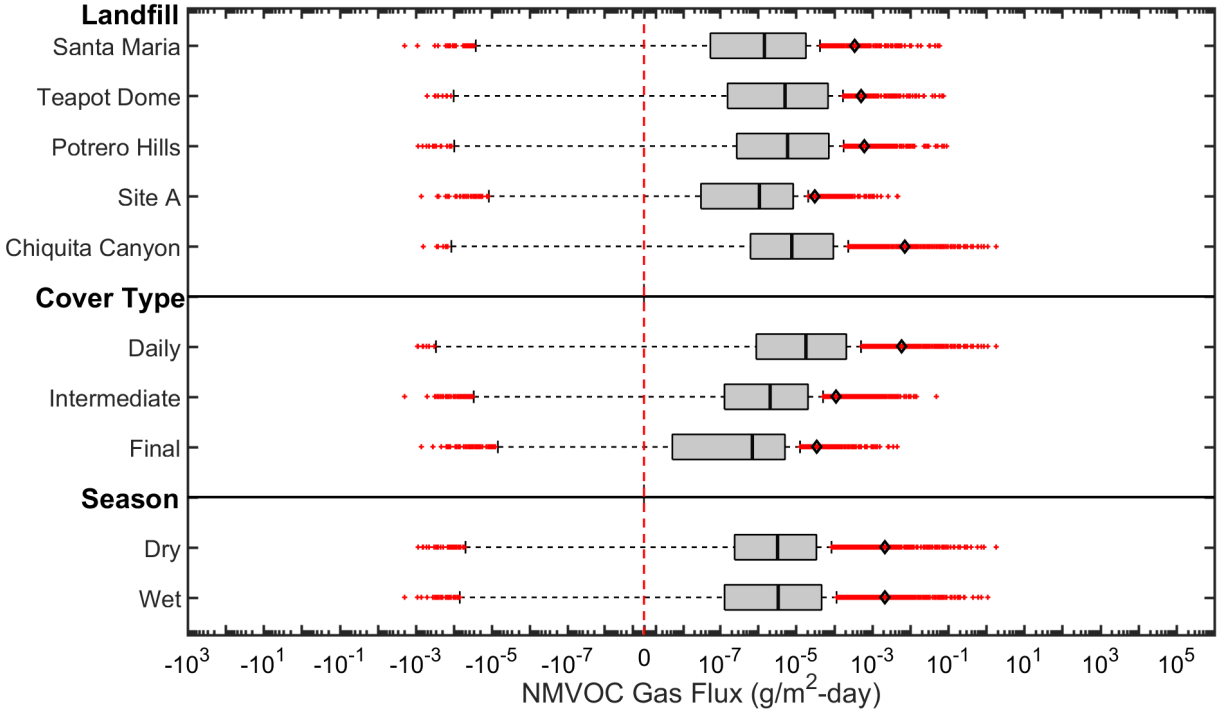

Overall, methane, nitrous oxide, and total NMVOC emissions are affected most by cover category/type, followed by site specific operational practices and scale, and then by season. The violin plots presented in Figures 5.5 and 5.6 provide probability density estimates for the different cover categories included in this investigation. For methane and GHGs, a higher probability of fluxes between 10^{-5} to 10^{0} g/m^2-day was observed for the daily covers compared to the intermediate and final covers. The intermediate and final cover systems demonstrated a wider range in probable flux between 10^{2} and 10^{-6} and 10^{1} and 10^{-6} g/m^2-day, respectively. The relative amount of negative fluxes increased from daily to intermediate to final covers. Chiquita Canyon and Site A Landfills were generally associated with the highest (most positive) and lowest (most negative) GHG fluxes, respectively (Figure 5.5). For NMVOCs, the highest probability density of positive fluxes was observed between 10^{-8} and 10^{-2}, 10^{-8} and 10^{-3}, and 10^{-8} and 10^{-4} g/m^2-day for the daily, intermediate, and final covers, respectively. The highest probability density of negative fluxes was observed between -10^{-8} and -10^{-3}, -10^{-8} and -10^{-4}, and -10^{-8} and -10^{-5} g/m^2-day for the daily, intermediate, and final covers, respectively. Chiquita Canyon, Potrero Hills, and Site A Landfills were associated with the majority of positive fluxes for daily, intermediate, and final covers, respectively. Negative fluxes were most likely associated with Site A Landfill for all cover categories.

Figure 5.5 Distribution of Methane Fluxes by Cover Category (open black diamonds, red lines, and solid red dots represent means, medians, and outliers, respectively).

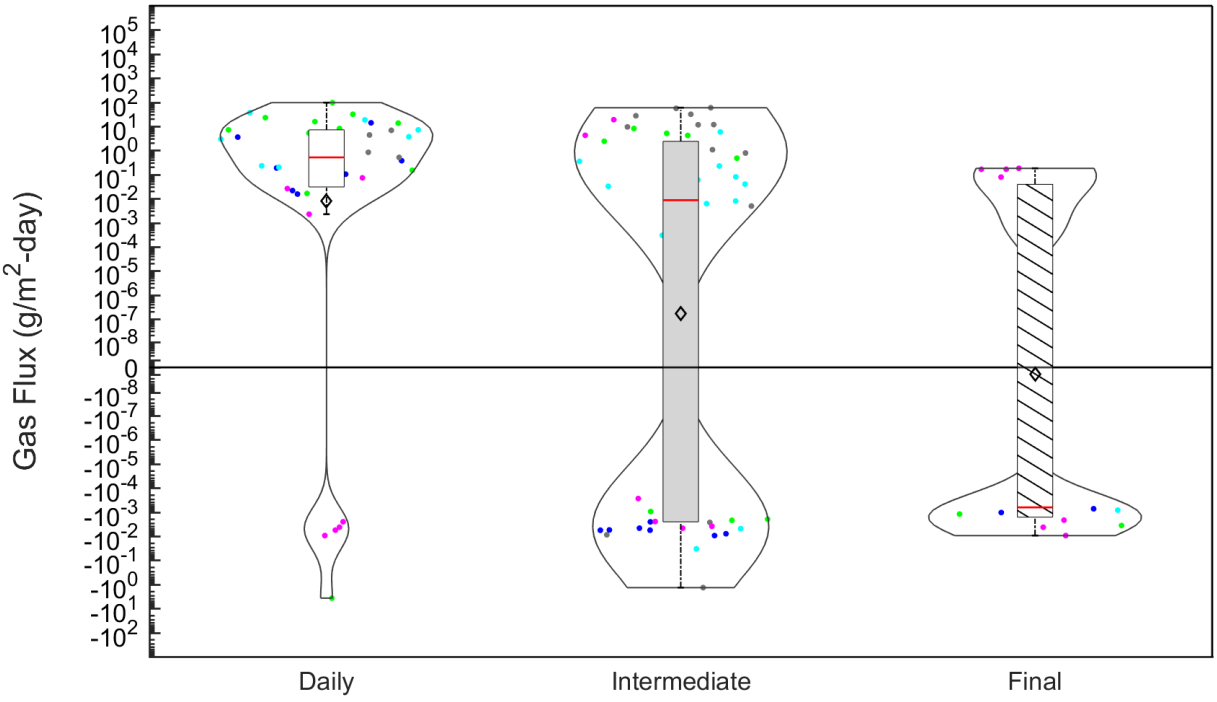

Figure 5.6 Distribution of a) GHG and b) NMVOC Fluxes by Cover Category (open black diamonds, red lines, and solid red dots represent means, medians, and outliers, respectively).

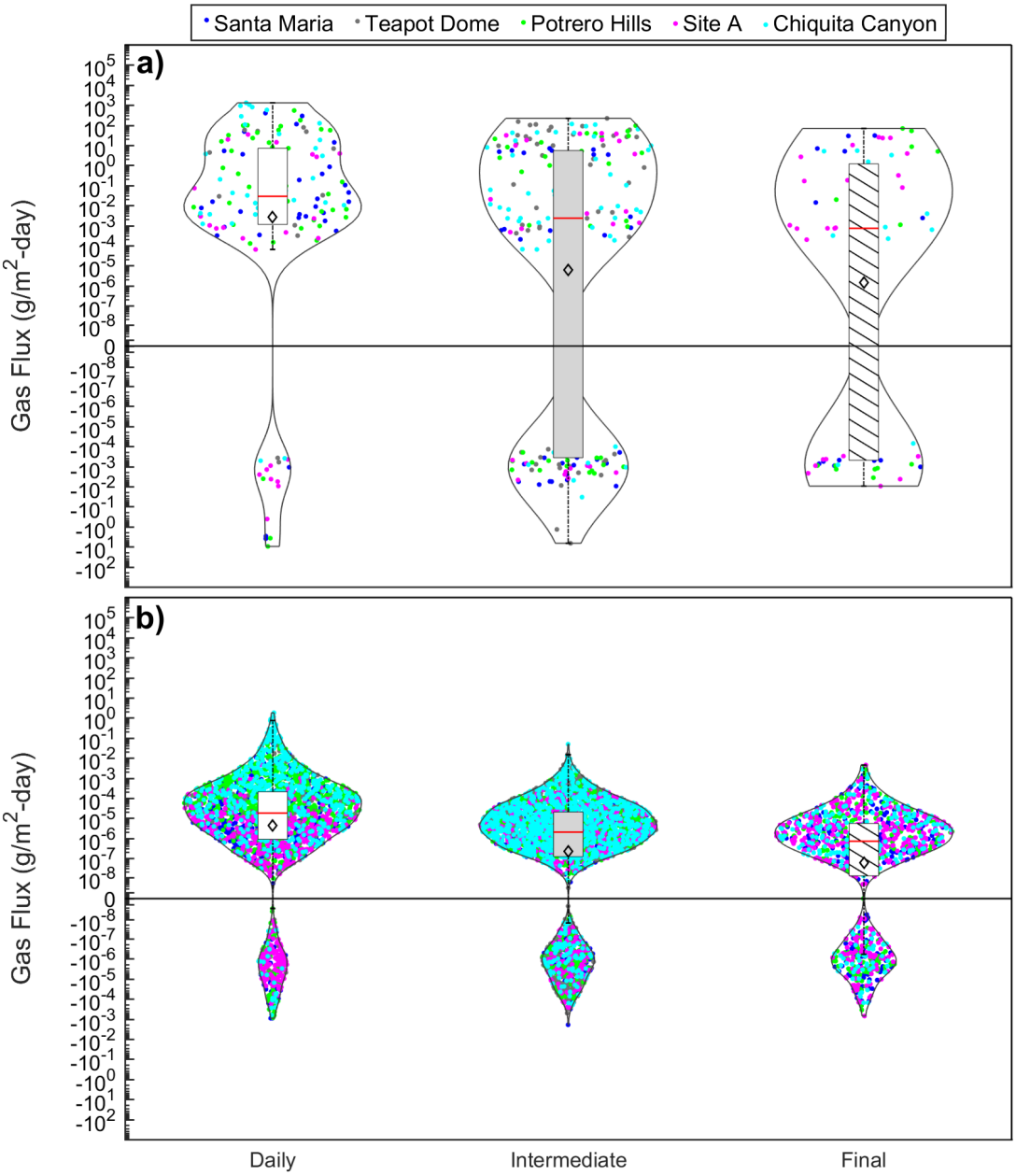

5.3 Influence of Cover Type on LFG Surface Fluxes

Analysis presented in Section 5.2 indicated that cover categories was the most significant factor affecting LFG surface fluxes as compared to site specific operational practices/scale and seasons. Thus, the influence of different cover types within each category (i.e., daily, intermediate, final) was further investigated herein. For daily cover categories, fluxes were grouped into cover types that included soils, green wastes, wood wastes, and autofluff. For intermediate cover categories, fluxes were grouped into cover types that included soils, soil/green wastes (green waste overlying soil), and

landfill areas receiving placement of waste during the wet season (referred to as wet waste). Final cover categories were grouped into cover types that included conventional compacted clay liners (CCLs), conventional geosynthetic clay liners (GCLs), and alternative final cover systems. Fluxes were combined across sites and seasons to investigate trends in LFG fluxes (i.e., methane, nitrous oxide, and total NMVOCs) with cover category and type.

Surface flux of methane decreased from daily to intermediate to final covers (Figure 5.7). The highest methane fluxes were generally from alternative daily covers and in particular typically from autofluff. The variations of methane flux within the individual alternative daily covers were low and the overall methane fluxes were high. The variations of flux through soil daily covers were higher than the variations through the alternative daily covers with overall lower methane fluxes for soil daily covers. For intermediate covers, methane fluxes through soil covers were lower (with potential for uptake) than covers with green waste and covers over wet waste. For final covers, the fluxes were lower through the conventional covers (CCL and GCL) than the alternative cover. The median methane fluxes from the alternative final cover had low variability and was significantly higher than the methane fluxes from the conventional covers (Figure 5.7).

Figure 5.7 Summary of CH_4 Fluxes as a Function of Daily, Intermediate, and Final Cover Categories/Types.

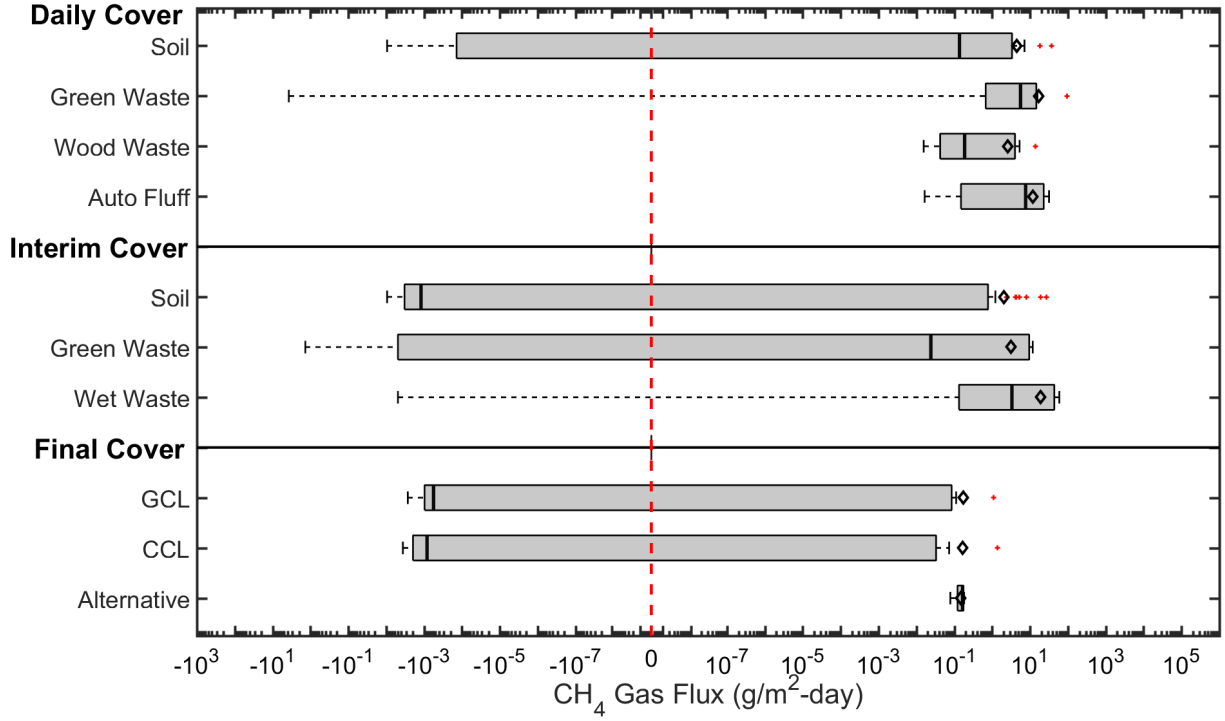

Surface fluxes of nitrous oxide were generally highest from daily cover locations and similar between the three daily cover types with somewhat lower values for autofluff (Figure 5.8). The intermediate cover N_2O fluxes were relatively similar between the three cover types and overall slightly lower than the daily cover nitrous oxide fluxes.

For final covers, the highest nitrous oxide fluxes were for the GCL cover and lower for the soil and alternative covers. The variation in flux was highest within the conventional CCL final covers.

Figure 5.8 Summary of N_2O Fluxes as a Function of Daily, Intermediate, and Final Cover Categories/Types.

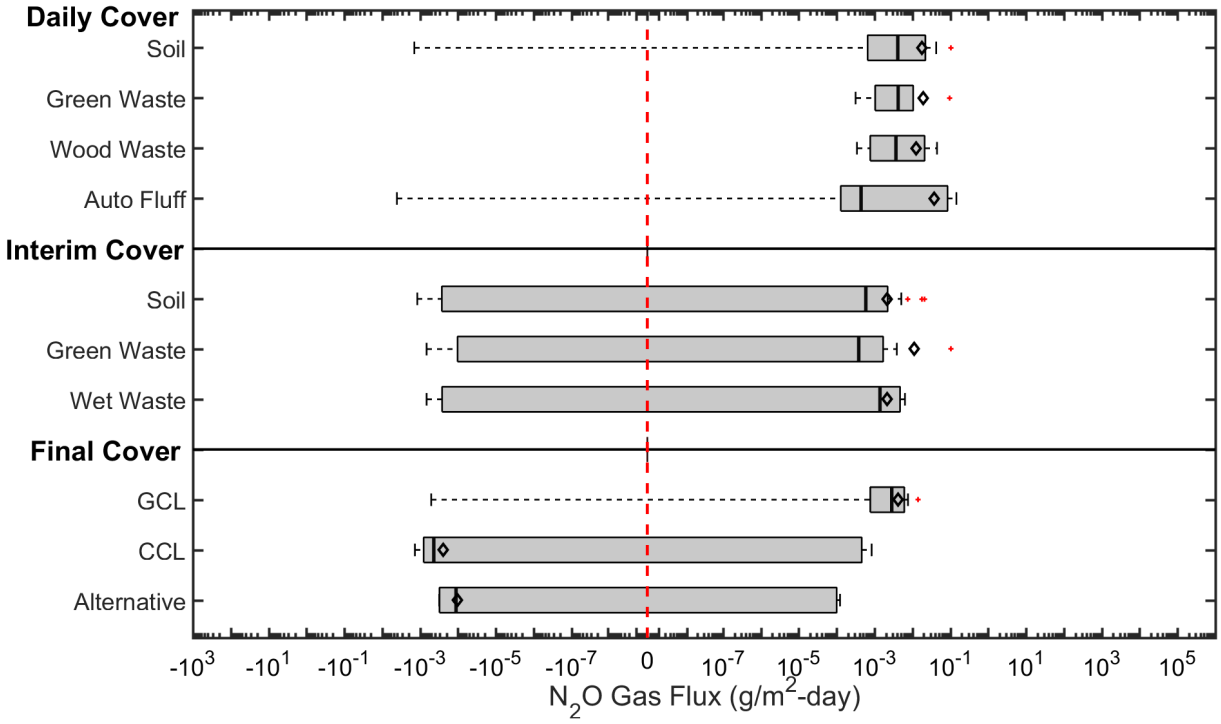

While the surface flux of NMVOCs decreased from daily to intermediate to final covers, the variations between the cover categories were low (Figure 5.9). The variation for a given cover type also was low for all three cover categories (daily, intermediate, and final). The lowest NMVOC fluxes were associated with soil materials for the three cover categories. All of the measured NMVOC median and mean fluxes were positive indicating high probability of emissions over uptake.

Figure 5.9 Summary of NMVOC Fluxes as a Function of Daily, Intermediate, and Final Cover Categories/Types.

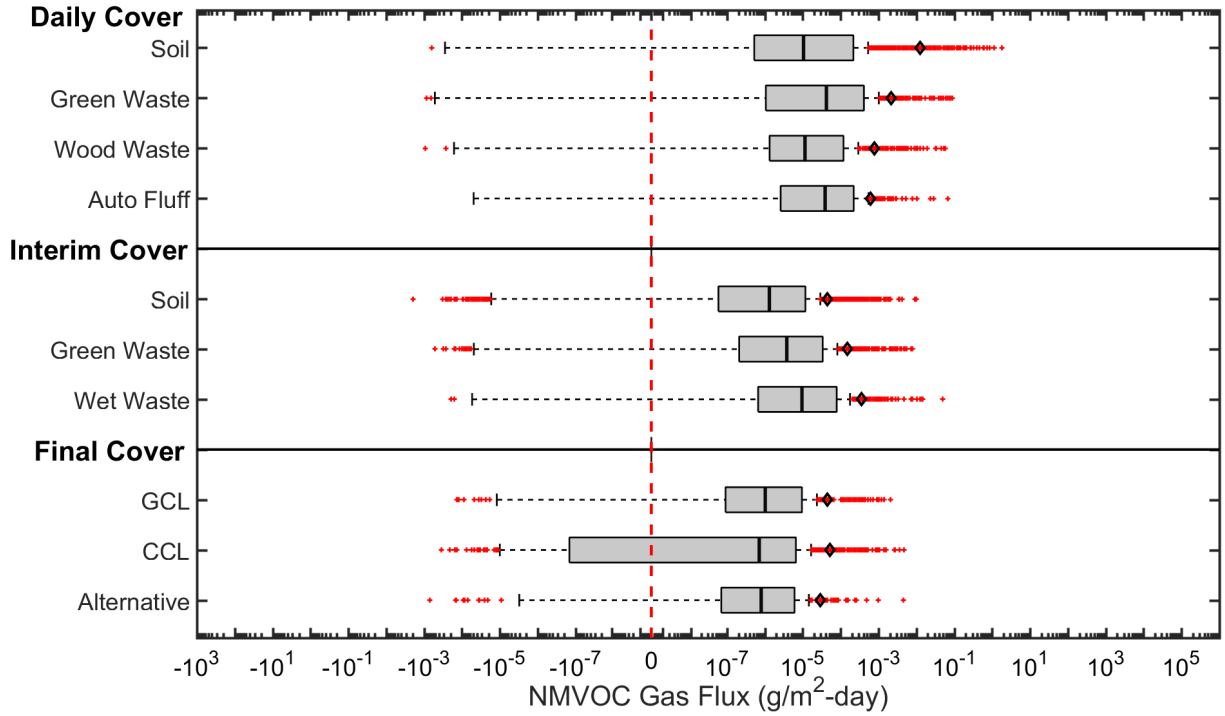

Overall fluxes of the GHGs and NMVOCs as a function of cover type indicated that for daily covers, locations with autofluff or green wastes had the highest surface fluxes. Both of these materials had low densities, high porosities, high void ratios, low solids content, low water content, and high volumetric air content both in the wet and dry seasons. Higher gaseous fluxes were associated with the lack of material (solids or water) to physically or chemically impede or retard gas transport in daily cover locations overlain with autofluff or green waste. The relatively low methane fluxes and large variations in soil daily covers resulted from mainly the data associated with thicker extended soil daily covers used in some cases at some of the study sites. For intermediate covers, the highest fluxes for the GHGs and NMVOCs were associated with the wet waste locations mainly due to the potential large amount of methane generation in the wet wastes as well as the coarser cover soils (high amount of interconnected pores for gaseous transport). For final covers, conventional covers were significantly more effective for impeding methane flux compared to the alternative cover due to the high fines content, clay content, and occluded pores resulting in tortuous gas transport paths. For nitrous oxide, the GCL cover had the highest flux with low nitrous oxide fluxes for both the CCL and the alternative final covers. The NMVOC fluxes were highly similar through the three final cover types. Overall cover categories and types had impacted GHG methane and nitrous oxide fluxes more than NMVOC fluxes. Methane undergoes potential transformations (oxidation, dissolves in soil water, and also attaches to soil solid surfaces) in the cover materials, which affect the surface flux. Similarly, nitrous oxide undergoes transformations in the cover materials as well as is produced through natural biological processes in soil and

vegetative covers. Potential transformations of NMVOCs in different landfill covers have not been investigated extensively. NMVOCs may not be affected by cover characteristics to the same extent as methane and nitrous oxide (observed low variation of NMVOC fluxes with cover category and type).

5.4 Aerial versus Ground-Based Methane Fluxes

The field investigation of flux included two types of measurement programs: aerial and ground. The aerial testing provided results only for methane (other gases of interest could not be measured with this method) and overall estimates for whole-site emissions. The ground-based testing provided direct flux results for all 82 target gas species and allowed for detailed assessment of the effects of variable surface conditions on the emissions of the target gases from the tested landfills. Methane emissions based on the two testing programs are compared in Table 5.1 and Figure 5.10. The ground-based methane emissions were consistently lower in magnitude compared to the aerial methane emissions estimates. Yearly methane emissions estimated from the ground-based field-testing campaigns for Santa Maria Regional Landfill resulted in a negative whole site emissions. The average ground-based methane emissions estimates for Santa Maria Regional Landfill (not depicted on the log scale presented in Figure 5.10) were -0.122 tonnes/year with 95% confidence intervals ranging from -0.201 to -0.043 tonnes/year and aerial estimates were 1684 tonnes/year with 95% confidence intervals ranging from -221 to 3589 tonnes/year. The inventory values generally were between the ground-based and aerial-based measured emissions, with the exception of Teapot Dome Landfill (lower inventory values) and Chiquita Canyon Landfill (higher inventory values). The variability in emissions estimates (95% confidence intervals) also is included in Figure 5.10. For a majority of the landfills, the variability in emissions estimates was lower for the ground-based measurement method compared to the aerial method. Emissions from the active waste placement surface (not measured in the ground tests) and the uncertainties in the aerial measurements likely collectively contributed to the differences between the aerial and ground measurements. Nevertheless, magnitude and variation of methane emissions were captured using both methodologies in the test program.

Table 5.1 Comparison of Ground, Aerial, and CARB Inventory of CH_4 Emissions

Site	Ground-Measured CH_4 Mean Direct Emissions (tonnes/year)	Aerial-Measured CH_4 Mean Emissions (tonnes/year)	CARB Inventory of CH_4 Emissions (tonnes/year)[a]
Santa Maria Regional Landfill	-0.122	1684	148
Teapot Dome Landfill	1220	3799	142
Potrero Hills Landfill	1344	16402	2941
Site A Landfill	945	14792	12627
Chiquita Canyon Landfill	381	5804	5916

[a]Spokas et al. (2015)

Figure 5.10 Comparison of Ground and Aerial Based Methane Emissions Estimates (dashed line indicates 1:1 reference, error bars represent 95% confidence intervals of overall estimates).

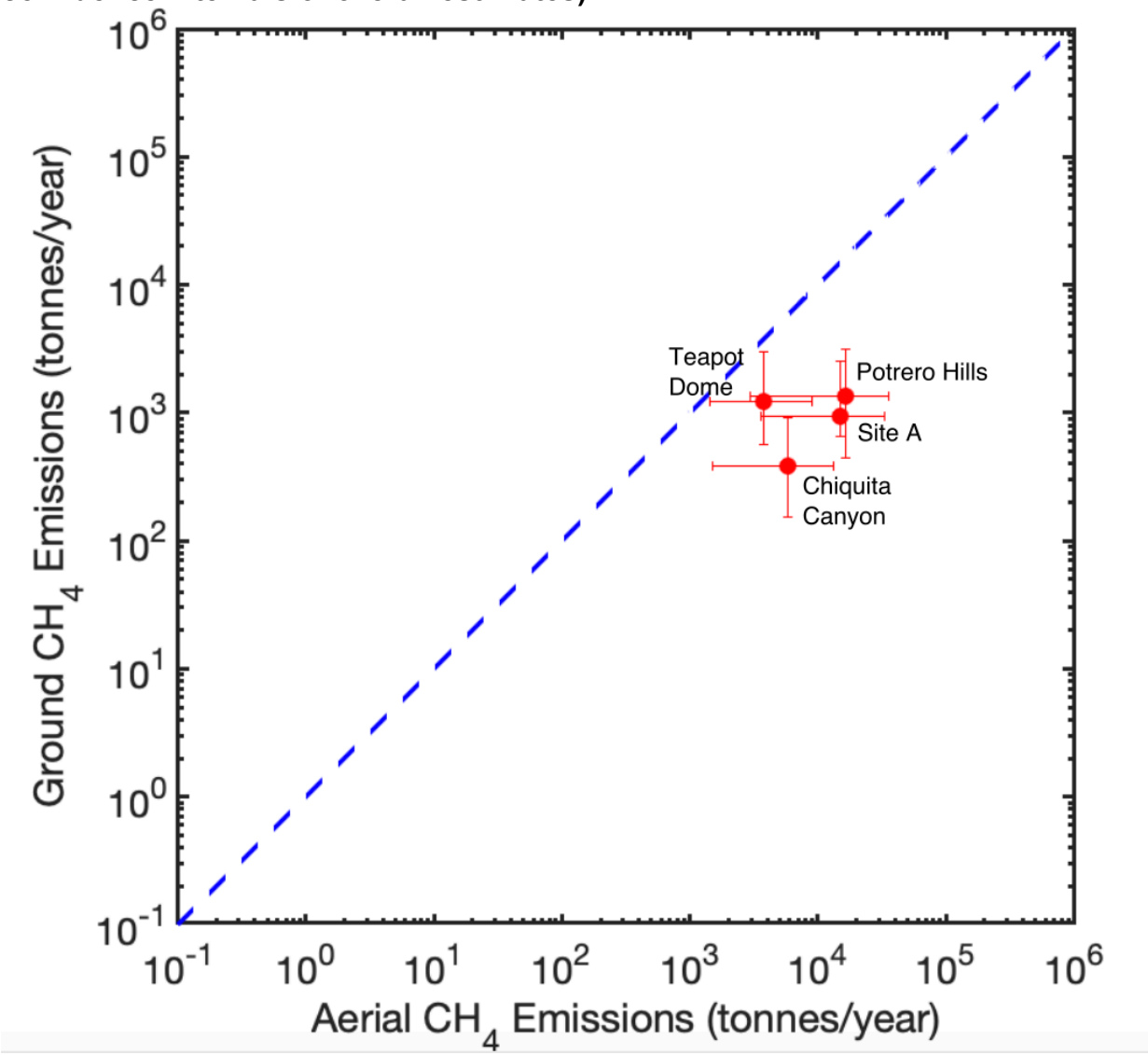

Estimates for flux of CH_4 from the active face region of the ground testing sites is summarized in Table 5.2. The estimates were calculated using an assumption that the difference in emissions between aerial- and ground-based measurements was entirely from the active face. This calculation assumes that both methods of measurement are valid and that no additional emissions sources are present. The active face flux values were relatively high compared to measured values of covered regions using ground-based techniques (ranging from one to several orders of magnitude higher than the daily cover direct measurements).

Table 5.2 Estimation of Flux from Active Face Regions

Site	Difference between Ground-Based and Aerial-Based Emissions (tonnes/year)	Active Face Size (m^2)	Estimated Flux from Active Face Region (g/m^2-day)
Santa Maria Regional Landfill	1684	700	$6.59x10^3$
Teapot Dome Landfill	2579	1200	$5.89x10^3$
Potrero Hills Landfill	15058	3000	$1.37\ x10^4$
Site A Landfill	13847	6100	$6.22\ x10^3$
Chiquita Canyon Landfill	5423	5600	$2.65\ x10^3$

5.5 Comparison to Literature Results

This study represents to the PIs knowledge, the most comprehensive field investigation of gas emissions from municipal solid waste landfills in California, the U.S. and internationally. Previous investigations have focused primarily on measuring fluxes of the major greenhouse gases (methane, nitrous oxide, carbon dioxide), with little emphasis placed on NMVOC flux determination. In addition, as reviewed in Section 1, few previous studies have measured fluxes of NMVOCs from daily cover systems (mainly data from a previous study conducted by the PIs for CARB). Out of the 82 chemicals analyzed in this study, 8 gases previously have not been measured in landfill settings. These chemicals consisted of dimethyl sulfide, dimethyl disulfide, carbon disulfide, HFC-365mfc, n-undecane, n-propyl benzene, 2-butanol, and butanone.

Analysis of data collected from the literature review indicated varying ranges of methane, nitrous oxide, carbon dioxide, and NMVOC flux measurements across MSW landfills around the world. The reported methane fluxes ranged from $-4.5x10^1$ to $4.15x10^4$ g/m^2-day as compared to $-3.73x10^0$ to $9.62x10^1$ g/m^2-day observed in this study. Nitrous oxide fluxes reported in the literature ranged from $-2.54x10^{-3}$ to $3.76x10^0$ g/m^2-day compared to $4.10x10^{-3}$ to $1.45x10^{-1}$ g/m^2-day observed in this study. Carbon dioxide fluxes reported in the literature ranged from $-4.5x10^1$ to $1.24x10^5$ g/m^2-day compared to $-9.60x10^0$ to $1.31x10^3$ g/m^2-day observed in this study. Total NMVOC fluxes reported in the literature ranged from $-1.66x10^{-3}$ to $3.00x10^{-1}$ g/m^2-day compared to $-1.93x10^{-3}$ to $1.81x10^0$ observed in this study. In general, the range of the major greenhouse gases observed from the literature was greater than the ranges reported from California landfills in this study. This result may be due to the wide range in landfills, climatic zones, and cover conditions associated with the sites reported in the literature, including several refuse disposal sites in Africa, India, and Asia where

cover systems were not in place. The range in total NMVOC emissions observed from California landfills was slightly larger than that reported in the literature. This result may be due to the higher number of NMVOC chemicals included under the scope of this study.

5.6 Anthropogenic vs. Biogenic Sources of LFG

The sources of the main chemical families investigated in this study are classified as anthropogenic, biogenic or both anthropogenic and biogenic in origin and presented in Table 5.3. The major greenhouse gases (methane, nitrous oxide, and carbon dioxide) are generally biogenic in origin due to anaerobic and aerobic waste degradation as well as oxidation processes occurring in the soil covers. On-site vehicle emissions, flaring and combustion of LFG, and operation of heavy equipment also may contribute to carbon monoxide, carbon dioxide, NOx and SOx emissions and therefore the GHGs were classified as both biogenic and anthropogenic in origin. The origin of RSC emissions is primarily biogenic from anaerobic or aerobic conversion processes of sulfur present in the organic fraction of MSW. However, sulfur can also be released during decomposition of waste tires and other C&D wastes, such as gypsum board. F-gases are strictly anthropogenic in origin and are present in foam insulation materials, refrigerants, fire suppressants (i.e., Halons), cleaning agents, and medical aerosols. The halogenated hydrocarbons are strictly anthropogenic and generally originate from pesticides, adhesives, plastic materials, and rubber. Even though the origin of the alkyl nitrates is not well documented in the landfill environment, the alkyl nitrates are potentially formed from chemical reactions involving byproducts of microbial metabolic processes and other inorganic nitrogen sources present in the landfill environment; thus, they are classified as both anthropogenic and biogenic in origin. The alkanes and alkenes mainly originate from manufactured products such as paper, plastic packaging, personal care products, cleaning solvents, and cooking fuels. As microbial production of low molecular weight alkanes and alkenes has been documented in soil ecosystems, these chemical families are classified as anthropogenic and biogenic in origin. The aldehydes and alkynes originate from biological conversion processes as well as off gassing from chemical products such as paints, adhesives, and plastic materials. The aromatics, in similarity to the halogenated hydrocarbons, are strictly anthropogenic in origin and enter the waste stream through household cleaning solvents, personal care products, household spray applications, paints, textiles, cooking fuels, and furniture. The monoterpenes, alcohols, and ketones are biogenic and anthropogenic in origin, where the production of alcohols and ketones is mostly due to anaerobic fermentation occurring within the landfill environment. Production of monoterpenes is approximately equally divided between off gassing from personal care products, household sprays and detergents and generation during decomposition of green and wood wastes (Table 5.3).

Table 5.3 – Classification of Chemical Family Sources in the Landfill Environment

Chemical Family	Anthropogenic	Biogenic	Both
GHGs			X
RSC			X
F-gas	X		
HH	X		
ON			X
Alk			X
Alke			X
Ald/Alky			X
Ar	X		
Mon			X
Alc			X
Ket			X

5.7 Indirect Effects of Landfill NMVOC Emissions on Human Health, Air Quality, and Climate Change

The indirect effects of fugitive NMVOC emissions on human health, air quality, and climate change are assessed in Figures 5.11 and 5.12. Overall, from the 5 ground-based test sites, large differences in indirect emissions were observed between sites and chemical families. The calculated O_3 and SOA formation potentials, along with the combined GWP (exclusive of the F-gases), HAP emissions, and ODS-weighted emissions (inclusive of F-gases) are provided for each site, categorized by chemical family in Figure 5.11. Overall, Potrero Hills Landfill contributed the most to overall ozone, SOA, CO_2-eq. emissions, and HAPs as compared to all other sites (Figure 5.11). Chiquita Canyon was associated with the highest ODS-weighted emissions (Figure 5.11) and Santa Maria Regional Landfill had low indirect effects overall. The alkenes contributed highly to ozone formation potentials at each landfill, as the measured fluxes and MIR values were relatively high compared to other chemical families (Figure 5.11a). SOA formation potentials across all sites were generally low in magnitude (< 1.4 tonnes/year) and were largely dominated by the monoterpene chemical family, as the FAC values were the highest (~30%) for the alpha and beta pinene NMVOC species (Figure 5.11b and Table 1.1). Even though greenhouse gas associated emissions had the highest y-axis scale over all other metrics (0-120 tonnes/year), the impacts on climate change were relatively low compared to the F-gases (up to 100,000 tonnes/year). The monoterpene chemical family contributed the most to net greenhouse gas emissions, which can be attributed to the high number of carbon atoms comprising each molecule in this particular chemical family (C# up to 10). In addition, the alkene chemical family indirectly contributed to climate change impacts due to the presence of indirect GWPs for ethene, propene, and isoprene (Figure 5.11c). In theory, indirect GWPs can be obtained for every reactive NMVOC involved in tropospheric O_3 production. However, to date, no studies have modeled the full range in indirect GWPs for each of the NMVOC species included in Table 1.1 (Collins et al. 2002).

Out of all metrics investigated, HAP emissions were the most comparable across all landfill sites (Figure 5.11d). Alcohols made up a significant fraction of the total HAP emissions, particularly for the Teapot Dome Landfill. Methanol was the only species within the alcohol family that was considered a HAP. Reduced sulfur compounds, halogenated and aromatic hydrocarbons, and alkanes were predominant HAPs at Teapot Dome, Potrero Hills, Site A, and Chiquita Canyon Landfills. Within these chemical families, BTEX (benzene, toluene, ethylene, xylene isomers) and methylene chloride and trichloroethylene (TCE) are acute and chronically toxic environmental pollutants. ODS-weighted emissions were dominated by the F-gas chemical family, which included chlorofluorocarbons (CFCs, Class I ODS), halons (H1211, Class I ODS), and hydrochlorofluorocarbons (HCFCs, Class II ODS) (Figure 5.11e). Of these species included in the analysis, H1211 had the highest ODS value and, based on the median value of flux estimates, contributed most to ODS-weighted emissions.

Figure 5.11 Summary of the net a) O_3 formation potential, b) SOA formation potential, c) indirect and direct global warming potential, d) HAP emissions, and e) ODS weighted emissions by NMVOC chemical family and landfill site.

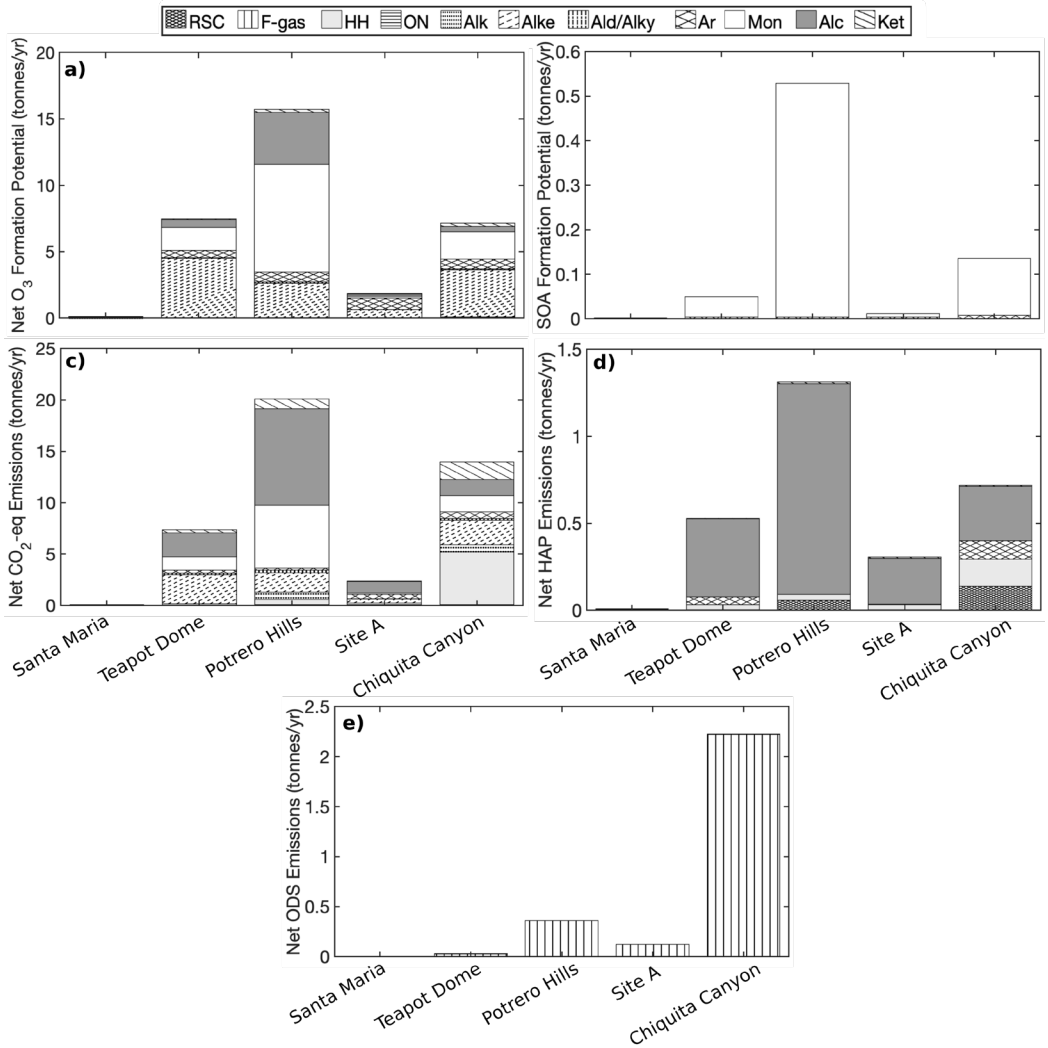

The calculated O_3 and SOA formation potentials, along with the combined GWP (exclusive of the F-gases), HAP emissions, and ODS-weighted emissions (inclusive of F-gases) are provided for each cover category, categorized by chemical family in Figure 5.12. Net ozone formation potential and ODS weighted emissions were highest from the daily cover categories, whereas SOA formation, net indirect/direct GWP weighted emissions, and HAP emissions were greater from the final cover categories. All indirect emissions were generally lowest from the intermediate cover categories (Figure 5.12). Similar to results presented in Figure 5.11 above, monoterpenes, alcohols, and alkenes were the chemical families that contributed most to indirect climate effects across the cover categories surveyed.

Figure 5.12 Summary of the net a) O_3 formation potential, b) SOA formation potential, c) indirect and direct global warming potential, d) HAP emissions, and e) ODS weighted emissions by NMVOC chemical family and cover category.

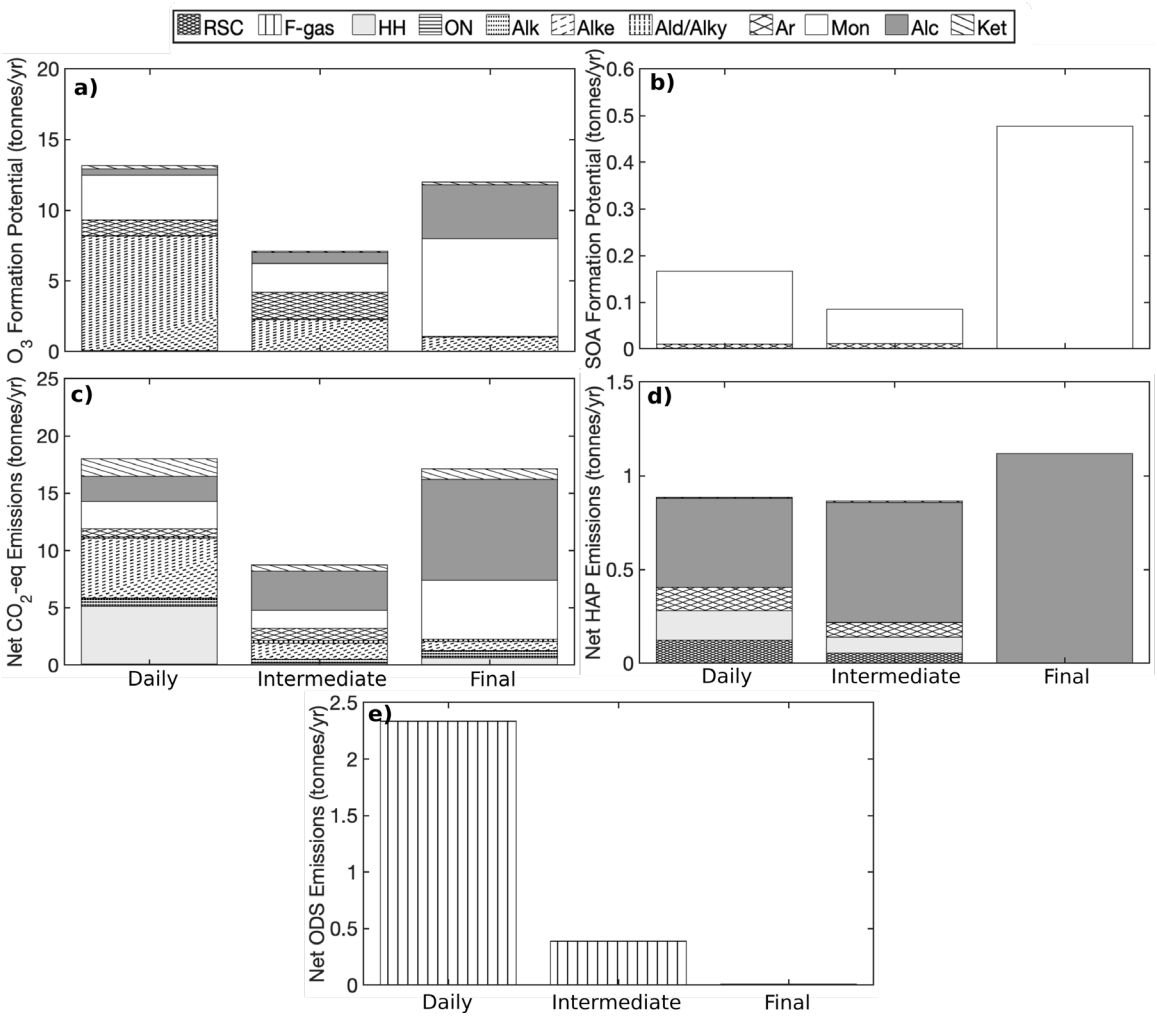

5.8 Additional Emission Control Measures

The recommendations for reducing emissions are provided under two main headings. First, potential measures are provided related to cover systems in landfill facilities. Second, discussion is provided related to other aspects of landfill operations, monitoring, and modeling.

5.8.1 Cover Category and Type

Soil covers were observed to be more effective than non-soil covers for a given cover category. For both daily and intermediate covers, emissions were generally lower from soil covers than for non-soil covers for cases investigated in this study. Higher material content in the covers (increased density, increased thickness) was directly aligned with lower fluxes [Sections 4.7 and 4.8]. While the use of non-soil materials as daily and/or interim cover allows for repurposing various waste and byproduct materials, these materials are not as effective as natural soils in reducing gas flux from landfill systems both for main (methane, carbon dioxide, nitrous oxide, and carbon monoxide) and trace NMVOC landfill gas constituents [Section 5.3]. In addition, for interim cover applications, natural soil covers were more effective at limiting gas emissions than composite soil/non-soil material covers (homogeneous mixtures or layered systems) [Section 5.3].

Flux decreased from daily to intermediate to final covers for all sites analyzed in this investigation [Section 5.1]. The decreases between daily and intermediate covers were greater than the decreases between intermediate and final covers. While the emissions were lower from thicker covers than thinner covers, increasing the thickness of the covers is not critical beyond certain limits [Section 4.13]. Proper use and management of the individual cover systems can be effective as control measures to reduce emissions from landfill facilities.

Daily and intermediate covers are temporary systems that affect emissions of a landfill in the relatively short-term. Final covers are used essentially in perpetuity as barriers against emissions and thus the performance and durability of these systems is critical.

Specific recommendations for the individual cover categories are provided below:

Daily Covers

- Minimize the areal extent of daily cover.
- Reduce duration of time period that daily cover is serving as barrier between the waste mass and the atmosphere.
- Avoid highly porous and open structure bulk materials (e.g., green waste, wood waste, and auto fluff [Section 5.3] as well as construction/demolition waste [Section 4.3.3.2]) for use in covers for extended periods (months, years).

Intermediate Covers

- Thickness – increasing thickness of intermediate covers is effective up to approximately 1 meter. Additional cover thickness beyond this value does not provide significant reduction in emissions [Section 4.13, Appendix A4].

- Place interim cover as quickly as possible (days to weeks, not months).
- Fines content for soil (% passing 0.075 mm) over 30% is more effective in controlling emissions compared to soils with lower fines content [Section 4.8].

Final Covers

- Based on comparison of a conventional cover and an alternative final (i.e., evapotranspirative) cover at one of the sites investigated, the gas flux from the alternative cover was higher than the flux through the conventional cover [Section 5.3]. The differences in flux were particularly significant for methane. To the PIs knowledge this was the first-time gas flux was measured through a water balance cover system.
- Higher plasticity soils (PI over 20%) are more effective in controlling emissions compared to soils with lower plasticity [Section 4.8].
- Based on thresholds developed for geotechnical landfill operations for soil covers, use long-term cover thickness of at least 150 cm (methane) and 75 cm (NMVOCs); compact soil in cover for maintaining at least 2000 kg of mass in long-term cover systems; and use soil with at least 60% fines content and 12% clay content for long-term covers [Appendix A4].

5.8.2 Other Aspects of Landfill Operations, Monitoring, and Modeling

- Minimize the size of active working face to reduce direct atmospheric exposure of freshly placed waste as well as all underlying wastes [Section 5.4].
- If specific regions of a landfill are designated for waste placement during wet weather conditions, apply more robust cover configurations for these regions than for other regions at the site to attain similar barrier function against gas flux [Section 5.3].
- Due to large uncertainty in modeling gas generation, the use of collection efficiency as a measure of emissions is not recommended [Section 4.9].
- Top-down aerial measurements can provide whole site emissions and may be used to estimate overall site data for methane emissions.
- Bottom-up ground measurements using flux chambers provide discrete measurements for individual cover types and categories for methane as well as a large number of additional gases, which cannot be obtained with aerial measurements. The ground-based measurements are effective for assessing individual cover systems and for comparing materials/designs for the individual covers. In addition, ground measurements provide data on the flux/emissions of trace gases.
- Both top-down and bottom-up measurements provide context for methane emissions from landfills and combining the methods has benefit of obtaining methane emissions information at different scales [Section 5.4].
- Specific to N_2O emissions, avoid concentrated placement of organic sludges (e.g., waste-water treatment plant sludge) within the landfill system [Section 4.3.3.2].
- NMVOCs are trace components in LFG yet are a significant and detectable fraction of landfill gas with net positive fluxes from all cover categories and appreciable portions of total emissions. NMVOC emissions can be included in

GHG inventories as well as used in air quality studies and impacts on public health and the environment.

- Emissions of different chemicals vary in magnitudes as well as in the underlying trends with physical, operational, and climatic conditions. Different physical, chemical, biological, thermal, and biochemical processes affect the different types of gas species that may be present in a landfill environment affecting the potential transformation of the chemical species. Therefore, from an analysis and modeling standpoint, investigations conducted for a given chemical/chemical family cannot be applied or scaled for other chemicals/chemical families. As methane does not serve as a surrogate for other chemicals, applying conventional methane modeling methods to other chemical species is not recommended [Part 5].
- The acceptance of waste tires was not determined to have significant effect on emissions overall [Section 4.10]. The two potential chemical families with direct tire relevance are RSCs and aromatic hydrocarbons. For RSC (reduced sulfur compounds) emissions, limited influence of presence of tires was measured. The presence of tires may potentially have sorptive capacity for aromatic hydrocarbons and resulted in the reduced emissions of these compounds [Section 4.10.3].
- Based on measured variability of emissions from different sized facilities, a holistic analysis approach is recommended for gas emissions from landfills, independent of facility size [Parts 4 and 5].

5.9 Future Research

Based on findings of the current investigation, the following future research priorities are identified:

- Quantify emissions of emerging chemicals and rank these chemicals for public health and climate change effects.
- Evaluate alternative final (evapotranspirative) covers from a gas emissions perspective. Significant analysis has been conducted for barrier performance against moisture infiltration of these systems, however commensurate analyses have not been conducted for gas transport. Preliminary results herein suggest that further investigation is warranted.
- Establish efficacy of specialty geomembranes that include devoted gas barrier layer.
- Investigate emissions of compost facilities.
- Improve modeling of gas transport through cover systems including multi-phase and multi-component analyses.
- Improve biological degradation and transformation of gases emitting from landfills using bio-cover principles.
- Similar to design methods for hydraulic performance of barriers, establish quantitative design parameters for performance of cover materials as gas barriers, ensuring quality control in construction and operations.
- Establish site-specific gas emissions performance for native soils typically used for cover applications and other cover materials, similar to requirements for hydraulic barrier performance. For example, in evaluating the use of green

waste erosion control cover over an interim soil cover on a slope, the potential additional biogenic VOC emissions (attributed to the presence of green waste cover) needs to be balanced against the erosion control function. Loss of integrity and effectiveness of the intermediate soil cover occurs due to erosion.

- Establish methodology for measurement of landfill gas flux at active working face locations. Direct adoption of static flux chamber method is difficult at these locations due to safety concerns in a heavy equipment work zone, large particle sizes of waste, difficulty with driving chamber into waste surface, and developing hydraulic seal around chamber perimeter in the highly porous waste material.

GLOSSARY

Term	Definition
abiotic	not biological
advective	transport caused by pressure differential
aerobic oxidation	term used to describe bacterial metabolism in an oxygenated (aerobic) environment.
aliphatic	of, relating to, or being an organic compound (such as an alkane) having an open-chain structure
anaerobic decomposition	breakdown of organic material into simpler compounds in environment free of oxygen
anaerobic soluble sugar fermentation	breakdown of sugar by enzymes in environment free of oxygen
anthropogenic	resulting from the influence/actions of human beings
autotrophic	requiring only carbon dioxide or carbonates as source of carbon and a simple inorganic nitrogen compound for metabolic synthesis of organic molecules
bandwidth	a range within a band of wavelengths, frequencies, or energies
biogenic	produced by living organisms
biological transformation	changing one configuration to another through processes of living organisms
BMP assays	analysis of biomethane potential
BMP protocols	set of established procedures for determining biomethane potential
decarboxylation	the removal or elimination of carboxyl from a molecule
diffusive	transport caused by pressure differential
electron acceptor	chemical entity that accepts electrons transferred to it from another compound
evapotranspirative cover system	monolithic or capillary break soil cover system that functions to balance water transport using evapotranspiration from the surface
extracellular byproducts	waste products released by bacterial cells during metabolism of different substrates present in the environment.
extracellular polymeric substances	sticky polysaccharides released by bacteria to improve flocculation and attachment to surfaces.
gas particle transfer	movement of gas particles
heterotrophic	requiring complex organic compounds of nitrogen and carbon (such as that obtained from plant or animal matter) for metabolic synthesis
hydraulic conductivity	the ease with which fluids pass through porous media under unit hydraulic gradient
hydrophilic	having strong affinity to water

Term	Definition
hydrophobic	lacking affinity to water
ionizable functional groups	any uncharged group in a molecular entity that is capable of dissociating by yielding an ion (usually an H+ ion) or an electron and itself becoming oppositely charged
kernel center	an empirical method to estimate probability distribution functions that relies on distance weighting to randomized points (kernel centers) in high dimensional space.
lipophilic	having an affinity to lipids (e.g., fats)
lysimeter	isolated zone installed beneath system to quantify leakage rate
methane oxidation	biologically mediated transformation of methane in cover materials in the presence of oxygen and methanotrophs
methanogenesis	formation of methane by microbes known as methanogens
methanotrophs	bacteria or archaea that metabolize methane as their only source of carbon and energy
non-parametric kernel density estimator	an empirical method to estimate probability distribution functions that relies on distance weighting to randomized points (kernel centers) in high dimensional space.
occluded	obstructed, isolated
parametric statistical model	A statistical model that has a direct, analytical procedure to calculate a probability distribution function.
physico-chemical	being physical and chemical
porosity	volumetric fraction of voids in a soil structure (quotient of volume of voids and total volume)
radiative forcing	difference between insolation (sunlight) absorbed by the Earth and energy radiated back to space
retardation	delay in transport of a chemical
sorption	act of holding by either adsorption or absorption
tensile strain	act of increasing in length due to application of tensile forces or stresses
tortuosity	state of being twisted or winding

REFERENCES

Abichou, T., Chanton, J., Powelson, D., Fleiger, J., Escoriaza, S., Lei, Y., and Stern, J., (2006a), "Methane Flux and Oxidation at Two Types of Intermediate Landfill Covers," *Waste Management*, 26(11), 1305–1312.

Abichou, T., Powelson, D., Chanton, J., Escoriaza, S., and Stern, Jennifer, (2006b), "Characterization of Methane Flux and Oxidation at a Solid Waste Landfill," *Journal of Environmental Engineering*, 132(2), 220–228.

Abichou, T., Clark, J., and Chanton, J., (2011), "Reporting Central Tendencies of Chamber Measured Surface Emission and Oxidation," *Waste Management, Landfill Gas Emission and Mitigation*, 31(5), 1002–1008.

Abushammala, M. F. M., Basri, N. E. A., Basri, H., Kadhum, A. A. H., and El-Shafie, A. H., (2012), "Methane and Carbon Dioxide Emissions from Sungai Sedu Open Dumping During Wet Season in Malaysia," *Ecological Engineering*, 49, 254–263.

Abushammala, M. F. M., Basri, N. E. A., and Elfithri, R., (2013), "Assessment of Methane Emission and Oxidation at Air Hitam Landfill Site Cover Soil in Wet Tropical Climate," *Environmental Monitoring and Assessment*, 185(12), 9967–9978.

Abushammala, M. F. M., Basri, N. E. A., Kadhum, A. A. H., Basri, H., El-Shafie, A. H., and Sharifah Mastura, S. A., (2014), "Evaluation of Methane Generation Rate and Potential from Selected Landfills in Malaysia," *International Journal of Environmental Science and Technology*, 11(2), 377–384.

Abushammala, M. F., Basri, N. E. A., and Younes, M. K., (2016), "Seasonal Variation of Landfill Methane and Carbon Dioxide Emissions in a Tropical Climate," *International Journal of Environmental Science and Development*, 7(8), 586.

Akerman, A., Budka, A., Hayward-Higham, S., Bour, O., and Rallu, D., (2007), "Methane Emissions Measurements on Different Landfills," *Proceedings Sardinia 2007, Eleventh International Waste Management and Landfill Symposium*, S. Margerita di Pula, Cagliari, Italy, October 1st-5th, 2007, 10.

Alamo-Nole, L., Perales-Perez, O., and Roman, F. R., (2012), "Use of Recycled Tires Crumb Rubber to Remove Organic Contaminants From Aqueous and Gaseous Phases," *Desalination and Water Treatment*, 49(1–3), 296–306.

Allen, M. R., Braithwaite, A., and Hills, C. C., (1997), "Trace Organic Compounds in Landfill Gas at Seven U.K. Waste Disposal Sites," *Environmental Science & Technology*, 31(4), 1054–1061.

Amini, H. R., Reinhart, D. R., and Mackie, K. R., (2012), “Determination of First-order Landfill Gas Modeling Parameters and Uncertainties,” *Waste Management*, 32(2), 305–316.

Amini, H. R., Reinhart, D. R., and Niskanen, A., (2013), “Comparison of First-Order-Decay Modeled and Actual Field Measured Municipal Solid Waste Landfill Methane Data,” *Waste Management*, 33(12), 2720–2728.

Andersland, O. B. and Ladanyi, B. (1994). *An Introduction to Frozen Ground Engineering*, Chapman and Hall, London.

Aprem, A. S., Joseph, K., Mathew, T., Altstaedt, V., and Thomas, S., (2003), “Studies on Accelerated Sulphur Vulcanization of Natural Rubber using 1-Phenyl-2, 4-Dithiobiuret/tertiary Butyl Benzothiazole Sulphenamide,” *European Polymer Journal*, 39(7), 1451–1460.

Archbold, M. E., Elliot, T., and Kalin, R. M., (2012), “Carbon Isotopic Fractionation of CFCs during Abiotic and Biotic Degradation,” *Environmental Science & Technology*, 46(3), 1764–1773.

Asadi, M., Yuen, S. T. S., Bogner, J., Chen, D., and Lightbody, P., (2014), “Seasonal Variation of Methane Emissions from Two Landfills in Australia,” *7th International Congress on Environmental Geotechnics*: *iceg2014*, 1355–1360.

Atkinson, R., and Arey, J. (2003), “Gas-phase Tropospheric Chemistry of Biogenic Volatile Organic Compounds: A Review,” *Atmospheric Environment, The 1997 Southern California Ozone Study (SCOS97-NARSTO)*, 37, 197–219.

Atkinson, R., Aschmann, S. M., Carter, W. P. L., Winer, A. M., and Pitts, J. N. J., (1982), “Alkyl Nitrate Formation from the NO_x-air Photooxidations of C_2-C_8 n-alkanes,” *J. Phys. Chem.*; (United States), 86:23.

Awad, N. H., Ali, M. Z., Suganthan, P. N., and Reynolds, R. G., (2016), “An Ensemble Sinusoidal Parameter Adaptation Incorporated with L-SHADE for solving CEC2014 benchmark problems,” Proceedings of the IEEE Congress on Evolutionary Computation (CEC), 2958–2965.

Aydilek, A. H., Madden, E. T., and Demirkan, M. M., (2006), “Field Evaluation of a Leachate Collection System Constructed with Scrap Tires,” *Journal of Geotechnical and Geoenvironmental Engineering*, 132(8), 990–1000.

Balsiger, C., Werner, D., and Holliger, C., (2002), “Reductive De-chlorination of CFCs and HCFCs under Methanogenic Conditions,” *In Proceedings of the Third International Conference on Remediation of Chlorinated and Recalcitrant Compounds*, 20–23.

Barlaz, M. A., Staley, B. F., and de los Reyes III, F. L., (2010a), “Anaerobic Biodegradation of Solid Waste,” In: Mitchell, R., Gu, J.D. (eds.), *Environmental Microbiology* (2nd edition), Wiley-Blackwell, New Jersey.

Barlaz, M. A., Bareither, C. A., Hossain, A., Saquing, J., Mezzari, I., Benson, C. H., Tolaymat, T. M., and Yazdani, R., (2010b), “Performance of North American Bioreactor Landfills. II: Chemical and Biological Characteristics,” *Journal of Environmental Engineering,* 136(8), 839–853.

Barlaz, M. A., Chanton, J. P., and Green, R. B., (2009), “Controls on Landfill Gas Collection Efficiency: Instantaneous and Lifetime Performance,” *Journal of the Air & Waste Management Association*, 59(12), 1399–1404.

Barlaz, M. A., Green, R. B., Chanton, J. P., Goldsmith, C. D., and Hater, G. R., (2004), “Evaluation of a Biologically Active Cover for Mitigation of Landfill Gas Emissions,” *Environmental Science & Technology*, 38(18), 4891–4899.

Barlaz, M. A., Ham, R. K., Schaefer, D. M., and Isaacson, R., (1990), “*Methane Production from Municipal Refuse: A Review of Enhancement Techniques and Microbial Dynamics*,” Critical Reviews in Environmental Control, 19(6), 557–584.
Barry, R. C., (2008), “Gas-Phase Mass Transfer Processes in Landfill Microbiology,” *Journal of Environmental Engineering*, 134(3), 191–199.

Barton, P. K., and Atwater, J. W. (2002). “Nitrous Oxide Emissions and the Anthropogenic Nitrogen in Wastewater and Solid Waste,” *Journal of Environmental Engineering*, 128(2), 137–150.

Baykal, G., Yesiller, N. and Koprulu, K., (1992), "Rubber-Clay Liners Against Petroleum Based Contaminants," *Environmental Geotechnology*, Usman and Acar (eds.), Balkema, Rotterdam, Netherlands, pp 477-481.

Bentley, H. W., Smith, S. J., and Schrauf, T., (2005), “Baro-Pneumatic Estimation of Landfill Gas Generation Rates at Four Landfills in the Southeastern United States,” *Proceedings from the SWANA 28th Annual Landfill Gas Symposium*, 1–16.

Bodelier, P. L. E., and Laanbroek, H. J., (2004), “Nitrogen as a Regulatory Factor of Methane Oxidation in Soils and Sediments,” *FEMS Microbiology Ecology*, 47(3), 265–277.
Boeckx, P., Cleemput, O. van, and Villaralvo, I., (1996), “Methane Emission from a Landfill and the Methane Oxidising Capacity of its Covering Soil,” *Soil Biology and Biochemistry*, 28(10), 1397–1405.

Boeckx, P., and Cleemput, O. van, (1996), “Methane Oxidation in a Neutral Landfill Cover Soil: Influence of Moisture Content, Temperature, and Nitrogen-Turnover,” *Journal of Environmental Quality*, 25(1), 178–183.

Boeckx, P., Van Cleemput, O., and Meyer, T., (1998), “The influence of Land Use and Pesticides on Methane Oxidation in some Belgian Soils,” *Biology and Fertility of Soils*, 27(3), 293–298.

Bogner, J. E., (1992), “Anaerobic Burial of Refuse in Landfills: Increased Atmospheric Methane and Implications for Increased Carbon Storage,” *Ecological Bulletins*, 42, 98–108.

Bogner, J., and Spokas, K., (1993), “Landfill CH_4: Rates, Fates, and Role in Global Carbon Cycle,” *Chemosphere*, 26(1), 369–386.

Bogner, J., Spokas, K. and Jolas, J., (1993), “Comparison of Measured and Calculated Methane Emissions at Mallard Lake Landfill, DuPage County, IL (USA),” *Proceedings of Sardinia ‘93 International Landfill Conference*, Univ. of Cagliari, Sardinia, 605-616.

Bogner, J., Spokas, K., Burton, E., Sweeney, R., and Corona, V., (1995), “Landfills as Atmospheric Methane Sources and Sinks,” *Chemosphere*, 31(9), 4119–4130.

Bogner, J., Meadows, M., and Czepiel, P., (1997a), “Fluxes of Methane Between Landfills and the Atmosphere: Natural and Engineered Controls,” *Soil Use and Management*, 13(s4), 268–277.

Bogner, J., Spokas, K., Niemann, M., Niemann, L., and Baker, J., (1997b). *Emissions of Nonmethane Organic Compounds at an Illinois (USA) Landfill: Preliminary Field Measurements*. Argonne National Lab., IL (United States).

Bogner, J. E., Spokas, K. A., and Burton, E. A., (1997c), “Kinetics of Methane Oxidation in a Landfill Cover Soil: Temporal Variations, a Whole-Landfill Oxidation Experiment, and Modeling of Net CH4 Emissions,” *Environmental Science & Technology*, 31(9), 2504–2514.

Bogner, J. E., Spokas, K. A., and Burton, E. A., (1999), “Temporal Variations in Greenhouse Gas Emissions at a Midlatitude Landfill,” *Journal of Environmental Quality*, 28(1), 278–288.

Bogner, J., Spokas, K., Chanton, J., Powelson, D., Fleiger, J., and Abichou, T., (2005), “Modeling Landfill Methane Emissions from Biocovers: A Combined Theoretical-Empirical Approach,” *Proceedings Sardinia 2005, Tenth International Waste Management and Landfill Symposium*, S. Margerita di Pula, Cagliari, Italy, October 1st-5th, 2005.

Bogner, J. E., Chanton, J. P., Blake, D., Abichou, T., and Powelson, D., (2010), “Effectiveness of a Florida Landfill Biocover for Reduction of CH_4 and NMHC Emissions,” *Environmental Science & Technology*, 44(4), 1197–1203.

Bogner, J. E., Spokas, K. A., and Chanton, J. P., (2011), “Seasonal Greenhouse Gas Emissions (Methane, Carbon Dioxide, Nitrous Oxide) from Engineered Landfills: Daily, Intermediate, and Final California Cover Soils,” *Journal of Environmental Quality*, 40(3), 1010–1020.

Börjesson, G., and Svensson, B. H., (1997a), “Seasonal and Diurnal Methane Emissions from a Landfill and their Regulation by Methane Oxidation,” *Waste Management & Research*, 15(1), 33–54.

Börjesson, G., and Svensson, B. H., (1997b), “Effects of a Gas Extraction Interruption on Emissions of Methane and Carbon Dioxide from a Landfill, and on Methane Oxidation in the Cover Soil,” *Journal of Environmental Quality*, 26(4), 1182–1190.

Börjesson, G., and Svensson, B. H., (1997c), “Nitrous Oxide Emissions from Landfill Cover Soils in Sweden,” *Tellus B*, 49(4), 357–363.

Börjesson, G., Sundh, I., Tunlid, A., and Svensson, B. H., (1998), “Methane Oxidation in Landfill Cover Soils, as Revealed by Potential Oxidation Measurements and Phospholipid Fatty Acid Analyses,” *Soil Biology and Biochemistry*, 30(10), 1423–1433.

Börjesson, G., Danielsson, Å., and Svensson, B. H., (2000), “Methane Fluxes from a Swedish Landfill Determined by Geostatistical Treatment of Static Chamber Measurements,” *Environmental Science & Technology*, 34(18), 4044–4050.

Börjesson, G., Chanton, J., and Svensson, B. H., (2001), “Methane Oxidation in Two Swedish Landfill Covers Measured with Carbon-13 to Carbon-12 Isotope Ratios,” *Journal of Environmental Quality*, 30(2), 369–376.

Börjesson, G., Samuelsson, J., and Chanton, J., (2007), “Methane Oxidation in Swedish Landfills Quantified with the Stable Carbon Isotope Technique in Combination with an Optical Method for Emitted Methane,” *Environmental Science & Technology*, 41(19), 6684–6690.

Börjesson, G., Samuelsson, J., Chanton, J., Adolfsson, R., Galle, B., and Svensson, B. H., (2009), “A National Landfill Methane Budget for Sweden Based on Field Measurements, and an Evaluation of IPCC models,” *Tellus B: Chemical and Physical Meteorology*, 61(2), 424–435.

Bredberg, K., Andersson, B. E., Landfors, E. and Holst, O., (2002), “Microbial Fetoxification of Waste Rubber Material by Wood-Rotting Fungi,” *Bioresource Technology*, 83: 221–224.

Brosseau, J., and Heitz, M., (1994), “Trace Gas Compound Emissions from Municipal Landfill Sanitary Sites,” *Atmospheric Environment*, 28(2), 285–293.

Buffiere, P., Loisel, D., Bernet, N., and Delgenes, J. P., (2006), "Towards New Indicators for the Prediction of Solid Waste Anaerobic Digestion Properties," *Water Science and Technology*, 53(8), 233–241.

Burton, D. A., (2016), "Composite Standard Deviations," http://www.burtonsys.com/climate/composite_standard_deviations.html, last accessed August 1st, 2019.

Budka, A., Aniel, D., Puglierin, L., Stoppioni, E., (2007), "Bioreactor and Conventional Landfill: LFG Modeling After Three Management Years of Two Compared Cells in Sonzay, France," *Proceedings of the Eleventh International Waste Management and Landfill Symposium*, Sardinia, Italy.
California Air Resources Board (CARB), (2009). "Almanac Emission Projection Data: 2015 Estimated Annual Average Emissions (Statewide)," https://www.arb.ca.gov/app/emsinv/emssumcat.php (July 2, 2019).

CalRecycle, (2017). *State of Disposal and Recycling in California: For Calendar Year 2017*. Department of Resources Recycling and Recovery, State of California, https://www2.calrecycle.ca.gov/Publications/Download/1399.

CalRecycle, (2018a), "Alternative Daily Cover (ADC)," https://www.calrecycle.ca.gov/lgcentral/basics/adcbasic#Approved.

CalRecycle, (2018b), "Tire Recycling and Market Development," https://www.calrecycle.ca.gov/Tires/Recycling/> (Dec. 20, 2019).

CalRecycle, (2019a), "Listing of Solid Waste Facilities and Disposal Sites Under Enforcement Orders," <https://www2.calrecycle.ca.gov/SWFacilities/Enforcement/Orders/> (Sep. 1, 2019).

CalRecycle, (2019b), "Waste Characterization Tool Limits and Background," https://www2.calrecycle.ca.gov/WasteCharacterization/StudyDesign

Capaccioni, B., Caramiello, C., Tatàno, F., and Viscione, A., (2011), "Effects of a Temporary HDPE Cover on Landfill Gas Emissions: Multiyear Evaluation with the Static Chamber Approach at an Italian Landfill," *Waste Management, Landfill Gas Emission and Mitigation*, 31(5), 956–965.

Cardellini, C., Chiodini, G., Frondini, F., Granieri, D., Lewicki, J., and Peruzzi, L., (2003), "Accumulation Chamber Measurements of Methane Fluxes: Application to Volcanic-Geothermal Areas and Landfills," *Applied Geochemistry*, 18(1), 45–54.

Carter, W. (2009). *Updated Maximum Incremental Reactivity Scale and Hydrocarbon Bin Reactivities for Regulatory Applications*. California Air Resources Board.

Caulton, D. R., Shepson, P. B., Santoro, R. L., Sparks, J. P., Howarth, R. W., Ingraffea, A. R., Cambaliza, M. O. L., Sweeney, C., Karion, A., Davis, K. J., Stirm, B. H., Montzka, S. A., and Miller, B. R., (2014), "Toward a Better Understanding and Quantification of Methane Emissions from Shale Gas Development," *Proceedings of the National Academy of Sciences*, 111(17), 6237–6242.

Cecchi, F., Pavan, P., Musacco, A., Alvarez, J. M., and Vallini, G., (1993). "Digesting The Organic Fraction Of Municipal Solid Waste: Moving From Mesophilic (37°C) To Thermophilic (55°C) Conditions," *Waste Management & Research*, 11(5), 403–414.

Celeiro, M., Lamas, J. P., Garcia-Jares, C., Dagnac, T., Ramos, L., and Llompart, M., (2014), "Investigation of PAH and Other Hazardous Contaminant Occurrence in Recycled Tyre Rubber Surfaces. Case-Study: Restaurant Playground in an Indoor Shopping Centre," *International Journal of Environmental Analytical Chemistry*, 94(12), 1264–1271.

Chakraborty, M., Sharma, C., Pandey, J., Singh, N., and Gupta, P. K., (2011), "Methane Emission Estimation from Landfills in Delhi: A Comparative Assessment of Different Methodologies," *Atmospheric Environment*, 45(39), 7135–7142.

Chang, R. Y.-W., Miller, C. E., Dinardo, S. J., Karion, A., Sweeney, C., Daube, B. C., Henderson, J. M., Mountain, M. E., Eluszkiewicz, J., Miller, J. B., Bruhwiler, L. M. P., and Wofsy, S. C., (2014), "Methane Emissions from Alaska in 2012 from CARVE Airborne Observations," *Proceedings of the National Academy of Sciences*, 111(47), 16694–16699.

Chanton, J., and Liptay, K., (2000), "Seasonal Variation in Methane Oxidation in a Landfill Cover Soil as Determined by an In Situ Stable Isotope Technique," *Global Biogeochemical Cycles*, 14(1), 51–60.

Chanton, J., Abichou, T., Langford, C., Spokas, K., Hater, G., Green, R., Goldsmith, D., and Barlaz, M. A., (2011), "Observations on the Methane Oxidation Capacity of Landfill Soils," *Waste Management, Landfill Gas Emission and Mitigation*, 31(5), 914–925.

Chaudhari, C. V., Bhardwaj, Y. K., Patil, N. D., Dubey, K. A., Kumar, V., and Sabharwal, S., (2005), "Radiation-Induced Vulcanisation of Natural Rubber Latex in Presence of Styrene-Butadiene Rubber Latex," *Radiation Physics and Chemistry*, 72(5), 613–618.

Chen, I. C., Hegde, U., Chang, C. H., and Yang, S. S. (2008)., "Methane and Carbon Dioxide Emissions from Closed Landfill in Taiwan," *Chemosphere*, 70(8), 1484–1491.

Chickering, G. W., Krause, M. J., and Townsend, T. G., (2018), "Determination of As-Discarded Methane Potential in Residential and Commercial Municipal Solid Waste," *Waste Management*, 76, 82–89.

Chiemchaisri, C., Chiemchaisri, W., and Sawat, A., (2006), “Mitigation of Methane Emission from Solid Waste Disposal Site in the Tropics by Vegetated Cover Soil,” *Asian Journal of Water, Environment and Pollution*, 3(2), 29–33.

Chiemchaisri, C., Chiemchaisri, W., Kumar, S., and Hettiaratchi, J. P. A., (2007), “Solid Waste Characteristics and their Relationship to Gas Production in Tropical Landfill,” *Environmental Monitoring and Assessment*, 135(1), 41–48.

Chiemchaisri, C., and Visvanathan, C., (2008), “Greenhouse Gas Emission Potential of the Municipal Solid Waste Disposal Sites in Thailand,” *Journal of the Air & Waste Management Association*, 58(5), 629–635.

Cho, J. K., Park, S. C., and Chang, H. N., (1995), “Biochemical Methane Potential and Solid State Anaerobic Digestion of Korean Food Wastes,” *Bioresource Technology*, 52(3), 245–253.

Cho, H. S., Moon, H. S., and Kim, J. Y., (2012), “Effect of Quantity and Composition of Waste on the Prediction of Annual Methane Potential from Landfills,” *Bioresource Technology,* 109, 86–92.

Christensen, T. H., Cossu, R., and Stegmann, R., (1996). *Landfilling of Waste: Biogas*. E & FN Spon, London; New York, NY.

Chritiansson, M., Stenberg, B., Wallenberg, L. R., and Holst, O., (1998), “Reduction of surface sulphur upon microbial devulcanization of rubber materials,” *Biotechnology Letters*, 20(7), 637–642.

Christophersen, M., and Kjeldsen, P., (2001), “Lateral Gas Transport in Soil Adjacent to an Old Landfill: Factors Governing Gas Migration,” *Waste Management & Research*, 19(6), 579–594.

Christophersen, M., Kjeldsen, P., Holst, H., and Chanton, J., (2001), “Lateral Gas transport in Soil Adjacent to an Old Landfill: Factors Governing Emissions and Methane Oxidation,” *Waste Management & Research*, 19(6), 595–612.

Collins, W. J., Derwent, R. G., Johnson, C. E., and Stevenson, D. S., (2002), “The Oxidation of Organic Compounds in the Troposphere and their Global Warming Potentials,” *Climatic Change*, 52(4), 453–479.

Conesa, J. A., Martín-Gullón, I., Font, R., and Jauhiainen, J., (2004), “Complete Study of the Pyrolysis and Gasification of Scrap Tires in a Pilot Plant Reactor,” *Environmental Science & Technology*, 38(11), 3189–3194.

Conley, S., Franco, G., Faloona, I., Blake, D. R., Peischl, J., and Ryerson, T. B., (2016), “Methane Emissions from the 2015 Aliso Canyon Blowout in Los Angeles, CA,” *Science*, 351(6279), 1317–1320.

Conley, S., Faloona, I., Mehrotra, S., Suard, M., Lenschow, D. H., Sweeney, C., Herndon, S., Schwietzke, S., Pétron, G., Pifer, J., Kort, E. A., and Schnell, R., (2017), “Application of Gauss’s Theorem to Quantify Localized Surface Emissions from Airborne Measurements of Wind and Trace Gases,” *Atmospheric Measurement Techniques*, 10, 3345–3358.

Crosson, E. R., (2008), “A Cavity Ring-Down Analyzer for Measuring Atmospheric Levels of Methane, Carbon Dioxide, and Water Vapor,” *Applied Physics B*, 92(3), 403–408.

Cusworth, D. H., Duren, R., Thorpe, A. K., Tseng, E., Thompson, D., Guha, A., Newman, S., Foster, K., and Miller, C. E., (2020), “Using Remote Sensing to Detect, Validate, and Quantify Methane Emissions from California Solid Waste Operations.” *Environmental Research Letters*.

Czepiel, P. M., Mosher, B., Harriss, R. C., Shorter, J. H., McManus, J. B., Kolb, C. E., Allwine, E., and Lamb, B. K., (1996), “Landfill Methane Emissions Measured by Enclosure and Atmospheric Tracer Methods,” *Journal of Geophysical Research: Atmospheres*, 101(D11), 16711–16719.

Czepiel, P. M., Shorter, J. H., Mosher, B., Allwine, E., McManus, J. B., Harriss, R. C., Kolb, C. E., and Lamb, B. K., (2003), “The Influence of Atmospheric Pressure on Landfill Methane Emissions,” *Waste Management, Second Intercontinental Landfill Research Symposium*, 23(7), 593–598.

Daniel, J. S., and Solomon, S., (1998), “On the Climate Forcing of Carbon Monoxide,” *Journal of Geophysical Research*: *Atmospheres*, 103(D11), 13249–13260.

Davidson, E. A., Savage, K., Verchot, L. V., and Navarro, R., (2002), “Minimizing Artifacts and Biases in Chamber-based Measurements of Soil Respiration,” *Agricultural and Forest Meteorology*, *FLUXNET 2000 Synthesis*, 113(1), 21–37.

Deipser, A., and Stegmann, R., (1997), “Biological Degradation of VCCs and CFCs under Simulated Anaerobic Landfill Conditions in Laboratory Test Digesters,” *Environmental Science and Pollution Research*, 4(4), 209–216.

De Visscher, A., Thomas, D., Boeckx, P., and Cleemput, O. van, (1999), “Methane Oxidation in Simulated Landfill Cover Soil Environments,” *Environmental Science & Technology*, 33(11), 1854–1859.

De Visscher, A., Schippers, M., and Cleemput, O. van, (2001), “Short-term Kinetic Response of Enhanced Methane Oxidation in Landfill Cover Soils to Environmental Factors,” *Biology and Fertility of Soils*, 33(3), 231–237.

De Visscher, A. and Cleemput, O. van, (2003), “Induction of Enhanced CH_4 Oxidation in Soils: NH_4+ Inhibition Patterns,” *Soil Biology and Biochemistry*, 35, 907-913.

DeWalle, F. B., Hammerberg, E., and Chian, E. S. K., (1978), “Gas Production from Solid Waste in Landfills,” *Journal of the Environmental Engineering Division*, 104(3), 415–432.
Di Bella, G., Di Trapani, D., and Viviani, G., (2011), “Evaluation of Methane Emissions from Palermo Municipal Landfill: Comparison between Field Measurements and Models,” *Waste Management*, 31(8), 1820–1826.

Dionisio, K. L., Frame, A. M., Goldsmith, M.-R., Wambaugh, J. F., Liddell, A., Cathey, T., Smith, D., Vail, J., Ernstoff, A. S., Fantke, P., Jolliet, O., and Judson, R. S., (2015), “Exploring Consumer Exposure Pathways and Patterns of use for Chemicals in the Environment,” *Toxicology Reports*, 2, 228–237.

Dionisio, K. L., Phillips, K., Price, P. S., Grulke, C. M., Williams, A., Biryol, D., Hong, T., and Isaacs, K. K., (2018), “The Chemical and Products Database, a Resource for Exposure-Relevant Data on Chemicals in Consumer Products,” *Scientific Data*, 5(1), 1–9.

Di Trapani, D., Di Bella, G., and Viviani, G., (2013), “Uncontrolled Methane Emissions from a MSW Landfill Surface: Influence of Landfill Features and Side Slopes,” *Waste Management*, Landfill Processes, 33(10), 2108–2115.

Dodds, J., Domenico, W. F., Evans, D. R., Fish, L. W., Lassahn, P. L., and Toth, W. J., (1983). *Scrap Tires: a Resource and Technology Evaluation of Tire Pyrolysis and Other Selected Alternate Technologies*. EG and G Idaho, Inc., Idaho Falls (USA).

Duan, J., Tan, J., Yang, L., Wu, S., and Hao, J., (2008), “Concentration, Sources and Ozone Formation Potential of Volatile Organic Compounds (VOCs) During Ozone Episode in Beijing,” *Atmospheric Research*, 88(1), 25–35.

Duan, Z., Lu, W., Li, D., and Wang, H., (2014), “Temporal Variation of Trace Compound Emission on the Working Surface of a Landfill in Beijing, China,” *Atmospheric Environment*, 88, 230–238.

Dunfield, P., Knowles, R., Dumont, R., and Moore, T. R., (1993), “Methane Production and Consumption in Temperate and Subarctic Peat Soils: Response to Temperature and pH,” *Soil Biology and Biochemistry*, 25(3), 321–326.

Duren, R. M., Thorpe, A. K., Foster, K. T., Rafiq, T., Hopkins, F. M., Yadav, V., Bue, B. D., Thompson, D. R., Conley, S., Colombi, N. K., Frankenberg, C., McCubbin, I. B.,

Eastwood, M. L., Falk, M., Herner, J. D., Croes, B. E., Green, R. O., and Miller, C. E., (2019), “California’s Methane Super-Emitters,” *Nature*, 575(7781), 180–184.

Edil, T. B., and Bosscher, P. J., (1994), “Engineering Properties of Tire Chips and Soil Mixtures,” *Geotechnical Testing Journal*, 17(4).

Edil, T. B., Park, J. K., and Kim, J. Y., (2004), “Effectiveness of Scrap Tire Chips as Sorptive Drainage Material,” *Journal of Environmental Engineering*, 130(7), 824–831.

Edil, T. B., (2008), “A Review of Environmental Impacts and Environmental Applications of Shredded Scrap Tires,” *Scrap Tire Derived Geomaterials—Opportunities and Challenges*; Hazarika, H., Yasuhara, K., Eds, 3-18.

Eggeman, T., and Verser, D., (2005), “Recovery of Organic Acids from Fermentation Broths,” *Twenty-Sixth Symposium on Biotechnology for Fuels and Chemicals, ABAB Symposium*, B. H. Davison, B. R. Evans, M. Finkelstein, and J. D. McMillan, eds., Humana Press, Totowa, NJ, 605–618.

Eitzer, B. D., (1995), “Emissions of Volatile Organic Chemicals from Municipal Solid Waste Composting Facilities,” *Environmental Science & Technology*, 29(4), 896–902.
Eleazer, W. E., Odle, W. S., Wang, Y.-S., and Barlaz, M. A., (1997), “Biodegradability of Municipal Solid Waste Components in Laboratory-Scale Landfills,” *Environmental Science & Technology*, 31(3), 911–917.

El-Fadel, M., Findikakis, A. N., and Leckie, J. O., (1997), “Environmental Impacts of Solid Waste Landfilling,” *Journal of Environmental Management*, 50(1), 1–25.
El-Fadel, M., Findikakis, A. N., and Leckie, J. O., (1996), “Numerical Modelling of Generation and Transport of Gas and Heat in Landfills I. Model Formulation,” *Waste Management & Research*, 14(5), 483–504.

El-Fadel, M., Abi-Esber, L., and Salhab, S., (2012), “Emission Assessment at the Burj Hammoud Inactive Municipal Landfill: Viability of Landfill Gas Recovery Under the Clean Development Mechanism,” *Waste Management*, *Special Thematic Issue: Waste Management in Developing Countries*, 32(11), 2106–2114.

Fang, J. J., Yang, N., Cen, D. Y., Shao, L. M., and He, P. J., (2012), “Odor Compounds from Different Sources of Landfill: Characterization and Source Identification,” *Waste Management*, 32(7), 1401–1410.

Farquhar, G. J., and Rovers, F. A., (1973), “Gas Production During Refuse Decomposition,” *Water, Air, and Soil Pollution*, 2(4), 483–495.

Fei, X., Zekkos, D., and Raskin, L., (2016), “Quantification of Parameters Influencing Methane Generation Due to Biodegradation of Municipal Solid Waste in Landfills and Laboratory Experiments,” *Waste Management*, 55, 276–287.

Faour, A. A., Reinhart, D. R., and You, H., (2007), “First-order Kinetic Gas Generation Model Parameters for Wet Landfills,” *Waste Management*, 27(7), 946–953.

Franzidis, J.-P., Héroux, M., Nastev, M., and Guy, C., (2008), “Lateral Migration and Offsite Surface Emission of Landfill Gas at City of Montreal Landfill Site,” *Waste Management & Research*, 26(2), 121–131.

Forney, F. W., and Markovetz, A. J., (1971), “The Biology of Methyl Ketones,” *Journal of Lipid Research*, 12(4), 383–395.

Fourie, A. B., and Morris, J. W. F., (2004), “Measured Gas Emissions from Four Landfills in South Africa and Some Implications for Landfill Design and Methane Recovery in Semi-Arid Climates,” *Waste Management & Research*, 22(6), 440–453.

Fredenslund, A., Scheutz, C., and Kjeldsen, P., (2005), “Disposal of Refrigerators and Freezers in the US: State of Practice, 2. Determination of Content of Blowing Agent in Pre- and Post-Shredded Foam and Modeling,” Environment & Resources DTU, Technical University of Denmark, 1-26.

Gallego, E., Perales, J. F., Roca, F. J., and Guardino, X., (2014), “Surface Emission Determination of Volatile Organic Compounds (VOC) from a Closed Industrial Waste Landfill using a Self-Designed Static Flux Chamber,” *Science of The Total Environment*, 470–471, 587–599.

Garg, A., Achari, G., and Joshi, R. C., (2006), “A Model to Estimate the Methane Generation Rate Constant in Sanitary Landfills using Fuzzy Synthetic Evaluation,” *Waste Management & Research*, 24(4), 363–375.

Gebert, J., Groengroeft, A., and Miehlich, G., (2003), “Kinetics of Microbial Landfill Methane Oxidation in Biofilters,” *Waste Management, Second Intercontinental Landfill Resarch Symposium*, 23(7), 609–619.

Gebert, J., and Groengroeft, A., (2006), “Passive Landfill Gas Emission – Influence of Atmospheric Pressure and Implications for the Operation of Methane-Oxidising Biofilters,” *Waste Management*, 26(3), 245–251.

Goldsmith, C. D., Chanton, J., Abichou, T., Swan, N., Green, R., and Hater, G., (2012), “Methane Emissions from 20 Landfills across the United States using Vertical Radial Plume Mapping,” *Journal of the Air & Waste Management Association*, 62(2), 183–197.

Gollapalli, M., and Kota, S. H., (2018), “Methane Emissions from a Landfill in North-East India: Performance of Various Landfill Gas Emission Models,” *Environmental Pollution*, 234, 174–180.

Gowing, A., (2001). *Measuring and Modelling of Landfill Gas Emissions*. Ph.D. Dissertation, University of Waterloo, Ontario, Canada.

Green, R. B., Hater, G. R., Thoma, E. D., DeWees, J., Rella, C. W., Crosson, E. R., ... and Swan, N., (2010), "Methane Emissions Measured at Two California Landfills by OTM-10 and an Acetylene Tracer Method," In *Proceedings of the Global Waste Management Symposium,* 3-6.

Grosjean, D., and Seinfeld, J. H., (1989), "Parameterization of the Formation Potential of Secondary Organic Aerosols," *Atmospheric Environment*, (1967), 23(8), 1733–1747. Grosjean, D. (1992), "In Situ Organic Aerosol Formation During a Smog Episode: Estimated Production and Chemical Functionality," *Atmospheric Environment. Part A. General Topics*, 26(6), 953–963.

Grossi, V., Cravo-Laureau, C., Guyoneaud, R., Ranchou-Peyruse, A., and Hirschler-Réa, A., (2008), "Metabolism of n-Alkanes and n-Alkenes by Anaerobic Bacteria: A Summary," *Organic Geochemistry, Advances in Organic Geochemistry 2007*, 39(8), 1197–1203.

Guo, H., Duan, Z., Zhao, Y., Liu, Y., Mustafa, M. F., Lu, W., and Wang, H., (2017), "Characteristics of Volatile Compound Emission and Odor Pollution from Municipal Solid Waste Treating/Disposal facilities of a City in Eastern China," *Environmental Science and Pollution Research*, 24(22), 18383–18391.

Haarstad, K., Bergersen, O., and Sørheim, R., (2006), "Occurrence of Carbon Monoxide during Organic Waste Degradation," *Journal of the Air & Waste Management Association*, 56(5), 575–580.

Hagan, M. T., Demuth, H. B., Beale, M. H., and De Jesus, O., (2014). *Neural Network Design (2nd ed.).*

Hallquist, M., Wenger, J. C., Baltensperger, U., Rudich, Y., Simpson, D., Claeys, M., Dommen, J., Donahue, N. M., George, C., Goldstein, A. H., Hamilton, J. F., Herrmann, H., Hoffmann, T., Iinuma, Y., Jang, M., Jenkin, M. E., Jimenez, J. L., Kiendler-Scharr, A., Maenhaut, W., McFiggans, G., Mentel, T. F., Monod, A., Prevot, A. S. H., Seinfeld, J. H., Surratt, J. D., Szmigielski, R., and Wildt, J., (2009), "The Formation, Properties and Impact of Secondary Organic Aerosol: Current and Emerging Issues," *Atmospheric Chemistry and Physics*, 9, 5155–5236.

Hanson, R. S., and Hanson, T. E., (1996), "Methanotrophic Bacteria," *Microbiological Reviews*, 60(2), 439–471.

Haroune, N., Combourieu, B., Besse, P., Sancelme, M., Kloepfer, A., Reemtsma, T., Wever, H. D., and Delort, A.-M., (2004), "Metabolism of 2-Mercaptobenzothiazole by *Rhodococcus rhodochrous*," *Applied and Environmental Microbiology*, 70(10), 6315–6319.

Harrison, R. M., and Yin, J., (2000), “Particulate Matter in the Atmosphere: Which Particle Properties are Important for its Effects on Health?” *Science of The Total Environment*, 249(1), 85–101.

Hartz, K. E., Klink, R. E., and Ham, R. K., (1982), “Temperature Effects: Methane Generation from Landfill Samples,” *Journal of the Environmental Engineering Division*, 108(4), 629–638.

Haywood, J., and Boucher, O., (2000). “Estimates of the Direct and Indirect Radiative Forcing Due to Tropospheric Aerosols: A Review,” *Reviews of Geophysics*, 38(4), 513–543.

He, P. J., Chen, M., and Zhang, H., (2008), “Effects of Leachate Irrigation and Cover Soil Type om N_2O Emission from Municipal Solid Waste Landfill,” *Chinese Journal of Applied Ecology*, 19(7), 1591–1596.

Hegde, U., Chang, T. C., and Yang, S. S. (2003), “Methane and Carbon Dioxide Emissions from Shan-Chu-Ku landfill Site in Northern Taiwan,” *Chemosphere*, 52(8), 1275–1285.

Henkelman, J., Sullivan, P., and Huff, R. H., (2016), “A Look at Fugitive GHG Emissions Reporting and the Effects on Regulated Facilities,” *Proceedings of the Air and Waste Management Associations 109th Annual Conference and Exhibition*, New Orleans, Louisiana, June 20th-23rd, 2016.

Hilger, H. A., Liehr, S. K., and Barlaz M. A., (1999), “Exopolysaccharide Control of Methane Oxidation in Landfill Cover Soil,” *Journal of Environmental Engineering*, 125(12), 1113–1123.

Hilger, H. A., Wollum, A. G., and Barlaz, M. A., (2000), “Landfill Methane Oxidation Response to Vegetation, Fertilization, and Liming,” *Journal of Environmental Quality*, 29(1), 324–334.

Hodson, E. L., Martin, D., and Prinn, R. G., (2010), “The Municipal Solid Waste Landfill as a Source of Ozone-Depleting Substances in the United States and United Kingdom,” *Atmospheric Chemistry and Physics*, 10(4), 1899–1910.
Hofstetter Gastechnik, A. G., (2014), “Production of LFG, Conditions for Gas Production, Quality, Quantity, Gas Yield, and Energy Value,” Retrieved March 23, 2019, from http://www.slideshare.net/HOFSTGAS/1-production-of-landfill-gas.
Holst, O., Stenberg, B., and Christiansson, M., (1998), “Biotechnological Possibilities for Waste Tyre-Rubber Treatment,” *Biodegradation*, 9(3–4), 301–310.

Hüffer, T., Wehrhahn, M., and Hofmann, T., (2020), “The Molecular Interactions of Organic Compounds with Tire Crumb Materials Differ Substantially From Those With Other Microplastics,” *Environmental Science: Processes & Impacts*.

Hütsch, B. W., (1998), “Methane Oxidation in Arable Soil as Inhibited by Ammonium, Nitrite, and Organic Manure with Respect to Soil pH,” *Biology and Fertility of Soils*, 28(1), 27–35.

Ikeguchi, T., and Watanabe, I., (1991), “Behaviour of Trace Components in Gases Generated from Municipal Solid Waste Landfills,” *Environmental Technology*, 12(10), 947–952.

Ishii, K., and Furuichi, T., (2013), “Estimation of Methane Emission Rate Changes Using Age-Defined Waste in a Landfill Site,” *Waste Management*, 33(9), 1861–1869.

IPCC, (2013). *Climate Change 2013: The Physical Science Basis. Contribution of Working Group I to the Fifth Assessment Report of the Intergovernmental Panel on Climate Change*. [Stocker, T.F., D. Qin, G.-K. Plattner, M. Tignor, S.K. Allen, J. Boschung, A. Nauels, Y. Xia, V. Bex and P.M. Midgley (eds.)], Cambridge University Press, Cambridge, United Kingdom and New York, NY, USA, 1535 p.

Isaacs, K. K., Goldsmith, M.-R., Egeghy, P., Phillips, K., Brooks, R., Hong, T., and Wambaugh, J. F., (2016), “Characterization and Prediction of Chemical Functions and Weight Fractions in Consumer Products,” *Toxicology Reports*, 3, 723–732.

Ishigaki, T., Yamada, M., Nagamori, M., Ono, Y., and Inoue, Y., (2005), “Estimation of Methane Emission from Whole Waste Landfill Site Using Correlation between Flux and Ground Temperature,” *Environmental Geology*, 48(7), 845–853.

Ishigaki, T., Chung, C. V., Sang, N. N., Ike, M., Otsuka, K., Yamada, M., and Inoue, Y., (2008), “Estimation and Field Measurement of Methane Emission from Waste Landfills in Hanoi, Vietnam,” *Journal of Material Cycles and Waste Management*, 10(2), 165.

Ishigaki, T., Nakagawa, M., Nagamori, M., and Yamada, M., (2016), “Anaerobic Generation and Emission of Nitrous Oxide in Waste Landfills,” *Environmental Earth Sciences*, 75(9), 750.

Jeon, E. J., Bae, S. J., Lee, D. H., Seo, D. C., Chun, S. K., Lee, N. H., and Kim, J. Y. (2007), “Methane Generation Potential and Biodegradability of MSW Components,” *Proceedings of the Eleventh International Waste Management and Landfill Symposium*, Sardinia, Italy.

Jeong, S., Park, J., Kim, Y. M., Park, M. H., and Kim, J. Y., (2019), “Innovation of Flux Chamber Network Design for Surface Methane Emission from Landfills using Spatial Interpolation Models,” *Science of The Total Environment*, 688, 18–25.

Jha, A. K., Sharma, C., Singh, N., Ramesh, R., Purvaja, R., and Gupta, P. K., (2008), “Greenhouse Gas Emissions from Municipal Solid Waste Management in Indian Mega-Cities: A Case Study of Chennai Landfill Sites,” *Chemosphere*, 71(4), 750–758.

Jokela, J. P. Y., Vavilin, V. A., and Rintala, J. A., (2005), “Hydrolysis Rates, Methane Production and Nitrogen Solubilisation of Grey Waste Components During Anaerobic Degradation,” *Bioresource Technology*, 96(4), 501–508.

Jones, H. A., and Nedwell, D. B., (1993), “Methane Emission and Methane Oxidation in Land-fill Cover Soil,” *FEMS Microbiology Ecology*, 11(3–4), 185–195.

Jung, Y., Imhoff, P. T., Augenstein, D., and Yazdani, R., (2011), “Mitigating Methane Emissions and Air Intrusion in Heterogeneous Landfills With a High Permeability Layer,” *Waste Management, Landfill Gas Emission and Mitigation*, 31(5), 1049–1058.

Kallistova, A. Y., Kevbrina, M. V., Nekrasova, V. K., Glagolev, M. V., Serebryanaya, M. I., and Nozhevnikova, A. N., (2005), “Methane Oxidation in Landfill Cover Soil,” *Microbiology*, 74(5), 608–614.

Kansal, A., (2009), “Sources and Reactivity of NMHCs and VOCs in the Atmosphere: A Review,” *Journal of Hazardous Materials*, 166(1), 17–26.

Karanjekar, R. V., Bhatt, A., Altouqui, S., Jangikhatoonabad, N., Durai, V., Sattler, M. L., Hossain, M. D. S., and Chen, V., (2015), “Estimating Methane Emissions from Landfills Based on Rainfall, Ambient Temperature, and Waste Composition: The CLEEN Model,” *Waste Management*, 46, 389–398.

Karion, A., Sweeney, C., Pétron, G., Frost, G., Hardesty, R. M., Kofler, J., Miller, B. R., Newberger, T., Wolter, S., Banta, R., Brewer, A., Dlugokencky, E., Lang, P., Montzka, S. A., Schnell, R., Tans, P., Trainer, M., Zamora, R., and Conley, S., (2013), “Methane Emissions Estimate from Airborne Measurements Over a Western United States Natural Gas Field,” *Geophysical Research Letters*, 40(16), 4393–4397.

Kesselmeier, J., and Staudt, M., (1999), “Biogenic Volatile Organic Compounds (VOC): An Overview on Emission, Physiology and Ecology,” *Journal of Atmospheric Chemistry*, 33(1), 23–88.

Kim, J. Y., Park, J. K., and Edil, T. B., (1997), “Sorption of Organic Compounds in the Aqueous Phase onto Tire Rubber,” *Journal of Environmental Engineering*, 123(9), 827–835.

Kim, K.-H., Choi, Y., Jeon, E., and Sunwoo, Y., (2005), “Characterization of Malodorous Sulfur Compounds in Landfill Gas,” *Atmospheric Environment*, 39(6), 1103–1112.

Kim, K.-H., (2006), “Emissions of Reduced Sulfur Compounds (RSC) as a Landfill Gas (LFG): A Comparative Study of Young and Old Landfill Facilities,” *Atmospheric Environment*, 40(34), 6567–6578.

Kim, K. H., Shon, Z. H., Kim, M. Y., Sunwoo, Y., Jeon, E. C., and Hong, J. H. (2008), "Major Aromatic VOC in the Ambient Air in the Proximity of an Urban Landfill Facility," *Journal of Hazardous Materials*, 150(3), 754–764.

Kim, H., and Townsend, T. G., (2012), "Wet Landfill Decomposition Rate Determination using Methane Yield Results for Excavated Waste Samples," *Waste Management*, 32(7), 1427–1433.

Kjeldsen, P., and Fischer, E. V., (1995), "Landfill Gas Migration—Field Investigations At Skellingsted Landfill, Denmark," *Waste Management & Research*, 13(5), 467–484.
Kjldsen, P., (1996), "Landfill Gas Migration in Soil," In: Christensen, T.H., Cossu, R. & Stegmann, R. (eds.): *Landfilling of Waste: Biogas*, Chapter 3.1. E. & FN Spon. London, UK.

Kjeldsen, P., Dalager, A., and Broholm, K., (1997), "Attenuation of Methane and Nonmethane Organic Compounds in Landfill Gas Affected Soils," *Journal of the Air & Waste Management Association*, 47(12), 1268–1275.

Kjeldsen, P., and Jensen, M. H., (2001), "Release of CFC-11 from Disposal of Polyurethane Foam Waste," *Environmental Science & Technology*, 35(14), 3055–3063.

Kjeldsen, P., and Christensen, T. H., (2001), "A Simple Model for the Distribution and Fate of Organic Chemicals in a Landfill: MOCLA," *Waste Management & Research*, 19(3), 201–216.

Klug, M. J., and Markovetz, A. J., (1971), "Utilization of Aliphatic Hydrocarbons by Micro-organisms," *Advances in Microbial Physiology*, A. H. Rose and J. F. Wilkinson, eds., Academic Press, 1–43.

Klusman, R. W., and Dick, C. J., (2000), "Seasonal Variability in CH_4 Emissions from a Landfill in a Cool, Semiarid Climate," *Journal of the Air & Waste Management Association*, 50(9), 1632–1636.

Ko, J. H., Xu, Q., and Jang, Y.-C., (2015), "Emissions and Control of Hydrogen Sulfide at Landfills: A Review," *Critical Reviews in Environmental Science and Technology*, 45(19), 2043–2083.

Krause, M. J., Chickering, G. W., Townsend, T. G., and Reinhart, D. R., (2016), "Critical Review of the Methane Generation Potential of Municipal Solid Waste," *Critical Reviews in Environmental Science and Technology*, 46(13), 1117–1182.

Krause, M. J., Chickering, G. W., Townsend, T. G., and Pullammanappallil, P., (2018), "Effects of Temperature and Particle Size on the Biochemical Methane Potential of Municipal Solid Waste Components," *Waste Management*, 71, 25–30.

Krautwurst, S., Gerilowski, K., Jonsson, H. H., Thompson, D. R., Kolyer, R. W., Iraci, L. T., Thorpe, A. K., Horstjann, M., Eastwood, M., Leifer, I., Vigil, S. A., Krings, T., Borchardt, J., Buchwitz, M., Fladeland, M. M., Burrows, J. P., and Bovensmann, H., (2017), "Methane Emissions from a Californian Landfill, Determined from Airborne Remote Sensing and In-situ Measurements," *Atmospheric Measurement Techniques*, 10, 3429–3452.

Kroll, J. H., and Seinfeld, J. H., (2008), "Chemistry of Secondary Organic Aerosol: Formation and Evolution of Low-Volatility Organics in the Atmosphere," *Atmospheric Environment*, 42(16), 3593–3624.
Lagos, D. A., Héroux, M., Gosselin, R., and Cabral, A. R., (2017), "Optimization of a Landfill Gas Collection Shutdown Based on an Adapted First-Order Decay Model," *Waste Management*, 63, 238–245.

Lamborn, J., (2012), "Observations from Using Models to Fit the Gas Production of Varying Volume Test cells and Landfills," *Waste Management*, 32(12), 2353–2363.

Latham, B. and Young, A., (1993), "Modellisation of the Effects of Barometric Pressure on Landfill Gas Migration," Proceedings of Sardinia 1993, Fourth International Landfill Symposium, CISA, Environmental Sanitary Engineering Centre, Cagliari, Italy, 681–689.

Leadbetter, E. R., and Foster, J. W., (1959), "Oxidation Products Formed from Gaseous Alkanes by the Bacterium *Pseudomonas methanica*," *Archives of biochemistry and biophysics*, 82(2), 491-492.

Lee, S., Xu, Q., Booth, M., Townsend, T. G., Chadik, P., and Bitton, G., (2006), "Reduced Sulfur Compounds in Gas from Construction and Demolition Debris Landfills," *Waste Management*, 26(5), 526–533.

Lee, D. H., Behera, S. K., Kim, J. W., and Park, H. S., (2009), "Methane Production Potential of Leachate Generated from Korean Food Waste Recycling Facilities: a Lab-Scale Study," *Waste Management*, 29(2), 876–882.

Lima, R., Salazar, J., Hernandez, P., and Perez, N., (2001), "Dynamics of Non-Controlled Emission of Biogas From Landfills," *AGU Fall Meeting Abstracts*, 42, B42A-0126.

Liu, Y., Lu, W., Guo, H., Ming, Z., Wang, C., Xu, S., Liu, Y., and Wang, H., (2016), "Aromatic Compound Emissions from Municipal Solid Waste Landfill: Emission Factors and their Impact on Air Pollution," *Atmospheric Environment*, 139, 205–213.

Livingston, G. P.; Hutchinson, G. L., (1995), "Enclosure-based measurement of trace gas exchange: Applications and sources of error," In *Biogenic Trace Gases: Measuring Emissions from Soil and Water*, Matson, P. A., Harris, R. C. (Eds); Blackwell Science Ltd.: Oxford, UK, 14–51.

Llompart, M., Sanchez-Prado, L., Pablo Lamas, J., Garcia-Jares, C., Roca, E., and Dagnac, T., (2013), “Hazardous Organic Chemicals in Rubber Recycled Tire Playgrounds and Pavers,” *Chemosphere*, 90(2), 423–431.

Long, X.-E., Huang, Y., Chi, H., Li, Y., Ahmad, N., and Yao, H., (2018), “Nitrous Oxide Flux, Ammonia Oxidizer and Denitrifier Abundance and Activity Across Three Different Landfill Cover Soils in Ningbo, China,” *Journal of Cleaner Production*, 170, 288–297.

Lowry, M. I., Bartelt-Hunt, S. L., Beaulieu, S. M., and Barlaz, M. A., (2008), “Development of a Coupled Reactor Model for Prediction of Organic Contaminant Fate in Landfills,” *Environmental Science & Technology*, 42(19), 7444–7451.

Machado, S. L., Carvalho, M. F., Gourc, J.-P., Vilar, O. M., and do Nascimento, J. C. F., (2009), “Methane Generation in Tropical Landfills: Simplified Methods and Field Results,” *Waste Management*, 29(1), 153–161.

Majumdar, D., and Srivastava, A., (2012), “Volatile Organic Compound Emissions from Municipal Solid Waste Disposal Sites: A Case Study of Mumbai, India,” *Journal of the Air & Waste Management Association*, 62(4), 398–407.

Majumdar, D., Ray, S., Chakraborty, S., Rao, P. S., Akolkar, A. B., Chowdhury, M., and Srivastava, A., (2014), “Emission, Speciation, and Evaluation of Impacts of Non-Methane Volatile Organic Compounds from Open Dump Site,” *Journal of the Air & Waste Management Association*, 64(7), 834–845.

Mandernack, K. W., Kinney, C. A., Coleman, D., Huang, Y.-S., Freeman, K. H., and Bogner, J., (2000), “The Biogeochemical Controls of N_2O Production and Emission in Landfill Cover Soils: the Role of Methanotrophs in the Nitrogen Cycle,” *Environmental Microbiology*, 2(3), 298–309.

Mansouri, K., Grulke, C. M., Judson, R. S., and Williams, A. J., (2018), “OPERA Models for Predicting Physicochemical Properties and Environmental Fate Endpoints,” *Journal of Cheminformatics*, 10(1), 10.

Manfredi, S., Tonini, D., and Christensen, T. H., (2010), “Contribution of Individual Waste fractions to the Environmental Impacts from Landfilling of Municipal Solid Waste,” *Waste Management*, 30(3), 433–440.

María Rosa, S. R., Mauricio, G. M., Gabriela, R. B., Nayla, C. P., Roger, M. N., and Stentiford Edward, I. (2013). “Superficial Methane Emissions from a Landfill in Merida, Yucatan, Mexico,” *Ingeniería, Investigación y Tecnología*, 14(3), 299–310.

Mata-Alvarez, J., and Martinez-Viturtia, A., (1986), “Laboratory Simulation of Municipal Solid Waste Fermentation with Leachate Recycle,” *Journal of Chemical Technology & Biotechnology*, 36(12), 547–556.

Maurice, C., and Lagerkvist, A., (1997), “Characterising Methane Emissions from Different Types of Landfill Sites,” *Proceedings Sardinia* 97, *Sixth International Waste Management and Landfill Symposium*, S. Margerita di Pula, Cagliari, Italy, October 13-17th, 1997, 87–93.

Maurice, C., and Lagerkvist, A., (2003), “LFG Emission Measurements in Cold Climatic Conditions: Seasonal Variations and Methane Emissions Mitigation,” *Cold Regions Science and Technology*, 36(1), 37–46.

McCulloch, A., (1992), “Global Production and Emissions of Bromochlorodifluoromethane and Bromotrifluoromethane (halons 1211 and 1301),” *Atmospheric Environment. Part A. General Topics*, 26(7), 1325–1329.

McKenna, E., and Kallio, R. E., (1965), “The Biology of Hydrocarbons,” *Annual Reviews in Microbiology*, 19(1), 183-208.

Meadows, M., Gregory, R., Fish, C., and Gronow, J., (1999), “Characterising Methane Emissions from Different Types of Landfill Sites,” *Proceedings Sardinia* 99, *Seventh International Waste Management and Landfill Symposium*, S. Margerita di Pula, Cagliari, Italy, October 4-8th, 1999, 25–32.

Mellouki, A., Wallington, T. J., and Chen, J. (2015), “Atmospheric Chemistry of Oxygenated Volatile Organic Compounds: Impacts on Air Quality and Climate,” *Chemical Reviews*, 115(10), 3984–4014.

Merz, R. C. and Stone, R., (1964), “Quantitative Study of Gas Produced by Decomposing Refuse,” *Public Works,* 99, 86–87.

Meyvantsdottir, G., (2014). *Methane Emissions from Icelandic Landfills*. M.S. Thesis, University of Iceland, Reykjavik, Iceland.

McCarthy, J., and Zachara, J., (1989), “ES&T Features: Subsurface transport of contaminants.” *Environmental Science & Technology*, 23(5), 496–502.

Molins, S., Mayer, K. U., Scheutz, C., and Kjeldsen, P., (2008), “Transport and Reaction Processes Affecting the Attenuation of Landfill Gas in Cover Soils,” *Journal of Environmental Quality*, 37(2), 459–468.

Moody, L. B., Burns, R. T., Bishop, G., Sell, S. T., and Spajic, R., (2011), “Using Biochemical Methane Potential Assays to Aid in Co-Substrate Selection for Co-Digestion,” *Applied Engineering in Agriculture*, 27(3), 433–439.

Moreira, J. M. L., and Candiani, G., (2016), “Assessment of Methane Generation, Oxidation, and Emission in a Subtropical Landfill Test Cell,” *Environmental Monitoring and Assessment*, 188(8), 464.

Mosher, B. W., Czepiel, P. C., Shorter, J., Allwine, E., Harriss, R. C., Kolb, C., and Lamb, B., (1996), “Mitigation of Methane Emissions at Landfill Sites in New England, USA,” *Energy Conversion and Management, Proceedings of the International Energy Agency Greenhouse Gases: Mitigation Options Conference*, 37(6), 1093–1098.

Mosher, B. W., Czepiel, P. M., Harriss, R. C., Shorter, J. H., Kolb, C. E., McManus, J. B., Allwine, E., and Lamb, B. K., (1999), “Methane Emissions at Nine Landfill Sites in the Northeastern United States,” *Environmental Science & Technology*, 33(12), 2088–2094.

Musat, F., (2015), “The Anaerobic Degradation of Gaseous, Nonmethane Alkanes — From In situ Processes to Microorganisms,” *Computational and Structural Biotechnology Journal*, 13, 222–228.

Muthuramu, K., Shepson, P. B., Bottenheim, J. W., Jobson, B. T., Niki, H., and Anlauf, K. G., (1994), “Relationships between organic nitrates and surface ozone destruction during Polar Sunrise Experiment 1992,” *Journal of Geophysical Research*: Atmospheres, 25369–25378.

Nair, A. T., Senthilnathan, J., and Nagendra, S. M. S., (2019), “Emerging Perspectives on VOC Emissions from Landfill Sites: Impact on Tropospheric Chemistry and Local Air Quality,” *Process Safety and Environmental Protection*, 121, 143–154.

Nagamori, M., Mowjood, M. I. M., Watanabe, Y., Isobe, Y., Ishigaki, T., and Kawamoto, K., (2016), “Characterization of Temporal Variations in Landfill Gas Components Inside an Open Solid Waste Dump Site in Sri Lanka,” *Journal of the Air & Waste Management Association*, 66(12), 1257–1267.

Nastev, M., Therrien, R., Lefebvre, R., and Gélinas, P., (2001), “Gas Production and Migration in Landfills and Geological Materials,” *Journal of Contaminant Hydrology*, 52(1), 187–211.

Ngwabie, N. M., Wirlen, Y. L., Yinda, G. S., and VanderZaag, A. C., (2019), “Quantifying Greenhouse Gas Emissions from Municipal Solid Waste Dumpsites in Cameroon,” *Waste Management*, 87, 947–953.

Nieto, P. P., Hidalgo, D., Irusta, R., and Kraut, D., (2012), “Biochemical Methane Potential (BMP) of Agro-Food Wastes from the Cider Region (Spain),” *Water Science and Technology,* 66(9), 1842–1848.

Nolasco, D., Lima, R. N., Hernández, P. A., and Pérez, N. M., (2008), “Non-Controlled Biogenic Emissions to the Atmosphere from Lazareto landfill, Tenerife, Canary Islands,” *Environmental Science and Pollution Research*, 15(1), 51–60.

Nozhevnikova, A. N., Lifshitz, A. B., Lebedev, V. S., and Zavarzin, G. A., (1993), "Emission of Methane into the Atmosphere from Landfills in the Former USSR," *Chemosphere*, 26(1), 401–417.
Nwaokorie, K. J., Bareither, C. A., Mantell, S. C., and Leclaire, D. J., (2018), "The Influence of Moisture Enhancement on Landfill Gas Generation in a Full-Scale Landfill," *Waste Management*, 79, 647–657.

Olivier, J. G., Schure, K. M., and Peters, J. A. H. W., (2017). *Trends in Global CO_2 and Total Greenhouse Gas Emissions*. PBL Netherlands Environmental Assessment Agency, 5.

Oonk, H., van Zomeren, A., Rees-White, T. C., Beaven, R. P., Hoekstra, N., Luning, L., Hannen, M., Hermkes, H., and Woelders, H., (2013), "Enhanced Biodegradation at the Landgraaf Bioreactor Test-Cell," *Waste Management*, 33(10), 2048–2060.

Owens, J. M., and Chynoweth, D. P., (1993), "Biochemical Methane Potential of Municipal Solid Waste (MSW) Components," *Water Science and Technology*, 27(2), 1–14.

Palmisano, A. C., and Barlaz, M. A., (1996). *Microbiology of solid waste* (Vol. 3). CRC press.
Park, J. K., Kim, J. Y., and Edil, T. B., (1996), "Mitigation of Organic Compound Movement in Landfills by Shredded Tires," *Water Environment Research*, 68(1), 4–10.

Park, J. W., and Shin, H. C., (2001), "Surface Emission of Landfill Gas from Solid Waste Landfill," *Atmospheric Environment*, 35(20), 3445–3451.

Perring, A. E., Pusede, S. E., and Cohen, R. C., (2013), "An Observational Perspective on the Atmospheric Impacts of Alkyl and Multifunctional Nitrates on Ozone and Secondary Organic Aerosol," *Chemical Reviews*, 113(8), 5848–5870.

Picarro, Inc., (2018), "G2401-m In-flight Gas Concentration Analyzer," <https://www.picarro.com/products/flight-co-co2-ch4-h2o-analyzer> (Jan. 13, 2020).

Pierini, V. I., Bartoloni, N., and Ratto, S. E., (2018), "Greenhouse Gases Emissions from a Closed Old Landfill Cultivated with Biomass Crops," *Environment, Development and Sustainability*, 20(6), 2795–2809.

Peischl, J., Ryerson, T. B., Brioude, J., Aikin, K. C., Andrews, A. E., Atlas, E., Blake, D., Daube, B. C., de Gouw, J. A., Dlugokencky, E., Frost, G. J., Gentner, D. R., Gilman, J. B., Goldstein, A. H., Harley, R. A., Holloway, J. S., Kofler, J., Kuster, W. C., Lang, P. M., Novelli, P. C., Santoni, G. W., Trainer, M., Wofsy, S. C., and Parrish, D. D., (2018), "Quantifying Sources of Methane using Light Alkanes in the Los Angeles Basin, California," *Journal of Geophysical Research: Atmospheres*, 4974–4990.

Powell, J. T., Townsend, T. G., and Zimmerman, J. B., (2016), “Estimates of Solid Waste Disposal Rates and Reduction Targets for Landfill Gas Emissions,” *Nature Climate Change*, 6(2), 162–165.

Powell, R. L., (2002), “CFC phase-out: have we met the challenge?” *Journal of Fluorine Chemistry, 13th European Symposium on Fluorine Chemistry (ESFC-13)*, 114(2), 237–250.

Pratt, C., Walcroft, A. S., Deslippe, J., and Tate, K. R., (2013), “CH_4/CO_2 Ratios Indicate Highly Efficient Methane Oxidation by a Pumice Landfill Cover-Soil,” *Waste Management*, 33(2), 412–419.
Primrose, S. B., (1979), “Ethylene and Agriculture: The Role of the Microbe,” *Journal of Applied Bacteriology*, 46(1), 1–25.

Qu, X., Vavilin, V. A., Mazeas, L., Lemunier, M., Duquennoi, C., He, P., and Bouchez, T., (2009), “Anaerobic Biodegradation of Cellulosic Material: Batch Experiments and Modelling Based on Isotopic Data and Focusing on Aceticlastic and Non-Aceticlastic Methanogenesis,” *Waste Management*, 29(6), 1828–1837.

Rachor, I. M., (2012). *Spatial and Temporal Patterns of Methane Fluxes on Old Landfills: Processes and Emission Reduction Potential*. Ph.D. Dissertation, University of Hamburg, Hamburg, Germany.

Rachor, I. M., Gebert, J., Gröngröft, A., and Pfeiffer, E. M., (2013), “Variability of Methane Emissions from an Old Landfill over Different Time-Scales,” *European Journal of Soil Science*, 64(1), 16–26.

Raco, B., Battaglini, R., and Lelli, M., (2010), “Gas Emission into the Atmosphere from Controlled Landfills: An Example from Legoli Landfill (Tuscany, Italy),” *Environmental Science and Pollution Research*, 17(6), 1197–1206.

Ramaswamy, J. N., (1970), “Nutritional Effects on Acid and Gas Production in Sanitary Landfills.” Ph.D. Dissertation: West Virginia University, Morgantown, West Virginia.
Rasi, S., Veijanen, A., and Rintala, J., (2007), “Trace Compounds of Biogas from Different Biogas Production Plants,” *Energy*, 32(8), 1375–1380.

Rawat, M., Singh, U. K., Mishra, A. K., and Subramanian, V., (2008), “Methane Emission and Heavy Metals Quantification from Selected Landfill Areas in India,” *Environmental Monitoring and Assessment*, 137(1), 67–74.

Reddy, K. R., Stark, T. D., and Marella, A., (2010), “Beneficial Use of Shredded Tires as Drainage Material in Cover Systems for Abandoned Landfills,” *Practice Periodical of Hazardous, Toxic, and Radioactive Waste Management*, 14(1), 47–60.

Reinhart, D. R., (1993), “A Review of Recent Studies on the Sources of Hazardous Compounds Emitted from Solid Waste Landfills: A U.S. Experience,” *Waste Management & Research*, 11(3), 257–268.

Rees, J. F., (1980a), “Optimisation of Methane Production and Refuse Decomposition in Landfills by Temperature Control,” *Journal of Chemical Technology and Biotechnology*, 30(1), 458–465.

Rees, J. F., (1980b), “The Fate of Carbon Compounds in the Landfill Disposal of Organic Matter,” *Journal of Chemical Technology and Biotechnology*, 30(1), 161–175.

Rinne, J., Pihlatie, M., Lohila, A., Thum, T., Aurela, M., Tuovinen, J. P., Laurila, T., and Vesala, T., (2005), “Nitrous Oxide Emissions from a Municipal Landfill,” *Environmental Science & Technology*, 39(20), 7790–7793.

Rolston, D. E., (1986), “47 - Gas flux,” In *Methods of Soil Analysis: Part I, Physical and Mineralogical Methods*, 2nd ed.; Klute, A. (Ed.); American Society of Agronomy/Soil Science Society of America: Madison, WI, 1103-1119.

Romine, R. A., and Romine, M. F. (1998). “Rubbercycle: a bioprocess for surface modification of waste tyre rubber.” Polymer Degradation and Stability, 1–3(59), 353–358.

Rose, K., and Steinbüchel, A., (2005), “Biodegradation of Natural Rubber and Related Compounds: Recent Insights into a Hardly Understood Catabolic Capability of Microorganisms,” *Applied and Environmental Microbiology*, 71(6), 2803–2812.

Rose, K., Tenberge, K. B., and Steinbüchel, A., (2005), “Identification and Characterization of Genes from *Streptomyces sp. Strain K30* Responsible for Clear Zone Formation on Natural Rubber Latex and Poly(cis-1,4-isoprene) Rubber Degradation,” *Biomacromolecules*, 6(1), 180–188.

Roy, R. V., Das, M., Banerjee, R., and Bhowmick, A. K., (2006), “Comparative Studies on Crosslinked and Uncrosslinked Natural Rubber Biodegradation by *Pseudomonas sp.*,” *Bioresource Technology*, 97(18), 2485–2488.

Salazar, J. C., Guerrero, V. H. B., Marín, J. F. R., and Murillo, J. H., (2017), “Greenhouse Gases, Carbonyls, and Volatile Organic Compounds Surface Flux Emissions at Three Final Waste Disposal Sites Located in the Metropolitan Area of Costa Rica,” *Open Journal of Air Pollution*, 6(4), 720–726.

Sanci, R., Panarello, H. O., and Ostera, H. A., (2012), “CO_2 Emissions from a Municipal Site for Final Disposal of Solid Waste in Gualeguaychu, Entre Rios Province, Argentina,” *Environmental Earth Sciences*, 66(2), 519–528.

Sanderson, J., (2001). *Quantitative Assessment of Methane Emissions from Landfills*. M.S. Thesis, University of Calgary, Calgary, Canada.

Saquing, J. M., Chanton, J. P., Yazdani, R., Barlaz, M. A., Scheutz, C., Blake, D. R., and Imhoff, P. T., (2014), "Assessing Methods to Estimate Emissions of Non-Methane Organic Compounds from Landfills," *Waste Management*, 34(11), 2260–2270.

Saral, A., Demir, S., and Yıldız, Ş., (2009), "Assessment of Odorous VOCs Released from a Main MSW Landfill Site in Istanbul-Turkey via a Modelling Approach," *Journal of Hazardous Materials*, 168(1), 338–345.

Sawamura, H., Yamada, M., Endo, K., Soda, S., Ishigaki, T., and Ike, M., (2010), "Characterization of Microorganisms at Different Landfill Depths using Carbon-Utilization Patterns and 16S rRNA Gene Based T-RFLP," *Journal of Bioscience and Bioengineering (Japan)*, 109(2), 130–137.

Scheutz, C., and Kjeldsen, P., (2003), "Capacity for Biodegradation of CFCs and HCFCs in a Methane Oxidative Counter-Gradient Laboratory System Simulating Landfill Soil Covers," *Environmental Science & Technology*, 37(22), 5143–5149.

Scheutz, C., Bogner, J., Chanton, J., Blake, D., Morcet, M., and Kjeldsen, P., (2003), "Comparative Oxidation and Net Emissions of Methane and Selected Non-Methane Organic Compounds in Landfill Cover Soils," *Environmental Science & Technology*, 37(22), 5150–5158.

Scheutz, C., and Kjeldsen, P., (2004), "Environmental Factors Influencing Attenuation of Methane and Hydrochlorofluorocarbons in Landfill Cover Soils," *Journal of Environmental Quality*, 33(1), 72–79.

Scheutz, C., and Kjeldsen, P., (2005), "Biodegradation of Trace Gases in Simulated Landfill Soil," *Journal of the Air & Waste Management Association*, 55(7), 878–885.
Scheutz, C., Dote, Y., Fredenslund, A. M., and Kjeldsen, P., (2007), "Attenuation of Fluorocarbons Released from Foam Insulation in Landfills," *Environmental Science & Technology*, 41(22), 7714–7722.

Scheutz, C., Bogner, J., Chanton, J. P., Blake, D., Morcet, M., Aran, C., and Kjeldsen, P., (2008), "Atmospheric Emissions and Attenuation of Non-Methane Organic Compounds in Cover Soils at a French Landfill," *Waste Management*, 28(10), 1892–1908.

Scheutz, C., Kjeldsen, P., Bogner, J. E., De Visscher, A., Gebert, J., Hilger, H. A., Huber-Humer, M., and Spokas, K., (2009a), "Microbial Methane Oxidation Processes and Technologies for Mitigation of Landfill Gas Emissions," *Waste Management & Research*, 27(5), 409–455.

Scheutz, C., Kjeldsen, P., and Gentil, E., (2009b), “Greenhouse Gases, Radiative Forcing, Global Warming Potential and Waste Management — an Introduction,” *Waste Management & Research*, 27(8), 716–723.

Scheutz, C., Fredenslund, A. M., Nedenskov, J., and Kjeldsen, P., (2010), “Release and Fate of Fluorocarbons in a Shredder Residue Landfill Cell: 2. Field Investigations,” *Waste Management, Special Thematic Section: Sanitary Landfilling*, 30(11), 2163–2169.

Schroth, M. H., Eugster, W., Gómez, K. E., Gonzalez-Gil, G., Niklaus, P. A., and Oester, P., (2012), “Above- and Below-Ground Methane Fluxes and Methanotrophic Activity in a Landfill-Cover Soil,” *Waste Management*, 32(5), 879–889.

Singhania, R. R., Patel, A. K., Christophe, G., Fontanille, P., and Larroche, C., (2013), “Biological Upgrading of Volatile Fatty Acids, Key Intermediates for the Valorization of Biowaste through Dark Anaerobic Fermentation,” *Bioresource Technology, Special Issue: IBS 2012 & Special Issue: IFIBiop*, 145, 166–174.

Shan, J., Iacoboni, M., and Ferrante, R., (2013), “Estimating Greenhouse Gas Emissions from Three Southern California Landfill Sites,” In *Proceedings of SWANA’s 2013 Landfill Gas Symposium,* Silver Springs, MD.

Sohn, A., (2016), “Field Emissions of (Hydro)Chlorofluorocarbons and Methane from a California Landfill.” M.S. Thesis, California Polytechnic State University, San Luis Obispo.

Sormunen, K., Laurila, T., and Rintala, J., (2013), “Determination of Waste Decay Rate for a Large Finnish Landfill by Calibrating Methane Generation Models on the Basis of Methane Recovery and Emissions,” *Waste Management & Research*, 31(10), 979–985.

Spokas, K., Bogner, J., Chanton, J. P., Morcet, M., Aran, C., Graff, C., Golvan, Y. M.-L., and Hebe, I., (2006), “Methane Mass Balance at Three Landfill Sites: What is the Efficiency of Capture by Gas Collection Systems?” *Waste Management*, 26(5), 516–525.

Spokas, K., Bogner, J., and Chanton, J., (2011), “A Process-Based Inventory Model for Landfill CH_4 Emissions Inclusive of Seasonal Soil Microclimate and CH_4 Oxidation,” *Journal of Geophysical Research: Biogeosciences*, 116(G4).

Spokas, K., Bogner, J., Corcoran, M., and Walker, S., (2015), “From California Dreaming to California Data: Challenging Historic Models for Landfill CH_4 Emissions,” *Elem Sci Anth*, 3(0), 000051.

Stevenson, K., Stallwood, B., and Hart, A. G., (2008), “Tire Rubber Recycling and Bioremediation: A Review,” *Bioremediation Journal*, 12(1), 1–11.

Stern, J. C., Chanton, J., Abichou, T., Powelson, D., Yuan, L., Escoriza, S., and Bogner, J., (2007), “Use of a Biologically Active Cover to Reduce Landfill Methane Emissions and Enhance Methane Oxidation,” *Waste Management*, 27(9), 1248–1258.

Sun, J., (2013). *Phytocaps as Biotic Systems to Mitigate Landfill Methane Emissions*. Ph.D. Dissertation, University of Melbourne, Australia.

Tassi, F., Montegrossi, G., Vaselli, O., Liccioli, C., Moretti, S., and Nisi, B., (2009), “Degradation of C_2–C_{15} Volatile Organic Compounds in a Landfill Cover Soil,” *Science of The Total Environment, Thematic Papers: Assessment of the chemical contamination in home-produced eggs in Belgium: general overview of the contegg study*, 407(15), 4513–4525.

Tassi, F., Montegrossi, G., Vaselli, O., Morandi, A., Capecchiacci, F., and Nisi, B., (2011), “Flux Measurements of Benzene and Toluene from Landfill Cover Soils,” *Waste Management & Research*, 29(1), 50–58.

Trégourès, A., Beneito, A., Berne, P., Gonze, M. A., Sabroux, J. C., Savanne, D., Pokryszka, Z., Tauziède, C., Cellier, P., Laville, P., Milward, R., Arnaud, A., Levy, F., and Burkhalter, R., (1999), “Comparison of Seven Methods for Measuring Methane Flux at a Municipal Solid Waste Landfill Site,” *Waste Management and Research*, 17(6), 453–458.

Tchobanoglous, G., Theisen, H., Vigil, S., (1993). *Integrated Solid Waste Management: Engineering Principles and Management Issues*. New York: Irwin McGraw-Hill.

Thompson, C. T., Stockwell, C., Smith, M., and Conley, S., (2019), “Statewide Airborne Methane Emissions Measurement Survey: Final Summary Report,” *California Air Resources Board Contract No. 16RD018*.

Thompson, S., Sawyer, J., Bonam, R., and Valdivia, J. E., (2009), “Building a Better Methane Generation Model: Validating Models with Methane Recovery Rates from 35 Canadian Landfills,” *Waste Management*, 29(7), 2085–2091.

Thorstenson, D. C., and Pollock, D. W., (1989), “Gas Transport in Unsaturated Porous Media: The Adequacy of Fick’s Law,” *Reviews of Geophysics*, 27(1), 61–78.

Tolaymat, T. M., Green, R. B., Hater, G. R., Barlaz, M. A., Black, P., Bronson, D., and Powell, J., (2010), “Evaluation of Landfill Gas Decay Constant for Municipal Solid Waste Landfills Operated as Bioreactors,” *Journal of the Air & Waste Management Association*, 60(1), 91–97.

Urbini, G., Viotti, P., and Gavasci, R., (2014), “Attenuation of Methane, PAHs and VOCs in the Soil Covers of an Automotive Shredded Residues Landfill: A Case Study,” *Journal of Chemical and Pharmaceutical Research*, 6(11), 618–625.

US EPA, (1993), "The Use of Alternative Materials for Daily Cover at Municipal Solid Waste Landfills," EPA Report # 68-C1-0018.

US EPA, (2005), “Landfill Gas Emissions Model (LandGEM) Version 3.02 User’s Guide.” https://www3.epa.gov/ttncatc1/dir1/landgem-v302-guide.pdf

US EPA, (2008), “Background Information Document for Updating AP42 Section 2.4 for Estimating Emissions from Municipal Solid Waste Landfills,” National Risk Management Research Laboratory, Air Pollution Prevention and Control Division, US EPA, https://www3.epa.gov/ttn/chief/ap42/ch02/draft/db02s04.pdf

US EPA, (2009), “US Emission Inventory 2009. Inventory of US Greenhouse Gas Emissions and Sinks: 1990-2007,” Public Review Draft, US EPA 430-R-09-004, http://www.epa.gov/climatechange/emissions/usinventoryreport.

US EPA, (2012), “Part 258-Criteria for Municipal Waste Landfill,” Title 40-Protection of the Environment, http://www.gpo.gov/fdsys/pkg/CFR-2012-title40-vol26/xml/CFR-2012-title40-vol26-part258.xml#seqnum258.21, Last Accessed, June, 1st, 2019.

US EPA, (2014b), "Guidance Note on Daily and Intermediate Cover at Landfills," http://www.epa.ie/pubs197/advice/waste/waste/EPA_Guidance_Note_On_Landfill_Daily_And_Intermediate_Cover_Final.pdf, Last Accessed June, 2nd, 2019.

US EPA, (2016a). *2014 National Emission Inventory Report*, https://www.epa.gov/air-emissions-inventories/2014-national-emission-inventory-nei-report.

US EPA, (2016b), “Initial List of Hazardous Air Pollutants with Modifications.” https://www.epa.gov/haps/initial-list-hazardous-air-pollutants-modifications#mods (July 3rd, 2019).

US EPA, (2017a), “National Overview: Facts and Figures on Materials, Wastes and Recycling,” US EPA, Overviews and Factsheets, <https://www.epa.gov/facts-and-figures-about-materials-waste-and-recycling/national-overview-facts-and-figures-materials>

US EPA, (2017b). “Project and Landfill Data by State.” US EPA, Overviews and Factsheets, <https://www.epa.gov/lmop/project-and-landfill-data-state> (Sep. 1, 2019).

US EPA, (2017c), “Facts and Figures about Materials, Waste, and Recyling: Durable Good - Product Specific Data,” https://www.epa.gov/facts-and-figures-about-materials-waste-and-recycling/durable-goods-product-specific-data#main-content (Dec. 23rd, 2019)

van Haaren, R., Themelis, N., and Goldstein, N., (2010), “The State of Garbage in America,” *BioCycle*, 51(10), 169–23.
Vermeulen, J., Huysmans, A., Crespo, M., Van Lierde, A., De Rycke, A., and Verstraete, W., (1993), “Processing of Biowaste by Anaerobic Composting to Plant Growth Substrates,” *Water Science and Technology*, 27(2), 109–119.

Vogel, T. M., Criddle, C. S., and McCarty, P. L., (1987), “ES Critical Reviews: Transformations of halogenated aliphatic compounds,” *Environmental Science & Technology*, 21(8), 722–736.

Vollhardt, P. C., and Schore, N., (1999). *Organic Chemistry: Structure and Function*. W.H. Freeman, New York.

Vu, H. L., Ng, K. T. W., and Richter, A., (2017), “Optimization of First Order Decay Gas Generation Model Parameters for Landfills Located in Cold Semi-Arid Climates,” *Waste Management*, 69, 315–324.

Walker, S., (2012), “Landfill Data Compilation,” Available as Supplemental Information from Spokas et al. 2015, https://www.elementascience.org/articles/10.12952/journal.elementa.000051/?utm_source=TrendMD&utm_medium=cpc&utm_campaign=TrendMD_Element

Wang-Yao, K., Towprayoon, S., Chiemchaisri, C., Gheewala, S. H., & Nopharatana, A., (2006), “Seasonal Variation of Landfill Methane Emissions from Seven Solid Waste Disposal Sites in Central Thailand,” *2nd Joint International Conference on Sustainable Energy and Environment* (SEE 2006), 21-23rd November, 2006, Bangkok, Thailand.

Wang, X., Padgett, J. M., De la Cruz, F. B., and Barlaz, M. A., (2011), “Wood Biodegradation in Laboratory-Scale Landfills,” *Environmental Science & Technology*, 45(16), 6864–6871.

Wang, X., Nagpure, A. S., DeCarolis, J. F., and Barlaz, M. A., (2013), “Using Observed Data To Improve Estimated Methane Collection from Select U.S. Landfills,” *Environmental Science & Technology*, 47(7), 3251–3257.

Wang, X., Nagpure, A. S., DeCarolis, J. F., and Barlaz, M. A., (2015), “Characterization of Uncertainty in Estimation of Methane Collection from Select U.S. Landfills,” *Environmental Science & Technology*, 49(3), 1545–1551.

Wangyao, K., Yamada, M., Endo, K., Ishigaki, T., Naruoka, T., Towprayoon, S., and Sutthasil, N., (2010), “Methane Generation Rate Constant in Tropical Landfill,” *Journal of Sustainable Energy & Environment*, 1(4), 181-184.

Warith, M. A., and Rao, S. M., (2006), “Predicting the Compressibility Behaviour of Tire Shred Samples for Landfill Applications,” *Waste Management*, 26(3), 268–276.

Williams, A. J., Grulke, C. M., Edwards, J., McEachran, A. D., Mansouri, K., Baker, N. C., Patlewicz, G., Shah, I., Wambaugh, J. F., Judson, R. S., and Richard, A. M., (2017), "The CompTox Chemistry Dashboard: A Community Data Resource for Environmental Chemistry," *Journal of Cheminformatics*, 9(1), 61.

Willumsen, H., and Terraza, H., (2007), "CDM Landfill Gas Projects – World Bank Report," World Bank Workshop, Washington DC, April 2007.
Wilson, J., Gering, S., Pinard, J., Lucas, R., and Briggs, B. R., (2018), "Bio-production of Gaseous Alkenes: Ethylene, Isoprene, Isobutene," *Biotechnology for Biofuels*, 11(1), 234.

WMO (World Meteorological Organization), (2014), "Update on Ozone-Depleting Substances (ODSs) and Other Gases of Interest to the Montreal Protocol," Chapter 1 in Scientific Assessment of Ozone Depletion: 2014, Global Ozone Research and Monitoring Project, L. J. Carpenter and S. Reimann, eds. WMO, Geneva, Switzerland.
Wood, J. A., and Porter, M. L., (1987), "Hazardous Pollutants in Class II Landfills," *JAPCA*, 37(5), 609–615.

Xie, S., Lazar, C. S., Lin, Y.-S., Teske, A., and Hinrichs, K.-U., (2013), "Ethane- and Propane-Producing Potential and Molecular Characterization of an Ethanogenic Enrichment in an Anoxic Estuarine Sediment," *Organic Geochemistry*, 59, 37–48.

Yacovitch, T. I., Herndon, S. C., Roscioli, J. R., Floerchinger, C., McGovern, R. M., Agnese, M., Pétron, G., Kofler, J., Sweeney, C., Karion, A., Conley, S. A., Kort, E. A., Nähle, L., Fischer, M., Hildebrandt, L., Koeth, J., McManus, J. B., Nelson, D. D., Zahniser, M. S., and Kolb, C. E., (2014), "Demonstration of an Ethane Spectrometer for Methane Source Identification," *Environmental Science & Technology*, 48(14), 8028–8034.

Yang, L., Chen, Z., Zhang, X., Liu, Y., and Xie, Y., (2015), "Comparison Study of Landfill Gas Emissions from Subtropical Landfill with Various Phases: A Case Study in Wuhan, China," *Journal of the Air & Waste Management Association*, 65(8), 980–986.

Yazdani, R., Barlaz, M. A., Augenstein, D., Kayhanian, M., and Tchobanoglous, G., (2012), "Performance Evaluation of an Anaerobic/Aerobic Landfill-Based Digester using Yard Waste for Energy and Compost Production," *Waste Management*, 32(5), 912–919.

Yeşiller N., Hanson J. L., and Liu W. L.., (2005), "Heat Generation in Municipal Solid Waste Landfills," *Journal of Geotechnical and Geoenvironmental Engineering*, 131(11), 1330–1344.

Yesiller, N., Hanson, J. L., Oettle, N. K., and Liu, W.-L. (2008). "Thermal Analysis of Cover Systems in Municipal Solid Waste Landfills," *Journal of Geotechnical and Geoenvironmental Engineering*, ASCE, Vol. 134, No. 11, 1655-1664.

Yesiller, N., and Shackelford, C. D., (2011), “Geoenvironmental Engineering (Chapter 13),” In: *Geotechnical Engineering Handbook*, Das, B, M. (ed.), J. Ross Publishing, Ft. Lauderdale, Florida.

Yesiller, N., Hanson, J., Sohn, A., and Tjan, S., (2017), “Emissions of Trace Gases from Landfills,” *Proceedings of the 19th International Conference on Soil Mechanics and Geotechnical Engineering*, Seoul, South Korea, 3211–3214.

Yeşiller, N., Hanson, J. L., Sohn, A. H., Bogner, J. E., and Blake, D. R. (2018), “Spatial and Temporal Variability in Emissions of Fluorinated Gases from a California Landfill,” *Environmental Science & Technology*, 52(12), 6789–6797.

Ying, D., Chuanyu, C., Bin, H., Yueen, X., Xuejuan, Z., Yingxu, C., and Weixiang, W., (2012), “Characterization and Control of Odorous Gases at a Landfill Site: A Case Study in Hangzhou, China,” *Waste Management*, 32(2), 317–326.

Yokouchi, Y., and Ambe, Y., (1988), “Diurnal Variations of Atmospheric Isoprene and Monoterpene Hydrocarbons in an Agricultural Area in Summertime,” *Journal of Geophysical Research: Atmospheres*, 93(D4), 3751–3759.

Zhang, H., He, P., and Qu, X., (2007a), “N2O Fluxes from Sanitary and Bioreactor MSW Landfill in the Summer,” *Research of Environmental Sciences*, 20(3), 108–112.

Zhang, R., El-Mashad, H. M., Hartman, K., Wang, F., Liu, G., Choate, C., and Gamble, P., (2007b). “Characterization of Food Waste as Feedstock for Anaerobic Digestion,” *Bioresource Technology*, 98(4), 929–935.

Zhang, H., He, P., and Shao, L., (2008a), “Methane Emissions from MSW landfill with Sandy Soil Covers under Leachate Recirculation and Subsurface Irrigation,” *Atmospheric Environment*, 42(22), 5579–5588.

Zhang, H., He, P., Shao, L., Qu, X., and Lee, D., (2008b), “Minimizing N_2O Fluxes from Full-Scale Municipal Solid Waste Landfill with Properly Selected Cover Soil,” *Journal of Environmental Sciences*, 20(2), 189–194.

Zhang, H. H., He, P. J., and Shao, L. M., (2008), “N_2O Emissions from Municipal Solid Waste Landfills with Selected Infertile Cover Soils and Leachate Subsurface Irrigation,” *Environmental Pollution*, 156(3), 959–965.

Zhang, H., He, P., and Shao, L., (2009), “N_2O Emissions at Municipal Solid Waste Landfill Sites: Effects of CH_4 Emissions and Cover Soil,” *Atmospheric Environment*, 43(16), 2623–2631.

Zhang, H., Yan, X., Cai, Z., and Zhang, Y., (2013), “Effect of Rainfall on the Diurnal Variations of CH_4, CO_2, and N_2O fluxes from a Municipal Solid Waste Landfill,” *Science of The Total Environment*, 442, 73–76.

Zhang, C., Guo, Y., Wang, X., and Chen, S., (2019), “Temporal and Spatial Variation of Greenhouse Gas Emissions from a Limited-Controlled Landfill Site,” *Environment International*, 127, 387–394.

Zhao X., Soong, T. Y., Subbarayan, M., and Williams, M., (2013), “Full-Scale Field Research and Demonstration of Septage Bioreactor Landfill Technology,” *Journal of Hazardous, Toxic, and Radioactive Waste*, 17(4), 295–306.

Ziemann, P. J., and Atkinson, R., (2012), “Kinetics, Products, and Mechanisms of Secondary Organic Aerosol Formation,” *Chemical Society Reviews*, 41(19), 6582–6605.

Zou, S. C., Lee, S. C., Chan, C. Y., Ho, K. F., Wang, X. M., Chan, L. Y., and Zhang, Z. X., (2003), “Characterization of Ambient Volatile Organic Compounds at a Landfill Site in Guangzhou, South China,” *Chemosphere*, 51(9), 1015–1022.

APPENDIX A

Chemical Family	Chemical Species	Min	Mean	Max	Standard Deviation	Number of Samples
Baseline GHGs	Methane	4.48E+01	1.60E+05	7.75E+05	1.62E+05	1109
	Carbon dioxide	2.92E+02	5.44E+05	3.52E+06	3.23E+05	497
	Nitrous oxide	4.92E-01	2.03E+01	2.43E+02	4.56E+01	59
	Carbon monoxide	3.14E+00	3.04E+01	8.97E+01	3.46E+01	8
Reduced sulfur compounds	Carbonyl sulfide	2.60E-04	6.33E-01	7.49E+00	1.65E+00	34
	Dimethyl sulfide	2.58E-05	7.69E+00	6.00E+01	1.28E+01	91
	Dimethyl disulfide	3.92E-05	8.93E-01	1.70E+00	4.59E+00	80
	Carbon disulfide	1.27E-04	8.64E-01	1.69E+01	2.17E+00	95
F-gases	CFC-11	4.05E-02	2.45E+00	7.40E+01	5.65E+00	223
	CFC-12	1.00E-03	1.11E+01	2.31E+02	2.35E+01	433
	CFC-113	1.00E-02	1.24E+00	4.90E+01	7.05E+00	225
	CFC-114	5.61E-02	8.43E-01	3.01E+00	8.22E-01	14
	HCFC-21	2.70E-02	2.55E+01	1.14E+02	3.01E+01	19
	HCFC-22	5.00E-01	7.58E+01	4.04E+02	1.18E+02	27
	HCFC-141b	2.16E+01	2.78E+01	5.77E+01	2.74E+01	3
	HCFC-142b	5.00E-01	1.06E+01	3.10E+01	1.13E+01	11
	HFC-134a	1.60E+00	4.49E+00	2.70E+00	4.09E+00	3
	HFC-152a	-	3.32E+00	-	0	1
	HFC-245fa	-	1.45E-01	-	0	1
	HFC-365mfc	-	-	-	-	-
	Halon-1211	8.10E-04	1.90E-03	1.70E-03	1.20E-03	3
Halogenated Hydrocarbons	Chloroform	0.00E+00	4.66E+01	9.13E+02	1.04E+02	97
	Methyl-Chloroform	1.66E-02	4.07E+00	3.13E+01	1.11E+01	251
	Carbon tetrachloride	0.00E+00	2.06E+01	7.95E+02	9.71E+01	74
	Methylene chloride	5.91E-03	2.29E+01	1.45E+02	3.21E+01	83
	Trichloroethylene	0.00E+00	1.37E+01	1.52E+02	3.38E+01	157
	Tetrachloroethylene	0.00E+00	2.39E+01	3.50E+02	5.66E+01	113
	Methyl chloride	0.00E+00	4.25E-01	2.43E+00	6.56E-01	23
	Bromomethane	0.00E+00	3.74E-01	1.45E+00	6.43E-01	13
	Dibromomethane	4.60E-03	6.03E-03	7.44E-03	2.03E-03	2
	Bromodichloromethane	1.87E-02	5.98E-02	1.01E-01	5.82E-02	2
	Bromoform	0.00E+00	3.97E-01	1.05E+00	7.74E-01	10
	Chloroethane	1.20E+00	3.98E+00	1.70E+01	5.76E+00	7
	1,2-Dichloroethane	0.00E+00	6.09E-01	1.07E+01	1.69E+01	60
	1,2-Dibromoethane	-	-	-	-	-
Organic Alkyl Nitrates	Methyl nitrate	9.80E-06	2.44E-05	3.90E-05	2.06E-05	2
	Ethyl nitrate	1.20E-05	2.75E-05	4.30E-05	2.19E-05	2
	Isopropyl nitrate	1.10E-05	3.16E-04	6.20E-04	4.31E-04	2
	N-propyl nitrate	4.00E-06	1.10E-05	1.80E-05	9.90E-06	2
	2-Butyl nitrate	1.30E-05	3.05E-05	4.80E-05	2.47E-05	2

Chemical Family	Chemical Species	Min	Mean	Max	Standard Deviation	Number of Samples
Alkanes	Ethane	2.10E+00	2.04E+02	1.75E+01	1.21E+02	276
	Propane	1.00E-03	2.24E+01	6.73E+01	1.10E+01	285
	i-Butane	4.70E-02	5.25E+01	2.24E+02	8.55E+01	70
	n-Butane	9.46E-01	2.08E+01	2.11E+02	4.31E+01	274
	i-Pentane	1.60E-02	1.04E+01	3.12E+01	6.72E+00	274
	n-Pentane	3.60E-02	4.91E+00	7.32E+01	9.36E+00	292
	n-Hexane	1.00E-03	5.08E+00	9.32E+01	8.91E+00	339
	n-Undecane	1.00E-03	2.97E+01	1.09E+02	1.63E+01	274
Alkenes	Ethene	1.70E+00	3.17E+00	2.80E+00	1.68E+00	3
	Propene	2.82E+00	5.93E+00	8.40E+00	1.95E+00	7
	1-Butene	1.00E-03	3.24E-01	1.27E+00	2.46E-01	71
	i-Butene	1.00E-03	2.52E-01	4.00E-01	1.49E-01	5
	trans-2-butene	-	-	-	-	-
	1-pentene	-	3.75E-01	-	0	1
	Isoprene	-	-	-	-	-
Aldehydes/Alkynes	Ethyne	3.29E-02	1.30E-01	1.00E-01	1.55E-01	6
	Acetaldehyde	1.00E-01	3.12E-01	2.00E-01	2.85E-01	3
	Butanal	3.66E-03	2.80E-01	1.55E+00	5.95E-01	70
Aromatic Hydrocarbons	Benzene	7.14E-04	4.21E+00	1.14E+02	1.04E+01	492
	Toluene	1.00E-03	6.42E+01	9.71E+02	9.46E+01	467
	Ethylbenzene	1.00E-03	2.21E+01	2.40E+02	2.94E+01	405
	m+p-Xylene	1.00E-03	4.52E+01	6.78E+02	7.37E+01	380
	o-Xylene	6.18E-04	9.34E+00	8.34E+01	1.37E+01	370
	i-Propylbenzene	-	-	-	-	-
	n-Propylbenzene	6.60E-01	1.17E+01	1.20E+02	1.24E+01	212
	3-Ethyltoluene	1.77E+00	1.32E+01	7.70E+00	5.13E+00	204
	4-Ethyltoluene	-	1.00E+01	-	5.00E+00	200
	2-Ethyltoluene	-	1.71E+01	-	5.00E+00	200
	1,3,5-Trimethylbenzene	6.00E-03	8.29E+00	5.30E+01	6.57E+00	260
	1,2,3-Trimethylbenzene	1.11E+00	8.56E+00	1.28E+01	6.85E+00	233
	1,2,4-Trimethylbenzene	3.20E-02	2.17E+01	7.75E+01	1.22E+01	270
	m+p+o-Xylene	2.08E-01	5.90E+01	4.40E+02	7.05E+01	113
Monoterpenes	alpha-Pinene	1.00E-03	3.48E+01	8.84E+01	1.94E+01	269
	beta-Pinene	3.90E-02	1.09E+00	1.16E+01	2.72E+00	27
	Limonene	1.00E-03	1.60E+02	2.59E+02	7.90E+01	273
Alcohols	Methanol	2.53E-02	4.93E+00	2.10E+02	2.58E+01	67
	Ethanol	7.66E-03	3.33E+01	8.00E+02	1.48E+02	76
	Isopropanol	2.92E-01	6.11E+00	1.43E+01	7.35E+00	10
	2-butanol	1.90E+01	7.45E+01	2.10E+02	7.70E+01	6
Ketones	Acetone	9.66E-03	1.68E+01	9.31E+01	1.90E+01	309
	Butanone	2.00E+01	3.86E+01	4.99E+01	9.55E+00	33
	Methylisobutylketone	2.20E-01	1.18E+01	2.95E+01	1.66E+01	59

Landfill gas concentrations are shown in micrograms per liter.

Study No.	Study Name	Location	Region	Climate Zone	Season	WIP (m3)	WIP (tonnes)	Waste Age (years)
1	Abichou et al. 2006a	Leon County, FL, USA	USA	Cfa	September 2003-February 2004	-	-	7
			USA	Cfa	February 2004-May 2004	-	-	1
2	Abichou et al. 2006b	Leon County, FL, USA	USA	Cfa	June 2003-September 2003	-	-	7
			USA	Cfa	June 2003-July 2003	-	-	14
			USA	Cfa	June 2003-November 2003	-	-	1
			USA	Cfa	September 2003-Feburary 2004	-	-	7
3,4	Bogner 1992 and	Brea-Olinda, CA, USA	USA	Csa	Mar-88	-	-	28
	Bogner and Spokas 1993[1]		USA	Csa	Mar-88	-	-	28
5	Bogner et al. 1995[1,3]		USA	Csa	1994 (Month unspecified)	-	-	34
			USA	Csa	1994 (Month unspecified)	-	-	34
6	Bogner et al. 1993[1,3,8]	Mallard Lake, Illinois, USA	USA	Dfa	1992-1993 (Month unspecified)	-	-	18
			USA	Dfa	1992-1993 (Month unspecified)	-	-	18
			USA	Dfa	1992-1993 (Month unspecified)	-	-	18
			USA	Dfa	1992-1993 (Month unspecified)	-	-	18
			USA	Dfa	1992-1993 (Month unspecified)	-	-	18
7	Bogner et al. 1995[1,3,8]	Mallard Lake, Illinois, USA 1994	USA	Dfa	1994 (Spring/Early Summer)	-	-	19
			USA	Dfa	1994 (Spring/Early Summer)	-	-	19
8,9	Bogner et al. 1997a, Bogner et al. 1999[1,3,8]	Mallard Lake, Illinois, USA 1994	USA	Dfa	June-December 1995	-	-	20
			USA	Dfa	June-December 1995	-	-	20
10	Czepiel et al. 1996 (some unpublished) as reported in Bogner et al. 1997a	Nashua, New Hampshire, USA	USA	Dfb	-	-	-	25
			USA	Dfb	-	-	-	25
			USA	Dfb	-	-	-	25
			USA	Dfb	-	-	-	25
			USA	Dfb	-	-	-	25
11	Mosher et al. 1999[3,8]	Rochester, New Hampshire, USA	USA	Dfb	Jul-94	-	2,780,000	17
		Nashua, New Hampshire, USA	USA	Dfb	Aug-95	-	2,230,000	24
		Wayland, Massachusetts, USA	USA	Dfb	Jun-95	-	-	16
		Sudbury, Massachusetts, USA	USA	Dfb	Aug-94	-	-	-
		Privately operated landfill-A	USA	-	Jul-95	-	5,700,000	34
		Privately operated landfill-E	USA	-	Jun-95	-	3,700,000	46
12	Gregory and Skennerton 1997 (unpublished) as reported in Bogner et al. 1997a[5]	United Kingdom, 26 sites	UK	Cfb	Winter and Summer	-	-	-
13	Svensson and Borjesson 1993 (unpublished) as	Hokhuvud, Sweden	Sweden	Dfb	-	-	-	-
		Hogbytorp, Sweden	Sweden	Dfb	-	-	-	-
14	Scott et al. 1992	Brogborough, U.K.	UK	Cfb	-	-	-	-
15	Nozhevnikova et al. 1993	Moscow, Russia	Russia	Dfb	-	24,000,000	17,086,648	-
			Japan	Cfa	Jun-01	1,450,000	1,032,318	19

Study No.	Study Name	Location	Region	Climate Zone	Season	WIP (m3)	WIP (tonnes)	Waste Age (years)
16	Ishigaki et al. 2005	Kanto, Japan	Japan	Cfa	Nov-01	1,450,000	1,032,318	19
			Russia	Cfa	Feb-01	1,450,000	1,032,318	19
17	Kallistova et al. (2005)[3]	Khmet'evo LF, Moscow, Russia	Russia	Dfb	Apr-02	-	-	-
			Russia	Dfb	Apr-02	-	-	-
			Russia	Dfb	Apr-02	-	-	-
			Russia	Dfb	Apr-02	-	-	-
			Russia	Dfb	Apr-02	-	-	-
			Russia	Dfb	Apr-02	-	-	-
			Russia	Dfb	Apr-02	-	-	-
			Russia	Dfb	Apr-02	-	-	-
			Russia	Dfb	Apr-02	-	-	-
			Russia	Dfb	Apr-02	-	-	-
			Russia	Dfb	Apr-02	-	-	-
			Russia	Dfb	Apr-02	-	-	-
			Russia	Dfb	Apr-02	-	-	-
			Russia	Dfb	Apr-02	-	-	-
			Russia	Dfb	Apr-02	-	-	-
			Russia	Dfb	Jun-02	-	-	-
			Russia	Dfb	Jun-02	-	-	-
			Russia	Dfb	Jun-02	-	-	-
			Russia	Dfb	Jun-02	-	-	-
			Russia	Dfb	Jun-02	-	-	-
			Russia	Dfb	Jun-02	-	-	-
			Russia	Dfb	Jun-02	-	-	-
			Russia	Dfb	Jun-02	-	-	-
			Russia	Dfb	Jun-02	-	-	-
			Russia	Dfb	Jun-02	-	-	-
			Russia	Dfb	Jun-02	-	-	-
			Russia	Dfb	Jun-02	-	-	-
			Sweden	Dfb	May-92	160,000	113,911	29
			Sweden	Dfb	Jun-92	160,000	113,911	29
			Sweden	Dfb	Jul-92	160,000	113,911	29
			Sweden	Dfb	Sep-92	160,000	113,911	29
			Sweden	Dfb	May-93	160,000	113,911	29
			Sweden	Dfb	Jun-93	160,000	113,911	29

Study No.	Study Name	Location	Region	Climate Zone	Season	WIP (m3)	WIP (tonnes)	Waste Age (years)
18	Borjesson and Svensson 1997a[3,6]	Hokhuvud LF, Sweden	Sweden	Dfb	Jul-93	160,000	113,911	29
			Sweden	Dfb	Aug-93	160,000	113,911	29
			Sweden	Dfb	Sep-93	160,000	113,911	29
			Sweden	Dfb	Nov-93	160,000	113,911	29
			Sweden	Dfb	Dec-93	160,000	113,911	29
			Sweden	Dfb	Jan-94	160,000	113,911	29
			Sweden	Dfb	Feb-94	160,000	113,911	29
			Sweden	Dfb	Mar-94	160,000	113,911	29
			Sweden	Dfb	Apr-94	160,000	113,911	29
			Sweden	Dfb	May-94	160,000	113,911	29
			Sweden	Dfb	Jun-94	160,000	113,911	29
			Sweden	Dfb	Jul-94	160,000	113,911	29
19	Borjesson et al. 2000[3]	Falevi LF, Sweden	Sweden	Dfb	6-May-97	325,000	231,382	35
			Sweden	Dfb	2-Jul-97	325,001	231,382	35
			Sweden	Dfb	21-Oct-97	325,002	231,383	35
20	Boeckx et al. 1996[3]	Antwerp, Belgium	Belgium	Cfb	Jun-94	-	-	-
			Belgium	Cfb	Jul-94	-	-	-
			Belgium	Cfb	Aug-94	-	-	-
			Belgium	Cfb	Sep-94	-	-	-
			Belgium	Cfb	Oct-94	-	-	-
			Belgium	Cfb	Nov-94	-	-	-
			Belgium	Cfb	Dec-94	-	-	-
21	Scheutz et al. 2003	Lapouyade Landfill, France	France	Cfb	Sep-01	-	310,000	6
			France	Cfb	Sep-01	-	-	6
22	Schuetz et al. 2008	Grand'Landes Landfill, France	France	Cfb	Sep-02	-	54,000	12
			France	Cfb	Sep-02	-	54,000	12
			Denmark	Dfb	May 1997-May 1998	-	420,000	25
			Denmark	Dfb	May 1997-May 1998	-	420,000	25
			Denmark	Dfb	May 1997-May 1998	-	420,000	25

Study No.	Study Name	Location	Region	Climate Zone	Season	WIP (m3)	WIP (tonnes)	Waste Age (years)
23,24	Christophersen et al. 2001, Christophersen & Kjeldsen 2001[3]	Skellingsted Landfill, Denmark	Denmark	Dfb	May 1997-May 1998	-	420,000	25
			Denmark	Dfb	May 1997-May 1998	-	420,000	25
			Denmark	Dfb	May 1997-May 1998	-	420,000	25
			Denmark	Dfb	May 1997-May 1998	-	420,000	25
			Denmark	Dfb	May 1997-May 1998	-	420,000	25
			Denmark	Dfb	May 1997-May 1998	-	420,000	25
			Denmark	Dfb	May 1997-May 1998	-	420,000	25
			Denmark	Dfb	May 1997-May 1998	-	420,000	25
			Denmark	Dfb	May 1997-May 1998	-	420,000	25
			Denmark	Dfb	May 1997-May 1998	-	420,000	25
			Denmark	Dfb	May 1997-May 1998	-	420,000	25
			Denmark	Dfb	May 1997-May 1998	-	420,000	25
			Denmark	Dfb	May 1997-May 1998	-	420,000	25
			Denmark	Dfb	May 1997-May 1998	-	420,000	25
			Denmark	Dfb	May 1997-May 1998	-	420,000	25
25	Jones and Nedwell 1993[8]	Martin's Farm LF, UK	UK	Cfb	-	-	-	-
			UK	Cfb	-	-	-	-
			UK	Cfb	-	-	-	-
			UK	Cfb	-	-	-	-
26	Meadows et al. 1999[8]	UK	UK	Cfb	-	-	-	-
27	Maurice and Lagerkvist 1997[8]	Lulea, Sweden	Sweden	Dfc	-	-	-	-
			Sweden	Dfc	-	-	-	-
28	Barlaz et al. 2004	Outer Loop LF, Louisville, KY, USA	USA	Cfa	Apr-02	-	-	4
			USA	Cfa	Apr-02	-	-	4
			USA	Cfa	Apr-02	-	-	4
			USA	Cfa	Jun-02	-	-	4
			USA	Cfa	Jun-02	-	-	4
			USA	Cfa	Jun-02	-	-	4
			USA	Cfa	Sep-02	-	-	4
			USA	Cfa	Sep-02	-	-	4
			USA	Cfa	Sep-02	-	-	4
			USA	Cfa	Jun-03	-	-	4
			USA	Cfa	Jun-03	-	-	4
			USA	Cfa	Jun-03	-	-	4
			USA	Cfa	Jun-03	-	-	4
			USA	Cfa	Jun-03	-	-	4
			USA	Cfa	Jun-03	-	-	4
29	Ishigaki et al. 2008	Nam Son/Tay Mo LF, Hanoi, Vietnam	Vietnam	Cwa	Jan-05	-	-	8
			Vietnam	Cwa	Jan-05	-	-	5
			Vietnam	Cwa	Jan-05	-	-	4
		Campbellton, Florida, USA	USA	Cfa	May 2006-December 2009	-	11,892,841	24.5
		Louisville, Kentucky, USA	USA	Cfa	May 2006-December 2009	-	31,368,908	38.5
		Campbellton, Florida, USA	USA	Cfa	May 2006-December 2009	-	11,892,841	24.5
		Glencoe, Minnesota, USA	USA	Dfa	May 2006-December 2009	-	6,794,033	36.5

Study No.	Study Name	Location	Region	Climate Zone	Season	WIP (m3)	WIP (tonnes)	Waste Age (years)
30	Abichou et al. 20111[1,7]	Louisville, Kentucky, USA	USA	Cfa	May 2006-December 2009	-	31,368,908	38.5
		Humble, Texas, USA	USA	Cfa	May 2006-December 2009	-	31,932,277	24.5
		Petersburg, Virginia, USA	USA	Cfa	May 2006-December 2009	-	2,522,329	30.4
		Jetersville, Virginia, USA	USA	Cfa	May 2006-December 2009	-	9,508,301	14.5
		Franklin, Wisconsin, USA	USA	Dfb	May 2006-December 2009	-	22,097,499	55.5
		Glencoe, Minnesota, USA	USA	Dfa	May 2006-December 2009	-	6,794,033	36.5
		Waverly, Virginia, USA	USA	Cfa	May 2006-December 2009	-	33,946,639	13.5
		Petersburg, Virginia, USA	USA	Cfa	May 2006-December 2009	-	2,522,329	30.5
		Jetersville, Virginia, USA	USA	Cfa	May 2006-December 2009	-	9,508,301	14.5
		Muskego, Wisconsin, USA	USA	Dfb	May 2006-December 2009	-	13,310,659	12.5
		Humble, Texas, USA	USA	Cfa	May 2006-December 2009	-	31,932,277	24.5
		Lake, Missippi, USA	USA	Cfa	May 2006-December 2009	-	6,713,437	16.5
		Glenford, Ohio, USA	USA	Dfa	May 2006-December 2009	-	11,815,593	25.5
			USA	Dfa	May 2006-December 2009	-	11,815,593	25.5
31	Capaccioni et al. 2011[1]	Fano LF site, Italy	Italy	Csa	May 2005-July 2009	-	1,400,000	27
			Italy	Csa	May 2005-July 2009	-	771,000	11
			Italy	Csa	May 2005-July 2009	-	1,400,000	27
			Italy	Csa	May 2005-July 2009	-	771,000	11
			Italy	Csa	May 2005-July 2009	-	1,400,000	27
			Italy	Csa	May 2005-July 2009	-	771,000	11
			Italy	Csa	May 2005-July 2009	-	1,400,000	27
			Italy	Csa	May 2005-July 2009	-	771,000	11
			Italy	Csa	May 2005-July 2009	-	771,000	11
			Italy	Csa	May 2005-July 2009	-	-	0.5
			Italy	Csa	May 2005-July 2009	-	1,400,000	27
			Italy	Csa	May 2005-July 2009	-	771,000	11
			Italy	Csa	May 2005-July 2009	-	771,000	11
			Italy	Csa	May 2005-July 2009	-	-	0.5
32	Di Trapani et al. 2013[1]	Bellolampo, Palermo LF site, Italy	Italy	Csa	April 2010-June 2010	-	-	16
			Italy	Csa	April 2010-June 2010	-	-	16
			Italy	Csa	April 2010-June 2010	-	-	14
			Italy	Csa	April 2010-June 2010	-	-	14
			Italy	Csa	April 2010-June 2010	-	-	14
			Italy	Csa	April 2010-June 2010	-	-	3
			Italy	Csa	April 2010-June 2010	-	-	16
			Italy	Csa	April 2010-June 2010	-	-	15
			Italy	Csa	April 2010-June 2010	-	-	14

Study No.	Study Name	Location	Region	Climate Zone	Season	WIP (m3)	WIP (tonnes)	Waste Age (years)
			Italy	Csa	April 2010-June 2010	-	-	14
			Italy	Csa	April 2010-June 2010	-	-	14
			Italy	Csa	April 2010-June 2010	-	-	3
33	Di Bella et al. 2011	Bellolampo, Palermo LF site, Italy	Italy	Csa	May-09	6,191,670	8,050,040	9.666666667
34	Klusman and Dick 2000	Rooney Rd LF site, CO, USA	USA	Dfb	Fall 1994, Winter 1994-1995, Summer 1995	-	-	-
			USA	Dfb	Fall 1994, Winter 1994-1995, Summer 1995	-	-	-
			USA	Dfb	Fall 1994, Winter 1994-1995, Summer 1995	-	-	-
35	Hedge et al. 2003[5]	Shan-Chu-Ku LF, Taipei City, Taiwan	Taiwan	Cfa	Feb-May 1998	-	1,022,000	0.5
			Taiwan	Cfa	Feb-May 1998	-	1,533,000	1
			Taiwan	Cfa	Feb-May 1998	-	2,555,000	5
36	Jeong et al. 2019[1,5]	10 LF Sites across South Korea	South Korea	Dwa	June-July 2015	7,650,683	5,446,855	19
			South Korea	Dwa	Aug-15	7,650,683	5,446,855	19
			South Korea	Dwa	Sep-15	7,650,683	5,446,855	19
			South Korea	Dwa	November-December 2015	7,650,683	5,446,855	19
			South Korea	Dwa	Mar-11	1,995,661	1,420,798	16
			South Korea	Dwa	April-May 2011	3,114,008	2,216,998	16
			South Korea	Dwa	Jun-15	1,800,302	1,281,714	17
			South Korea	Dwa	July-August 2015	1,800,302	1,281,714	17
			South Korea	Dwa	Sep-15	1,800,302	1,281,714	17
			South Korea	Dwa	Nov-15	1,800,302	1,281,714	17
			South Korea	Dwa	Mar-11	2,085,229	1,484,566	23
			South Korea	Dwa	Jun-14	2,085,229	1,484,566	23
			South Korea	Dwa	Jul-14	2,085,229	1,484,566	23
			South Korea	Dwa	Aug-14	2,085,229	1,484,566	23
			South Korea	Dwa	Aug-14	2,085,229	1,484,566	23
			South Korea	Dwa	Sep-11	450,662	320,846	11
			South Korea	Dwa	Mar-11	139,283	99,162	8
			South Korea	Dwa	Sep-11	314,207	223,698	17
			South Korea	Dwa	Aug-11	344,304	245,125	13
			South Korea	Dwa	Jul-15	321,539	228,918	16
			South Korea	Dwa	Aug-15	321,539	228,918	16
			South Korea	Dwa	Sep-15	321,539	228,918	16
37	Raco et al. 2010[3]	Legoli LF, Tuscany, Italy	Italy	Csa	May 2004-January 2009	-	3,100,000	-
			Italy	Csa	May 2004-January 2009	-	3,100,000	-
			Italy	Csa	May 2004-January 2009	-	3,100,000	-
			Italy	Csa	May 2004-January 2009	-	3,100,000	-
			Italy	Csa	May 2004-January 2009	-	3,100,000	-
			Italy	Csa	May 2004-January 2009	-	3,100,000	-
			Italy	Csa	May 2004-January 2009	-	3,100,000	-
			Italy	Csa	May 2004-January 2009	-	3,100,000	-
			Italy	Csa	May 2004-January 2009	-	3,100,000	-

Study No.	Study Name	Location	Region	Climate Zone	Season	WIP (m3)	WIP (tonnes)	Waste Age (years)
			Italy	Csa	May 2004-January 2009	-	3,100,000	-
38	Fourie and Morris 2004[1,6]	4-Landfills near Johannesburg, South Africa	South Africa	Cwb	March/September 1999	115,500	82,229	4
			South Africa	Cwb	March/September 1999	115,500	82,229	4
			South Africa	Cwb	March/September 1999	100,500	71,550	10
			South Africa	Cwb	March/September 1999	1,830,000	1,302,857	10
			South Africa	Cwb	March/September 1999	2,190,000	1,559,157	-
			South Africa	Cwb	March/September 1999	4,500,000	3,203,747	71
39	Stern et al. 2007	Leon County, FL, USA	USA	Cfa	March 2004-May 2005	-	-	8
			USA	Cfa	March 2004-May 2005	-	-	8
			USA	Cfa	March 2004-May 2005	-	-	8
			USA	Cfa	March 2004-May 2005	-	-	8
			USA	Cfa	March 2004-May 2005	-	-	8
			USA	Cfa	March 2004-May 2005	-	-	8
			USA	Cfa	March 2004-May 2005	-	-	8
			USA	Cfa	March 2004-May 2005	-	-	8
			USA	Cfa	March 2004-May 2005	-	-	8
			USA	Cfa	March 2004-May 2005	-	-	8
			USA	Cfa	March 2004-May 2005	-	-	8
			USA	Cfa	March 2004-May 2005	-	-	8
			USA	Cfa	March 2004-May 2005	-	-	8
			USA	Cfa	March 2004-May 2005	-	-	8
			USA	Cfa	March 2004-May 2005	-	-	8
40	Bogner et al. 2011[1]	Marina LF, Monterey,CA, USA	USA	Csa	March and August 2007/2008	-	-	-
			USA	Csa	March and August 2007/2008	-	-	-
			USA	Csa	March and August 2007/2008	-	-	-
			USA	Csa	March and August 2007/2008	-	-	-
			USA	Csa	March and August 2007/2008	-	-	-
			USA	Csa	March and August 2007/2008	-	-	-
			USA	Csa	March and August 2007/2008	-	-	40.5
			USA	Csa	March and August 2007/2008	-	-	40.5
		Scholl Canyon LF, Los Angeles, USA	USA	Csb	March and August 2007/2008	-	-	-
			USA	Csb	March and August 2007/2008	-	-	-
			USA	Csb	March and August 2007/2008	-	-	-
			USA	Csb	March and August 2007/2008	-	-	-
			USA	Csb	March and August 2007/2008	-	-	45.5
			USA	Csb	March and August 2007/2008	-	-	45.5
41	Tregoures et al. 1999[1]	LF Site North of Paris, France	France	Cfb	Jul-96	-	-	7
			France	Cfb	Jul-96	-	-	7
			France	Cfb	Jul-96	-	-	7
			USA	Cfa	December 1996-January 1998	-	-	20
			USA	Cfa	December 1996-January 1998	-	-	20
			USA	Cfa	December 1996-January 1998	-	-	20
			USA	Cfa	December 1996-January 1998	-	-	20
			USA	Cfa	December 1996-January 1998	-	-	20

Study No.	Study Name	Location	Region	Climate Zone	Season	WIP (m3)	WIP (tonnes)	Waste Age (years)
42	Chanton and Liptay 2000[1]	Leon County, FL, USA	USA	Cfa	December 1996-January 1998	-	-	20
			USA	Cfa	December 1996-January 1998	-	-	20
			USA	Cfa	December 1996-January 1998	-	-	20
			USA	Cfa	December 1996-January 1998	-	-	20
			USA	Cfa	December 1996-January 1998	-	-	20
			USA	Cfa	December 1996-January 1998	-	-	20
			USA	Cfa	December 1996-January 1998	-	-	20
			USA	Cfa	December 1996-January 1998	-	-	20
			USA	Cfa	December 1996-January 1998	-	-	20
			USA	Cfa	December 1996-January 1998	-	-	20
			USA	Cfa	December 1996-January 1998	-	-	20
			USA	Cfa	December 1996-January 1998	-	-	20
			USA	Cfa	December 1996-January 1998	-	-	20
			USA	Cfa	December 1996-January 1998	-	-	20
			USA	Cfa	December 1996-January 1998	-	-	20
			USA	Cfa	December 1996-January 1998	-	-	20
			USA	Cfa	December 1996-January 1998	-	-	20
			USA	Cfa	December 1996-January 1998	-	-	20
			USA	Cfa	December 1996-January 1998	-	-	20
			USA	Cfa	December 1996-January 1998	-	-	20
			USA	Cfa	December 1996-January 1998	-	-	20
			USA	Cfa	December 1996-January 1998	-	-	20
			USA	Cfa	December 1996-January 1998	-	-	20
43	Zhang et al. 2013[6]	Nanjing City, Eastern China	China	Cwa	Apr-12	100,000	71,194	7
			China	Cwa	Apr-12	100,000	71,194	7
			China	Cwa	Apr-12	100,000	71,194	7
			China	Cwa	Apr-12	100,000	71,194	7
			China	Cwa	Apr-12	100,000	71,194	7
			China	Cwa	Apr-12	100,000	71,194	7
			China	Cwa	Apr-12	1,300,000	925,527	3
			China	Cwa	Apr-12	1,300,000	925,527	3
			China	Cwa	Apr-12	1,300,000	925,527	3
			China	Cwa	Apr-12	1,300,000	925,527	3
			China	Cwa	Apr-12	1,300,000	925,527	3
			China	Cwa	Apr-12	1,300,000	925,527	3
			China	Cwa	Apr-12	5,000,000	3,559,718	3
			China	Cwa	Apr-12	5,000,000	3,559,718	3
			China	Cwa	Apr-12	5,000,000	3,559,718	3
			China	Cwa	Apr-12	5,000,000	3,559,718	3
			China	Cwa	Apr-12	5,000,000	3,559,718	3
			China	Cwa	Apr-12	5,000,000	3,559,718	3
44	Bogner et al. 1997b[1]	Green Valley LF, Illinois, USA	USA	Dfa	May-96	-	32,259,540	22
			USA	Dfa	May-96	-	32,259,540	22
			USA	Dfa	May-96	-	32,259,540	22

Study No.	Study Name	Location	Region	Climate Zone	Season	WIP (m3)	WIP (tonnes)	Waste Age (years)
44	Bogner et al. 1997b	Green Valley LF, Illinois, USA	USA	Dfa	May-96	-	32,259,540	22
			USA	Dfa	May-96	-	32,259,540	22
			USA	Dfa	May-96	-	32,259,540	22
45	Bogner et al. 2010	Leon County, FL, USA	USA	Cfa	May-November 2005	-	-	2
46	Salazar et al. 2017[1]	Three LF sites in Costa Rica	Costa Rica	Aw	October/July 2014	-	-	12
			Costa Rica	Aw	October/July 2014	-	-	9
			Costa Rica	Aw	October/July 2014	-	-	49
47	Bogner et al. 2005[1]	Leon County, FL, USA	USA	Cfa	June-September 2003	-	-	26
			USA	Cfa	-	-	-	7
			USA	Cfa	-	-	-	7
48	Scheutz et al. 2010[1]	AV-Miljo LF, Denmark	Denmark	Dfb	February 2005-June 2006	-	155,000	15.5
			Denmark	Dfb	February 2005-June 2006	-	155,000	15.5
			Denmark	Dfb	February 2005-June 2006	-	155,000	15.5
			Denmark	Dfb	February 2005-June 2006	-	155,000	15.5
			Denmark	Dfb	February 2005-June 2006	-	155,000	15.5
49	Borjesson et al. 2001[1]	Falkoping, Sweden	Sweden	Dfb	August 1997-March 1998	325,000	231,382	32
			Sweden	Dfb	August 1997-March 1998	325,000	231,382	32
			Sweden	Dfb	August 1997-March 1998	325,000	231,382	32
			Sweden	Dfb	August 1997-March 1998	325,000	231,382	32
			Sweden	Dfb	August 1997-March 1998	325,000	231,382	32
			Sweden	Dfb	August 1997-March 1998	325,000	231,382	32
			Sweden	Dfb	August 1997-March 1998	325,000	231,382	32
		Hokhuvud, Sweden	Sweden	Dfb	August 1997-March 1998	100,000	71,194	29
			Sweden	Dfb	August 1997-March 1998	100,000	71,194	29
			Sweden	Dfb	August 1997-March 1998	100,000	71,194	29
			Sweden	Dfb	August 1997-March 1998	100,000	71,194	29
			Sweden	Dfb	August 1997-March 1998	100,000	71,194	29
			Sweden	Dfb	August 1997-March 1998	100,000	71,194	29
		Hogbytorp LF, Sweden	Sweden	Dfb	November 1991-November 1994	-	-	9
			Sweden	Dfb	November 1991-November 1994	-	-	9
			Sweden	Dfb	November 1991-November 1994	-	-	9
			Sweden	Dfb	November 1991-November 1994	-	-	9
			Sweden	Dfb	November 1991-November 1994	-	-	9
			Sweden	Dfb	November 1991-November 1994	-	-	9
			Sweden	Dfb	November 1991-November 1994	-	-	9
		Hagby LF, Uppper, Sweden	Sweden	Dfb	November 1991-November 1994	-	-	1
			Sweden	Dfb	November 1991-November 1994	-	-	1
			Sweden	Dfb	November 1991-November 1994	-	-	1
			Sweden	Dfb	November 1991-November 1994	-	-	1
			Sweden	Dfb	November 1991-November 1994	-	-	1
			Sweden	Dfb	November 1991-November 1994	-	-	1
			Sweden	Dfb	November 1991-November 1994	-	12,100	1
			Sweden	Dfb	November 1991-November 1994	-	12,100	1

Study No.	Study Name	Location	Region	Climate Zone	Season	WIP (m3)	WIP (tonnes)	Waste Age (years)
50	Borjesson et al. 1998	Hogbytorp LF, Sweden	Sweden	Dfb	November 1991-November 1994	-	12,100	1
			Sweden	Dfb	November 1991-November 1994	-	12,100	1
			Sweden	Dfb	November 1991-November 1994	-	12,100	1
			Sweden	Dfb	November 1991-November 1994	-	12,100	1
			Sweden	Dfb	November 1991-November 1994	-	12,100	1
			Sweden	Dfb	November 1991-November 1994	-	12,100	1
			Sweden	Dfb	November 1991-November 1994	-	12,100	1
			Sweden	Dfb	November 1991-November 1994	-	12,100	1
			Sweden	Dfb	November 1991-November 1994	-	12,100	1
			Sweden	Dfb	November 1991-November 1994	-	12,100	1
			Sweden	Dfb	November 1991-November 1994	-	12,100	1
			Sweden	Dfb	November 1991-November 1994	-	12,100	1
			Sweden	Dfb	November 1991-November 1994	-	12,100	1
			Sweden	Dfb	November 1991-November 1994	-	12,100	1
			Sweden	Dfb	November 1991-November 1994	-	12,100	1
			Sweden	Dfb	November 1991-November 1994	-	12,100	1
			Sweden	Dfb	November 1991-November 1994	-	12,100	1
			Sweden	Dfb	November 1991-November 1994	-	12,100	1
			Sweden	Dfb	November 1991-November 1994	-	12,100	1
			Sweden	Dfb	November 1991-November 1994	-	12,100	1
51	Tassi et al. 2011[1]	Case Passerini LF, Tuscany, Italy	Italy	Csa	May-09	2,100,000	1,495,082	34
52	Gowing 2001	Waterloo LF, Canada	Canada	Dfb	June 1997-October 1997	-	-	1.75
		Cambridge LF, Canada	Canada	Dfb	June 1997-October 1997	-	-	4.5
		Stratford LF, Canada	Canada	Dfb	June 1997-October 1997	-	-	5.25
53	Sanderson 2001	Loma Los Colorados LF, Santiago, Chile	Chile	Csb	May-00	4,400,000	-	4
54	Ngwabie et al. 2019[6]	Mussaka Dumpsite, Cameroon	Cameroon	Am	May-15	3,308	-	3
		Mbellewa Dumpsite, Cameroon	Cameroon	Am	Aug-16	3,700	-	2.5
55,56,57	Abushammala et al. 2012, 2013, 2014	Air Hitam LF, Malaysia	Malaysia	Af	Oct-10	-	6,527,640	15
		Jeram LF, Malaysia	Malaysia	Af	September-December 2010	-	-	3
			Malaysia	Af	February-June 2010	-	-	3
		Sungai Sedu LF, Malaysia	Malaysia	Af	September-December 2010	-	1,613,300	7
			Malaysia	Af	February-June 2010	-	1,613,300	7

Study No.	Study Name	Location	Region	Climate Zone	Season	WIP (m3)	WIP (tonnes)	Waste Age (years)
58	El-Fadel et al. 2012	LF in Beirut, Lebanon	Lebanon	Csa	Jun-01	-	4,196,438	26
59	Maurice and Lagerkvist 2003[4]	Lulea, Sweden	Sweden	Dfc	February 1996-March 1997	-	-	-
			Sweden	Dfc	February 1996-March 1997	-	-	-
			Sweden	Dfc	February 1996-March 1997	-	-	-
			Sweden	Dfc	February 1996-March 1997	-	-	-
			Sweden	Dfc	February 1996-March 1997	-	-	-
			Sweden	Dfc	February 1996-March 1997	-	-	-
			Sweden	Dfc	February 1996-March 1997	-	-	-
			Sweden	Dfc	February 1996-March 1997	-	-	-
			Sweden	Dfc	February 1996-March 1997	-	-	-
			Sweden	Dfc	February 1996-March 1997	-	-	-
			Sweden	Dfc	February 1996-March 1997	-	-	-
		Kemi, Northern Finland	Finland	Dfc	Summer 1999-Spring 2000	-	-	-
			Finland	Dfc	Summer 1999-Spring 2000	-	-	-
			Finland	Dfc	Summer 1999-Spring 2000	-	-	-
60	Park and Shin 2001[6]	Sudokwon LF, Inchon City, South Korea	South Korea	Dwa	Winter-Summer 1997	3,200,000	2,278,220	5
			South Korea	Dwa	Winter-Summer 1997	3,200,000	2,278,220	5
			South Korea	Dwa	Winter-Summer 1997	3,200,000	2,278,220	5
			South Korea	Dwa	Winter-Summer 1997	3,200,000	2,278,220	5
			South Korea	Dwa	Winter-Summer 1997	3,200,000	2,278,220	5
			South Korea	Dwa	Winter-Summer 1997	3,200,000	2,278,220	5
			South Korea	Dwa	Winter-Summer 1997	3,200,000	2,278,220	5
			South Korea	Dwa	Winter-Summer 1997	3,200,000	2,278,220	5
			South Korea	Dwa	Winter-Summer 1997	3,200,000	2,278,220	5
61	Jha et al. 2008[1,4,6]	KDG LF, Chennai, India	India	Aw	December 2003-September 2004	1,315,230	-	24
		PGD LF, Chennai, India	India	Aw	December 2003-September 2004	704,000	-	17
	Chiemchaisriet al. 2007,	Nakornprathom LF, Thailand	Thailand	Aw	January-June 2002 and July-October 2002	48,000	-	3
			Thailand	Aw	January-June 2002 and July-October 2002	-	-	3
			Thailand	Aw	January-June 2002 and July-October 2002	-	-	3
			Thailand	Aw	January-June 2002 and July-October 2002	-	-	3
			Thailand	Aw	January-June 2002 and July-October 2002	-	-	3
			Thailand	Aw	January-June 2002 and July-October 2002	-	-	3
			Thailand	Aw	January-June 2002 and July-October 2002	-	-	3
			Thailand	Aw	January-June 2002 and July-October 2002	-	-	3

Study No.	Study Name	Location	Region	Climate Zone	Season	WIP (m3)	WIP (tonnes)	Waste Age (years)
62,63	Chiemchaisri & Visvanathan 2008[5,6]	Nonthaburi dumpsite, Thailand	Thailand	Aw	January-June 2002 and July-October 2002	-	-	10
			Thailand	Aw	January-June 2002 and July-October 2002	-	-	10
			Thailand	Aw	January-June 2002 and July-October 2002	-	-	10
			Thailand	Aw	January-June 2002 and July-October 2002	-	-	10
			Thailand	Aw	January-June 2002 and July-October 2002	-	-	10
			Thailand	Aw	January-June 2002 and July-October 2002	-	-	10
			Thailand	Aw	January-June 2002 and July-October 2002	-	-	10
			Thailand	Aw	January-June 2002 and July-October 2002	-	-	10
64	Chiemchaisriet et al. 2006[5]	Nonthaburi dumpsite, Thailand	Thailand	Aw	November 2002-March 2003 and April 2003-	-	-	10
			Thailand	Aw	November 2002-March 2003 and April 2003-July 2003	-	-	10
			Thailand	Aw	November 2002-March 2003 and April 2003-July 2003	-	-	10
			Thailand	Aw	November 2002-March 2003 and April 2003-July 2003	-	-	10
			Thailand	Aw	November 2002-March 2003 and April 2003-July 2003	-	-	10
			Thailand	Aw	November 2002-March 2003 and April 2003-July 2003	-	-	10
			Thailand	Aw	November 2002-March 2003 and April 2003-July 2003	-	-	10
			Thailand	Aw	November 2002-March 2003 and April 2003-July 2003	-	-	10
			Thailand	Aw	November 2002-March 2003 and April 2003-July 2003	-	-	10
			Thailand	Aw	November 2002-March 2003 and April 2003-July 2003	-	-	10
65	Pierini et al. 2018	Villa Dominico LF, Buenos Aires Argentina	Argentina	Cfa	July 2014-July 2015	-	469,490	28.5
66	Chanton et al. 2011[5]	Northwest Florida, USA (anonymous)	USA	Cfa	May and June 2011	-	-	-
			USA	Cfa	May and June 2011	-	-	-
			USA	Cfa	May and June 2011	-	-	-
			USA	Cfa	May and June 2011	-	-	-
			USA	Cfa	May and June 2011	-	-	-

Study No.	Study Name	Location	Region	Climate Zone	Season	WIP (m3)	WIP (tonnes)	Waste Age (years)
			USA	Cfa	May and June 2011	-	-	-
67	Wang-yao et al. 2006[5]	Pattaya LF, Thailand	Thailand	Aw	Dry and Wet Season 2006	-	350,000	4
			Thailand	Aw	Dry and Wet Season 2006	-	350,000	4
		Cha Am LF, Thailand	Thailand	Aw	Dry and Wet Season 2006	-	50,000	6
			Thailand	Aw	Dry and Wet Season 2006	-	50,000	6
		Hua Hin LF, Thailand	Thailand	Aw	Dry and Wet Season 2006	-	160,000	8
			Thailand	Aw	Dry and Wet Season 2006	-	160,000	8
		Nothaburi LF, Thailand	Thailand	Aw	Dry and Wet Season 2006	-	5,500,000	20
			Thailand	Aw	Dry and Wet Season 2006	-	5,500,000	20
		Nakhonpathom LF, Thailand	Thailand	Aw	Dry and Wet Season 2006	-	590,000	9
			Thailand	Aw	Dry and Wet Season 2006	-	590,000	9
		Samutprakan LF, Thailand	Thailand	Aw	Dry and Wet Season 2006	-	180,000	7
			Thailand	Aw	Dry and Wet Season 2006	-	180,000	7
		Rayong LF, Thailand	Thailand	Aw	Dry and Wet Season 2006	-	114,000	8
			Thailand	Aw	Dry and Wet Season 2006	-	114,000	8
68	Zhang et al. 2019*[5]	Nanjing LF, China	China	Cwa	April 2015-March 2016	-	-	7.5
			China	Cwa	April 2015-March 2017	-	-	7.5
			China	Cwa	April 2015-March 2018	-	-	7.5
			China	Cwa	April 2015-March 2019	-	-	7.5
			China	Cwa	April 2015-March 2020	-	-	7.5
			China	Cwa	April 2015-March 2021	-	-	7.5
69	Meyvantsdottir 2014[6]	Kirkjuferjuhjaleiga LF, Iceland	Iceland	Dfc	August 2012-March 2013	780,000	555,316	7
			Iceland	Dfc	August 2012-March 2014	780,000	555,316	7
			Iceland	Dfc	August 2012-March 2015	780,000	555,316	7
			Iceland	Dfc	August 2012-March 2016	780,000	555,316	7
		Fiflhol LF, Iceland	Iceland	Dfc	October 2013-February 2013	47,000	34,770	8
			Iceland	Dfc	October 2013-February 2014	-	34,770	8
			Iceland	Dfc	October 2013-February 2015	-	34,770	8
			Iceland	Dfc	October 2013-February 2016	-	34,770	8
			Iceland	Dfc	October 2013-February 2017	-	34,770	8
70	Popita et al. 2015	Cluj-Nopaca LF, Romania	Romania	Dfb	March-August 2011	-	107,550	38
			Romania	Dfb	March-August 2012	-	107,550	38
71	Wang et al. 2017*	Dongbu LF, China	China	Cfa	April 2012-April 2013	-	2,299,500	3
			China	Cfa	April 2012-April 2014	-	2,299,500	3
72	Einola et al. 2009	Aikkala LF, Finland	Finland	Dfb	October 2004-June 2006	-	200,000	18
73	Chu Chen et al. 2008[6]	Fu-Der-Kan LF, Taiwan	Taiwan	Cfa	October 1999-January 2006	8,473,000	6,032,299	14.5
			Taiwan	Cfa	October 1999-January 2007	8,473,000	6,032,299	14.5
			Taiwan	Cfa	October 1999-January 2008	8,473,000	6,032,299	14.5
			Taiwan	Cfa	October 1999-January 2009	8,473,000	6,032,299	14.5
			Taiwan	Cfa	October 1999-January 2010	8,473,000	6,032,299	14.5
			Taiwan	Cfa	October 1999-January 2011	8,473,000	6,032,299	14.5
			Taiwan	Cfa	October 1999-January 2012	8,473,000	6,032,299	14.5
			Taiwan	Cfa	October 1999-January 2013	8,473,000	6,032,299	1.5
			Taiwan	Cfa	October 1999-January 2014	8,473,000	6,032,299	1.5

Study No.	Study Name	Location	Region	Climate Zone	Season	WIP (m3)	WIP (tonnes)	Waste Age (years)
74	Akerman et al. 2007	Different LFs in UK	UK	Cfb	-	-	-	20
			UK	Cfb	-	-	-	14
			UK	Cfb	-	-	-	4
			UK	Cfb	-	-	-	4
			UK	Cfb	-	-	-	19.5
75	Maria Rosa et al. 2013	Merida LF, Mexico	Mexico	Aw	September 2004-April 2005	-	1,850,000	7.5
76	Ranchor 2012, Rachor et al. 2013[1,5]	Lower Saxony, Germany	Germany	Cfb	July 2008-January 2010	140000-180000	-	39.5
			Germany	Cfb	July 2008-January 2011	-	-	39.5
			Germany	Cfb	July 2008-January 2012	-	-	39.5
			Germany	Cfb	July 2008-January 2013	-	-	39.5
			Germany	Cfb	July 2008-January 2014	-	-	39.5
			Germany	Cfb	July 2008-January 2015	-	-	39.5
			Germany	Cfb	July 2008-January 2016	-	-	39.5
		Berlin, Germany	Germany	Cfb	July 2008-January 2017	-	-	53
			Germany	Cfb	July 2008-January 2018	-	-	53
			Germany	Cfb	July 2008-January 2019	-	-	53
			Germany	Cfb	July 2008-January 2020	-	-	53
			Germany	Cfb	July 2008-January 2021	-	-	53
			Germany	Cfb	July 2008-January 2022	-	-	53
		Saxony-Anhalt, Germany	Germany	Cfb	July 2008-January 2023	-	-	26
			Germany	Cfb	July 2008-January 2024	-	-	26
			Germany	Cfb	July 2008-January 2025	-	-	26
			Germany	Cfb	July 2008-January 2026	-	-	26
			Germany	Cfb	July 2008-January 2027	-	-	26
			Germany	Cfb	July 2008-January 2028	-	-	26
		Hamburg, Germany	Germany	Cfb	July 2008-January 2029	-	-	64
			Germany	Cfb	July 2008-January 2030	-	-	64
			Germany	Cfb	July 2008-January 2031	-	-	64
			Germany	Cfb	July 2008-January 2032	-	-	64
			Germany	Cfb	July 2008-January 2033	-	-	64
			Germany	Cfb	July 2008-January 2034	-	-	64
		Sckeswig-Holstein, Germany	Germany	Cfb	July 2008-January 2035	-	-	49
			Germany	Cfb	July 2008-January 2036	-	-	49
			Germany	Cfb	July 2008-January 2037	-	-	49
			Germany	Cfb	July 2008-January 2038	-	-	49
			Germany	Cfb	July 2008-January 2039	-	-	49
			Germany	Cfb	July 2008-January 2040	-	-	49
		Dandenong LF, Melbourne, Australia	Australia	Cfb	February 2013-July 2013	-	3,912,000	24

Study No.	Study Name	Location	Region	Climate Zone	Season	WIP (m3)	WIP (tonnes)	Waste Age (years)
77	Asadi et al. 2014[1]	Dandenong LF, Melbourne, Australia	Australia	Cfb	February 2013-July 2014	-	3,912,000	24
		Garden Isle LF, Adelaide, Australia	Australia	Bsk	February 2013-July 2015	-	-	-
			Australia	Bsk	February 2013-July 2016	-	-	-
78	Chakraborty et al. 2011[1]	Gazipur LF, Delhi, India	India	BSh	November 2008-December 2009	-	11,000,000	24.5
			India	BSh	November 2008-December 2010	-	11,000,000	24.5
			India	BSh	November 2008-December 2011	-	11,000,000	24.5
		Bhalswa LF, Delhi, India	India	BSh	November 2008-December 2012	-	9,200,000	16.5
			India	BSh	November 2008-December 2013	-	9,200,000	16.5
			India	BSh	November 2008-December 2014	-	9,200,000	16.5
		Okhla LF, Delhi, India	India	BSh	November 2008-December 2015	-	6,100,000	12.5
			India	BSh	November 2008-December 2016	-	6,100,000	12.5
			India	BSh	November 2008-December 2017	-	6,100,000	12.5
79	Maciel & Juca 2011	Muribeca LF, Recife, Brazil	Brazil	Am	September-December 2008	-	36,659	0.5
			Brazil	Am	September-December 2009	-	36,659	0.5
80	Schroth et al. 2012[1,5]	Lindenstock LF, Liestal, Switzerland	Switzerland	Dfb	Jul-08	3,200,000	2,278,220	59
			Switzerland	Dfb	Aug-08	3,200,000	2,278,220	59
			Switzerland	Dfb	Sep-08	3,200,000	2,278,220	59
			Switzerland	Dfb	Oct-08	3,200,000	2,278,220	59
			Switzerland	Dfb	Nov-08	3,200,000	2,278,220	59
81	Moreira and Candiani 2016[5]	CTR-Caieiras LF, Sao Paolo, Brazil	Brazil	Cwa	October-November 2010	-	3,786	1.12
82	Borjesson and Svensson 1997b[5]	Hagby LF, Uppper, Sweden	Sweden	Dfb	Oct-95	-	12,000	4
			Sweden	Dfb	Nov-95	-	12,000	4
			Sweden	Dfb	Dec-95	-	12,000	4
83	Gollapalli and Kota 2018[1]	Guwahati, India	India	Cwa	September 2015-August 2016	-	-	7.5
			India	Cwa	September 2015-August 2017	-	-	7.5
			India	Cwa	September 2015-August 2018	-	-	7.5
84	Rawat et al. 2008	6 LF sites across India	India	BSh	April 2002-May 2003	-	-	-
			India	BSh	April 2002-May 2004	-	-	-
			India	Aw	April 2002-May 2005	-	-	-
			India	Cwb	April 2002-May 2006	-	-	-
			India	BSh	April 2002-May 2007	-	-	-
			India	Aw	April 2002-May 2008	-	-	-
85	Pratt et al. 2013[6]	Taupo LF, North Island, New Zealand	New Zealand	Cfb	August 2010-March 2012	-	-	-
			New Zealand	Cfb	August 2010-March 2013	-	-	-
			New Zealand	Cfb	August 2010-March 2014	-	-	-
86	Mosher et al. 1996[1,5]	Nashua LF, New Hampshire, USA	USA	Dfb	Sep-94	-	-	25
			USA	Dfb	Sep-94	-	-	25
			China	Cfa	April 2007-January 2008	-	-	0.167
			China	Cfa	April 2007-January 2008	-	-	0.167
			China	Cfa	April 2007-January 2008	-	-	0.167
			China	Cfa	April 2007-January 2008	-	-	0.167
			China	Cfa	April 2007-January 2008	-	-	4

Appendix A, Table A-2
Surface Flux of Landfill Gas by Chemical Families from Literature.

Study No.	Study Name	Location	Region	Climate Zone	Season	WIP (m3)	WIP (tonnes)	Waste Age (years)
87	Zhang et al. 2009	Three landfill sites, Eastern China	China	Cfa	April 2007-January 2008	-	-	4
			China	Cfa	April 2007-January 2008	-	-	4
			China	Cfa	April 2007-January 2008	-	-	4
			China	Cfa	April 2007-January 2008	-	5,110,000	4
			China	Cfa	April 2007-January 2008	-	5,110,000	4
			China	Cfa	April 2007-January 2008	-	5,110,000	4
			China	Cfa	April 2007-January 2008	-	5,110,000	4
88	Zhang et al. 2008a	Tianziling MSW LF, Eastern China	China	Cfa	December 2006-June 2007	-	5,110,000	0.25
			China	Cfa	December 2006-June 2007	-	5,110,000	0.25
			China	Cfa	December 2006-June 2007	-	5,110,000	0.25
			China	Cfa	December 2006-June 2007	-	5,110,000	0.25
			China	Cfa	December 2006-June 2007	-	5,110,000	2.5
			China	Cfa	December 2006-June 2007	-	5,110,000	2.5
			China	Cfa	December 2006-June 2007	-	5,110,000	2.5
			China	Cfa	December 2006-June 2007	-	5,110,000	2.5
			China	Cfa	December 2006-June 2007	-	5,110,000	4
			China	Cfa	December 2006-June 2007	-	5,110,000	4
			China	Cfa	December 2006-June 2007	-	5,110,000	4
			China	Cfa	December 2006-June 2007	-	5,110,000	4
			China	Cfa	December 2006-June 2007	-	5,110,000	4
			China	Cfa	December 2006-June 2007	-	5,110,000	4
89	Long et al. 2018[1]	Fenghua LF, Nigbo, China	China	Cfa	2017	-	4,818,000	24
			China	Cfa	2018	-	4,818,000	24
		Xiangshan LF, Nigbo, China	China	Cfa	2019	-	3,832,500	21
			China	Cfa	2020	-	3,832,500	21
		Ninghai LF, Nigbo, China	China	Cfa	2021	-	1,642,500	15
			China	Cfa	2022	-	1,642,500	15
90	Kjeldsen et al. 1997[1,3,4]	Skellingsted Landfill, Denmark	Denmark	Dfb	Oct-94	-	420,000	23
			Denmark	Dfb	Oct-94	-	420,000	23
			Denmark	Dfb	Oct-94	-	420,000	23
			Denmark	Dfb	Oct-94	-	420,000	23
91	Sun 2013[1,3]	Melbourne A-ACAP LF site, Australia	Australia	Cfb	August 2009-August 2011	-	-	19
			Australia	Cfb	December 2009-July 2010	-	-	19
92	Nolasco et al. 2008	Lazareto LF, Tenerife, Canary Islands	Spain	Bwk	February-March 2002	-	-	-
93	Sanci et al. 2012[9]	Gualeguaychu LF, Argentina	South America	Cfa	2012	-	-	-
94	Abushammala et al. 2016[1]	Jeram LF, Malaysia	Malaysia	Af	September-December 2010	-	-	3
				Af	January-April 2010	-	-	3
95	Lima et al. 2002	Arico LF, Tenerife, Canary Islands	Spain	Bwk	May 1999-March 2000	-	-	-
96	Cardellini et al. 2003[3]	Palma Campania LF, Italy	Italy	Csa	-	-	-	-
97	Zhang et al. 2008b*,[6]	Tianziling LF, Eastern China, No subsurface irrigation	China	Cfa	Aug-06	-	5,110,000	0
			China	Cfa	Aug-06	-	5,110,000	0.020833333
			China	Cfa	Aug-06	-	5,110,000	1
			China	Cfa	Aug-06	-	5,110,000	2.5

Study No.	Study Name	Location	Region	Climate Zone	Season	WIP (m3)	WIP (tonnes)	Waste Age (years)
			China	Cfa	Aug-06	-	5,110,000	4
98	Borjesson and Svensson 1997c[1,5]	Hagby LF, Sweden	Sweden	Dfb	November 1991-November 1994	-	12,250	1
		Hokhuvuf LF, Sweden	Sweden	Dfb	November 1991-November 1994	-	60,000	24
		Hogbytrop LF, Sweden	Sweden	Dfb	November 1991-November 1994	-	100,000	8.5
			Sweden	Dfb	November 1991-November 1994	-	12,100	2.5
			Sweden	Dfb	November 1991-November 1994	-	12,100	16
99	Rinne et al. 2005*[1]	Ammassuo LF, Helsinki, Finland	Finland	Dfb	August-October 2003	-	5,600,000	16
			Finland	Dfb	August-October 2003	-	5,600,000	16
			Finland	Dfb	August-October 2003	-	5,600,000	16
100	Mandernack et al. 2000*[1,5]	Brea-Olinda LF, CA, USA	USA	Csa	June-December 1995	-	-	34
		UCI LF, CA, USA	USA	BSk	July-December 1995	-	-	34
		San Joaquin LF, CA, USA	USA	BSk	July-February 1995	-	-	34
		Houghton, WA, USA	USA	Csb	March-October 1995	-	-	34
101	Ishigaki et al. 2016[3,4]	Site A2, Japan	Japan	-	2008-2012	-	-	-
			Japan	-	2008-2012	-	-	-
			Japan	-	2008-2012	-	-	-
		Site B, Japan	Japan	-	2008-2012	-	-	-
			Japan	-	2008-2012	-	-	-
			Japan	-	2008-2012	-	-	-
		Site C, Japan	Japan	-	2008-2012	-	-	-
			Japan	-	2008-2012	-	-	-
			Japan	-	2008-2012	-	-	-
		Site D, Malaysia	Malaysia	-	2008-2012	-	-	-
			Japan	-	2008-2012	-	-	-

Study No.	Study Name	Location	Region	Climate Zone	Season	WIP (m3)	WIP (tonnes)	Waste Age (years)
		Site F, Japan	Japan	-	2008-2012	-	-	-
		Site G, Thailand	Thailand	-	2008-2012	-	-	-
		Site H, Sri Lanka	India	-	2008-2012	-	-	-
		Site I, Sri Lanka	India	-	2008-2012	-	-	-
102	Zhang et al. 2008c	Tianziling LF, Eastern China, Site A, No subsurface irrigation	China	Cfa	November 2006-June 2007	-	51,100,006	0.25
			China	Cfa	November 2006-June 2007	-	51,100,006	2.5
			China	Cfa	November 2006-June 2007	-	51,100,006	4
			China	Cfa	November 2006-June 2007	-	51,100,006	0.25
			China	Cfa	November 2006-June 2007	-	51,100,006	2.5
			China	Cfa	November 2006-June 2007	-	51,100,006	4
			China	Cfa	November 2006-June 2007	-	51,100,006	0.25
			China	Cfa	November 2006-June 2007	-	51,100,006	2.5
			China	Cfa	November 2006-June 2007	-	51,100,006	4
			China	Cfa	November 2006-June 2007	-	51,100,006	0.25
			China	Cfa	November 2006-June 2007	-	51,100,006	2.5
			China	Cfa	November 2006-June 2007	-	51,100,006	4
103	He et al. 2008	Landfill in China	China	Cfa	2007	-	-	-
104	Zhang et al. 2007	Landfill in China	China	Cfa	2006	-	-	-
105	Gallego et al. 2014[1,3]	Landfill in Spain	Spain	Csa	Jul-12	2,450,000	1,744,262	30
106	Archbold et al. 2012[1,3]	Belfast, Northern Ireland	UK	Cfb	March 2004-May 2004	-	-	9
						-	-	43
107	Majumdar et al. 2014	Dhapa LF site, India	India	Aw	-	-	-	-
108	Yesiller et al. 2017, Yesiller et al. 2018	Potrero Hills LF, CA, USA	USA	Csa	February 2014-April 2014	-	-	7.9
			USA	Csa	February 2014-April 2014	-	-	22
			USA	Csa	February 2014-April 2014	-	-	22
			USA	Csa	Aug-14	-	-	7.9
			USA	Csa	Aug-14	-	-	22
			USA	Csa	Aug-14	-	-	22

Study No.	Active Gas Extraction System?	Cover Type	Cover Depth (cm)	Cover Material Texture	Moisture Content (%) Mean	Moisture Content (%) Standard Deviation	Moisture Content (%) No. Measuements
1	N	Daily	15	Non-vegetated sandy clay cover	-	-	-
	N	Interim	45	Vegetated sandy clay and sandy loam	-	-	-
2	N	Interim	45	Vegetated sandy clay and sandy loam	9.2	-	-
	N	Interim	45	Vegetated sandy clay	9.2	-	-
	N	Daily	22.5	Non-vegetated sandy clay cover	9.2	-	-
	N	Interim	70	Vegetated sandy clay and sandy loam	9.2	-	-
3,4	N	Final	50	Dry, unvegetated sandy silt cover	9.625709861	4.835457631	13
	N	Final	50	Dry, unvegetated sandy silt cover	9.625709861	4.835457631	13
5	Y	Final	150	Dry, unvegetated sandy silt cover	7.4	-	-
	Y	Final	150	Fine clayey silt overlaying sandy silt	12.2	-	-
6	Y	Final	150	Silty clay soil, vegetated	-	-	-
	Y	Final	150	Silty clay soil, vegetated	-	-	-
	Y	Final	150	Silty clay soil, vegetated	-	-	-
	Y	Final	150	Silty clay soil, vegetated	-	-	-
	Y	Final	150	Silty clay soil, vegetated	-	-	-
7	Y	Final	150	Silty clay soil, vegetated	12.72727273	6.794957758	6
	Y	Final	150	Silty clay soil, vegetated	18.91608392	7.738292304	6
8,9	Y	Final	150	Silty clay soil, vegetated	19.26247757	6.625697501	21
	Y	Final	150	Silty clay soil, vegetated	21.73413543	6.287564655	25
10	N	-	-	-	-	-	-
	N	-	-	-	-	-	-
	N	-	-	-	-	-	-
	N	-	-	-	-	-	-
	N	-	-	-	-	-	-
11	Y	Final	-	Geomembrane and soil cover	-	-	-
	N	-	-	Soil cover	-	-	-
	N	Final	-	Geomembrane and soil cover	-	-	-
	N	-	-	Soil Cover	-	-	-
	N	Final	-	Geomembrane and soil cover	-	-	-
	Y	Final	-	Geomembrane and soil cover	-	-	-
12	Y	-	-	Clay cover, sand/LDPE, other soil covers	-	-	-
13	-	-	-	-	-	-	-
	-	-	-	-	-	-	-
14	-	-	-	-	-	-	-
15	-	-	-	-	-	-	-
	N	-	10	Loamy soil without vegetation	-	-	-

Appendix A, Table A-2
Surface Flux of Landfill Gas by Chemical Families from Literature.

Study No.	Active Gas Extraction System?	Cover Type	Cover Depth (cm)	Cover Material Texture	Moisture Content (%) Mean	Moisture Content (%) Standard Deviation	Moisture Content (%) No. Measuements
16	N	-	10	Loamy soil without vegetation	-	-	-
	N	-	10	Loamy soil without vegetation	-	-	-
17	N	Final	45	Sand/clay, small stones cover	-	-	-
	N	Final	45	Sand/clay, small stones cover	-	-	-
	N	Final	45	Sand/clay, small stones cover	-	-	-
	N	Final	45	Sand/clay, small stones cover	-	-	-
	N	Final	45	Sand/clay, small stones cover	-	-	-
	N	Final	45	Sand/clay, small stones cover	-	-	-
	N	Final	45	Sand/clay, small stones cover	-	-	-
	N	Final	45	Sand/clay, small stones cover	-	-	-
	N	Final	45	Sand/clay, small stones cover	-	-	-
	N	Final	45	Sand/clay, small stones cover	-	-	-
	N	Final	45	Sand/clay, small stones cover	-	-	-
	N	Final	45	Sand/clay, small stones cover	-	-	-
	N	Final	45	Sand/clay, small stones cover	-	-	-
	N	Final	45	Sand/clay, small stones cover	-	-	-
	N	Final	45	Sand/clay, small stones cover	-	-	-
	N	Final	45	Sand/clay, small stones cover	-	-	-
	N	Final	45	Sand/clay, small stones cover	-	-	-
	N	Final	45	Sand/clay, small stones cover	-	-	-
	N	Final	45	Sand/clay, small stones cover	-	-	-
	N	Final	45	Sand/clay, small stones cover	-	-	-
	N	Final	45	Sand/clay, small stones cover	-	-	-
	N	Final	45	Sand/clay, small stones cover	-	-	-
	N	Final	45	Sand/clay, small stones cover	-	-	-
	N	Final	45	Sand/clay, small stones cover	-	-	-
	N	Final	45	Sand/clay, small stones cover	-	-	-
	N	Final	45	Sand/clay, small stones cover	-	-	-
	N	Final	45	Sand/clay, small stones cover	-	-	-
	N	Final	45	Sand/clay, small stones cover	-	-	-
	N	Final	45	Sand/clay, small stones cover	-	-	-
	N	Final	45	Sandy loam[2] cover soil overlain by ashes, bark and glass wool	22	9.02	8
	N	Final	45	Sandy loam[2] cover soil overlain by ashes, bark and glass wool	12	8.4	8
	N	Final	45	Sandy loam[2] cover soil overlain by ashes, bark and glass wool	15	11.25	8
	N	Final	45	Sandy loam[2] cover soil overlain by ashes, bark and glass wool	18	8.82	8
	N	Final	45	Sandy loam[2] cover soil overlain by ashes, bark and glass wool	6.9	5.451	8
	N	Final	45	Sandy loam[2] cover soil overlain by ashes, bark and glass wool	12	7.08	8

Study No.	Active Gas Extraction System?	Cover Type	Cover Depth (cm)	Cover Material Texture	Moisture Content (%) Mean	Moisture Content (%) Standard Deviation	Moisture Content (%) No. Measuements
18	N	Final	45	Sandy loam[2] cover soil overlain by ashes, bark and glass wool	5	3.25	8
	N	Final	45	Sandy loam[2] cover soil overlain by ashes, bark and glass wool	6.8	2.244	8
	N	Final	45	Sandy loam[2] cover soil overlain by ashes, bark and glass wool	13	17.55	8
	N	Final	45	Sandy loam[2] cover soil overlain by ashes, bark and glass wool	12	8.88	8
	N	Final	45	Sandy loam[2] cover soil overlain by ashes, bark and glass wool	18	9.36	8
	N	Final	45	Sandy loam[2] cover soil overlain by ashes, bark and glass wool	22	0	8
	N	Final	45	Sandy loam[2] cover soil overlain by ashes, bark and glass wool	39	18.33	8
	N	Final	45	Sandy loam[2] cover soil overlain by ashes, bark and glass wool	14	8.12	8
	N	Final	45	Sandy loam[2] cover soil overlain by ashes, bark and glass wool	9.1	5.824	8
	N	Final	45	Sandy loam[2] cover soil overlain by ashes, bark and glass wool	5.9	4.661	8
	N	Final	45	Sandy loam[2] cover soil overlain by ashes, bark and glass wool	6.8	3.808	8
	N	Final	45	Sandy loam[2] cover soil overlain by ashes, bark and glass wool	5.8	5.568	8
19	Y	Final	40	Rough soil (including stones) and Sand[2]	14.16666667	0.929157324	2
	Y	Final	41	Rough soil (including stones) and Sand[2]	7.566666667	4.491720779	2
	Y	Final	42	Rough soil (including stones) and Sand[2]	14.16666667	0.929157324	2
20	N	Final	30	Sandy loam/Loamy soil	8.1	0	1
	N	Final	30	Sandy loam/Loamy soil	5.5	0	1
	N	Final	30	Sandy loam/Loamy soil	3.8	0	1
	N	Final	30	Sandy loam/Loamy soil	16	0	1
	N	Final	30	Sandy loam/Loamy soil	29.8	0	1
	N	Final	30	Sandy loam/Loamy soil	22.3	0	1
	N	Final	30	Sandy loam/Loamy soil	33.1	0	1
21	Y	Final	115	Sandy silt, Silty sand, and Coarse sand	8.4	3.577708764	9
	Y	Interim	40	Coarse sand	-	-	-
22	Y	Final	100	Compacted clay overlain by topsoil	14.52142857	2.017625903	7
	Y	Final	100	HDPE geomembrane, compacted clay, topsoil	10.558	0.757377053	5
	N	Final	100	Sand overlain by mould, vegetated	11.40875912	8.125937884	25
	N	Final	100	Sand overlain by mould, vegetated	11.40875912	8.125937884	25
	N	Final	100	Sand overlain by mould, vegetated	11.40875912	8.125937884	25

Appendix A, Table A-2
Surface Flux of Landfill Gas by Chemical Families from Literature.

Study No.	Active Gas Extraction System?	Cover Type	Cover Depth (cm)	Cover Material Texture	Moisture Content (%) Mean	Moisture Content (%) Standard Deviation	Moisture Content (%) No. Measuements
23,24	N	Final	100	Sand overlain by mould, vegetated	11.40875912	8.125937884	25
	N	Final	100	Sand overlain by mould, vegetated	11.40875912	8.125937884	25
	N	Final	100	Sand overlain by mould, vegetated	11.40875912	8.125937884	25
	N	Final	100	Sand overlain by mould, vegetated	11.40875912	8.125937884	25
	N	Final	100	Sand overlain by mould, vegetated	11.40875912	8.125937884	25
	N	Final	100	Sand overlain by mould, vegetated	11.40875912	8.125937884	25
	N	Final	100	Sand overlain by mould, vegetated	11.40875912	8.125937884	25
	N	Final	100	Sand overlain by mould, vegetated	11.40875912	8.125937884	25
	N	Final	100	Sand overlain by mould, vegetated	11.40875912	8.125937884	25
	N	Final	100	Sand overlain by mould, vegetated	11.40875912	8.125937884	25
	N	Final	100	Sand overlain by mould, vegetated	11.40875912	8.125937884	25
	N	Final	100	Sand overlain by mould, vegetated	11.40875912	8.125937884	25
	N	Final	100	Sand overlain by mould, vegetated	11.40875912	8.125937884	25
	N	Final	100	Sand overlain by mould, vegetated	11.40875912	8.125937884	25
	N	Final	100	Sand overlain by mould, vegetated	11.40875912	8.125937884	25
25	-	Final	50	Sandy loam ontop of clay	19.40135648	11.31442322	44
	-	Final	50	Sandy loam ontop of clay	19.40135648	11.31442322	44
	-	Final	50	Sandy loam ontop of clay	19.40135648	11.31442322	44
	-	Final	50	Sandy loam ontop of clay	19.40135648	11.31442322	44
26	-	-	-	-	-	-	-
27	-	-	-	-	-	-	-
	-	-	-	-	-	-	-
28	Y	-	100	Compacted Clay	16.6	-	1
	Y	-	100	Compacted Clay	16.6	-	1
	Y	-	100	Compacted Clay	16.6	-	1
	Y	-	100	Compacted Clay	-	-	-
	Y	-	100	Compacted Clay	-	-	-
	Y	-	100	Compacted Clay	-	-	-
	Y	-	100	Compacted Clay	-	-	-
	Y	-	100	Compacted Clay	-	-	-
	Y	-	100	Compacted Clay	-	-	-
	Y	-	100	Compacted Clay	14.6	-	3
	Y	-	100	Compacted Clay	14.6	-	3
	Y	-	100	Compacted Clay	14.6	-	3
	Y	-	100	Compacted Clay	22.5	-	3
	Y	-	100	Compacted Clay	22.5	-	3
	Y	-	100	Compacted Clay	22.5	-	3
29	-	-	-	No daily cover, geological or artificial liner	-	-	-
	-	-	-	Daily cover, geological and artificial liner	-	-	-
	-	-	-	Daily cover, geological and artificial liner	-	-	-
	Y	-	-	-	-	-	-
	Y	-	-	-	-	-	-
	Y	-	-	-	-	-	-
	Y	-	-	-	-	-	-

Study No.	Active Gas Extraction System?	Cover Type	Cover Depth (cm)	Cover Material Texture	Moisture Content (%) Mean	Moisture Content (%) Standard Deviation	Moisture Content (%) No. Measuements
30	Y	-	-	-	-	-	-
	Y	-	-	-	-	-	-
	N	-	-	-	-	-	-
	Y	-	-	-	-	-	-
	Y	-	-	-	-	-	-
	Y	-	-	-	-	-	-
	Y	-	-	-	-	-	-
	N	-	-	-	-	-	-
	Y	-	-	-	-	-	-
	Y	-	-	-	-	-	-
	Y	-	-	-	-	-	-
	Y	-	-	-	-	-	-
	Y	-	-	-	-	-	-
	Y	-	-	-	-	-	-
31	Y	-	-	-	-	-	-
	Y	-	50	Section 1: Final composite cover, substratum non-compacted clay, compacted clay, geotextile-geonet-geotextile drainage layer, top soil; Section 2A: 1mm HDPE geomembrane, 50 cm clay layer; Section 2B: 50 cm clay layer; Section 3: Active waste placement	-	-	-
	Y	-	-		-	-	-
	Y	-	50		-	-	-
	Y	-	-		-	-	-
	Y	-	50		-	-	-
	Y	-	-		-	-	-
	Y	-	50		-	-	-
	Y	-	50		-	-	-
	Y	-	-		-	-	-
	Y	-	-		-	-	-
	Y	-	50		-	-	-
	Y	-	50		-	-	-
	Y	-	-		-	-	-
32	Y	-	-	Zones 1 and 2: 1 mm HDPE geomembrane and 50 cm compacted clay; Zones 3 and 4: non-compacted + compacted clay layer	-	-	-
	Y	-	-		-	-	-
	Y	-	50		-	-	-
	Y	-	50		-	-	-
	Y	-	-		-	-	-
	Y	-	-		-	-	-
	Y	-	-		-	-	-
	Y	-	50		-	-	-
	Y	-	50		-	-	-

Appendix A, Table A-2
Surface Flux of Landfill Gas by Chemical Families from Literature.

Study No.	Active Gas Extraction System?	Cover Type	Cover Depth (cm)	Cover Material Texture	Moisture Content (%) Mean	Moisture Content (%) Standard Deviation	Moisture Content (%) No. Measuements
	Y	-	50		-	-	-
	Y	-	-		-	-	-
	Y	-	-		-	-	-
33	Y	-	50	Non-compacted + compacted clay layer	-	-	-
34	N	Final	-	Sandy loam, cracked, vegetated	-	-	-
	N	Final	-	-	-	-	-
	N	Final	-	-	-	-	-
35	N	-	130	Loam, sandy loam	23.09	4.02	15
	N	-	140	Loam, clay loam	22.72	3.98	15
	N	-	180	Loam	22.16	2.25	15
36	Y	All	-	-	-	-	-
	Y	All	-	-	-	-	-
	Y	All	-	-	-	-	-
	Y	All	-	-	-	-	-
	Y	All	-	-	-	-	-
	N	All	-	-	-	-	-
	N	All	-	-	-	-	-
	N	All	-	-	-	-	-
	N	All	-	-	-	-	-
	N	All	-	-	-	-	-
	Y	All	-	-	-	-	-
	N	All	-	-	-	-	-
	Y	All	-	-	-	-	-
	Y	All	-	-	-	-	-
	Y	All	-	-	-	-	-
	Y	All	-	-	-	-	-
	N	All	-	-	-	-	-
	N	All	-	-	-	-	-
	N	All	-	-	-	-	-
	N	All	-	-	-	-	-
	N	All	-	-	-	-	-
	N	All	-	-	-	-	-
37	Y	Final	-	-	-	-	-
	Y	Final	-	-	-	-	-
	Y	Final	-	-	-	-	-
	Y	Final	-	-	-	-	-
	Y	Final	-	-	-	-	-
	Y	Final	-	-	-	-	-
	Y	Final	-	-	-	-	-
	Y	Final	-	-	-	-	-
	Y	Final	-	-	-	-	-
	Y	Final	-	-	-	-	-

Study No.	Active Gas Extraction System?	Cover Type	Cover Depth (cm)	Cover Material Texture	Moisture Content (%) Mean	Moisture Content (%) Standard Deviation	Moisture Content (%) No. Measuements
	Y	Final	-	-	-	-	-
38	Y	Interim	10	Gravelly clayey sand (SC), Sparse-No vegetation	9	0	1
	Y	Final	10	Gravelly clayey sand (SC), Sparse-No vegetation	6	0	1
	N	-	35	Gravelly clayey sandy silt (SC/CL), Sparse-No vegetation	24	1.414213562	2
	N	-	35	-	23	2.828427125	2
	N	Final	15	Gravelly silty sand (SW), Fully vegetated	3.5	0.707106781	2
	N	-	37.5	Clayey silty sand (SC/CL), Fully vegetated	20.5	9.192388155	2
39	N	Interim	75	Sandy clay overlain by fine sandy loam, vegetated	6.536964981	2.80	3
	N	Interim	75	Sandy clay overlain by fine sandy loam, vegetated	5.60311284	2.33	3
	N	Interim	75	Sandy clay overlain by fine sandy loam, vegetated	14.94163424	2.33	3
	N	Interim	75	Sandy clay overlain by fine sandy loam, vegetated	48.09338521	38.29	3
	N	Interim	75	Sandy clay overlain by fine sandy loam, vegetated	-	-	3
	N	Interim	75	Sandy clay overlain by fine sandy loam, vegetated	45.75875486	35.49	3
	N	Interim	75	Sandy clay overlain by fine sandy loam, vegetated	12.14007782	2.80	3
	N	Interim	75	Sandy clay overlain by fine sandy loam, vegetated	18.6770428	1.87	3
	N	Interim	75	Sandy clay overlain by fine sandy loam, vegetated	14.47470817	2.33	3
	N	Interim	75	Sandy clay overlain by fine sandy loam, vegetated	22.41245136	1.87	3
	N	Interim	75	Sandy clay overlain by fine sandy loam, vegetated	25.21400778	3.74	3
	N	Interim	75	Sandy clay overlain by fine sandy loam, vegetated	19.61089494	1.87	3
	N	Interim	75	Sandy clay overlain by fine sandy loam, vegetated	23.3463035	4.67	3
	N	Interim	75	Sandy clay overlain by fine sandy loam, vegetated	25.21400778	2.80	3
	N	Interim	75	Sandy clay overlain by fine sandy loam, vegetated	24.28015564	1.87	3
40	Y	Daily	30	Sand	8	8	-
	Y	Daily	30	Sand	8	8	-
	Y	Daily	30	Sand	8	8	-
	Y	Daily	30	Sand	17	12	-
	Y	Interim	50	Sandy Loam	1	3	-
	Y	Interim	50	Sandy Loam	18	34	-
	Y	Final	250	Sandy Loam	19	-	-
	Y	Final	250	Sandy Loam	11	7	-
	Y	Daily	30	Sand	11	6	-
	Y	Daily	30	Sand	5	-	-
	Y	Interim	75	Sandy Loam	-	-	-
	Y	Interim	75	Sandy Loam	3	1	-
	Y	Final	270	Sandy Loam	3	-	-
	Y	Final	270	Sandy Loam	5	5	-
41	N	Final	110	Silt and peat soil	-	-	-
	N	Final	110	Silt and peat soil	-	-	-
	N	Final	110	Silt and peat soil	-	-	-
	N	Final	109	Clay and mulch/top soil	54.3	0	1
	N	Final	109	Clay and mulch/top soil	55.4	0	1
	N	Final	109	Clay and mulch/top soil	47.8	0	1
	N	Final	109	Clay and mulch/top soil	46.3	0	1
	N	Final	109	Clay and mulch/top soil	58.5	0	1

Study No.	Active Gas Extraction System?	Cover Type	Cover Depth (cm)	Cover Material Texture	Moisture Content (%) Mean	Moisture Content (%) Standard Deviation	Moisture Content (%) No. Measuements
42	N	Final	109	Clay and mulch/top soil	51.6	0	1
	N	Final	109	Clay and mulch/top soil	48.6	0	1
	N	Final	109	Clay and mulch/top soil	35.7	0	1
	N	Final	109	Clay and mulch/top soil	29.6	0	1
	N	Final	109	Clay and mulch/top soil	13.7	0	1
	N	Final	109	Clay and mulch/top soil	15.2	0	1
	N	Final	109	Clay and mulch/top soil	42.5	0	1
	N	Final	109	Clay and mulch/top soil	47.5	0	1
	N	Final	109	Clay and mulch/top soil	44.8	0	1
	N	Final	100	Clay soil	20.5	0	1
	N	Final	100	Clay soil	20.9	0	1
	N	Final	100	Clay soil	21.3	0	1
	N	Final	100	Clay soil	15.2	0	1
	N	Final	100	Clay soil	24.3	0	1
	N	Final	100	Clay soil	12.2	0	1
	N	Final	100	Clay soil	20.5	0	1
	N	Final	100	Clay soil	13.7	0	1
	N	Final	100	Clay soil	15.2	0	1
	N	Final	100	Clay soil	11.4	0	1
	N	Final	100	Clay soil	9.9	0	1
	N	Final	100	Clay soil	23.5	0	1
	N	Final	100	Clay soil	25.1	0	1
	N	Final	100	Clay soil	22.0	0	1
43	Y	-	-	Fine sandy, sparsely vegetated, geomembrane HDPE	10	0.666666667	5
	Y	-	-	Fine sandy, sparsely vegetated, geomembrane HDPE	15.55555556	0.666666667	5
	Y	-	-	Fine sandy, sparsely vegetated, geomembrane HDPE	12	0.444444444	5
	Y	-	-	Fine sandy, sparsely vegetated, geomembrane HDPE	13.77777778	0.444444444	5
	Y	-	-	Fine sandy, sparsely vegetated, geomembrane HDPE	12.44444444	0.444444444	5
	Y	-	-	Fine sandy, sparsely vegetated, geomembrane HDPE	12	0.222222222	5
	N	-	-	Coarse Sandy, no vegetation	10.66666667	0.666666667	5
	N	-	-	Coarse Sandy, no vegetation	15.11111111	0.444444444	5
	N	-	-	Coarse Sandy, no vegetation	10	0.444444444	5
	N	-	-	Coarse Sandy, no vegetation	9.333333333	0.444444444	5
	N	-	-	Coarse Sandy, no vegetation	7.111111111	0.444444444	5
	N	-	-	Coarse Sandy, no vegetation	6.222222222	0.444444444	5
	Y	-	-	Coarse Sandy, no vegetation	14.07166124	0.260586319	5
	Y	-	-	Coarse Sandy, no vegetation	20.06514658	0.521172638	5
	Y	-	-	Coarse Sandy, no vegetation	10.68403909	0.260586319	5
	Y	-	-	Coarse Sandy, no vegetation	11.59609121	0.521172638	5
	Y	-	-	Coarse Sandy, no vegetation	10.16286645	0.260586319	5
	Y	-	-	Coarse Sandy, no vegetation	14.07166124	0.260586319	5
44	N	Interim	45	Silty clay+stones and rubble	-	-	-
	N	Interim	45	Silty clay+stones and rubble	-	-	-
	N	Interim	45	Silty clay+stones and rubble	-	-	-

Study No.	Active Gas Extraction System?	Cover Type	Cover Depth (cm)	Cover Material Texture	Moisture Content (%) Mean	Moisture Content (%) Standard Deviation	Moisture Content (%) No. Measuements
44	N	Interim	45	Silty clay+stones and rubble	-	-	-
	N	Interim	45	Silty clay+stones and rubble	-	-	-
	N	Interim	45	Silty clay+stones and rubble	-	-	-
45	N	Interim	15	Compacted sandy clay	-	-	-
46	-	-	-	-	-	-	-
	-	-	-	-	-	-	-
	-	-	-	-	-	-	-
47	N	All	62.5	S1 test sites: lower sandy clay and an upper fine sandy loam; S4 test sites: compacted sandy clay	-	-	-
	N	Interim	75		-	-	-
	N	Interim	75		-	-	-
48	N	Interim	-	Shredder residue cell, NO COVER SOILS	-	-	-
	N	Interim	-		-	-	-
	N	Interim	-		-	-	-
	N	Interim	-		-	-	-
	N	Interim	-		-	-	-
49	Y	-	75	Loamy Sand	12	-	3
	Y	-	75	Loamy Sand	-	-	-
	Y	-	75	Loamy Sand	10	-	3
	Y	-	75	Loamy Sand	12	-	3
	Y	-	75	Loamy Sand	-	-	-
	Y	-	75	Loamy Sand	10	-	3
	Y	-	75	Loamy Sand	-	-	-
	N	-	55	Sandy Loam	13	-	3
	N	-	55	Sandy Loam	15	-	3
	N	-	55	Sandy Loam	-	-	-
	N	-	55	Sandy Loam	13	-	3
	N	-	55	Sandy Loam	15	-	3
	N	-	55	Sandy Loam	-	-	-
	Y	-	40	A Loam, with old sewage sludge as cover material	-	-	-
	Y	-	40	A Loam, with old sewage sludge as cover material	-	-	-
	Y	-	40	A Loam, with old sewage sludge as cover material	-	-	-
	Y	-	40	A Loam, with old sewage sludge as cover material	-	-	-
	Y	-	40	A Loam, with old sewage sludge as cover material	-	-	-
	Y	-	40	A Loam, with old sewage sludge as cover material	-	-	-
	Y	-	40	A Loam, with old sewage sludge as cover material	-	-	-
	N	-	65	Mineral soil, Sandy Loam	-	-	-
	N	-	65	Mineral soil, Sandy Loam	-	-	-
	N	-	65	Mineral soil, Sandy Loam	-	-	-
	N	-	65	Mineral soil, Sandy Loam	-	-	-
	N	-	65	Mineral soil, Sandy Loam	-	-	-
	N	-	65	Mineral soil, Sandy Loam	-	-	-
	N	-	100	A Loam, with fresh sewage sludge as cover material	-	-	-
	N	-	100	A Loam, with fresh sewage sludge as cover material	-	-	-

Study No.	Active Gas Extraction System?	Cover Type	Cover Depth (cm)	Cover Material Texture	Moisture Content (%) Mean	Moisture Content (%) Standard Deviation	Moisture Content (%) No. Measuements
50	N	-	100	A Loam, with fresh sewage sludge as cover material	-	-	-
	N	-	100	A Loam, with fresh sewage sludge as cover material	-	-	-
	N	-	100	A Loam, with fresh sewage sludge as cover material	-	-	-
	N	-	100	A Loam, with fresh sewage sludge as cover material	-	-	-
	N	-	100	A Loam, with fresh sewage sludge as cover material	-	-	-
	N	-	100	A Loam, with fresh sewage sludge as cover material	-	-	-
	N	-	100	A Loam, with fresh sewage sludge as cover material	-	-	-
	N	-	100	A Loam, with fresh sewage sludge as cover material	-	-	-
	N	-	100	A Loam, with fresh sewage sludge as cover material	-	-	-
	N	-	100	A Loam, with fresh sewage sludge as cover material mixed with clay	-	-	-
	N	-	100	A Loam, with fresh sewage sludge as cover material mixed with clay	-	-	-
	N	-	100	A Loam, with fresh sewage sludge as cover material mixed with clay	-	-	-
	N	-	100	A Loam, with fresh sewage sludge as cover material mixed with clay	-	-	-
	N	-	100	A Loam, with fresh sewage sludge as cover material mixed with clay	-	-	-
	N	-	100	A Loam, with fresh sewage sludge as cover material mixed with clay	-	-	-
	N	-	100	A Loam, with fresh sewage sludge as cover material mixed with clay	-	-	-
	N	-	100	A Loam, with fresh sewage sludge as cover material mixed with clay	-	-	-
	N	-	100	A Loam, with fresh sewage sludge as cover material mixed with clay	-	-	-
	N	-	100	A Loam, with fresh sewage sludge as cover material mixed with clay	-	-	-
	N	-	100	A Loam, with fresh sewage sludge as cover material mixed with clay	-	-	-
51	Y	Interim	100	Clay rich cover	-	-	-
52	Y	Interim	-	Vegetated	-	-	-
	Y	Interim	-	Vegetated	-	-	-
	N	Final	-	Compacted clay, vegetated	-	-	-
53	Y	All	15-40	Soils unspecified	-	-	-
54	N	-	-	Soils unspecified, open dumpsite	-	-	-
	N	-	-	Soils unspecified, open dumpsite	-	-	-
55,56,57	N	Interim	30-40	Poorly graded sand, some vegetation	16.5	4.123105626	4
	N	-	-	Soils unspecified, borderline open dumpsite	-	-	-
	N	-	-	Soils unspecified, borderline open dumpsite	-	-	-
	N	Interim	15-30	Poorly graded sand, some vegetation	-	-	-
	N	Interim	15-30	Poorly graded sand, some vegetation	-	-	-

Study No.	Active Gas Extraction System?	Cover Type	Cover Depth (cm)	Cover Material Texture	Moisture Content (%) Mean	Moisture Content (%) Standard Deviation	Moisture Content (%) No. Measuements
58	N	-	-	Soils unspecified	-	-	-
59	N	-	120	Silty soil	-	-	-
	N	-	120	Silty soil	-	-	-
	N	-	120	Silty soil	-	-	-
	N	-	120	Silty soil	-	-	-
	N	-	120	Silty soil	-	-	-
	N	-	120	Silty soil	-	-	-
	N	-	120	Silty soil	-	-	-
	N	-	120	Silty soil	-	-	-
	N	-	120	Silty soil	-	-	-
	N	-	120	Silty soil	-	-	-
	N	-	120	Silty soil	-	-	-
	N	-	-	-	-	-	-
	N	-	-	-	-	-	-
	N	-	-	-	-	-	-
60	Y	Interim	60	Sandy Loam[2]	-	-	-
	Y	Interim	60	Sandy Loam[2]	-	-	-
	Y	Interim	60	Sandy Loam[2]	-	-	-
	Y	Interim	60	Sandy Loam[2]	-	-	-
	Y	Interim	60	Sandy Loam[2]	-	-	-
	Y	Interim	60	Sandy Loam[2]	-	-	-
	Y	Interim	60	Sandy Loam[2]	-	-	-
	Y	Interim	60	Sandy Loam[2]	-	-	-
61	N	Interim	-	Clayey soil	-	-	-
	N	Interim	-	Silty clay soil	-	-	-
	N	Final	-	Clay[2]	25.52123552	8.254064132	9
	N	Final	-	Clay[2]	25.52123552	8.254064132	9
	N	Final	-	Clay[2]	25.52123552	8.254064132	9
	N	Final	-	Clay[2]	25.52123552	8.254064132	9
	N	Final	-	Clay[2]	30.42471042	8.103349403	9
	N	Final	-	Clay[2]	30.42471042	8.103349403	9
	N	Final	-	Clay[2]	30.42471042	8.103349403	9
	N	Final	-	Clay[2]	30.42471042	8.103349403	9

Study No.	Active Gas Extraction System?	Cover Type	Cover Depth (cm)	Cover Material Texture	Moisture Content (%) Mean	Moisture Content (%) Standard Deviation	Moisture Content (%) No. Measuements
62,63	-	-	-	-	-	-	-
	-	-	-	-	-	-	-
	-	-	-	-	-	-	-
	-	-	-	-	-	-	-
	-	-	-	-	-	-	-
	-	-	-	-	-	-	-
	-	-	-	-	-	-	-
	-	-	-	-	-	-	-
64	N	-	55	Clay	23.97413061	3.872061191	14
	N	-	55	-	24.69631477	5.662851377	13
	N	-	55	Sandy Loam+Water	9.221890329	1.912427298	14
	N	-	55	-	11.7090351	2.423363368	10
	N	-	55	Sandy Loam+Leachate	9.221890329	1.912427298	14
	N	-	55	-	11.7090351	2.423363368	10
	N	-	55	Sandy Loam+Vegatation+Water	9.221890329	1.912427298	14
	N	-	55	-	11.7090351	2.423363368	10
	N	-	55	Sandy Loam+Vegatation+Leachate	9.221890329	1.912427298	14
	N	-	55	-	11.7090351	2.423363368	10
65	N	Final	60	Compacted Clay loam	-	-	-
66	Y	Final	145	Compacted clay, geomembrane (LLDPE), sandy loam, vegetated	14.5	9.192388155	2
	Y	Final	145	Compacted clay, geomembrane (LLDPE), sandy loam, vegetated	14.5	9.192388155	2
	Y	Final	145	Compacted clay, NO geomembrane (LLDPE), sandy loam, vegetated	14.5	9.192388155	2
	N	Interim	37.5	Sandy loam soil, no vegetation	14.5	9.192388155	2
	N	Interim	37.5	Sandy loam soil, no vegetation	14.5	9.192388155	2

Study No.	Active Gas Extraction System?	Cover Type	Cover Depth (cm)	Cover Material Texture	Moisture Content (%) Mean	Moisture Content (%) Standard Deviation	Moisture Content (%) No. Measuements
	N	Interim	37.5	Sandy loam soil, no vegetation	14.5	9.192388155	2
67	N	-	-	-	-	-	-
	N	-	-	-	-	-	-
	N	-	-	-	-	-	-
	N	-	-	-	-	-	-
	N	-	-	-	-	-	-
	N	-	-	-	-	-	-
	N	-	-	-	-	-	-
	N	-	-	-	-	-	-
	N	-	-	-	-	-	-
	N	-	-	-	-	-	-
	N	-	-	-	-	-	-
	N	-	-	-	-	-	-
	N	-	-	-	-	-	-
	N	-	-	-	-	-	-
68	N	-	-	-	-	-	-
	N	-	-	-	-	-	-
	N	-	-	-	-	-	-
	N	-	-	-	-	-	-
	N	-	-	-	-	-	-
	N	-	-	-	-	-	-
69	N	Final	100	Final: gravel, sand, local topsoil (histic andosol)	-	-	-
	N	Final	100	Final: gravel, sand, local topsoil (histic andosol)	-	-	-
	N	Final	100	Final: gravel, sand, local topsoil (histic andosol)	-	-	-
	N	Final	100	Final: gravel, sand, local topsoil (histic andosol)	-	-	-
	N	Final	110	Final: woodchips and soil (vitrisol/histol soils)	-	-	-
	N	Final	110	Final: woodchips and soil (vitrisol/histol soils)	-	-	-
	N	Final	110	Final: woodchips and soil (vitrisol/histol soils)	-	-	-
	N	Final	110	Final: woodchips and soil (vitrisol/histol soils)	-	-	-
	N	Final	110	Final: woodchips and soil (vitrisol/histol soils)	-	-	-
70	N	Daily	-	No cover (daily at best)	-	-	-
	N	Daily	-	No cover (daily at best)	-	-	-
71	N	Final	-	HDPE geomembrane, No cover soil	-	-	-
	N	Daily	-	No soil cover	-	-	-
72	Y	Final	160	clay, drainage layer, mineral soil	-	-	-
73	Y	Final	275	Waste LF soil and loam-clay loam soil with vegetation	31.1	1.7	4
	Y	Final	275	Waste LF soil and loam-clay loam soil with vegetation	29.6	1.8	4
	Y	Final	275	Waste LF soil and loam-clay loam soil with vegetation	19.6	2.2	4
	Y	Final	275	Waste LF soil and loam-clay loam soil with vegetation	24	0.3	4
	Y	Final	275	Waste LF soil and loam-clay loam soil with vegetation	29.3	2.2	4
	Y	Final	275	Waste LF soil and loam-clay loam soil with vegetation	26.5	3	4
	Y	Final	275	Waste LF soil and loam-clay loam soil with vegetation	17.5	1	4
	Y	Final	275	Waste LF soil and loam-clay loam soil with vegetation	33.6	2.9	4
	Y	Final	275	Waste LF soil and loam-clay loam soil with vegetation	22.5	2	4

Study No.	Active Gas Extraction System?	Cover Type	Cover Depth (cm)	Cover Material Texture	Moisture Content (%) Mean	Moisture Content (%) Standard Deviation	Moisture Content (%) No. Measuements
74	Y	-	100	Clay and geomembrane	-	-	-
	Y	-	100-200	Compacted soil + vegetation	-	-	-
	Y	-	130	Bottom ashes and clay or limestone	-	-	-
	Y	-	50-70	Clay	-	-	-
	Y	-	50-100	Clay and soil	-	-	-
75	N	Final	15	Non-consolidated calcite soil (sahcab), no geomembrane	-	-	-
76	-	Final	110	organic rich cultivation layer, cover soil of variable properties,	-	-	-
	-	Final	110	organic rich cultivation layer, cover soil of variable properties, vegetated	-	-	-
	-	Final	110	organic rich cultivation layer, cover soil of variable properties, vegetated	-	-	-
	-	Final	110	organic rich cultivation layer, cover soil of variable properties, vegetated	-	-	-
	-	Final	110	organic rich cultivation layer, cover soil of variable properties, vegetated	-	-	-
	-	Final	110	organic rich cultivation layer, cover soil of variable properties, vegetated	-	-	-
	-	Final	110	organic rich cultivation layer, cover soil of variable properties, vegetated	-	-	-
	-	Final	50	Sandy soil	-	-	-
	-	Final	50	Sandy soil	-	-	-
	-	Final	50	Sandy soil	-	-	-
	-	Final	50	Sandy soil	-	-	-
	-	Final	50	Sandy soil	-	-	-
	-	Final	50	Sandy soil	-	-	-
	-	Final	50	Sandy soil	-	-	-
	-	Final	50	Sandy soil	-	-	-
	-	Final	50	Sandy soil	-	-	-
	-	Final	50	Sandy soil	-	-	-
	-	Final	120	Mostly sand and silt, some clay	-	-	-
	-	Final	120	Mostly sand and silt, some clay	-	-	-
	-	Final	120	Mostly sand and silt, some clay	-	-	-
	-	Final	120	Mostly sand and silt, some clay	-	-	-
	-	Final	120	Mostly sand and silt, some clay	-	-	-
	-	Final	120	Mostly sand and silt, some clay	-	-	-
	-	Final	120	Sandy soil	-	-	-
	-	Final	120	Sandy soil	-	-	-
	-	Final	120	Sandy soil	-	-	-
	-	Final	120	Sandy soil	-	-	-
	-	Final	120	Sandy soil	-	-	-
	-	Final	120	Sandy soil	-	-	-
	-	Final	115	Sandy to loamy soil	-	-	-
	-	Final	115	Sandy to loamy soil	-	-	-
	-	Final	115	Sandy to loamy soil	-	-	-
	-	Final	115	Sandy to loamy soil	-	-	-
	-	Final	115	Sandy to loamy soil	-	-	-
	-	Final	115	Sandy to loamy soil	-	-	-
	Y	Final	100	Compacted clay, sandy clay, top soil	30.26	-	-

Study No.	Active Gas Extraction System?	Cover Type	Cover Depth (cm)	Cover Material Texture	Moisture Content (%) Mean	Moisture Content (%) Standard Deviation	Moisture Content (%) No. Measuements
77	Y	Final	100	Compacted clay, sandy clay, top soil	21.1	-	-
	N	Final	150	Compacted clay, sandy clay and top soil	27.88	-	-
	N	Final	150	Compacted clay, sandy clay and top soil	20.27	-	-
78	N	-	-	-	-	-	-
	N	-	-	-	-	-	-
	N	-	-	-	-	-	-
	N	-	-	-	-	-	-
	N	-	-	-	-	-	-
	N	-	-	-	-	-	-
	N	-	-	-	-	-	-
	N	-	-	-	-	-	-
	N	-	-	-	-	-	-
79	Y	Final	50	Compacted soil (sandy clay), geotextile, gravel	16.9	0.6	-
	Y	Final	67.5	Compacted soil (sandyclay)	14.9	1	-
80	N	Final	225	Sily loam, clay lenses, gravel and boulders	0.27	0.056568542	6-^8
	N	Final	225	Sily loam, clay lenses, gravel and boulders	0.25	0.04472136	6
	N	Final	225	Sily loam, clay lenses, gravel and boulders	0.22	0.025298221	6
	N	Final	225	Sily loam, clay lenses, gravel and boulders	0.32	0.035777088	6
	N	Final	225	Sily loam, clay lenses, gravel and boulders	0.32	0.050990195	6
81	N	Interim	50	Silty soil cover	-	-	-
82	Y	-	60	Sandy loam soil, some vegetation	12.25	4.87903679	2
	N	-	60	-	-	-	-
	Y	-	60	-	-	-	-
83	N	-	-	-	-	-	-
	N	-	-	-	-	-	-
	N	-	-	-	-	-	-
84	-	-	-	-	-	-	-
	-	-	-	-	-	-	-
	-	-	-	-	-	-	-
	-	-	-	-	-	-	-
	-	-	-	-	-	-	-
	-	-	-	-	-	-	-
85	-	Final	100	Pumic cover (volcanic) soil	-	-	-
	-	Final	100	Pumic cover (volcanic) soil	-	-	-
	-	Final	100	Pumic cover (volcanic) soil	-	-	-
86	N	-	150	Sandy-clay loam, no membrane cover	-	-	-
	N	-	150	Sandy-clay loam, no membrane cover	-	-	-
	N	-	-	Silty clay[2]	-	-	-
	N	-	-	Silty clay[2]	-	-	-
	N	-	-	Silty clay[2]	-	-	-
	N	-	-	Silty clay[2]	-	-	-
	N	-	-	Silty clay loam[2]	-	-	-

Appendix A, Table A-2
Surface Flux of Landfill Gas by Chemical Families from Literature.

Study No.	Active Gas Extraction System?	Cover Type	Cover Depth (cm)	Cover Material Texture	Moisture Content (%) Mean	Moisture Content (%) Standard Deviation	Moisture Content (%) No. Measuements
87	N	-	-	Silty clay loam[2]	-	-	-
	N	-	-	Silty clay loam[2]	-	-	-
	N	-	-	Silty clay loam[2]	-	-	-
	Y	-	90	Silt loam[2]	-	-	-
	Y	-	90	Silt loam[2]	-	-	-
	Y	-	90	Silt loam[2]	-	-	-
	Y	-	90	Silt loam[2]	-	-	-
88	Y	-	90	Loam-silt loam[2]	17.50588235	0.465330101	5
	Y	-	90	Loam-silt loam[2]	16.90980392	0.513111443	5
	Y	-	90	Loam-silt loam[2]	19.57894737	1.660190557	5
	Y	-	90	Loam-silt loam[2]	24.44444444	3.692955055	5
	Y	-	90	Loam-silt loam[2]	17.50588235	0.465330101	5
	Y	-	90	Loam-silt loam[2]	16.90980392	0.513111443	5
	Y	-	90	Loam-silt loam[2]	19.57894737	1.660190557	5
	Y	-	90	Loam-silt loam[2]	24.44444444	3.692955055	5
	Y	-	90	Loam-silt loam[2]	17.50588235	0.465330101	5
	Y	-	90	Loam-silt loam[2]	16.90980392	0.513111443	5
	Y	-	90	Loam-silt loam[2]	19.57894737	1.660190557	5
	Y	-	90	Loam-silt loam[2]	24.44444444	3.692955055	5
89	Y	Final	125	C&D waste+clay soil	-	-	-
	Y	Final	125	C&D waste+clay soil	-	-	-
	Y	Interim	-	-	-	-	-
	Y	Interim	-	-	-	-	-
	Y	Interim	-	-	-	-	-
	Y	Interim	-	-	-	-	-
90	N	Final	80	Clay soil layer	-	-	-
	N	Final	80	Clay soil layer	-	-	-
	N	Final	80	Clay soil layer	-	-	-
	N	Final	80	Clay soil layer	-	-	-
91	Y	Final	100	Sandy Loam/Loam soil layer	0	0	12
	N	Final	100	Sandy Loam/Loam soil layer	0	0	33
92	Y	Final	-	Soil cover	-	-	-
93	N	-	-	Permeable top soil	-	-	-
94	N	-	40	-	-	-	-
	N	-	40	-	-	-	-
95	N	-	-	-	18.2	15.2	7920
96	-	Final	210	Soil cover	-	-	-
97	Y	Final	75	Sandy clay	22.9	11.7	3
	Y	Final	75	Sandy clay	22.9	11.7	3
	Y	Final	75	Sandy clay	13.4	1.62	3
	Y	Final	75	Sandy clay	15.7	1.27	3

Study No.	Active Gas Extraction System?	Cover Type	Cover Depth (cm)	Cover Material Texture	Moisture Content (%) Mean	Moisture Content (%) Standard Deviation	Moisture Content (%) No. Measuements
	Y	Final	75	Sandy clay	13.9	5.88	3
98	Y	Final	75	Sandy Loam	16	0	1
	N	Final	45	Ashes, bark, glass wool+sand	16.33333333	5.131601439	3
	Y	Final	40	Mineral soil and sewage sludge	75	35.35533906	2
	Y	Final	100	Clay and sewage sludge	64	0	1
	Y	Final	100	Pure sewage sludge	64	0	1
99	Y	Interim	20	Organic/mineral soil	28	7.937253933	3
	Y	Interim	20	Organic/mineral soil	28	7.937253933	3
	Y	Interim	20	Organic/mineral soil	28	7.937253933	3
100	Y	-	-	Sandy clay loam/sandy loam	5.9	2.19317122	5
	-	-	-	Sandy clay loam	11.2875	5.050159121	8
	-	-	-	-	-	-	-
	-	-	-	-	-	-	-
101	-	Final	125	Aerobic conversion in process, soil layer	-	-	-
	-	Final	125	Aerobic conversion in process, soil layer	-	-	-
	-	Final	125	Aerobic conversion in process, soil layer	-	-	-
	-	-	-	-	-	-	-
	-	-	-	-	-	-	-
	-	-	-	-	-	-	-
	-	-	100	Well compacted soil layer	-	-	-
	-	-	100	Well compacted soil layer	-	-	-
	-	-	100	Well compacted soil layer	-	-	-
	-	-	40	Clay-sand mixture, local soil	-	-	-
	-	-	100	Well compacted soil layer	-	-	-
	-	-	40	Clay-sand mixture, local soil	-	-	-
	-	Final	100	Highly compacted soil, vegetation	-	-	-

Study No.	Active Gas Extraction System?	Cover Type	Cover Depth (cm)	Cover Material Texture	Moisture Content (%) Mean	Moisture Content (%) Standard Deviation	Moisture Content (%) No. Measuements
	-	-	15	Soil cover	-	-	-
	-	-	40	Clay-sand mixture, local soil	-	-	-
	-	-	-	No cover soil	-	-	-
	-	-	10	Thin cover soil	-	-	-
102	Y	-	90	Loam/silt loam[2]	17.50588235	0.465330101	5
	Y	-	90	Loam/silt loam[2]	16.90980392	0.513111443	5
	Y	-	90	Loam/silt loam[2]	19.57894737	1.660190557	5
	Y	-	90	Loam/silt loam[2]	24.44444444	3.692955055	5
	Y	-	90	Loam/silt loam[2]	17.50588235	0.465330101	5
	Y	-	90	Loam/silt loam[2]	16.90980392	0.513111443	5
	Y	-	90	Loam/silt loam[2]	19.57894737	1.660190557	5
	Y	-	90	Loam/silt loam[2]	24.44444444	3.692955055	5
	Y	-	90	Loam/silt loam[2]	17.50588235	0.465330101	5
	Y	-	90	Loam/silt loam[2]	16.90980392	0.513111443	5
	Y	-	90	Loam/silt loam[2]	19.57894737	1.660190557	5
	Y	-	90	Loam/silt loam[2]	24.44444444	3.692955055	5
103	Y	-	-	Clay soil	-	-	-
104	Y	-	-	Sandy soil	-	-	-
105	N	Final	240	Clay, gravel, topsoil	-	-	-
106	N	Final	-	-	-	-	-
	N	Final	-	-	-	-	-
107	-	-	-	-	-	-	-
108	Y	Daily	30	Loamy-sand	-	-	-
	Y	Interim	80	Sandy-loam to Clay	-	-	-
	Y	Final	90	Clay	-	-	-
	Y	Daily	30	Loamy-sand	-	-	-
	Y	Interim	80	Sandy-loam to Clay	-	-	-
	Y	Final	90	Clay	-	-	-

Study No.	Soil Temperature (°C) Mean	Soil Temperature (°C) Standard Deviation	Soil Temperature (°C) No. Measuements	Air Temp (°C) Mean	Air Temp (°C) Standard Deviation	Air Temp (°C) No. Measuements	Barometric Pressure (kPa) Mean	Barometric Pressure (kPa) Standard Deviation	Barometric Pressure (kPa) No. Measuements
1	-	-	-	-	-	-	-	-	-
	-	-	-	-	-	-	-	-	-
2	22.3	-	-	-	-	-	-	-	-
	22.3	-	-	-	-	-	-	-	-
	22.3	-	-	-	-	-	-	-	-
	22.3	-	-	-	-	-	-	-	-
3,4	-	-	-	-	-	-	-	-	-
	-	-	-	-	-	-	-	-	-
5	-	-	-	-	-	-	-	-	-
	-	-	-	-	-	-	-	-	-
6	-	-	-	-	-	-	-	-	-
	-	-	-	-	-	-	-	-	-
	-	-	-	-	-	-	-	-	-
	-	-	-	-	-	-	-	-	-
	-	-	-	-	-	-	-	-	-
7	8.375803432	7.048684775	6	-	-	-	-	-	-
	9.227992958	7.539408075	6	-	-	-	-	-	-
8,9	15	8.9	24	14.3	11.4	24	-	-	-
	16.6	10.6	29	16.2	12.6	29	-	-	-
10	-	-	-	-	-	-	-	-	-
	-	-	-	-	-	-	-	-	-
	-	-	-	-	-	-	-	-	-
	-	-	-	-	-	-	-	-	-
	-	-	-	-	-	-	-	-	-
11	-	-	-	-	-	-	-	-	-
	-	-	-	-	-	-	-	-	-
	-	-	-	-	-	-	-	-	-
	-	-	-	-	-	-	-	-	-
	-	-	-	-	-	-	-	-	-
	-	-	-	-	-	-	-	-	-
12	-	-	-	-	-	-	-	-	-
13	-	-	-	-	-	-	-	-	-
	-	-	-	-	-	-	-	-	-
14	-	-	-	-	-	-	-	-	-
15	-	-	-	-	-	-	-	-	-
	-	-	-	22.15	1.626345597	2	97.7	0.141421356	2

Study No.	Soil Temperature (°C) Mean	Soil Temperature (°C) Standard Deviation	Soil Temperature (°C) No. Measuements	Air Temp (°C) Mean	Air Temp (°C) Standard Deviation	Air Temp (°C) No. Measurements	Barometric Pressure (kPa) Mean	Barometric Pressure (kPa) Standard Deviation	Barometric Pressure (kPa) No. Measuements
16	-	-	-	4.65	3.040559159	2	100.05	0.070710678	2
	-	-	-	-0.9	6.222539674	2	99.4	0	1
	-	-	-	-	-	-	-	-	-
	-	-	-	-	-	-	-	-	-
	-	-	-	-	-	-	-	-	-
	-	-	-	-	-	-	-	-	-
	-	-	-	-	-	-	-	-	-
	-	-	-	-	-	-	-	-	-
	-	-	-	-	-	-	-	-	-
	-	-	-	-	-	-	-	-	-
	-	-	-	-	-	-	-	-	-
	-	-	-	-	-	-	-	-	-
	-	-	-	-	-	-	-	-	-
	-	-	-	-	-	-	-	-	-
	-	-	-	-	-	-	-	-	-
	-	-	-	-	-	-	-	-	-
17	-	-	-	-	-	-	-	-	-
	-	-	-	-	-	-	-	-	-
	-	-	-	-	-	-	-	-	-
	-	-	-	-	-	-	-	-	-
	-	-	-	-	-	-	-	-	-
	-	-	-	-	-	-	-	-	-
	-	-	-	-	-	-	-	-	-
	-	-	-	-	-	-	-	-	-
	-	-	-	-	-	-	-	-	-
	-	-	-	-	-	-	-	-	-
	-	-	-	-	-	-	-	-	-
	-	-	-	-	-	-	-	-	-
	-	-	-	-	-	-	-	-	-
	-	-	-	-	-	-	-	-	-
	-	-	-	-	-	-	-	-	-
	-	-	-	1.5	0	1	-	-	-
	-	-	-	5.5	0	1	-	-	-
	19.5	0	1	33	0	1	-	-	-
	16.8	0	1	27	0	1	-	-	-
	12.8	0	1	24	0	1	-	-	-
	14.8	0	1	18.5	0	1	-	-	-

Study No.	Soil Temperature (°C) Mean	Soil Temperature (°C) Standard Deviation	Soil Temperature (°C) No. Measuements	Air Temp (°C) Mean	Air Temp (°C) Standard Deviation	Air Temp (°C) No. Measuements	Barometric Pressure (kPa) Mean	Barometric Pressure (kPa) Standard Deviation	Barometric Pressure (kPa) No. Measuements
18	19.8	0	1	24.5	0	1	-	-	-
	18	0	1	17.5	0	1	-	-	-
	12.1	0	1	10.5	0	1	-	-	-
	4.5	0	1	-2.8	0	1	-	-	-
	2.1	0	1	-2	0	1	-	-	-
	0.4	0	1	-7	0	1	-	-	-
	-	-	-	-6	0	1	-	-	-
	0.6	0	1	4	0	1	-	-	-
	3.4	0	1	5	0	1	-	-	-
	10.4	0	1	12.2	0	1	-	-	-
	14.1	0	1	16.5	0	1	-	-	-
	22.6	0	1	26	0	1	-	-	-
19	9.9	0.848528137	2	11.85	1.343502884	2	98.465	0.035355339	2
	18.15	0.777817459	2	18	5.939696962	2	101.075	0.120208153	2
	2.15	0.25	2	5.2	1.4	2	101.72	0.16	2
20	20	0	1	-	-	-	-	-	-
	24.5	0	1	-	-	-	-	-	-
	24	0	1	-	-	-	-	-	-
	18.5	0	1	-	-	-	-	-	-
	13.5	0	1	-	-	-	-	-	-
	8	0	1	-	-	-	-	-	-
	10	0	1	-	-	-	-	-	-
21	19.7	6.861000899	4	-	-	-	-	-	-
	25	0	1	-	-	-	-	-	-
22	-	-	-	20	9.899494937	2	-	-	-
	-	-	-	20	9.899494937	2	-	-	-
	-	-	-	12.653	10.45898942	26	101.6016132	13.51752879	26
	-	-	-	12.653	10.45898942	26	101.6016132	13.51752879	26
	-	-	-	12.653	10.45898942	26	101.6016132	13.51752879	26

Appendix A, Table A-2
Surface Flux of Landfill Gas by Chemical Families from Literature.

Study No.	Soil Temperature (°C) Mean	Soil Temperature (°C) Standard Deviation	Soil Temperature (°C) No. Measuements	Air Temp (°C) Mean	Air Temp (°C) Standard Deviation	Air Temp (°C) No. Measuements	Barometric Pressure (kPa) Mean	Barometric Pressure (kPa) Standard Deviation	Barometric Pressure (kPa) No. Measuements
23,24	-	-	-	12.653	10.45898942	26	101.6016132	13.51752879	26
	-	-	-	12.653	10.45898942	26	101.6016132	13.51752879	26
	-	-	-	12.653	10.45898942	26	101.6016132	13.51752879	26
	-	-	-	12.653	10.45898942	26	101.6016132	13.51752879	26
	-	-	-	12.653	10.45898942	26	101.6016132	13.51752879	26
	-	-	-	12.653	10.45898942	26	101.6016132	13.51752879	26
	-	-	-	12.653	10.45898942	26	101.6016132	13.51752879	26
	-	-	-	12.653	10.45898942	26	101.6016132	13.51752879	26
	-	-	-	12.653	10.45898942	26	101.6016132	13.51752879	26
	-	-	-	12.653	10.45898942	26	101.6016132	13.51752879	26
	-	-	-	12.653	10.45898942	26	101.6016132	13.51752879	26
	-	-	-	12.653	10.45898942	26	101.6016132	13.51752879	26
	-	-	-	12.653	10.45898942	26	101.6016132	13.51752879	26
	-	-	-	12.653	10.45898942	26	101.6016132	13.51752879	26
	-	-	-	12.653	10.45898942	26	101.6016132	13.51752879	26
25	15	10	3	-	-	-	-	-	-
	15	10	3	-	-	-	-	-	-
	15	10	3	-	-	-	-	-	-
	15	10	3	-	-	-	-	-	-
26	-	-	-	-	-	-	-	-	-
27	-	-	-	-	-	-	-	-	-
	-	-	-	-	-	-	-	-	-
28	-	-	-	28.6	7.495331881	2	101.791347	0.471364451	2
	-	-	-	28.6	7.495331881	2	101.791347	0.471364451	2
	-	-	-	28.6	7.495331881	2	101.791347	0.471364451	2
	-	-	-	31.45	12.37436867	2	101.32472	0.377091561	2
	-	-	-	31.45	12.37436867	2	101.32472	0.377091561	2
	-	-	-	31.45	12.37436867	2	101.32472	0.377091561	2
	-	-	-	29.15	9.203079195	4	101.191398	0.79249061	4
	-	-	-	29.15	9.203079195	4	101.191398	0.79249061	4
	-	-	-	29.15	9.203079195	4	101.191398	0.79249061	4
	-	-	-	22.2	8.766983518	4	758.75	4.924428901	4
	-	-	-	22.2	8.766983518	4	758.75	4.924428901	4
	-	-	-	22.2	8.766983518	4	758.75	4.924428901	4
	-	-	-	22.2	8.766983518	4	758.75	4.924428901	4
	-	-	-	22.2	8.766983518	4	758.75	4.924428901	4
	-	-	-	22.2	8.766983518	4	758.75	4.924428901	4
29	-	-	-	-	-	-	-	-	-
	-	-	-	-	-	-	-	-	-
	-	-	-	-	-	-	-	-	-
	-	-	-	-	-	-	-	-	-
	-	-	-	-	-	-	-	-	-
	-	-	-	-	-	-	-	-	-
	-	-	-	-	-	-	-	-	-

Study No.	Soil Temperature (°C) Mean	Soil Temperature (°C) Standard Deviation	Soil Temperature (°C) No. Measuements	Air Temp (°C) Mean	Air Temp (°C) Standard Deviation	Air Temp (°C) No. Measuements	Barometric Pressure (kPa) Mean	Barometric Pressure (kPa) Standard Deviation	Barometric Pressure (kPa) No. Measuements
30	-	-	-	-	-	-	-	-	-
	-	-	-	-	-	-	-	-	-
	-	-	-	-	-	-	-	-	-
	-	-	-	-	-	-	-	-	-
	-	-	-	-	-	-	-	-	-
	-	-	-	-	-	-	-	-	-
	-	-	-	-	-	-	-	-	-
	-	-	-	-	-	-	-	-	-
	-	-	-	-	-	-	-	-	-
	-	-	-	-	-	-	-	-	-
	-	-	-	-	-	-	-	-	-
	-	-	-	-	-	-	-	-	-
	-	-	-	-	-	-	-	-	-
31	-	-	-	-	-	-	-	-	-
	-	-	-	-	-	-	-	-	-
	-	-	-	-	-	-	-	-	-
	-	-	-	-	-	-	-	-	-
	-	-	-	-	-	-	-	-	-
	-	-	-	-	-	-	-	-	-
	-	-	-	-	-	-	-	-	-
	-	-	-	-	-	-	-	-	-
	-	-	-	-	-	-	-	-	-
	-	-	-	-	-	-	-	-	-
	-	-	-	-	-	-	-	-	-
	-	-	-	-	-	-	-	-	-
32	-	-	-	14.4	1.272792206	2	95.25	0.353553391	2
	-	-	-	14.4	1.272792206	2	95.25	0.353553391	2
	-	-	-	14.4	1.272792206	2	95.25	0.353553391	2
	-	-	-	14.4	1.272792206	2	95.25	0.353553391	2
	-	-	-	14.4	1.272792206	2	95.25	0.353553391	2
	-	-	-	14.4	1.272792206	2	95.25	0.353553391	2
	-	-	-	22.4	0.282842712	2	96.35	0.212132034	2
	-	-	-	22.4	0.282842712	2	96.35	0.212132034	2
	-	-	-	22.4	0.282842712	2	96.35	0.212132034	2

Study No.	Soil Temperature (°C) Mean	Soil Temperature (°C) Standard Deviation	Soil Temperature (°C) No. Measuements	Air Temp (°C) Mean	Air Temp (°C) Standard Deviation	Air Temp (°C) No. Measuements	Barometric Pressure (kPa) Mean	Barometric Pressure (kPa) Standard Deviation	Barometric Pressure (kPa) No. Measuements
	-	-	-	22.4	0.282842712	2	96.35	0.212132034	2
	-	-	-	22.4	0.282842712	2	96.35	0.212132034	2
	-	-	-	22.4	0.282842712	2	96.35	0.212132034	2
33	-	-	-	23.86666667	4.219399641	3	96.52666667	0.192959409	3
34	5.65	3.040559159	2	3.7	0	1	-	-	-
	5.65	0.353553391	2	4.8	0	1	-	-	-
	20.65	3.323401872	2	22.2	0	1	-	-	-
35	21.5	3.2	15	27.5	7.071067812	2	-	-	-
	22.4	4.1	15	17.1	9.616652224	2	-	-	-
	21	2.8	15	26.75	8.131727984	2	-	-	-
36	-	-	-	-	-	-	-	-	-
	-	-	-	-	-	-	-	-	-
	-	-	-	-	-	-	-	-	-
	-	-	-	-	-	-	-	-	-
	-	-	-	-	-	-	-	-	-
	-	-	-	-	-	-	-	-	-
	-	-	-	-	-	-	-	-	-
	-	-	-	-	-	-	-	-	-
	-	-	-	-	-	-	-	-	-
	-	-	-	-	-	-	-	-	-
	-	-	-	-	-	-	-	-	-
	-	-	-	-	-	-	-	-	-
	-	-	-	-	-	-	-	-	-
	-	-	-	-	-	-	-	-	-
	-	-	-	-	-	-	-	-	-
	-	-	-	-	-	-	-	-	-
	-	-	-	-	-	-	-	-	-
	-	-	-	-	-	-	-	-	-
	-	-	-	-	-	-	-	-	-
	-	-	-	-	-	-	-	-	-
	-	-	-	-	-	-	-	-	-
	-	-	-	-	-	-	-	-	-
37	-	-	-	-	-	-	-	-	-
	-	-	-	-	-	-	-	-	-
	-	-	-	-	-	-	-	-	-
	-	-	-	-	-	-	-	-	-
	-	-	-	-	-	-	-	-	-
	-	-	-	-	-	-	-	-	-
	-	-	-	-	-	-	-	-	-
	-	-	-	-	-	-	-	-	-
	-	-	-	-	-	-	-	-	-
	-	-	-	-	-	-	-	-	-

Appendix A, Table A-2
Surface Flux of Landfill Gas by Chemical Families from Literature.

Study No.	Soil Temperature (°C) Mean	Soil Temperature (°C) Standard Deviation	Soil Temperature (°C) No. Measuements	Air Temp (°C) Mean	Air Temp (°C) Standard Deviation	Air Temp (°C) No. Measuements	Barometric Pressure (kPa) Mean	Barometric Pressure (kPa) Standard Deviation	Barometric Pressure (kPa) No. Measuements
	-	-	-	-	-	-	-	-	-
38	36	4.25	3	23.5	0.707106781	2	83.9	0.707106781	2
	25	5	3	22	8.485281374	2	84.85	0.636396103	2
	25.5	1.75	3	26.5	4.949747468	2	83.6	0.282842712	2
	26	3.25	3	26.5	4.949747468	2	83.6	0.282842712	2
	26.5	3	3	25.75	5.303300859	2	83.6	0.282842712	2
	23	1.5	3	24.5	3.535533906	2	82.6	0.707106781	2
39	19.96197719	3.422053232	3	-	-	-	-	-	-
	27.56653992	4.372623574	3	-	-	-	-	-	-
	26.80608365	5.513307985	3	-	-	-	-	-	-
	40.11406844	1.711026616	3	-	-	-	-	-	-
	45.05703422	1.901140684	3	-	-	-	-	-	-
	28.8973384	0.950570342	3	-	-	-	-	-	-
	30.98859316	0.950570342	3	-	-	-	-	-	-
	29.46768061	1.140684411	3	-	-	-	-	-	-
	24.90494297	0.950570342	3	-	-	-	-	-	-
	17.4904943	0.950570342	3	-	-	-	-	-	-
	19.96197719	0.950570342	3	-	-	-	-	-	-
	10.8365019	0.760456274	3	-	-	-	-	-	-
	11.21673004	0.760456274	3	-	-	-	-	-	-
	19.20152091	0.760456274	3	-	-	-	-	-	-
	21.29277567	0.950570342	3	-	-	-	-	-	-
40	-	-	-	-	-	-	-	-	-
	-	-	-	-	-	-	-	-	-
	-	-	-	-	-	-	-	-	-
	15.8	1.1	-	-	-	-	-	-	-
	28.3	4.4	-	-	-	-	-	-	-
	15.8	1.1	-	-	-	-	-	-	-
	25.6	4.6	-	-	-	-	-	-	-
	15.8	1.1	-	-	-	-	-	-	-
	36.2	1.2	-	-	-	-	-	-	-
	31	1.7	-	-	-	-	-	-	-
	36	11.3	-	-	-	-	-	-	-
	17.3	1.1	-	-	-	-	-	-	-
	35.9	9.4	-	-	-	-	-	-	-
	28.1	7.3	-	-	-	-	-	-	-
41	-	-	-	-	-	-	-	-	-
	-	-	-	-	-	-	-	-	-
	-	-	-	-	-	-	-	-	-
	10.85443038	0	1	-	-	-	-	-	-
	3.544303797	0	1	-	-	-	-	-	-
	13.9556962	0	1	-	-	-	-	-	-
	20.37974684	0	1	-	-	-	-	-	-
	19.93670886	0	1	-	-	-	-	-	-

Study No.	Soil Temperature (°C) Mean	Soil Temperature (°C) Standard Deviation	Soil Temperature (°C) No. Measuements	Air Temp (°C) Mean	Air Temp (°C) Standard Deviation	Air Temp (°C) No. Measuements	Barometric Pressure (kPa) Mean	Barometric Pressure (kPa) Standard Deviation	Barometric Pressure (kPa) No. Measuements
42	24.81012658	0	1	-	-	-	-	-	-
	27.02531646	0	1	-	-	-	-	-	-
	33.44936709	0	1	-	-	-	-	-	-
	32.56329114	0	1	-	-	-	-	-	-
	34.55696203	0	1	-	-	-	-	-	-
	27.02531646	0	1	-	-	-	-	-	-
	9.303797468	0	1	-	-	-	-	-	-
	5.981012658	0	1	-	-	-	-	-	-
	7.088607595	0	1	-	-	-	-	-	-
	10.85443038	0	1	-	-	-	-	-	-
	3.544303797	0	1	-	-	-	-	-	-
	13.9556962	0	1	-	-	-	-	-	-
	20.37974684	0	1	-	-	-	-	-	-
	19.93670886	0	1	-	-	-	-	-	-
	24.81012658	0	1	-	-	-	-	-	-
	27.02531646	0	1	-	-	-	-	-	-
	33.44936709	0	1	-	-	-	-	-	-
	32.56329114	0	1	-	-	-	-	-	-
	34.55696203	0	1	-	-	-	-	-	-
	27.02531646	0	1	-	-	-	-	-	-
	34.55696203	0	1	-	-	-	-	-	-
	27.02531646	0	1	-	-	-	-	-	-
	9.303797468	0	1	-	-	-	-	-	-
	5.981012658	0	1	-	-	-	-	-	-
	7.088607595	0	1	-	-	-	-	-	-
43	24.22222222	1.555555556	5	-	-	-	-	-	-
	22.22222222	0.888888889	5	-	-	-	-	-	-
	24	0.666666667	5	-	-	-	-	-	-
	18.22222222	1.111111111	5	-	-	-	-	-	-
	26.22222222	0.888888889	5	-	-	-	-	-	-
	23.33333333	2	5	-	-	-	-	-	-
	18.88888889	3.333333333	5	-	-	-	-	-	-
	19.77777778	1.111111111	5	-	-	-	-	-	-
	21.77777778	0.666666667	5	-	-	-	-	-	-
	20	2.222222222	5	-	-	-	-	-	-
	28	0.666666667	5	-	-	-	-	-	-
	29.77777778	1.333333333	5	-	-	-	-	-	-
	31.27035831	1.563517915	5	-	-	-	-	-	-
	21.49837134	1.824104235	5	-	-	-	-	-	-
	23.45276873	0.912052117	5	-	-	-	-	-	-
	22.14983713	2.996742671	5	-	-	-	-	-	-
	30.48859935	0.521172638	5	-	-	-	-	-	-
	29.44625407	0.781758958	5	-	-	-	-	-	-
44	-	-	-	-	-	-	-	-	-
	-	-	-	-	-	-	-	-	-
	-	-	-	-	-	-	-	-	-

Study No.	Soil Temperature (°C) Mean	Soil Temperature (°C) Standard Deviation	Soil Temperature (°C) No. Measuements	Air Temp (°C) Mean	Air Temp (°C) Standard Deviation	Air Temp (°C) No. Measuements	Barometric Pressure (kPa) Mean	Barometric Pressure (kPa) Standard Deviation	Barometric Pressure (kPa) No. Measuements
44	-	-	-	-	-	-	-	-	-
	-	-	-	-	-	-	-	-	-
	-	-	-	-	-	-	-	-	-
45	25	7	-	-	-	-	-	-	-
46	-	-	-	20.5	4.949747468	2	-	-	-
	-	-	-	24.5	0.707106781	2	-	-	-
	-	-	-	20.5	4.949747468	2	-	-	-
47	-	-	-	-	-	-	-	-	-
	-	-	-	-	-	-	-	-	-
	-	-	-	-	-	-	-	-	-
48	-	-	-	-	-	-	-	-	-
	-	-	-	-	-	-	-	-	-
	-	-	-	-	-	-	-	-	-
	-	-	-	-	-	-	-	-	-
	-	-	-	-	-	-	-	-	-
49	26.8	-	3	28.2	-	3	-	-	-
	4.4	-	3	10	-	3	-	-	-
	-0.3	-	3	-1.9	-	3	-	-	-
	-	-	-	-	-	-	-	-	-
	-	-	-	-	-	-	-	-	-
	-	-	-	-	-	-	-	-	-
	-	-	-	-	-	-	-	-	-
	-	-	-	-	-	-	-	-	-
	24.8	-	3	24.8	-	3	-	-	-
	1.4	-	3	1.2	-	3	-	-	-
	0.4	-	3	-1.1	-	3	-	-	-
	-	-	-	-	-	-	-	-	-
	-	-	-	-	-	-	-	-	-
	-	-	-	-	-	-	-	-	-
	-	-	-	-	-	-	-	-	-
	-	-	-	-	-	-	-	-	-
	-	-	-	-	-	-	-	-	-
	-	-	-	-	-	-	-	-	-
	-	-	-	-	-	-	-	-	-
	-	-	-	-	-	-	-	-	-
	-	-	-	-	-	-	-	-	-
	-	-	-	-	-	-	-	-	-
	-	-	-	-	-	-	-	-	-
	-	-	-	-	-	-	-	-	-
	-	-	-	-	-	-	-	-	-
	-	-	-	-	-	-	-	-	-
	-	-	-	-	-	-	-	-	-
	-	-	-	-	-	-	-	-	-
	-	-	-	-	-	-	-	-	-

Study No.	Soil Temperature (°C) Mean	Soil Temperature (°C) Standard Deviation	Soil Temperature (°C) No. Measuements	Air Temp (°C) Mean	Air Temp (°C) Standard Deviation	Air Temp (°C) No. Measuements	Barometric Pressure (kPa) Mean	Barometric Pressure (kPa) Standard Deviation	Barometric Pressure (kPa) No. Measuements
50	-	-	-	-	-	-	-	-	-
	-	-	-	-	-	-	-	-	-
	-	-	-	-	-	-	-	-	-
	-	-	-	-	-	-	-	-	-
	-	-	-	-	-	-	-	-	-
	-	-	-	-	-	-	-	-	-
	-	-	-	-	-	-	-	-	-
	-	-	-	-	-	-	-	-	-
	-	-	-	-	-	-	-	-	-
	-	-	-	-	-	-	-	-	-
	-	-	-	-	-	-	-	-	-
	-	-	-	-	-	-	-	-	-
	-	-	-	-	-	-	-	-	-
	-	-	-	-	-	-	-	-	-
	-	-	-	-	-	-	-	-	-
	-	-	-	-	-	-	-	-	-
	-	-	-	-	-	-	-	-	-
	-	-	-	-	-	-	-	-	-
	-	-	-	-	-	-	-	-	-
51	25.13888889	2.987141756	36	-	-	-	101.1722222	0.364582823	36
52	-	-	-	19.81666667	6.423304491	24	98.10654029	0.850148217	24
	-	-	-	24.4	2.121320344	2	98.543949	0	2
	-	-	-	18.85	0.636396103	2	97.0200735	1.676177533	2
53	-	-	-	-	-	-	-	-	-
54	-	-	-	21.28365385	2.06004952	24	-	-	-
	-	-	-	-	-	-	-	-	-
55,56,57	-	-	-	33.4	4.95665422	20	100.2	0.081649658	10
	-	-	-	27.2	-	-	-	-	-
	-	-	-	27.2	-	-	-	-	-
	-	-	-	32.96428571	4.662554878	28	100.8928571	0.126881445	14
	-	-	-	32.96428571	4.662554878	29	100.8928571	0.126881445	15

Appendix A, Table A-2
Surface Flux of Landfill Gas by Chemical Families from Literature.

Study No.	Soil Temperature (°C) Mean	Soil Temperature (°C) Standard Deviation	Soil Temperature (°C) No. Measuements	Air Temp (°C) Mean	Air Temp (°C) Standard Deviation	Air Temp (°C) No. Measuements	Barometric Pressure (kPa) Mean	Barometric Pressure (kPa) Standard Deviation	Barometric Pressure (kPa) No. Measuements
58	-	-	-	-	-	-	-	-	-
59	4.249963361	6.076155095	5	-	-	-	-	-	-
	1.106982861	1.645485921	5	-	-	-	-	-	-
	14.34593858	6.773542437	5	-	-	-	-	-	-
	-	-	-	-	-	-	-	-	-
	-	-	-	-	-	-	-	-	-
	-	-	-	-	-	-	-	-	-
	-	-	-	-	-	-	-	-	-
	-	-	-	-	-	-	-	-	-
	-	-	-	-	-	-	-	-	-
	-	-	-	-	-	-	-	-	-
	-	-	-	-	-	-	-	-	-
	-	-	-	-	-	-	-	-	-
	-	-	-	-	-	-	-	-	-
	-	-	-	-	-	-	-	-	-
60	-	-	-	-	-	-	-	-	-
	-	-	-	-	-	-	-	-	-
	-	-	-	-	-	-	-	-	-
	-	-	-	-	-	-	-	-	-
	-	-	-	-	-	-	-	-	-
	-	-	-	-	-	-	-	-	-
	-	-	-	-	-	-	-	-	-
	-	-	-	-	-	-	-	-	-
	-	-	-	-	-	-	-	-	-
61	34.5	6.363961031	2^6	40.5	7.778174593	2	-	-	-
	34.5	6.363961031	2^6	40.5	7.778174593	2	-	-	-
	-	-	-	-	-	-	-	-	-
	-	-	-	-	-	-	-	-	-
	-	-	-	-	-	-	-	-	-
	-	-	-	-	-	-	-	-	-
	-	-	-	-	-	-	-	-	-
	-	-	-	-	-	-	-	-	-
	-	-	-	-	-	-	-	-	-

Study No.	Soil Temperature (°C) Mean	Soil Temperature (°C) Standard Deviation	Soil Temperature (°C) No. Measuements	Air Temp (°C) Mean	Air Temp (°C) Standard Deviation	Air Temp (°C) No. Measuements	Barometric Pressure (kPa) Mean	Barometric Pressure (kPa) Standard Deviation	Barometric Pressure (kPa) No. Measuements
62,63	-	-	-	-	-	-	-	-	-
	-	-	-	-	-	-	-	-	-
	-	-	-	-	-	-	-	-	-
	-	-	-	-	-	-	-	-	-
	-	-	-	-	-	-	-	-	-
	-	-	-	-	-	-	-	-	-
	-	-	-	-	-	-	-	-	-
	-	-	-	-	-	-	-	-	-
64	31.15530958	2.689495265	14	37.45935662	5.141454118	14	-	-	-
	30.31476998	1.804555577	9	34.26841923	4.695832662	9	-	-	-
	32.27084054	3.184593713	14	37.45935662	5.141454118	14	-	-	-
	32.25450632	2.477242669	9	34.26841923	4.695832662	9	-	-	-
	32.27084054	3.184593713	14	37.45935662	5.141454118	14	-	-	-
	32.25450632	2.477242669	9	34.26841923	4.695832662	9	-	-	-
	32.27084054	3.184593713	14	37.45935662	5.141454118	14	-	-	-
	32.25450632	2.477242669	9	34.26841923	4.695832662	9	-	-	-
	32.27084054	3.184593713	14	37.45935662	5.141454118	14	-	-	-
	32.25450632	2.477242669	9	34.26841923	4.695832662	9	-	-	-
65	-	-	-	-	-	-	-	-	-
66	30.25	5.057996968	4	-	-	-	-	-	-
	30.25	5.057996968	4	-	-	-	-	-	-
	30.25	5.057996968	4	-	-	-	-	-	-
	30.25	5.057996968	4	-	-	-	-	-	-
	30.25	5.057996968	4	-	-	-	-	-	-

Study No.	Soil Temperature (°C) Mean	Soil Temperature (°C) Standard Deviation	Soil Temperature (°C) No. Measuements	Air Temp (°C) Mean	Air Temp (°C) Standard Deviation	Air Temp (°C) No. Measuements	Barometric Pressure (kPa) Mean	Barometric Pressure (kPa) Standard Deviation	Barometric Pressure (kPa) No. Measuements
	30.25	5.057996968	4	-	-	-	-	-	-
67	-	-	-	-	-	-	-	-	-
	-	-	-	-	-	-	-	-	-
	-	-	-	-	-	-	-	-	-
	-	-	-	-	-	-	-	-	-
	-	-	-	-	-	-	-	-	-
	-	-	-	-	-	-	-	-	-
	-	-	-	-	-	-	-	-	-
	-	-	-	-	-	-	-	-	-
	-	-	-	-	-	-	-	-	-
	-	-	-	-	-	-	-	-	-
	-	-	-	-	-	-	-	-	-
	-	-	-	-	-	-	-	-	-
	-	-	-	-	-	-	-	-	-
68	-	-	-	-	-	-	-	-	-
	-	-	-	-	-	-	-	-	-
	-	-	-	-	-	-	-	-	-
	-	-	-	-	-	-	-	-	-
	-	-	-	-	-	-	-	-	-
	-	-	-	-	-	-	-	-	-
	-	-	-	-	-	-	-	-	-
69	-	-	-	15	0	1	-	-	-
	-	-	-	1.4	0	1	-	-	-
	-	-	-	-2.4	0	1	-	-	-
	-	-	-	4	0	1	-	-	-
	-	-	-	3.3	0	1	-	-	-
	-	-	-	1.9	0	1	-	-	-
	-	-	-	0.1	0	1	-	-	-
	-	-	-	3.6	0	1	-	-	-
	-	-	-	2.1	0	1	-	-	-
70	-	-	-	16	0	1	98.2	0	1
	-	-	-	25	0	1	97.9	0	1
71	-	-	-	-	-	-	-	-	-
	-	-	-	-	-	-	-	-	-
72	12.8	-	22	10.15	2.333452378	2	101.67	0.848528137	2
73	31.9	1	4	29.14933333	2.397306425	15	101.5	0.1	4
	30.9	1	4	34.57869688	3.32489986	15	101.4	0.1	4
	20.5	0.8	4	20.70347513	4.540881988	10	101.8	0.4	4
	31.1	1	4	26.28528529	1.014387821	15	101.5	0.1	4
	26.9	0.6	4	23.53535354	1.581401342	15	101.4	0.1	4
	29.5	2.3	4	24.85195737	4.386477753	18	100.7	0.1	4
	20.6	0.7	4	11.17790077	1.173768799	9	1018.5	0.4	4
	33.6	2.1	4	-	-	-	100.7	0.1	4
	20	0.9	4	23.48591961	2.671242182	9	100.8	0.4	4

Study No.	Soil Temperature (°C) Mean	Soil Temperature (°C) Standard Deviation	Soil Temperature (°C) No. Measuements	Air Temp (°C) Mean	Air Temp (°C) Standard Deviation	Air Temp (°C) No. Measuements	Barometric Pressure (kPa) Mean	Barometric Pressure (kPa) Standard Deviation	Barometric Pressure (kPa) No. Measuements
74	-	-	-	-	-	-	-	-	-
	-	-	-	-	-	-	-	-	-
	-	-	-	-	-	-	-	-	-
	-	-	-	-	-	-	-	-	-
	-	-	-	-	-	-	-	-	-
75	-	-	-	-	-	-	-	-	-
76	-	-	-	15.6	21.92031022	2	100.19	3.337544007	2
	-	-	-	-	-	-	-	-	-
	-	-	-	-	-	-	-	-	-
	-	-	-	-	-	-	-	-	-
	-	-	-	-	-	-	-	-	-
	-	-	-	-	-	-	-	-	-
	-	-	-	-	-	-	-	-	-
	-	-	-	-	-	-	-	-	-
	-	-	-	-	-	-	-	-	-
	-	-	-	-	-	-	-	-	-
	-	-	-	-	-	-	-	-	-
	-	-	-	-	-	-	-	-	-
	-	-	-	-	-	-	-	-	-
	-	-	-	-	-	-	-	-	-
	-	-	-	-	-	-	-	-	-
	-	-	-	-	-	-	-	-	-
	-	-	-	-	-	-	-	-	-
	-	-	-	-	-	-	-	-	-
	-	-	-	-	-	-	-	-	-
	-	-	-	-	-	-	-	-	-
	-	-	-	-	-	-	-	-	-
	-	-	-	-	-	-	-	-	-
	-	-	-	-	-	-	-	-	-
	-	-	-	-	-	-	-	-	-
	-	-	-	-	-	-	-	-	-
	-	-	-	-	-	-	-	-	-
	-	-	-	-	-	-	-	-	-
	-	-	-	-	-	-	-	-	-
	-	-	-	-	-	-	-	-	-
	-	-	-	-	-	-	-	-	-
	-	-	-	-	-	-	-	-	-
	10.3	-	-	-	-	-	-	-	-

Study No.	Soil Temperature (°C) Mean	Soil Temperature (°C) Standard Deviation	Soil Temperature (°C) No. Measuements	Air Temp (°C) Mean	Air Temp (°C) Standard Deviation	Air Temp (°C) No. Measuements	Barometric Pressure (kPa) Mean	Barometric Pressure (kPa) Standard Deviation	Barometric Pressure (kPa) No. Measuements
77	27.1	-	-	-	-	-	-	-	-
	12.9	-	-	-	-	-	-	-	-
	29.9	-	-	-	-	-	-	-	-
78	-	-	-	-	-	-	-	-	-
	-	-	-	-	-	-	-	-	-
	-	-	-	-	-	-	-	-	-
	-	-	-	-	-	-	-	-	-
	-	-	-	-	-	-	-	-	-
	-	-	-	-	-	-	-	-	-
	-	-	-	-	-	-	-	-	-
	-	-	-	-	-	-	-	-	-
	-	-	-	-	-	-	-	-	-
79	34.4	1.9	-	23.8	4.666904756	2	1013.1	4.384062043	2
	33.2	2	-	23.8	4.666904756	2	1013.1	4.384062043	2
80	19.83472785	2.042591767	57	-	-	-	-	-	-
	-	-	-	-	-	-	-	-	-
	-	-	-	-	-	-	-	-	-
	-	-	-	-	-	-	-	-	-
	-	-	-	-	-	-	-	-	-
81	-	-	-	-	-	-	-	-	-
82	-	-	-	9.4	8.485281374	2	100.835	2.510229073	2
	-	-	-	9.4	8.485281374	2	100.835	2.510229073	2
	-	-	-	9.4	8.485281374	2	100.835	2.510229073	2
83	-	-	-	19.7	2.6	-	-	-	-
	-	-	-	30.5	2.4	-	-	-	-
	-	-	-	32.6	1.3	-	-	-	-
84	-	-	-	35	7.071067812	2	-	-	-
	-	-	-	35	7.071067812	2	-	-	-
	-	-	-	35	7.071067812	2	-	-	-
	-	-	-	35	7.071067812	2	-	-	-
	-	-	-	35	7.071067812	2	-	-	-
	-	-	-	35	7.071067812	2	-	-	-
85	-	-	-	5.3	13.43502884	2	-	-	-
	-	-	-	5.3	13.43502884	2	-	-	-
	-	-	-	13.35	16.05132393	2	-	-	-
86	-	-	-	-	-	-	-	-	-
	-	-	-	-	-	-	-	-	-
	16.25101351	2.315483646	5	-	-	-	-	-	-
	36.36363636	3.335451753	5	-	-	-	-	-	-
	15.45454545	1.72005229	5	-	-	-	-	-	-
	5.138888889	0.380362887	5	-	-	-	-	-	-
	16.14814815	2.200511226	5	-	-	-	-	-	-

Appendix A, Table A-2
Surface Flux of Landfill Gas by Chemical Families from Literature.

Study No.	Soil Temperature (°C) Mean	Soil Temperature (°C) Standard Deviation	Soil Temperature (°C) No. Measuements	Air Temp (°C) Mean	Air Temp (°C) Standard Deviation	Air Temp (°C) No. Measuements	Barometric Pressure (kPa) Mean	Barometric Pressure (kPa) Standard Deviation	Barometric Pressure (kPa) No. Measuements
87	34.88372093	3.088639041	5	-	-	-	-	-	-
	14.76923077	1.039173545	5	-	-	-	-	-	-
	4.962406015	0.314533845	5	-	-	-	-	-	-
	18.43283582	2.483516611	5	-	-	-	-	-	-
	27.81954887	1.527074888	5	-	-	-	-	-	-
	9.708029197	2.429133035	5	-	-	-	-	-	-
	6.015037594	2.143186889	5	-	-	-	-	-	-
88	9.726315789	2.369999474	5	13.42745098	5.775872871	5	-	-	-
	6.094736842	2.160909319	5	8.188235294	3.363233829	5	-	-	-
	18.47368421	2.547335798	5	26.36842105	6.300419895	5	-	-	-
	27.92207792	1.655525816	5	33.44155844	8.44779989	5	-	-	-
	9.726315789	2.369999474	5	13.42745098	5.775872871	5	-	-	-
	6.094736842	2.160909319	5	8.188235294	3.363233829	5	-	-	-
	18.47368421	2.547335798	5	26.36842105	6.300419895	5	-	-	-
	27.92207792	1.655525816	5	33.44155844	8.44779989	5	-	-	-
	9.726315789	2.369999474	5	13.42745098	5.775872871	5	-	-	-
	6.094736842	2.160909319	5	8.188235294	3.363233829	5	-	-	-
	18.47368421	2.547335798	5	26.36842105	6.300419895	5	-	-	-
	27.92207792	1.655525816	5	33.44155844	8.44779989	5	-	-	-
89	-	-	-	-	-	-	-	-	-
	-	-	-	-	-	-	-	-	-
	-	-	-	-	-	-	-	-	-
	-	-	-	-	-	-	-	-	-
	-	-	-	-	-	-	-	-	-
	-	-	-	-	-	-	-	-	-
90	-	-	-	-	-	-	-	-	-
	-	-	-	-	-	-	-	-	-
	-	-	-	-	-	-	-	-	-
	-	-	-	-	-	-	-	-	-
91	-	-	-	15.38126892	3.54956652	7	101.8120435	0.684638031	7
	-	-	-	16.05748276	3.915809979	11	1014.985325	5.760533215	11
92	-	-	-	-	-	-	-	-	-
93	25	7.071067812	2	-	-	-	-	-	-
94	-	-	-	-	-	-	-	-	-
	-	-	-	-	-	-	-	-	-
95	29.2	2.3	7920	19.8	3.6	7920	100.49	0.36	-
96	33.4	21.77888886	2	-	-	-	-	-	-
97	33.2	0	1	33.1	1.272792206	2	-	-	-
	33.2	0	1	33.1	1.272792206	2	-	-	-
	27.9	0	1	33.1	1.272792206	2	-	-	-
	32.2	0	1	33.1	1.272792206	2	-	-	-

Study No.	Soil Temperature (°C) Mean	Soil Temperature (°C) Standard Deviation	Soil Temperature (°C) No. Measuements	Air Temp (°C) Mean	Air Temp (°C) Standard Deviation	Air Temp (°C) No. Measuements	Barometric Pressure (kPa) Mean	Barometric Pressure (kPa) Standard Deviation	Barometric Pressure (kPa) No. Measuements
	37.2	0	1	33.1	1.272792206	2	-	-	-
98	21	0	1	-	-	-	-	-	-
	13.33333333	17.14885808	3	-	-	-	-	-	-
	14	21.92031022	2	-	-	-	-	-	-
	-	-	-	-	-	-	-	-	-
	-	-	-	-	-	-	-	-	-
99	21	8.485281374	2	-	-	-	-	-	-
	21	8.485281374	2	-	-	-	-	-	-
	21	8.485281374	2	-	-	-	-	-	-
100	-	-	-	-	-	-	-	-	-
	-	-	-	-	-	-	-	-	-
	-	-	-	-	-	-	-	-	-
	-	-	-	-	-	-	-	-	-
101	-	-	-	-	-	-	-	-	-
	-	-	-	-	-	-	-	-	-
	-	-	-	-	-	-	-	-	-
	-	-	-	-	-	-	-	-	-
	-	-	-	-	-	-	-	-	-
	-	-	-	-	-	-	-	-	-
	-	-	-	-	-	-	-	-	-
	-	-	-	-	-	-	-	-	-
	-	-	-	-	-	-	-	-	-
	-	-	-	-	-	-	-	-	-
	-	-	-	-	-	-	-	-	-

Study No.	Soil Temperature (°C) Mean	Soil Temperature (°C) Standard Deviation	Soil Temperature (°C) No. Measuements	Air Temp (°C) Mean	Air Temp (°C) Standard Deviation	Air Temp (°C) No. Measuements	Barometric Pressure (kPa) Mean	Barometric Pressure (kPa) Standard Deviation	Barometric Pressure (kPa) No. Measuements
	-	-	-	-	-	-	-	-	-
	-	-	-	-	-	-	-	-	-
	-	-	-	-	-	-	-	-	-
	-	-	-	-	-	-	-	-	-
102	9.726315789	2.369999474	5	13.42745098	5.775872871	5	-	-	-
	6.094736842	2.160909319	5	8.188235294	3.363233829	5	-	-	-
	18.47368421	2.547335798	5	26.36842105	6.300419895	5	-	-	-
	27.92207792	1.655525816	5	33.44155844	8.44779989	5	-	-	-
	9.726315789	2.369999474	5	13.42745098	5.775872871	5	-	-	-
	6.094736842	2.160909319	5	8.188235294	3.363233829	5	-	-	-
	18.47368421	2.547335798	5	26.36842105	6.300419895	5	-	-	-
	27.92207792	1.655525816	5	33.44155844	8.44779989	5	-	-	-
	9.726315789	2.369999474	5	13.42745098	5.775872871	5	-	-	-
	6.094736842	2.160909319	5	8.188235294	3.363233829	5	-	-	-
	18.47368421	2.547335798	5	26.36842105	6.300419895	5	-	-	-
	27.92207792	1.655525816	5	33.44155844	8.44779989	5	-	-	-
103	-	-	-	-	-	-	-	-	-
104	-	-	-	-	-	-	-	-	-
105	-	-	-	-	-	-	-	-	-
106	-	-	-	-	-	-	-	-	-
	-	-	-	-	-	-	-	-	-
107	-	-	-	-	-	-	-	-	-
108	-	-	-	-	-	-	-	-	-
	-	-	-	-	-	-	-	-	-
	-	-	-	-	-	-	-	-	-
	-	-	-	-	-	-	-	-	-
	-	-	-	-	-	-	-	-	-
	-	-	-	-	-	-	-	-	-

Study No.	OM (food waste) Composition (%) Mean	OM (food waste) Composition (%) Standard Deviation	OM (food waste) Composition (%) No. Measurements	Total No. of Flux Measurements Methane	Total No. of Flux Measurements CO2	Total No. of Flux Measurements N2O	Total No. of Flux Measurements NMVOCs	Total No. of Flux Measurements CO	Total No. of Flux Measurements
1	-	-	-	76					76
	-	-	-	88					88
2	-	-	-	62					62
	-		-	18					18
	-	-	-	28					28
	-	-	-	112					112
3,4	-	-	-	4					4
	-	-	-	4					4
5	-	-	-	18					18
	-	-	-	9					9
6	-	-	-	12					12
	-	-	-	29					29
	-	-	-	1					1
	-	-	-	1					1
	-	-	-	1					1
7	-	-	-	5					5
	-	-	-	6					6
8,9	-	-	-	22	26				48
	-	-	-	25	27				52
10	-	-	-	139					139
	-	-	-	92					92
	-	-	-	111					111
	-	-	-	106					106
	-	-	-	124					124
11	-	-	-	1					1
	-	-	-	1					1
	-	-	-	1					1
	-	-	-	1					1
	-	-	-	1					1
	-	-	-	1					1
12	-	-	-	26					26
13	-	-	-	1					1
	-	-	-	1					1
14	-	-	-	1					1
15	-	-	-	1	1	0	0	1	3
	-	-	-	45					45

Appendix A, Table A-2
Surface Flux of Landfill Gas by Chemical Families from Literature.

Study No.	OM (food waste) Composition (%) Mean	OM (food waste) Composition (%) Standard Deviation	OM (food waste) Composition (%) No. Measurements	Total No. of Flux Measurements Methane	Total No. of Flux Measurements CO2	Total No. of Flux Measurements N2O	Total No. of Flux Measurements NMVOCs	Total No. of Flux Measurements CO	Total No. of Flux Measurements
16	-	-	-	14					14
	-	-	-	42					42
	-	-	-	17					17
	-	-	-	17					17
	-	-	-	17					17
	-	-	-	17					17
	-	-	-	17					17
	-	-	-	17					17
	-	-	-	17					17
	-	-	-	17					17
	-	-	-	17					17
	-	-	-	17					17
	-	-	-	17					17
	-	-	-	17					17
	-	-	-	17					17
	-	-	-	17					17
17	-	-	-	17					17
	-	-	-	17					17
	-	-	-	17					17
	-	-	-	17					17
	-	-	-	17					17
	-	-	-	17					17
	-	-	-	17					17
	-	-	-	17					17
	-	-	-	17					17
	-	-	-	17					17
	-	-	-	17					17
	-	-	-	17					17
	-	-	-	17					17
	-	-	-	17					17
	-	-	-	17					17
	-	-	-	4	4				8
	-	-	-	4	4				8
	-	-	-	4	4				8
	-	-	-	4	4				8
	-	-	-	4	4				8
	-	-	-	4	4				8

Appendix A, Table A-2
Surface Flux of Landfill Gas by Chemical Families from Literature.

Study No.	OM (food waste) Composition (%) Mean	OM (food waste) Composition (%) Standard Deviation	OM (food waste) Composition (%) No. Measurements	Total No. of Flux Measurements Methane	Total No. of Flux Measurements CO2	Total No. of Flux Measurements N2O	Total No. of Flux Measurements NMVOCs	Total No. of Flux Measurements CO	Total No. of Flux Measurements
18	-	-	-	4	4				8
	-	-	-	4	4				8
	-	-	-	4	4				8
	-	-	-	4	4				8
	-	-	-	4	4				8
	-	-	-	4	4				8
	-	-	-	4	4				8
	-	-	-	4	4				8
	-	-	-	4	4				8
	-	-	-	4	4				8
	-	-	-	4	4				8
	-	-	-	4	4				8
19	-	-	-	81					81
	-	-	-	101					101
	-	-	-	83					83
20	-	-	-	6					6
	-	-	-	6					6
	-	-	-	6					6
	-	-	-	6					6
	-	-	-	6					6
	-	-	-	6					6
	-	-	-	6					6
21	-	-	-	4	4	0	123		131
	-	-	-	1	1	0	31		33
22	-	-	-	6			266		272
	-	-	-	1			45		46
	-	-	-	7	7				14
	-	-	-	7	7				14
	-	-	-	24	24				48

Appendix A, Table A-2
Surface Flux of Landfill Gas by Chemical Families from Literature.

Study No.	OM (food waste) Composition (%) Mean	OM (food waste) Composition (%) Standard Deviation	OM (food waste) Composition (%) No. Measurements	Total No. of Flux Measurements Methane	Total No. of Flux Measurements CO2	Total No. of Flux Measurements N2O	Total No. of Flux Measurements NMVOCs	Total No. of Flux Measurements CO	Total No. of Flux Measurements
23,24	-	-	-	25	25				50
	-	-	-	25	25				50
	-	-	-	25	25				50
	-	-	-	20	20				40
	-	-	-	9	9				18
	-	-	-	3	3				6
	-	-	-	7	7				14
	-	-	-	9	9				18
	-	-	-	24	24				48
	-	-	-	24	24				48
	-	-	-	24	24				48
	-	-	-	24	24				48
	-	-	-	17	17				34
	-	-	-	6	6				12
	-	-	-	1	1				2
25	-	-	-	1					1
	-	-	-	1					1
	-	-	-	1					1
	-	-	-	1					1
26	-	-	-	1					1
27	-	-	-	1					1
	-	-	-	1					1
28	-	-	-	3			8		10.93333333
	-	-	-	3			8		10.93333333
	-	-	-	3			8		10.93333333
	-	-	-	4			8		11.93333333
	-	-	-	4			8		11.93333333
	-	-	-	4			8		11.93333333
	-	-	-	5			8		12.93333333
	-	-	-	4			8		11.93333333
	-	-	-	4			8		11.93333333
	-	-	-	3			8		10.93333333
	-	-	-	3			8		10.93333333
	-	-	-	3			8		10.93333333
	-	-	-	2			8		9.933333333
	-	-	-	2			8		9.933333333
	-	-	-	2			8		9.933333333
29	47.85	11.9501046	2	13					13
	47.85	11.9501046	2	14					14
	47.85	11.9501046	2	18					18
	-	-	-	33					33
	-	-	-	8					8
	-	-	-	9					9
	-	-	-	6					6

Appendix A, Table A-2

Surface Flux of Landfill Gas by Chemical Families from Literature.

Study No.	OM (food waste) Composition (%) Mean	OM (food waste) Composition (%) Standard Deviation	OM (food waste) Composition (%) No. Measurements	Total No. of Flux Measurements Methane	Total No. of Flux Measurements CO2	Total No. of Flux Measurements N2O	Total No. of Flux Measurements NMVOCs	Total No. of Flux Measurements CO	Total No. of Flux Measurements
30	-	-	-	17					17
	-	-	-	19					19
	-	-	-	12					12
	-	-	-	21					21
	-	-	-	11					11
	-	-	-	56					56
	-	-	-	37					37
	-	-	-	46					46
	-	-	-	32					32
	-	-	-	18					18
	-	-	-	51					51
	-	-	-	13					13
	-	-	-	21					21
	-	-	-	18					18
31	-	-	-	45	45				90
	-	-	-	57	57				114
	-	-	-	79	79				158
	-	-	-	103	103				206
	-	-	-	45	45				90
	-	-	-	180	180				360
	-	-	-	78	78				156
	-	-	-	78	78				156
	-	-	-	31	31				62
	-	-	-	81	81				162
	-	-	-	80	80				160
	-	-	-	49	49				98
	-	-	-	50	50				100
	-	-	-	92	92				184
32	-	-	-	15					15
	-	-	-	20					20
	-	-	-	12					12
	-	-	-	7					7
	-	-	-	50					50
	-	-	-	13					13
	-	-	-	18					18
	-	-	-	16					16
	-	-	-	12					12

Appendix A, Table A-2
Surface Flux of Landfill Gas by Chemical Families from Literature.

Study No.	OM (food waste) Composition (%) Mean	OM (food waste) Composition (%) Standard Deviation	OM (food waste) Composition (%) No. Measurements	Total No. of Flux Measurements Methane	Total No. of Flux Measurements CO2	Total No. of Flux Measurements N2O	Total No. of Flux Measurements NMVOCs	Total No. of Flux Measurements CO	Total No. of Flux Measurements
	-	-	-	7					7
	-	-	-	35					35
	-	-	-	14					14
33	36.91	0	1	82					82
34	-	-	-	60					60
	-	-	-	60					60
	-	-	-	60					60
35	30.18142857	0	7	16	16				32
	-	-	-	16	16				32
	-	-	-	16	16				32
36	-	-	-	45					45
	-	-	-	45					45
	-	-	-	45					45
	-	-	-	45					45
	-	-	-	29					29
	-	-	-	42					42
	-	-	-	40					40
	-	-	-	31					31
	-	-	-	40					40
	-	-	-	31					31
	-	-	-	40					40
	-	-	-	40					40
	-	-	-	31					31
	-	-	-	31					31
	-	-	-	31					31
	-	-	-	31					31
	-	-	-	18					18
	-	-	-	30					30
	-	-	-	25					25
	-	-	-	20					20
	-	-	-	26					26
	-	-	-	26					26
	-	-	-	26					26
37	-	-	-	42	100				142
	-	-	-	166	161				327
	-	-	-	113	89				202
	-	-	-	189	192				381
	-	-	-	158	188				346
	-	-	-	152	187				339
	-	-	-	159	210				369
	-	-	-	148	227				375
	-	-	-	150	235				385
	-	-	-	204	342				546

Appendix A, Table A-2
Surface Flux of Landfill Gas by Chemical Families from Literature.

Study No.	OM (food waste) Composition (%) Mean	OM (food waste) Composition (%) Standard Deviation	OM (food waste) Composition (%) No. Measurements	Total No. of Flux Measurements Methane	Total No. of Flux Measurements CO2	Total No. of Flux Measurements N2O	Total No. of Flux Measurements NMVOCs	Total No. of Flux Measurements CO	Total No. of Flux Measurements
	-	-	-	180	269				449
38	-	-	-	56					56
	-	-	-	40					40
	-	-	-	40					40
	-	-	-	46					46
	-	-	-	43					43
	-	-	-	32					32
39	-	-	-	3					3
	-	-	-	3					3
	-	-	-	3					3
	-	-	-	3					3
	-	-	-	3					3
	-	-	-	3					3
	-	-	-	3					3
	-	-	-	3					3
	-	-	-	3					3
	-	-	-	3					3
	-	-	-	3					3
	-	-	-	3					3
	-	-	-	3					3
	-	-	-	3					3
	-	-	-	3					3
	-	-	-	3					3
	-	-	-	3					3
40	-	-	-	50	0	0			50
	-	-	-	50	0	0			50
	-	-	-	50	50	50	50		200
	-	-	-	50	50	50	50		200
	-	-	-	61	61	61	61		244
	-	-	-	61	61	61	61		244
	-	-	-	30	30	30	30		120
	-	-	-	30	30	30	30		120
	-	-	-	33	33	33	33		132
	-	-	-	33	33	33	33		132
	-	-	-	60	60	60	60		240
	-	-	-	60	60	60	60		240
	-	-	-	23	23	23	23		92
	-	-	-	23	23	23	23		92
41	-	-	-	480					480
	-	-	-	360					360
	-	-	-	240					240
	-	-	-	6					6
	-	-	-	6					6
	-	-	-	6					6
	-	-	-	6					6
	-	-	-	6					6

Study No.	OM (food waste) Composition (%) Mean	OM (food waste) Composition (%) Standard Deviation	OM (food waste) Composition (%) No. Measurements	Total No. of Flux Measurements Methane	Total No. of Flux Measurements CO2	Total No. of Flux Measurements N2O	Total No. of Flux Measurements NMVOCs	Total No. of Flux Measurements CO	Total No. of Flux Measurements
42	-	-	-	6					6
	-	-	-	6					6
	-	-	-	6					6
	-	-	-	6					6
	-	-	-	6					6
	-	-	-	6					6
	-	-	-	6					6
	-	-	-	6					6
	-	-	-	6					6
	-	-	-	4					4
	-	-	-	4					4
	-	-	-	4					4
	-	-	-	4					4
	-	-	-	4					4
	-	-	-	4					4
	-	-	-	4					4
	-	-	-	4					4
	-	-	-	4					4
	-	-	-	4					4
	-	-	-	4					4
	-	-	-	4					4
	-	-	-	4					4
	-	-	-	4					4
	-	-	-	4					4
	-	-	-	4					4
	-	-	-	4					4
	-	-	-	4					4
43	-	-	-	5	5	5			15
	-	-	-	5	5	5			15
	-	-	-	5	5	5			15
	-	-	-	5	5	5			15
	-	-	-	5	5	5			15
	-	-	-	5	5	5			15
	-	-	-	5	5	5			15
	-	-	-	5	5	5			15
	-	-	-	5	5	5			15
	-	-	-	5	5	5			15
	-	-	-	5	5	5			15
	-	-	-	5	5	5			15
	-	-	-	5	5	5			15
	-	-	-	5	5	5			15
	-	-	-	5	5	5			15
	-	-	-	5	5	5			15
	-	-	-	5	5	5			15
44	-	-	-	1					1
	-	-	-	1					1
	-	-	-	1					1

Study No.	OM (food waste) Composition (%) Mean	OM (food waste) Composition (%) Standard Deviation	OM (food waste) Composition (%) No. Measurements	Total No. of Flux Measurements Methane	Total No. of Flux Measurements CO2	Total No. of Flux Measurements N2O	Total No. of Flux Measurements NMVOCs	Total No. of Flux Measurements CO	Total No. of Flux Measurements
44	-	-	-	1					1
	-	-	-	1					1
	-	-	-	1					1
45	-	-	-	4			361		365
46	-	-	-	19	19		160		197.6666667
	-	-	-	10	10		160		179.6666667
	-	-	-	20	20		160		199.6666667
47	-	-	-	92					92
	-	-	-	108					108
	-	-	-	73					73
48	-	-	-	14			3		17
	-	-	-	14			0		14
	-	-	-	14			0		14
	-	-	-	14			0		14
	-	-	-	14			0		14
49	-	-	-	26					26
	-	-	-	16					16
	-	-	-	4					4
	-	-	-	26					26
	-	-	-	16					16
	-	-	-	4					4
	-	-	-	23					23
	-	-	-	16					16
	-	-	-	6					6
	-	-	-	23					23
	-	-	-	16					16
	-	-	-	6					6
	-	-	-	4					4
	-	-	-	4					4
	-	-	-	4					4
	-	-	-	4					4
	-	-	-	4					4
	-	-	-	4					4
	-	-	-	4					4
	-	-	-	4					4
	-	-	-	4					4
	-	-	-	4					4
	-	-	-	4					4
	-	-	-	4					4
	-	-	-	4					4
	-	-	-	4					4

Study No.	OM (food waste) Composition (%) Mean	OM (food waste) Composition (%) Standard Deviation	OM (food waste) Composition (%) No. Measurements	Total No. of Flux Measurements Methane	Total No. of Flux Measurements CO2	Total No. of Flux Measurements N2O	Total No. of Flux Measurements NMVOCs	Total No. of Flux Measurements CO	Total No. of Flux Measurements
50	-	-	-	4					4
	-	-	-	4					4
	-	-	-	4					4
	-	-	-	4					4
	-	-	-	4					4
	-	-	-	4					4
	-	-	-	4					4
	-	-	-	4					4
	-	-	-	4					4
	-	-	-	4					4
	-	-	-	4					4
	-	-	-	4					4
	-	-	-	4					4
	-	-	-	4					4
	-	-	-	4					4
	-	-	-	4					4
	-	-	-	4					4
	-	-	-	4					4
	-	-	-	4					4
	-	-	-	4					4
51	-	-	-	36	36		74		146
52	-	-	-	24					24
	-	-	-	2					2
	-	-	-	2					2
53	53.145	10.66750346	6	232	232				464
54	75	0	1	36	36	36			108
	-	-	-	24	25	24			73
55,56,57	48.32	0	1	73	0				73
	-	-	-	81	81				162
	-	-	-	81	0				81
	-	-	-	81	0				81
	-	-	-	80	0				80

Study No.	OM (food waste) Composition (%) Mean	OM (food waste) Composition (%) Standard Deviation	OM (food waste) Composition (%) No. Measurements	Total No. of Flux Measurements Methane	Total No. of Flux Measurements CO2	Total No. of Flux Measurements N2O	Total No. of Flux Measurements NMVOCs	Total No. of Flux Measurements CO	Total No. of Flux Measurements
58	52	0	1	40	40				80
59	-	-	-	9	9				18
	-	-	-	11	11				22
	-	-	-	12	12				24
	-	-	-	6	6				12
	-	-	-	10	10				20
	-	-	-	8	8				16
	-	-	-	3	3				6
	-	-	-	3	3				6
	-	-	-	3	3				6
	-	-	-	3	3				6
	-	-	-	12	12				24
	-	-	-	11	11				22
	-	-	-	8	8				16
	-	-	-	11	1				12
60	-	-	-	6	6				12
	-	-	-	7	7				14
	-	-	-	6	6				12
	-	-	-	6	6				12
	-	-	-	7	7				14
	-	-	-	6	6				12
	-	-	-	6	6				18
	-	-	-	6	6				12
	-	-	-	6	6				12
61	46.562	2.489943774	5	12	12	12			36
	46.562	2.489943774	5	13	13	13			39
	32.4	0.674199862	12	5					5
	32.4	0.674199862	12	5					5
	32.4	0.674199862	12	5					5
	32.4	0.852802865	12	5					5
	32.4	0.852802865	12	8					8
	32.4	0.852802865	12	8					8
	32.4	0.852802865	12	8					8
	32.4	0.674199862	12	8					8

Appendix A, Table A-2
Surface Flux of Landfill Gas by Chemical Families from Literature.

Study No.	OM (food waste) Composition (%) Mean	OM (food waste) Composition (%) Standard Deviation	OM (food waste) Composition (%) No. Measurements	Total No. of Flux Measurements Methane	Total No. of Flux Measurements CO2	Total No. of Flux Measurements N2O	Total No. of Flux Measurements NMVOCs	Total No. of Flux Measurements CO	Total No. of Flux Measurements
62,63	-	-	-	5					5
	-	-	-	5					5
	-	-	-	5					5
	-	-	-	5					5
	-	-	-	8					8
	-	-	-	8					8
	-	-	-	8					8
	-	-	-	8					8
64	-	-	-	13	14				27
	-	-	-	9	9				18
	-	-	-	13	14				27
	-	-	-	9	9				18
	-	-	-	13	14				27
	-	-	-	9	9				18
	-	-	-	13	13				26
	-	-	-	9	8				17
65	-	-	-	6	6	6			18
66	-	-	-	2					2
	-	-	-	2					2
	-	-	-	2					2
	-	-	-	3					3
	-	-	-	2					2

Study No.	OM (food waste) Composition (%) Mean	OM (food waste) Composition (%) Standard Deviation	OM (food waste) Composition (%) No. Measurements	Total No. of Flux Measurements Methane	Total No. of Flux Measurements CO2	Total No. of Flux Measurements N2O	Total No. of Flux Measurements NMVOCs	Total No. of Flux Measurements CO	Total No. of Flux Measurements
	-	-	-	2					2
67	-	-	-	40					40
	-	-	-	41					41
	-	-	-	30					30
	-	-	-	31					31
	-	-	-	30					30
	-	-	-	40					40
	-	-	-	30					30
	-	-	-	32					32
	-	-	-	20					20
	-	-	-	20					20
	-	-	-	22					22
	-	-	-	20					20
	-	-	-	16					16
	-	-	-	16					16
68	-	-	-	37	37	37			111
	-	-	-	37	37	37			111
	-	-	-	37	37	37			111
	-	-	-	37	37	37			111
	-	-	-	37	37	37			111
	-	-	-	37	37	37			111
	-	-	-	37	37	37			111
69	30.60575396	3.798074186	3	17	17				34
	30.60575396	3.798074186	3	18	18				36
	30.60575396	3.798074186	3	4	4				8
	30.60575396	3.798074186	3	30	30				60
	20.94878444	5.288754695	4	10	10				20
	20.94878444	5.288754695	4	8	8				16
	20.94878444	5.288754695	4	7	7				14
	20.94878444	5.288754695	4	12	12				24
	20.94878444	5.288754695	4	17	17				34
70	55	20	-	88	88				176
	55	20	-	64	64				128
71	-	-	-	73	73	73			219
	-	-	-	100	100	100			300
72	-	-	-	22	22	22			66
73	-	-	-	4	4				8
	-	-	-	4	4				8
	-	-	-	4	4				8
	-	-	-	4	4				8
	-	-	-	4	4				8
	-	-	-	4	4				8
	-	-	-	4	4				8
	-	-	-	9	9				18
	-	-	-	4	4				8

Appendix A, Table A-2

Surface Flux of Landfill Gas by Chemical Families from Literature.

Study No.	OM (food waste) Composition (%) Mean	OM (food waste) Composition (%) Standard Deviation	OM (food waste) Composition (%) No. Measurements	Total No. of Flux Measurements Methane	Total No. of Flux Measurements CO2	Total No. of Flux Measurements N2O	Total No. of Flux Measurements NMVOCs	Total No. of Flux Measurements CO	Total No. of Flux Measurements
74	-	-	-	1					1
	-	-	-	1					1
	-	-	-	1					1
	-	-	-	1					1
	-	-	-	1					1
75	-	-	-	24					24
76	-	-	-	1118					1118
	-	-	-	43					43
	-	-	-	43					43
	-	-	-	43					43
	-	-	-	43					43
	-	-	-	43					43
	-	-	-	43					43
	-	-	-	31					31
	-	-	-	31					31
	-	-	-	31					31
	-	-	-	31					31
	-	-	-	31					31
	-	-	-	31					31
	-	-	-	31					31
	-	-	-	39					39
	-	-	-	39					39
	-	-	-	39					39
	-	-	-	39					39
	-	-	-	39					39
	-	-	-	39					39
	-	-	-	9					9
	-	-	-	9					9
	-	-	-	9					9
	-	-	-	9					9
	-	-	-	9					9
	-	-	-	9					9
	-	-	-	31					31
	-	-	-	31					31
	-	-	-	31					31
	-	-	-	31					31
	-	-	-	31					31
	-	-	-	31					31
	-	-	-	40					40

Study No.	OM (food waste) Composition (%) Mean	OM (food waste) Composition (%) Standard Deviation	OM (food waste) Composition (%) No. Measurements	Total No. of Flux Measurements Methane	Total No. of Flux Measurements CO2	Total No. of Flux Measurements N2O	Total No. of Flux Measurements NMVOCs	Total No. of Flux Measurements CO	Total No. of Flux Measurements
77	-	-	-	40					40
	-	-	-	81					81
	-	-	-	51					51
78	55	20	-	32					32
	55	20	-	32					32
	55	20	-	32					32
	55	20	-	48					48
	55	20	-	48					48
	55	20	-	48					48
	55	20	-	24					24
	55	20	-	24					24
	55	20	-	24					24
79	44.4	0	1	10					10
	44.4	0	1	10					10
80	-	-	-	16					16
	-	-	-	16					16
	-	-	-	16					16
	-	-	-	16					16
	-	-	-	16					16
81	58.3	0	1	55					55
82	-	-	-	9	9				18
	-	-	-	36	36				72
	-	-	-	4	4				8
83	64.9	0	1	32	32				64
	64.9	0	1	32	32				64
	64.9	0	1	32	32				64
84	35.4	0	1	5					5
	47.5	0	1	4					4
	34.9	0	1	4					4
	36.8	0	1	5					5
	39.6	0	1	5					5
	30.2	0	1	5					5
85	-	-	-	17	24				41
	-	-	-	14	25				39
	-	-	-	15	28				43
86	-	-	-	139					139
	-	-	-	139					139
	-	-	-	30		30			60
	-	-	-	30		30			60
	-	-	-	30		30			60
	-	-	-	30		30			60
	-	-	-	30		30			60

Study No.	OM (food waste) Composition (%) Mean	OM (food waste) Composition (%) Standard Deviation	OM (food waste) Composition (%) No. Measurements	Total No. of Flux Measurements Methane	Total No. of Flux Measurements CO2	Total No. of Flux Measurements N2O	Total No. of Flux Measurements NMVOCs	Total No. of Flux Measurements CO	Total No. of Flux Measurements
87	-	-	-	30		30			60
	-	-	-	30		30			60
	-	-	-	30		30			60
	-	-	-	30		30			60
	-	-	-	30		30			60
	-	-	-	30		30			60
	-	-	-	30		30			60
88	57.13333333	1.936491673	9	30					30
	57.13333333	1.936491673	9	30					30
	57.13333333	1.936491673	9	30					30
	57.13333333	1.936491673	9	30					30
	57.13333333	1.936491673	9	30					30
	57.13333333	1.936491673	9	30					30
	57.13333333	1.936491673	9	30					30
	57.13333333	1.936491673	9	30					30
	57.13333333	1.936491673	9	30					30
	57.13333333	1.936491673	9	30					30
	57.13333333	1.936491673	9	30					30
	57.13333333	1.936491673	9	30					30
89	-	-	-	6	6	6			18
	-	-	-	6	6	6			18
	-	-	-	6	6	6			18
	-	-	-	6	6	6			18
	-	-	-	6	6	6			18
	-	-	-	6	6	6			18
90	-	-	-	2					2
	-	-	-	2					2
	-	-	-	2					2
	-	-	-	1					1
91	-	-	-	0					0
	-	-	-	0					0
92	-	-	-	0	281				281
93	-	-	-	0	107				107
94	-	-	-	0	81				81
	-	-	-	0	81				81
95	-	-	-	0	7920				7920
96	-	-	-	0	1038				1038
97	-	-	-	0	0	4			4
	-	-	-	0	0	4			4
	-	-	-	0	0	4			4
	-	-	-	0	0	4			4

Study No.	OM (food waste) Composition (%) Mean	OM (food waste) Composition (%) Standard Deviation	OM (food waste) Composition (%) No. Measurements	Total No. of Flux Measurements Methane	Total No. of Flux Measurements CO2	Total No. of Flux Measurements N2O	Total No. of Flux Measurements NMVOCs	Total No. of Flux Measurements CO	Total No. of Flux Measurements
	-	-	-	0	0	4			4
98	-	-	-	0	0	16			16
	-	-	-	0	0	12			12
	-	-	-	0	0	28			28
	-	-	-	0	0	20			20
	-	-	-	0	0	20			20
99	-	-	-	0	0	9			9
	-	-	-	0	0	7			7
	-	-	-	0	0	10			10
100	-	-	-	0	0	12			12
	-	-	-	0	0	16			16
	-	-	-	0	0	5			5
	-	-	-	0	0	6			6
101	-	-	-	0	0	39			39
	-	-	-	0	0	17			17
	-	-	-	0	0	12			12
	-	-	-	0	0	26			26
	-	-	-	0	0	13			13
	-	-	-	0	0	14			14
	-	-	-	0	0	37			37
	-	-	-	0	0	14			14
	-	-	-	0	0	37			37
	-	-	-	0	0	22			22
	-	-	-	0	0	7			7
	-	-	-	0	0	88			88
	-	-	-	0	0	38			38

Study No.	OM (food waste) Composition (%) Mean	OM (food waste) Composition (%) Standard Deviation	OM (food waste) Composition (%) No. Measurements	Total No. of Flux Measurements Methane	Total No. of Flux Measurements CO2	Total No. of Flux Measurements N2O	Total No. of Flux Measurements NMVOCs	Total No. of Flux Measurements CO	Total No. of Flux Measurements
	-	-	-	0	0	14			14
	-	-	-	0	0	48			48
	-	-	-	0	0	8			8
	-	-	-	0	0	6			6
102	-	-	-	0	0	30			30
	-	-	-	0	0	30			30
	-	-	-	0	0	30			30
	-	-	-	0	0	30			30
	-	-	-	0	0	30			30
	-	-	-	0	0	30			30
	-	-	-	0	0	30			30
	-	-	-	0	0	30			30
	-	-	-	0	0	30			30
	-	-	-	0	0	30			30
	-	-	-	0	0	30			30
	-	-	-	0	0	30			30
103	-	-	-	0	0	**3**			3
104	-	-	-	0	0	**3**			3
105	-	-	-	0	0	0	344		344
106	-	-	-	0	0	0	24		24
	-	-	-	0	0	0	24		24
107	-	-	-	0	0	0	700		700
108	-	-	-	0	0	0	340		340
	-	-	-	0	0	0	340		340
	-	-	-	0	0	0	340		340
	-	-	-	0	0	0	513		513.3333333
	-	-	-	0	0	0	513		513.3333333
	-	-	-	0	0	0	513		513.3333333
			Total:	16193	15613	2444	5667	1	39918

Footnotes:

[1]If not given in study, estimated using time period between start of landfilling to beginning of testing period

[2]Soil texture deduced using USDA standard soil classification triangle

[3]If landfill site was closed, it was assumed that the soil cover was Final

[4]If flux units were volumetric, the conversion to g/m2/day was conducted using 0.716 g/L density at NTP for methane, 1.96 g/L for CO2, and 1.83 g/L for N2O (applies to all remaining rows in the study)

[5]If a standard deviation was not given, the range rule technique was used to estimate SD (applies to all remaining rows in the study)

[6]The volumetric WIP was estimated for this LF site given the area and depth of the waste

[7]The gravimetric WIP and presence of a gas extraction system was included based on US EPA site specific LF data for the year 2017

[8]If standard deviation or a range was not given, the mean value was assume to be a point estimate (no. of measurements = 1 and SD = 0)

[9]Estimated using the group mean/stdev method

[*]Indicates the flux units were given in mg-C/m2/day, or mg-N/m2/day and needed to be converted to mg-CH4/m2/day, mg-CO2/m2/day or mg-N2O/m2/day

Chemical Family	Chemical Name	Min	Mean	Max	Standard Deviation	Number of Samples
Baseline GHGs	Methane	-45	7.85E+01	4.15E+04	4.78E+02	15873
	Carbon dioxide	-21.38	2.81E+02	1.24E+05	1.40E+03	14249
	Nitrous Oxide	-0.002544	6.50E-02	3.76E+00	3.26E+01	2344
	Carbon Monoxide	-	-	-	-	-
Reduced sulfur compounds	Carbonyl sulfide	-0.001655708	1.40E-03	1.28E-02	3.02E-03	24
	Dimethyl sulfide	-	-	-	-	-
	Dimethyl disulfide	-	-	-	-	-
	Carbon disulfide	-	-	-	-	-
F-gases	CFC-11	-0.000184	5.29E-05	2.57E-01	2.93E-04	47
	CFC-12	-1.68E-05	1.97E-04	5.14E-03	8.81E-04	34
	CFC-113	-5.96E-07	8.34E-06	6.31E-05	1.16E-05	34
	CFC-114	-8.14E-08	3.22E-05	2.53E-04	7.80E-05	10
	HCFC-21	-	5.00E-03	-	-	1
	HCFC-22	-4.89E-06	7.43E-06	3.43E-03	1.72E-05	12
	HCFC-141b	3.63E-06	1.54E-05	6.66E-05	2.27E-05	7
	HCFC-142b	-3.50E-07	-	4.93E-03	-	56
	HFC-134a	-2.59E-06	1.25E-06	5.49E-06	3.04E-06	7
	HFC-152a	4.00E-07	-	6.76E-02	-	56
	HFC-245fa	9.74E-09	-	5.21E-02	-	56
	HFC-365mfc	-	-	-	-	-
	H-1211	-1.09E-08	-2.80E-06	2.61E-07	1.32E-05	20
Halogenated Hydrocarbons	Chloroform	-0.000162038	9.74E-05	8.10E-04	2.53E-04	118
	Methyl-Chloroform	-6.69E-08	4.87E-05	2.61E-05	1.15E-04	84
	Carbon tetrachloride	-1.88E-06	1.62E-04	7.00E-06	3.91E-04	83
	Methylene chloride	-2.10E-05	-7.52E-07	5.14E-06	5.02E-06	25
	Trichloroethylene	-4.92E-06	7.19E-05	2.14E-04	3.04E-04	91
	Tetrachloroethylene	-6.24E-07	9.73E-05	1.15E-04	3.12E-04	92
	Methyl chloride	-8.09E-06	6.04E-06	8.29E-05	1.70E-05	29
	Bromomethane	-5.89E-08	8.19E-07	3.23E-06	1.05E-06	8
	Dibromomethane	1.10E-08	1.47E-08	2.10E-08	5.42E-09	3
	Bromodichloromethane	-	1.56E-04	-	4.14E-04	50
	Bromoform	1.24E-07	1.97E-07	3.40E-07	7.67E-08	9
	Chloroethane	1.58E-06	2.87E-06	3.33E-06	8.61E-07	4
	1,2-Dichloroethane	2.00E-07	1.05E-06	3.10E-06	6.75E-07	15
	1,2-Dibromoethane	-9.48E-06	1.62E-04	-	4.70E-04	52
Organic Alkyl Nitrates	Methyl nitrate	-3.48E-08	3.22E-08	3.29E-07	1.31E-07	7
	Ethyle nitrate	-2.18E-08	2.64E-08	2.03E-07	7.93E-08	7
	Isopropyl nitrate	-5.33E-08	9.70E-08	2.59E-07	1.17E-07	7
	N-propyl nitrate	-1.80E-08	-4.35E-09	4.88E-09	8.32E-09	7
	2-Butyl nitrate	-9.54E-08	-2.04E-08	7.08E-08	5.46E-08	7
	Ethane	1.42E-06	3.22E-03	7.70E-02	1.19E-02	54
	Propane	-6.45E-05	4.09E-03	7.39E-02	1.60E-02	21

Chemical Family	Chemical Name	Min	Mean	Max	Standard Deviation	Number of Samples
Alkanes	i-Butane	-0.000115	6.16E-04	7.21E-03	1.57E-03	21
	n-Butane	-0.000145	2.95E-04	2.05E-03	5.08E-04	21
	i-Pentane	-2.57E-05	5.20E-04	2.95E-03	8.86E-04	21
	n-Pentane	-3.64E-06	5.85E-05	3.13E-04	7.69E-05	36
	n-Hexane	1.76E-07	8.41E-05	8.64E-04	2.36E-04	35
	n-Undecane	-	-	-	-	-
Alkenes	Ethene	2.30E-07	1.12E-04	1.00E-03	2.36E-04	48
	Propene	-3.85E-06	1.66E-04	7.22E-04	2.61E-04	21
	1-Butene	-6.46E-07	2.16E-05	8.98E-05	3.23E-05	21
	i-Butene	-7.15E-07	4.35E-05	1.87E-04	6.14E-05	21
	trans-2-Butene	1.56E-06	8.21E-06	1.90E-05	6.28E-06	9
	cis-2-Butene	-2.27E-06	3.39E-06	1.84E-05	5.26E-06	18
	1-Pentene	2.09E-06	7.70E-06	1.78E-05	5.42E-06	9
	Isoprene	-3.00E-06	1.36E-05	6.22E-05	1.99E-05	19
Aldehydes/	Ethyne	-3.70E-06	1.43E-05	2.92E-04	5.21E-05	43
Alkynes	Acetaldehyde	-	1.12E-03	-	1.83E-03	99
	Butanal	-	1.81E-04	-	5.00E-04	50
Aromatic Hydrocarbons	Benzene	-8.57E-06	2.72E-03	2.04E-02	1.63E-02	199
	Toluene	-9.49E-05	7.00E-03	2.90E-02	3.06E-02	181
	Ethylbenzene	-8.56E-05	1.01E-02	2.07E-02	4.75E-02	145
	m+p-Xylene	1.00E-06	1.42E-05	7.20E-05	1.86E-05	17
	o-Xylene	3.00E-07	7.27E-03	1.97E-03	2.69E-02	63
	m-Xylene	6.49E-06	2.39E-02	2.96E-03	7.74E-02	57
	p-Xylene	2.24E-06	6.31E-03	1.12E-03	2.04E-02	57
	m+p+o-Xylene	-0.000404	1.90E-03	9.64E-02	1.16E-02	69
	i-Propylbenzene	1.43E-06	5.91E-05	1.30E-04	4.70E-05	8
	n-Propylbenzene	-	-	-	-	-
	3-Ethyltoluene	1.54E-06	3.22E-04	6.06E-04	2.69E-04	8
	4-Ethyltoluene	3.63E-06	5.19E-04	5.75E-03	1.51E-03	14
	2-Ethyltoluene	7.30E-06	1.11E-04	2.28E-04	8.30E-05	7
	1,3,5-Trimethylbenzene	-3.13E-06	3.78E-04	6.78E-03	1.44E-03	22
	1,2,3-Trimethylbenzene	1.00E-07	5.20E-07	2.30E-06	5.68E-07	15
	1,2,4-Trimethylbenzene	-4.39E-05	2.76E-04	5.59E-03	1.16E-03	23
Monoterpenes	alpha-Pinene	-0.000107776	9.28E-03	3.00E-01	4.48E-02	46
	beta-Pinene	-9.13E-05	6.63E-05	8.10E-04	1.81E-04	24
	Limonene	1.00E-07	5.57E-05	3.15E-04	9.53E-05	24
Alcohols	Methanol	-1.90E-05	5.60E-04	4.48E-03	1.13E-03	26
	Ethanol	4.60E-06	1.01E-01	7.75E-05	5.18E-01	44
	Isopropanol	3.00E-09	1.27E-02	9.00E-06	4.49E-02	33
	2-Butanol	-	-	-	-	-
Ketones	Acetone	3.47E-05	1.86E-03	1.74E-02	3.51E-03	136
	Butanone	-	-	-	-	-
	Methylisobutylketone	9.00E-07	1.96E-06	4.50E-06	1.32E-06	15

Gas flux measurements in grams per cubic meter per day.

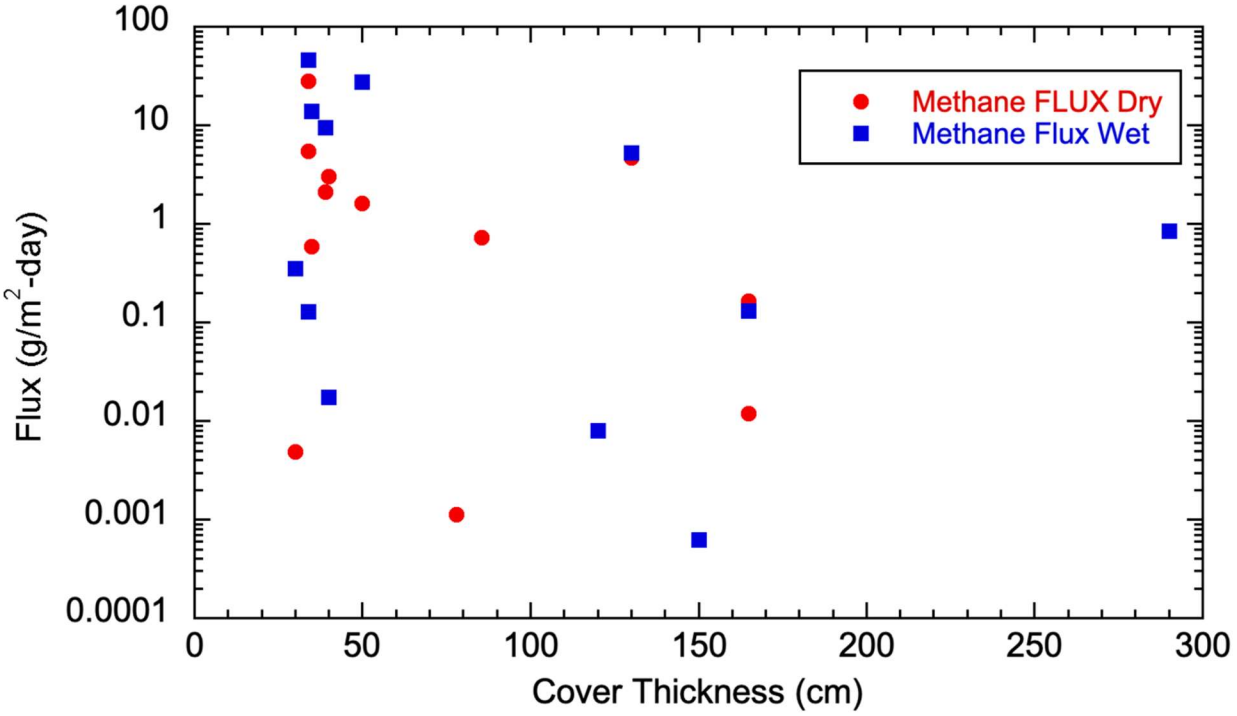

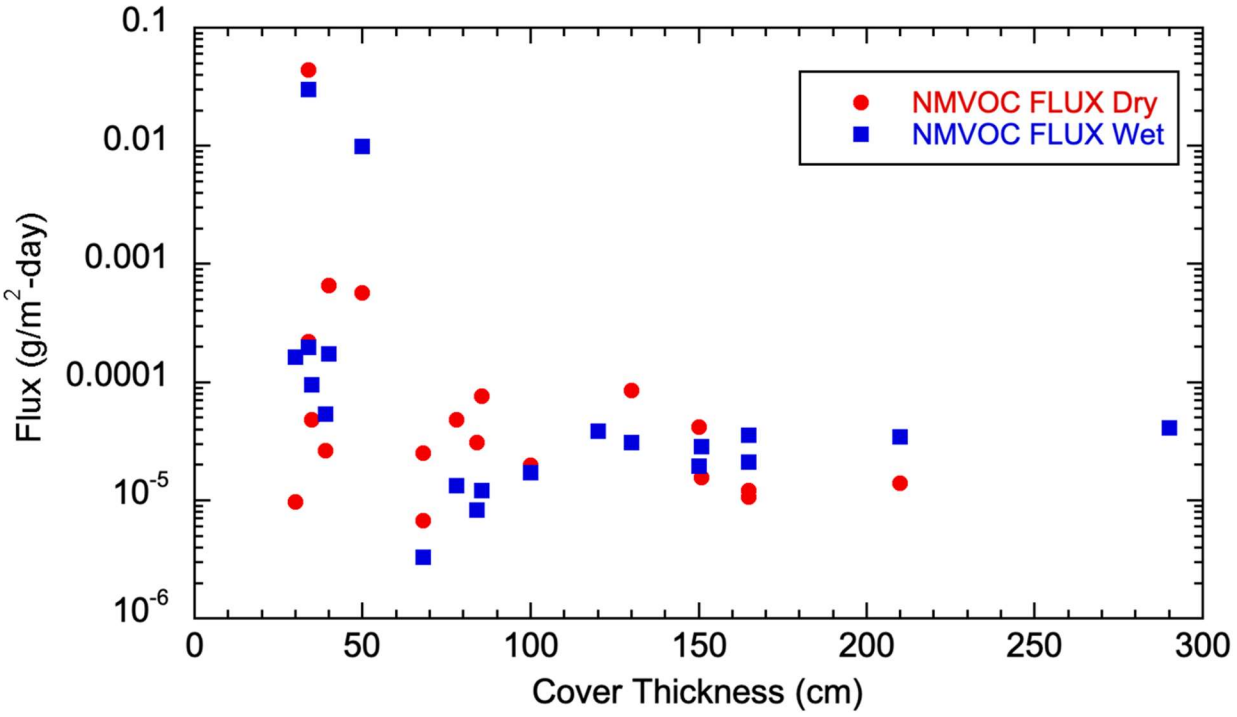

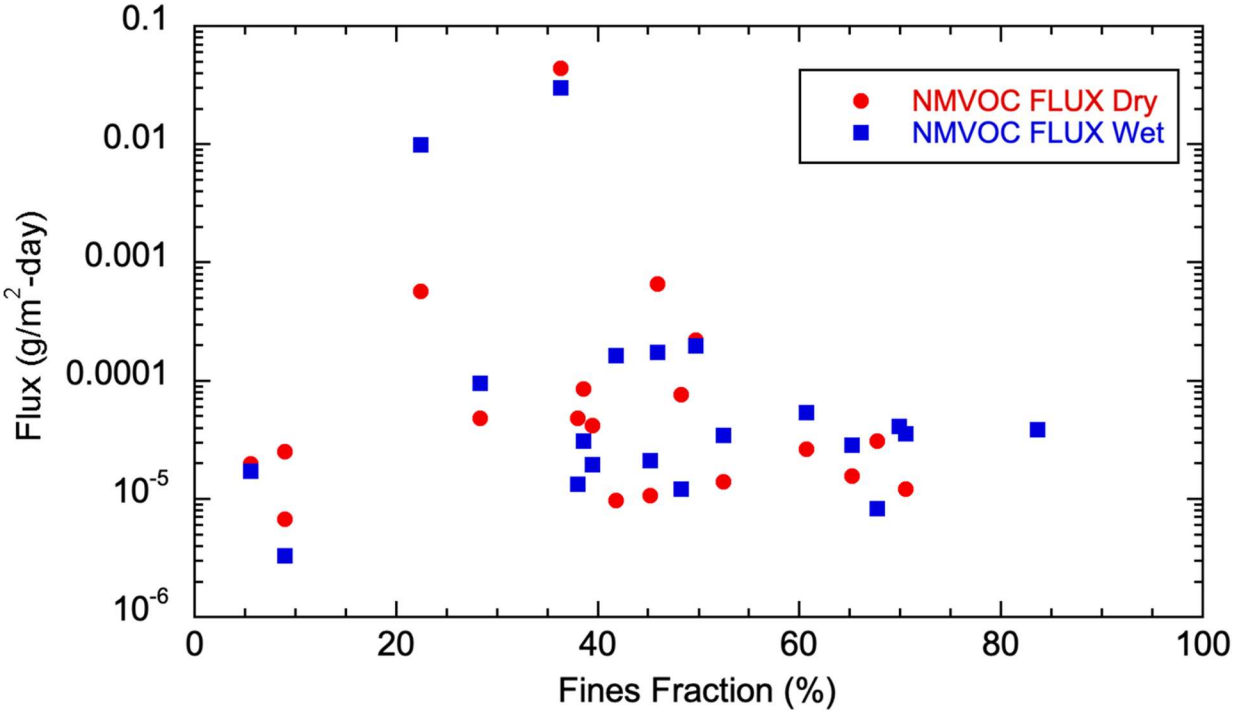

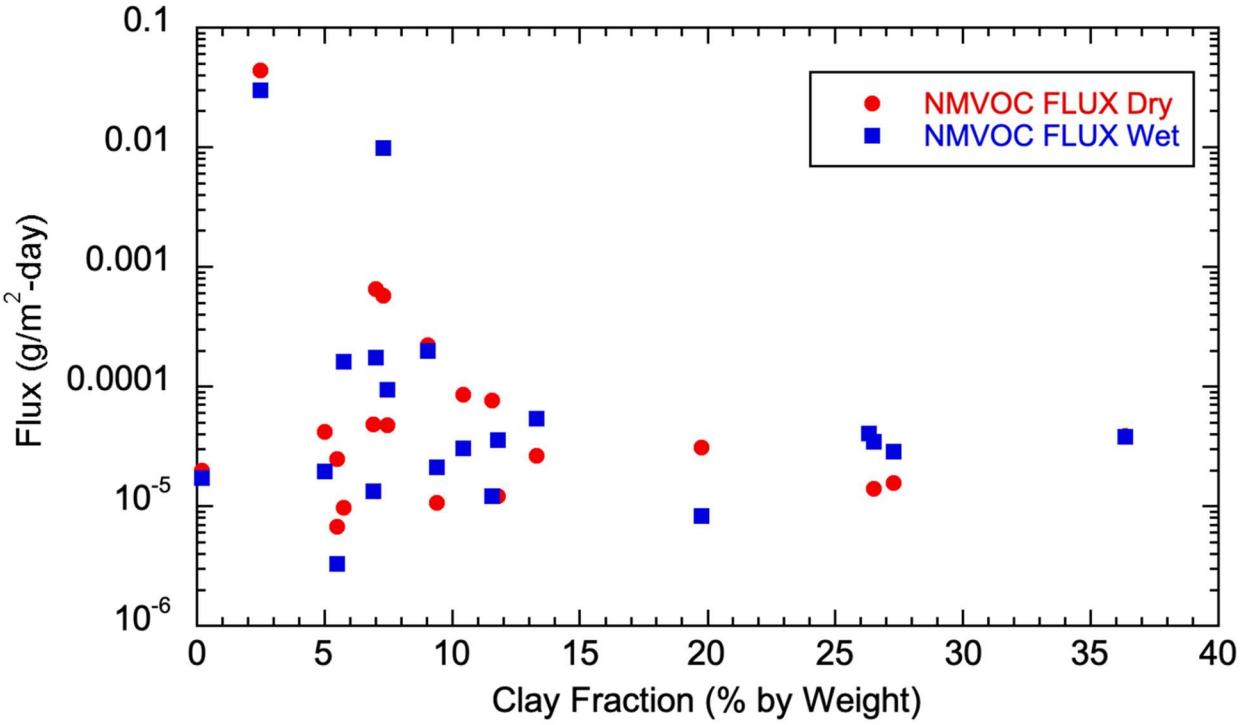

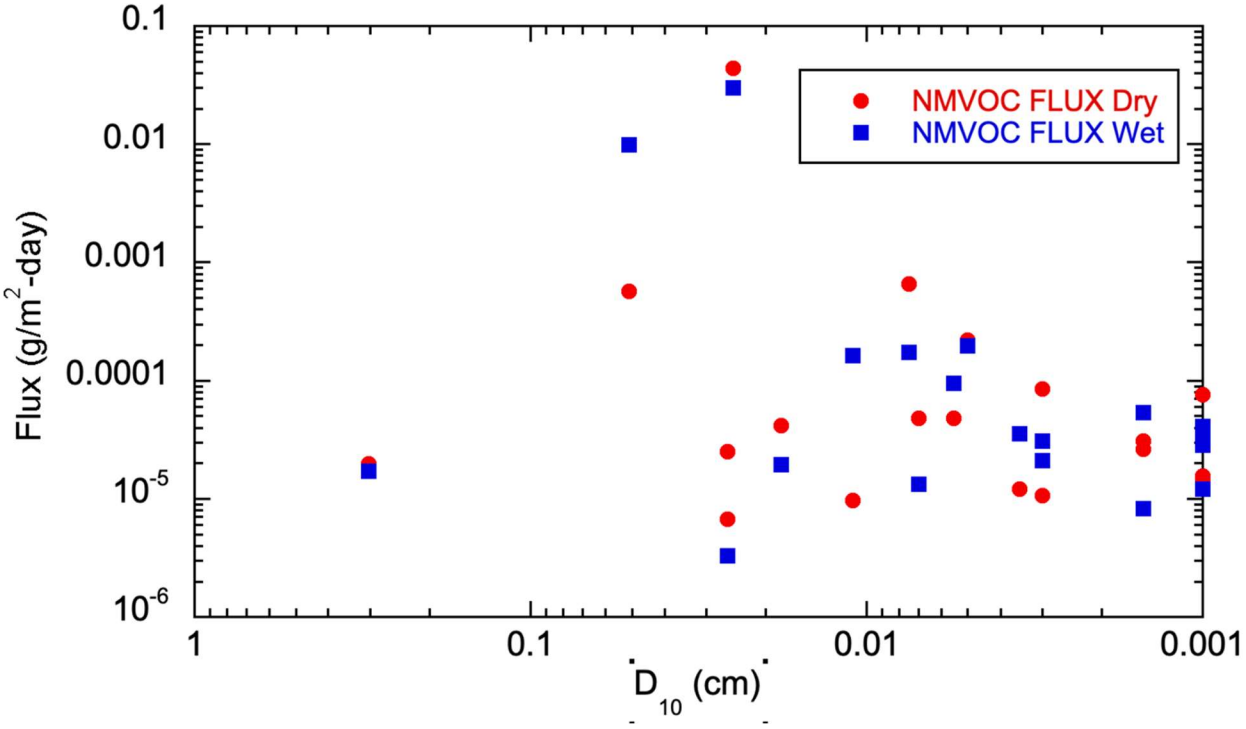

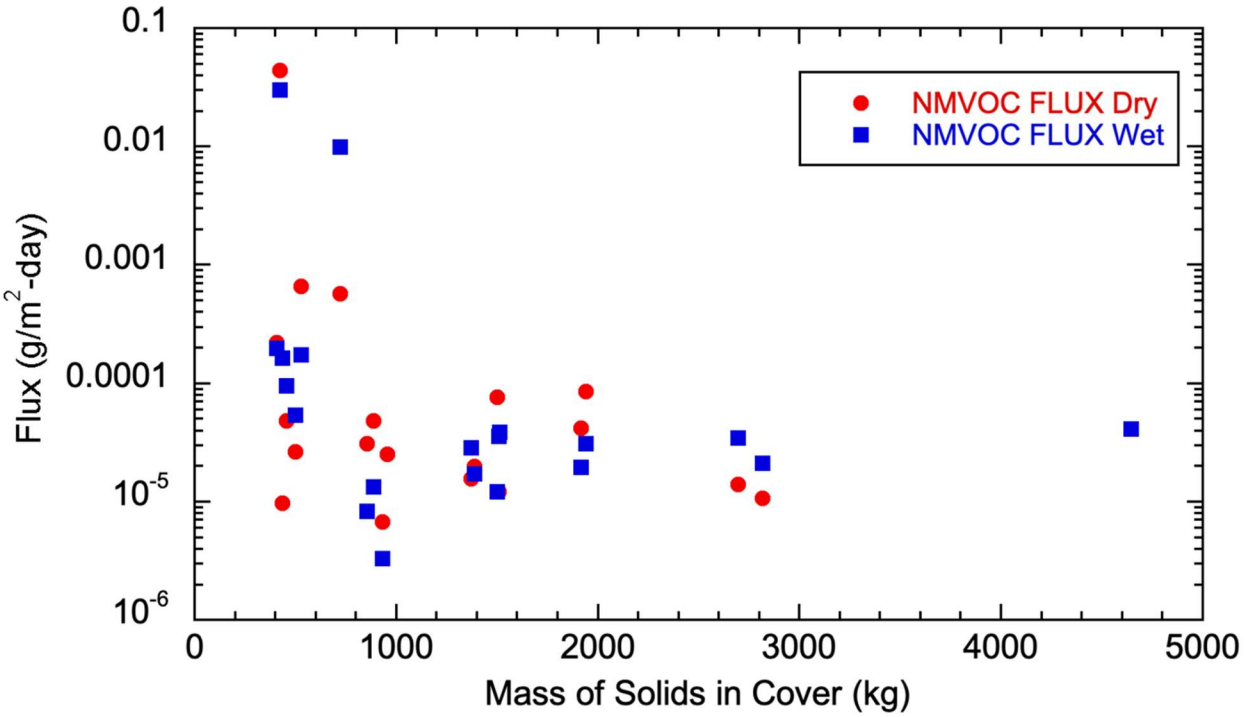

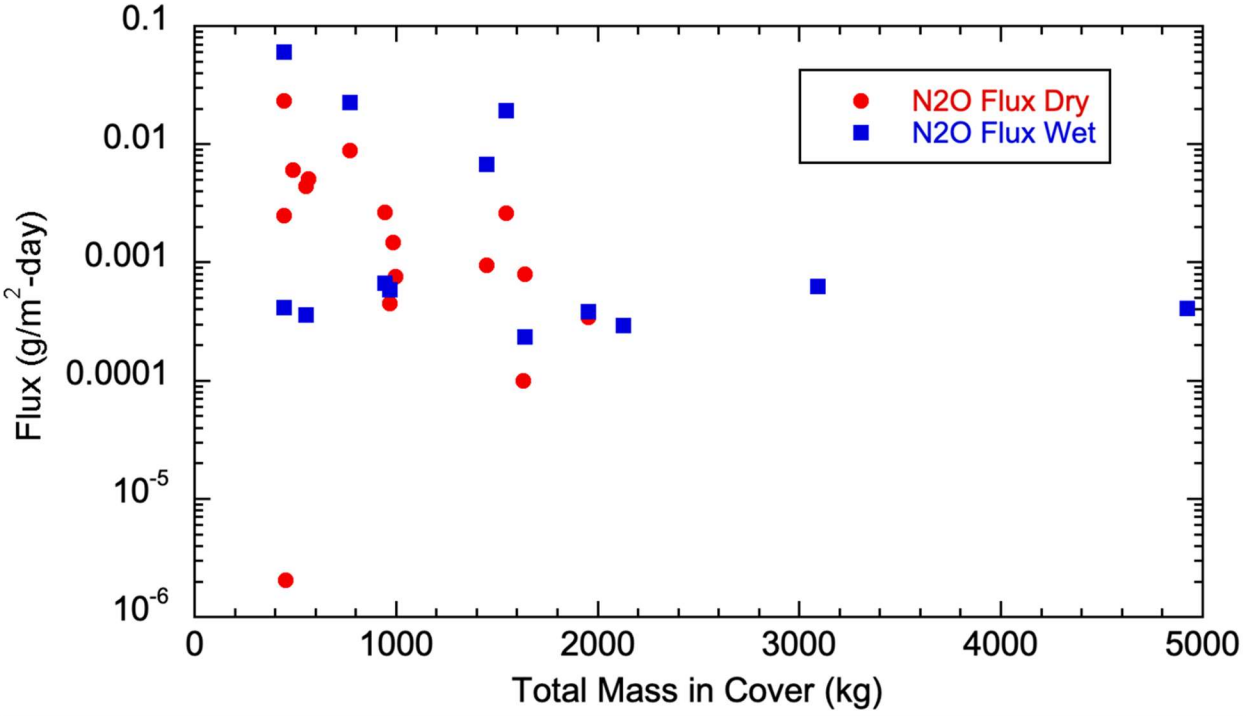

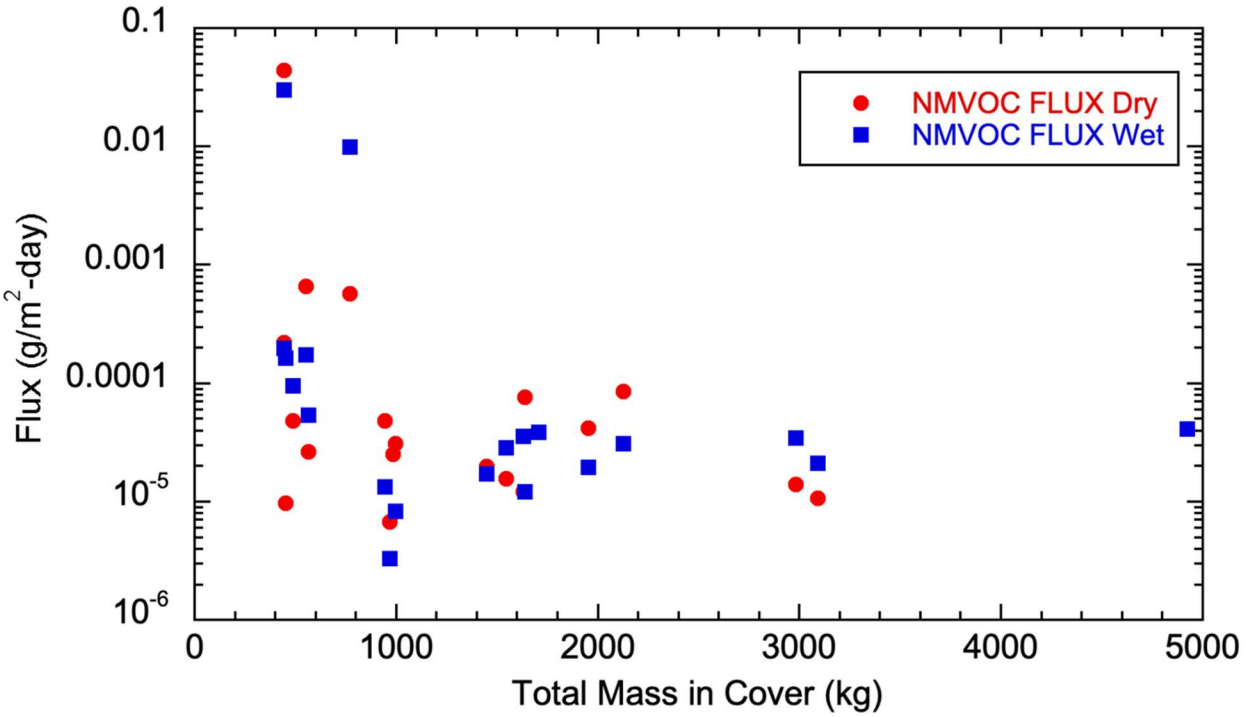

APPENDIX B

SWIS No	Name	Total LFG Collected (scf) (1)	Category	Unit No	Regulatory Status	Operational Status	Accepted Waste	Tires (Y/)
01-AA-0009	Site A	2,619,948,500	Disposal	01	Permitted	Active	Ash,Construction/demolition,Contaminated soil,Green Materials,Industrial,Mixed municipal,Other designated,Tires, Shreds	Y
01-AA-0010	Vasco Road Sanitary Landfill	111,447,852	Disposal	01	Permitted	Active	Construction/demolition,Contaminated soil,Green Materials,Industrial,Mixed municipal,Other designated	
04-AA-0002	Neal Road Recycling and Waste Facility	377,106,426	Disposal	01	Permitted	Active	Construction/demolition,Green Materials,Inert,Metals,Mixed municipal,Sludge (BioSolids),Tires,Wood waste	Y
05-AA-0023	Rock Creek Landfill	55,562,289	Disposal	01	Permitted	Active	Agricultural,Ash,Construction/demolition,Mixed municipal,Sludge (BioSolids),Tires	Y
06-AA-0002	Stonyford Disposal Site	-	Disposal	01	Permitted	Active	Agricultural,Construction/demolition,Mixed municipal,Tires	Y
07-AA-0002	Acme Landfill	183,000,000	Disposal	01	Permitted	Active	Construction/demolition,Green Materials	
07-AA-0032	Keller Canyon Landfill	1,124,204,392	Disposal	01	Permitted	Active	Agricultural,Construction/demolition,Industrial,Mixed municipal,Other designated,Sludge (BioSolids)	
07-AC-0042	USS-Posco Industries Waste Mgmt Unit II	-	Disposal	01	Exempt	Active	Contaminated soil,Inert	
09-AA-0003	Union Mine Disposal Site	111,081,705	Disposal	01	Permitted	Active	Agricultural,Asbestos,Ash,Construction/demolition,Industrial,Mixed municipal,Other designated,Sludge (BioSolids),Tires	Y
10-AA-0004	City Of Clovis Landfill	105,611,917	Disposal	01	Permitted	Active	Industrial,Mixed municipal	
10-AA-0009	American Avenue Disposal Site	857,752,305	Disposal	01	Permitted	Active	Agricultural,Asbestos,Construction/demolition,Industrial,Mixed municipal,Tires,Tires, Shreds	Y

SWIS No	Name	Total LFG Collected (scf) (1)	Category	Unit No	Regulatory Status	Operational Status	Accepted Waste	Tires (Y/)
11-AA-0001	Glenn County Landfill Site	-	Disposal	01	Permitted	Active	Agricultural,Construction/demolition,Dead Animals,Industrial,Inert,Mixed municipal,Tires	Y
13-AA-0001	Imperial Solid Waste Site	-	Disposal	01	Permitted	Active	Construction/demolition,Dead Animals,Mixed municipal	
13-AA-0004	Calexico Solid Waste Site	-	Disposal	01	Permitted	Active	Agricultural,Construction/demolition,Mixed municipal	
13-AA-0009	Niland Solid Waste Site	-	Disposal	01	Permitted	Active	Construction/demolition,Mixed municipal	
13-AA-0010	Hot Spa Solid Waste Site	-	Disposal	01	Permitted	Active	Construction/demolition,Mixed municipal	
13-AA-0011	Salton City Solid Waste Site	-	Disposal	01	Permitted	Active	Construction/demolition,Green Materials,Mixed municipal	
13-AA-0019	Imperial Landfill	4,178,184	Disposal	01	Permitted	Active	Agricultural,Asbestos,Ash,Construction/demolition,Dead Animals,Green Materials,Industrial,Inert,Mixed municipal,Sludge (BioSolids),Tires,Wood waste	Y
13-AA-0022	Monofill Facility	-	Disposal	01	Permitted	Active	Industrial	
14-AA-0003	Lone Pine Landfill	-	Disposal	01	Permitted	Active	Agricultural,Ash,Construction/demolition,Dead Animals,Industrial,Mixed municipal	
14-AA-0004	Independence Landfill	-	Disposal	01	Permitted	Active	Agricultural,Ash,Construction/demolition,Dead Animals,Industrial,Mixed municipal,Tires	Y
14-AA-0005	Bishop Sunland Solid Waste Site	-	Disposal	01	Permitted	Active	Agricultural,Asbestos,Ash,Construction/demolition,Contaminated soil,Dead Animals,Industrial,Mixed municipal,Other designated,Sludge (BioSolids)	
14-AA-0006	Shoshone Landfill	-	Disposal	01	Permitted	Active	Construction/demolition,Dead Animals,Green Materials,Mixed municipal	
14-AA-0007	Tecopa Landfill	-	Disposal	01	Permitted	Active	Construction/demolition,Dead Animals,Green Materials,Mixed municipal	

SWIS No	Name	Total LFG Collected (scf) (1)	Category	Unit No	Regulatory Status	Operational Status	Accepted Waste	Tires (Y/)
15-AA-0045	Boron Sanitary Landfill	-	Disposal	01	Permitted	Active	Ash,Construction/demolition,Dead Animals,Industrial,Mixed municipal	
15-AA-0057	Shafter-Wasco Recycling & Sanitary LF	131,192,695	Disposal	01	Permitted	Active	Construction/demolition,Dead Animals,Green Materials,Inert,Metals,Mixed municipal	
15-AA-0058	Mojave-Rosamond Sanitary Landfill	-	Disposal	01	Permitted	Active	Agricultural,Construction/demolition,Dead Animals,Industrial,Mixed municipal	
15-AA-0059	Ridgecrest Recycling & Sanitary Landfill	-	Disposal	01	Permitted	Active	Agricultural,Ash,Construction/demolition,Industrial,Mixed municipal	
15-AA-0061	Taft Recycling & Sanitary Landfill	-	Disposal	01	Permitted	Active	Ash,Construction/demolition,Dead Animals,Green Materials,Industrial,Inert,Metals,Mixed municipal,Tires	Y
15-AA-0062	Tehachapi Sanitary Landfill	-	Disposal	01	Permitted	Active	Construction/demolition,Dead Animals,Industrial,Mixed municipal	
15-AA-0105	McKittrick Waste Treatment Site	-	Disposal	01	Permitted	Active	Contaminated soil,Industrial,Other designated	
15-AA-0150	Main Base Sanitary Landfill, Edwards AFB	-	Disposal	01	Permitted	Active	Construction/demolition,Dead Animals,Green Materials,Mixed municipal	
15-AA-0273	Bakersfield Metropolitan (Bena) SLF	515,314,977	Disposal	01	Permitted	Active	Construction/demolition,Industrial,Mixed municipal	
15-AA-0278	U.S. Borax Inc-Gangue/Refuse Waste Pile	-	Disposal	01	Permitted	Active	Construction/demolition,Industrial	
15-AA-0308	H.M. Holloway Inc.	-	Disposal	01	Permitted	Active	Ash,Inert,Other designated,Sludge (BioSolids)	
16-AA-0004	Avenal Regional Landfill	-	Disposal	01	Permitted	Active	Agricultural,Ash,Construction/demolition,Dead Animals,Industrial,Inert,Mixed municipal,Other designated	
16-AA-0021	CWMI, KHF (MSW Landfill B-19)	128,204,000	Disposal	01	Permitted	Active	Dead Animals,Industrial,Mixed municipal,Other designated,Sludge (BioSolids)	

SWIS No	Name	Total LFG Collected (scf) (1)	Category	Unit No	Regulatory Status	Operational Status	Accepted Waste	Tires (Y/)
16-AA-0027	Chemical Waste Management, Inc.Unit B-17	-	Disposal	01	Permitted	Active	Mixed municipal	
17-AA-0001	Eastlake Sanitary Landfill	131,018,400	Disposal	01	Permitted	Active	Mixed municipal	
18-AA-0009	Bass Hill Landfill	-	Disposal	01	Permitted	Active	Agricultural,Ash,Construction/demolition,Dead Animals,Mixed municipal,Other designated,Sludge (BioSolids)	
18-AA-0010	Westwood Landfill	-	Disposal	01	Permitted	Active	Construction/demolition,Dead Animals,Mixed municipal,Tires	Y
18-AA-0013	Sierra Army Depot	-	Disposal	01	Permitted	Active	Construction/demolition,Industrial,Mixed municipal,Other designated,Tires	Y
19-AA-0012	Scholl Canyon Landfill	3,232,430,000	Disposal	01	Permitted	Active	Construction/demolition,Industrial,Inert,Manure,Mixed municipal,Tires	Y
19-AA-0040	Burbank Landfill Site No. 3	146,988,703	Disposal	01	Permitted	Active	Construction/demolition,Industrial,Inert,Mixed municipal	
19-AA-0050	Lancaster Landfill and Recycling Center	492,800,000	Disposal	01	Permitted	Active	Agricultural,Asbestos,Construction/demolition,Contaminated soil,Green Materials,Industrial,Inert,Mixed municipal,Sludge (BioSolids),Tires	Y
19-AA-0052	Chiquita Canyon Sanitary Landfill	2,684,566,829	Disposal	01	Permitted	Active	Construction/demolition,Green Materials,Industrial,Inert,Mixed municipal	
19-AA-0056	Calabasas Landfill	2,245,000,000	Disposal	01	Permitted	Active	Construction/demolition,Green Materials,Industrial,Mixed municipal,Tires	Y
19-AA-0061	Pebbly Beach (Avalon) Disposal Site	-	Disposal	01	Permitted	Active	Ash,Green Materials,Inert,Metals,Mixed municipal,Sludge (BioSolids)	

SWIS No	Name	Total LFG Collected (scf) (1)	Category	Unit No	Regulatory Status	Operational Status	Accepted Waste	Tires (Y/)
19-AA-0063	San Clemente Island Landfill	-	Disposal	01	Permitted	Active	Construction/demolition,Industrial,Inert,Mixed municipal	
19-AA-2000	Sunshine Canyon City/County Landfill	2,889,387,207	Disposal	01	Permitted	Active	Construction/demolition,Green Materials,Industrial,Inert,Mixed municipal	
19-AA-5624	Antelope Valley Public Landfill	422,300,000	Disposal	01	Permitted	Active	Agricultural,Asbestos,Construction/demolition,Contaminated soil,Green Materials,Industrial,Inert,Mixed municipal	
19-AH-0001	Savage Canyon Landfill	3,229,986	Disposal	01	Permitted	Active	Construction/demolition,Green Materials,Industrial,Inert,Mixed municipal	
19-AR-0004	Bradley East Landfill	1,847,512,000	Disposal	01	Permitted	Absorbed		
20-AA-0002	Fairmead Solid Waste Disposal Site	460,141,920	Disposal	01	Permitted	Active	Agricultural,Asbestos,Construction/demolition,Green Materials,Industrial,Mixed municipal,Tires,Wood waste	Y
21-AA-0001	Redwood Landfill	1,195,146,000	Disposal	01	Permitted	Active	Agricultural,Asbestos,Ash,Construction/demolition,Mixed municipal,Other designated,Sludge (BioSolids),Tires,Wood waste	Y
22-AA-0001	Mariposa County Sanitary Landfill	-	Disposal	01	Permitted	Active	Construction/demolition,Dead Animals,Mixed municipal,Sludge (BioSolids),Tires	Y
24-AA-0001	Highway 59 Disposal Site	428,802,480	Disposal	01	Permitted	Active	Green Materials,Mixed municipal,Other designated,Other hazardous,Tires,Wood waste	Y
24-AA-0002	Billy Wright Disposal Site	-	Disposal	01	Permitted	Active	Agricultural,Construction/demolition,Mixed municipal	
25-AA-0001	Alturas Sanitary Landfill	-	Disposal	01	Permitted	Active	Dead Animals,Mixed municipal,Sludge (BioSolids),Tires	Y
26-AA-0001	Walker Landfill	-	Disposal	01	Permitted	Active	Construction/demolition,Inert	

SWIS No	Name	Total LFG Collected (scf) (1)	Category	Unit No	Regulatory Status	Operational Status	Accepted Waste	Tires (Y/)
26-AA-0003	Pumice Valley Landfill	-	Disposal	01	Permitted	Active	Construction/demolition,Green Materials,Mixed municipal	
26-AA-0004	Benton Crossing Landfill	-	Disposal	01	Permitted	Active	Construction/demolition,Dead Animals,Green Materials,Metals,Mixed municipal,Other designated,Sludge (BioSolids)	
27-AA-0005	Johnson Canyon Sanitary Landfill	454,686,811	Disposal	01	Permitted	Active	Agricultural,Construction/demolition,Sludge (BioSolids),Tires	Y
27-AA-0010	Monterey Peninsula Landfill	405,852,728	Disposal	01	Permitted	Active	Agricultural,Construction/demolition,Mixed municipal,Sludge (BioSolids)	
28-AA-0002	Clover Flat Resource Recovery Park	130,808,503	Disposal	01	Permitted	Active	Agricultural,Construction/demolition,Industrial,Mixed municipal,Sludge (BioSolids),Tires	Y
30-AB-0019	Prima Deshecha Sanitary Landfill	1,414,787,819	Disposal	01	Permitted	Active	Construction/demolition,Industrial,Mixed municipal	
30-AB-0035	Olinda Alpha Sanitary Landfill	4,590,639,570	Disposal	01	Permitted	Active	Agricultural,Construction/demolition,Industrial,Mixed municipal,Tires,Wood waste	Y
30-AB-0360	Frank R. Bowerman Sanitary LF	3,649,894,950	Disposal	01	Permitted	Active	Construction/demolition,Industrial,Mixed municipal	
31-AA-0210	Western Regional Landfill	893,534,274	Disposal	01	Permitted	Active	Ash,Construction/demolition,Mixed municipal,Sludge (BioSolids)	
32-AA-0009	Chester Sanitary Landfill	-	Disposal	01	Permitted	Active	Construction/demolition,Mixed municipal,Tires	Y

SWIS No	Name	Total LFG Collected (scf) (1)	Category	Unit No	Regulatory Status	Operational Status	Accepted Waste	Tires (Y/)
33-AA-0006	Badlands Sanitary Landfill	619,324,587	Disposal	01	Permitted	Active	Agricultural,Asbestos,Ash,Construction/demolition,Contaminated soil,Dead Animals,Green Materials,Industrial,Inert,Liquid Waste,Metals,Mixed municipal,Sludge (BioSolids),Tires,Wood waste	Y
33-AA-0007	Lamb Canyon Sanitary Landfill	621,640,984	Disposal	01	Permitted	Active	Agricultural,Asbestos,Ash,Construction/demolition,Contaminated soil,Dead Animals,Green Materials,Industrial,Inert,Liquid Waste,Metals,Mixed municipal,Sludge (BioSolids),Tires	Y
33-AA-0015	Oasis Sanitary Landfill	-	Disposal	01	Permitted	Active	Agricultural,Construction/demolition,Green Materials,Inert,Metals,Mixed municipal,Wood waste	
33-AA-0016	Desert Center Landfill	-	Disposal	01	Permitted	Active	Agricultural,Construction/demolition,Green Materials,Inert,Metals,Mixed municipal,Tires,Wood waste	Y
33-AA-0017	Blythe Sanitary Landfill	-	Disposal	01	Permitted	Active	Agricultural,Construction/demolition,Contaminated soil,Dead Animals,Green Materials,Industrial,Inert,Liquid Waste,Metals,Mixed municipal,Tires,Wood waste	Y
33-AA-0071	Mecca Landfill II	-	Disposal	01	Permitted	Active	Agricultural,Construction/demolition,Dead Animals,Green Materials,Inert,Metals,Mixed municipal,Tires,Wood waste	Y
33-AA-0217	El Sobrante Landfill	1,865,719,000	Disposal	01	Permitted	Active	Construction/demolition,Mixed municipal,Tires	Y
33-AA-0231	Philadelphia Recycling Mine	-	Disposal	01	Pre-regulations	Absorbed	Construction/demolition	
34-AA-0001	Sacramento County Landfill (Kiefer)	3,639,052,672	Disposal	01	Permitted	Active	Construction/demolition,Mixed municipal,Other designated,Sludge (BioSolids)	
34-AA-0020	L and D Landfill	248,130,000	Disposal	01	Permitted	Active	Asphalt Shingles,Construction/demolition,Green Materials,Industrial,Inert,Mixed municipal,Other designated	
35-AA-0001	John Smith Road Landfill	171,796,607	Disposal	01	Permitted	Active	Agricultural,Construction/demolition,Dead Animals,Green Materials,Industrial,Inert,Manure,Mixed municipal,Tires,Wood waste	Y
36-AA-0017	California Street Landfill	228,604,819	Disposal	01	Permitted	Active	Construction/demolition,Mixed municipal,Other designated,Sludge (BioSolids)	
36-AA-0028	Oro Grande Kiln Waste Dust Dump	-	Disposal	01	Exempt	Active	Other designated	

SWIS No	Name	Total LFG Collected (scf) (1)	Category	Unit No	Regulatory Status	Operational Status	Accepted Waste	Tires (Y/)
36-AA-0045	Victorville Sanitary Landfill	153,363,803	Disposal	01	Permitted	Active	Agricultural,Ash,Construction/demolition,Dead Animals,Green Materials,Industrial,Mixed municipal,Sludge (BioSolids),Tires,Wood waste	Y
36-AA-0046	Barstow Sanitary Landfill	-	Disposal	01	Permitted	Active	Agricultural,Construction/demolition,Industrial,Mixed municipal,Other designated,Sludge (BioSolids)	
36-AA-0055	Mid-Valley Sanitary Landfill	827,661,684	Disposal	01	Permitted	Active	Construction/demolition,Industrial,Mixed municipal,Tires	Y
36-AA-0057	Landers Sanitary Landfill	-	Disposal	01	Permitted	Active	Construction/demolition,Industrial,Mixed municipal,Other designated,Sludge (BioSolids),Tires	Y
36-AA-0067	USMC - 29 Palms Disposal Facility	-	Disposal	01	Permitted	Active	Agricultural,Construction/demolition,Dead Animals,Industrial,Inert,Mixed municipal,Sludge (BioSolids),Tires, Shreds	Y
36-AA-0068	Fort Irwin Sanitary Landfill	-	Disposal	01	Permitted	Active	Contaminated soil,Dead Animals,Mixed municipal,Sludge (BioSolids)	
36-AA-0074	Mitsubishi Cement Plant Cushenbury L.F.	-	Disposal	01	Permitted	Active	Industrial	
36-AA-0087	San Timoteo Sanitary Landfill	277,865,760	Disposal	01	Permitted	Active	Agricultural,Construction/demolition,Dead Animals,Industrial,Inert,Mixed municipal,Sludge (BioSolids)	
37-AA-0006	Borrego Landfill	-	Disposal	01	Permitted	Active	Agricultural,Construction/demolition,Mixed municipal,Sludge (BioSolids),Tires,Wood waste	Y
37-AA-0010	Otay Landfill	2,432,170,648	Disposal	01	Permitted	Active	Agricultural,Ash,Construction/demolition,Contaminated soil,Dead Animals,Green Materials,Industrial,Inert,Mixed municipal,Other designated,Sludge (BioSolids),Tires	Y
37-AA-0020	West Miramar Sanitary Landfill	2,665,116,934	Disposal	01	Permitted	Active	Construction/demolition,Mixed municipal,Tires	Y
37-AA-0023	Sycamore Landfill	1,700,649,579	Disposal	01	Permitted	Active	Agricultural,Asbestos,Contaminated soil,Dead Animals,Mixed municipal,Other designated,Sludge (BioSolids),Tires, Shreds,Wood waste	Y

SWIS No	Name	Total LFG Collected (scf) (1)	Category	Unit No	Regulatory Status	Operational Status	Accepted Waste	Tires (Y/)
37-AA-0902	San Onofre Landfill	-	Disposal	01	Permitted	Active	Construction/demolition,Industrial,Mixed municipal,Sludge (BioSolids)	
37-AA-0903	Las Pulgas Landfill	-	Disposal	01	Permitted	Active	Construction/demolition,Industrial,Mixed municipal,Sludge (BioSolids)	
39-AA-0004	Foothill Sanitary Landfill	299,700,000	Disposal	01	Permitted	Active	Agricultural,Construction/demolition,Dead Animals,Industrial,Mixed municipal,Tires,Wood waste	Y
39-AA-0015	Forward Landfill, Inc.	1,594,038,126	Disposal	01	Permitted	Active	Agricultural,Asbestos,Asbestos, friable,Ash,Construction/demolition,Contaminated soil,Green Materials,Industrial,Mixed municipal,Sludge (BioSolids),Tires, Shreds	Y
39-AA-0022	North County Landfill & Recycling Center	124,700,000	Disposal	01	Permitted	Active	Agricultural,Construction/demolition,Industrial,Metals,Mixed municipal,Other designated,Tires,Wood waste	Y
40-AA-0001	City Of Paso Robles Landfill	56,780,066	Disposal	01	Permitted	Active	Agricultural,Construction/demolition,Green Materials,Industrial,Metals,Mixed municipal,Sludge (BioSolids),Tires,Wood waste	Y
40-AA-0002	Camp Roberts Landfill	-	Disposal	01	Permitted	Active	Construction/demolition,Mixed municipal	
40-AA-0004	Cold Canyon Landfill, Inc.	330,262,073	Disposal	01	Permitted	Active	Agricultural,Construction/demolition,Contaminated soil,Dead Animals,Industrial,Inert,Mixed municipal,Sludge (BioSolids),Tires	Y
40-AA-0008	Chicago Grade Landfill	127,510,195	Disposal	01	Permitted	Active	Agricultural,Asbestos,Construction/demolition,Contaminated soil,Dead Animals,Food Wastes,Green Materials,Industrial,Inert,Metals,Mixed municipal,Other designated,Sludge (BioSolids),Tires	Y
41-AA-0002	Corinda Los Trancos Landfill (Ox Mtn)	35,643,304	Disposal	01	Permitted	Active	Asbestos,Construction/demolition,Mixed municipal,Other designated,Sludge (BioSolids),Tires	Y

SWIS No	Name	Total LFG Collected (scf) (1)	Category	Unit No	Regulatory Status	Operational Status	Accepted Waste	Tires (Y/)
42-AA-0012	Vandenberg AFB Landfill	-	Disposal	01	Permitted	Active	Agricultural,Asbestos,Ash,Construction/demolition,Dead Animals,Mixed municipal,Sludge (BioSolids),Tires	Y
42-AA-0015	Tajiguas Sanitary Landfill	520,906,156	Disposal	01	Permitted	Active	Agricultural,Asbestos,Construction/demolition,Industrial,Mixed municipal,Sludge (BioSolids),Tires	Y
42-AA-0016	Santa Maria Regional Landfill	330,700,847	Disposal	01	Permitted	Active	Agricultural,Construction/demolition,Green Materials,Industrial,Metals,Mixed municipal,Tires, Cut,Tires, Shreds	Y
42-AA-0017	City Of Lompoc Sanitary Landfill	-	Disposal	01	Permitted	Active	Construction/demolition,Mixed municipal	
43-AN-0001	Zanker Material Processing Facility	-	Disposal	01	Permitted	Active	Construction/demolition,Other designated	
43-AN-0003	Newby Island Sanitary Landfill	1,898,044,453	Disposal	01	Permitted	Active	Construction/demolition,Contaminated soil,Green Materials,Industrial,Mixed municipal,Sludge (BioSolids),Tires	Y
43-AN-0008	Kirby Canyon Recycl.& Disp. Facility	957,026,200	Disposal	01	Permitted	Active	Construction/demolition,Green Materials,Industrial,Mixed municipal,Tires	Y
43-AN-0015	Guadalupe Sanitary Landfill	1,049,536	Disposal	01	Permitted	Active	Construction/demolition,Green Materials,Industrial,Mixed municipal	
44-AA-0001	City of Santa Cruz Resource Recovery Fac	275,125,170	Disposal	01	Permitted	Active	Construction/demolition,Dead Animals,Green Materials,Industrial,Inert,Metals,Mixed municipal,Sludge (BioSolids),Tires,Wood waste	Y
44-AA-0002	City Of Watsonville Landfill	-	Disposal	01	Permitted	Active	Agricultural,Construction/demolition,Mixed municipal,Sludge (BioSolids)	

SWIS No	Name	Total LFG Collected (scf) (1)	Category	Unit No	Regulatory Status	Operational Status	Accepted Waste	Tires (Y/)
44-AA-0004	Buena Vista Drive Sanitary Landfill	561,756,068	Disposal	01	Permitted	Active	Agricultural,Construction/demolition,Contaminated soil,Dead Animals,Green Materials,Industrial,Inert,Metals,Mixed municipal,Sludge (BioSolids),Tires,Wood waste	Y
45-AA-0020	Anderson Landfill, Inc.	387,626,000	Disposal	01	Permitted	Active	Agricultural,Asbestos,Asbestos, friable,Ash,Construction/demolition,Industrial,Mixed municipal,Sludge (BioSolids),Tires,Wood waste	Y
45-AA-0043	West Central Landfill	299,487,842	Disposal	01	Permitted	Active	Agricultural,Construction/demolition,Industrial,Mixed municipal,Sludge (BioSolids),Tires	Y
46-AA-0001	Loyalton Landfill	-	Disposal	01	Permitted	Active	Ash,Construction/demolition,Inert,Mixed municipal,Tires	Y
48-AA-0002	Recology Hay Road	421,324,792	Disposal	01	Permitted	Active	Agricultural,Asbestos,Asbestos, friable,Ash,Construction/demolition,Mixed municipal,Sludge (BioSolids),Tires	Y
48-AA-0075	Potrero Hills Landfill	1,014,064,587	Disposal	01	Permitted	Active	Agricultural,Ash,Construction/demolition,Industrial,Mixed municipal,Sludge (BioSolids),Tires	Y
48-AA-0078	Tonnesen Pet Cemetery	-	Disposal	01	Unpermitted	Active	Dead Animals	
49-AA-0001	Central Disposal Site	684,162,713	Disposal	01	Permitted	Active	Agricultural,Construction/demolition,Industrial,Mixed municipal,Other designated,Sludge (BioSolids),Tires,Wood waste	Y
50-AA-0001	Blue Mountain Minerals	195,678,773	Disposal	01	Permitted	Active	Agricultural,Asbestos,Ash,Construction/demolition,Contaminated soil,Dead Animals,Industrial,Inert,Mixed municipal,Other designated,Sludge (BioSolids),Tires,Wood waste	Y
52-AA-0001	Tehama County/Red Bluff Landfill	110,482,677	Disposal	01	Permitted	Active	Agricultural,Construction/demolition,Dead Animals,Green Materials,Industrial,Mixed municipal,Tires	Y
52-AA-0028	Pactiv Disposal Site	-	Disposal	01	Exempt	Active	Industrial	

SWIS No	Name	Total LFG Collected (scf) (1)	Category	Unit No	Regulatory Status	Operational Status	Accepted Waste	Tires (Y/)
54-AA-0004	Teapot Dome Disposal Site	70,171,930	Disposal	01	Permitted	Active	Agricultural,Construction/demolition,Industrial,Mixed municipal	
54-AA-0009	Visalia Disposal Site	215,446,456	Disposal	01	Permitted	Active	Agricultural,Construction/demolition,Industrial,Mixed municipal	
55-AA-0012		-	Disposal	01	Exempt	Active		
56-AA-0005	Toland Road Landfill	859,627,956	Disposal	01	Permitted	Active	Agricultural,Construction/demolition,Industrial,Mixed municipal,Sludge (BioSolids)	
56-AA-0007	Simi Valley Landfill & Recycling Center	1,973,900,000	Disposal	01	Permitted	Active	Construction/demolition,Industrial,Mixed municipal,Sludge (BioSolids)	
57-AA-0001	Yolo County Central Landfill	389,090,000	Disposal	01	Permitted	Active	Agricultural,Construction/demolition,Mixed municipal,Sludge (BioSolids),Tires	Y
58-AA-0011	Recology Ostrom Road LF Inc.	660,270,758	Disposal	01	Permitted	Active	Agricultural,Asbestos,Ash,Construction/demolition,Contaminated soil,Industrial,Mixed municipal,Other designated,Sludge (BioSolids),Tires	Y

SWIS No	Program Type	Closure Date	ClosureType	Throughput	Throughput Units	Throughput (tonnes/day)	Capacity	Capacity Units	Acreage	Disposal Acreage	Disposal Acreage in Sq. Ft.
01-AA-0009	AB2296 LF,BOE Reporting Disposal Facility,Composite_Lined _LF_Cell(s),Financial Assurance Responsibilities,PaleoDS,Remaining Capacity Landfill,Treated Wood Waste Acceptance	1/1/2025	Estimated	11,150	Tons/day	10,115	124,400,000	Cubic Yards	2,170	472	20,560,320
01-AA-0010	BOE Reporting Disposal Facility,Composite_Lined _LF_Cell(s),Financial Assurance Responsibilities,PaleoDS,Remaining Capacity Landfill	12/31/2022	Estimated	2,518	Tons/day	2,284	32,970,000	Cubic Yards	323	246	10,715,760
04-AA-0002	AB2296 LF,BOE Reporting Disposal Facility,Financial Assurance Responsibilities,Remaining Capacity Landfill	1/1/2033	Estimated	1,500	Tons/day	1,361	25,271,900	Cubic Yards	190	140	6,098,400
05-AA-0023	BOE Reporting Disposal Facility,Composite_Lined _LF_Cell(s),Financial Assurance Responsibilities,Remaining Capacity Landfill,Treated Wood Waste Acceptance	9/30/2035	Estimated	500	Tons/day	454	7,651,000	Cubic Yards	201	57	2,482,920
06-AA-0002	BOE Reporting Disposal Facility,Financial Assurance Responsibilities,Remaining Capacity Landfill	1/1/2064	Estimated	10	Tons/day	9	149,219	Cubic Yards	47	3	143,748
07-AA-0002	BOE Reporting Disposal Facility,Financial Assurance Responsibilities,Remaining Capacity Landfill	7/1/2021	Estimated	1,500	Tons/day	1,361	6,195,000	Cubic Yards	109	109	4,748,040
07-AA-0032	BOE Reporting Disposal Facility,Composite_Lined _LF_Cell(s),Financial Assurance Responsibilities,Remaining Capacity Landfill,Treated Wood Waste Acceptance	12/31/2030	Estimated	3,500	Tons/day	3,175	75,018,280	Cubic Yards	1,399	244	10,628,640
07-AC-0042		1/1/2118	Estimated	8	Tons/day	7	86,000	Cubic Yards	7	7	304,920
09-AA-0003	BOE Reporting Disposal Facility,Financial Assurance Responsibilities,Remaining Capacity Landfill,Treated Wood Waste Acceptance	1/1/2040	Estimated	300	Tons/day	272	195,000	Cubic Yards	322	22	949,608
10-AA-0004	BOE Reporting Disposal Facility,Composite_Lined _LF_Cell(s),Financial Assurance Responsibilities,Remaining Capacity Landfill	4/30/2047	Estimated	2,000	Tons/day	1,814	7,800,000	Cubic Yards	210	76	3,323,628
10-AA-0009	BOE Reporting Disposal Facility,Composite_Lined _LF_Cell(s),Financial Assurance Responsibilities,Remaining Capacity Landfill,Treated Wood Waste Acceptance	8/31/2031	Estimated	2,200	Tons/day	1,996	32,700,000	Cubic Yards	440	361	15,725,160

SWIS No	Program Type	Closure Date	ClosureType	Throughput	Throughput Units	Throughput (tonnes/day)	Capacity	Capacity Units	Acreage	Disposal Acreage	Disposal Acreage in Sq. Ft.
11-AA-0001	BOE Reporting Disposal Facility,Financial Assurance Responsibilities,Remaining Capacity Landfill	7/1/2016	Estimated	200	Tons/day	181	2,400,000	Cubic Yards	356	83	3,615,480
13-AA-0001	BOE Reporting Disposal Facility,Financial Assurance Responsibilities,Remaining Capacity Landfill	3/1/2019	Estimated	18	Tons/day	16	1,936,000	Cubic Yards	69	18	784,080
13-AA-0004	BOE Reporting Disposal Facility,Composite_Lined _LF_Cell(s),Financial Assurance Responsibilities,Remaining Capacity Landfill	11/1/2077	Estimated	150	Tons/day	136	3,437,800	Cubic Yards	82	40	1,746,756
13-AA-0009	BOE Reporting Disposal Facility,Composite_Lined _LF_Cell(s),Financial Assurance Responsibilities,Remaining Capacity Landfill	2/1/2056	Estimated	55	Tons/day	50	131,000	Cubic Yards	100	14	605,484
13-AA-0010	BOE Reporting Disposal Facility,Composite_Lined _LF_Cell(s),Financial Assurance Responsibilities,Remaining Capacity Landfill	9/1/2021	Estimated	10	Tons/day	9	233,150	Cubic Yards	40	6	278,784
13-AA-0011	BOE Reporting Disposal Facility,Financial Assurance Responsibilities,Remaining Capacity Landfill	12/31/2038	Estimated	6,000	Tons/day	5,443	65,100,000	Cubic Yards	320	284	12,371,040
13-AA-0019	BOE Reporting Disposal Facility,Financial Assurance Responsibilities,Remaining Capacity Landfill,Treated Wood Waste Acceptance	12/31/2040	Estimated	1,700	Tons/day	1,542	19,514,700	Cubic Yards	337	162	7,056,720
13-AA-0022	BOE Reporting Disposal Facility,Financial Assurance Responsibilities	1/31/2025	Estimated	750	Tons/day	680	1,729,800	Cubic Yards	182	29	1,258,884
14-AA-0003	BOE Reporting Disposal Facility,Financial Assurance Responsibilities,Remaining Capacity Landfill	12/31/2052	Estimated	22	Tons/day	20	996,620	Cubic Yards	60	26	1,132,560
14-AA-0004	BOE Reporting Disposal Facility,Financial Assurance Responsibilities,Remaining Capacity Landfill	12/31/2068	Estimated	10	Tons/day	9	317,900	Cubic Yards	90	18	784,080
14-AA-0005	BOE Reporting Disposal Facility,Financial Assurance Responsibilities,Remaining Capacity Landfill	12/31/2064	Estimated	120	Tons/day	109	4,039,760	Cubic Yards	118	68	2,962,080
14-AA-0006	BOE Reporting Disposal Facility,Financial Assurance Responsibilities,Remaining Capacity Landfill	12/31/2069	Estimated	1	Tons/day	1	42,960	Cubic Yards	20	5	196,020
14-AA-0007	BOE Reporting Disposal Facility,Financial Assurance Responsibilities,Remaining Capacity Landfill	12/31/2190	Estimated	1	Tons/day	1	119,090	Cubic Yards	29	9	405,108

SWIS No	Program Type	Closure Date	ClosureType	Throughput	Throughput Units	Throughput (tonnes/day)	Capacity	Capacity Units	Acreage	Disposal Acreage	Disposal Acreage in Sq. Ft.
15-AA-0045	BOE Reporting Disposal Facility,Financial Assurance Responsibilities,Remaining Capacity Landfill	1/1/2048	Estimated	200	Tons/day	181	1,057,000	Cubic Yards	120	14	614,196
15-AA-0057	BOE Reporting Disposal Facility,Composite_Lined _LF_Cell(s),Financial Assurance Responsibilities,Remaining Capacity Landfill	12/31/2053	Estimated	1,500	Tons/day	1,361	21,895,179	Cubic Yards	358	135	5,880,600
15-AA-0058	BOE Reporting Disposal Facility,Financial Assurance Responsibilities,Remaining Capacity Landfill	12/31/2123	Estimated	3,000	Tons/day	2,722	78,000,000	Cubic Yards	1,689	544	23,696,640
15-AA-0059	BOE Reporting Disposal Facility,Financial Assurance Responsibilities,Remaining Capacity Landfill	12/31/2045	Estimated	701	Tons/day	636	10,500,000	Cubic Yards	320	105	4,573,800
15-AA-0061	BOE Reporting Disposal Facility,Financial Assurance Responsibilities,Remaining Capacity Landfill	12/31/2076	Estimated	800	Tons/day	726	11,000,000	Cubic Yards	172	85	3,702,600
15-AA-0062	BOE Reporting Disposal Facility,Financial Assurance Responsibilities,Remaining Capacity Landfill	6/1/2020	Estimated	1,000	Tons/day	907	4,000,000	Cubic Yards	240	32	1,380,852
15-AA-0105	BOE Reporting Disposal Facility,Composite_Lined _LF_Cell(s),Financial Assurance Responsibilities,Remaining Capacity Landfill,Treated Wood Waste Acceptance	12/31/2059	Estimated	3,500	Tons/day	3,175	5,474,900	Cubic Yards	51	90	3,920,400
15-AA-0150	BOE Reporting Disposal Facility,Financial Assurance Responsibilities	12/31/2028	Estimated	120	Tons/day	109	2,250,000	Cubic Yards	137	73	3,179,880
15-AA-0273	BOE Reporting Disposal Facility,Composite_Lined _LF_Cell(s),Financial Assurance Responsibilities,Remaining Capacity Landfill	4/1/2046	Estimated	4,500	Tons/day	4,082	53,000,000	Cubic Yards	2,285	229	9,975,240
15-AA-0278	BOE Reporting Disposal Facility,Financial Assurance Responsibilities	1/1/2023	Estimated	443	Tons/day	402	8,500,000	Cubic Yards	60	60	2,613,600
15-AA-0308	BOE Reporting Disposal Facility,Financial Assurance Responsibilities	12/1/2030	Estimated	2,000	Tons/day	1,814	12,600,000	Cubic Yards	331	172	7,505,388
16-AA-0004	BOE Reporting Disposal Facility,Financial Assurance Responsibilities,Remaining Capacity Landfill	12/31/2020	Estimated	6,000	Tons/day	5,443	36,300,000	Cubic Yards	173	123	5,366,592
16-AA-0021	BOE Reporting Disposal Facility,Financial Assurance Responsibilities,PaleoDS,Remaining Capacity Landfill,Treated Wood Waste Acceptance	12/31/2010	Estimated	2,000	Tons/day	1,814	4,200,000	Cubic Yards	1,600	29	1,263,240

SWIS No	Program Type	Closure Date	ClosureType	Throughput	Throughput Units	Throughput (tonnes/day)	Capacity	Capacity Units	Acreage	Disposal Acreage	Disposal Acreage in Sq. Ft.
16-AA-0027	BOE Reporting Disposal Facility,Financial Assurance Responsibilities	1/1/2030	Estimated	2,000	Tons/day	1,814	18,400,000	Cubic Yards	1,600	62	2,700,720
17-AA-0001	BOE Reporting Disposal Facility,Composite_Lined _LF_Cell(s),Financial Assurance Responsibilities,Remaining Capacity Landfill	12/31/2023	Estimated	200	Tons/day	181	6,050,000	Cubic Yards	80	31	1,350,360
18-AA-0009	BOE Reporting Disposal Facility,Financial Assurance Responsibilities,Remaining Capacity Landfill	12/30/2019	Estimated	300	Tons/day	272	2,150,000	Cubic Yards	200	32	1,393,920
18-AA-0010	BOE Reporting Disposal Facility,Financial Assurance Responsibilities,Remaining Capacity Landfill	1/1/2027	Estimated	10	Tons/day	9	89,369	Cubic Yards	40	9	392,040
18-AA-0013	BOE Reporting Disposal Facility,Financial Assurance Responsibilities	1/1/2067	Estimated	42	Tons/day	38	665,000	Cubic Yards	40		-
19-AA-0012	BOE Reporting Disposal Facility,Financial Assurance Responsibilities,Remaining Capacity Landfill	4/1/2030	Estimated	3,400	Tons/day	3,084	58,900,000	Cubic Yards	440	314	13,677,840
19-AA-0040	BOE Reporting Disposal Facility,Financial Assurance Responsibilities,Remaining Capacity Landfill,Treated Wood Waste Acceptance	1/1/2053	Estimated	240	Tons/day	218	5,933,365	Cubic Yards	86	48	2,090,880
19-AA-0050	Bio Reactor (LF),BOE Reporting Disposal Facility,Composite_Lined _LF_Cell(s),Financial Assurance Responsibilities,Remaining Capacity Landfill	3/1/2044	Estimated	5,100	Tons/day	4,627	27,700,000	Cubic Yards	276	210	9,160,668
19-AA-0052	BOE Reporting Disposal Facility,Financial Assurance Responsibilities,Remaining Capacity Landfill,Treated Wood Waste Acceptance	11/24/2019	Estimated	6,000	Tons/day	5,443	63,900,000	Cubic Yards	592	257	11,194,920
19-AA-0056	BOE Reporting Disposal Facility,Composite_Lined _LF_Cell(s),Financial Assurance Responsibilities,Remaining Capacity Landfill,Treated Wood Waste Acceptance	1/1/2029	Estimated	3,500	Tons/day	3,175	69,300,000	Cubic Yards	491	305	13,285,800
19-AA-0061	BOE Reporting Disposal Facility,Financial Assurance Responsibilities	1/1/2020	Estimated	49	Tons/day	44	143,142	Cubic Yards	8	6	261,360

SWIS No	Program Type	Closure Date	ClosureType	Throughput	Throughput Units	Throughput (tonnes/day)	Capacity	Capacity Units	Acreage	Disposal Acreage	Disposal Acreage in Sq. Ft.
19-AA-0063	BOE Reporting Disposal Facility,Financial Assurance Responsibilities	1/1/2032	Estimated	10	Tons/day	9	235,459	Cubic Yards	20	20	871,200
19-AA-2000	BOE Reporting Disposal Facility,Composite_Lined _LF_Cell(s),Financial Assurance Responsibilities,Remaining Capacity Landfill	12/31/2037	Estimated	12,100	Tons/day	10,977	140,900,000	Cubic Yards	1,036	363	15,812,280
19-AA-5624	BOE Reporting Disposal Facility,Composite_Lined _LF_Cell(s),Financial Assurance Responsibilities	1/1/2042	Estimated	3,564	Tons/day	3,233		Cubic Yards	185	125	5,445,000
19-AH-0001	BOE Reporting Disposal Facility,Composite_Lined _LF_Cell(s),Financial Assurance Responsibilities,Remaining Capacity Landfill,Treated Wood Waste Acceptance	12/31/2055	Estimated	3,350	Tons/day	3,039	19,337,450	Cubic Yards	132	102	4,443,120
19-AR-0004		12/31/1980	Estimated			-			-	-	-
20-AA-0002	BOE Reporting Disposal Facility,Composite_Lined _LF_Cell(s),Financial Assurance Responsibilities,PaleoDS,Remaining Capacity Landfill	12/31/2028	Estimated	1,100	Tons/day	998	9,400,000	Cubic Yards	121	77	3,354,120
21-AA-0001	BOE Reporting Disposal Facility,Composite_Lined _LF_Cell(s),Financial Assurance Responsibilities,Remaining Capacity Landfill	7/1/2024	Estimated	2,300	Tons/day	2,087	19,100,000	Cubic Yards	420	223	9,692,100
22-AA-0001	BOE Reporting Disposal Facility,Financial Assurance Responsibilities,Remaining Capacity Landfill	12/31/2065	Estimated	100	Tons/day	91	1,971,000	Cubic Yards	58	40	1,742,400
24-AA-0001	BOE Reporting Disposal Facility,Composite_Lined _LF_Cell(s),Financial Assurance Responsibilities,PaleoDS,Remaining Capacity Landfill,Treated Wood Waste Acceptance	1/1/2030	Estimated	1,500	Tons/day	1,361	30,012,352	Cubic Yards	610	255	11,107,800
24-AA-0002	BOE Reporting Disposal Facility,Financial Assurance Responsibilities,Remaining Capacity Landfill	12/31/2054	Estimated	1,500	Tons/day	1,361	14,800,000	Cubic Yards	172	102	4,434,408
25-AA-0001	BOE Reporting Disposal Facility,Financial Assurance Responsibilities,Remaining Capacity Landfill	1/1/2028	Estimated	16	Tons/day	15	1,600,000	Cubic Yards	162	28	1,197,900
26-AA-0001	BOE Reporting Disposal Facility,Financial Assurance Responsibilities,Remaining Capacity Landfill	12/30/2120	Estimated	1	Tons/day	1	340,716	Cubic Yards	44	10	453,024

SWIS No	Program Type	Closure Date	ClosureType	Throughput	Throughput Units	Throughput (tonnes/day)	Capacity	Capacity Units	Acreage	Disposal Acreage	Disposal Acreage in Sq. Ft.
26-AA-0003	BOE Reporting Disposal Facility,Financial Assurance Responsibilities,Remaining Capacity Landfill	1/1/2048	Estimated	110	Tons/day	100	741,360	Cubic Yards	48	24	1,028,016
26-AA-0004	BOE Reporting Disposal Facility,Financial Assurance Responsibilities,Remaining Capacity Landfill	12/31/2023	Estimated	500	Tons/day	454	2,617,900	Cubic Yards	145	72	3,114,540
27-AA-0005	BOE Reporting Disposal Facility,Composite_Lined _LF_Cell(s),Financial Assurance Responsibilities,Remaining Capacity Landfill,Treated Wood Waste Acceptance	12/21/2040	Estimated	1,574	Tons/day	1,428	13,834,328	Cubic Yards	163	96	4,194,828
27-AA-0010	BOE Reporting Disposal Facility,Financial Assurance Responsibilities,Remaining Capacity Landfill,Treated Wood Waste Acceptance	2/28/2107	Estimated	3,500	Tons/day	3,175	49,700,000	Cubic Yards	466	315	13,721,400
28-AA-0002	BOE Reporting Disposal Facility,Financial Assurance Responsibilities,Remaining Capacity Landfill	1/1/2047	Estimated	600	Tons/day	544	4,900,000	Cubic Yards	79	44	1,916,640
30-AB-0019	BOE Reporting Disposal Facility,Composite_Lined _LF_Cell(s),Financial Assurance Responsibilities,PaleoDS,Remaining Capacity Landfill,Treated Wood Waste Acceptance	12/31/2067	Estimated	4,000	Tons/day	3,629	172,900,000	Cubic Yards	1,530	698	30,404,880
30-AB-0035	BOE Reporting Disposal Facility,Composite_Lined _LF_Cell(s),Financial Assurance Responsibilities,PaleoDS,Remaining Capacity Landfill	12/31/2021	Estimated	8,000	Tons/day	7,257	148,800,000	Cubic Yards	565	420	18,295,200
30-AB-0360	BOE Reporting Disposal Facility,Composite_Lined _LF_Cell(s),Financial Assurance Responsibilities,PaleoDS,Remaining Capacity Landfill	12/31/2053	Estimated	11,500	Tons/day	10,433	266,000,000	Cubic Yards	725	534	23,261,040
31-AA-0210	BOE Reporting Disposal Facility,Composite_Lined _LF_Cell(s),Financial Assurance Responsibilities,Remaining Capacity Landfill,Treated Wood Waste Acceptance	1/1/2058	Estimated	1,900	Tons/day	1,724	36,350,000	Cubic Yards	281	231	10,062,360
32-AA-0009	BOE Reporting Disposal Facility,Financial Assurance Responsibilities	1/1/2024	Estimated	0	Tons/day	0	710,000	Cubic Yards	40	27	1,176,120

SWIS No	Program Type	Closure Date	ClosureType	Throughput	Throughput Units	Throughput (tonnes/day)	Capacity	Capacity Units	Acreage	Disposal Acreage	Disposal Acreage in Sq. Ft.
33-AA-0006	BOE Reporting Disposal Facility,Financial Assurance Responsibilities,Remaining Capacity Landfill	1/1/2022	Estimated	4,800	Tons/day	4,354	34,400,000	Cubic Yards	278	150	6,534,000
33-AA-0007	BOE Reporting Disposal Facility,Composite_Lined _LF_Cell(s),Financial Assurance Responsibilities,Remaining Capacity Landfill	4/1/2029	Estimated	5,500	Tons/day	4,990	38,935,653	Cubic Yards	581	145	6,298,776
33-AA-0015	BOE Reporting Disposal Facility,Financial Assurance Responsibilities,Remaining Capacity Landfill	9/1/2055	Estimated	400	Tons/day	363	1,097,152	Cubic Yards	165	23	1,014,948
33-AA-0016	BOE Reporting Disposal Facility,Financial Assurance Responsibilities,Remaining Capacity Landfill	4/1/2087	Estimated	60	Tons/day	54	115,341	Cubic Yards	162	7	304,920
33-AA-0017	BOE Reporting Disposal Facility,Financial Assurance Responsibilities,Remaining Capacity Landfill	8/1/2047	Estimated	400	Tons/day	363	6,229,670	Cubic Yards	335	78	3,397,680
33-AA-0071	BOE Reporting Disposal Facility,Financial Assurance Responsibilities,Remaining Capacity Landfill	1/1/2098	Estimated	400	Tons/day	363	452,182	Cubic Yards	80	19	827,640
33-AA-0217	BOE Reporting Disposal Facility,Composite_Lined _LF_Cell(s),Financial Assurance Responsibilities,Remaining Capacity Landfill	1/1/2045	Estimated	16,054	Tons/day	14,564	184,930,000	Tons	1,322	485	21,126,600
33-AA-0231		1/1/1995	Estimated	400	Tons/day	363			29	13	566,280
34-AA-0001	BOE Reporting Disposal Facility,Composite_Lined _LF_Cell(s),Financial Assurance Responsibilities,Remaining Capacity Landfill	1/1/2064	Estimated	10,815	Tons/day	9,811	117,400,000	Cubic Yards	1,084	660	28,749,600
34-AA-0020	BOE Reporting Disposal Facility,Composite_Lined _LF_Cell(s),Financial Assurance Responsibilities,Remaining Capacity Landfill	1/1/2023	Estimated	2,540	Tons/day	2,304	6,031,055	Cubic Yards	177	157	6,838,920
35-AA-0001	BOE Reporting Disposal Facility,Composite_Lined _LF_Cell(s),Financial Assurance Responsibilities,Remaining Capacity Landfill	1/1/2032	Estimated	1,000	Tons/day	907	9,354,000	Cubic Yards	90	58	2,526,480
36-AA-0017	BOE Reporting Disposal Facility,Financial Assurance Responsibilities,Remaining Capacity Landfill	1/1/2042	Estimated	829	Tons/day	752	10,000,000	Cubic Yards	115	106	4,617,360
36-AA-0028		12/31/2019	Estimated	220	Tons/day	200			161	104	4,530,240

SWIS No	Program Type	Closure Date	ClosureType	Throughput	Throughput Units	Throughput (tonnes/day)	Capacity	Capacity Units	Acreage	Disposal Acreage	Disposal Acreage in Sq. Ft.
36-AA-0045	BOE Reporting Disposal Facility,Financial Assurance Responsibilities,Remaining Capacity Landfill	10/1/2047	Estimated	3,000	Tons/day	2,722	83,200,000	Cubic Yards	491	341	14,853,960
36-AA-0046	BOE Reporting Disposal Facility,Financial Assurance Responsibilities,Remaining Capacity Landfill	5/1/2071	Estimated	1,500	Tons/day	1,361	80,354,500	Cubic Yards	645	331	14,418,360
36-AA-0055	BOE Reporting Disposal Facility,Composite_Lined _LF_Cell(s),Financial Assurance Responsibilities,Remaining Capacity Landfill,Treated Wood Waste Acceptance	4/1/2033	Estimated	7,500	Tons/day	6,804	101,300,000	Cubic Yards	498	408	17,772,480
36-AA-0057	BOE Reporting Disposal Facility,Financial Assurance Responsibilities,Remaining Capacity Landfill	1/1/2072	Estimated	1,200	Tons/day	1,089	13,983,500	Cubic Yards	637	92	4,007,520
36-AA-0067	BOE Reporting Disposal Facility,Financial Assurance Responsibilities	10/1/2066	Estimated	100	Tons/day	91	10,945,000	Cubic Yards	128	69	3,005,640
36-AA-0068	BOE Reporting Disposal Facility,Financial Assurance Responsibilities	1/1/2405	Estimated	100	Tons/day	91	19,000,000	Cubic Yards	467	460	20,037,600
36-AA-0074	BOE Reporting Disposal Facility,Financial Assurance Responsibilities	1/1/2034	Estimated	40	Tons/day	36	520,400	Cubic Yards	15	15	653,400
36-AA-0087	BOE Reporting Disposal Facility,Composite_Lined _LF_Cell(s),Financial Assurance Responsibilities,PaleoDS,Remaining Capacity Landfill	1/1/2043	Estimated	2,000	Tons/day	1,814	20,400,000	Cubic Yards	366	114	4,965,840
37-AA-0006	BOE Reporting Disposal Facility,Financial Assurance Responsibilities,Remaining Capacity Landfill	12/31/2046	Estimated	50	Tons/day	45	476,098	Cubic Yards	46	19	827,640
37-AA-0010	BOE Reporting Disposal Facility,Composite_Lined _LF_Cell(s),Financial Assurance Responsibilities,Remaining Capacity Landfill,Treated Wood Waste Acceptance	2/28/2030	Estimated	6,700	Tons/day	6,078	61,154,000	Cubic Yards	409	230	10,018,800
37-AA-0020	BOE Reporting Disposal Facility,Composite_Lined _LF_Cell(s),Financial Assurance Responsibilities,Remaining Capacity Landfill,Treated Wood Waste Acceptance	8/31/2025	Estimated	8,000	Tons/day	7,257	87,760,000	Cubic Yards	802	476	20,747,628
37-AA-0023	BOE Reporting Disposal Facility,Composite_Lined _LF_Cell(s),Financial Assurance Responsibilities,Remaining Capacity Landfill,Treated Wood Waste Acceptance	12/31/2042	Estimated	5,000	Tons/day	4,536	71,233,171	Cubic Yards	603	349	15,211,152

SWIS No	Program Type	Closure Date	ClosureType	Throughput	Throughput Units	Throughput (tonnes/day)	Capacity	Capacity Units	Acreage	Disposal Acreage	Disposal Acreage in Sq. Ft.
37-AA-0902	BOE Reporting Disposal Facility,Composite_Lined _LF_Cell(s),Financial Assurance Responsibilities,Treated Wood Waste Acceptance	5/31/2045	Estimated	100	Tons/day	91	1,920,000	Cubic Yards	64	29	1,245,816
37-AA-0903	BOE Reporting Disposal Facility,Composite_Lined _LF_Cell(s),Financial Assurance Responsibilities	9/1/2059	Estimated	400	Tons/day	363	14,600,000	Cubic Yards	133	89	3,863,772
39-AA-0004	BOE Reporting Disposal Facility,Composite_Lined _LF_Cell(s),Financial Assurance Responsibilities,Remaining Capacity Landfill	12/31/2082	Estimated	1,500	Tons/day	1,361	138,000,000	Cubic Yards	800	674	29,359,440
39-AA-0015	BOE Reporting Disposal Facility,Composite_Lined _LF_Cell(s),Financial Assurance Responsibilities,Remaining Capacity Landfill,Treated Wood Waste Acceptance	1/1/2020	Estimated	8,668	Tons/day	7,863	51,040,000	Cubic Yards	567	355	15,442,020
39-AA-0022	BOE Reporting Disposal Facility,Composite_Lined _LF_Cell(s),Financial Assurance Responsibilities,Remaining Capacity Landfill	12/31/2048	Estimated	825	Tons/day	748	41,200,000	Cubic Yards	320	185	8,058,600
40-AA-0001	BOE Reporting Disposal Facility,Composite_Lined _LF_Cell(s),Financial Assurance Responsibilities,Remaining Capacity Landfill	10/1/2051	Estimated	450	Tons/day	408	6,495,000	Cubic Yards	80	65	2,831,400
40-AA-0002	BOE Reporting Disposal Facility,Composite_Lined _LF_Cell(s),DOD,Financial Assurance Responsibilities	1/1/2045	Estimated	618	Tons/day	561	1,004,579	Cubic Yards	85	13	579,348
40-AA-0004	BOE Reporting Disposal Facility,Composite_Lined _LF_Cell(s),Financial Assurance Responsibilities,Remaining Capacity Landfill,Treated Wood Waste Acceptance	12/31/2040	Estimated	1,650	Tons/day	1,497	23,900,000	Cubic Yards	209	121	5,270,760
40-AA-0008	BOE Reporting Disposal Facility,Composite_Lined _LF_Cell(s),Financial Assurance Responsibilities,Remaining Capacity Landfill,Treated Wood Waste Acceptance	12/31/2039	Estimated	500	Tons/day	454	10,548,980	Cubic Yards	188	77	3,358,476
41-AA-0002	BOE Reporting Disposal Facility,Composite_Lined _LF_Cell(s),Financial Assurance Responsibilities,Remaining Capacity Landfill,Treated Wood Waste Acceptance	1/1/2034	Estimated	3,598	Tons/day	3,264	60,500,000	Cubic Yards	2,786	173	7,535,880

SWIS No	Program Type	Closure Date	ClosureType	Throughput	Throughput Units	Throughput (tonnes/day)	Capacity	Capacity Units	Acreage	Disposal Acreage	Disposal Acreage in Sq. Ft.
42-AA-0012	BOE Reporting Disposal Facility,Financial Assurance Responsibilities	9/1/2060	Estimated	400	Tons/day	363	4,721,017	Cubic Yards	217	46	2,003,760
42-AA-0015	BOE Reporting Disposal Facility,Composite_Lined _LF_Cell(s),Financial Assurance Responsibilities,PaleoDS,Remaining Capacity Landfill	1/1/2036	Estimated	1,500	Tons/day	1,361	23,300,000	Cubic Yards	357	118	5,140,080
42-AA-0016	BOE Reporting Disposal Facility,Composite_Lined _LF_Cell(s),Financial Assurance Responsibilities,Remaining Capacity Landfill	1/1/2018	Estimated	858	Tons/day	778	13,998,400	Cubic Yards	291	247	10,763,676
42-AA-0017	BOE Reporting Disposal Facility,Composite_Lined _LF_Cell(s),Financial Assurance Responsibilities,Remaining Capacity Landfill	1/1/2045	Estimated	400	Tons/day	363	7,970,000	Cubic Yards	115	39	1,698,840
43-AN-0001	BOE Reporting Disposal Facility,Financial Assurance Responsibilities,Remaining Capacity Landfill	11/1/2025	Estimated	350	Tons/day	318	640,000	Cubic Yards	53	25	1,089,000
43-AN-0003	BOE Reporting Disposal Facility,Composite_Lined _LF_Cell(s),Financial Assurance Responsibilities,Remaining Capacity Landfill,Treated Wood Waste Acceptance	1/1/2041	Estimated	4,000	Tons/day	3,629	57,500,000	Cubic Yards	342	298	12,980,880
43-AN-0008	BOE Reporting Disposal Facility,Composite_Lined _LF_Cell(s),Financial Assurance Responsibilities,Remaining Capacity Landfill,Treated Wood Waste Acceptance,UltraMafic	12/31/2022	Estimated	2,600	Tons/day	2,359	36,400,000	Cubic Yards	827	311	13,547,160
43-AN-0015	BOE Reporting Disposal Facility,Composite_Lined _LF_Cell(s),Financial Assurance Responsibilities,Remaining Capacity Landfill,Treated Wood Waste Acceptance	1/1/2048	Estimated	1,300	Tons/day	1,179	28,600,000	Cubic Yards	411	115	5,009,400
44-AA-0001	BOE Reporting Disposal Facility,Composite_Lined _LF_Cell(s),Financial Assurance Responsibilities,Remaining Capacity Landfill,Treated Wood Waste Acceptance	1/1/2058	Estimated	535	Tons/day	485	7,118,000	Cubic Yards	100	67	2,918,520
44-AA-0002	BOE Reporting Disposal Facility,Composite_Lined _LF_Cell(s),Financial Assurance Responsibilities,Remaining Capacity Landfill,Treated Wood Waste Acceptance	12/31/2029	Estimated	275	Tons/day	249	2,437,203	Cubic Yards	103	48	2,090,880

SWIS No	Program Type	Closure Date	ClosureType	Throughput	Throughput Units	Throughput (tonnes/day)	Capacity	Capacity Units	Acreage	Disposal Acreage	Disposal Acreage in Sq. Ft.
44-AA-0004	BOE Reporting Disposal Facility,Composite_Lined _LF_Cell(s),Financial Assurance Responsibilities,Remaining Capacity Landfill,Treated Wood Waste Acceptance	7/1/2031	Estimated	838	Tons/day	760	7,537,700	Cubic Yards	126	61	2,657,160
45-AA-0020	BOE Reporting Disposal Facility,Composite_Lined _LF_Cell(s),Financial Assurance Responsibilities,Remaining Capacity Landfill,Treated Wood Waste Acceptance	1/1/2093	Estimated	1,850	Tons/day	1,678	16,840,000	Cubic Yards	246	130	5,662,800
45-AA-0043	BOE Reporting Disposal Facility,Composite_Lined _LF_Cell(s),Financial Assurance Responsibilities,Remaining Capacity Landfill,Treated Wood Waste Acceptance	3/1/2032	Estimated	700	Tons/day	635	13,115,844	Cubic Yards	1,250	122	5,314,320
46-AA-0001	BOE Reporting Disposal Facility,Financial Assurance Responsibilities,Remaining Capacity Landfill	1/1/2016	Estimated	8	Tons/day	7	744,000	Cubic Yards	27	11	457,380
48-AA-0002	BOE Reporting Disposal Facility,Composite_Lined _LF_Cell(s),Financial Assurance Responsibilities,Remaining Capacity Landfill,Treated Wood Waste Acceptance	1/1/2077	Estimated	2,400	Tons/day	2,177	37,000,000	Cubic Yards	640	256	11,151,360
48-AA-0075	BOE Reporting Disposal Facility,Composite_Lined _LF_Cell(s),Financial Assurance Responsibilities,Remaining Capacity Landfill	2/14/2048	Estimated	4,330	Tons/day	3,928	83,100,000	Cubic Yards	526	340	14,810,400
48-AA-0078	Financial Assurance Responsibilities					-			15	-	-
49-AA-0001	BOE Reporting Disposal Facility,Composite_Lined _LF_Cell(s),Financial Assurance Responsibilities,Remaining Capacity Landfill	1/1/2034	Estimated	2,500	Tons/day	2,268	32,650,000	Cubic Yards	398	172	7,492,320
50-AA-0001	BOE Reporting Disposal Facility,Composite_Lined _LF_Cell(s),Financial Assurance Responsibilities,Remaining Capacity Landfill	12/1/2023	Estimated	2,400	Tons/day	2,177	14,640,000	Cubic Yards	203	203	8,820,900
52-AA-0001	BOE Reporting Disposal Facility,Financial Assurance Responsibilities,Remaining Capacity Landfill	1/1/2040	Estimated	600	Tons/day	544	5,097,000	Cubic Yards	102	54	2,352,240
52-AA-0028						-				12	500,940

SWIS No	Program Type	Closure Date	ClosureType	Throughput	Throughput Units	Throughput (tonnes/day)	Capacity	Capacity Units	Acreage	Disposal Acreage	Disposal Acreage in Sq. Ft.
54-AA-0004	BOE Reporting Disposal Facility,Financial Assurance Responsibilities,Remaining Capacity Landfill	12/31/2022	Estimated	800	Tons/day	726	7,880,307	Cubic Yards	122	71	3,092,760
54-AA-0009	BOE Reporting Disposal Facility,Financial Assurance Responsibilities,Remaining Capacity Landfill	1/1/2024	Estimated	2,000	Tons/day	1,814	18,630,666	Cubic Yards	631	247	10,759,320
55-AA-0012				-		-	-		-	-	-
56-AA-0005	BOE Reporting Disposal Facility,Composite_Lined _LF_Cell(s),Financial Assurance Responsibilities,PaleoDS,Remaining Capacity Landfill,Treated Wood Waste Acceptance	5/31/2027	Estimated	1,500	Tons/day	1,361	30,000,000	Cubic Yards	217	91	3,981,384
56-AA-0007	BOE Reporting Disposal Facility,Composite_Lined _LF_Cell(s),Financial Assurance Responsibilities,PaleoDS,Remaining Capacity Landfill,Treated Wood Waste Acceptance	1/31/2052	Estimated	9,250	Tons/day	8,391	119,600,000	Cubic Yards	887	368	16,030,080
57-AA-0001	Bio Reactor (LF),BOE Reporting Disposal Facility,Composite_Lined _LF_Cell(s),Financial Assurance Responsibilities,Remaining Capacity Landfill	1/1/2081	Estimated	1,800	Tons/day	1,633	49,035,200	Cubic Yards	725	473	20,603,880
58-AA-0011	BOE Reporting Disposal Facility,Composite_Lined _LF_Cell(s),Financial Assurance Responsibilities,Remaining Capacity Landfill,Treated Wood Waste Acceptance	12/31/2066	Estimated	3,000	Tons/day	2,722	43,467,231	Cubic Yards	261	225	9,801,000

SWIS No	Disposal Area in m2	Remaining Capacity	WDRNo	WIP (cubic yards)	WIP (tons)	WIP (metric tons, tonnes)	Fraction of Total Waste (m3)	Size	Amount of Waste (ft3)	Waste Column Height (ft)	Waste Column Height (m)	Tonnage (2)	ADC (Users) (3)	ADC Amnt
01-AA-0009	1,910,054	65,400,000	II,III	59,000,000	49,701,600	45,108,745	0.03733	L	1,593,000,000	77	24	865,868	Y*	
01-AA-0010	995,494	7,959,079	II,III	25,010,921	21,069,200	19,122,225	0.01582	M	675,294,867	63	19	185,419	Y	131,846
04-AA-0002	566,541	20,847,970	II,III	4,423,930	3,726,719	3,382,338	0.00280	S	119,446,110	20	6	116,389	Y*	
05-AA-0023	230,663	6,624,226	II	1,026,774	864,954	785,025	0.00065	S	27,722,898	11	3	18,257	Y	5,337
06-AA-0002	13,354	55,683	III	93,536	78,795	71,513	0.00006	S	2,525,472	18	5	-	Y*	
07-AA-0002	441,093	506,590	III	5,688,410	4,791,917	4,349,102	0.00360	M	153,587,070	32	10	12,186	Y	3,803
07-AA-0032	987,401	63,408,410	II	11,609,870	9,780,154	8,876,384	0.00735	M	313,466,490	29	9	593,250	Y	86,974
07-AC-0042	28,327		I	86,000		65,752	0.00005	S	2,322,000	8	2	-	N	
09-AA-0003	88,219	135,000	II,III	60,000	50,544	45,873	0.00004	S	1,620,000	2	1	1,885	Y*	
10-AA-0004	308,765	7,740,000	III	60,000	50,544	45,873	0.00004	S	1,620,000	0	0	39,763	Y*	
10-AA-0009	1,460,867	29,358,535	II,III	3,341,465	2,814,850	2,554,734	0.00211	S	90,219,555	6	2	380,576	Y*	

SWIS No	Disposal Area in m2	Remaining Capacity	WDRNo	WIP (cubic yards)	WIP (tons)	WIP (metric tons, tonnes)	Fraction of Total Waste (m3)	Size	Amount of Waste (ft3)	Waste Column Height (ft)	Waste Column Height (m)	Tonnage (2)	ADC (Users) (3)	ADC Amnt
11-AA-0001	335,878	866,521	III	1,533,479	1,291,803	1,172,429	0.00097	S	41,403,933	11	3	14,931	Y	3,730
13-AA-0001	72,841	180,000	III	1,756,000	1,479,254	1,342,559	0.00111	S	47,412,000	60	18	1,144	Y*	
13-AA-0004	162,274	1,808,802	III	1,628,998	1,372,268	1,245,459	0.00103	S	43,982,946	25	8	881	Y*	
13-AA-0009	56,249	318,669	III	(187,669)	28,368	33,368	0.00003	S	(5,067,063)	(8)	(3)	-	Y*	
13-AA-0010	25,899	47,263	III	185,887	156,591	142,121	0.00012	S	5,018,949	18	5	95	Y*	
13-AA-0011	1,149,270	65,100,000	III	-	129,295	152,082	0.00013	S	-	-	-	71,798	Y*	
13-AA-0019	655,569	15,485,200	III	4,029,500	3,394,451	3,080,774	0.00255	S	108,796,500	15	5	78,852	Y	27,386
13-AA-0022	116,950	1,058,252	II	671,548		513,435	0.00042	S	18,131,796	14	4	38,432	Y*	
14-AA-0003	105,215	1,002,586	III	(5,966)	183,600	215,957	0.00018	S	(161,082)	(0)	(0)	3,175	Y*	
14-AA-0004	72,841	126,513	III	191,387	161,224	146,326	0.00012	S	5,167,449	7	2	626	Y	6
14-AA-0005	275,177	3,314,752	III	725,008	610,747	554,308	0.00046	S	19,575,216	7	2	9,015	Y	435
14-AA-0006	18,210	8,038	III	34,922	29,418	26,700	0.00002	S	942,894	5	1	-	N	
14-AA-0007	37,635	37,048	III	82,042	69,112	62,726	0.00005	S	2,215,134	5	2	-	N	

SWIS No	Disposal Area in m2	Remaining Capacity	WDRNo	WIP (cubic yards)	WIP (tons)	WIP (metric tons, tonnes)	Fraction of Total Waste (m3)	Size	Amount of Waste (ft3)	Waste Column Height (ft)	Waste Column Height (m)	Tonnage (2)	ADC (Users) (3)	ADC Amnt
15-AA-0045	57,059	94,851	III	962,149	810,514	735,616	0.00061	S	25,978,023	42	13	2,105	Y*	
15-AA-0057	546,308	7,901,339	III	13,993,840	11,788,411	10,699,060	0.00885	M	377,833,680	64	20	102,293	N	
15-AA-0058	2,201,418	76,310,297	III	1,689,703	1,423,406	1,291,871	0.00107	S	45,621,981	2	1	9,036	Y*	
15-AA-0059	424,906	5,037,428	III	5,462,572	4,601,671	4,176,437	0.00346	M	147,489,444	32	10	37,183	Y*	
15-AA-0061	343,972	7,380,708	III	3,619,292	3,048,892	2,767,148	0.00229	S	97,720,884	26	8	26,686	Y*	
15-AA-0062	128,281	522,298	III	3,477,702	2,929,616	2,658,894	0.00220	S	93,897,954	68	21	40,944	Y*	
15-AA-0105	364,205	769,790	II	4,705,110		3,597,315	0.00298	S	127,037,970	32	10	87,351	Y*	
15-AA-0150	295,411	1,078,875	III	1,171,125	986,556	895,389	0.00074	S	31,620,375	10	3	2,590	Y	22
15-AA-0273	926,700	32,808,260	III	20,191,740	17,009,522	15,437,696	0.01277	M	545,176,980	55	17	326,664	Y	17,441
15-AA-0278	242,803	995,196	III	7,504,804		5,737,835	0.00475	M	202,629,708	78	24	-	Y*	
15-AA-0308	697,251	7,522,934	II,III	5,077,066		3,881,696	0.00321	S	137,080,782	18	6	83,514	Y*	
16-AA-0004	498,556	30,300,000	III	6,000,000	5,054,400	4,587,330	0.00380	M	162,000,000	30	9	88,482	Y	128,955
16-AA-0021	117,355	303,125	II,III	3,896,875	3,282,728	2,979,375	0.00247	S	105,215,625	83	25	129,122	Y*	

SWIS No	Disposal Area in m2	Remaining Capacity	WDRNo	WIP (cubic yards)	WIP (tons)	WIP (metric tons, tonnes)	Fraction of Total Waste (m3)	Size	Amount of Waste (ft3)	Waste Column Height (ft)	Waste Column Height (m)	Tonnage (2)	ADC (Users) (3)	ADC Amnt
16-AA-0027	250,897	17,468,595	III	931,405		712,110	0.00059	S	25,147,935	9	3	-	Y	66,980
17-AA-0001	125,448	2,859,962	III	3,190,038	2,687,288	2,438,960	0.00202	S	86,131,026	64	19	48,827	Y*	
18-AA-0009	129,495	603,404	III	1,546,596	1,302,852	1,182,458	0.00098	S	41,758,092	30	9	4858,11027 ?	Y	2,099
18-AA-0010	36,421	62,207	III	27,162	22,881	20,767	0.00002	S	733,374	2	1	0,57?	Y*	
18-AA-0013	-	244,500	II	420,500		321,495	0.00027	S	11,353,500	-	-	-	N	
19-AA-0012	1,270,671	9,900,000	III	49,000,000	41,277,600	37,463,195	0.03100	M	1,323,000,000	97	29	202,089	Y	81,940
19-AA-0040	194,243	5,174,362	III	759,003	639,384	580,300	0.00048	S	20,493,081	10	3	24,594	Y*	
19-AA-0050	851,026	14,514,648	III	13,185,352	11,107,341	10,080,927	0.00834	M	356,004,504	39	12	84,855	Y	49,934
19-AA-0052	1,040,008	8,617,126	III	55,282,874	46,570,293	42,266,798	0.03498	L	1,492,637,598	133	41	795,252	Y	60,351
19-AA-0056	1,234,251	14,500,000	III	54,800,000	46,163,520	41,897,614	0.03467	L	1,479,600,000	111	34	195,908	Y	44,619
19-AA-0061	24,280	75,924	III	67,218	56,624	51,392	0.00004	S	1,814,886	7	2	3,076	Y	739

SWIS No	Disposal Area in m2	Remaining Capacity	WDRNo	WIP (cubic yards)	WIP (tons)	WIP (metric tons, tonnes)	Fraction of Total Waste (m3)	Size	Amount of Waste (ft3)	Waste Column Height (ft)	Waste Column Height (m)	Tonnage (2)	ADC (Users) (3)	ADC Amnt
19-AA-0063	80,934	209,816	III	25,643	21,602	19,605	0.00002	S	692,361	1	0	230	Y*	
19-AA-2000	1,468,961	96,800,000	III	44,100,000	37,149,840	33,716,876	0.02790	M	1,190,700,000	75	23	1,270,704	Y*	
19-AA-5624	505,841	18,303,272	III	(18,303,272)	7,604,521	8,944,730	0.00740	M	(494,188,344)	(91)	(28)	366,600	Y	25,055
19-AH-0001	412,766	9,510,833	III	9,826,617	8,277,942	7,512,989	0.00622	M	265,318,659	60	18	66,949	Y*	
19-AR-0004	-		III	-	62,292,575	73,270,923	0.06063	L	-	-	-	-	N	
20-AA-0002	311,598	5,552,894	III	3,847,106	3,240,802	2,941,324	0.00243	S	103,871,862	31	9	123,300	Y	36,772
21-AA-0001	900,396	26,000,000	III	(6,900,000)	15,000,000	17,643,577	0.01460	M	(186,300,000)	(19)	(6)	154,199	Y	65,674
22-AA-0001	161,869	1,193,088	III	777,912	655,313	594,757	0.00049	S	21,003,624	12	4	8,439	Y	998
24-AA-0001	1,031,915	28,025,334	III	1,987,018	1,673,864	1,519,185	0.00126	S	53,649,486	5	1	47137,118109?	Y	1,487
24-AA-0002	411,957	11,370,000	III	3,430,000	2,889,432	2,622,424	0.00217	S	92,610,000	21	6	12414,31922?	Y	533
25-AA-0001	111,285	176,931	III	1,423,069	1,198,793	1,088,015	0.00090	S	38,422,863	32	10	-	N	
26-AA-0001	42,086	279,036	III	61,680	51,959	47,158	0.00004	S	1,665,360	4	1	80	Y	138

SWIS No	Disposal Area in m2	Remaining Capacity	WDRNo	WIP (cubic yards)	WIP (tons)	WIP (metric tons, tonnes)	Fraction of Total Waste (m3)	Size	Amount of Waste (ft3)	Waste Column Height (ft)	Waste Column Height (m)	Tonnage (2)	ADC (Users) (3)	ADC Amnt
26-AA-0003	95,503	358,790	III	382,570	322,277	292,496	0.00024	S	10,329,390	10	3	521	Y	169
26-AA-0004	289,341	695,047	III	1,922,853	1,619,811	1,470,127	0.00122	S	51,917,031	17	5	14,721	Y	4,846
27-AA-0005	389,700	6,923,297	III	6,911,031	5,821,853	5,283,863	0.00437	M	186,597,837	44	14	130,427	Y	4,636
27-AA-0010	1,274,718	48,560,000	III	1,140,000	960,336	871,593	0.00072	S	30,780,000	2	1	322,763	Y	60,896
28-AA-0002	178,056	2,870,000	III	2,030,000	1,710,072	1,552,047	0.00128	S	54,810,000	29	9	24,104	Y	98
30-AB-0019	2,824,613	87,384,799	III	85,515,201	72,038,005	65,381,075	0.05410	L	2,308,910,427	76	23	291,654	Y	46,077
30-AB-0035	1,699,624	34,200,000	III	114,600,000	96,539,040	87,618,003	0.07250	L	3,094,200,000	169	52	1,584,376	Y	318,197
30-AB-0360	2,160,951	205,000,000	III	61,000,000	51,386,400	46,637,855	0.03859	L	1,647,000,000	71	22	1,618,956	Y	192,608
31-AA-0210	934,793	29,093,819	II,III	7,256,181	6,112,607	5,547,749	0.00459	M	195,916,887	19	6	58,410	Y	32,282
32-AA-0009	109,262	388,150	III	321,850	271,126	246,072	0.00020	S	8,689,950	7	2	-	N	

SWIS No	Disposal Area in m2	Remaining Capacity	WDRNo	WIP (cubic yards)	WIP (tons)	WIP (metric tons, tonnes)	Fraction of Total Waste (m3)	Size	Amount of Waste (ft3)	Waste Column Height (ft)	Waste Column Height (m)	Tonnage (2)	ADC (Users) (3)	ADC Amnt
33-AA-0006	607,009	15,748,799	III	18,651,201	15,711,772	14,259,869	0.01180	M	503,582,427	77	23	636,448	Y	2,006
33-AA-0007	585,156	19,242,950	III	19,692,703	16,589,133	15,056,155	0.01246	M	531,702,981	84	26	403,841	Y	1,765
33-AA-0015	94,289	433,779	III	663,373	558,825	507,185	0.00042	S	17,911,071	18	5	7,662	Y*	-
33-AA-0016	28,327	35,714	III	79,627	67,078	60,879	0.00005	S	2,149,929	7	2	28	Y*	-
33-AA-0017	315,644	3,834,470	III	2,395,200	2,017,716	1,831,262	0.00152	S	64,670,400	19	6	13,147	Y*	-
33-AA-0071	76,888	6,371	III	445,811	375,551	340,847	0.00028	S	12,036,897	15	4	-	Y*	-
33-AA-0217	1,962,661	145,530,000	III	39,400,000	33,190,560	30,123,467	0.02493	M	1,063,800,000	50	15	1,690,862	Y	188,659
33-AA-0231	52,607		UC	-		-	-	-	-	-	-	-	N	
34-AA-0001	2,670,838	112,900,000	III	4,500,000	3,790,800	3,440,498	0.00285	S	121,500,000	4	1	477,648	Y	21,428
34-AA-0020	635,336	4,100,000	II,III	1,931,055	1,626,721	1,476,398	0.00122	S	52,138,485	8	2	146,313	Y	63,701
35-AA-0001	234,710	4,625,827	III	4,728,173	3,983,013	3,614,948	0.00299	S	127,660,671	51	15	197,150	Y*	-
36-AA-0017	428,953	6,800,000	III	3,200,000	2,695,680	2,446,576	0.00202	S	86,400,000	19	6	37,075	Y*	-
36-AA-0028	420,859		II	-	100,000	90,759	0.00008	S	-	-	-	-	N	

SWIS No	Disposal Area in m2	Remaining Capacity	WDRNo	WIP (cubic yards)	WIP (tons)	WIP (metric tons, tonnes)	Fraction of Total Waste (m3)	Size	Amount of Waste (ft3)	Waste Column Height (ft)	Waste Column Height (m)	Tonnage (2)	ADC (Users) (3)	ADC Amnt
36-AA-0045	1,379,933	81,510,000	III	1,690,000	1,423,656	1,292,098	0.00107	S	45,630,000	3	1	194,262	Y	10,765
36-AA-0046	1,339,466	71,481,660	III	8,872,840	7,474,480	6,783,774	0.00561	M	239,566,680	17	5	46,859	Y	8,397
36-AA-0055	1,651,063	67,520,000	III	33,780,000	28,456,272	25,826,668	0.02137	M	912,060,000	51	16	805,014	Y	120,504
36-AA-0057	372,299		III	13,983,500	11,779,700	10,691,155	0.00885	M	377,554,500	94	29	35,235	Y	2,033
36-AA-0067	279,224	8,302,400	III	2,642,600	2,226,126	2,020,413	0.00167	S	71,350,200	24	7	2706,4982?	Y*	-
36-AA-0068	1,861,493	18,935,202	III	64,798	54,586	49,542	0.00004	S	1,749,546	0	0	7,619	Y*	-
36-AA-0074	60,701	221,600	III	298,800		228,449	0.00019	S	8,067,600	12	4	-	Y*	-
36-AA-0087	461,327	13,605,488	III	6,794,512	5,723,697	5,194,778	0.00430	M	183,451,824	37	11	190,059	Y	20,362
37-AA-0006	76,888	111,504	III	364,594	307,134	278,752	0.00023	S	9,844,038	12	4	1,668	Y*	-
37-AA-0010	930,747	21,194,008	III	39,959,992	33,662,297	30,551,612	0.02528	M	1,078,919,784	108	33	1,072,468	Y	215,153
37-AA-0020	1,927,455	15,527,878	III	72,232,122	60,848,340	55,225,430	0.04570	L	1,950,267,294	94	29	642,013	Y	11,917
37-AA-0023	1,413,116	39,608,998	III	31,624,173	26,640,203	24,178,420	0.02001	M	853,852,671	56	17	693,347	Y	80,188

SWIS No	Disposal Area in m2	Remaining Capacity	WDRNo	WIP (cubic yards)	WIP (tons)	WIP (metric tons, tonnes)	Fraction of Total Waste (m3)	Size	Amount of Waste (ft3)	Waste Column Height (ft)	Waste Column Height (m)	Tonnage (2)	ADC (Users) (3)	ADC Amnt
37-AA-0902	115,736	1,064,500	III	855,500	720,673	654,077	0.00054	S	23,098,500	19	6	390	Y*	-
37-AA-0903	358,944	9,503,985	III	5,096,015	4,292,883	3,896,184	0.00322	S	137,592,405	36	11	19,380	Y*	-
39-AA-0004	2,727,492	125,000,000	III	13,000,000	10,951,200	9,939,215	0.00822	M	351,000,000	12	4	124,640	Y*	-
39-AA-0015	1,434,564	22,100,000	I,II,III	28,940,000	24,379,056	22,126,222	0.01831	M	781,380,000	51	15	619,130	Y*	-
39-AA-0022	748,644	35,400,000	III	5,800,000	4,885,920	4,434,419	0.00367	M	156,600,000	19	6	167,150	Y*	-
40-AA-0001	263,037	5,190,000	III	1,305,000	1,099,332	997,744	0.00083	S	35,235,000	12	4	29,204	Y	338
40-AA-0002	53,821	450,156	III	554,423	467,046	423,887	0.00035	S	14,969,421	26	8	542	Y*	-
40-AA-0004	489,654	14,500,000	III	9,400,000	7,918,560	7,186,817	0.00595	M	253,800,000	48	15	125,467	Y	7,637
40-AA-0008	312,002	6,124,976	III	4,424,004	3,726,781	3,382,394	0.00280	S	119,448,108	36	11	71,426	Y	10,894
41-AA-0002	700,083	22,180,000	III	38,320,000	32,280,768	29,297,748	0.02424	M	1,034,640,000	137	42	396,325	Y	23,534

SWIS No	Disposal Area in m2	Remaining Capacity	WDRNo	WIP (cubic yards)	WIP (tons)	WIP (metric tons, tonnes)	Fraction of Total Waste (m3)	Size	Amount of Waste (ft3)	Waste Column Height (ft)	Waste Column Height (m)	Tonnage (2)	ADC (Users) (3)	ADC Amnt
42-AA-0012	186,149	1,880,930	III	2,840,087	2,392,489	2,171,403	0.00180	S	76,682,349	38	12	253	Y	528
42-AA-0015	477,513	4,867,490	III	18,432,510	15,527,546	14,092,668	0.01166	M	497,677,770	97	30	141,998	Y	30,269
42-AA-0016	999,946	3,030,720	III	10,967,680	9,239,174	8,385,395	0.00694	M	296,127,360	28	8	67,863	Y	15,973
42-AA-0017	157,822	2,146,779	III	5,823,221	4,905,481	4,452,173	0.00368	M	157,226,967	93	28	27,873	Y	5,838
43-AN-0001	101,168	640,000	III	-	178,000	161,551	0.00013	S	-	-	-	13,170	Y	20,276
43-AN-0003	1,205,924	21,200,000	III	36,300,000	30,579,120	27,753,347	0.02297	M	980,100,000	76	23	476,640	Y	134,322
43-AN-0008	1,258,531	16,191,600	III	20,208,400	17,023,556	15,450,433	0.01279	M	545,626,800	40	12	137,123	Y	8,574
43-AN-0015	465,373	11,055,000	III	17,545,000	14,779,908	13,414,117	0.01110	M	473,715,000	95	29	121,937	Y	26,982
44-AA-0001	271,131	6,150,000	III	968,000	815,443	740,089	0.00061	S	26,136,000	9	3	34,726	Y	1,829
44-AA-0002	194,243	2,100,000	III	337,203	284,060	257,810	0.00021	S	9,104,481	4	1	32,129	Y	5,701

SWIS No	Disposal Area in m2	Remaining Capacity	WDRNo	WIP (cubic yards)	WIP (tons)	WIP (metric tons, tonnes)	Fraction of Total Waste (m3)	Size	Amount of Waste (ft3)	Waste Column Height (ft)	Waste Column Height (m)	Tonnage (2)	ADC (Users) (3)	ADC Amnt
44-AA-0004	246,850	3,303,649	II,III	4,234,051	3,566,765	3,237,165	0.00268	S	114,319,377	43	13	53,691	Y	117
45-AA-0020	526,074	11,914,025	III	4,925,975	4,149,641	3,766,179	0.00312	S	133,001,325	23	7	54,239	Y	6,594
45-AA-0043	493,700	6,589,044	III	6,526,800	5,498,176	4,990,098	0.00413	M	176,223,600	33	10	93,776	Y	138
46-AA-0001	42,491	30,541	III	713,459	601,018	545,479	0.00045	S	19,263,393	42	13	1,630	Y	8
48-AA-0002	1,035,961	30,433,000	II,III	6,567,000	5,532,041	5,020,833	0.00415	M	177,309,000	16	5	196,864	Y	60,290
48-AA-0075	1,375,886	13,872,000	III	69,228,000	58,317,667	52,928,614	0.04380	L	1,869,156,000	126	38	486,935	Y	265,635
48-AA-0078	-			-		-	-	-	-	-	-	-	N	
49-AA-0001	696,037	9,076,760	III	23,573,240	19,858,097	18,023,039	0.01491	M	636,477,480	85	26	138213,52013?	Y*	-
50-AA-0001	819,462	8,240,435	II,III	6,399,565	5,390,994	4,892,819	0.00405	M	172,788,255	20	6	155,413	Y	9,825
52-AA-0001	218,523	2,148,557	III	2,948,443	2,483,768	2,254,247	0.00187	S	79,607,961	34	10	35,993	Y	1,054
52-AA-0028	46,537			-		-	-	-	-	-	-	-	N	

SWIS No	Disposal Area in m2	Remaining Capacity	WDRNo	WIP (cubic yards)	WIP (tons)	WIP (metric tons, tonnes)	Fraction of Total Waste (m3)	Size	Amount of Waste (ft3)	Waste Column Height (ft)	Waste Column Height (m)	Tonnage (2)	ADC (Users) (3)	ADC Amnt
54-AA-0004	287,317	857,757	III	7,022,550	5,915,796	5,369,126	0.00444	M	189,608,850	61	19	81,671	Y	561
54-AA-0009	999,541	14,815,501	III	3,815,165	3,213,895	2,916,903	0.00241	S	103,009,455	10	3	169,195	Y	11,857
55-AA-0012	-	-		-		-	-	-	-	-	-	-	N	
56-AA-0005	369,871	21,983,000	III	8,017,000	6,753,521	6,129,437	0.00507	M	216,459,000	54	17	330,097	Y	34,685
56-AA-0007	1,489,194	119,600,000	III	-	23,547,852	27,697,889	0.02292	M	-	-	-	422404,203609?	Y	184,927
57-AA-0001	1,914,100		II,III	49,035,200	41,307,252	37,490,107	0.03102	M	1,323,950,400	64	20	134,705	Y	35,461
58-AA-0011	910,513	39,223,000	II,III	4,244,231	3,575,340	3,244,948	0.00269	S	114,594,237	12	4	132,104	Y	14,384

SWIS No	AIC (Y/N)	AIC Amnt	Disposal Start Date	Age of Waste	Final Cover System (4)	Liner System	Leachate Recirculation (Y/N)	LFG System Type (Y/N)	2010 Avg. Total System Flow	2010 Avg. Total % Methane by Volume	Climate Zone	Climate #	Climate Zone (title)
01-AA-0009	Y*	0	1980	37	Water Balance-CCL	Unlined/CCL Canyon Bottom (122)- Composite	No	Active-Flare/LFGTE	8,104	50%	Csb	2	Warm temperature, summer dry, warm summer
01-AA-0010	Y*	0	1962	55	Water Balance-CCL	Composite- Unlined (87)	Yes	Active-Flare/LFGTE Planned	1,875	44%	Csb	2	Warm temperature, summer dry, warm summer
04-AA-0002	Y*	0	1970	47	Composite	Unlined (49.5)- CCL-Composite (double floor, single sideslopes)	No	Active-Flare	882	40%	Csa	1	Warm temperature, summer dry, hot summer
05-AA-0023	Y	221	1990	27	Composite	Composite- CCL	No	Active-Flare Proposed			Csb	2	Warm temperature, summer dry, warm summer
06-AA-0002	Y*	0	1974	43	CCL	Unlined	No	No System			Csb	2	Warm temperature, summer dry, warm summer
07-AA-0002	Y*	0	1954	63	Composite- CCL	Unlined (141)- CCL	No	Active-Flare/LFGTE- No flow data			Csb	2	Warm temperature, summer dry, warm summer
07-AA-0032	Y*	0	1992	25	Composite	Composite	No	Active-Flare/LFGTE	1,849	57%	Csb	2	Warm temperature, summer dry, warm summer
07-AC-0042	N		-	-	-	-					Csb	2	Warm temperature, summer dry, warm summer
09-AA-0003	Y*	0	1962	55	CCL - Composite	Unlined (25)-Composite	No	Active-Flare/LFGTE- No flow data			Csa	1	Warm temperature, summer dry, hot summer
10-AA-0004	Y*	0	1960	57	FML- CCL	Composite- CCL	Yes	Active-Flare- No flow data			BSk	6	Arid, steppe, cold arid
10-AA-0009	Y*	0	1992	25	Composite	Composite- Unlined (30)	Yes	Active-Flare	1,100	48%	BSk	6	Arid, steppe, cold arid

SWIS No	AIC (Y/N)	AIC Amnt	Disposal Start Date	Age of Waste	Final Cover System (4)	Liner System	Leachate Recirculation (Y/N)	LFG System Type (Y/N)	2010 Avg. Total System Flow	2010 Avg. Total % Methane by Volume	Climate Zone	Climate #	Climate Zone (title)
11-AA-0001	Y*	0	1972	45	FML	Unlined	No	No System			Csa	1	Warm temperature, summer dry, hot summer
13-AA-0001	Y*	0	1970	47	Water Balance	Unlined	No	No System			BWh	4	Arid, desert, hot arid
13-AA-0004	Y*	0	1971	46	Water Balance	Unlined	No	No System			BWh	4	Arid, desert, hot arid
13-AA-0009	Y*	0	1971	46	Water Balance	Unlined	No	No System			BWh	4	Arid, desert, hot arid
13-AA-0010	Y*	0	1970	47	Water Balance	Unlined	No	No System			BWh	4	Arid, desert, hot arid
13-AA-0011	Y*	0	1970	47	Water Balance	Unlined	No	No System			BWh	4	Arid, desert, hot arid
13-AA-0019	Y*	0	1971	46	Water Balance	Composite- Unlined (31)	No	Active-Flare	151	35%	BWh	4	Arid, desert, hot arid
13-AA-0022	Y*	0	-	-	-	-					BWh	4	Arid, desert, hot arid
14-AA-0003	Y*	0	1965	52	Water Balance	Unlined	No	No System			Csb	2	Warm temperature, summer dry, warm summer
14-AA-0004	Y*	0	1965	52	Water Balance	Unlined	No	No System			Csb	2	Warm temperature, summer dry, warm summer
14-AA-0005	Y*	0	1955	62	Water Balance	Unlined	No	No System			Csb	2	Warm temperature, summer dry, warm summer
14-AA-0006	N		1972	45	Water Balance	Unlined	No	No System			BWh	4	Arid, desert, hot arid
14-AA-0007	N		1965	52	Water Balance	Unlined	No	No System			BWh	4	Arid, desert, hot arid

SWIS No	AIC (Y/N)	AIC Amnt	Disposal Start Date	Age of Waste	Final Cover System (4)	Liner System	Leachate Recirculation (Y/N)	LFG System Type (Y/N)	2010 Avg. Total System Flow	2010 Avg. Total % Methane by Volume	Climate Zone	Climate #	Climate Zone (title)
15-AA-0045	Y*	0	1973	44	Water Balance	Unlined	No	No System			BSk	6	Arid, steppe, cold arid
15-AA-0057	N		1972	45	Water Balance	Unlined (48)-Composite	No	Active-Flare	197	37%	BSk	6	Arid, steppe, cold arid
15-AA-0058	Y*	0	1972	45	Water Balance	Unlined	No	No System			BSk	6	Arid, steppe, cold arid
15-AA-0059	Y*	0	1968	49	GCL	Unlined	No	Active-Carbon	60	12%	BWk	3	Arid, desert, cold arid
15-AA-0061	Y*	0	1968	49	Water Balance	Unlined	No	No System			BWk	3	Arid, desert, cold arid
15-AA-0062	Y*	0	1969	48	Water Balance	Unlined	No	No System			BSk	6	Arid, steppe, cold arid
15-AA-0105	Y*	0	-	-	-	-					BSk	6	Arid, steppe, cold arid
15-AA-0150	Y*	0	1973	44	CCL- FML (21)	Unlined	No	No System			BSk	6	Arid, steppe, cold arid
15-AA-0273	Y*	0	1992	25	Water Balance	Composite- CCL	Yes	Active-Flare/LFGTE Planned	696	43%	BSk	6	Arid, steppe, cold arid
15-AA-0278	Y*	0	-	-	-	-					BSk	6	Arid, steppe, cold arid
15-AA-0308	Y*	0	-	-	-	-					BSk	6	Arid, steppe, cold arid
16-AA-0004	Y*	0	1992	25	Water Balance	Composite- Unlined (44)	No	Active-Carbon Proposed			Csb	2	Warm temperature, summer dry, warm summer
16-AA-0021	Y*	0	-	-	-	-					Csb	2	Warm temperature, summer dry, warm summer

SWIS No	AIC (Y/N)	AIC Amnt	Disposal Start Date	Age of Waste	Final Cover System (4)	Liner System	Leachate Recirculation (Y/N)	LFG System Type (Y/N)	2010 Avg. Total System Flow	2010 Avg. Total % Methane by Volume	Climate Zone	Climate #	Climate Zone (title)
16-AA-0027	Y*	0	1998	19	Water Balance	Triple Composite	Yes- RD&D project adds additional liquids and liquid wastes from outside unit.	Active-Flare	468	49%	Csb	2	Warm temperature, summer dry, warm summer
17-AA-0001	Y*	0	1971	46	Composite	Unlined	No	No System			Csb	2	Warm temperature, summer dry, warm summer
18-AA-0009	Y*	0	1967	50	GCL	Unlined	No	No System			Csb	2	Warm temperature, summer dry, warm summer
18-AA-0010	Y*	0	1972	45	CCL	Unlined	No	No System			Csb	2	Warm temperature, summer dry, warm summer
18-AA-0013	N		1968	49	CCL	Unlined	No	No System			Csb	2	Warm temperature, summer dry, warm summer
19-AA-0012	Y*	0	1952	65	Water Balance	Unlined	No	Active-Flare/LFGTE	6,242	34%	Csb	2	Warm temperature, summer dry, warm summer
19-AA-0040	Y*	0	1958	59	Water-Balance-Soil (Units 1 and 2)	Unlined (Unit 3-27.4; Unit 1- 31; Unit 2-15)- Composite	No	Active-Flare/LFGTE	335	47%	Csb	2	Warm temperature, summer dry, warm summer
19-AA-0050	Y*	0	1957	60	Water Balance	Composite- Unlined (78)	Yes	Active-Flare	444	44%	BSk	6	Arid, steppe, cold arid
19-AA-0052	Y*	0	1971	46	Water Balance	Unlined (154)-Composite (103)	No	Active-Flare/LFGTE	4,116	46%	Csb	2	Warm temperature, summer dry, warm summer
19-AA-0056	Y*	0	1972	45	Water Balance	Composite- CCL-Unlined (est. 160)	No	Active-Flare/LFGTE	5,693	30%	Csb	2	Warm temperature, summer dry, warm summer
19-AA-0061	Y*	0	1961	56	Water Balance	Unlined	No	No System			Csb	2	Warm temperature, summer dry, warm summer

SWIS No	AIC (Y/N)	AIC Amnt	Disposal Start Date	Age of Waste	Final Cover System (4)	Liner System	Leachate Recirculation (Y/N)	LFG System Type (Y/N)	2010 Avg. Total System Flow	2010 Avg. Total % Methane by Volume	Climate Zone	Climate #	Climate Zone (title)
19-AA-0063	Y	20	1940	77	Water Balance	Unlined	No	No System			Csb	2	Warm temperature, summer dry, warm summer
19-AA-2000	Y*	0	1948	69	Composite	Composite- Unlined (Unit I- 125 acres; overlain by composite liner for vertical expansion)	No	Active-Flare/LFGTE	7,679	41%	Csb	2	Warm temperature, summer dry, warm summer
19-AA-5624	Y*	0	1960	57	Water Balance	Composite (90)-Unlined (35)	Yes	Active-Flare	812	45%	BSk	6	Arid, steppe, cold arid
19-AH-0001	Y*	0	1963	54	Water Balance	Unlined (62)-Composite	No	Active-Flare	600	45%	Csb	2	Warm temperature, summer dry, warm summer
19-AR-0004	N		-	-	-	-					Csb	2	Warm temperature, summer dry, warm summer
20-AA-0002	Y*	0	1958	59	Water Balance	Unlined (29)- CCL-Composite	No	Active-Flare	344	23%	Csa	1	Warm temperature, summer dry, hot summer
21-AA-0001	Y*	0	1958	59	FML	Unlined (209)-Composite	No	Active-Flare/LFGTE Planned	2,774	50%	Csb	2	Warm temperature, summer dry, warm summer
22-AA-0001	Y*	0	1973	44	CCL	Unlined	No	No System			Csa	1	Warm temperature, summer dry, hot summer
24-AA-0001	Y*	0	1972	45	Water Balance	Unlined (89)-Composite	No	Active-Flare Proposed			Csb	2	Warm temperature, summer dry, warm summer
24-AA-0002	Y*	0	1940	77	GCL	Unlined (40)-Composite	No	No System			Csa	1	Warm temperature, summer dry, hot summer
25-AA-0001	N		1973	44	CCL	Unlined	No	No System			Csb	2	Warm temperature, summer dry, warm summer
26-AA-0001	Y*	0	1970	47	GCL	Unlined	No	No System			Csb	2	Warm temperature, summer dry, warm summer

SWIS No	AIC (Y/N)	AIC Amnt	Disposal Start Date	Age of Waste	Final Cover System (4)	Liner System	Leachate Recirculation (Y/N)	LFG System Type (Y/N)	2010 Avg. Total System Flow	2010 Avg. Total % Methane by Volume	Climate Zone	Climate #	Climate Zone (title)
26-AA-0003	Y*	0	1972	45	Composite	Unlined	No	No System			Csb	2	Warm temperature, summer dry, warm summer
26-AA-0004	Y*	0	1973	44	GCL	Unlined	No	No System			Csb	2	Warm temperature, summer dry, warm summer
27-AA-0005	Y*	0	1976	41	Composite	Composite- Unlined (11)	No	Active-Flare- No flow data			Csb	2	Warm temperature, summer dry, warm summer
27-AA-0010	Y	4340.8	1966	51	CCL- Composite	Composite- Unlined (52 acres; Modules 1 and 2)	No	Active-Flare/LFGTE	1,244	52%	Csb	2	Warm temperature, summer dry, warm summer
28-AA-0002	Y*	0	1963	54	Composite- CCL	Composite- Unlined (12)	Yes	No System			Csb	2	Warm temperature, summer dry, warm summer
30-AB-0019	Y*	0	1976	41	Water Balance	Composite- Unlined (139)	No	Active-Flare/LFGTE	2,056	46%	Csb	2	Warm temperature, summer dry, warm summer
30-AB-0035	Y*	0	1960	57	Water Balance	Unlined	No	Active-Flare/LFGTE	8,066	52%	Csb	2	Warm temperature, summer dry, warm summer
30-AB-0360	Y*	0	1989	28	Water Balance	Composite	No	Active-Flare/LFGTE	6,331	49%	Csb	2	Warm temperature, summer dry, warm summer
31-AA-0210	Y*	0	1980	37	Composite- CCL	Composite- Double Composite- CCL	No	Active-Flare/LFGTE	1,382	50%	Csa	1	Warm temperature, summer dry, hot summer
32-AA-0009	N		1978	39	GCL	Unlined	No	No System			Csb	2	Warm temperature, summer dry, warm summer

SWIS No	AIC (Y/N)	AIC Amnt	Disposal Start Date	Age of Waste	Final Cover System (4)	Liner System	Leachate Recirculation (Y/N)	LFG System Type (Y/N)	2010 Avg. Total System Flow	2010 Avg. Total % Methane by Volume	Climate Zone	Climate #	Climate Zone (title)
33-AA-0006	Y*	0	1966	51	Water Balance	CCL- Unlined (38)	Yes	Active-Flare/LFGTE	1,027	43%	Csb	2	Warm temperature, summer dry, warm summer
33-AA-0007	Y*	0	1970	47	Water Balance	Unlined (74)-Composite	No	Active-Flare/LFGTE	842	42%	Csb	2	Warm temperature, summer dry, warm summer
33-AA-0015	Y*	0	1972	45	Water Balance	Unlined	No	No System			BWh	4	Arid, desert, hot arid
33-AA-0016	Y*	0	1975	42	Water Balance	Unlined	No	No System			Csb	2	Warm temperature, summer dry, warm summer
33-AA-0017	Y*	0	1956	61	Water Balance	Unlined	No	Active-Carbon	55	13%	Csb	2	Warm temperature, summer dry, warm summer
33-AA-0071	Y*	0	1982	35	Water Balance	Unlined	No	No System			BWh	4	Arid, desert, hot arid
33-AA-0217	Y*	0	1983	34	Water Balance	Composite- CCL-Unlined (est. 100)	Yes	Active-Flare/LFGTE	2,617	45%	Csb	2	Warm temperature, summer dry, warm summer
33-AA-0231	N		-	-	-	-					BWh	4	Arid, desert, hot arid
34-AA-0001	Y*	0	1967	50	GCL- Water Balance	Composite- Unlined (165)	Yes	Active-Flare/LFGTE	6,032	49%	Csa	1	Warm temperature, summer dry, hot summer
34-AA-0020	Y	32326.8	1977	40	FML- Composite	Unlined (100)-Composite	No	Active-Carbon-No flow data			Csa	1	Warm temperature, summer dry, hot summer
35-AA-0001	Y*	0	1968	49	CCL- FML	Unlined (29)-Composite	No	Active-Flare	189	38%	Csb	2	Warm temperature, summer dry, warm summer
36-AA-0017	Y	2511	1963	54	Water Balance	Unlined (63)- Double Composite-Composite	No	Active-Flare/LFGTE- No flow data			BSk	6	Arid, steppe, cold arid
36-AA-0028	N		-	-	-	-					BSk	6	Arid, steppe, cold arid

SWIS No	AIC (Y/N)	AIC Amnt	Disposal Start Date	Age of Waste	Final Cover System (4)	Liner System	Leachate Recirculation (Y/N)	LFG System Type (Y/N)	2010 Avg. Total System Flow	2010 Avg. Total % Methane by Volume	Climate Zone	Climate #	Climate Zone (title)
36-AA-0045	Y*	0	1955	62		Unlined	No	Active-Flare	297	32%	BSk	6	Arid, steppe, cold arid
36-AA-0046	Y*	0	1963	54		Unlined	No	Active-Carbon	141	7%	Csa	1	Warm temperature, summer dry, hot summer
36-AA-0055	Y*	0	1958	59	Water Balance	Composite- Unlined (142)	No	Active-Flare/LFGTE	2,221	44%	Csb	2	Warm temperature, summer dry, warm summer
36-AA-0057	Y*	0	1963	54		Unlined	No	No System			BSk	6	Arid, steppe, cold arid
36-AA-0067	Y*	0	1972	45		Unlined	No	No System			Csb	2	Warm temperature, summer dry, warm summer
36-AA-0068	Y*	0	1940	77		Unlined	No	No System			BSk	6	Arid, steppe, cold arid
36-AA-0074	Y*	0	-	-	-	-					BSk	6	Arid, steppe, cold arid
36-AA-0087	Y*	0	1978	39	Water Balance	Composite- Unlined (52)	No	Active-Flare/LFGTE Planned	227	40%	Csb	2	Warm temperature, summer dry, warm summer
37-AA-0006	Y*	0	1973	44	Water Balance	Unlined	No	No System			BSk	6	Arid, steppe, cold arid
37-AA-0010	Y*	0	1963	54	Water Balance-CCL	Unlined (est. 150)-FML (Canyon 3)	No	Active-Flare/LFGTE	6,054	44%	Csb	2	Warm temperature, summer dry, warm summer
37-AA-0020	Y*	0	1973	44	Water Balance	Unlined (239)-Composite	Yes	Active-Flare/LFGTE	4,585	47%	Csb	2	Warm temperature, summer dry, warm summer
37-AA-0023	Y*	0	1976	41	Water Balance	Composite- Unlined (110)	No	Active-Flare/LFGTE	2,564	43%	Csb	2	Warm temperature, summer dry, warm summer

SWIS No	AIC (Y/N)	AIC Amnt	Disposal Start Date	Age of Waste	Final Cover System (4)	Liner System	Leachate Recirculation (Y/N)	LFG System Type (Y/N)	2010 Avg. Total System Flow	2010 Avg. Total % Methane by Volume	Climate Zone	Climate #	Climate Zone (title)
37-AA-0902	Y*	0	1974	43	CCL	Unlined	No	No System			Csb	2	Warm temperature, summer dry, warm summer
37-AA-0903	Y*	0	1971	46	CCL	Composite- Unlined (39)	Yes	No System			Csb	2	Warm temperature, summer dry, warm summer
39-AA-0004	Y*	0	1965	52	Water Balance	Unlined (74)- Composite	Yes	No System			Csa	1	Warm temperature, summer dry, hot summer
39-AA-0015	Y*	0	1973	44	Water Balance	Composite- Unlined (139)- CCL	No	Active-Flare/LFGTE	1,533	42%	Csa	1	Warm temperature, summer dry, hot summer
39-AA-0022	Y*	0	1990	27	GCL	Composite	Yes	Active-Flare	320	55%	Csa	1	Warm temperature, summer dry, hot summer
40-AA-0001	Y*	0	1970	47	Composite	Unlined (est. 25)- Composite	Yes	Active-Flare	200	47%	Csb	2	Warm temperature, summer dry, warm summer
40-AA-0002	Y*	0	1941	76	Water Balance	Unlined	No	No System			Csb	2	Warm temperature, summer dry, warm summer
40-AA-0004	Y*	0	1965	52	Composite- GCL	Unlined (66)- Composite	Yes	Active-Flare/LFGTE	510	39%	Csb	2	Warm temperature, summer dry, warm summer
40-AA-0008	Y*	0	1970	47	CCL or GCL	Composite- Unlined (19)	No	Active-Flare	230	30%	Csb	2	Warm temperature, summer dry, warm summer
41-AA-0002	Y*	0	1976	41	Composite	Unlined (70)- Composite	No	Active-Flare/LFGTE	3,623	55%	Csb	2	Warm temperature, summer dry, warm summer

SWIS No	AIC (Y/N)	AIC Amnt	Disposal Start Date	Age of Waste	Final Cover System (4)	Liner System	Leachate Recirculation (Y/N)	LFG System Type (Y/N)	2010 Avg. Total System Flow	2010 Avg. Total % Methane by Volume	Climate Zone	Climate #	Climate Zone (title)
42-AA-0012	Y*	0	1941	76	CCL	Unlined	No	No System			Csb	2	Warm temperature, summer dry, warm summer
42-AA-0015	Y*	0	1967	50	Composite-Water Balance	Unlined (89)-Composite	No	Active-Flare/LFGTE	1,188	53%	Csb	2	Warm temperature, summer dry, warm summer
42-AA-0016	Y*	0	1960	57	CCL- Composite	Unlined (186)-Composite	No	Active-Flare	101	47%	Csb	2	Warm temperature, summer dry, warm summer
42-AA-0017	Y	13276	1960	57	CCL	Unlined	No	No System			Csb	2	Warm temperature, summer dry, warm summer
43-AN-0001	Y*	0	-	-	-	-					Csb	2	Warm temperature, summer dry, warm summer
43-AN-0003	Y	1352.8	1932	85	Water Balance	Unlined (205)-Composite	No	Active-Flare/LFGTE	2,857	46%	Csb	2	Warm temperature, summer dry, warm summer
43-AN-0008	Y*	0	1986	31	Composite	Composite- Unlined (22 Unit-C1)	No	Active-Flare/LFGTE Planned	1,589	48%	Csb	2	Warm temperature, summer dry, warm summer
43-AN-0015	Y*	0	1929	88	FML (topdeck)-CCL (sideslopes)	Composite- Unlined (26)	No	Active-Flare/LFGTE	1,816	49%	Csb	2	Warm temperature, summer dry, warm summer
44-AA-0001	Y*	0	1966	51	FML- CCL- Water Balance (6)	Unlined (40)-Composite	No	Active-Flare/LFGTE	578	46%	Csb	2	Warm temperature, summer dry, warm summer
44-AA-0002	Y	7728	1956	61	CCL	Unlined	No	Active-Flare- No flow data			Csb	2	Warm temperature, summer dry, warm summer

SWIS No	AIC (Y/N)	AIC Amnt	Disposal Start Date	Age of Waste	Final Cover System (4)	Liner System	Leachate Recirculation (Y/N)	LFG System Type (Y/N)	2010 Avg. Total System Flow	2010 Avg. Total % Methane by Volume	Climate Zone	Climate #	Climate Zone (title)
44-AA-0004	Y*	0	1966	51	FML- CCL	Composite- Unlined (57)	No	Active-Flare/LFGTE	1,110	45%	Csb	2	Warm temperature, summer dry, warm summer
45-AA-0020	Y*	0	1976	41	FML- CCL	Composite- Unlined (40)	No	Active-Flare	539	51%	Csa	1	Warm temperature, summer dry, hot summer
45-AA-0043	Y*	0	1981	36	CCL	Composite-CCL	No	Active-Flare Proposed			Csb	2	Warm temperature, summer dry, warm summer
46-AA-0001	Y*	0	1977	40	CCL	Unlined	No	No System			Csb	2	Warm temperature, summer dry, warm summer
48-AA-0002	Y*	0	1964	53	Composite	Composite- Unlined (35)- CCL	Yes	Active-Flare	236	48%	Csa	1	Warm temperature, summer dry, hot summer
48-AA-0075	Y*	0	1986	31	Water Balance	Composite- CCL	Yes	Active-Flare/LFGTE Planned	1,846	51%	Csa	1	Warm temperature, summer dry, hot summer
48-AA-0078	N		-	-	-	-					Csb	2	Warm temperature, summer dry, warm summer
49-AA-0001	Y*	0	1972	45	Composite	Unlined (110)- Composite	No	Active-Flare/LFGTE	1,625	54%	Csb	2	Warm temperature, summer dry, warm summer
50-AA-0001	Y*	0	1973	44	FML- CCL	Composite- Unlined (18)- CCL	No	Active-Flare	360	24%	Csb	2	Warm temperature, summer dry, warm summer
52-AA-0001	Y*	0	1962	55	CCL- Composite	Unlined (32) - Composite	No	Active-Flare	250	35%	Csa	1	Warm temperature, summer dry, hot summer
52-AA-0028	N		-	-	-	-					Csa	1	Warm temperature, summer dry, hot summer

SWIS No	AIC (Y/N)	AIC Amnt	Disposal Start Date	Age of Waste	Final Cover System (4)	Liner System	Leachate Recirculation (Y/N)	LFG System Type (Y/N)	2010 Avg. Total System Flow	2010 Avg. Total % Methane by Volume	Climate Zone	Climate #	Climate Zone (title)
54-AA-0004	Y*	0	1972	45	Water Balance	Unlined	No	Active-Flare/LFGTE Planned	112	41%	BSk	6	Arid, steppe, cold arid
54-AA-0009	Y*	0	1952	65	Water Balance	Unlined (127)-Composite	No	Active-Flare/LFGTE- No flow data			BSk	6	Arid, steppe, cold arid
55-AA-0012	N		-	-	-	-					Csb	2	Warm temperature, summer dry, warm summer
56-AA-0005	Y*	0	1970	47	Water Balance	Composite- Unlined (Phase 1- est. 50 acres; CCL overlies)	Yes	Active-Flare/LFGTE	1,500	52%	Csb	2	Warm temperature, summer dry, warm summer
56-AA-0007	Y*	0	1970	47	Water Balance	Composite- Unlined (est. 25)	Yes	Active-Flare/LFGTE	2,860	47%	Csb	2	Warm temperature, summer dry, warm summer
57-AA-0001	Y*	0	1975	42	CCL- Composite	Composite- CCL-Unlined (94)	Yes- includes RD&D and bioreactor Project XL projects which add leachate and ground water from units.	Active-Flare/LFGTE	1,085	49%	Csa	1	Warm temperature, summer dry, hot summer
58-AA-0011	Y*	0	1995	22	Composite	Composite	Yes	Active-Flare/LFGTE	509	50%	Csa	1	Warm temperature, summer dry, hot summer
	All data from CalRecycle SWIS Database with the exception of the data in columns listed with the following notes:												
	(1) From CARB Landfill Methane Reports (2017-2018).												
	(2) From CalRecycle 2015 Q3 Tonnage Report.												
	(3) From Disposal ADC AIC (only columns X-AA in those data).												
	(4) From Scott Walker Master 2012 Master List (only columns AA-AH in those data).												

Gas	Units	Level of Detection (LOD)
CH4	ppmv	0.1
CO	ppbv	1
CO2	ppmv	50
N2O	ppbv	50
OCS	pptv	50
DMS	pptv	1
DMDS	pptv	0.1
CS2	pptv	1
CFC-12	pptv	5
CFC-11	pptv	5
CFC-113	pptv	5.0
CFC-114	pptv	1
H-1211	pptv	0.1
HFC-152a	pptv	0.2
HFC-134a	pptv	1
HCFC-22	pptv	1
HCFC-142b	pptv	1
HCFC-141b	pptv	1
HCFC-245fa	pptv	0.1
HFC365mfc	pptv	0.1
HCFC-21	pptv	0.1
CHCl3	pptv	1
CH3CCl3	pptv	0.1
CCl4	pptv	1.0
CH2Cl2	pptv	1.0
C2Cl4	pptv	0.1
CH3Cl	pptv	50
CH3Br	pptv	0.1
CH2Br2	pptv	0.05
CHBrCl2	pptv	0.05
CHBr3	pptv	0.05
CH3CH2Cl	pptv	1
1,2-DCE	pptv	1
1,2- DBE	pptv	1
MeONO2	pptv	0.1
EtONO2	pptv	0.1
i-PrONO2	pptv	0.1
n-PrONO2	pptv	0.1
2-BuONO2	pptv	0.1
Ethane	pptv	5

Gas	Units	Level of Detection (LOD)
Ethene	pptv	5
Ethyne	pptv	5
Propane	pptv	5
Propene	pptv	5
i-Butane	pptv	5
n-Butane	pptv	5
1-Butene	pptv	5
i-Butene	pptv	5
trans-2-Butene	pptv	5
cis-2-Butene	pptv	5
i-Pentane	pptv	5
n-Pentane	pptv	5
1-Pentene	pptv	5
Isoprene	pptv	5
n-Hexane	pptv	5
n-Undecane	pptv	5
Benzene	pptv	5
Toluene	pptv	5
Ethylbenzene	pptv	5
m+p-xylene	pptv	5
o-Xylene	pptv	5
i-Propylbenzene	pptv	5
n-Propylbenzene	pptv	5
3-Ethyltoluene	pptv	5
4-Ethyltoluene	pptv	5
2-Ethyltoluene	pptv	5
1,3,5-Trimethylbenzene	pptv	5
1,2,4-Trimethylbenzene	pptv	5
1,2,3-Trimethylbenzene	pptv	5
alpha-pinene	pptv	5
beta-Pinene	pptv	5
Limonene	pptv	5
Methanol	pptv	50
Ethanol	pptv	50
Isopropanol	pptv	5
2-Butanol	pptv	5
Acetaldehyde	pptv	10
Butanal	pptv	1
Acetone	pptv	50
Butanone	pptv	10
Methylisobutylketone	pptv	1
pptv = parts per trillion by volume		

Study	Food Wastes (1)	L_0 for Waste Fraction i (2)
Zhang et al. 2007	USA food waste	105
Lee et al. 2009	Korean food waste	11
Buffiere et al. 2006	Salad	26
	Carrots	47
	Potato	69
	Banana	32
	Apple	53
	Orange	65
Cho et al. 2012	Korean food waste	100
Cho et al. 1995	Boiled rice	102
	cooked meat	248
	cabbage	12
	Korean food waste	117
Nieto et al. 2012	beverage waste	54
	Apple waste	43
	milk waste	52
	yogurt waste	79
	fats/oils waste	25
Elezer et al. 1997	Food Wastes	300.7
Manfredi et al. 2009	Kitchen organics	59.8
		71.7
Ishii and Furuichi 2013	Kitchen Waste	126.7
Wangyao et al. 2010	Kitchen Waste	45.5
Jeon et al. 2007	Food Wastes	117.1
Moody et al. 2011	Potato Peel	23
	Food Scraps	79
	Food Grease	340
Karanjekar et al. 2015	Food Wastes	36.30413214
Tchnobanoglous et al. 1993/Machado	Food Wastes	151.503
	Food/Soiled Paper	387
	Food/Soiled Paper	304
	Food/Soiled Paper	333
	Food/Soiled Paper	318
	Food/Soiled Paper	374
	Food/Soiled Paper	293
	Food/Soiled Paper	322
	Food/Soiled Paper	272
	Food/Soiled Paper	294
	Food/Soiled Paper	375
	Food/Soiled Paper	333

Study	Food Wastes (1)	L_0 for Waste Fraction i (2)
Krause et al. 2018b	Food/Soiled Paper	347
	Food/Soiled Paper	257
	Food/Soiled Paper	262
	Food/Soiled Paper	271
	Food/Soiled Paper	258
	Food/Soiled Paper	347
	Food/Soiled Paper	310
	Food/Soiled Paper	216
	Food/Soiled Paper	393
	Food/Soiled Paper	401
	Food/Soiled Paper	351
	Food/Soiled Paper	326
	Food/Soiled Paper	336
	Food/Soiled Paper	538
	Food/Soiled Paper	338
	Food/Soiled Paper	315
	Food/Soiled Paper	144
	Food/Soiled Paper	73
	Food/Soiled Paper	364
	Food/Soiled Paper	295
	Food/Soiled Paper	334
	Food/Soiled Paper	311
	Food/Soiled Paper	461
	Food/Soiled Paper	322
	Food/Soiled Paper	377
	Food/Soiled Paper	489
	Food/Soiled Paper	322
	Food/Soiled Paper	386
Vermeulen et al. 1993	Cardboard	387
	Brochures	80
	Cardboard	183
Jokela et al. 2005	Cardboard	146
Owens and Chynoweth	Cellophane	325
Vermeulen et al. 1993	Office paper	308
Owens and Chynoweth	Coated Paper	325
	Cardboard	257
	Cardboard	300
	Cardboard	324
	Office paper	214
	Magazines	154

Study	Food Wastes (1)	L_0 for Waste Fraction i (2)
Vermuelen et al. 1993	Magazines	123
	Paperboard	304
Owens and Chynoweth	News paper	90
	News paper	75
Vermuelen et al. 1993	News paper	66
	News paper	102
Owens and Chynoweth	Office paper	329
Vermuelen et al. 1993	Cardboard	217
	Misc. Paper	186
Jeon et al. 2007	Office Paper	239
Vermeulen et al. 1993	Office Paper	115
	Cardboard	169
Owens and Chynoweth	Misc. Paper	326
Vermeulen et al. 1993	Misc. Paper	270
Eleazer et al. 1997	News paper	74.3
	Cardboard	152.3
	Office paper	217.3
	PhoneBooks	74.3
	Books	217.3
	Magazines	84.4
	Mail	150.8
Ishii and Furuichi 2013	Office Paper	214.4
Wangyao et al. 2010	Office Paper	121.4
Jeon et al. 2007	Office Paper	239.1
Karanjekar et al. 2015	Misc. Paper	241.4602722
Krause et al. 2018a	Office paper	255.1838814
		283.958325
		276.386103
		256.6983258
	News paper	40.5150796
		53.7265186
		60.7726194
		51.0842308
	Cardboard	207.3014255
		255.140216
		176.346914
		160.4006505
	Paperboard	211.10144
		238.14336
		221.56928

Study	Food Wastes (1)	L_0 for Waste Fraction i (2)
		204.9952
	Coated Paper	137.0774265
		141.948198
		160.7354595
		142.6440225
Qu et al. 2009	Office paper	258
	Cardboard	164
Tchnobanoglous et al. 1993/Machado	Office paper	188.3295
	Cardboard	197.415
	Cardboard	255
	News paper	79
	Office paper	369
	Junk Mail	307
	Paperboard	200
	Misc. Paper	219
	Cartons	299
	Cardboard	169
	538	82
	Office paper	317
	Junk Mail	328
	Paperboard	263
	Misc. Paper	303
	Cartons	286
	Cardboard	175
	News paper	43
	Office paper	315
	Junk Mail	267
	Paperboard	240
	Misc. Paper	106
	Cartons	260
	Cardboard	187
	News paper	73
	Office paper	313
	Junk Mail	250
	Paperboard	267
	Misc. Paper	179
	Cartons	300
	Cardboard	167
	News paper	22
	Office paper	349

Study	Food Wastes (1)	L_0 for Waste Fraction i (2)
	Junk Mail	285
	Paperboard	300
	Misc. Paper	164
	Cartons	282
	Cardboard	166
	News paper	-
	Office paper	229
	Junk Mail	318
	Paperboard	261
	Misc. Paper	303
	Cartons	272
	Cardboard	-
	News paper	84
	Office paper	287
	Junk Mail	-
	Paperboard	175
	Misc. Paper	132
	Cartons	-
	Cardboard	224
	News paper	184
	Office paper	294
	Junk Mail	-
	Paperboard	246
	Misc. Paper	209
	Cartons	208
	Cardboard	217
	News paper	149
	Office paper	289
	Junk Mail	311
	Paperboard	246
	Misc. Paper	290
	Cartons	252
	Cardboard	235
	News paper	111
	Office paper	338
	Junk Mail	319
	Paperboard	269
	Misc. Paper	279
	Cartons	264
	Cardboard	249

Study	Food Wastes (1)	L_0 for Waste Fraction i (2)
	News paper	126
	Office paper	0
	Junk Mail	0
	Paperboard	242
	Misc. Paper	273
	Cartons	248
	Cardboard	170
	News paper	92
	Office paper	335
	Junk Mail	310
	Paperboard	232
	Misc. Paper	222
	Cartons	262
	Cardboard	227
	News paper	55
	Office paper	275
	Junk Mail	240
	Paperboard	297
	Misc. Paper	213
	Cartons	232
	Cardboard	225
	News paper	83
	Office paper	275
	Junk Mail	298
	Paperboard	226
	Misc. Paper	324
	Cartons	286
	Cardboard	280
	News paper	78
	Office paper	304
	Junk Mail	224
	Paperboard	221
	Misc. Paper	213
	Cartons	255
	Cardboard	194
	News paper	116
	Office paper	289
	Junk Mail	218
	Paperboard	252
	Misc. Paper	274

Study	Food Wastes (1)	L_0 for Waste Fraction i (2)
Krause et al. 2018b	Cartons	260
	Cardboard	199
	News paper	38
	Office paper	148
	Junk Mail	273
	Paperboard	218
	Misc. Paper	219
	Cartons	242
	Cardboard	234
	News paper	116
	Office paper	314
	Junk Mail	283
	Paperboard	249
	Misc. Paper	301
	Cartons	273
	Cardboard	232
	News paper	77
	Office paper	311
	Junk Mail	333
	Paperboard	231
	Misc. Paper	212
	Cartons	273
	Cardboard	239
	News paper	40
	Office paper	306
	Junk Mail	303
	Paperboard	218
	Misc. Paper	315
	Cartons	244
	Cardboard	224
	News paper	73
	Office paper	281
	Junk Mail	351
	Paperboard	228
	Misc. Paper	327
	Cartons	303
	Cardboard	227
	News paper	40
	Office paper	281
	Junk Mail	140

Study	Food Wastes (1)	L_0 for Waste Fraction i (2)
	Paperboard	214
	Misc. Paper	234
	Cartons	293
	Cardboard	263
	News paper	38
	Office paper	303
	Junk Mail	194
	Paperboard	194
	Misc. Paper	281
	Cartons	283
	Cardboard	175
	News paper	0
	Office paper	276
	Junk Mail	289
	Paperboard	177
	Misc. Paper	196
	Cartons	259
	Cardboard	243
	News paper	32
	Office paper	314
	Junk Mail	235
	Paperboard	347
	Misc. Paper	280
	Cartons	285
	Cardboard	194
	News paper	18
	Office paper	308
	Junk Mail	226
	Paperboard	208
	Misc. Paper	310
	Cartons	364
	Cardboard	233
	News paper	56
	Office paper	276
	Junk Mail	288
	Paperboard	184
	Misc. Paper	232
	Cartons	273
	Cardboard	226
	News paper	56

Study	Food Wastes (1)	L_0 for Waste Fraction i (2)
	Office paper	312
	Junk Mail	194
	Paperboard	319
	Misc. Paper	185
	Cartons	275
	Cardboard	178
	News paper	73
	Office paper	295
	Junk Mail	319
	Paperboard	256
	Misc. Paper	367
	Cartons	280
	Cardboard	215
	News paper	183
	Office paper	203
	Junk Mail	366
	Paperboard	299
	Misc. Paper	281
	Cartons	243
	Cardboard	241
	News paper	-
	Office paper	253
	Junk Mail	-
	Paperboard	206
	Misc. Paper	305
	Cartons	-
	Cardboard	193
	News paper	-
	Office paper	215
	Junk Mail	361
	Paperboard	201
	Misc. Paper	292
	Cartons	-
	Cardboard	234
	News paper	-
	Office paper	280
	Junk Mail	-
	Paperboard	265
	Misc. Paper	312
	Cartons	198

Study	Food Wastes (1)	L_0 for Waste Fraction i (2)
	Cardboard	189
	News paper	49
	Office paper	305
	Junk Mail	308
	Paperboard	293
	Misc. Paper	349
	Cartons	260
	Cardboard	236
	News paper	322
	Office paper	293
	Junk Mail	302
	Paperboard	281
	Misc. Paper	291
	Cartons	130
	Cardboard	198
	News paper	59
	Office paper	323
	Junk Mail	308
	Paperboard	145
	Misc. Paper	298
	Cartons	245
	Cardboard	218
	News paper	122
	Office paper	295
	Junk Mail	-
	Paperboard	119
	Misc. Paper	272
	Cartons	163
	Cardboard	236
	News paper	322
	Office paper	293
	Junk Mail	302
	Paperboard	281
	Misc. Paper	291
	Cartons	130
	Cardboard	206
	News paper	28
	Office paper	317
	Junk Mail	238
	Paperboard	191

Study	Food Wastes (1)	L_0 for Waste Fraction i (2)
	Misc. Paper	282
	Cartons	160
Elezer et al. 1997	Leaves	30.6
	Grass	136
	Branches	62.6
Bufiere et al. 2006	Grass	104
Karanjekar et al. 2015	Yard Wastes	39.14087845
Yazdani et al. 2012	Yard Wastes	49
Tchnobanoglous et al. 1993/Machado	Yard Wastes	192.688
	Leaves/branches	337.204
Krause et al. 2018b	Yard Wastes	175
	Yard Wastes	97
	Yard Wastes	134
	Yard Wastes	61
	Yard Wastes	105
	Yard Wastes	72
	Yard Wastes	172
	Yard Wastes	115
	Yard Wastes	226
	Yard Wastes	124
	Yard Wastes	144
	Yard Wastes	87
	Yard Wastes	174
	Yard Wastes	134
	Yard Wastes	345
	Yard Wastes	62
	Yard Wastes	237
	Yard Wastes	161
	Yard Wastes	216
	Yard Wastes	80
	Yard Wastes	171
	Yard Wastes	35
	Yard Wastes	80
Manfredi et al. 2009	Wood	85.9
		96.6
Wangyao et al. 2010	Wood	130.5
Jeon et al. 2007	Wood	116
	Hard wood	211.4760648
		35.776026
		129.5887164

Study	Food Wastes (1)	L_0 for Waste Fraction i (2)
Krause et al. 2018a		38.9561172
	Soft wood	48.25392
		27.197664
		41.235168
		28.952352
Krause et al. 2018b	Wood	49
	Wood	46
	Wood	82
	Wood	72
	Wood	36
	Wood	44
	Wood	26
	Wood	16
	Wood	34
	Wood	171
	Wood	46
	Wood	17
	Wood	20
	Wood	57
	Wood	66
	Wood	27
	Wood	20
	Wood	69
	Wood	108
	Wood	40
	31	45
	Wood	51
	Wood	11
	Wood	9
	Wood	142
	Wood	11
	Wood	109
Wang et al. 2011	Wood	29.133
	Wood	6.723
	Wood	0.4482
	Wood	75.7458
	Wood	5.64732
	Wood	5.01984
	Wood	4.12344
	Wood	0

Study	Food Wastes (1)	L_0 for Waste Fraction i (2)
	Wood	0
Tchnobanoglous et al. 1993/Machado	Wood	310.3616
Karanjekar et al. 2015	Textile Wastes	80.67869136
Wangyao et al. 2010	Textile Wastes	130.5
Jeon et al. 2007	Textile Wastes	215.8
	Leather	124
	Rubber	36
Jokela et al. 2005	Textile Wastes	191
	Diaper	59
Krause et al. 2018a	Cotton	166.7765792
		104.235362
		200.8899704
		147.8246952
Krause et al. 2018b	Textile Wastes	212
	Textile Wastes	212
	Textile Wastes	287
	Textile Wastes	193
	Textile Wastes	143
	Textile Wastes	20
	Textile Wastes	3
	Textile Wastes	299
	Textile Wastes	207
	Textile Wastes	177
	Textile Wastes	207
	Textile Wastes	212
	Textile Wastes	212
	Textile Wastes	212
	Textile Wastes	266
	Textile Wastes	171
	Textile Wastes	365
	Textile Wastes	246
	Textile Wastes	337
	Textile Wastes	302
	Textile Wastes	309
	Textile Wastes	212
	Textile Wastes	238
	Textile Wastes	298
	Textile Wastes	346
	Textile Wastes	325
	Textile Wastes	216

Study	Food Wastes (1)	L_0 for Waste Fraction i (2)
	Textile Wastes	80
	Textile Wastes	171
	Textile Wastes	35
	Textile Wastes	80
Tchnobanoglous et al. 1993/Machado	Textiles	269.7189
Vermeulen et al. 1993	Misc. Paper	186
Owens and Chynoweth	Misc. Paper	326
Vermuelen et al. 1993	Misc. Paper	270
Karanjekar et al. 2015	Misc. Paper	241.4602722
Krause et al. 2018b	Misc. Paper	219
	Misc. Paper	303
	Misc. Paper	106
	Misc. Paper	179
	Misc. Paper	164
	Misc. Paper	303
	Misc. Paper	132
	Misc. Paper	209
	Misc. Paper	290
	Misc. Paper	279
	Misc. Paper	273
	Misc. Paper	222
	Misc. Paper	213
	Misc. Paper	324
	Misc. Paper	213
	Misc. Paper	274
	Misc. Paper	219
	Misc. Paper	301
	Misc. Paper	212
	Misc. Paper	315
	Misc. Paper	327
	Misc. Paper	234
	Misc. Paper	281
	Misc. Paper	196
	Misc. Paper	280
	Misc. Paper	310
	Misc. Paper	232
	Misc. Paper	185
	Misc. Paper	367
	Misc. Paper	281
	Misc. Paper	305

Study	Food Wastes (1)	L_0 for Waste Fraction i (2)
	Misc. Paper	292
	Misc. Paper	312
	Misc. Paper	349
	Misc. Paper	291
	Misc. Paper	298
	Misc. Paper	272
	Misc. Paper	291
	Misc. Paper	282
Owens & Chynoweth 1993	Coated Paper	325
	Magazines	154
Vermuelen et al. 1993	Magazines	123
Elezer et al. 1997	Magazines	84.4
Krause et al. 2018b	Junk Mail	150.8
	Junk Mail	307
	Junk Mail	328
	Junk Mail	267
	Junk Mail	250
	Junk Mail	285
	Junk Mail	318
	Junk Mail	311
	Junk Mail	319
	Junk Mail	310
	Junk Mail	240
	Junk Mail	298
	Junk Mail	224
	Junk Mail	218
	Junk Mail	273
	Junk Mail	283
	Junk Mail	333
	Junk Mail	303
	Junk Mail	351
	Junk Mail	140
	Junk Mail	194
	Junk Mail	289
	Junk Mail	235
	Junk Mail	226
	Junk Mail	288
	Junk Mail	194
	Junk Mail	319
	Junk Mail	366

Study	Food Wastes (1)	L_0 for Waste Fraction i (2)
	Junk Mail	361
	Junk Mail	308
	Junk Mail	302
	Junk Mail	308
	Junk Mail	302
	Junk Mail	238
Vermuelen et al. 1993	Cardboard	387
	Cardboard	183
Jokela et al. 2005	Cardboard	146
Owens & Chynoweth	Cardboard	257
	Cardboard	300
	Cardboard	324
Vermuelen et al. 1993	Paperboard	304
Eleazer et al. 1997	Cardboard	217
Krause et al. 2018a	Cardboard	169
Qu et al. 2009	Cardboard	152.3
	Cardboard	164
Tch/Machado et al. 2009	Cardboard	197.415
	Cardboard	255
	Paperboard	200
	Paperboard	299
	Cardboard	169
	Paperboard	263
	Paperboard	286
	Cardboard	175
	Paperboard	240
	Paperboard	260
	Cardboard	187
	Paperboard	267
	Paperboard	300
	Cardboard	167
	Paperboard	300
	Paperboard	282
	Cardboard	166
	Paperboard	261
	Paperboard	272
	Paperboard	175
	Cardboard	224
	Paperboard	246
	Paperboard	208

Study	Food Wastes (1)	L_0 for Waste Fraction i (2)
Krause et al. 2018b	Cardboard	217
	Paperboard	246
	Paperboard	252
	Cardboard	235
	Paperboard	269
	Paperboard	264
	Cardboard	249
	Paperboard	242
	Paperboard	248
	Cardboard	170
	Paperboard	232
	Paperboard	262
	Cardboard	227
	Paperboard	297
	Paperboard	232
	Cardboard	225
	Paperboard	226
	Paperboard	286
	Cardboard	280
	Paperboard	221
	Paperboard	255
	Cardboard	194
	Paperboard	252
	Paperboard	260
	Cardboard	199
	Paperboard	218
	Paperboard	242
	Cardboard	234
	Paperboard	249
	Paperboard	273
	Cardboard	232
	Paperboard	231
	Paperboard	273
	Cardboard	239
	Paperboard	218
	Paperboard	244
	Cardboard	224
	Paperboard	228
	Paperboard	303
	Cardboard	227

Study	Food Wastes (1)	L_0 for Waste Fraction i (2)
	Paperboard	214
	Paperboard	293
	Cardboard	263
	Paperboard	194
	Paperboard	283
	Cardboard	175
	Paperboard	177
	Paperboard	259
	Cardboard	243
	Paperboard	347
	Paperboard	285
	Cardboard	194
	Paperboard	208
	Paperboard	364
	Cardboard	233
	Paperboard	184
	Paperboard	273
	Cardboard	226
	Paperboard	319
	Paperboard	275
	Cardboard	178
	Paperboard	256
	Paperboard	280
	Cardboard	215
	Paperboard	299
	Paperboard	243
	Cardboard	241
	Paperboard	206
	Cardboard	193
	Paperboard	201
	Cardboard	234
	Paperboard	265
	Paperboard	198
	Cardboard	189
	Paperboard	293
	Paperboard	260
	Cardboard	236
	Paperboard	281
	Paperboard	130
	Cardboard	198

Study	Food Wastes (1)	L_0 for Waste Fraction i (2)
	Paperboard	145
	Paperboard	245
	Cardboard	218
	Paperboard	119
	Paperboard	163
	Cardboard	236
	Paperboard	281
	Paperboard	130
	Cardboard	206
	Paperboard	191
	Paperboard	160
Vermuelen et al. 1993	Office paper	308
Owens & Chynoweth	Office paper	214
Jeon et al. 2007	Office paper	329
Eleazer et al. 1997	Office Paper	239
Ishii and Furuichi 2013	Office Paper	115
Wangyao et al. 2010	Office paper	217.3
Krause et al. 2018a	Office Paper	214.4
Qu et al. 2009	Office Paper	121.4
	Office Paper	239.1
	Office paper	258
Tch/Machado et al. 2009	Office paper	188.3295
	Office paper	369
	Office paper	317
	Office paper	315
	Office paper	313
	Office paper	349
	Office paper	229
	Office paper	287
	Office paper	294
	Office paper	289
	Office paper	338
	Office paper	335
	Office paper	275
	Office paper	275
	Office paper	304
	Office paper	289
	Office paper	148
	Office paper	314
	Office paper	311

Study	Food Wastes (1)	L_0 for Waste Fraction i (2)
Krause et al. 2018b	Office paper	306
	Office paper	281
	Office paper	281
	Office paper	303
	Office paper	276
	Office paper	314
	Office paper	308
	Office paper	276
	Office paper	312
	Office paper	295
	Office paper	203
	Office paper	253
	Office paper	215
	Office paper	280
	Office paper	305
	Office paper	293
	Office paper	323
	Office paper	295
	Office paper	293
	Office paper	317
Vermuelen et al. 1993	News paper	90
Owens & Chynoweth	News paper	75
Eleazer et al. 1997	News paper	66
Krause et al. 2018a	News paper	102
	News paper	74.3
	News paper	79
	News paper	82
	News paper	43
	News paper	73
	News paper	22
	News paper	84
	News paper	184
	News paper	149
	News paper	111
	News paper	126
	News paper	92
	News paper	55
	News paper	83
	News paper	78
	News paper	116

Study	Food Wastes (1)	L_0 for Waste Fraction i (2)
Krause et al. 2018b	News paper	38
	News paper	116
	News paper	77
	News paper	40
	News paper	73
	News paper	40
	News paper	38
	News paper	32
	News paper	18
	News paper	56
	News paper	56
	News paper	73
	News paper	183
	News paper	49
	News paper	322
	News paper	59
	News paper	122
	News paper	322
	News paper	28
Notes:		
(1) paperboard = milk cartons		
(2) All units in cubic meters CH_4/Mg wet waste.		

Study	Site	Geographic Location	Landfill Depth (m)	WIP (tons)	AVG Annual Precip (mm)	AVG Daily Temp (deg C)	Throughput (tons/day)	Areal Coverage (m2)	B0 (%)	Aprox. Waste Age	k value (1/yr)
Garg et al. 2006	Calabassas	California	36.58536585	26,805,695	431.80	17.83	1,044.12	1,275,165	71.5	45	0.0335
	Mission Hills	California	60.97560976	21,310,000	431.80	15.33	463,260.87	809,371	72.5	46	0.032
	Palos Verdes	California	60.97560976	24,048,240	355.60	17.06	3,794.77	121,001	71.5	54	0.018
	Puente Hills	California	69.9695122	142,250,454	406.40	19.72	5,850.19	2,388,000	72.4	49	0.042
	Scholl Canyon	California	91.46341463	32,886,801	406.40	18.22	1,274.37	853,887	72.8	45	0.023
	Coyote Canyon	California	76.2195122	38,999,999	304.80	17.94	586.56	1,315,000	72.0	43	0.028
	Spadra LF	California	45.72	17,268,344	406.40	17.50	463.34	700,106	73.0	49	0.033
	Bakersfield LF	California	30.48780488	9,448,923	145.29	18.56	1,219.02	463,365	72.7	14	0.025
	Prince William Co	Virginia	51.82926829	10,032,942	1,016.00	13.33	1,147.05	511,118	60.7	38	0.061
	Atlanta	Georgia	21.06867779	4,861,702	1,289.56	16.28	745.70	331,842	56.3	21	0.054
	Birmingham	Alabama	23.17073171	4,602,414	1,386.33	16.56	538.11	283,280	56.3	25	0.076
	Smithtown	Long Island, NY, USA	30.48	1,700,000	1,193.80	11.33	861.92	146,496	69.6	27	0.09
Barlaz et al. 2010a	Yolo County-Full Scale Cell 1 (NE)	California	18.29268293	76,324	581.00	17.12	544.61	14,200	51.0	9	0.15
	Yolo County-Full Scale Cell 2 (W)	California	18.29268293	194,271	581.00	17.12	544.61	24,300	51.0	9	0.09
	CSWMC-Cell A/B	Delaware	30.48780488	707,738	1,096.00	13.84	328.77	170,980	47.0	30	0.14
	CSWMC-Cell C	Delaware	30.48780488	17,246,450	1,096.00	13.84	328.77	170,980	47.0	22	0.17
	CSWMC-Cell D	Delaware	30.48780488	567,902	1,096.00	13.84	328.77	97,125	47.0	17	0.12
	CSWMC-Cell C/D	Delaware	30.48780488	120,999	1,096.00	13.84	328.77	26,305	47.0	12	0.15
	CSWMC-Cell E	Delaware	30.48780488	1,103,914	1,096.00	13.84	328.77	137,593	47.0	11	0.08
	Old-Lycoming County	Pennsylvania	36.58536585	5,302,531	1,233.00	10.87	729.83	306,556	48.0	24	0.05
	Expansion-Lycoming County	Pennsylvania	36.58536585	6,970,213	1,233.00	10.87	729.83	306,758	48.0	10	0.09
Zhao et al. 2013	Smiths Creek LF-Septage	Michigan	21.34146341	245,028	790.00	7.97	456.64	15,400	25.0	46	0.296
	Smiths Creek LF-Leachate	Michigan	21.34146341	139,206	790.00	7.97	456.64	250,000	25.0	46	0.082
El-Fadel et al. 1996	Shoreline LF, Mountain View	California	9.146341463	12,727,050	401.83	16.40	732.44	1,386,858	55.0	28	0.11
Faour et al. 2007	Yolo County-Pilot Cell	California	9.146341463	48,412	581.00	17.12	3.18	10,117	61.0	6	0.23
	Yolo County-Full Scale Cell 1 (NE)	California	18.29268293	76,324	581.00	17.12	98.15	14,200	61.0	6	0.2
	Yolo County-Full Scale Cell 2 (W)	California	18.29268293	194,271	581.00	17.12	320.88	24,300	61.0	6	2.2
	SSWMC	Delaware	28.96341463	5,966,310	1,111.76	13.45	6.71	502,620	54.0	23	0.21
	New-River-Landfill A	Florida	13.62686456	4,739,178	1,308.86	19.96	710.59	312,822	57.0	15	0.11
	CSWMC	Delaware	30.48780488	5,526,995	1,096.00	13.84	39.76	602,982	54.0	27	0.12
	Brogborough LF	UK	20	14,000	568.45	9.74	4.03	6,000	54.0	21	0.39
Tolaymat et al. 2010	Outer Loop LF-Control Cell	Kentucky	1.113558073	558,871	1,231.65	13.39	218.74	451,429	44.0	12	0.06
	Outer Loop LF-Cell A	Kentucky	2.455538315	616,191	1,231.65	13.39	337.64	225,714	44.0	9	0.11
	Outer Loop LF-Cell B	Kentucky	3.492223543	876,336	1,231.65	13.39	480.18	225,714	44.0	9	0.11
Wang et al. 2013, 2015	S	North Carolina	23.17073171	1,425,570	1,271.00	15.20	100.15	271,139	38.0	39	0.15
	G	Wisconsin	24.3902439	4,484,675	833.00	6.60	455.07	327,795	33.0	27	0.112
	H	Wisconsin	24.3902439	1,981,344	833.00	6.60	387.74	327,795	16.0	14	0.154
	T	Pennsylvania	29.87804878	28,729,729	1,143.00	9.60	3,148.46	457,295	51.0	25	0.0764
	C1	New York	35.06097561	5,224,091	1,110.00	7.80	260.23	477,529	45.0	55	0.17
	P1	North Carolina	23.17073171	4,301,015	1,271.00	15.20	512.33	271,139	50.0	23	0.062

Study	Site	Geographic Location	Landfill Depth (m)	WIP (tons)	AVG Annual Precip (mm)	AVG Daily Temp (deg C)	Throughput (tons/day)	Areal Coverage (m2)	B0 (%)	Aprox. Waste Age	k value (1/yr)
	Mission Hills	Virginia	30.18292683	6,112,009	1,136.00	13.10	930.29	307,561	52.0	18	0.17
	Q	Illinois	20.12195122	1,693,606	1,032.00	11.30	309.33	376,358	23.0	15	0.136
	C2	Michigan	26.2195122	2,829,063	840.00	7.30	322.95	424,920	23.0	24	0.15
	P2	Montana	22.86585366	5,142,714	1,118.00	12.70	1,083.82	279,233	48.0	13	0.132
	N	North Carolina	23.17073171	5,517,278	1,271.00	15.20	559.85	271,139	50.0	27	0.138
Amini et al. 2012	LF1-Phase 1	Florida	29.57317073	15,432,340	1,387.93	22.27	766.44	554,419	45.0	34	0.063333333
	LF1-Phase 2	Florida	29.57317073	3,527,392	1,387.93	22.27	766.44	554,419	45.0	34	0.03
	LF2	Florida	29.57317073	7,605,939	1,387.93	22.27	481.08	554,419	57.0	34	0.133333333
	LF3-Phase1	Florida	29.57317073	2,425,082	1,387.93	22.27	130.38	554,419	57.0	40	0.06
	LF3-Phase 2	Florida	29.57317073	2,425,082	1,387.93	22.27	217.30	554,419	57.0	24	0.183333333
	Landfill 4	Florida	29.57317073	15,432,340	1,387.93	22.27	766.44	554,419	57.0	34	0.086666667
	Landfill 5	Florida	29.57317073	9,479,866	1,387.93	22.27	766.44	554,419	57.0	34	0.060333333
Bentley et al. 2005	St. Landry Parish LF	Louisiana	27.43902439	1,060,000	1,509.27	20.37	290.95	133,546	58.0	19	0.2
	North Shelby LF	Tennessee	24.3902439	7,760,000	1,359.41	16.76	995.65	311,608	58.0	15	0.078
	Decatur LF	Georgia	6.17898483	973,000	1,348.49	19.42	165.55	141,640	58.0	23	0.179
	Houser's Mill Rd LF	Georgia	5.042668427	726,000	1,160.27	18.09	76.50	129,499	58.0	26	0.148
Karanjekar et al. 2015	LA County	California	23.17073171	6,427,347	316.82	18.08	624.35	494,813	72.6	50	0.0095
	Unknown	Texas	35.06097561	8,505,518	781.10	21.40	929.51	562,513	64.0	34	0.0129
Sormunen et al. 2013	Ammassuo LF	Finland	14.99128831	9,000,000	650.00	5.30	1,232.88	540,000	20.0	26	0.18
Oonk et al. 2013	Landgraaf Test Cell	Netherlands	8	27,558	752.38	10.57	18.88	3,500	15.0	4	1.37
Wangyao et al. 2010	4 Landfill sites	Thailand	7.360287498	354,121	1,581.93	28.13	165.44	47,704	69.0	8.25	0.33
Machado et al. 2009	MCL LF, Salvador	Brazil	45	6,490,882	1,928.97	25.30	2,535.31	230,898	38.0	12	0.2
Lamborn et al. 2012	Narre Warren LF, Melbourne	Australia	30	5,015,511	754.40	14.51	458.04	450,000	60.0	30	0.02
Vu et al. 2017	Regina LF, Saskatchewan	Canada	19.21036715	3,417,161	389.70	3.10	167.18	160,000	64.0	56	0.0115
	Saskatoon LF, Saskatchewan	Canada	19.46283315	5,842,243	353.70	3.30	258.16	270,000	64.0	62	0.0115
Nwaokorie et al. 2018	Phase 3+4	Wisconsin	27.57134796	855,208	835.91	5.26	123.32	27,900	56.7	22	0.037
	Phase 5	Wisconsin	30.38247033	533,691	835.91	5.26	97.48	15,800	56.7	18	0.118
	Phase 6	Wisconsin	13.85213016	803,890	835.91	5.26	137.65	52,200	56.7	16	0.127
	Phase 7	Wisconsin	4.954733506	149,279	835.91	5.26	34.08	27,100	56.7	12	0.025
	Sitewide	Wisconsin	12.6008497	2,517,432	835.91	5.26	313.50	179,700	56.7	23	0.078
Garg et al. 2006	W12A London, CA	Canada	8	276,624	987.10	7.50	1,812.02	1,070,000	56.7	33	0.02
Willumsen 2007	Sao Paoulo	Brazil	50	22,046,200	1,370.00	20.83	2,157.16	1,500,000	60.0	28	0.11
	Olavarria	Argentina	8	198,416	1,028.00	14.32	67.95	80,000	19.0	8	0.1
	Monterrey	Mexico	20	9,590,097	470.00	23.18	1,545.54	1,050,000	67.0	17	0.07
	Maldonado	Uruguay	13	391,320	1,400.00	16.41	107.21	125,000	70.0	10	0.28
Amini et al. 2013	Landfill A	USA	10.90653103	2,425,082	818.34	12.56	415.25	200,000	65.0	16	0.06
	Landfill B	USA	21.36675331	8,267,325	818.34	12.56	1,742.32	348,030	63.0	13	0.09
	Landfill C	USA	24.82295129	8,487,787	818.34	12.56	567.18	307,561	68.0	41	0.04
Lagos et al. 2017	Montreal-CESM	Canada	80	40,000,000	1,024.23	7.42	2,236.51	720,000	64.6	49	0.197
Budka et al. 2007	Conventional-Sonyaz	France	1.19998488	53,989	684.10	11.87	49.30	40,469	60.0	3	0.24
	Bioreactor-Sonyaz	France	1.11989105	50,385	684.10	11.87	46.01	40,469	59.0	3	1.36